NAC INTERNATIONAL

Atlanta Corporate Headquarters
3930 East Jones Bridge Road, Suite 200
Norcross, GA 30092
Phone 770-447-1144
Fax 770-447-1797
www.nacintl.com

March 23, 2009

U.S. Nuclear Regulatory Commission
11555 Rockville Pike
Rockville, MD 20852-2738

Attn: Document Control Desk

Subject: Submittal of a Request for an Amendment of Certificate of Compliance (CoC) No. 9225 for the NAC-LWT Cask to Incorporate Alternate Shipping Configurations for TPBARs and Fuel Rods

Docket No. 71-9225

Reference:
1. Model No. NAC-LWT Package, U.S. Nuclear Regulatory Commission (NRC) Certificate of Compliance (CoC) No. 9225, Revision 50, December 2008
2. Safety Analysis Report (SAR) for the NAC Legal Weight Truck Cask, Revision 39, NAC International, October 2008

NAC International (NAC) hereby submits a request to amend the Model NAC-LWT Package CoC to incorporate the following changes:

- Include the shipping configuration of up to 25 Tritium Producing Burnable Absorber Rods (TPBARs) in a PWR/BWR Rod Transport Canister utilizing a 5×5 rod insert;
- Allow use of an alternate design of the 5×5 rod insert for the PWR/BWR Rod Transport Canister that accommodates an oversize nonfuel-bearing component (e.g., CE guide tube or BWR water rod) and up to 21 fuel rods.

These proposed changes to the approved content conditions were presented and discussed with the NRC Spent Fuel Storage and Transportation staff during the March 17, 2009, presubmittal meeting in Rockville, MD.

This submittal includes eight copies of this transmittal letter and Revision LWT-09A changed pages to the Reference 2 SAR. The changed pages incorporate the requested amendment and the applicable evaluations performed to justify the addition of the proposed contents to the authorized shipping configurations of the CoC. Attachment 1 contains a brief summary of the changes to the SAR for the amendment. Consistent with NAC administrative practice, this proposed SAR revision is numbered to uniquely identify the applicable changed pages. Revision bars mark the SAR text changes on the Revision LWT-09A pages. Minor editorial changes have been made throughout the document. These changes do not affect the technical content of this submittal or the existing information in Reference 2. This submittal includes five revised license drawings. Attachment 2 to this transmittal letter lists all drawing changes in detail. The included List of Effective Pages identifies the current revision level of all pages in the Reference 2 SAR.



NMSS01

ED20090021

In order to better facilitate the review process, NAC is providing the Revision LWT-09A change pages as complete sections of the SAR. Consequently, a considerable number of Revision LWT-09A pages with no revision bars are included. In accordance with NAC's administrative practices, upon final acceptance of this application, the LWT-09A changed pages will be reformatted and incorporated into the next revision of the NAC-LWT SAR.

In this amendment request, the proposed changes to the authorized shipping configurations are described in Chapter 1. The structural, thermal, containment, shielding and criticality evaluations documenting the suitability of the NAC-LWT packaging for the requested configurations are presented in SAR Chapters 2, 3, 4, 5 and 6, respectively. Chapter 4, Containment, has also been revised to delete information that became nonapplicable after the implementation of leaktight (no credible leakage) shipping criteria for all contents. Chapter 7 has been revised to address the operational and loading requirements; and Chapter 8, Acceptance Tests and Maintenance Program, has been modified to clarify the acceptance criteria for helium leakage rate tests.

Attachment 3 to this transmittal letter includes the requested changes to Reference 1.

Approval of the amendment to Reference 1 is requested by November 30, 2009, to support shipping schedules planned for December 2009/January 2010.

If you have any comments or questions, please contact me on my direct line at 678-328-1274.

Sincerely,

Anthony L. Patko
Director, Licensing
Engineering

Attachment 1 – List of Changes, NAC-LWT SAR, Revision LWT-09A, Incorporation and Analysis of TPBAR Amendment
Attachment 2 – List of Drawing Changes, NAC-LWT SAR, Revision LWT-09A, TPBAR Amendment
Attachment 3 – Proposed Changes for Revision 51 of Certificate of Compliance No. 9225 for the NAC-LWT Cask

Enclosure

NAC INTERNATIONAL

Attachment 1

List of Changes

NAC-LWT SAR, Revision LWT-09A

Incorporation and Analysis of TPBAR Amendment

List of Changes, NAC-LWT SAR, Revision LWT-09A

Note: The List of Effective Pages and the Chapter Tables of Contents, including the List of Figures and the List of Tables, were revised as needed to incorporate the following changes.

Chapter 1

- Pages 1-iii & 1-iv – revised License Drawings 315-40-10 (Rev. 8), 315-40-098 (Rev. 6), 315-40-102 (Rev. 2), 315-40-104 (Rev. 5) and 315-40-128 (Rev. 3) and they are included in this amendment request
- Page 1-1, Section 1, General Information, 2nd paragraph, 4th bullet – added footnote 2 to the list of contents
- Page 1-3, Table 1.1-1, Terminology and Notation – added footnote 1 to 3rd bullet in list of contents
- Page 1.1-1 – added footnote 1 to 6th and 7th bullets in list of contents
- Page 1.1-2 – added "in a consolidation canister" to 300 TPBAR content and added "up to 25 TPBARs (of which two can be prefailed) in a rod holder" to NAC-LWT list of contents; 1st full paragraph – added new 2nd, 3rd & 4th sentences to describe the fuel rod holders; 2nd full paragraph, 1st sentence – deleted "and transported in a leaktight configuration NAC-LWT"; 3rd paragraph – deleted "and transported in a leaktight configuration NAC-LWT"
- Page 1.1-3 – added new 2nd paragraph to describe TPBAR content configuration and TPBAR containment configuration; added new last paragraph to describe TPBAR shipping configurations
- Page 1.2-5, Section 1.2.3, Contents of Packaging – added footnote 1 to 8th and 9th bullets in list of contents; added "in a consolidation canister" to 300 TPBAR content; added "up to 25 TPBARs (of which two can be prefailed) in a rod holder" to NAC-LWT list of contents
- Page 1.2-6, Item 4 – added "0.058 kW for 25 TPBARs"; Item 7 – deleted "in a leaktight configuration NAC-LWT"; Item 8 – deleted "in a leaktight configuration NAC-LWT"
- Page 1.2-7, Item 13 – revised throughout; Item 19 – deleted "and transported in a leaktight configuration NAC-LWT"
- Page 1.2-9, Item 2 – deleted "and transported in a leaktight configuration NAC-LWT"; Item 3 – deleted "and transported in a leaktight configuration NAC-LWT"
- Page 1.2-10, 2nd paragraph, last sentence – deleted "and transported in a leaktight configuration NAC-LWT"
- Page 1.2-13, Section 1.2.3.4 – added "Assembly" to section title and added new 2nd paragraph; Section 1.2.3.5 – added "Assembly" to section title and added new 2nd paragraph; Section 1.2.3.6, TPBARs, 1st paragraph, 1st sentence – changed "two" to "three"; added 2 new sentences to end of paragraph; 2nd paragraph, 1st sentence – changed "second" to "third"
- Page 1.2-14, 1st full paragraph, 1st sentence – changed "both" to "the consolidation canister and waste container"; added new last sentence; Section 1.2.3.7 – changed title to "PWR/BWR Fuel Rods"; added new 1st paragraph
- Page 1.2-18, Section 1.2.3.11, PWR MOX Fuel Rods, 1st paragraph, 1st sentence – deleted "and transported … helium)"

Chapter 2

- Page 2.2.1-2, Table 2.2.1-1, Weights of the NAC-LWT Cask Major Components – revised TPBAR Basket and Spacer weight for consistency; added two new rows to bottom of table and footnote 4
- Page 2.2.1-3, Table 2.2.1-2, Weights and Center of Gravity Locations for the NAC-LWT Cask Shipping Configurations – revised Package – Loaded for Shipment (TPBARs and Basket) and Package – Empty for Shipment (TPBAR Basket) weights for consistency
- Page 2.2.1-4, Table 2.2.1-2, Weights and Center of Gravity Locations for the NAC-LWT Cask Shipping Configurations (cont'd) – added two new rows
- Page 2.6.7-47, Section 2.6.7.10 – changed the title to "PWR/BWR Rod Transport Canister Assembly Analysis"; Section 2.6.7.10.1, Discussion, 1st sentence – changed "rod shipment can assembly" to "PWR/BWR Rod Transport Canister"; 3rd sentence – added "(rod holder)"; added three new sentences to discuss the BWR water tube
- Pages 2.6.12-91 through 2.6.12-93 – added new Section 2.6.12.12, TPBAR Basket with the PWR/BWR Rod Transport Canister
- Page 2.7.7-59, Section 2.7.7.12.4, TPBAR Spacer – 9th sentence – added "bounded by"
- Pages 2.7.7-70 through 2.7.7-72 – added new Section 2.7.7.14, TPBAR Basket with the PWR/BWR Rod Transport Canister
- Page 2.9-6, Section 2.9.4, ANSTO Fuels – added text as stated in NAC letter #ED20080143 dated 12/4/08 to clarify ANSTO HIFAR amendment request
- Page 2.10.14-4, Section 2.10.14.3, Inner Shell Buckling, 1st paragraph, 1st bullet – changed "TPBAR contents of 1,000 lbs envelops the weight" to "TPBAR contents of 1,000 lbs is enveloped by the weight"; 2nd bullet, 2nd sentence – revised for clarity
- Pages 2.10.16-1 through 2.10.16.5 – added new Section 2.10.16, Structural Evaluation of the NAC-LWT Cask Body with TPBARs in the PWR/BWR Rod Transport Canister

Chapter 3

- Page 3.4-15, Section 3.4.1.7 – changed title to "High Burnup PWR or BWR Rods in a PWR/BWR Rod Transport Canister; 1st paragraph – added last three sentences to discuss BWR water rod; 2nd paragraph – 1st sentence – revised throughout to list three configurations
- Page 3.4-25, Section 3.4.1.11, High Burnup PWR and BWR Fuel Rods in a Rod Holder with Damaged Fuel Rods, 2nd paragraph, 1st sentence – revised throughout to list three configurations; 3rd sentence – editorial change
- Pages 3.4-31 through 3.4-34 – added new Section 3.4.1.16, Thermal Evaluation for TPBARs in the PWR/BWR Rod Transport Canister
- Page 3.4-44, last paragraph, 1st sentence – changed "canister cavity" to "cask cavity"
- Page 3.4-45 – added new 2nd paragraph to address TPBAR content condition of 25 TPBARs contained in a 5×5 rod holder
- Page 3.4-46, Combustible Hazard Assessment – added new 4th paragraph to address 25 TPBAR payload

- Pages 3.5.12 & 3.5.13 – added new Section 3.5.3.14, Evaluation for TPBARs in the PWR/BWR Rod Transport Canister
- Pages 3.5-16 & 3.5-17, Section 3.5.4.4, TPBAR Shipment Cask Cavity Internal Pressure—Accident Conditions, 1st paragraph – added two new sentences to the end of the paragraph to address TPBAR content condition of up to 25 TPBARs contained in a 5×5 rod holder

Chapter 4

- Page 4.1-1, Section 4.1, Containment Boundary, 1st paragraph – revised throughout and split into two paragraphs; 2nd paragraph – deleted last sentence; Section 4.1.2.1, Seals, 1st paragraph, 1st sentence – revised throughout; deleted 4th sentence and moved it into a 2nd paragraph on following page
- Page 4.1-2, 1st paragraph – moved from previous page; Section 4.1.2.1.1, Fabrication Leakage Rate Test – revised throughout; Section 4.1.2.1.2, Fabrication Pressure Test, 1st paragraph, last sentence – deleted "for fissile material shipments"; 2nd paragraph, last sentence – added "for the TPBAR content conditions"; moved last sentence of this paragraph to a new paragraph; Section 4.1.2.1.3, Preshipment Leakage Rate Test, 2nd paragraph – changed "If the alternate port cover" to "If an alternate port cover's"; changed "Section 8.1.3" to "Section 8.1.3.2.2"
- Page 4.1-3, Closure, 2nd paragraph – revised throughout; 3rd paragraph, last sentence – revised throughout
- Page 4.2-1, Section 4.2, Containment Requirements for Normal Conditions of Transport – revised throughout; Section 4.2.1, Containment of Radioactive Material – revised throughout; eliminated subsections 4.2.1.1 and 4.2.1.2
- Page 4.2-2, Section 4.2.2, Pressurization of Containment Vessel – entire section revised throughout; Section 4.2.3, Containment Criteria, 1st paragraph – revised throughout; deleted 2nd and 3rd paragraphs and added new paragraph
- Page 4.2-3, last paragraph – revised throughout
- Deleted Tables 4.2-1, 4.2-2 and 4.2-4
- Page 4.2-4 – old Table 4.2-3 became Table 4.2-1 and added "Containment Analysis Basis" to title; footnote 1 – deleted last sentence; footnote 3 – deleted last sentence
- Page 4.3-1, Section 4.3, Containment Requirements for Hypothetical Accident Conditions – revised throughout; Section 4.3.1, Fission Gas Products – revised throughout; Section 4.3.2, Containment of Radioactive Materials – revised throughout; deleted old Sections 4.3.2.1 and 4.3.2.2
- Page 4.3-2, old Section 4.3.2.3 became Section 4.3.2.1, Containment Criteria and text changed throughout; old Section 4.3.2.4 became Section 4.3.2.2, Tritium Permeation Rate of Seals for TPBAR Shipment
- Deleted Tables 4.3-1 through 4.3-4; deleted entire Section 4.5.4, SAS2H Output and Group A_2 Values for Design Basis PWR, BWR, TRIGA MTR and DIDO Fuel, and Tables 4.5-2 through 4.5-24; deleted Section 4.5.5, Containment Analysis of MTR Fuel Elements, and subsections; deleted Section 4.5.6, Evaluation of Normal Conditions Allowable Leakage Rate for 25 BWR High Burnup Rods with up to 14 Damaged Rods; deleted Section 4.5.7,

Containment Analysis of DIDO Fuel Assemblies and subsections; deleted Section 4.5.8, Containment Analysis for PULSTAR Fuel Elements, and Tables 4.5-25 through 4.5-31

- Page 4.5-29, old Section 4.5.9, Metallic Face Seal, became Section 4.5.4

Chapter 5

- Page 5.1.1-1, Section 5.1.1, NAC-LWT Contents – added footnote 1 to 9th bullet in list of contents; added "in a consolidation canister" and "Up to 25 TPBARs (of which two can be prefailed) in a rod holder"
- Page 5.1.1-9, Table 5.1.1-1, Type, Form, Quantity and Potential Sources of Design Basis Fuel, TPBAR section, Material Type – added "(max. for 300 TPBARs)"; Quantity – added "in consolidation canister" and "Up to 25 TPBARs (of which two can be prefailed) in rod holder"; Maximum Activity – added "max. for 300 TPBARs"
- Page 5.3.13-1, Section 5.3.13, TPBAR Shielding Evaluation, 1st paragraph – revised throughout
- Page 5.3.13-2 – added new 4th paragraph to address 25 TPBAR configuration

Chapter 6

- Page 6.7.1-1, Section 6.7.1.1, Package Fuel Loading, 3rd sentence – changed "Table 6.7.1-1 and Table 6.7.1-2" to "Table 6.7.1-12 and table 6.7.1-13"
- Page 6.7.1-19 – added new Table 6.7.1-12, B&W, CE and Westinghouse PWR Fuel Assembly Data, and new Table 6.7.1-13, Exxon/ANF PWR Fuel Assembly Data

Chapter 7

- Page 7.1-1, Section 7, Operating Procedures – 4th paragraph, 1st sentence – added "in a leaktight containment boundary configuration"; deleted remainder of paragraph; 5th paragraph, 1st sentence – added "in a leaktight containment boundary configuration"; deleted last sentence
- Page 7.1-2, Section 7.1, Procedures for Loading Packages, 1st paragraph, last sentence – deleted "or 7.1.1"; 2nd paragraph – revised throughout; 4th paragraph, 1st sentence -- added "TPBAR"; last sentence – added "following component removal"
- Page 7.1-3, 1st paragraph, 1st sentence – changed "vacuum dried and verified as dry" to "vacuum dried, verified as dry"
- Page 7.1-6, Item 36, Note – deleted "torque the high-strength bolts to 285 ±15 inch-pounds" and changed "Section 8.1.3.3" to "Section 8.1.3.3.2"; Item 42 – revised throughout
- Page 7.1-9, Item 26, Note – deleted "torque the high-strength bolts to 285 ±15 inch-pounds" and changed "Section 8.1.3.3" to "Section 8.1.3.3.2"
- Page 7.1-10, Item 32 – revised throughout
- Page 7.1-17, first Note – deleted "torque the high-strength bolts to 285 ±15 inch-pounds" and changed "Section 8.1.3.3" to "Section 8.1.3.3.2"; Item 37 – revised throughout

- Page 7.1-33, Section 7.1.6, Procedure for Dry Loading of TRIGA Fuel Basket Modules and GA IFM Modules into the NAC-LWT Cask, 2nd paragraph, last sentence – deleted "shall be loaded and transported in an NAC-LWT assembled and tested in a leaktight containment configuration"
- Page 7.1-34, 1st partial sentence/paragraph – deleted last sentence of that paragraph
- Page 7.1-37, Item 29 – deleted last sentence; Item 32, Note, 1st sentence – deleted "to provide a leaktight containment boundary"; 2nd sentence – deleted "torque the high-strength bolts to 285 ±15 inch-pounds" and changed "Section 8.1.3.3" to "Section 8.1.3.3.2"; Item 36, 3rd sentence – revised throughout
- Page 7.1-39, Section 7.1.8 – added "or TPBARs" to title; 1st paragraph, 1st sentence – added "For the shipment of PWR and BWR fuel rods," and moved last sentence of paragraph to 3rd paragraph; added new 2nd paragraph
- Page 7.1-40, Item 6 – revised throughout for clarity
- Page 7.1-41, Section7.1.9 – added "or PWR/BWR Rod Transport Canister" to title; 1st paragraph, 1st sentence – added "or with a screened or free flow PWR/BWR Rod Transport Canister"; added new 2nd paragraph; 4th paragraph – revised throughout
- Page 7.1-42, Item 11, last sentence – added "for consolidation canister transports"; Item 12 – revised throughout and Note added; Item 16 – added "or the PWR/BWR Rod Transport Canister containing TPBARs"; Item 17 – added "or the PWR/BWR Rod Transport Canister"
- Page 7.1-43, Item 18, 2nd sentence – added "consolidation"; Item 20 – revised 1st and 2nd sentences for clarity
- Page 7.1-44, Item 33 – deleted "torque the high-strength bolts to 285 ±15 inch-pounds" and changed "Section 8.1.3.3" to "Section 8.1.3.3.2"; Item 39 – revised throughout
- Page 7.1-48, Item 33, Note, 1st sentence – deleted "to confirm the leaktight seal condition"; 2nd sentence – deleted ""torque the high-strength bolts to 285 ±15 inch-pounds" and changed "Section 8.1.3.3" to "Section 8.1.3.3.2"; Item 39 – revised throughout
- Page 7.1-50, Item 23, 2nd sentence – changed "Section 8.1.3.3" to "Section 8.1.3.3.2"
- Page 7.1-51, Item 27 – revised throughout
- Page 7.1-52, 1st partial sentence/paragraph – deleted remainder of that sentence and last sentence of that paragraph; 2nd full paragraph – deleted "including Alternate B port covers"
- Page 7.1-53, Item 10 – revised throughout and added Note
- Page 7.1-54, Item 32 – deleted "with leakage rate acceptance criteria per 8.1.3.1, Step 9(b); added new Item 33
- Page 7.1-55 – added new Items 34 and 35 with Note; renumbered subsequent items; new Item 41 (formerly 39) – revised throughout
- Page 7.2-1, Section 7.2.1, Procedures for Wet Unloading of LWR Fuel and PWR, PWR MOX an BWR Fuel Rods in Transport Canisters, Item 5 – revised throughout
- Page 7.2-2, Item 10 – changed "fill/drain" to "drain"
- Page 7.2-4, Item 5 – revised throughout
- Page 7.2-6, Section 7.2.3, Procedure for Wet Unloading of MTR, TRIGA, DIDO, ANSTO or PULSTAR Fuel Basket Content, Item 5 – revised throughout
- Page 7.2-9, Item 5 – revised throughout; Item 18 – deleted "or TPBAR consolidation canister"

- Page 7.2-10, Item 21 – deleted "(not required for TPBAR configuration)"; Section 7.2.5, Procedure for Dry Unloading of TPBAR Contents, 1st paragraph – revised throughout; added new Item 5 and renumbered items 6-9
- Page 7.2-11, Item 10 – combined former Items 9 and 10
- Page 7.2-13, Item 10 – combined former Items 10 and 11 and renumbered subsequent items; Item 21, Note – added "Inspection or"; Item 22 – revised throughout

Chapter 8

- Page 8.1-1, Section 8.1, Acceptance Tests, 1st paragraph, 5th sentence – revised throughout; added new last sentence
- Page 8.1-4, Section 8.1.3.1, Closure Lid Leakage Rate Test, Item 9 – revised throughout
- Page 8.1-5, Section 8.1.3.2.1, Fabrication and Periodic Leakage Rate Tests, Item 8 – revised throughout
- Page 8.1-6, Item 10 – revised throughout; Section 8.1.3.3.1, Fabrication and Periodic Leakage Rate Tests, Item 8 – revised throughout
- Page 8.1-7, Section 8.1.3.3.2, Maintenance and Preshipment Leakage Rate Tests, Item 10 – added "under test conditions"
- Page 8.1-8, Section 8.1.4.2, Gaskets – deleted 2nd paragraph
- Page 8.2-1, Section 8.2, Maintenance Program, 5th paragraph – revised throughout; 6th paragraph – deleted "and/or for a leaktight containment condition"
- Page 8.2-4, Table 8.2-1, Maintenance Program Schedule, last line of table – deleted "as applicable"

NAC INTERNATIONAL

Attachment 2

List of Drawing Changes

NAC-LWT SAR, Revision LWT-09A

TPBAR Amendment

Drawing 315-40-10, LWT Cask, PWR Basket, Revision 8

- Sheet 1: Revise BO.M. on sheet 1 to reflect the added Assembly 95 "ALT. TPBAR BASKET ASSEMBLY" on sheet 2. Assembly 95 includes items 1, 2, 3, 4, 5, 6, 8, 9, 10, 11, 12 and 14 as follows:
  - B.O.M. #1, Qty 1, RING, 304 ST. STL., ASTM A240, 1/4 X 4
  - B.O.M. #2, Qty 2, SIDE, 6061-T651, ASTM B209, 2-1/2 PLATE
  - B.O.M. #3, Qty 2, SIDE, 6061-T651, ASTM B209, 2-1/2 PLATE
  - B.O.M. #4, Qty 2, LUG, 304 ST. STL., ASTM A276, 1/2 X 1-5/8 BAR
  - B.O.M. #5, Qty 1, FLANGE, 304 ST. STL., ASTM A240, 5/8 PLATE
  - B.O.M. #6, Qty 1, FLANGE, 304 ST. STL., ASTM A240, 7/8 PLATE
  - B.O.M. #8, Qty 10, HEX HD BOLT, 18-8, COML, 1/2-13 UNC X 1-1/2 LG
  - B.O.M. #9, Qty 10, THREAD INSERT, ST. STL., COML, 3585-8CN1000 HELI-COIL
  - B.O.M. #10, Qty 10, BAND, 6061-T651, ASTM B211, 1/2 BAR
  - B.O.M. #11, Qty 10, LOCK WASHER, 18-8, COML, 1/2 REGULAR
  - B.O.M. #12, Qty 1, ALTERNATE SPACER, 304 ST. STL., ASTM A312, 8" SCH 80
  - B.O.M. #14, Qty 4, SPACER GUIDE, 304 ST. STL., ASTM A240/A276, 1 PLATE/BAR
- Sheet 2:
  - Zone B5, add assembly callout for assembly 95 (ALT. TPBAR BASKET ASSEMBLY)
  - Zone C1, add identification balloon 12 for the new spacer
  - Zone D1, add -96, to 7.0 dimension identifying Item 7 used for Assembly 96 and 6.5 –95 dimension identifying Item 12 used for new Assembly 95
  - Zone E4, remove (176.7) referenced basket overall length

Drawing 315-40-098, PWR/BWR Transport Canister Assembly, Revision 6

- Revise B.O.M. to add Item 19 "5X5 INSERT W/WATER ROD" on sheet 1 as follows:
  - B.O.M. #19, Qty A/R for Assemblies 99, 98, 97, 95 and 94, Drawing No. 315-40-102-98
- Zone F-4, replace identification balloon 8 with 19 and revise view to show 5x5 w/ water rod assembly
- Change verbiage of Assembly 97 to "SCREENED CAN (SHOWN WITH 5X5 INSERT W/ WATER ROD) was "SCREENED CAN (SHOWN WITH 5X5 INSERT)"

Drawing 315-40-102, 5×5 Insert, PWR/BWR Transport Canister, Revision 2

- Sheet 1:
  1. Revise BOM to add Assembly 98 which includes 21 of Item 1 and 1 of Item 2 as follows:
     - Item 1 named "Pin Tube", previously used for Assembly 99; Quantity is 21 for assembly 98
     - Item 2 named "Water Rod Tube"

       Quantity: 1 (assembly 98 only)

       Material: 304 ST. STL.

       Spec.: ASME SA249/ASTM 269

       Description: 1 7/16 OD TUBE X .049 WALL
  2. Zone D-5, add Assembly 98 identification balloon and the name "5X5 INSERT WITH WATER ROD", Weight: 68#.
  3. Revise delta note 1 as follows: "TACK WELD ITEM 1, PIN TUBE(S), FOR ASSEMBLY 99, AND ITEM 1 AND 2, PIN AND WATER ROD TUBE(S) FOR ASSEMBLY 98, TOGETHER ON AT LEAST TWO QUADRANTS OF EACH TUBE. INCLUDE AT LEAST 1" OF WELD FOR EVERY 12" OF MATERIAL THE LENGTH OF THE TUBE."
  4. Zone A-7, add Section A-A to show Assembly 98 with the tube for water rod
  5. Zone A-5, add Assembly 99 wording to Section A-A
  6 Update title block group names

Drawing 315-40-104, Legal Weight Truck Transport Cask Assy., PWR/BWR Rod Transport Canister, Revision 5

Sheet 1:

- Add Assembly 95 "PWR/BWR ROD TRANSPORT CANISTER FOR TPBARS" on sheet 3 and revise B.O.M. on sheet 1 to add Assembly 95 which includes items 1, 2, 4, 6, 7, 8, 9, 11, 12, 20 and 21 as follows:
  - B.O.M. #1, Qty 1, Impact Limiter, 315-40-05-99
  - B.O.M. #2, Qty 1, Impact Limiter, 315-0-06-99
  - B.O.M. #4, Qty A/R, Free Flow Can, 315-40-98-99
  - B.O.M. #6, Qty 1, PWR Insert, 315-40-105-99
  - B.O.M. #7, Qty 8, Ball Lock-Pin, 315-40-01-8
  - B.O.M. #8, Qty A/R, Wire, 315-40-01-10
  - B.O.M. #9, Qty 1, Tamper Indicating Device (TID), 315-40-01-11
  - B.O.M. #11, Qty A/R, Pin Spacer, 315-40-103-1
  - B.O.M. #12, Qty A/R, Screen Can, 315-40-98-97

- B.O.M. #20, Qty 1, ALT. TPBAR Basket Assembly, 315-40-10-95
- B.O.M. #21, Qty 1, Cask Assembly, 315-40-02-97

- Delete delta note 3 and add "DELETED" and delta note 3 symbol from the B.O.M. pointing to Item 3
- Revise delta note 4 to insert "..OR TPBARS.." wording after "MOX FUEL RODS"

Sheet 3:

- Add Assembly 95 "PWR/BWR ROD TRANSPORT CANISTER FOR TPBARS"

Drawing 315-40-128, Legal Weight Truck Transport Cask Assy., TPBAR Shipment, Revision 3

Sheet 1:

- Revise B.O.M. as follows:
  - Add Item #13, Qty A/R, ALT. TPBAR BASKET ASSEMBLY, Drawing No. 315-40-10-95
  - Revise quantity of Item 10 (TPBAR BASKET ASSEMBLY) for Assembly 99, **is** A/R, **was** 1

NAC INTERNATIONAL

Attachment 3

Proposed Changes for Revision 51 of

Certificate of Compliance No. 9225

for the NAC-LWT Cask

Proposed Changes for Revision 51 of Certificate of Compliance No. 9225 for the NAC-LWT Cask (changes are highlighted)

Page No.	Description of Change
1-27	CoC heading – 1.b.: Revision Number 51. Remove previous revision bars throughout.
2 of 27	5.(a)(3) Drawings (ii) LWT 315-40-10, Rev. 8 (Sheets 1-2) PWR Basket
3 of 27	5.(a)(3)(ii) Drawings (continued) LWT 315-40-098, Rev. 6 (Sheets 1-3) PWR/BWR Rod Transport Canister Assembly LWT 315-40-102, Rev. 2 5 × 5 Insert, PWR/BWR Transport Canister LWT 315-40-104, Rev. 5 (Sheets 1-3) LWT Cask Assembly, PWR/BWR Rod Transport Canister
20 of 27	5.(b)(2) Maximum quantity of material per package (continued) Revise the next-to-last sentence of the 3rd paragraph of item (ix) as follows: (ix) Guide/instrument tubes and tube segments may be placed in the fuel rod insert.
21 of 27	5.(b)(2) Maximum quantity of material per package (continued) Insert the following new sentence into the last paragraph of item (x) as the next-to-last sentence: (x) … fuel rod insert. Water rods and inert rods may be placed in the fuel rod insert. The fuel rod insert must be transported ….
22 of 27	5.(b)(2) Maximum quantity of material per package (continued) Revise item (xiii) to include a second paragraph as follows: (xiii) Up to 300 TPBARs, … volume of 300 TPBARs. Up to 25 TPBARs, including a maximum of 2 prefailed rods, positioned within a PWR/BWR Rod Transport Canister. The PWR/BWR Rod Transport Canister is transported in a TPBAR basket assembly. The maximum decay heat is 2.31 watts per rod and 58 watts per package.

Proposed Changes for Revision 51 of Certificate of Compliance No. 9225 for the NAC-LWT Cask (changes are highlighted) (cont'd)

Page No.	Description of Change
26 of 27	Revise item 14 (c) as follows: (c) The package must be configured as shown in NAC International Drawing No. 315-40-128, Rev. 3, for the applicable TPBAR contents; and
27 of 27	Revise items 18 and 19 as follows: 18. Revision 50 of this certificate may be used until TBD. 20. Expiration Date: TBD. Under REFERENCES, change application date to March XX, 2009. NAC International, Inc., supplements dated: TBD, TBD.

March 2009

Revision LWT-09A

NAC-LWT

Legal Weight Truck Cask System

SAFETY ANALYSIS REPORT

Volume 1 of 2

Docket No. 71-9225

NAC INTERNATIONAL

Atlanta Corporate Headquarters: 3930 East Jones Bridge Road, Norcross, Georgia 30092 USA
Phone 770-447-1144, Fax 770-447-1797, www.nacintl.com

List of Effective Pages

LIST OF EFFECTIVE PAGES

Chapter 1

1-i thru 1-iv ..... Revision LWT-09A
1-1 thru 1-5 ..... Revision LWT-09A
1.1-1 thru 1.1-3 ..... Revision LWT-09A
1.2-1 thru 1.2-50 ..... Revision LWT-09A
1.3-1 ..... Revision 39
1.4-1 ..... Revision 39
1.5-1 ..... Revision 39

73 drawings in the
Chapter 1 List of Drawings

Chapter 1 Appendices 1-A
through 1-G

Chapter 2

2-i thru 2-xxiv ..... Revision LWT-09A
2-1 ..... Revision 39
2.1.1-1 thru 2.1.1-2 ..... Revision 39
2.1.2-1 thru 2.1.2-3 ..... Revision 39
2.1.3-1 thru 2.1.3-8 ..... Revision 39
2.2.1-1 thru 2.2.1-4 ..... Revision LWT-09A
2.3-1 ..... Revision 39
2.3.1-1 thru 2.3.1-13 ..... Revision 39
2.4-1 ..... Revision 39
2.4.1-1 ..... Revision 39
2.4.2-1 ..... Revision 39
2.4.3-1 ..... Revision 39
2.4.4-1 ..... Revision 39
2.4.5-1 ..... Revision 39
2.4.6-1 ..... Revision 39
2.5.1-1 thru 2.5.1-11 ..... Revision 39
2.5.2-1 thru 2.5.2-17 ..... Revision 39
2.6.1-1 thru 2.6.1-7 ..... Revision 39
2.6.2-1 thru 2.6.2-7 ..... Revision 39
2.6.3-1 ..... Revision 39
2.6.4-1 ..... Revision 39
2.6.5-1 thru 2.6.5-2 ..... Revision 39
2.6.6-1 ..... Revision 39
2.6.7-1 thru 2.6.7-136 . Revision LWT-09A
2.6.8-1 ..... Revision 39
2.6.9-1 ..... Revision 39
2.6.10-1 thru 2.6.10-15 ..... Revision 39
2.6.11-1 thru 2.6.11-12 ..... Revision 39
2.6.12-1 thru 2.6.12-91 ..... Revision 39
2.7-1 ..... Revision 39
2.7.1-1 thru 2.7.1-117 ..... Revision 39
2.7.2-1 thru 2.7.2-23 ..... Revision 39
2.7.3-1 thru 2.7.3-5 ..... Revision 39
2.7.4-1 ..... Revision 39
2.7.5-1 thru 2.7.5-5 ..... Revision 39
2.7.6-1 thru 2.7.6-4 ..... Revision 39
2.7.7-1 thru 2.7.7-50 ..... Revision 39
2.7.7-51 thru 2.7.7-72 . Revision LWT-09A
2.8-1 ..... Revision 39
2.9-1 thru 2.9-14 ..... Revision LWT-09A
2.10.1-1 thru 2.10.1-3 ..... Revision 39
2.10.2-1 thru 2.10.2-49 ..... Revision 39
2.10.3-1 thru 2.10.3-18 ..... Revision 39
2.10.4-1 thru 2.10.4-11 ..... Revision 39
2.10.5-1 ..... Revision 39
2.10.6-1 thru 2.10.6-19 ..... Revision 39
2.10.7-1 thru 2.10.7-66 ..... Revision 39
2.10.8-1 thru 2.10.8-67 ..... Revision 39
2.10.9-1 thru 2.10.9-9 ..... Revision 39
2.10.10-1 thru 2.10.10-97 ..... Revision 39
2.10.11-1 thru 2.10.11-10 ..... Revision 39
2.10.12-1 thru 2.10.12-31 ..... Revision 39

LIST OF EFFECTIVE PAGES (Continued)

2.10.13-1 thru 2.10.13-17 ..... Revision 39
2.10.14-1 thru 2.10.14-38 .. Revision LWT-09A
2.10.15-1 thru 2.10.15-10 ..... Revision 39
2.10.16-1 thru 2.10.16-5 .... Revision LWT-09A

Chapter 3
3-i thru 3-v ..... Revision LWT-09A
3.1-1 thru 3.1-2 ..... Revision 39
3.2-1 thru 3.2-11 ..... Revision 39
3.3-1 ..... Revision 39
3.4-1 thru 3.4-88 ..... Revision LWT-09A
3.5-1 thru 3.5-35 ..... Revision LWT-09A
3.6-1 thru 3.6-12 ..... Revision 39

Chapter 4
4-i thru 4-iii ..... Revision LWT-09A
4.1-1 thru 4.1-3 ..... Revision LWT-09A
4.2-1 thru 4.2-4 ..... Revision LWT-09A
4.3-1 thru 4.3-4 ..... Revision LWT-09A
4.4-1 ..... Revision 39
4.5-1 thru 4.5-28 ..... Revision 39
4.5-29 thru 4.5-40 ..... Revision LWT-09A

Chapter 5
5-i thru 5-xii ..... Revision LWT-09A
5-1 thru 5-3 ..... Revision 39
5.1.1-1 thru 5.1.1-17 ..... Revision LWT-09A
5.2.1-1 thru 5.2.1-7 ..... Revision 39
5.3.1-1 thru 5.3.1-2 ..... Revision 39
5.3.2-1 ..... Revision 39
5.3.3-1 thru 5.3.3-8 ..... Revision 39
5.3.4-1 thru 5.3.4-19 ..... Revision 39
5.3.5-1 thru 5.3.5-4 ..... Revision 39
5.3.6-1 thru 5.3.6-18 ..... Revision 39
5.3.7-1 thru 5.3.7-19 ..... Revision 39
5.3.8-1 thru 5.3.8-25 ..... Revision 39
5.3.9-1 thru 5.3.9-26 ..... Revision 39
5.3.10-1 thru 5.3.10-14 ..... Revision 39
5.3.11-1 thru 5.3.11-48 ..... Revision 39
5.3.12-1 thru 5.3.12-26 ..... Revision 39
5.3.13-1 thru 5.3.13-18 .. Revision LWT-09A
5.3.14-1 thru 5.3.14-21 ..... Revision 39
5.3.15-1 thru 5.3.15-9 ..... Revision 39
5.3.16-1 thru 5.3.16-5 ..... Revision 39
5.3.17-1 thru 5.3.17-9 ..... Revision 39
5.3.18-1 thru 5.3.18-40 ..... Revision 39
5.4.1-1 thru 5.4.1-6 ..... Revision 39

Chapter 6
6-i thru 6-xiii ..... Revision LWT-09A
6-1 ..... Revision 39
6.1-1 thru 6.1-5 ..... Revision 39
6.2-1 ..... Revision 39
6.2.1-1 thru 6.2.1-3 ..... Revision 39
6.2.2-1 thru 6.2.2-3 ..... Revision 39
6.2.3-1 thru 6.2.3-7 ..... Revision 39
6.2.4-1 ..... Revision 39
6.2.5-1 thru 6.2.5-5 ..... Revision 39
6.2.6-1 thru 6.2.6-3 ..... Revision 39
6.2.7-1 thru 6.2.7-2 ..... Revision 39
6.2.8-1 thru 6.2.8-3 ..... Revision 39
6.2.9-1 thru 6.2.9-4 ..... Revision 39
6.2.10-1 thru 6.2.10-3 ..... Revision 39
6.2.11-1 thru 6.2.11-3 ..... Revision 39
6.2.12-1 thru 6.2.12-4 ..... Revision 39
6.3.1-1 thru 6.3.1-6 ..... Revision 39
6.3.2-1 thru 6.3.2-4 ..... Revision 39
6.3.3-1 thru 6.3.3-9 ..... Revision 39
6.3.4-1 thru 6.3.4-9 ..... Revision 39
6.3.5-1 thru 6.3.5-12 ..... Revision 39

LIST OF EFFECTIVE PAGES (Continued)

6.3.6-1 thru 6.3.6-9 ..... Revision 39
6.3.7-1 thru 6.3.7-4 ..... Revision 39
6.3.8-1 thru 6.3.8-7 ..... Revision 39
6.3.9-1 thru 6.3.9-7 ..... Revision 39
6.4.1-1 thru 6.4.1-10 ..... Revision 39
6.4.2-1 thru 6.4.2-10 ..... Revision 39
6.4.3-1 thru 6.4.3-34 ..... Revision 39
6.4.4-1 thru 6.4.4-24 ..... Revision 39
6.4.5-1 thru 6.4.5-32 ..... Revision 39
6.4.6-1 thru 6.4.6-23 ..... Revision 39
6.4.7-1 thru 6.4.7-14 ..... Revision 39
6.4.8-1 thru 6.4.8-14 ..... Revision 39
6.4.9-1 thru 6.4.9-10 ..... Revision 39
6.4.10-1 thru 6.4.10-18 ..... Revision 39
6.5.1-1 thru 6.5.1-13 ..... Revision 39
6.5.2-1 thru 6.5.2-4 ..... Revision 39
6.5.3-1 thru 6.5.3-2 ..... Revision 39
6.7.1-1 thru 6.7.1-19 ..... Revision LWT-09A
6.7.2-1 thru 6.7.2-47 ..... Revision 39

Appendix 6.6

6.6-i thru 6.6-iii ..... Revision 39
6.6-1 ..... Revision 39
6.6.1-1 thru 6.6.1-111 ..... Revision 39
6.6.2-1 thru 6.6.2-56 ..... Revision 39
6.6.3-1 thru 6.6.3-73 ..... Revision 39
6.6.4.-1 thru 6.6.4-77 ..... Revision 39
6.6.5-1 thru 6.6.5-101 ..... Revision 39
6.6.6-1 thru 6.6.6-158 ..... Revision 39
6.6.7-1 thru 6.6.7-84 ..... Revision 39
6.6.8-1 thru 6.6.8-183 ..... Revision 39
6.6.9-1 thru 6.6.9-52 ..... Revision 39
6.6.10-1 thru 6.6.10-33 ..... Revision 39
6.6.11-1 thru 6.6.11-47 ..... Revision 39
6.6.12-1 thru 6.6.12-20 ..... Revision 39
6.6.13-1 thru 6.6.13-22 ..... Revision 39
6.6.14-1 thru 6.6.14-7 ..... Revision 39
6.6.15-1 thru 6.6.15-45 ..... Revision 39

Chapter 7

7-i thru 7-ii ..... Revision LWT-09A
7.1-1 thru 7.1-56 ..... Revision LWT-09A
7.2-1 thru 7.2-13 ..... Revision LWT-09A
7.3-1 thru 7.3-2 ..... Revision 39

Chapter 8

8-i ..... Revision 39
8.1-1 thru 8.1-11 ..... Revision LWT-09A
8.2-1 thru 8.2-4 ..... Revision LWT-09A
8.3-1 thru 8.3-4 ..... Revision 39

Chapter 9

9-i ..... Revision 39
9-1 thru 9-10 ..... Revision 39

Chapter 1

Table of Contents

1 GENERAL INFORMATION 1-1

1.1 Introduction 1.1-1

1.2 Package Description 1.2-1
1.2.1 Packaging 1.2-1
1.2.2 Operational Features 1.2-4
1.2.3 Contents of Packaging 1.2-5

1.3 Quality Assurance 1.3-1

1.4 License Drawings 1.4-1

1.5 Unclassified DOE Reference Documents and Drawings 1.5-1

Chapter 1 Appendices

Appendix 1-A – TTQP-1-015, "Description of the Tritium-Producing Burnable Absorber Rod for the Commercial Light Water Reactor," Revision 14

Appendix 1-B – TTQP-1-091, "Unclassified TPBAR Releases, Including Tritium," Revision 11

Appendix 1-C – TTQP-1-111, "Unclassified Bounding Source Term, Radionuclide Concentrations, Decay Heat, and Dose Rates for the Production TPBAR," Revision 5

Appendix 1-D – DOE Drawing H-3-307845, "Production TPBAR Reactor Interface Dimensions Watts Bar," Revision 10, Sheet 1 of 2

Appendix 1-E – DOE Drawing H-3-308875, "Production TPBAR Reactor Interface Dimensions Sequoyah," Revision 5, Sheet 1 of 2

Appendix 1-F – DOE Drawing H-3-310568, "Mark 8 Multi-Pencil TPBAR – Watts Bar Reactor Interface," Revision 0, Sheet 1 of 2

Appendix 1-G – PNNL Letter, TTP-06-056, Subject: Exposure of Shipping Cask to Tritium, February 21, 2006

List of Figures

Figure 1.2.3-1 Aluminum Clad TRIGA Fuel Element 1.2-19
Figure 1.2.3-2 Aluminum Clad Instrumented Fuel Element 1.2-20
Figure 1.2.3-3 Stainless Steel Clad TRIGA Fuel Element 1.2-21
Figure 1.2.3-4 Stainless Steel Clad Instrumented Fuel Element 1.2-22
Figure 1.2.3-5 Standard Fuel Follower Control Rod Element 1.2-23
Figure 1.2.3-6 TRIGA Fuel Cluster and Rod Details 1.2-24
Figure 1.2.3-7 HTGR Fuel Handling Unit 1.2-25
Figure 1.2.3-8 RERTR Fuel Handling Unit 1.2-26
Figure 1.2.3-9 Typical TPBAR Assembly 1.2-27
Figure 1.2.3-10 TPBAR Consolidation Canister Sketch 1.2-28
Figure 1.2.3-11 Failed PWR/BWR Fuel Rod Capsule 1.2-29
Figure 1.2.3-12 NAC-LWT with TPBAR Consolidation Canister Payload 1.2-30
Figure 1.2.3-13 PULSTAR Fuel Assembly 1.2-31
Figure 1.2.3-14 Spiral Fuel Assembly Cross-Section Sketch 1.2-32
Figure 1.2.3-15 MOATA Plate Bundle Sketches 1.2-33
Figure 1.2.3-16 TPBAR Waste Container and Extension Weldment Sketch 1.2-34
Figure 1.2.3-17 NAC-LWT with TPBAR Waste Container Payload 1.2-35

List of Tables

Table 1.1-1 Terminology and Notation 1-3
Table 1.2-1 Characteristics of Design Basis TRIGA Fuel Elements Acceptable for Loading in the Poisoned TRIGA Basket 1.2-36
Table 1.2-2 Characteristics of Design Basis TRIGA Fuel Elements Acceptable for Loading in the Nonpoisoned TRIGA Basket 1.2-37
Table 1.2-3 Characteristics of Design Basis TRIGA Fuel Cluster Rods 1.2-38
Table 1.2-4 Fuel Characteristics 1.2-39
Table 1.2-5 PWR Fuel Characteristics 1.2-42
Table 1.2-6 BWR Fuel Characteristics 1.2-43
Table 1.2-7 Characteristics of General Atomics Irradiated Fuel Material (GA IFM) 1.2-44
Table 1.2-8 Typical Production TPBAR Characteristics 1.2-45
Table 1.2-9 PULSTAR Fuel Characteristics 1.2-46
Table 1.2-10 Spiral Fuel Assembly Characteristics 1.2-47
Table 1.2-11 MOATA Plate Bundle Characteristics 1.2-48
Table 1.2-12 Typical TPBAR Segment Characteristics in Waste Container 1.2-49
Table 1.2-13 Solid, Irradiated Hardware Characteristics 1.2-50

List of Drawings

315-40-01		Rev 7	Legal Weight Truck Transport Cask Assembly
315-40-02	Sheets 1 – 2	Rev 24	NAC-LWT Cask Body Assembly
315-40-03	Sheets 1 – 6	Rev 6*	NAC-LWT Transport Cask Body
315-40-03	Sheets 1 – 7	Rev 22	NAC-LWT Transport Cask Body
315-40-04		Rev 10	NAC-LWT Transport Cask Lid Assembly
315-40-05		Rev 9	NAC-LWT Transport Cask Upper Impact Limiter
315-40-06		Rev 9	NAC-LWT Transport Cask Lower Impact Limiter
315-40-08	Sheets 1 – 5	Rev 18	NAC-LWT Transport Cask Parts Detail
315-40-09		Rev 2	NAC-LWT PWR Basket Spacer
315-40-10	Sheets 1 – 2	Rev 8	NAC-LWT Cask PWR Basket
315-40-11		Rev 2	NAC-LWT BWR Fuel Basket Assembly
315-40-12		Rev 3	NAC-LWT Metal Fuel Basket Assembly
315-40-045		Rev 5	Weldment, 7 Element Basket, 42 MTR Fuel Base Module
315-40-046		Rev 5	Weldment, 7 Element Basket, 42 MTR Fuel Intermediate Module
315-40-047		Rev 5	Weldment, 7 Element Basket, 42 MTR Fuel Top Module
315-40-048		Rev 3	Legal Weight Truck Transport Cask Assembly, 42 MTR Element
315-40-049		Rev 5	Weldment, 7 Element Basket, 28 MTR Fuel Base Module
315-40-050		Rev 5	Weldment, 7 Element Basket, 28 MTR Fuel Intermediate Module
315-40-051		Rev 5	Weldment, 7 Element Basket, 28 MTR Fuel Top Module
315-40-052		Rev 3	Legal Weight Truck Transport Cask Assembly, 28 MTR Element
315-40-070		Rev 5	Weldment, 7 Cell Basket, TRIGA Fuel Base Module
315-40-071		Rev 5	Weldment, 7 Cell Basket, TRIGA Fuel Intermediate Module
315-40-072		Rev 5	Weldment, 7 Cell Basket, TRIGA Fuel Top Module
315-40-079		Rev 5	Legal Weight Truck Transport Cask Assy, 120 TRIGA Fuel Elements or 480 Cluster Rods
315-040-080		Rev 3	Weldment, 7 Cell Poison Basket, TRIGA Fuel Base Module
315-040-081		Rev 3	Weldment, 7 Cell Poison Basket, TRIGA Fuel Intermediate Module
315-040-082		Rev 3	Weldment, 7 Cell Poison Basket, TRIGA Fuel Top Module
315-040-083		Rev 0	Spacer, LWT Cask Assembly, TRIGA Fuel
315-40-084		Rev 4	Legal Weight Truck Transport Cask Assy, 140 TRIGA Elements
315-40-085		Rev 0	Axial Fuel and Cell Block Spacers, MTR and TRIGA Fuel Baskets, NAC-LWT Cask
315-40-086		Rev 1	Assembly, Sealed Failed Fuel Can, TRIGA Fuel
315-40-087		Rev 6	Canister Lid Assembly, Sealed Failed Fuel Can, TRIGA Fuel
315-40-088		Rev 2	Canister Body Assembly, Sealed Failed Fuel Can, TRIGA Fuel
315-40-090		Rev 3	Weldment, 7 Element Basket, 35 MTR Fuel Base Module
315-40-091		Rev 3	Weldment, 7 Element Basket, 35 MTR Fuel Intermediate Module
315-40-092		Rev 3	Weldment, 7 Element Basket, 35 MTR Fuel Top Module
315-40-094		Rev 4	Legal Weight Truck Transport Cask Assembly, 35 MTR Element
315-40-096		Rev 3	Fuel Cluster Rod Insert, TRIGA Fuel
315-40-098	Sheets 1 - 3	Rev 6	PWR/BWR Rod Transport Canister Assembly
315-40-099	Sheets 1 - 3	Rev 3	Can Weldment, PWR/BWR Transport Canister

* Packaging Unit Nos. 1, 2, 3, 4 and 5 are constructed in accordance with this revision of drawing.

List of Drawings (continued)

315-40-100	Sheets 1 - 3	Rev 4	Lids, PWR/BWR Transport Canister
315-40-101		Rev 0	4 × 4 Insert, PWR/BWR Transport Canister
315-40-102		Rev 2	5 × 5 Insert, PWR/BWR Transport Canister
315-40-103		Rev 0	Pin Spacer, PWR/BWR Transport Canister
315-40-104	Sheets 1 - 3	Rev 5	Legal Weight Truck Transport Cask Assy, PWR/BWR Rod Transport Canister
315-40-105	Sheets 1 - 2	Rev 3	PWR Insert PWR/BWR Transport Canister
315-40-106	Sheets 1 - 3	Rev 1	MTR Plate Canister, LWT Cask
315-40-108	Sheets 1 - 3	Rev 1	Weldment, 7 Cell Basket, Top Module, DIDO Fuel
315-40-109	Sheets 1 - 3	Rev 1	Weldment, 7 Cell Basket, Intermediate Module, DIDO Fuel
315-40-110	Sheets 1 - 3	Rev 1	Weldment, 7 Cell Basket, Base Module, DIDO Fuel
315-40-111		Rev 2	Legal Weight Truck, Transport Cask Assy, DIDO Fuel
315-40-113		Rev 0	Spacers, Top Module, DIDO Fuel
315-40-120	Sheets 1 - 3	Rev 2	Top Module, General Atomics IFM, LWT Cask
315-40-123	Sheets 1 - 2	Rev 1	Spacer, General Atomics IFM, LWT Cask
315-40-124		Rev 1	Transport Cask Assembly, General Atomics IFM, LWT Cask
315-40-125	Sheets 1 - 3	Rev 3	Transport Cask Assembly, Framatome/EPRI, LWT Cask
315-40-126	Sheets 1 - 2	Rev 2	Weldments, Framatome/EPRI, LWT Cask
315-40-127	Sheets 1 - 2	Rev 2	Spacer Assembly, TPBAR Shipment, LWT Cask
315-40-128	Sheets 1 - 2	Rev 3	Legal Weight Truck, Transport Cask Assy, TPBAR Shipment
032230		Rev A	RERTR Secondary Enclosure, General Atomics
032231		Rev A	HTGR Secondary Enclosure, General Atomics
032236		Rev B	RERTR Primary Enclosure, General Atomics
032237		Rev B	HTGR Primary Enclosure, General Atomics
315-40-129		Rev 1	Canister Body Assembly, Failed Fuel Can, PULSTAR
315-40-130		Rev 1	Assembly, Failed Fuel Can, PULSTAR
315-40-133	Sheets 1 - 2	Rev 1	Transport Cask Assembly, PULSTAR Shipment, LWT Cask
315-40-134		Rev 1	Body Weldment, Screened Fuel Can, PULSTAR Fuel
315-40-135		Rev 1	Assembly, Screened Fuel Can, PULSTAR Fuel
315-40-139		Rev 1	Legal Weight Truck Transport Cask Assy, ANSTO Fuel
315-40-140	Sheets 1 - 2	Rev 1	Weldment, 7 Cell Basket, Top Module, ANSTO Fuel
315-40-141	Sheets 1 - 2	Rev 1	Weldment, 7 Cell Basket, Intermediate Module, ANSTO Fuel
315-40-142	Sheets 1 - 2	Rev 1	Weldment, 7 Cell Basket, Base Module, ANSTO Fuel
315-40-145		Rev 0	Irradiated Hardware Lid Spacer Assembly, LWT Cask
315-40-148		Rev 0	Legal Weight Truck Transport Cask Assembly, ANSTO-DIDO Combination Basket

1 GENERAL INFORMATION

This chapter of the NAC International, Legal Weight Truck spent fuel shipping cask (NAC-LWT) Safety Analysis Report (SAR) presents a general introduction to, and description of, the NAC-LWT cask. Terminology used throughout this report is presented in Table 1.1-1.

Shipment of the NAC-LWT cask by truck, ISO container, and/or by railcar, as a Type B(U)F-96 package, as defined in 10 CFR 71.4, is authorized for the following contents:

- PWR and BWR fuel assemblies[1];
- MTR fuel assemblies and plates;
- DIDO fuel assemblies, metallic fuel rods;
- 25 high burnup PWR and BWR fuel rods (including up to 14 fuel rods classified as damaged)[2];
- 16 PWR MOX fuel rods (or mixed load of up to 16 PWR MOX and UO_2 PWR fuel rods) and up to 9 burnable poison rods (BRPs);
- TRIGA fuel elements and TRIGA fuel cluster rods;
- General Atomics (GA) High-Temperature Gas-Cooled Reactor (HTGR) and Reduced-Enrichment Research and Test Reactor (RERTR) Irradiated Fuel Materials (IFM);
- up to 700 PULSTAR fuel elements;
- spiral fuel assemblies; and
- MOATA plate bundles.

The authorized contents previously listed include both irradiated and unirradiated forms of the materials.

Irradiated hardware is also authorized to be shipped in the NAC-LWT cask by truck, ISO container, and/or by railcar, as a Type B(U)F-96 package, as defined in 10 CFR 71.4. Irradiated hardware is defined as solid, irradiated and contaminated fuel assembly structural or reactor internal component hardware, which may include fissile material, provided the quantity of fissile material does not exceed a Type A quantity and does not exceed the exemptions of 10 CFR 71.15, paragraphs (a), (b) and (c).

Shipment of the NAC-LWT cask by truck, ISO container, and/or by railcar, as a Type B(M)-96 package, as defined in 10 CFR 71.4, is also authorized for the following contents:

[1] NAC-LWT casks containing PWR and BWR fuel assemblies are to be transported on an open trailer with a personnel barrier.

[2] PWR and BWR fuel rods may be transported in either a fuel assembly lattice (skeleton) or in a fuel rod insert. The fuel rod insert may contain PWR instrument/guide tubes and BWR water/inert rods in addition to the fuel rods.

- up to 300 Tritium Producing Burnable Absorber Rods (TPBARs), of which two can be prefailed; and
- up to 55 TPBARs segmented during PIE, including segmentation debris.

In accordance with 10 CFR 71.59, the NAC-LWT cask is assigned a Criticality Safety Index (CSI) for criticality control of the approved contents as follows:

- 100 for PWR fuel assemblies;
- 33.4 for package with any number of canned PULSTAR fuel;
- 12.5 for DIDO fuel assemblies and TRIGA payloads in a nonpoisoned basket and no canisters, or a canister loaded with up to two equivalent TRIGA elements;
- 5 for BWR fuel assemblies; and
- 0 for metallic fuels, spiral fuel assemblies, MOATA plate bundles, PWR and BWR rods, PWR MOX rods, MTR fuel assemblies, TRIGA fuel elements and fuel cluster rods, GA IFM elements, and intact PULSTAR fuel elements.

TPBARs do not contain fissile material and criticality assessments are not required. Solid, irradiated and contaminated hardware contents could include fissile material not exceeding a Type A quantity and the exemptions of 10 CFR 71.15, paragraphs (a), (b) and (c). A CSI of 0 is assigned for these contents for documentation purposes.

The estimated Transport Index (TI) for shielding for the prior listed contents is shown in Table 5.1.1-1. The actual TI for individual shipments will be determined in accordance with 10 CFR 71.4 by the licensee.

Table 1.1-1 Terminology and Notation

Cask Model	NAC-LWT
Package	The Packaging with its radioactive contents (payload), as presented for transportation (10 CFR 71.4). Within this report, the Package is denoted as the NAC-LWT cask or simply as the cask.
Packaging	The assembly of components necessary to ensure compliance with packaging requirements (10 CFR 71.4). Within this report, the Packaging is denoted as the NAC-LWT cask.
NAC-LWT Cask	This packaging consists of a spent-fuel shipping cask body and closure lid with energy absorbing impact limiters.
Contents (Payload)	• 1 PWR assembly • up to 2 BWR assemblies • up to 25 PWR or BWR rods (including high burnup fuel rods and up to 14 fuel rods classified as damaged)[1] • up to 16 PWR MOX fuel rods (or mixed contents of up to 16 PWR MOX and UO_2 PWR fuel rods) and up to 9 BPRs • up to 42 MTR fuel elements (including plates) • up to 42 DIDO fuel assemblies • up to 15 sound (cladding intact) metallic fuel rods • up to 9 damaged metallic fuel rods or 3 severely damaged metallic fuel rods in filters • up to 140 intact or damaged TRIGA fuel elements/debris • up to 560 intact or damaged TRIGA fuel cluster rods • 2 GA IFM packages • up to 300 TPBARs (including up to 2 prefailed TPBARs) • up to 55 TPBARs segmented into individual segments and segmentation debris • up to 700 intact or damaged PULSTAR fuel elements in either assembly or element form, including fuel debris • up to 42 intact spiral fuel assemblies (also referred to as Mark III spiral fuel). Spiral fuel assemblies may be cropped. • up to 42 intact MOATA plate bundles • any combination of individual ANSTO basket modules containing either spiral fuel assemblies or MOATA plate bundles up to a total of 42 assemblies/bundles • irradiated hardware

[1] PWR and BWR fuel rods may be transported in either a fuel assembly lattice (skeleton) or in a fuel rod insert. The fuel rod insert may contain PWR instrument/guide tubes and BWR water/inert rods in addition to the fuel rods.

Table 1.1-1 Terminology and Notation (cont'd)

Impact Limiters	Aluminum honeycomb energy absorbers located at the ends of the cask.
Intact LWR Fuel (Assembly or Rod)	Spent nuclear fuel that is not Damaged LWR Fuel, as defined herein. To be classified as intact, fuel must meet the criteria for both intact cladding and structural integrity. An intact fuel assembly can be handled using normal handling methods, and any missing fuel rods have been replaced by solid filler rods that displace a volume equal to, or greater than, that of the original fuel rod.
Damaged LWR Fuel (Assembly or Rod)	Spent nuclear fuel that includes any of the following conditions that result in either compromise of cladding confinement integrity or recognition of fuel assembly geometry. 1. The fuel contains known or suspected cladding defects greater than a pinhole leak or a hairline crack that have the potential for release of significant amounts of fuel particles. 2. The fuel assembly: i. is damaged in such a manner as to impair its structural integrity; ii. has missing or displaced structural components such as grid spacers; iii. is missing fuel pins that have not been replaced by filler rods that displace a volume equal to, or greater than, that of the original fuel rod; iv. cannot be handled using normal handling methods. 3. The fuel is no longer in the form of an intact fuel assembly and consists of, or contains, debris such as loose pellets, rod segments, etc.
Damaged Fuel (TRIGA)	TRIGA fuel (elements and cluster rods) with known or suspected clad breach (i.e., cladding defects that permit the release of gas from the interior of the rod and/or allow water intrusion into the clad to fuel gap while submerged).
Fuel Debris (TRIGA)	TRIGA damaged fuel that does not maintain its structural integrity, including fuel particles, fuel debris, and broken fuel rods.
TPBAR	Tritium Producing Burnable Absorber Rod

Table 1.1-1 Terminology and Notation (cont'd)

Irradiated Fuel Material (IFM)	High-Temperature Gas-Cooled Reactor (HTGR/IFM) and Reduced-Enrichment Research and Test Reactor (RERTR/IFM) type TRIGA fuel entities produced by General Atomics.
PULSTAR Fuel Element	PULSTAR fuel rod. May be contained in either assembly, rod holder or can form for shipment. PULSTAR fuel elements may be intact or damaged.
Damaged PULSTAR Fuel Element	PULSTAR fuel rods having cladding failures greater than hairline cracks or pinhole leaks. The damaged fuel definition for PULSTAR fuel elements includes fuel debris. Damaged PULSTAR fuel elements may also be referred to as failed and must be transported in either of two types of PULSTAR cans.
Irradiated Hardware	Solid, irradiated and contaminated fuel assembly structural or reactor internal component hardware, which may include fissile material, provided the quantity of fissile material does not exceed a Type A quantity and does not exceed the exemptions of 10 CFR 71.15, paragraphs (a), (b) and (c). Authorized quantity of irradiated hardware and components is limited to 4,000 lbs (including spacers, dunnage and containers) and a gamma source term as defined in Table 1.2-13.
MOX Fuel Rods	The term as used in this SAR is defined as irradiated or unirradiated mixed uranium-plutonium oxide (MOX) fuel rods. The MOX fuel rods can be made with plutonium having various compositions of plutonium isotopes. The evaluated mixes of the various grades of plutonium are defined in the shielding (Chapter 5) and criticality (Chapter 6) evaluations.

1.1 Introduction

The NAC-LWT spent-fuel shipping cask has been developed by NAC International (NAC) as a safe means of transporting radioactive materials authorized as approved contents. The cask design is optimized for legal weight over the road transport, with a gross weight of less than 80,000 pounds. The cask provides maximum safety during the loading, transport, and unloading operations required for spent-fuel shipment. The NAC-LWT cask assembly is composed of a package that provides a containment vessel that prevents the release of radioactive material. The actual containment boundary provided by the package consists of a 4.0-inch thick bottom plate, a 0.75-inch thick, 13.375-inch inner diameter shell, an upper ring forging, and an 11.3-inch thick closure lid. The cask lid closure is accomplished using twelve, 1-inch diameter bolts. The cask has an outer shell, 1.20 inches thick, to protect the containment shell and also to enclose the 5.75-inch thick lead gamma shield. Neutron shielding is provided by a 5.0-inch thick neutron shield tank with a 0.24-inch (6mm) thick outer wall, containing a water/ethylene glycol mixture and 1.0 minimum weight percent (wt %) boron (58 wt % ethylene glycol; 39 wt % demineralized water; 3 wt % potassium tetraborate [$K_2B_4O_7$]). The neutron shield tank system includes an expansion tank to permit the expansion and contraction of the shield tank liquid without compromising the shielding or overstressing the shield tank structure. Aluminum honeycomb impact limiters are attached to each end of the cask to absorb kinetic energy developed during a cask drop, and limit the consequences of normal operations and hypothetical accident events.

The NAC-LWT is a legal weight truck cask designed to transport the following contents:

- 1 PWR assembly;
- up to 2 BWR assemblies;
- up to 15 sound metallic fuel rods;
- up to 42 MTR fuel elements;
- up to 42 DIDO fuel assemblies;
- up to 25 high burnup PWR fuel rods (including up to 14 rods classified as damaged)[1];
- up to 25 high burnup BWR fuel rods (including up to 14 rods classified as damaged)[1];
- up to 16 PWR MOX fuel rods (or a combination of 16 PWR MOX and UO_2 PWR rods) and up to 9 BPRs
- up to 9 damaged metallic fuel rods;
- up to 3 severely damaged metallic fuel rods in filters;
- up to 140 TRIGA intact or damaged fuel elements/fuel debris ("TRIGA" is a Trademark of General Atomics);
- up to 560 TRIGA fuel cluster rods;

[1] PWR and BWR fuel rods may be transported in either a fuel assembly lattice (skeleton) or in a fuel rod insert. The fuel rod insert may contain PWR instrument/guide tubes and BWR water/inert rods in addition to the fuel rods.

- 2 GA IFM packages;
- up to 300 TPBARs (of which two can be prefailed) in a consolidation canister;
- up to 25 TPBARs (of which two can be prefailed) in a rod holder;
- up to 55 TPBARs segmented during post-irradiation examination (PIE), including segmentation debris; ,
- up to 700 PULSTAR fuel elements (intact or damaged);
- up to 42 spiral fuel assemblies;
- up to 42 MOATA plate bundles; or
- up to 4,000 lbs of solid, irradiated and contaminated hardware, which may include fissile material less than a Type A quantity and meeting the exemptions of 10 CFR 71.15, paragraphs (a), (b) and (c). Total allowed mass includes the weight of spacers, shoring and dunnage.

PWR or BWR fuel rods may be placed in a fuel rod insert (also referred to as a rod holder) or in a fuel assembly lattice. The fuel rod holder is composed of a 4×4 or a 5×5 rod array. An alternate 5×5 rod holder is designed to contain an oversize nonfuel-bearing component (e.g., CE guide tube or BWR water rod). The alternative configuration reduces fuel-bearing capacity to a maximum of 21 fuel rods. The lattice may be irradiated or unirradiated. Up to 14 of the fuel rods may be classified as damaged. Damaged fuel rods must be placed in a rod holder. Damaged fuel rods or rod sections may be encapsulated to facilitate handling prior to placement in the rod holder. PWR rods may include Integral Fuel Burnable Absorber (IFBA) rods.

PWR MOX fuel rods (or a combination of PWR MOX and UO_2 PWR fuel rods) are required to be loaded in a screened or free flow PWR/BWR Rod Transport Canister with a 5×5 insert. PWR MOX/UO_2 rods may include Integral Fuel Burnable Absorber (IFBA) rods.

Damaged TRIGA fuel elements, cluster rods and fuel debris are required to be loaded in a sealed damaged fuel canister (DFC).

PULSTAR fuel elements may be configured as intact fuel assemblies, may be placed into a fuel rod insert, i.e., a 4×4 rod holder (intact elements only), or may be loaded into one of two can designs, designated as the PULSTAR screened fuel can or the PULSTAR failed fuel can. Damaged PULSTAR fuel elements and nonfuel components of PULSTAR fuel assemblies must be loaded into cans. PULSTAR fuel cans may only be loaded into the top or base module of the 28 MTR basket assembly. Intact PULSTAR fuel assemblies and intact PULSTAR fuel elements in a TRIGA fuel rod insert may be loaded in any basket module.

Irradiated hardware may be loaded directly into the NAC-LWT cavity or preloaded into a canister or cage. Stainless steel dunnage may be used to limit the movement of the irradiated hardware within the cask cavity. The maximum gamma source term of the irradiated hardware shall be

limited to that defined for the authorized PWR content condition as described in Chapter 5.

The NAC-LWT cask provides a testable containment for the contents during both normal operations and hypothetical accident conditions, satisfying the requirements of 10 CFR 71.51. Any number of NAC-LWT casks may be shipped at one time, each on its own vehicle.

The NAC-LWT has two leaktight configurations as defined by ANSI N14.5. The standard configuration is provided by a closure lid with a metal containment seal and alternate vent and drain port covers provided with Viton® containment O-rings. The second configuration is provided by a closure lid with a metal containment seal and Alternate B vent and drain port covers provided with metal seals. The metal port cover seal containment configuration is required to be utilized for all TPBAR contents and may be used for other contents. The NAC-LWT standard, Viton® O-ring containment configuration is not authorized for TPBAR contents.

NAC-LWT casks may be shipped in a closed International Shipping Organization (ISO) container when containing all fuel contents other than PWR and BWR fuel assemblies. NAC-LWT casks containing PWR and BWR fuel assemblies are to be transported on an open trailer with a personnel barrier.

The terminology of MTR, DIDO and TRIGA fuel elements will be used independent of whether the element contains low, medium or high enriched uranium (i.e., LEU, MEU or HEU), except when required for analysis or loading purposes.

TPBAR contents may be placed into a consolidation canister, waste container or 5×5 rod insert (also referred to as a rod holder) in a PWR/BWR Rod Transport Canister. Segmented TPBARs are only permitted within the waste container. The three TPBAR shipping configurations are individually placed within one of the two TPBAR basket assemblies (one with a 7-inch bottom spacer and the alternative TPBAR basket assembly with a 6.5-inch alternative bottom spacer), depending on container configuration.

1.2 Package Description

This section presents a basic description of the NAC-LWT cask and the contents that may be transported. Drawings of the cask are presented within Section 1.4.

1.2.1 Packaging

1.2.1.1 Gross Weight

Gross shipping weight of the NAC-LWT spent-fuel shipping cask is approximately 52,000 pounds for the package. When mounted on the transport vehicle, the cask and vehicle weight is less than the 80,000-pound maximum for legal weight transport. A summary of overall component weights, detailed in Table 2.2.1-1, is listed below:

Component	Weight (pounds)
Cask Body	43,412
Closure Lid and Bolts	941
Payload and Basket	4,000 maximum
Impact Limiters	2,855
Total	51,208
SAR Analysis Weight	52,000

1.2.1.2 Materials of Construction, Dimensions, and Fabrication

The NAC-LWT cask body consists of Type 304 stainless steel forgings and closure lid with Type XM-19 stainless steel shells. Type XM-19 is a high strength stainless steel and is used in the inner and outer structural shells, which are more highly stressed than other cask components that use the more common Type 304 stainless steel. A lead gamma shield and a borated ethylene glycol/water solution neutron shield are utilized for radiation shielding. The cask provides the containment boundary for the payload and also acts as an environmental barrier. The cask is protected at each end by energy absorbing impact limiters, which consist of crushable aluminum honeycomb material with a thin aluminum shell. The impact limiters also provide thermal insulation, which protects the lid seals during the hypothetical fire transient event, although this thermal protection is conservatively neglected in this report. The cask is passively cooled because of its relatively low maximum heat loading of 2.5 kilowatts (kW). The overall arrangement of the NAC-LWT cask and design details are presented in the drawings within Section 1.4. The cask body, closure lid, and impact limiters are more fully described in the following sections.

1.2.1.2.1 Cask Body

The cask body is fabricated from Type 304 and Type XM-19 stainless steel. A poured lead gamma shield forms an annulus 5.75 inches thick and 174.9 inches long. The lead is enclosed between a 0.75-inch thick, 13.375-inch inner diameter Type XM-19 stainless steel inner shell and a 1.20-inch thick, 28.78-inch outer diameter Type XM-19 stainless steel outer shell. The Type 304 stainless steel bottom end forging of the cask is 4.0 inches thick, and the bottom also contains a 3.0-inch thick, 20.75-inch diameter lead disk enclosed by a 3.5-inch thick Type 304 stainless steel end cover.

As discussed in Chapter 8, installation of the lead into the cask is done in a carefully controlled manner. Temperatures of the inner and outer shells are continuously monitored and controlled during the lead pour and cooldown process. In addition, the welds connecting the inner and outer shells to the bottom end forging are not made until after the cooldown process is complete and the entire cask has reached a uniform temperature. Dimensional checks for straightness and ovality are also made before and after lead pour.

The upper ring forging is a Type 304 stainless steel ring 14.25 inches thick. This forging is machined to accept the closure lid and contains the penetrations to the cask cavity for the vent and fill/drain valves. Four lifting trunnions are welded to the forging to permit cask lifting and handling with a nonredundant or redundant lifting yoke.

Neutron shielding is provided by an ethylene glycol/water jacket that surrounds the 1.20-inch thick Type XM-19 stainless steel outer shell and is designed to axially blanket the active fuel length of the more common light water reactor fuels. The neutron shield region is 5.00 inches thick and 164.0 inches long. The external surface of the shield tank is a 0.24-inch thick Type 304 stainless steel shell with 0.50-inch thick end plates. An expansion tank for the neutron shield is provided to allow for thermal expansion and contraction of the liquid and is connected to the shield tank by a siphon tube. The liquid contains a solution of ethylene glycol/water and 1.0 wt % boron, which is added to reduce the secondary gamma radiation component.

The inner shell, end forgings, and the closure lid establish a cask cavity that is 177.9 inches long and 13.375 inches in diameter.

The weight of the cask body is approximately 43,412 pounds. The overall length of the cask body is 199.8 inches, and the maximum outside diameter is 44.24 inches at the neutron shield expansion tank.

1.2.1.2.2 Closure Lid

The cask closure lid is a Type 304 stainless steel forging 11.3 inches thick. The lid is machined to recess into the upper ring forging when it is installed on the cask. The closure lid and upper end forging are machined to provide a series of steps to prevent radiation streaming through the gap between the components. The closure lid attaches to the cask using 12 bolts with a 1-inch diameter. The containment boundary seal is achieved by a metallic O-ring captured in a groove machined on the underside of the closure lid (a second O-ring is provided to allow seal testing of the containment boundary O-ring). The O-rings mate against a machined sealing surface of the cask upper ring forging.

1.2.1.2.3 Impact Limiters

The impact limiters are fabricated from aluminum. The aluminum "honeycomb" has a crush strength of 3,500 psi. The honeycomb is a multidirectional crushable material that does not actually resemble a hexagonal honeycomb structure. The impact limiter is attached to the cask body at four locations. The outside diameter of the top end impact limiter is 65.25 inches and the bottom end impact limiter has a 60.25-inch diameter. The top and bottom impact limiters are 27.8 and 28.3 inches long, respectively, and both overlap the ends of the cask body by 12.0 inches.

1.2.1.3 Valves and Testing

The closure lid and the alternate and Alternate B drain and vent port covers each have a seal test port. The seal test port accesses the volume between the two O-ring seals on the cover or lid permitting leakage testing to verify proper sealing. The vent and drain valves are not considered part of the containment boundary and are used during in-plant loading operations to access the cask cavity for water filling and draining, vacuum drying, helium backfilling, etc.

1.2.1.4 Heat Dissipation

There are no special devices utilized on the NAC-LWT cask for the transfer or dissipation of heat. The package is passively cooled, which is possible because of its relatively low maximum heat load of 2.5 kW. A more detailed discussion of the package thermal characteristics is provided in Chapter 3.

1.2.1.5 Coolants

There are no coolants utilized within the package other than the normal transportation atmosphere of air or helium, depending on content conditions.

1.2.1.6 Protrusions

There are no outer protrusions on the package other than the four external lifting trunnions, the longitudinal shear ring at the upper end of the cask, and the eight impact limiter attachment lugs, four near each end of the package. All of these protrusions are located within the envelope protected by the impact limiters. The closure lid and valve port covers are recessed into the cask body and do not protrude from the cask surface. Refer to the drawings in Section 1.4 for more detail.

1.2.1.7 Lifting and Tiedown Devices

Of the four trunnions located on the exterior of the package at the upper end forging, two are intended for lifting with a nonredundant lifting yoke and the other two are used with a redundant lifting yoke. The package lifting and tiedown features are described in more detail in Section 2.5.

1.2.1.8 Shielding

A 5.75-inch annulus of lead and 2.19 inches of steel are maintained between the cask contents and the exterior radial surface of the package for the attenuation of radiation. Five inches of borated water are also provided for neutron shielding. The bottom end of the cask provides 7.5 inches of steel and 3.0 inches of lead shielding, and the closure lid provides 11.3 inches of steel shielding. Further detail is provided in Chapter 5.

1.2.2 Operational Features

The NAC-LWT cask is intended to be simple to operate. The cask is designed to be easily loaded and handled at any nuclear facility. The outer surface of the cask is electropolished and the configuration of the exposed surfaces aids in decontamination. An optional sleeving arrangement is available to limit contact between the cask and the contaminated pool water during wet loading and unloading.

The closure lid of the cask and the two valve port covers (alternate and Alternate B designs) are one-piece fixtures designed for ease of handling and to maintain personnel dose rates as low as reasonably achievable (ALARA). The closure lid has built-in alignment grooves (i.e. key ways) to facilitate installation. The alternate and Alternate B port cover designs provide clearance for valves underneath the port cover. The inner O-rings on the closure lid and the vent and drain valve port covers are components of the cask containment boundary. For the transport of TPBAR contents and other contents requiring a leaktight transport containment configuration (i.e., damaged TRIGA fuel in sealed DFCs or PWR MOX fuel rods), the cask is required to be

configured with Alternate B drain and vent port covers incorporating metallic seals. The transport arrangement drawings for approved contents are presented in Section 1.4.

An alternative drain tube, including a drain tube alignment ring, is required to be installed and utilized when loading and transporting modular fuel baskets (i.e., not full length) and canisters.

The impact limiters and the personnel barrier are designed to be removed and installed without the aid of supplemental lifting gear or fixtures. All approved content may be transported in an International Shipping Organization (ISO) container, except for PWR and BWR fuel assemblies. All operational features are readily apparent from the drawings provided in Section 1.4. Operational procedures are delineated in Chapter 7.

1.2.3 Contents of Packaging

The NAC-LWT cask is analyzed as presented in this SAR for the transport of the following contents:

- 1 PWR assembly;
- up to 2 BWR assemblies;
- up to 15 sound metallic fuel rods;
- up to 9 failed metallic fuel rods;
- up to 3 severely failed metallic fuel rods in filters;
- up to 42 MTR fuel elements;
- up to 42 DIDO fuel assemblies;
- up to 25 PWR fuel rods (including up to 14 rods classified as damaged)[1];
- up to 25 BWR fuel rods (including up to 14 rods classified as damaged)[1];
- up to 16 PWR MOX fuel rods (or a combination of up to 16 PWR MOX and UO_2 fuel rods) plus up to 9 BPRs;
- up to 140 TRIGA fuel elements;
- up to 560 TRIGA fuel cluster rods;
- 2 GA IFM packages;
- up to 300 TPBARs (of which two can be prefailed) in a consolidation canister;
- up to 25 TPBARs (of which two can be prefailed) in a rod holder;
- up to 55 TPBARs segmented during PIE, including segmentation debris;
- up to 700 PULSTAR fuel elements (intact or damaged);
- up to 42 spiral fuel assemblies;
- up to 42 MOATA plate bundles;
- any combination of individual ANSTO basket modules containing either spiral fuel assemblies or MOATA plate bundles up to a total of 42 assemblies/bundles; or

[1] PWR and BWR fuel rods may be transported in either a fuel assembly lattice (skeleton) or in a fuel rod insert. The fuel rod insert may contain PWR instrument/guide tubes and BWR water/inert rods in addition to the fuel rods.

- up to 4,000 lbs of solid, irradiated and contaminated hardware, which may include fissile material less than a Type A quantity and meeting the exemptions of 10 CFR 71.15, paragraphs (a), (b) and (c). Total allowed mass includes the weight of spacers, shoring and dunnage.

Shipments in the NAC-LWT package shall not exceed the following limits:

1. The maximum contents weight shall not exceed 4,000 pounds.
2. The limits specified in Table 1.2-1 through Table 1.2-13 for the fuel and other radioactive contents shall not be exceeded.
3. Any number of casks may be shipped at one time, one cask per tractor/trailer vehicle.
4. The maximum decay heat shall not exceed the following: 2.5 kW for PWR fuel assemblies, 2.2 kW for BWR fuel assemblies, 2.3 kW for 25 high burnup PWR fuel rods, 2.1 kW for 25 high burnup BWR fuel rods, 2.3 kW for 16 PWR MOX/UO_2 fuel rods; 1.26 kW for MTR fuel, 1.05 kW for DIDO fuel assemblies, 1.05 kW for TRIGA fuel elements or fuel cluster rods, 13.05 W for GA IFM packages, 0.693 kW for 300 TPBARs, 0.127 kW for TPBAR segments; 0.058 kW for 25 TPBARs; 0.84 kW for the PULSTAR fuel contents, 0.756 kW for spiral fuel assemblies (0.126 kW per basket), 0.126 kW for MOATA plate bundles (21 W per basket), and 1.26 kW for solid, nonfissile, irradiated hardware.
5. Radiation levels shall meet the requirements delineated in 10 CFR 71.47 or 49 CFR 173.441. The neutron shield tank may be drained for shipment of metallic fuel rods.
6. Surface contamination levels shall meet the requirements of 10 CFR 71.87(i) or 49 CFR 173.443.
7. Damaged TRIGA fuel elements and fuel debris (up to two equivalent elements) will be shipped in a sealed damaged fuel canister.
8. Damaged TRIGA cluster rod and fuel debris will be transported in a sealed damaged fuel canister (maximum of up to six equivalent fuel cluster rods).
9. MTR fuel elements may consist of any combination of intact or damaged highly enriched uranium (HEU), medium enriched uranium (MEU) or low enriched uranium (LEU) fuel elements that are enveloped by the parameters listed in Table 1.2-4, as supported by information presented in Table 5.1.1-2, Table 6.4.3-21, Table 6.4.3-22, Table 6.4.3-25 and Table 6.4.3-28.
10. High burnup PWR fuel rods will be shipped in either a sealed, free flow or screened can.
11. High burnup BWR fuel rods will be shipped in either a sealed, free flow or screened can.
12. Up to 25 high burnup PWR or BWR fuel rods in a fuel assembly lattice or rod holder. Up to 14 of the fuel rods in a rod holder may be classified as damaged. Damaged fuel rods or rod sections may be placed into fuel rod capsules prior to placing them in the fuel rod holder. Typical failed fuel rod capsule configuration is shown in Figure 1.2-11.

13. Production TPBARs will either be shipped in an open top consolidation canister as shown in Figure 1.2.3-10 and assembled in the cask as shown in Figure 1.2.3-12, or shipped in a PWR/BWR Rod Transport Canister in accordance with License Drawing No. 315-40-104.
14. Intact PULSTAR fuel elements may be loaded into a fuel rod insert or the PULSTAR screened or failed fuel can.
15. Damaged PULSTAR fuel elements and nonfuel components of PULSTAR fuel assemblies shall be loaded into either a PULSTAR failed fuel or screened fuel can, and placed into the top or base module of the 28 MTR fuel basket. Damaged fuel, including fuel debris, may be placed in an encapsulating rod prior to loading in a PULSTAR can.
16. Any combination of spiral fuel assemblies or MOATA plate bundles, each loaded into separate ANSTO basket modules containing up to a total of 42 assemblies/bundles.
17. Segmented TPBARs will be shipped in a sealed, dry Waste Container as shown in Figure 1.2.3-16 and assembled in the cask as shown in Figure 1.2.3-17.
18. Solid, irradiated and contaminated hardware containing less than a Type A quantity of fissile material and meeting the exemptions of 10 CFR 71.15, paragraphs (a), (b) and (c), loaded directly into the cask or contained in a secondary container or basket. The irradiated hardware spacer will be installed to limit the axial movement of the hardware above the lead shielded region of the cask body. As needed, additional secondary containers, dunnage and shoring may be used to limit the movement of the contents during normal and accident conditions of transport.
19. PWR MOX fuel rods (or a combination of PWR MOX and UO_2 PWR fuel rods) are required to be loaded in a screened or free flow PWR/BWR Rod Transport Canister provided with a 5×5 insert.

1.2.3.1 TRIGA Fuel and Basket Description

Two basic types of TRIGA fuel are to be transported in the NAC-LWT cask: TRIGA fuel elements and smaller fuel rods from TRIGA fuel cluster assemblies. TRIGA fuel elements are approximately 1-1/2 inches in diameter and are described in Section 1.2.3.1.1. TRIGA fuel cluster rods are smaller; approximately 1/2-inch in diameter and are also described in Section 1.2.3.1.1.

Up to 140 TRIGA fuel elements in the form of: a) standard fuel elements – either aluminum clad or stainless steel clad; b) instrumented fuel elements – similar to standard fuel elements (aluminum clad or stainless steel clad), but containing thermocouple instrumentation; and c) fuel follower control rod elements (aluminum or stainless steel clad) – poison rods with a fuel follower in a single tube may be shipped in the NAC-LWT cask. Up to 560 TRIGA fuel cluster rods may be shipped.

Up to six equivalent TRIGA fuel cluster rods may be loaded and transported in a sealed damaged fuel can (DFC). Up to the equivalent of two TRIGA damaged fuel elements and debris may be loaded and shipped in a sealed DFC. The TRIGA transport baskets and DFCs are described in Section 1.2.3.1.2.

1.2.3.1.1 TRIGA Fuel

TRIGA Fuel Elements

The characteristics of the design basis TRIGA fuel element are presented in Table 1.2-4 and in Table 1.2-1 for the poisoned basket and in Table 1.2-2 for the nonpoisoned basket.

The fuel material in a TRIGA fuel element is a solid, homogeneous mixture of uranium-zirconium hydride alloy, i.e., a metal alloy fuel. Both the aluminum-clad and the stainless steel-clad TRIGA fuel elements are approximately 1.5-inch diameter rods by approximately 30 inches long. The fuel follower control rod elements range in length from 45 inches to 66.5 inches and are cut, as required, to fit the basket length. Instrumented fuel elements are identical to standard fuel elements with the exception of thermocouples and wires and lead-out tubing. The lead-out tubing needs to be detached prior to shipment in order for the instrumented fuel elements to fit into the standard element height envelope. The aluminum-clad TRIGA fuel element and instrumented fuel element, the stainless steel-clad TRIGA fuel element and instrumented fuel element, and the standard fuel follower control rod element are shown in Figure 1.2.3-1 through Figure 1.2.3-5, respectively.

TRIGA Fuel Cluster Rods

The fuel material in TRIGA fuel cluster rods is a solid, homogeneous mixture of uranium-zirconium-erbium hydride alloy, i.e., a metal alloy fuel. Erbium is a burnable neutron poison that is used in the fuel to enhance the flux profile along the length of the fuel rod, and conservatively ignored in the nuclear evaluations. The rods have a nominal diameter of 0.54 inch and are approximately 31 inches long. The rod cladding is Incoloy 800 material and is 0.015-inch thick, minimum. Instrumented rods are identical to the standard rods, with the exception of thermocouples and wires. A diagram of the TRIGA fuel cluster rods, and the individual fuel pin (cluster rod) making up the cluster, is shown in Figure 1.2.3-6.

The active fuel region of a TRIGA fuel cluster rod is a maximum of 0.53 inch in diameter, 22.5 inches in length, and has an initial uranium enrichment of up to 95 percent for HEU material and 20 percent for LEU material. A compression spring is utilized to fill the space in the plenum region of the rod, and top and bottom plugs are used to seal the fuel within the rod. The design-

basis TRIGA fuel cluster rod characteristics are summarized in Table 1.2-3, Table 1.2-4, and Tables 5.1.1-1, 5.1.1-2, 6.2.6-1 and 6.2.6-2.

Axial fuel spacers, as shown on Drawing 315-40-085, may be used to axially position the TRIGA fuel elements, fuel inserts and DFCs. The axial spacers do not provide a safety function and are dunnage used to position the fuel elements to facilitate fuel handling. The total weight per basket module cell for the TRIGA fuel elements or cluster rods, inserts, spacer(s) and fuel cans, as applicable, shall be limited to a maximum of 80 pounds.

TRIGA Fuel Classification

The TRIGA fuel contents are divided into three categories based on fuel condition for evaluation, loading configuration and transport in the NAC-LWT:

1. Intact fuel (i.e., no cladding breach) is loaded directly into the TRIGA fuel basket modules (Section 1.2.3.1.2) with a maximum of four TRIGA fuel elements per loading position. Up to 16 intact cluster rods are loaded into fuel rod inserts (Drawing 315-40-096) that are inserted into the TRIGA fuel basket module cell openings. Intact TRIGA fuel elements and cluster rods may be loaded into a sealed DFC, if length permits.
2. Damaged TRIGA fuel elements and TRIGA fuel debris (up to the equivalent of two fuel elements) shall be loaded into a sealed DFC (Section 1.2.3.1.2), and then loaded into a top or base basket module.
3. Damaged TRIGA cluster rods and cluster rod fuel debris (up to the equivalent of six cluster rods) shall be loaded into a sealed DFC and then loaded into a top or base basket module.

1.2.3.1.2 TRIGA Fuel Baskets and Damaged Fuel Cans

The TRIGA fuel basket assembly configurations consist of five modules – a base module, three intermediate modules, and a top module. The three intermediate modules are interchangeable, but the base and top modules are required to be in their proper positions. Two basket configurations are available, "nonpoisoned" and "poisoned," where the poisoned basket configuration utilizes borated steel plates for additional criticality control. Each module has up to seven cells (fuel positions) for loading TRIGA fuel elements or cluster rods. The center cell of each module of the nonpoisoned basket configuration is blocked by a welded stainless steel baffle that prevents loading of that cell. The nonpoisoned configuration is also referred to as the 24-element basket or the 120-element loading, based on the maximum of 120 intact TRIGA fuel elements that may be loaded into the baskets in this configuration. The poisoned configuration is also referred to as the 28-element basket or the 140-element loading, based on the maximum of 140 intact TRIGA fuel elements that may be loaded into the baskets in this configuration. Additionally, the nonpoisoned configuration can accommodate up to 480 intact TRIGA fuel cluster rods, while the poisoned basket can hold up to 560 intact TRIGA fuel cluster rods.

Each basket module is a Type 304 stainless steel weldment consisting of longitudinal divider plates with circular support plates near each end; the top module also has a support plate at its midpoint due to its longer length. The poisoned basket modules contain four borated stainless steel plates that are seal welded to surfaces of the divider plates in the central region of the basket cross-section. The nonpoisoned basket modules are shown in Drawings 315-40-070, -071, and -072 and the poisoned basket modules are shown in Drawings 315-40-080, -081, and -082.

The nonpoisoned TRIGA fuel basket assembly in the NAC-LWT cask is shown in Drawing 315-40-079. The poisoned basket assembly in the NAC-LWT cask is shown in Drawing 315-40-084. In the poisoned basket configuration, an alternate assembly is presented that utilizes one base module and four intermediate modules, along with a spacer (Drawing 315-40-083). The spacer is utilized to fill the space differential in the cask cavity resulting from the use of an additional intermediate module, rather than a top module. This additional assembly configuration is provided for flexibility in situations where the extra length provided by the top module is not needed. The fuel basket modules are described in further detail in Section 2.6.12.8. Damaged TRIGA fuel and fuel debris shall be loaded into sealed DFCs.

The sealed DFC is a 3.25-inch outside diameter tube with a 0.065-inch thick wall. The bottom of the sealed fuel can includes a check valve and drain plug to facilitate draining of the can. The top of the sealed DFC is closed by a bolted lid that is sealed with a metallic O-ring and includes a diaphragm valve to facilitate draining, drying, and helium backfilling of the can. The sealed DFC is constructed of austenitic stainless steel as shown on Drawings 315-40-086, -087, and -088.

1.2.3.2 MTR and DIDO Fuel and Basket Description

The MTR fuel elements to be shipped are 33 to 57 inches long, including the upper and lower nonfuel-bearing hardware, which may be removed from the element prior to transport. The MTR element fuel plates consist of a U-Al, U_3O_8-Al, or U_3Si_2-Al fuel meat clad with aluminum. The fuel plates are held in a parallel arrangement with two thick aluminum slotted pieces to form a fuel element. The active fuel region is typically 22.75 inches in height, and the fuel meat is typically 0.023-inch thick. MTR elements/plates may contain cadmium wires. A maximum 100-gram cadmium source is addressed in the shielding evaluations documented in Chapter 5. Axial fuel spacers and plates may be used in the cells of the basket modules to position MTR elements to facilitate fuel unloading and handling. The axial fuel spacers do not perform a safety function and are considered dunnage. The axial fuel spacers and plates are shown on Drawing 315-40-085.

A maximum of 42 MTR fuel elements has been analyzed for transport in the NAC-LWT cask. This configuration consists of up to seven fuel elements placed radially in each of the six axial fuel basket modules. Two alternate configurations of MTR fuel element loading provide for loads of 35 elements in five basket modules or 28 elements in four basket modules. HEU MTR fuel elements having > 380 g ^{235}U, but less than 460 g ^{235}U, shall have a minimum of 2.0 cm (0.8 inch) of nonfuel hardware and/or spacers/plates at both ends of the fuel element. The minimum 2.0 cm nonfuel hardware and/or spacer/plate dimension assures criticality control. The axial fuel spacer and plate design is shown on Drawing 315-40-085. For the shipment of MTR fuel elements (or an equivalent number of plates in a plate canister) having ^{235}U greater than 470 g per element, or greater than 22 g per plate (up to a maximum of 640 g per element or 32 g per plate), the maximum quantity of elements per basket module is limited to four, which are to be loaded in basket positions 4, 5, 6 and 7. Cell block spacers shall be installed in basket openings 1, 2 and 3 to block these cells from being inadvertently loaded with fuel elements. The cell block spacer design is shown on Drawing 315-40-085. Therefore, for the transport of elements of greater than 470 g ^{235}U, if only one element exceeds the 470 g (22 g per plate) limit, a maximum of four elements shall be loaded into the seven-element basket module and cell block spacers shall be placed in basket opening positions 1, 2 and 3.

Loose MTR fuel plates may be shipped in an MTR plate canister to facilitate handling. The contents of the canister are limited to the number of plates in the original intact fuel assembly, and the fuel plate dimensions and fuel masses must be bounded by the MTR fuel element limits in Table 1.2-4. The total weight per basket module cell for the fuel element, spacer(s) and fuel plate canister, as applicable, shall be limited to a maximum of 80 pounds.

A maximum of 42 DIDO fuel assemblies has been analyzed for transport in the NAC-LWT cask. Again, up to seven fuel assemblies may be placed radially in each of six axial fuel basket modules.

DIDO fuel assemblies are similar to MTR fuel elements in that the fuel bearing hardware consists of plates of fuel meat sandwiched by cladding. However, in DIDO fuel, the plates have been formed into tubular elements that are arranged in a concentric configuration. Typical DIDO assemblies contain four of the concentric tubes.

MTR and DIDO fuel characteristics are presented in Table 1.2-4.

1.2.3.3 General Atomics Irradiated Fuel Material (GA IFM) and Basket Description

The GA IFM is made up of two separate types of fuel material—the High-Temperature Gas-Cooled Reactor (HTGR) type fuel and the Reduced-Enrichment Research and Test Reactor (RERTR) type fuel. Each type of IFM is packaged in its own unique Fuel Handling Unit (FHU). Figures 1.2-7 and 1.2-8 illustrate the HTGR and RERTR FHUs. Detailed drawings for the GA and IFM FHUs are in Section 1.4.

The HTGR IFM is comprised of fuel in four forms: fuel particles (kernels), fuel particles (coatings), fuel compacts (rods), and fuel pebbles. Fuel kernels are solid, spheridized, high-temperature sintered fully-densified, ceramic kernel substrate, composed of: UC_2, UCO, UO_2, $(Th,U)C_2$, or $(Th,U)O_2$. The as-manufactured enrichment of the HTGR fuel varies from ~10.0 to 93.15 wt % ^{235}U. Fuel coatings are solid, spheridized, isotropic, discrete multi-layered fuel particle coatings with chemical composition including pyrolitic-carbon (PyC) and silicon carbide (SiC). Fuel compacts are multi-coated ceramic fuel particles, bound in solid, cylindrical, injection-molded, high-temperature heat-treated compacts. The fuel compact matrix is composed of carbonized graphite shim, coke, and graphite powder. Fuel pebbles are multi-coated fuel particles, bound in solid, spherical injection-molded, high-temperature heat-treated pebbles. The fully-cured binding matrix is composed of carbonized graphite shim, coke , and graphite powder.

The RERTR IFM is comprised of 20 irradiated TRIGA fuel elements; 13 of the elements are intact and the remaining seven have been previously sectioned for examination purposes. Parameters characterizing the RERTR/TRIGA fuel elements are shown in Table 6.2.9-1. Three distinct mass loadings of uranium were used in the 20 TRIGA elements: 20, 30, and 45 wt % U; the average mass of the fueled portion of these elements is 551g with an enrichment of 19.7 wt % ^{235}U. The RERTR IFM consists of U-ZrH metal alloy fuel material and as a solid meets the requirement of 10 CFR 71.63.

Two GA IFM Fuel Handling Units (FHU) are intended for a single shipment in the NAC-LWT. The first IFM FHU contains HTGR type fuel and the second contains RERTR type fuel. Each IFM FHU consists of stainless steel weld-encapsulated primary and secondary enclosures. The FHUs are filled and sealed with air at atmospheric pressure. The two IFM FHUs are placed in the top of the NAC-LWT cavity with a bottom spacer to facilitate unloading of the IFM packages.

The GA IFM fuel characteristics are presented in Table 1.2-7.

1.2.3.4 PWR Fuel Assembly

The NAC-LWT cask is analyzed for the PWR fuel assemblies listed in Table 1.2-5. This table provides the dimensional and enrichment constraints for the PWR fuel. The burnup and decay heat limits are specified in Table 1.2-4.

The PWR fuel rod cladding is a zirconium alloy type (Zircaloy-2, Zircaloy-4, Zirlo, M-5, etc.). Minor variations of alloy composition have no impact on performance of cladding material.

1.2.3.5 BWR Fuel Assembly

The NAC-LWT cask is analyzed for the BWR fuel assemblies listed in Table 1.2-6. This table provides the dimensional constraints for the BWR fuel. The enrichment, burnup and decay heat limits are specified in Table 1.2-4.

The BWR fuel rod cladding is a Zirconium alloy type (Zircaloy-2, Zircaloy-4, Zirlo, M-5, etc.). Minor variations of alloy composition have no impact on performance of cladding material.

1.2.3.6 TPBARs

The NAC-LWT cask is analyzed for the transport of three separate Tritium Producing Burnable Absorber Rod (TPBAR) content configurations. For the transport of production TPBARs from the reactor facility to the DOE processing facility, an open (i.e., unsealed) stainless steel consolidation canister is utilized to contain up to 300 TPBARs, two of which can be prefailed. The characteristics of the production TPBARs are listed in Table 1.2-8. The consolidation canister assembly is shown in Figure 1.2.3-10. Up to 25 TPBARs may also be transported within the 5×5 rod holder located within the PWR/BWR Rod Ttransport Canister. For a TPBAR shipment, the transport canister is located within the TPBAR basket. Up to two of the 25 TPBARs located within the rod holder may be classified as prefailed.

The third transport configuration is for the shipment of segmented TPBARs, following post-irradiation examination (PIE), contained in a welded stainless steel waste container containing segments and debris from up to 55 TPBARs. The characteristics of the TPBAR PIE segments are provided in Table 1.2-12. The waste container and extension weldment assembly is shown in Figure 1.2.3-16.

TPBARs are similar in size and nuclear characteristics to standard, commercial PWR, stainless steel-clad burnable absorber rods. The exterior of a typical TPBAR is a stainless steel clad tube. The internal components of the TPBAR are designed and selected to produce and retain tritium. Internal configurations differ for various TPBAR designs (see DOE reports provided in the

Chapter 1 Appendices). The internal components of a typical TPBAR include a plenum spacer tube (getter tube), a spring clip or a plenum (compression) spring, pellet stack assemblies (pencils), and a bottom spacer tube. A pencil consists of a zirconium alloy liner around which lithium aluminate absorber pellets are stacked and then confined in a getter tube as shown in Figure 1.2.3-9. The unclassified design details of the various TPBAR designs are provided in the unclassified DOE documents and drawings provided in the Chapter 1 Appendices.

The transport assembly arrangements for the consolidation canister and waste container TPBAR content configurations are identical and include a closure lid spacer assembly, a TPBAR basket and Alternate B port covers with bolting installed. The detailed requirements for the NAC-LWT assembly are provided in license drawing 315-40-128 in Section 1.4. The overall payload arrangement for the NAC-LWT with the consolidation canister and waste container are shown in Figure 1.2.3-12 and Figure 1.2.3-17, respectively. For the transport of fewer than 300 TPBARs in the consolidation canister, stainless steel dunnage may be used to align and protect the contents. The weight and volume of the dunnage and the reduced TPBAR contents of the consolidation canister must be less than, or equal to, the weight and volume of 300 TPBARs. Up to 25 TPBAR rods may also be transported in a PWR/BWR Rod Transport Canister in a NAC-LWT assembly as shown in License Drawing No. 315-40-104 (assembly 95).

The TPBAR content conditions are analyzed and evaluated for compliance with structural, thermal, containment and shielding conditions of the NAC-LWT in the appropriate SAR chapters. TPBARs do not contain fissile material and, therefore, criticality evaluations have not been performed. The operating procedures for the wet and dry loading and dry unloading of the TPBAR contents are provided in Chapter 7. The special leakage and pressure testing requirements for NAC-LWT casks intended for the transport of TPBAR contents are provided in Chapter 8.

1.2.3.7 PWR/BWR Fuel Rods

PWR and BWR fuel rods are transported within the fuel lattice (skeleton) or 4×4 or 5×5 inserts (rod holder). The rod holder is located within a free flow, screened or sealed PWR/BWR transport canister. (The rod holder may also contain a nonfuel-bearing irradiated hardware component [e.g., BWR water rod, PWR instrument/guide tube]).

The PWR and BWR fuel rod cladding is of Zirconium alloy type (Zircaloy-2, Zircaloy-4, Zirlo, M-5, etc.). Minor variations of alloy composition have no impact on performance of cladding material.

1.2.3.8 PULSTAR Fuel Element and Transport Configuration Description

PULSTAR fuel elements are transported in the NAC-LWT in the 28 MTR fuel basket assembly, which contains four modules with seven cells per module. The basket assembly is composed of a top module, a base module, and two intermediate modules (Dwgs 315-40-051, -049, and -050, respectively).

PULSTAR fuel elements may be loaded into the module cells in one of four configurations: a) intact PULSTAR fuel assemblies b) intact PULSTAR fuel elements loaded into the 4×4 TRIGA fuel rod insert (Dwg. 315-40-096); c) intact or damaged PULSTAR fuel elements, fuel debris and nonfuel-bearing components of PULSTAR fuel assemblies in the PULSTAR screened can (Dwg. 315-40-135); or d) intact or damaged PULSTAR fuel elements, fuel debris and nonfuel-bearing components of PULSTAR fuel assemblies in the PULSTAR sealed can (Dwg. 315-40-130). The contents of either can type are restricted to a quantity of fissile material and a total volume of material equivalent to 25 PULSTAR fuel elements. The sealed cask contents are restricted to the displaced volume of 25 intact PULSTAR fuel elements. The total cask payload shall not exceed 700 PULSTAR fuel elements. Loading of modules with mixed PULSTAR payload configurations is allowed, but PULSTAR cans, either screened or sealed, are restricted to loading in the base and top modules.

PULSTAR fuel elements are low enriched (< 7 wt %) uranium oxide rods, with zirconium alloy cladding. During reactor operation, 25 PULSTAR fuel elements are arranged in a rectangular 5×5 lattice, surrounded by a zirconium alloy box, and capped by top- and bottom-end fittings to form a PULSTAR fuel assembly. The nonfuel components of a PULSTAR fuel assembly are primarily aluminum and zirconium alloy and do not contain a significant activation source. A sketch of a PULSTAR fuel assembly is provided in Figure 1.2.3-13. Key physical, radiation protection and thermal characteristics of the PULSTAR fuel assembly/elements are listed in Table 1.2-9.

The sealed and screened PULSTAR cans are stainless steel containers that: a) minimize the dispersal of gross fuel particles that may escape from damaged fuel element cladding and/or fuel debris; b) facilitate retrieval of the contents from the transportation cask; and c) confine damaged fuel and/or debris within a known volume to facilitate criticality control, maintain dose limits, and control thermal loads within the cask. PULSTAR fuel pellets, pieces, and debris may be placed in an encapsulating rod for handling purposes prior to placement into either a sealed or screened can. The encapsulating rod is not required and has no safety significance. In addition to fuel elements, the cans may contain fuel assembly hardware up to the total content weight limit specified in Table 1.2-9. For operational/retrievability purposes, stainless steel rod inserts

may be used to position the PULSTAR fuel elements within the fuel rod insert. Total content weight shall not exceed the total weight limit specified in Table 1.2-9. The fuel rod insert is composed of a 4×4 grid of 0.75-inch OD × 0.065-inch wall stainless steel tubes. The tubes provide structural support for individual intact PULSTAR fuel elements during transport in the NAC-LWT.

Spacers may be used to axially position PULSTAR fuel contents near the top of the module for ease of loading and unloading operations. The spacers are provided for ease of operations and do not provide a safety function.

1.2.3.9 ANSTO Basket and Payload Description

Two basic fuel types are to be transported in the ANSTO baskets within the NAC-LWT cask: spiral fuel assemblies and MOATA plate bundles. Spiral fuel assemblies are composed of cylindrical aluminum inner and outer shells connected by curved metallic fuel plates. Further detail on the spiral fuel assemblies is provided in Section 1.2.3.9.1. MOATA plate bundles are comprised of up to 14 MTR fuel plates. Further detail on the plate bundles is provided in Section 1.2.3.9.2. Spiral fuel assemblies and MOATA plate bundles shall be intact. Note that spiral assemblies may be cropped by removing nonfuel-bearing hardware to fit within the basket tubes. Cropped spiral fuel assemblies are classified as intact fuel.

Up to 42 spiral fuel assemblies or 42 MOATA plate bundles may be loaded. A full cask load contains 6 baskets of up to 7 fuel assemblies or plate bundles per basket. The mixed loading of ANSTO basket modules containing either spiral fuel assemblies or MOATA plate bundles is authorized.

1.2.3.9.1 Spiral Fuel Assemblies

The design basis characteristics of spiral fuel assemblies are presented in Table 1.2-10. The fuel material in spiral fuel assembly plates is a solid, homogeneous mixture of uranium-aluminum alloy, i.e., a metal alloy fuel. The fuel meat of each plate is clad in aluminum. A set of 10 curved fuel plates is located between an inner and outer cylindrical aluminum shell. Fuel elements are cropped to fit axially within the basket envelope. Fuel material is not cut during the cropping operation. The fuel plates are located in a spiral pattern, maintaining a constant pitch between fuel plate centers. A sketch of the assembly cross-section is provided in Figure 1.2.3-14.

1.2.3.9.2 MOATA Plate Bundles

The design basis characteristics of MOATA plate bundles are presented in Table 1.2-4. The fuel material in the plate bundle is a solid, homogeneous mixture of uranium-aluminum alloy, i.e., a metal alloy fuel. Each plate is clad in aluminum. A plate bundle is comprised of up to 14 fuel plates. Two thick (0.635 cm) aluminum nonfuel side plates support the fuel plate stack from two sides, making a possible total of 16 plates per bundle. At each axial end, the plates in the stack are connected by a pin. Spacing between plates is maintained by disk spacers placed onto the top and bottom pins between each fuel plate and the aluminum side plates. A sketch of a typical MOATA plate bundle is provided in Figure 1.2.3-15.

1.2.3.10 Solid, Irradiated and Contaminated Hardware

The design basis characteristics of the solid, irradiated and contaminated hardware are provided in Table 1.2-13. As described in the content definition, the solid, irradiated and contaminated hardware may contain small quantities of fissile materials. Fissile materials in the irradiated hardware contents are acceptable if the quantity of fissile material does not exceed a Type A quantity and does not exceed the exemptions of 10 CFR 71.15, paragraphs (a), (b) and (c).

The irradiated hardware may be directly loaded into the NAC-LWT cask cavity, or may be contained in a secondary container or basket. As needed, appropriate component spacers, dunnage and shoring may be used to limit the movement of the contents during normal and accident conditions of transport.

To ensure that the movement of the irradiated hardware contents above the lead shielded length of the NAC-LWT cask body (i.e., the approximately upper 6.25 inches of the cavity length) is precluded, an Irradiated Hardware Lid Spacer as shown on Drawing No. 315-40-145 shall be installed for all irradiated hardware content configurations. The total installed height of the spacer is 6.5 inches. Therefore, the available cavity length for the irradiated hardware is approximately 171 inches. The NAC-LWT cask shall be assembled for transport as shown on NAC Drawing No. 315-40-01 with the irradiated hardware spacer installed on the lid.

A comparative shielding evaluation for a conservatively selected irradiated hardware transport configuration (i.e., a single line source with no self-shielding) or consideration of the additional shielding provided by additional spacers, dunnage, inserts or secondary containers is presented in Chapter 5. The evaluations show that the regulatory dose rate requirements per 10 CFR 71.47 for normal conditions of transport, or 10 CFR 71.51(b) under hypothetical accident conditions, are not exceeded.

1.2.3.11 PWR MOX Fuel Rods

The NAC-LWT cask is analyzed and evaluated for the transport of up to 16 PWR MOX fuel rods (or a combination of up to 16 PWR MOX and UO_2 fuel rods) loaded into a 5×5 insert placed in a screened or free flow PWR/BWR Rod Transport Canister. The authorized characteristics of the evaluated PWR MOX fuel rods are provided in Table 1.2-4. For mixed PWR MOX and UO_2 PWR fuel rod combinations, the UO_2 PWR fuel rods may have the identical heat load, burnup and cool time characteristics as the PWR MOX fuel rods.

In addition to the 16 PWR MOX fuel rods (or a combination of PWR MOX and UO_2 PWR fuel rods), up to 9 burnable poison rods (BPRs) may be loaded in the remaining openings in the 5×5 insert in the PWR/BWR Rod Transport Canister.

Figure 1.2.3-1 Aluminum Clad TRIGA Fuel Element

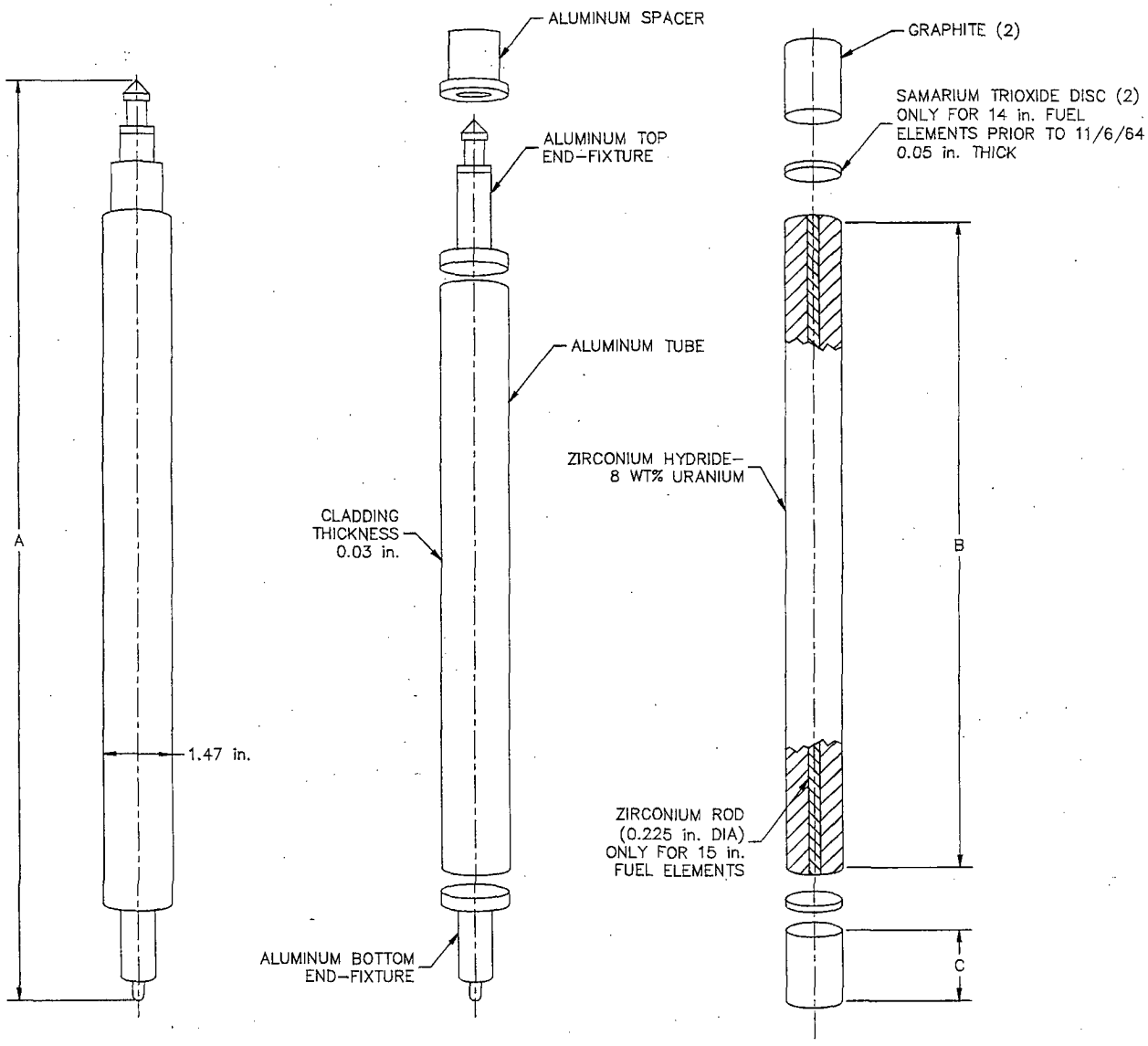


Figure 1.2.3-2 Aluminum Clad Instrumented Fuel Element

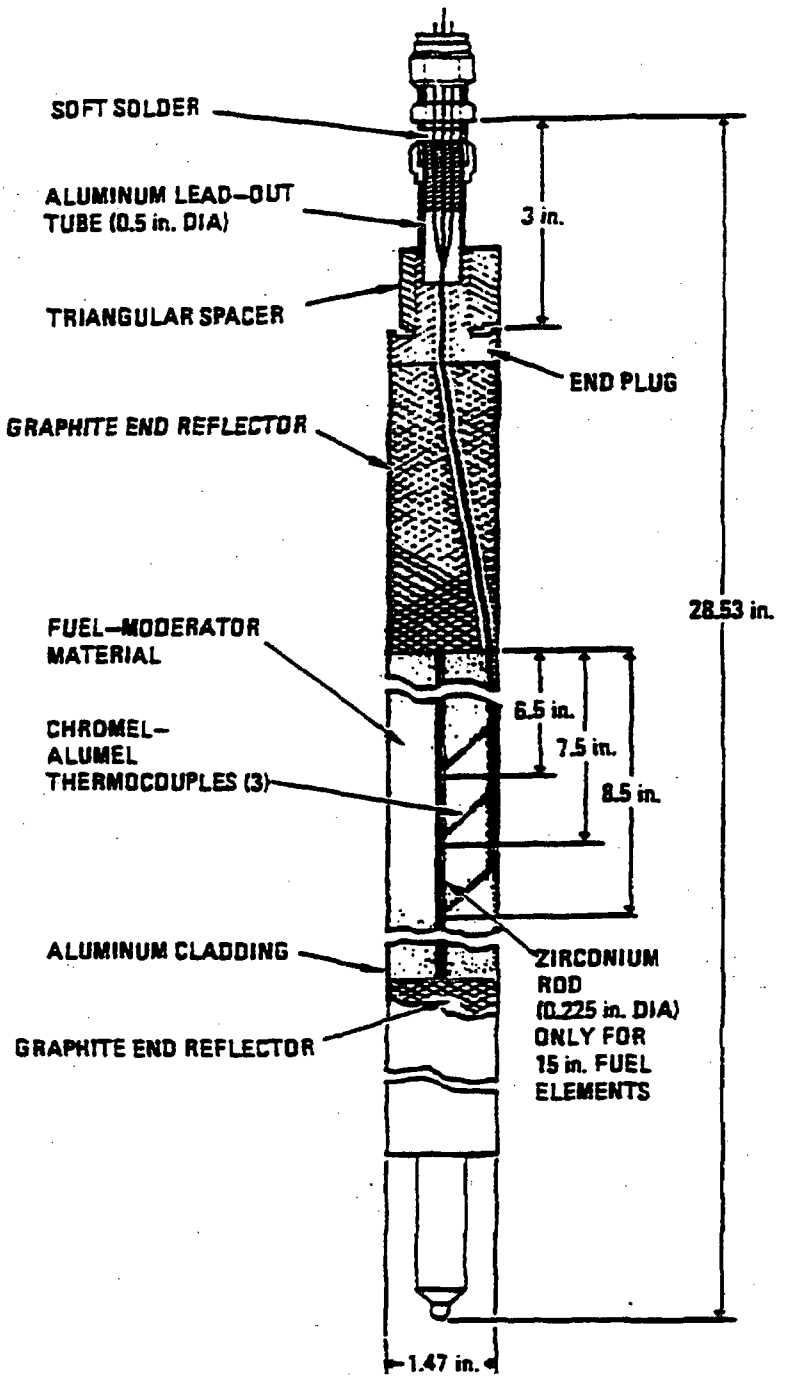


Figure 1.2.3-3 Stainless Steel Clad TRIGA Fuel Element

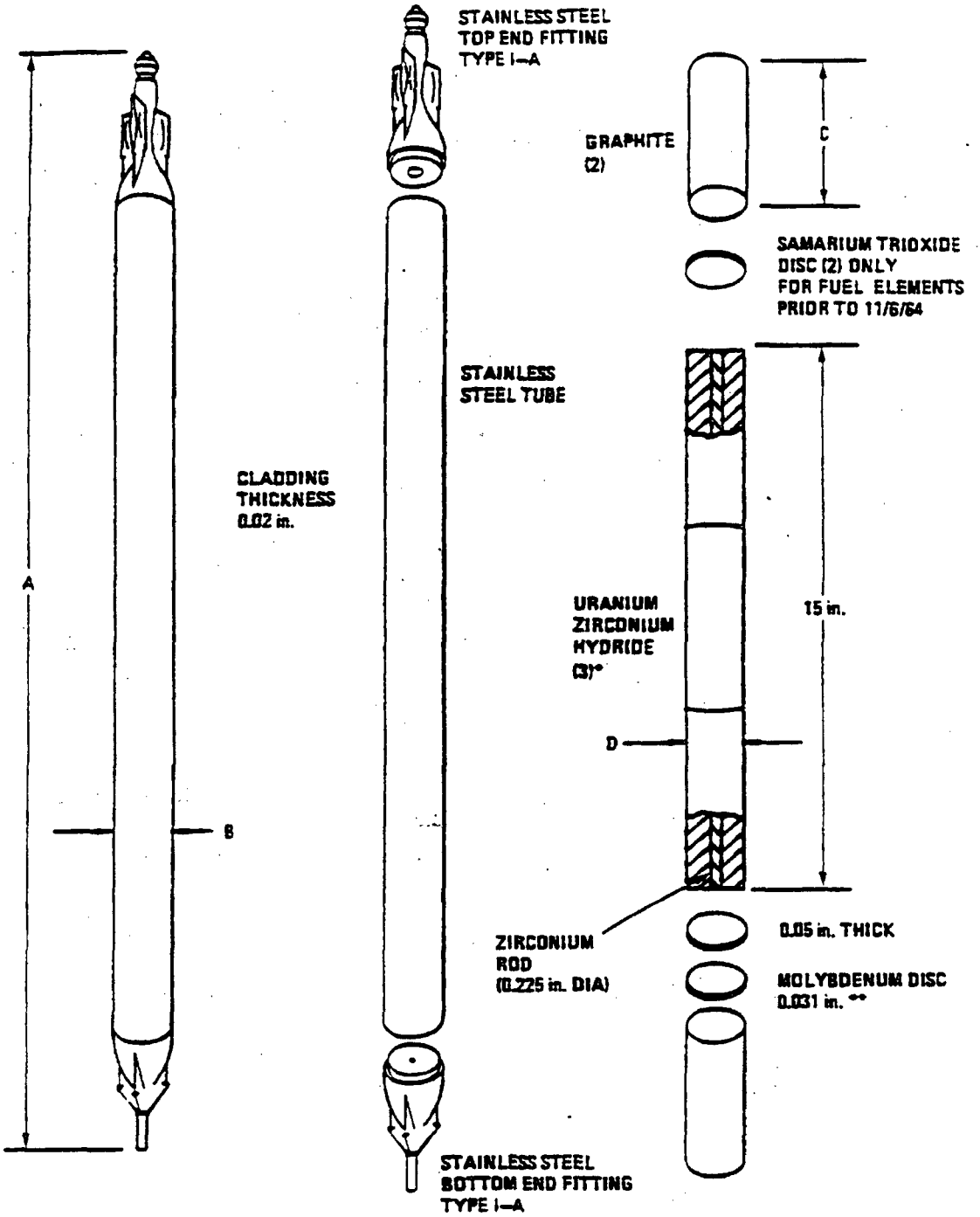


Figure 1.2.3-4 Stainless Steel Clad Instrumented Fuel Element

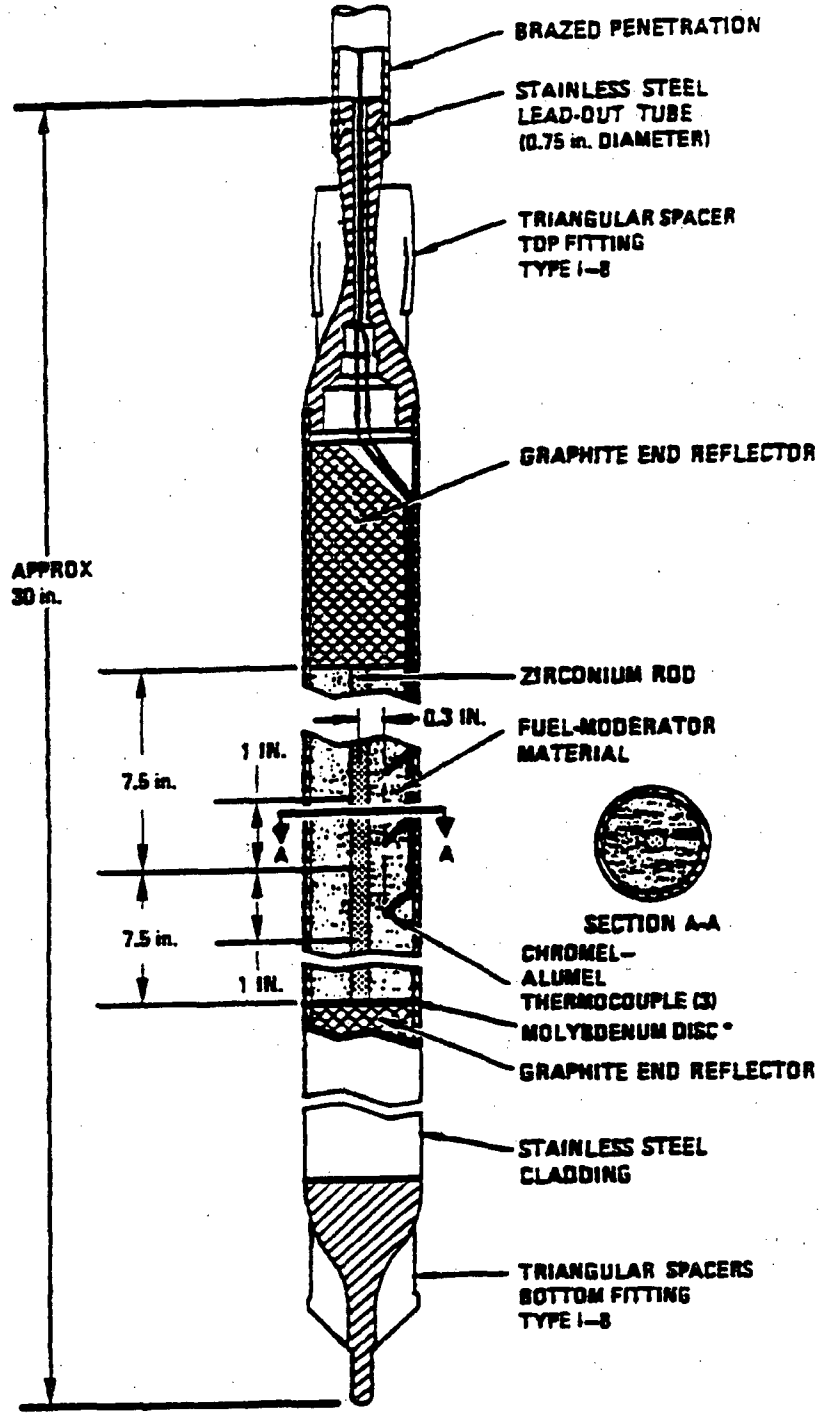


Figure 1.2.3-5 Standard Fuel Follower Control Rod Element

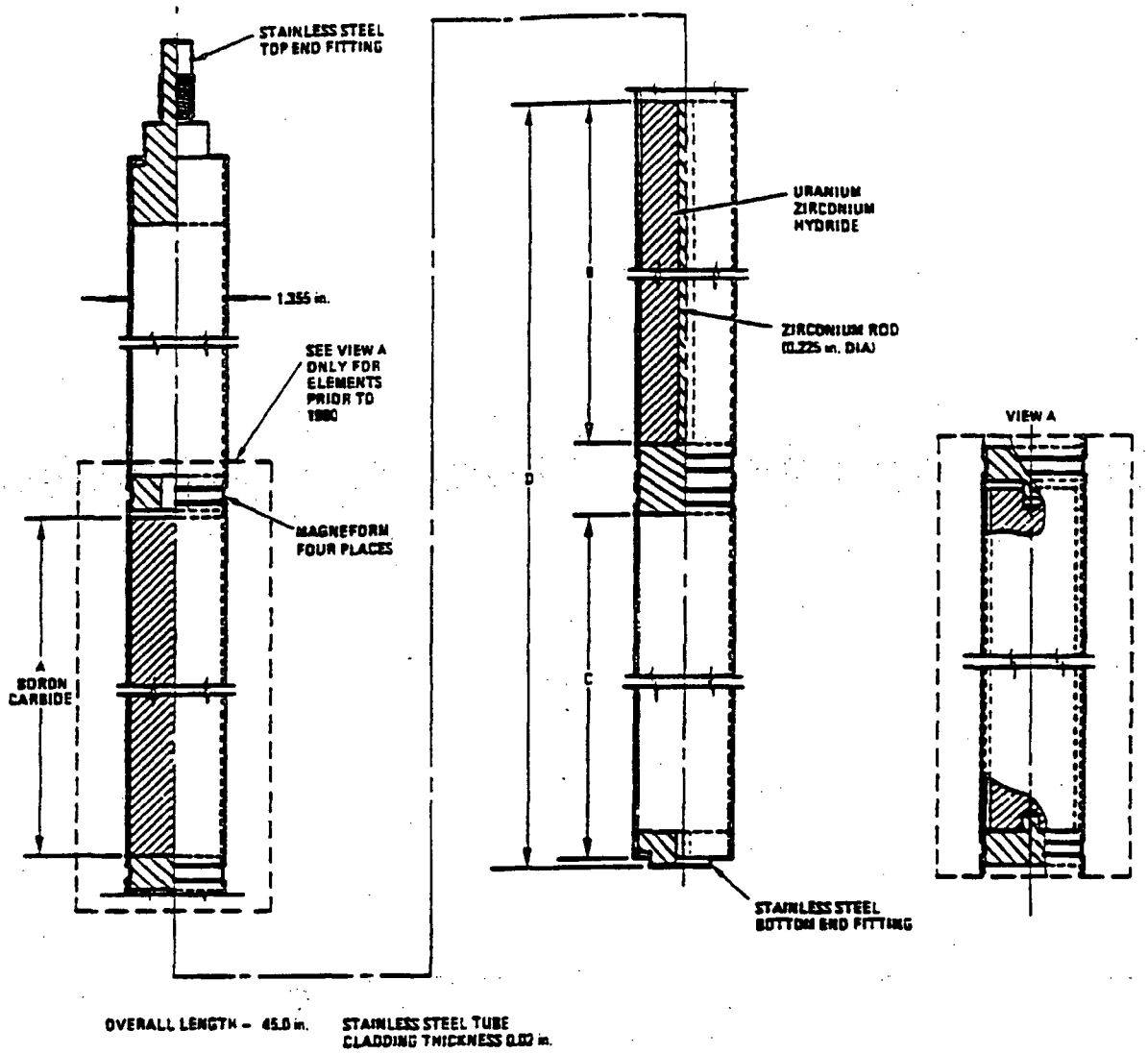
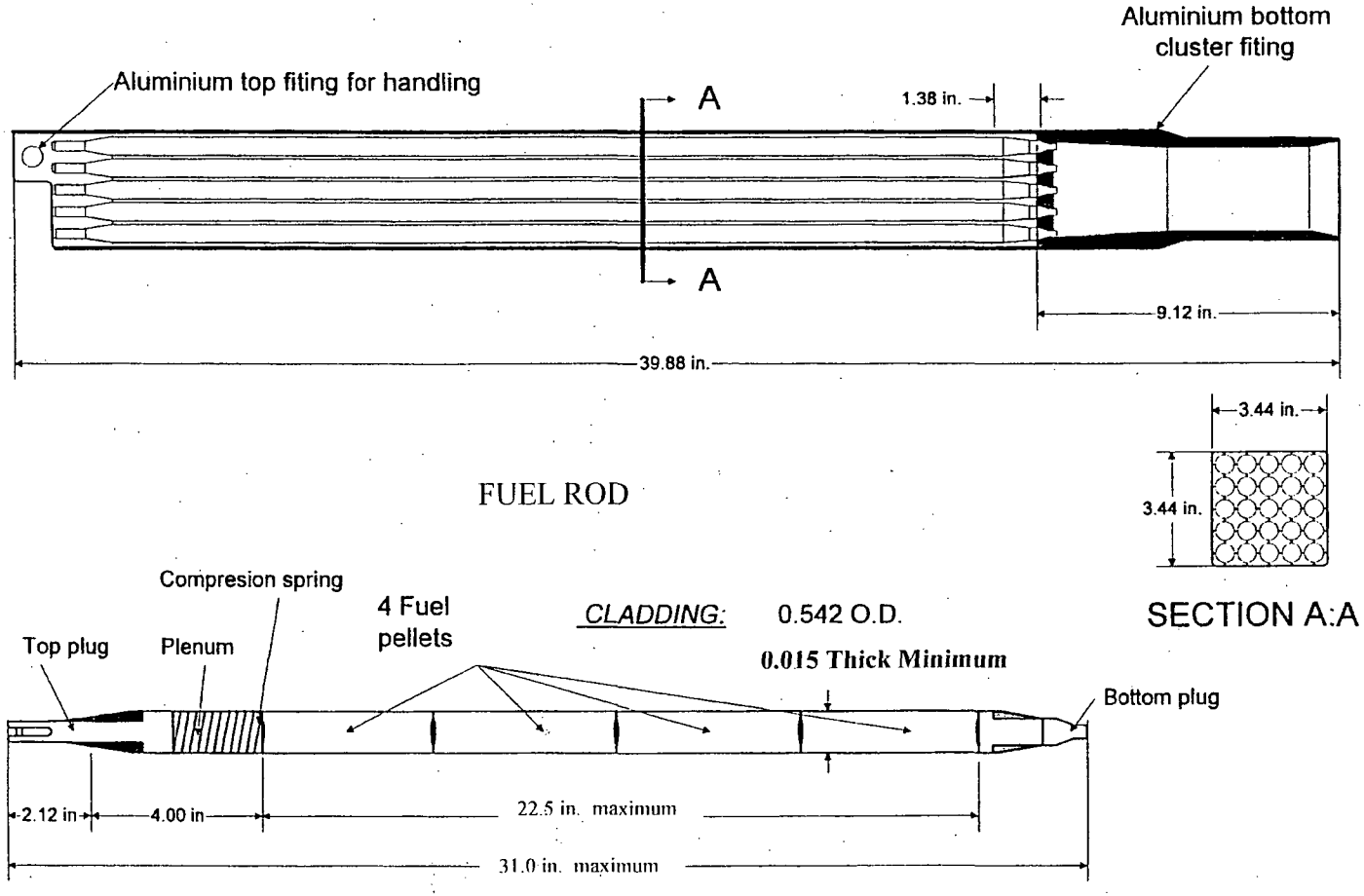


Figure 1.2.3-6 TRIGA Fuel Cluster and Rod Details



Fuel bundle and fuel element

Figure 1.2.3-7 HTGR Fuel Handling Unit

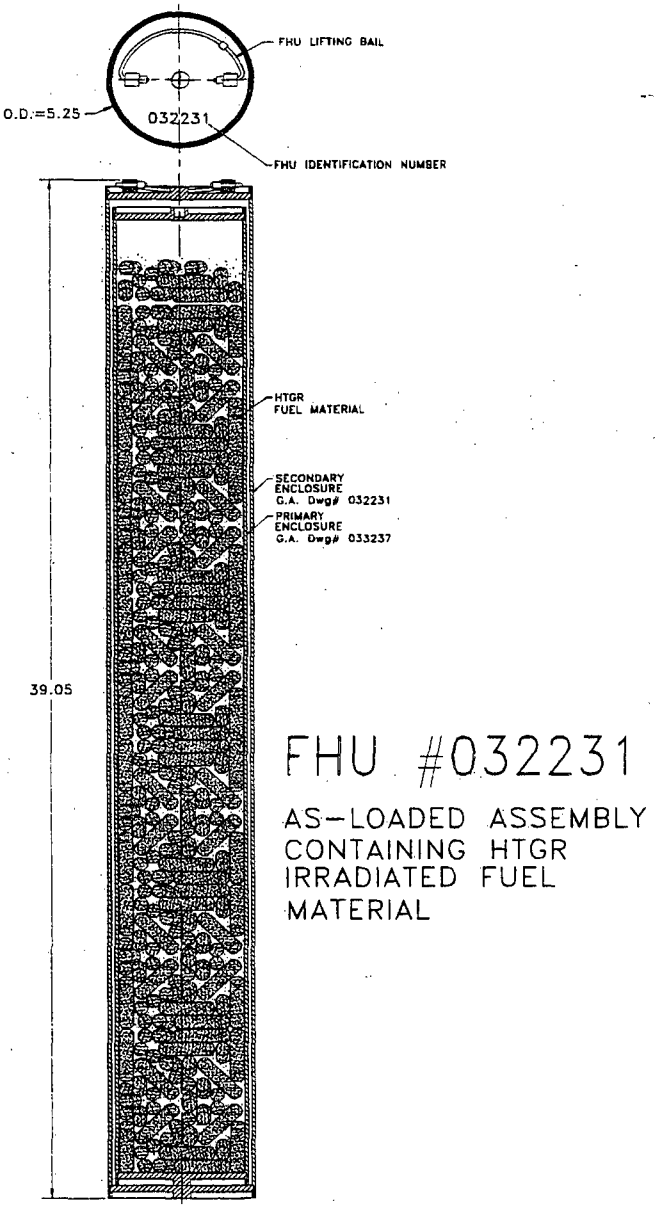


Figure 1.2.3-8 RERTR Fuel Handling Unit

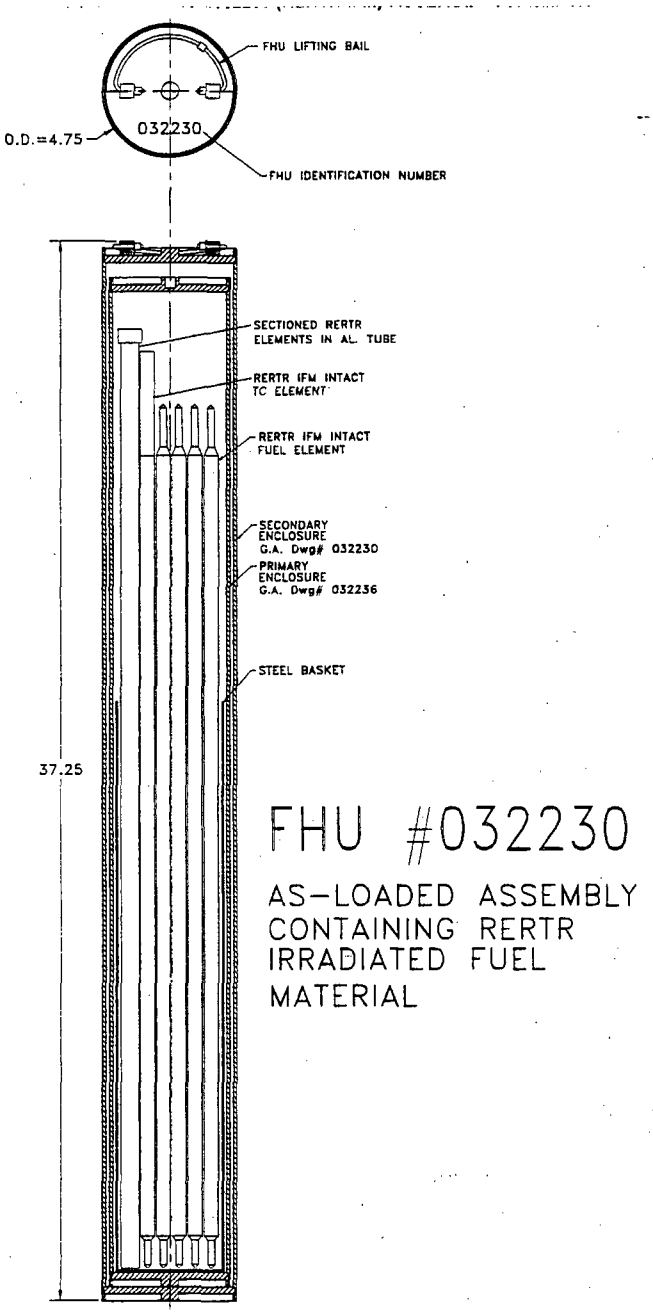
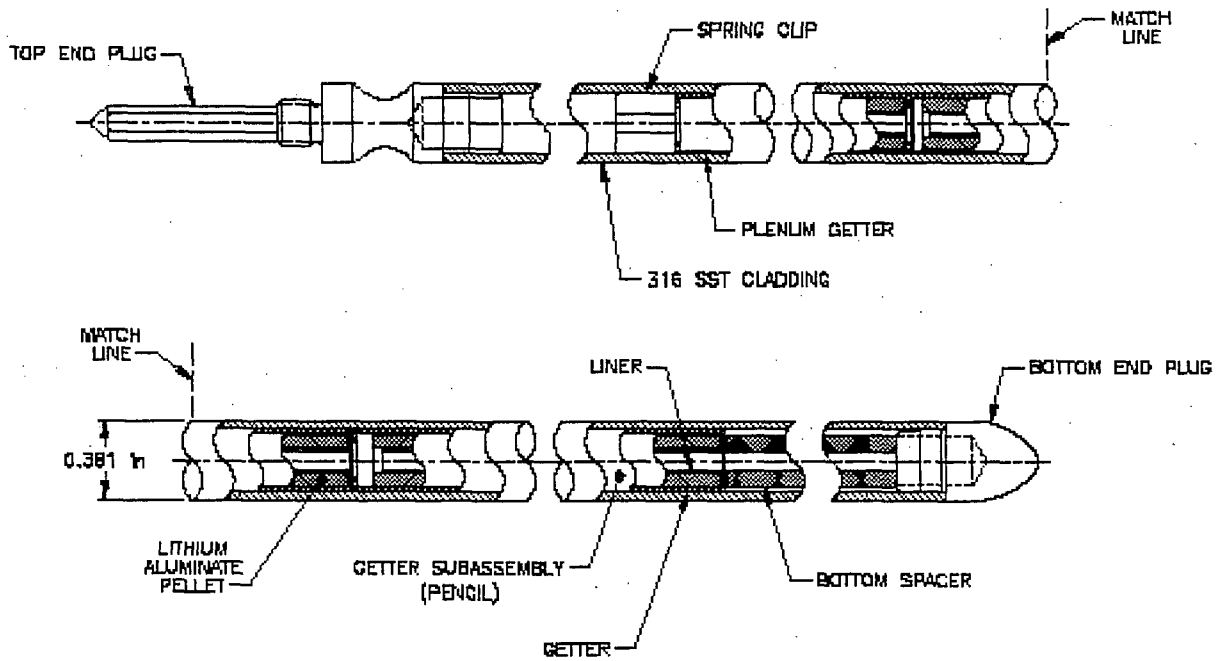


Figure 1.2.3-9 Typical TPBAR Assembly



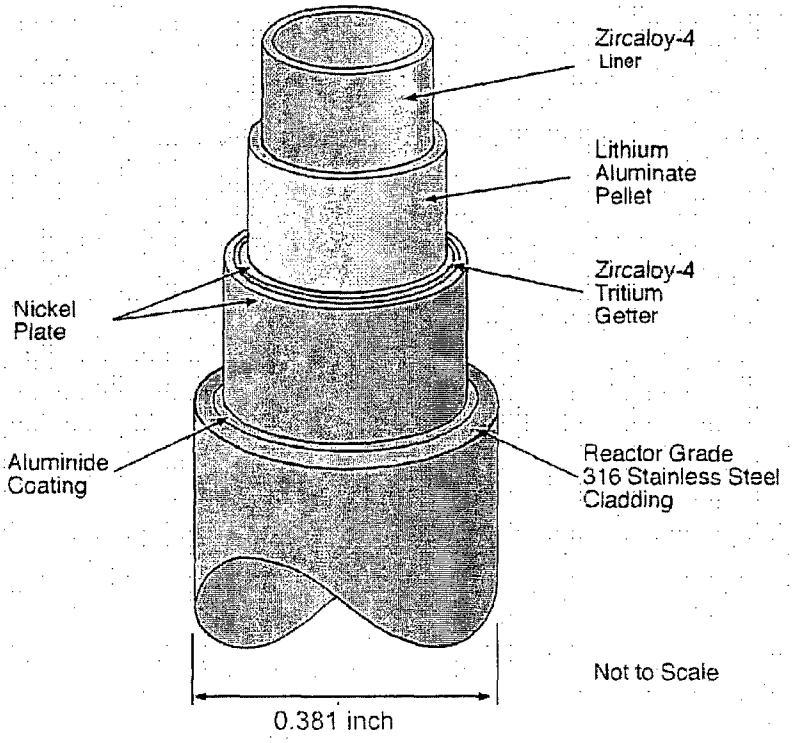
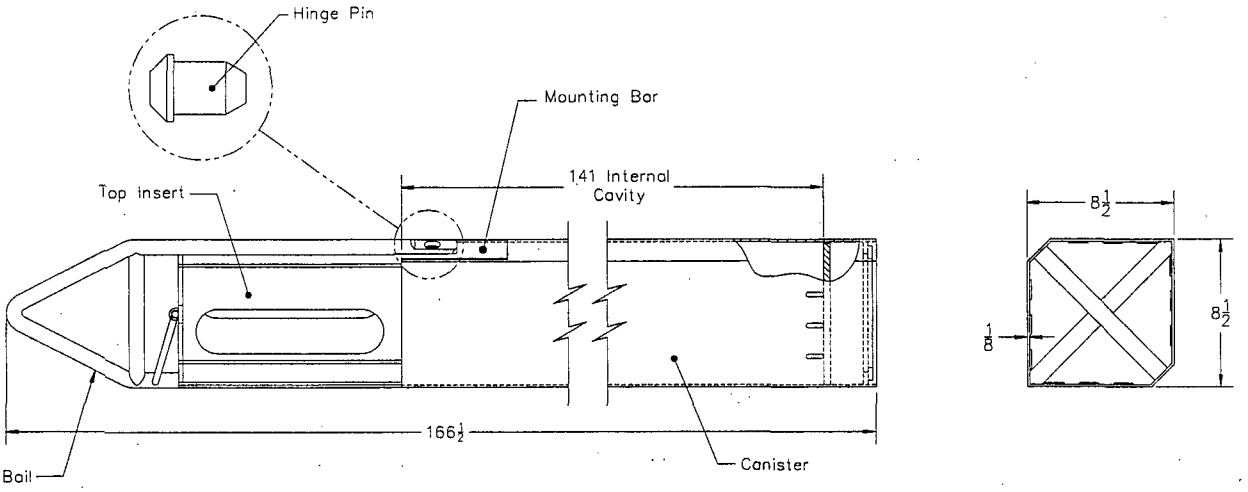


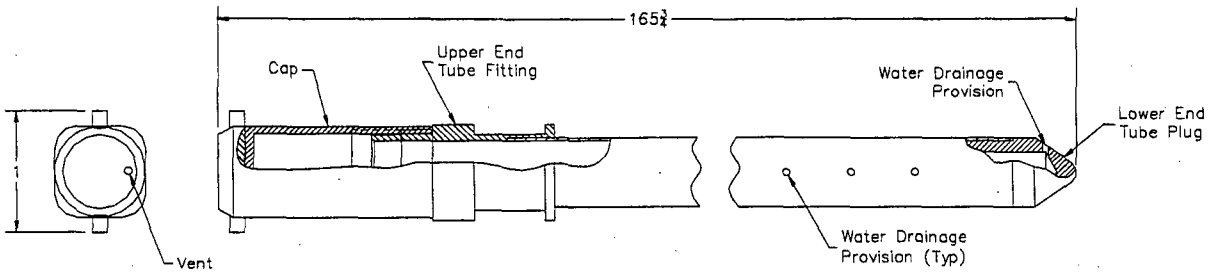
Figure 1.2.3-10 TPBAR Consolidation Canister Sketch



Conceptual Layout with Approximate Dimensions

Note: Material of construction is stainless steel.

Figure 1.2.3-11 Failed PWR/BWR Fuel Rod Capsule



Failed Fuel Rod Capsule Conceptual Layout

All Dimensions Approximate

Note: Material of construction is stainless steel.

Figure 1.2.3-12 NAC-LWT with TPBAR Consolidation Canister Payload

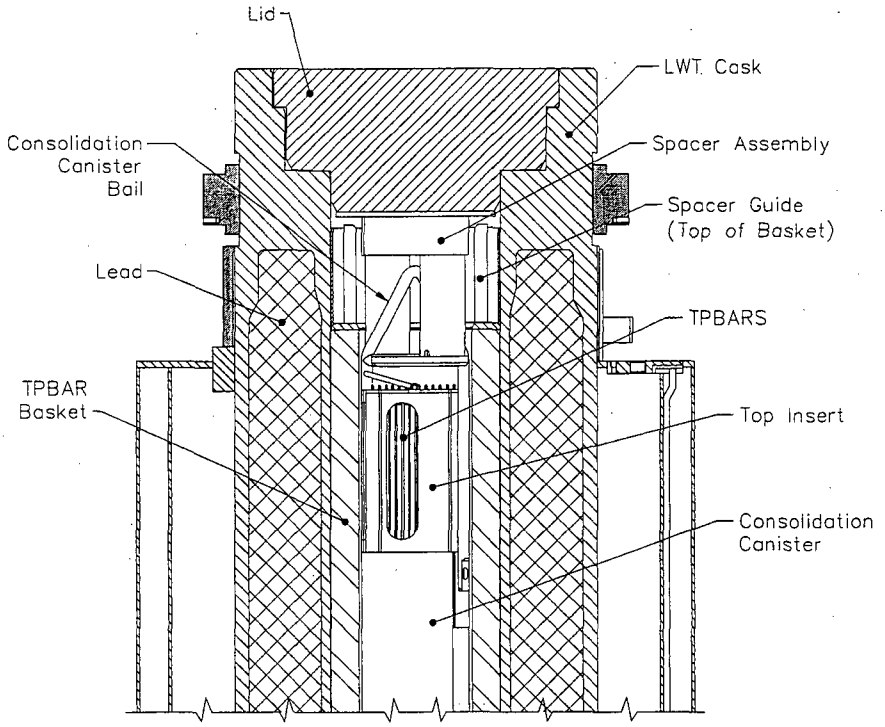


Figure 1.2.3-13 PULSTAR Fuel Assembly

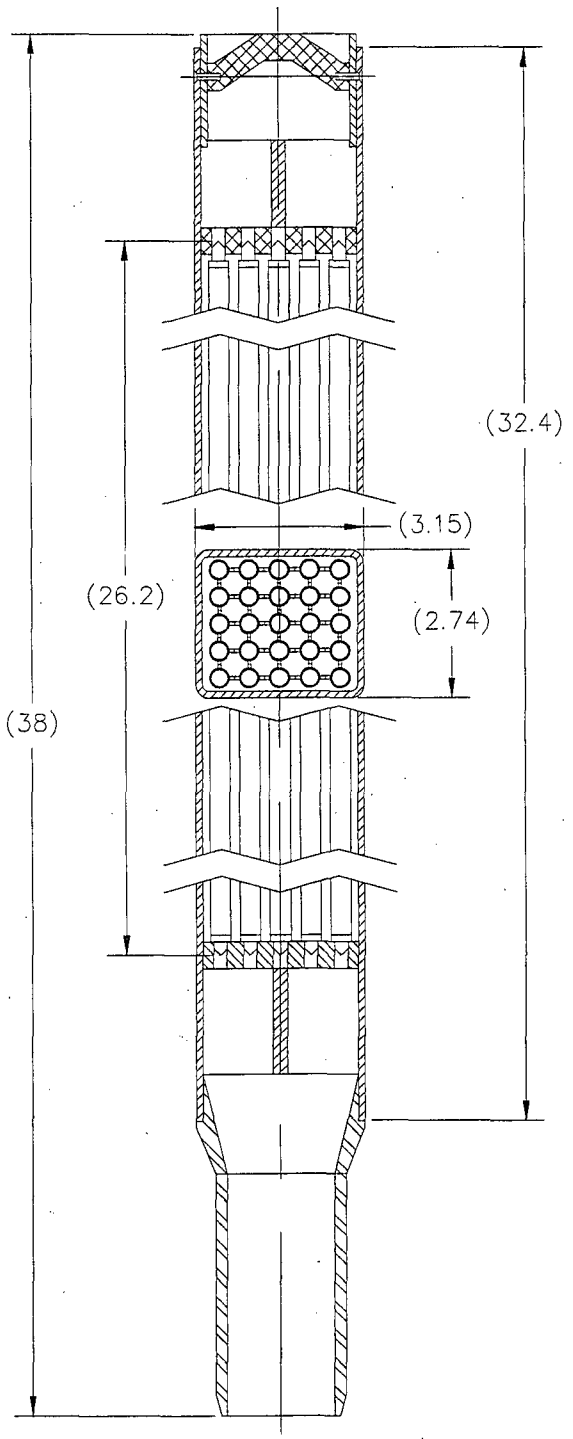
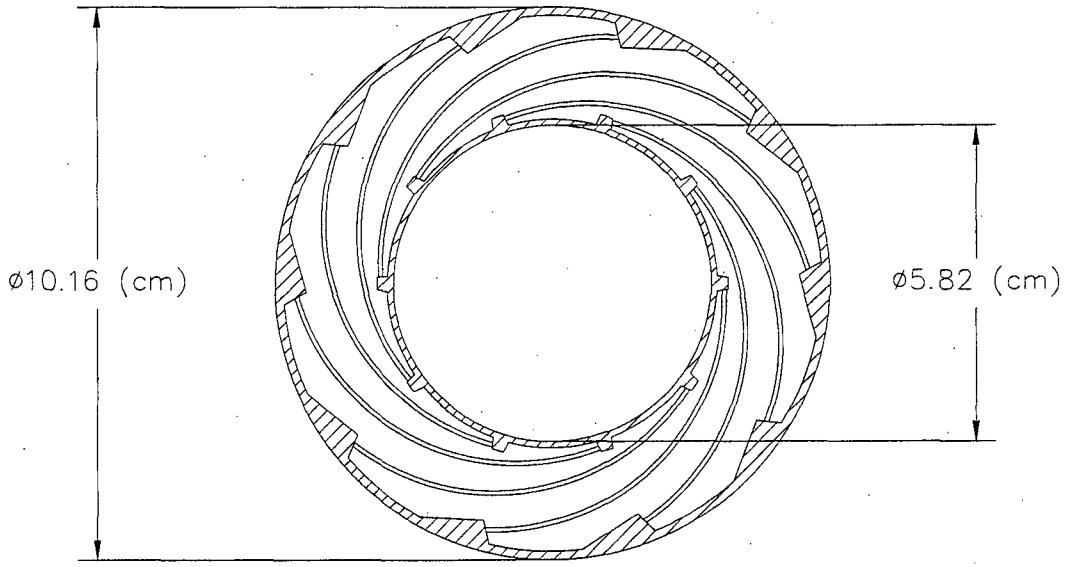
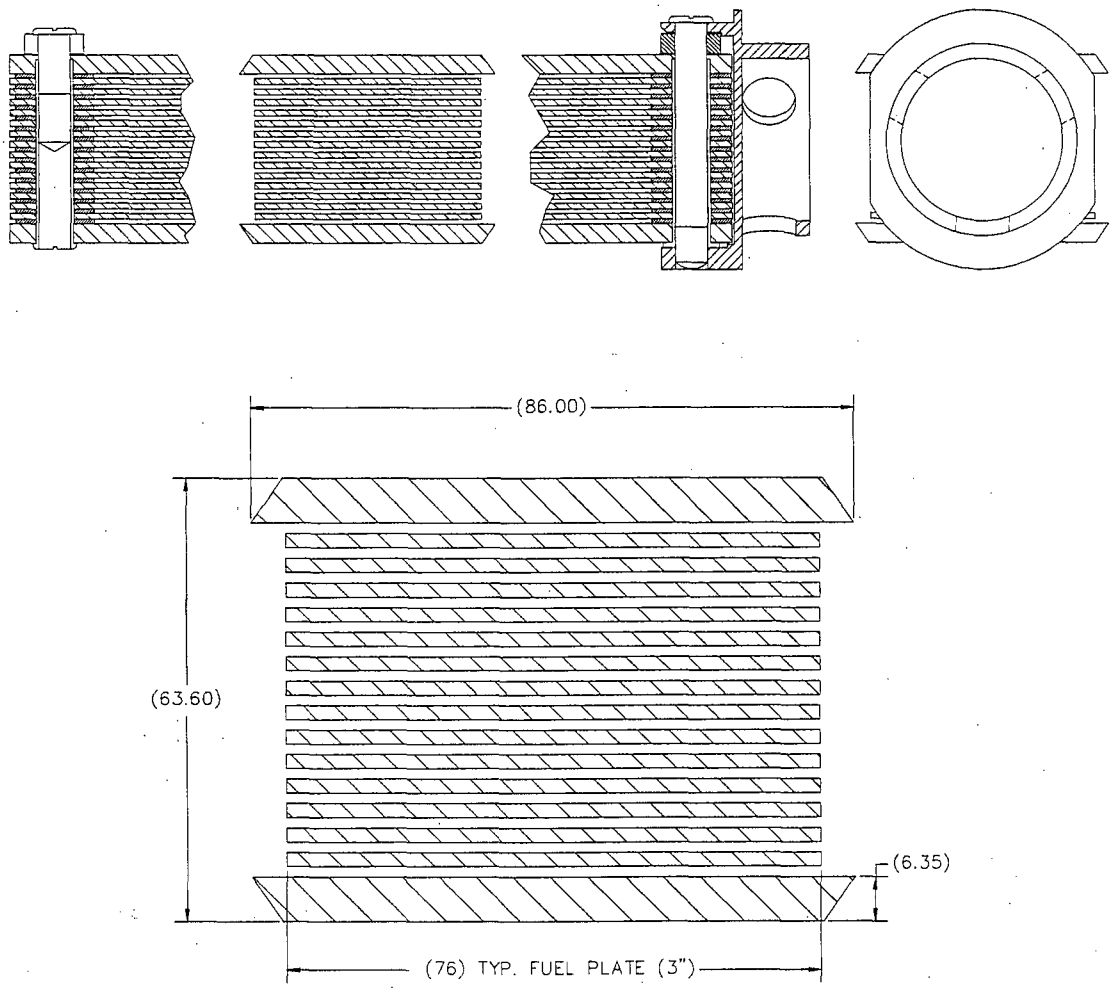


Figure 1.2.3-14 Spiral Fuel Assembly Cross-Section Sketch



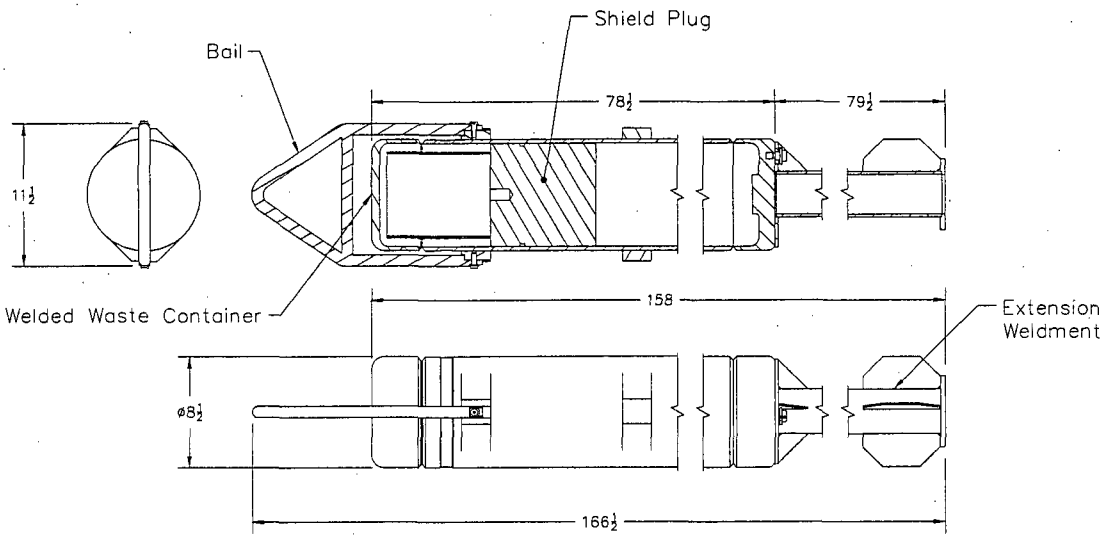
Note: Nominal dimensions

Figure 1.2.3-15 MOATA Plate Bundle Sketches



Note: 14-plate bundle configuration. Dimensions are reference values. Bundles with a reduced number of plates retain the plate pitch and compensate by wider side plates and outside spacers to retain overall bundle dimensions.

Figure 1.2.3-16 TPBAR Waste Container and Extension Weldment Sketch



Conceptual Layout with Approximate Dimensions

Note: Material of construction is stainless steel.

Figure 1.2.3-17 NAC-LWT with TPBAR Waste Container Payload

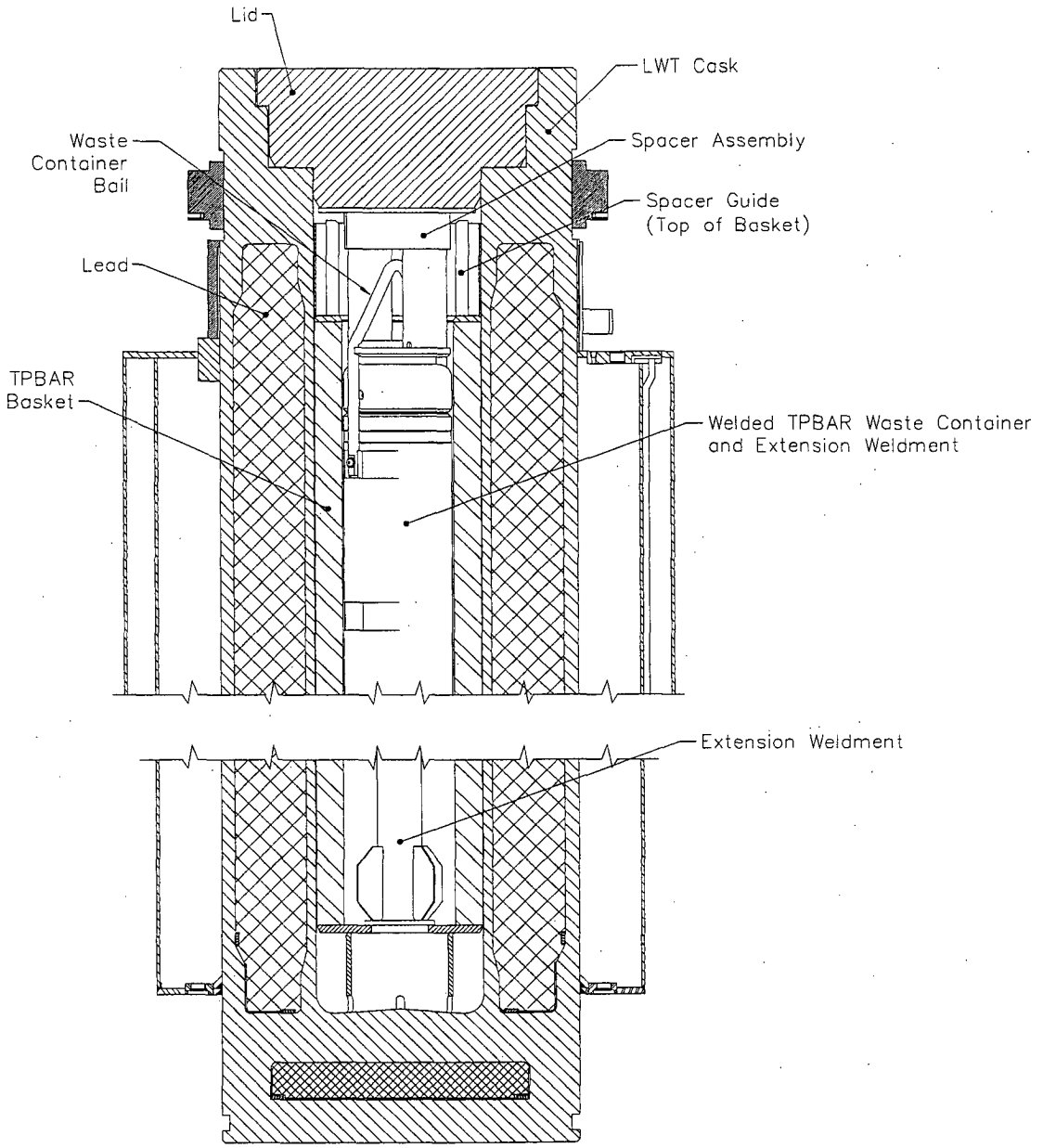


Table 1.2-1 Characteristics of Design Basis TRIGA Fuel Elements Acceptable for Loading in the Poisoned TRIGA Basket

	TRIGA HEU (Notes 1, 2, 6 & 7)	TRIGA LEU (Notes 1, 2, 6 & 7)	TRIGA LEU (Notes 1, 2, 6 & 7)
Fuel Form	Clad U-ZrH rod	Clad U-ZrH rod	Clad U-ZrH rod
Maximum Element Weight, lbs	13.2	13.2	13.2
Maximum Element Length, in	47.74	47.74	47.74
Element Cladding	Stainless Steel	Stainless Steel	Aluminum
Clad Thickness, in	0.02	0.02	0.03
Active Fuel Length, in	15	15	14-15 (Note 4)
Element Diameter, in	1.478 max.	1.478 max.	1.47 max.
Fuel Diameter, in	1.435 max.	1.435 max.	1.41 max.
Maximum Initial U Content/Element, kilograms	0.196	0.845	0.205
Maximum Initial ^{235}U Mass, grams	137	169	41
Maximum Initial ^{235}U Enrichment, weight percent	70	20	20
Zirconium Mass, grams (Note 5)	2060	1886-2300	2300
Hydrogen to Zirconium Ratio, max. (Note 5)	1.6	1.7	1.0
Maximum Average Burnup, MWd/MTU	460,000 (80% ^{235}U)	151,100 (80% ^{235}U)	151,100 (80% ^{235}U)
Minimum Cooling Time	90 days (Note 3)	90 days (Note 3)	90 days (Note 3)

Notes:

1. Mixed TRIGA LEU and HEU contents authorized.
2. TRIGA Standard, instrumented and fuel follower control rod type elements authorized.
3. Maximum decay heat of any element is 7.5 watts.
4. Aluminum clad fuel with 14-inch active fuel is solid and has no central hole with a zirconium rod.
5. Zirconium mass and H/Zr ratio apply to the fuel material (U-Zr-H_x) and do not include the center zirconium rod.
6. Listed TRIGA fuel elements have a 0.225-inch diameter zirconium rod in the center.
7. Dimensions listed are as-fabricated (unirradiated) nominal values.

Table 1.2-2 Characteristics of Design Basis TRIGA Fuel Elements Acceptable for Loading in the Nonpoisoned TRIGA Basket

	TRIGA HEU (Notes 1, 2, 6)	TRIGA LEU (Notes 1, 2, 6)	TRIGA LEU (Notes 1, 2, 6)
Fuel Form	Clad U-ZrH rod (Note 4)	Clad U-ZrH rod (Note 4)	Clad U-ZrH rod (Note 4)
Maximum Element Weight, lbs	13.2	13.2	13.2
Maximum Element Length, in	47.74	47.74	47.74
Element Cladding	Stainless Steel	Stainless Steel	Aluminum
Minimum Clad Thickness, in	0.01	0.01	0.01
Active Fuel Length, in	(Note 5)	(Note 5)	(Note 5)
Maximum Element Diameter, in	1.5 max.	1.5 max.	1.5 max.
Fuel Diameter, in	(Note 5)	(Note 5)	(Note 5)
Maximum Initial U Content/Element, kilograms	0.196	0.845	0.205
Maximum Initial ^{235}U Mass, grams	137	169	41
Maximum Initial ^{235}U Enrichment, weight percent	70	20	20
Zirconium Mass, grams	(Note 5)	(Note 5)	(Note 5)
Hydrogen to Zirconium Ratio, max.	(Note 5)	(Note 5)	(Note 5)
Maximum Average Burnup, MWd/MTU	460,000 (80% ^{235}U)	151,100 (80% ^{235}U)	151,100 (80% ^{235}U)
Minimum Cooling Time	90 days (Note 3)	90 days (Note 3)	90 days (Note 3)

Notes:

1. Mixed TRIGA LEU and HEU contents authorized.
2. TRIGA Standard, instrumented and fuel follower control rod type elements authorized.
3. Maximum decay heat of any element is 7.5 watts.
4. Element may contain zirconium rod in the center.
5. See criticality analyses in Chapter 6, Section 6.4.5.6, for the evaluations determining critical fuel characteristics.
6. Dimensions listed are as-fabricated (unirradiated) nominal values.

Table 1.2-3 Characteristics of Design Basis TRIGA Fuel Cluster Rods

Element Type	TRIGA Fuel Cluster Rod
Max. Rod Length (in)	31.0
Max. Active Length (in)	22.5
Clad Material	Incoloy 800
Min. Clad Thickness (in)	0.015
Fuel Material	U-ZrH
Max. Pellet Diameter (in)	0.53
Max. Rod Weight (kg)	0.65
Min. U in U-ZrH (wt %)	43.0 (LEU) or 9.5 (HEU)[1]
Max. ^{235}U in U (wt %)	19.9 to 93.3
^{235}U Mass (g)	55.0 (LEU) or 46.5 (HEU)
Max. H to Zr Ratio	1.7

[1] Equivalent to a maximum zirconium mass of 357 g for LEU fuel and 457 g for HEU fuel material. Lower weight percents are permitted, provided the maximum zirconium mass limits are not exceeded.

Table 1.2-4 Fuel Characteristics

Parameter	PWR Fuel Assembly	BWR Fuel Assembly	PWR Rods	High Burnup PWR Rods	PWR MOX Fuel Rods[6]	High Burnup BWR Rods 7 × 7	High Burnup BWR Rods[1] 8 × 8[2]
Maximum Number of Assemblies, Elements or Rods	[1]	[2]	25 rods	25 rods	16 rods	25 rods	25 rods
Maximum Overall Weight, lbs	1650	750	N/A	N/A	N/A	N/A	N/A
Maximum Overall Length, in	178.25	176.1	162	162	162	176.1	176.1
Maximum Active Fuel Length, in	150	150	150	150	153.5	150	150
Fuel Rod Cladding	Zirc	Zirc	Zirc	Zirc	Zirc	Zirc	Zirc
Maximum Uranium, kg U	475	198	58.2	65.6	41.6[7]	198	198
Maximum Initial ^{235}U, wt %	*See below*[3]	4.0	5.0	5.0	7.0 max/2.0 min, fissile Pu[8]	5.0	5.0
Maximum Burnup, MWd/MTU	35,000	30,000	60,000[4]	80,000	62,500	60,000 - 80,000	80,000
Maximum Unit Decay Heat, kW	2.5	1.1	0.564	0.92	0.143	0.84	0.84
Maximum Cask Decay Heat, kW	2.5	2.2	1.41	2.3	2.3	2.1	2.1
Minimum Cool Time, yr	2	2	150 days	150 days	90 days	210 - 270 days[5]	150 days

[1] High burnup rods are loaded in a fuel assembly lattice or rod holder. Up to 14 rods, loaded in a rod holder, may be classified as damaged. The lattice may be irradiated.
[2] Includes rods from all larger BWR assembly arrays (e.g., 9×9, 10×10).
[3] See Table 1.2-5 for maximum PWR fuel enrichment by fuel type.
[4] Up to 2 of the 25 PWR rods may have a maximum burnup of 65,000 MWd//MTU.
[5] Minimum cool time for high burnup BWR 7×7 rods is determined by extent of burnup. See Section 5.3.8 and Table 5.3.8-23.
[6] Up to 16 PWR MOX fuel rods or a combination of up to 16 MOX PWR and UO_2 PWR fuel rods can be loaded.
[7] Maximum fuel mass is 2.6 kg HM/rod.
[8] Maximum 5.0 wt % ^{235}U for UO_2 rods.

Table 1.2-4 Fuel Characteristics (Continued)

Parameter	Metallic Fuel	Metallic Fuel	Metallic Fuel	MTR HEU	MTR MEU	MTR LEU	TRIGA LEU Element	TRIGA HEU Element	TRIGA Cluster Rod
Maximum Number of Assemblies, Elements or Rods	15 rods (sound)	9 rods (failed)	3 rods (severely failed in filters)	42[1]	42	42[2]	140	140	560
Maximum Overall Weight, lbs	1805	1805	1805	30 (max)[3]	30 (max)[3]	30 (max)[3]	13.2 (max)[3]	8.82 (nom.) 13.2 (max)[3]	1.5[3]
Maximum Overall Length, in	120.5	120.5	120.5	25.4[4]	26.1[4]	26.1[4]	47.74[5]	47.74[5]	31.0
Maximum Active Fuel Length, in	120.0	120.0	120.0	24.8	25.6	25.6	15	15	22.5
Fuel Rod Cladding	Al	Al	Al	Al	Al	Al	Al or SS	Al or SS	Incoloy 800
Maximum Uranium, kg U	54.5	54.5	54.5	0.422 0.511	0.950	2.474 3.368[2]	0.824	0.196	0.0505 (HEU) 0.2894 (LEU)
Maximum Initial ^{235}U, wt %	Natural	Natural	Natural	94	94[6]	25	20	70	95 (HEU)/20 (LEU)
Maximum Burnup, MWd/MTU	1,600	1,600	1,600	Variable up to 660,000[7]	Variable up to 293,300	Variable up to 139,300	151,100 (80% ^{235}U)	460,000 (80% ^{235}U)	600,000 (HEU)/ 140,000 (LEU) (80% ^{235}U)
Maximum Unit Decay Heat, kW	0.036	0.036	0.036	Variable[8]	0.030[8]	0.030[8]	0.0075	0.0075	0.001875
Maximum Cask Decay Heat, kW	0.54	0.54	0.54	1.26	1.26	1.26	1.05	1.05	1.05
Minimum Cool Time, yr	1	1	1	Variable[8]	Variable[8]	Variable[8]	Variable[9]	Variable[9]	Variable[9]

[1] For NISTR fuel, 42 assemblies may be cut in half, producing 84 fuel-bearing pieces. Each fuel-bearing piece may contain up to 0.211 kgU.

[2] MTR fuel elements having ^{235}U content >470 g (>22 g per plate) are limited to a total of 4 elements in a 7-element basket. Basket openings 1, 2 and 3 shall be blocked by cell block spacers to ensure that MTR elements are not loaded in these openings. Therefore, depending on the number of such 4-element baskets, the maximum number of elements per cask will be reduced accordingly.

[3] Maximum weight of fuel element(s), spacer(s) and fuel can, as applicable, per basket module cell shall be 80 pounds.

[4] For MTR fuel elements, which are cut to remove nonfuel-bearing hardware prior to transport, a nominal 0.28 inch of nonfuel or spacer hardware will remain above and below the active fuel region to allow for fuel handling operations. The HFBR element, with an element length of 57.24 inches, must be cut prior to shipment. For HEU MTR elements having >380 g ^{235}U but less than 460 g ^{235}U, a minimum of 2.0 cm (0.8 inch) of nonfuel hardware and/or spacers/plates shall be provided at the ends of the element.

[5] Permissible fuel element length is limited to basket cavity length, which is a minimum 47.74 inches for the basket top module, 30.94 inches for the intermediate modules, and 32.64 inches for thebottom module.

[6] Typical MEU enrichment is 45 wt% ^{235}U. Criticality analysis supports up to 94 wt% under the MEU fuel definition.

[7] Maximum burnup is 660,000 MWd/MTU for 380g ^{235}U and 577,500 MWd/MTU for 460g ^{235}U.

[8] Minimum cool times for MTR fuel, down to 30 days, shall be determined using the procedure presented in Section 7.1.5.

[9] Minimum cool times for TRIGA fuel elements and fuel cluster rods, down to 90 days, are determined so that the maximum decay heat of any element to be shipped is $\leq$ 7.5 watts and any fuel cluster rod is $\leq$ 1.875 watts.

Table 1.2-4 Fuel Characteristics (Continued)

Parameter	DIDO HEU	DIDO MEU	DIDO LEU
Number of Fuel Cylinders per Assembly	4	4	4
Maximum Overall Weight (lb)[1]	15	15	15
Minimum Plate Thickness, in	0.051	0.051	0.051
Minimum Clad Thickness (Al), in	0.00984	0.00984	0.00984
Maximum ^{235}U per Element, g	190	190	190
Maximum Initial ^{235}U, wt %	94	94	94
Minimum Initial ^{235}U, wt %	90	40	19
Maximum Uranium, kg U	0.2111	0.4750	1.0000
Minimum Active Fuel Height, in	23.13	23.13	23.13
Minimum Element Height[2], in	24.21	24.21	24.21
Maximum Burnup, MWd/MTU	577,460	256,650	121,910
Maximum Unit Decay Heat[3], kW	0.025	0.025	0.025
Maximum Cask Decay Heat, kW	1.05	1.05	1.05
Minimum Cool Time[4], yr	Variable	Variable	Variable

1 Maximum weight of fuel element(s), spacer(s) and fuel can, as applicable, per basket module cell shall be 80 pounds.

2 Element height provides for spacing of fissile material. An optional spacer may be used to maintain spacing if the element is cut shorter than 24.21 inches.

3 Maximum unit decay heat of 0.025 kW allowed only in conjunction with spacers for top basket (see Section 7.1.4), otherwise the limit is 0.018 kW.

4 Minimum cool times for DIDO fuel assemblies, down to 180 days, shall be determined using the procedure presented in Section 7.1.4.

Table 1.2-5 PWR Fuel Characteristics

Fuel Type	No. of Fuel Rods	Max. Assembly Length (in.)	Max. Assembly Weight (lb)	Max. Enrich. (wt %)	Max. MTU	Pitch (in.)	Rod Dia. (in.)	Clad Thick. (in.)	Pellet Dia.(in.)	Max. Active Length (in.)
B&W 15 × 15	208	165.63	1515	3.5	0.4750	0.5680	0.430	0.0265	0.3686	144.0
B&W 17 × 17	264	165.72	1505	3.5	0.4658	0.5020	0.379	0.0240	0.3232	143.0
CE 14 × 14	176	157.00	1270	3.7	0.4037	0.5800	0.440	0.0280	0.3765	137.0
CE 16 × 16	236	178.25	1430	3.7	0.4417	0.5060	0.382	0.0250	0.3250	150.0
WE 14 × 14 Std	179	159.71	1302	3.7	0.4144	0.5560	0.422	0.0225	0.3674	145.2
WE 14 × 14 OFA	179	159.71	1177	3.7	0.3612	0.5560	0.400	0.0243	0.3444	144.0
WE 15 × 15	204	159.71	1472	3.5	0.4646	0.5630	0.422	0.0242	0.3659	144.0
WE 17 × 17 Std	264	159.77	1482	3.5	0.4671	0.4960	0.374	0.0225	0.3225	144.0
WE 17 × 17 OFA	264	160.10	1373	3.5	0.4282	0.4960	0.360	0.0225	0.3088	144.0
Ex/ANF 14 × 14 WE	179	160.13	1271	3.7	0.3741	0.5560	0.424	0.0300	0.3505	144.0
Ex/ANF 14 × 14 CE	176	157.24	1292	3.7	0.3814	0.5800	0.440	0.0310	0.3700	134.0
Ex/ANF 15 × 15 WE	204	159.70	1433	3.7	0.4410	0.5630	0.424	0.0300	0.3565	144.0
Ex/ANF 17 × 17 WE	264	159.71	1348	3.5	0.4123	0.4960	0.360	0.0250	0.3030	144.0

Table 1.2-6 BWR Fuel Characteristics

Fuel Type	No. of Fuel Rods	No. of Water Rods	Max. Assembly Length (in.)	Max. Assembly Weight (lb)	Max. MTU	Pitch (in.)	Rod Dia. (in.)	Clad Thick. (in.)	Pellet Dia. (in.)	Max. Active Length (in.)
GE 7 x 7	49	0	175.9	678.9	0.1923	0.738	0.563	0.037	0.477	146
GE 8 x 8-1	63	1	175.9	681.0	0.1880	0.640	0.493	0.034	0.416	146
GE 8 x 8-2	62	2	175.9	681.0	0.1847	0.640	0.483	0.032	0.410	150[1]
GE 8 x 8-4	60	4	176.1	665.0	0.1787	0.640	0.484	0.032	0.410	150[1,2]
GE 9 x 9	74	2[3]	176.1	646.0	0.1854	0.566	0.441	0.028	0.376	150[1,4]
	79	2	176.1	646.0	0.1979	0.566	0.441	0.028	0.376	150[1,4]
Ex/ANF 7 x 7	49	0	171.3	619.1	0.1960	0.738	0.570	0.036	0.490	144
Ex/ANF 8 x 8-1	63	1	171.3	562.3	0.1764	0.641	0.484	0.036	0.4045	145.2
Ex/ANF 8 x 8-2	62	2	176.1	587.8	0.1793	0.641	0.484	0.036	0.4045	150
Ex/ANF 9 x 9	79	2	176.1	575.3	0.1779	0.572	0.424	0.03	0.3565	150
	74	2[3]	176.1	575.3	0.1666	0.572	0.424	0.03	0.3565	150

[1] 6" natural uranium blankets on top and bottom.
[2] May have 1 large water hole - 3.2 cm ID, 0.1 cm thickness.
[3] 2 large water holes occupying 7 fuel rod locations - 2.5 cm ID, 0.07 cm thickness.
[4] Shortened active fuel length in some rods.

Table 1.2-7 Characteristics of General Atomics Irradiated Fuel Material (GA IFM)

Parameter	RERTR	HTGR
Maximum Number of Assemblies, Elements or Rods	13 intact; 7 sectioned	N/A
Maximum Loaded Enclosure Weight, lbs	76.0	71.5
Maximum Fuel Weight, lbs	23.73	23.52
Maximum Overall Length, in	29.92	N/A
Maximum Active Fuel Length, in	22.05	N/A
Fuel Material	U-ZrH	UC_2, UCO, UO_2, $(Th,U)C_2$, $(Th,U)O_2$
Fuel Rod Cladding	Incoloy 800	N/A
Maximum Uranium, kg U	3.86	0.21
Maximum Initial ^{235}U, wt %	19.7	93.15
Maximum Burnup, MWd/MTU	N/A	N/A
Maximum Unit Decay Heat, W	11.0	2.05
Maximum Cask Decay Heat, W	13.05	13.05
Earliest Shipment Date	1/1/96	1/1/96
Maximum Activity, Ci	2920	483

Table 1.2-8 Typical Production TPBAR Characteristics[1]

Parameter Description	Value
Maximum Number of TPBARs per Consolidation Canister	300
Number of Consolidation Canisters per Cask	1
TPBAR Clad Material	316 L Stainless Steel
Rod Length[2], in	153.04
Rod Diameter[2], in	0.381
Maximum Rod Heat Load, W	2.31
Maximum Cask Heat Load, kW	0.693
Maximum Tritium Content per Rod, gram	1.2
Maximum Activity per Cask[3], Ci	3.84×10^6
Loaded TPBAR Consolidation Canister Maximum Weight, pounds[4]	1,000
Maximum Event Failed Tritium Release (Ci/rod)	<55
Minimum Cooling Time, days	30

1 Refer to Section 1.5, Chapter 1 Appendices, Unclassified DOE Reference Documents and Drawings.
2 Beginning of life, nominal, unirradiated dimensions.
3 Primary dose contribution: 1.1×10^4 Ci ^{60}Co/cask
4 The bounding weight employed in the structural analysis.

Table 1.2-9 PULSTAR Fuel Characteristics

Description	Value
Maximum Pellet Diameter (inch)	0.423
Minimum Element (Rod) Cladding Thickness (inch)	0.0185
Minimum Element (Rod) Diameter (inch)	0.470
Maximum Active Fuel Height (inch)	24.1
Element (Rod) Length (inch)	26.2
Rod Pitch (inch)	0.525 × 0.607
Assembly Length (inch)	38
Box Outside Width (inch)	2.745 × 3.155
Box Thickness (inch)	0.06
Maximum Assembly or Loaded Can Weight (lb) [1]	80
Maximum PULSTAR Can Content Weight (lb)[2]	39.6
Maximum Enrichment (wt % ^{235}U)	6.5
Maximum ^{235}U Content per Element (g)	33
No. of Elements (Rods) per Assembly	25
No. of Elements (Rods) per Can[2]	25
Maximum Depletion (%^{235}U)	45
Minimum Cool Time (yrs)	1.5
Maximum Heat Load per Assembly (W)	30
Maximum Heat Load per Element (W)	1.2

[1] Listed weight is the maximum weight evaluated for the structural calculation to bound all payload configurations, including loaded cans, and spacers. Nominal PULSTAR assembly weight is 45 pounds.

[2] The contents of a PULSTAR can are restricted to the equivalent of the fuel material in 25 PULSTAR fuel elements and of the displaced volume of 25 intact PULSTAR fuel elements. Fuel material may be in damaged form including fuel debris. The listed weight represents the can content limit established by the structural analyses.

Table 1.2-10 Spiral Fuel Assembly Characteristics

Parameter	Value
Number of elements per assembly	10
Fuel element type	Curved plate
Nominal dimensions of element (cm)	0.147 × 7.33 × 63.5 (individual plate)
Chemical form of fuel meat	U-Al_x-alloy
Cladding material	Aluminum
Nominal over-all dimensions (cm)	63.818 (height) × 10.16 diameter[1]
Max total weight of ^{235}U (g)	160 (total per assembly)
Maximum enrichment (wt % ^{235}U)	85
Side plate material	Aluminum (inner and outer tubes)
Nominal side plate – dimensions (cm)	Inner 6.045 OD, 5.82 ID × 63.818 Outer 10.16 OD, 9.85 ID × 63.818[2]
Max. assembly weight (lb)	18[3]
Assembly maximum heat load (W)	15.7[4]
Burnup/cool time limit	Variable[5]

1 Cropped to fit within ANSTO fuel basket module nominal height of 28.3 inches.
2 Criticality evaluations reduced inner and outer shell thickness to 0.01 cm to provide additional moderator within the assembly.
3 Typical assembly weight is 7.9 pounds. Bounding structural analysis weight is listed.
4 Thermal and shielding evaluation employed 18 W per element. Based on cool time constraint, 15.7 W represents maximum heat load.
5 Spiral fuel is contrained to DIDO MEU cool time limits as a function of burnup. Minimum cool times for the spiral assembly, down to 270 days, shall be determined using the procedure presented in Section 7.1.4 for 18 W DIDO MEU fuel.

Table 1.2-11 MOATA Plate Bundle Characteristics

Parameter	Value
Maximum number of elements per assembly	14
Nominal dimensions of element (cm)	66 cm long, 7.6 cm wide and 0.203 cm thick
Nominal dimensions of fuel meat (cm)	58.4 cm long, 6.99 cm wide and 0.1016 cm thick (bounding active fuel width evaluated to a maximum of 7.32 cm)
Chemical form of fuel meat	U-Al_x-alloy
Cladding material	Aluminum
Nominal clad thickness (cm)	0.05 cm (evaluated to 0.01 cm minimum)
Plate spacer thickness (cm)	0.147 min, 0.152 max (evaluated to 0.18 maximum)
Maximum weight of ^{235}U (g) per plate	22.3
Maximum enrichment (wt % ^{235}U)	92
Nominal side plate thickness (cm)	0.635 (bounding evaluation replaced by cavity moderator)
Max. assembly weight (lb)	18[1]
Maximum heat load per assembly (W)[2]	3 (total for 14 fuel plates)
Maximum burnup	30,000 MWd/MTU or 4.1 % depletion ^{235}U
Minimum cool time (years)	10

[1] Typical assembly weight is 13.6 pounds. Bounding structural analysis weight is listed.
[2] Actual heat load at limiting burnup and cool time < 1 Watt. Thermal evaluations at 3 Watt per bundle.

Table 1.2-12 Typical TPBAR Segment Characteristics in Waste Container

Parameter/Description	Value
Maximum Number of TPBAR Segments and Debris per Waste Container, equivalent number of TPBARs	55
Number of Waste Containers per Cask	1
Waste Container Material	316L Stainless Steel
Maximum Tritium Content per TPBAR equivalent, gram	1.2
Maximum Activity per Cask, Ci	6.66 ×10+5
Maximum Heat Load per Waste Container, watts	127
Maximum Loaded Waste Container Weight, pounds	700[1]
Minimum Cooling Time, years	90

[1] Design basis weight of a loaded waste container is 700 pounds. Applying a maximum payload of 55 TPBARs, with storage canister, yields a maximum weight of 662 pounds. Use of shrouds to contain segments and/or TPBAR debris reduces overall waste container weight due to a reduction in TPBAR payload capacity resulting from the reduced container free volume.

Table 1.2-13 Solid, Irradiated Hardware Characteristics[1]

Parameter	Value
Maximum Content Weight	4,000 pounds [2]
Maximum Content Length	171.5 inches [3]
Hardware Material	Solid, irradiated and contaminated fuel assembly structural or reactor internal component hardware [4]
Maximum Cask Heat Load	1.0 KW
Maximum Activity per Cask, Ci	6.0 x 10E+6
Maximum Source Term, gamma/sec	6.0 x 10E+15
Maximum Source Term, MeV/sec	1.0 x 10E+15

1 Maximum content weight includes any spacers, containers or dunnage loaded in the cavity with the irradiated hardware.

2 Length of cavity is limited to 171.5 inches by the installation and use of an irradiated hardware spacer bolted to the underside of the closure lid.

3 Appropriate secondary containers will be used to prevent any contact and cross-contamination between the carbon steel contents and the stainless steel internals of the cask cavity.

4 The irradiated hardware contents may contain fissile material, provided the quantity of fissile material does not exceed a Type A quantity and does not exceed the mass limits of 10 CFR 71.53.

Figure Withheld Under 10 CFR 2.390

NAC INTERNATIONAL

LWT CASK
PWR BASKET
SAFETY ANALYSIS
REPORT

PROJECT 315-40	DRAWING 10	REV 8
SCALE 1/4	WEIGHT NOTED	SH 1 OF 2

Figure Withheld Under 10 CFR 2.390

NAC INTERNATIONAL

LWT CASK
PWR BASKET
SAFETY ANALYSIS
REPORT

PROJECT 315-40	DRAWING 10	REV 8
SCALE 1/4	EST.WT. NOTED	SH 2 OF 2	3:24PM 1-26-2009

Figure Withheld Under 10 CFR 2.390

NAC INTERNATIONAL

PWR/BWR ROD
TRANSPORT CANISTER
ASSEMBLY

PROJECT 315-40		DRAWING 098	REV 6
SCALE	WEIGHT	SH 1 OF 3	3:01PM 2-11-2009

8 7 6 5 4 3 2 1

F E D C B A

Figure Withheld Under 10 CFR 2.390

NAC INTERNATIONAL

PWR/BWR ROD
TRANSPORT CANISTER
ASSEMBLY

PROJECT	DRAWING	REV
315-40	098	6
	SH 2 OF 3	1:56PM 7-11-2000

8 7 6 5 4 3 2 1

F E D C B A

Figure Withheld Under 10 CFR 2.390

NAC INTERNATIONAL

PWR/BWR ROD
TRANSPORT CANISTER
ASSEMBLY

PROJECT		DRAWING		REV
315-40		098		6
1/2	NOTED	SH 3 OF 3	1:56PM 2-11-2009	

Figure Withheld Under 10 CFR 2.390

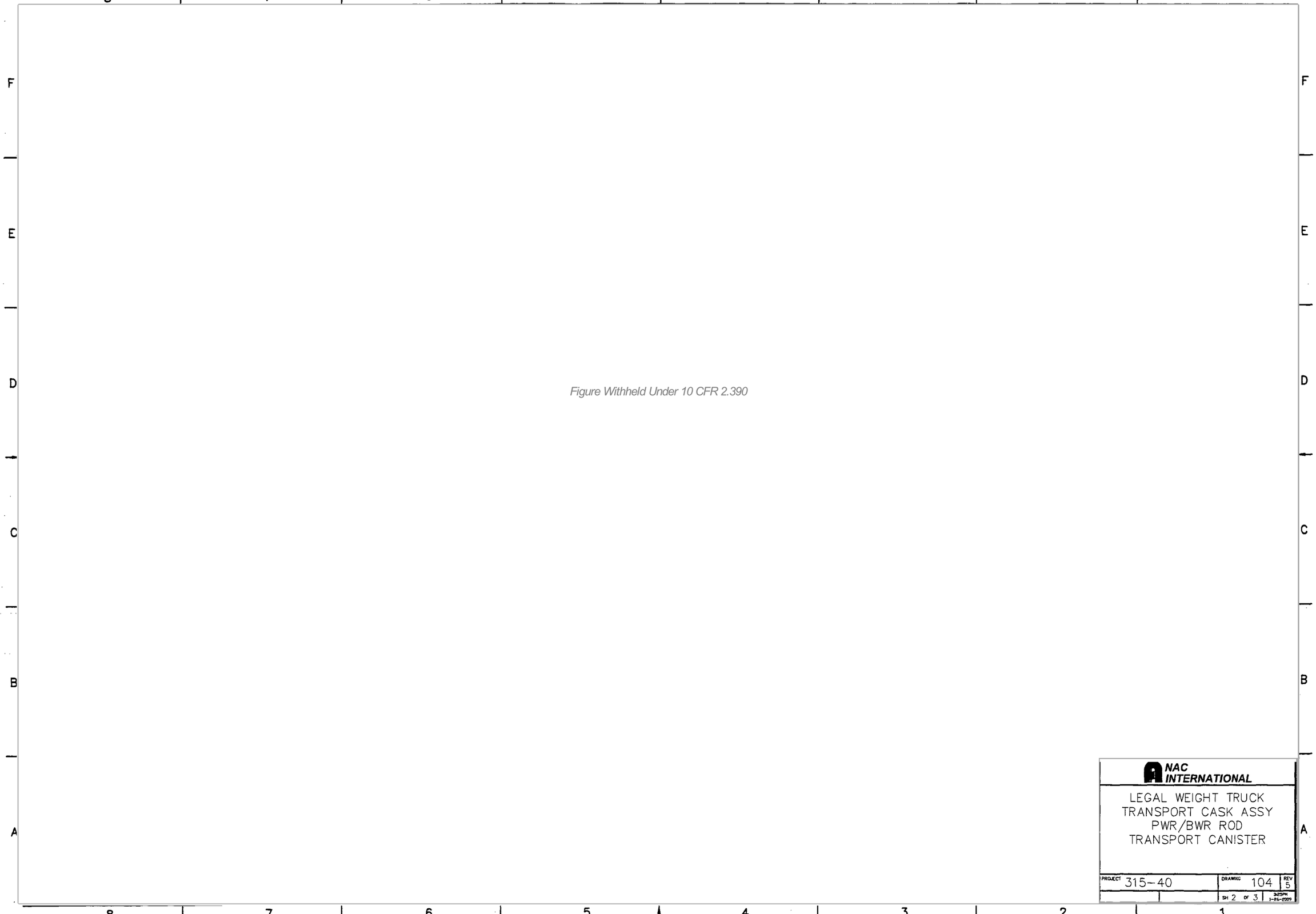
NAC INTERNATIONAL

5 X 5 INSERT
PWR/BWR TRANSPORT
CANISTER

PROJECT	DRAWING	REV
315-40	102	2
SCALE 1/1 | EST.WT. NOTED	SH 1 OF 1	12:28PM 2-25-2009

M:\ACADFILE\315\License\315410231.dwg, 2/25/2009 12:28:39 PM

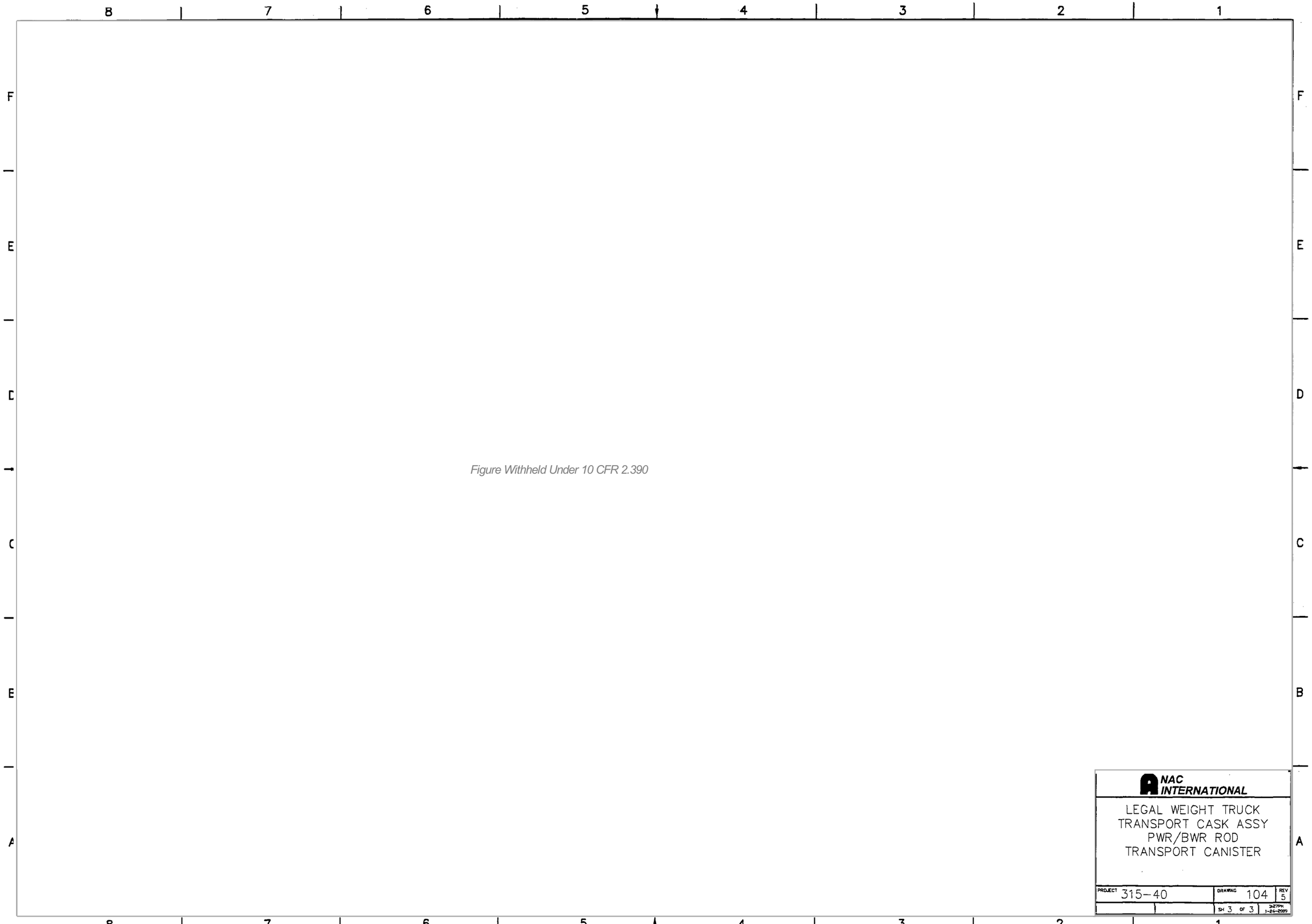

8
7
6
5
4
3
2
1
F
E
D
C
B
A
Figure Withheld Under 10 CFR 2.390
NAC INTERNATIONAL
LEGAL WEIGHT TRUCK
TRANSPORT CASK ASSY,
PWR/BWR ROD
TRANSPORT CANISTER
PROJECT 315-40
DRAWING 104
REV 5
SCALE
WEIGHT
SH 1 OF 3
3:25PM
1-26-2009



NAC INTERNATIONAL

LEGAL WEIGHT TRUCK
TRANSPORT CASK ASSY
PWR/BWR ROD
TRANSPORT CANISTER

PROJECT	DRAWING	REV
315-40	104	5
	SH 2 OF 3	3:25PM 1-26-2009



NAC INTERNATIONAL

LEGAL WEIGHT TRUCK
TRANSPORT CASK ASSY
PWR/BWR ROD
TRANSPORT CANISTER

PROJECT 315-40 | DRAWING 104 | REV 5

SH 3 OF 3 | 3:27PM 1-26-2009

Figure Withheld Under 10 CFR 2.390

NAC INTERNATIONAL

LEGAL WEIGHT TRUCK
TRANSPORT CASK ASSY
TPBAR SHIPMENT
SAFETY ANALYSIS REPORT

PROJECT	DRAWING	REV
315-40	128	3
	SH 1 OF 2	9164P 1-28-2009

Figure Withheld Under 10 CFR 2.390

NAC INTERNATIONAL

LEGAL WEIGHT TRUCK
TRANSPORT CASK ASSY
TPBAR SHIPMENT
SAFETY ANALYSIS REPORT

PROJECT	DRAWING	REV
315-40	128	3
1/8	SH 2 OF 2	Bridge 1-29-2009

Chapter 2

Table of Contents

2 STRUCTURAL EVALUATION 2-1
2.1 Structural Design 2.1.1-1
2.1.1 Discussion 2.1.1-1
2.1.2 Basic Design Criteria 2.1.2-1
2.1.2.1 Containment Structures 2.1.2-1
2.1.2.2 Noncontainment Structures 2.1.2-1
2.1.3 Miscellaneous Structural Failure Modes 2.1.3-1
2.1.3.1 Brittle Fracture 2.1.3-1
2.1.3.2 Fatigue – Normal Operating Cycles 2.1.3-1
2.1.3.3 Extreme Total Stress Intensity Range 2.1.3-5
2.1.3.4 Buckling 2.1.3-5
2.2 Weights and Centers of Gravity 2.2.1-1
2.2.1 Major Component Statistics 2.2.1-1
2.3 Properties of Materials 2.3.1
2.3.1 Mechanical Properties of Materials 2.3.1-1
2.3.1.1 Cask Body Materials 2.3.1-1
2.3.1.2 Port Cover Materials 2.3.1-1
2.3.1.3 Fuel Basket Materials 2.3.1-1
2.3.1.4 Bolting Material 2.3.1-2
2.3.1.5 Shielding Material (Gamma Radiation) 2.3.1-2
2.4 General Standards for All Packages 2.4-1
2.4.1 Minimum Package Size 2.4.1-1
2.4.2 Tamperproof Feature 2.4.2-1
2.4.3 Positive Closure 2.4.3-1
2.4.4 Chemical and Galvanic Reactions 2.4.4-1
2.4.5 Cask Design 2.4.5-1
2.4.6 Continuous Venting 2.4.6-1
2.5 Lifting and Tiedown Standards 2.5.1-1
2.5.1 Lifting Devices 2.5.1-1
2.5.1.1 Lifting Trunnion 2.5.1-1
2.5.1.2 Lid Lifting Bolts 2.5.1-7
2.5.1.3 Can Assembly (315-40-98) 2.5.1-8
2.5.2 Tiedown Devices 2.5.2-1
2.5.2.1 Discussion and Loads 2.5.2-1
2.5.2.2 Rear Support 2.5.2-5
2.5.2.3 Front Support 2.5.2-11
2.6 Normal Conditions of Transport 2.6.1-1
2.6.1 Hot Case 2.6.1-1
2.6.1.1 Discussion 2.6.1-1
2.6.1.2 Analysis Description 2.6.1-1
2.6.1.3 Detailed Analysis 2.6.1-2
2.6.1.4 Conclusion 2.6.1-3
2.6.2 Cold Case 2.6.2-1

Table of Contents (continued)

2.6.2.1 Discussion 2.6.2-1
2.6.2.2 Analysis Description 2.6.2-1
2.6.2.3 Detailed Analysis 2.6.2-2
2.6.2.4 Conclusion 2.6.2-3
2.6.3 Reduced External Pressure 2.6.3-1
2.6.4 Increased External Pressure 2.6.4-1
2.6.5 Vibration 2.6.5-1
2.6.6 Water Spray 2.6.6-1
2.6.7 Free Drop (1 Foot) 2.6.7-1
2.6.7.1 End Drop (1 Foot) 2.6.7-1
2.6.7.2 Side Drop (1 Foot) 2.6.7-2
2.6.7.3 Corner Drop (1 Foot) 2.6.7-3
2.6.7.4 Impact Limiters 2.6.7-4
2.6.7.5 Closure Lid 2.6.7-20
2.6.7.6 Bolts – Closure Lid (Normal Conditions of Transport) 2.6.7-22
2.6.7.7 Neutron Shield Tank 2.6.7-24
2.6.7.8 Expansion Tank 2.6.7-39
2.6.7.9 Upper Ring/Outer Shell Intersection Analysis 2.6.7-42
2.6.7.10 PWR/BWR Rod Transport Canister Assembly Analysis 2.6.7-47
2.6.8 Corner Drop 2.6.8-1
2.6.9 Compression 2.6.9-1
2.6.10 Penetration 2.6.10-1
2.6.10.1 Impact Limiter – Penetration 2.6.10-1
2.6.10.2 Expansion Tank – Penetration 2.6.10-1
2.6.10.3 Neutron Shield Tank – Penetration 2.6.10-5
2.6.10.4 Port Cover – Penetration 2.6.10-6
2.6.10.5 Alternate Port Cover – Penetration 2.6.10-8
2.6.11 Fabrication Conditions 2.6.11-1
2.6.11.1 Lead Pour 2.6.11-1
2.6.11.2 Cooldown 2.6.11-3
2.6.11.3 Lead Creep 2.6.11-12
2.6.12 Fuel Basket Analysis 2.6.12-1
2.6.12.1 Discussion 2.6.12-1
2.6.12.2 PWR Basket Construction 2.6.12-1
2.6.12.3 PWR Basket Analysis 2.6.12-2
2.6.12.4 BWR Basket Construction 2.6.12-4
2.6.12.5 Metallic Fuel Basket Construction 2.6.12-5
2.6.12.6 MTR Fuel Basket Construction 2.6.12-7
2.6.12.7 TRIGA Fuel Basket One-Foot Drop Evaluation 2.6.12-25
2.6.12.8 DIDO Fuel Basket Construction 2.6.12-52
2.6.12.9 General Atomics IFM Basket Construction 2.6.12-61
2.6.12.10 TPBAR Basket Analysis 2.6.12-70
2.6.12.11 ANSTO Basket Analysis 2.6.12-84

Table of Contents (continued)

2.6.12.12 TPBAR Basket with the PWR/BWR Rod Transport Canister 2.6.12-91
2.6.12.13 Conclusion 2.6.12-93
2.7 Hypothetical Accident Conditions 2.7-1
2.7.1 Free Drop (30 Feet) 2.7.1-1
2.7.1.1 End Drop 2.7.1-2
2.7.1.2 Side Drop 2.7.1-5
2.7.1.3 Oblique Drops 2.7.1-10
2.7.1.4 Shielding for Lead Slump Accident 2.7.1-18
2.7.1.5 Bolts - Closure Lid (Hypothetical Accident - Free Drop) 2.7.1-19
2.7.1.6 Crush 2.7.1-20
2.7.1.7 Rod Shipment Can Assembly Analysis 2.7.1-21
2.7.2 Puncture 2.7.2-1
2.7.2.1 Puncture - Cask Side Midpoint 2.7.2-1
2.7.2.2 Puncture - Center of Cask Closure Lid 2.7.2-3
2.7.2.3 Puncture - Center of Cask Bottom 2.7.2-6
2.7.2.4 Puncture - Port Cover 2.7.2-9
2.7.2.5 Puncture Accident - Shielding Consequences 2.7.2-17
2.7.2.6 Puncture - Conclusion 2.7.2-17
2.7.3 Fire 2.7.3-1
2.7.3.1 Discussion 2.7.3-1
2.7.3.2 Thermal Stress Evaluation 2.7.3-1
2.7.3.3 Bolts - Closure Lid (Hypothetical Accident - Fire) 2.7.3-3
2.7.3.4 Inner Shell Evaluation 2.7.3-4
2.7.3.5 Conclusion 2.7.3-5
2.7.4 Immersion - Fissile Material 2.7.4-1
2.7.5 Immersion – Irradiated Nuclear Fuel Packages 2.7.5-1
2.7.5.1 Method of Analysis 2.7.5-1
2.7.5.2 Closure Lid Stresses 2.7.5-1
2.7.5.3 Outer Bottom Head Forging Stresses 2.7.5-2
2.7.5.4 Cask Cylindrical Shell Stresses 2.7.5-3
2.7.5.5 Containment Seal Evaluation 2.7.5-5
2.7.6 Damage Summary 2.7.6-1
2.7.7 Fuel Basket Accident Analysis 2.7.7-1
2.7.7.1 Discussion 2.7.7-1
2.7.7.2 PWR Basket Construction 2.7.7-1
2.7.7.3 PWR Basket Analysis 2.7.7-1
2.7.7.4 BWR Basket Construction 2.7.7-3
2.7.7.5 Metallic Fuel Basket Analysis 2.7.7-6
2.7.7.6 MTR Fuel Basket Construction 2.7.7-8
2.7.7.7 Conclusion 2.7.7-18
2.7.7.8 PWR Spacer 2.7.7-18
2.7.7.9 TRIGA Fuel Basket Thirty-Foot Drop Evaluation 2.7.7-23

Table of Contents (continued)

2.7.7.10 DIDO Fuel Basket Construction 2.7.7-46
2.7.7.11 General Atomics IFM Basket Construction 2.7.7-51
2.7.7.12 TPBAR Basket Analysis 2.7.7-54
2.7.7.13 ANSTO Basket Analysis 2.7.7-66
2.7.7.14 TPBAR Basket with the PWR/BWR Rod Transport Canister 2.7.7-70
2.8 Special Form 2.8-1
2.9 Spent Fuel Contents 2.9-1
2.9.1 PWR and BWR Fuel Rods 2.9-1
2.9.2 TRIGA Fuel Elements 2.9-1
2.9.2.1 End Drop 2.9-2
2.9.2.2 Side Drop 2.9-3
2.9.3 PULSTAR Intact Fuel Elements 2.9-5
2.9.4 ANSTO Fuels 2.9-6
2.9.4.1 MARK III Spiral Fuel Assemblies 2.9-6
2.9.4.2 MOATA Plate Bundles 2.9-10
2.10 Appendices 2.10.1-1
2.10.1 Computer Program Descriptions 2.10.1-1
2.10.1.1 ANSYS 2.10.1-1
2.10.1.2 RBCUBED - A Program to Calculate Impact Limiter Dynamics 2.10.1-2
2.10.2 Finite Element Model Description 2.10.2-1
2.10.2.1 Boundary and Loading Conditions Used in the 30-Foot Drop Finite Element Analysis 2.10.2-2
2.10.3 Finite Element Evaluations 2.10.3-1
2.10.3.1 Isothermal Plot - Hot Case 2.10.3-1
2.10.3.2 Isothermal Plot - Cold Case 2.10.3-1
2.10.3.3 Determination of Component Critical Stresses 2.10.3-1
2.10.4 Oblique Drop Slapdown 2.10.4-1
2.10.4.1 Discussion 2.10.4-1
2.10.4.2 Analysis 2.10.4-1
2.10.4.3 Energy Calculation 2.10.4-3
2.10.4.4 Rotational Velocity Change 2.10.4-4
2.10.5 Lead Slump - End Drop 2.10.5-1
2.10.6 Inner Shell Buckling Design Criteria and Evaluation 2.10.6-1
2.10.6.1 Code Case N-284 ..... 2.10.6-1
2.10.6.2 Theoretical Elastic Buckling Stresses 2.10.6-1
2.10.6.3 Capacity Reduction Factors 2.10.6-2
2.10.6.4 Plasticity Reduction Factors 2.10.6-3
2.10.6.5 Upper Bound Magnitudes for Compressive Stresses and In-Plane Shear Stresses 2.10.6-3
2.10.6.6 Interaction Equations 2.10.6-4
2.10.6.7 Detailed Buckling Evaluation - Sample Calculation 2.10.6-4

Table of Contents (continued)

2.10.6.8 Conclusion 2.10.6-7
2.10.7 Detailed Finite Element Stress Summary 2.10.7-1
2.10.7.1 Finite Element Stress Tables – Normal Operation Hot Condition 2.10.7-1
2.10.7.2 Finite Element Stress Tables - Normal Operation Cold Condition 2.10.7-1
2.10.7.3 Finite Element Stress Tables – 1-Foot End Drop 2.10.7-1
2.10.7.4 Finite Element Stress Tables – 1-Foot Side Drop 2.10.7-1
2.10.7.5 Finite Element Stress Tables – 1-Foot Corner Drop 2.10.7-1
2.10.7.6 Finite Element Stress Tables – 30-Foot End Drop 2.10.7-1
2.10.7.7 Finite Element Stress Tables – 30-Foot Side Drop 2.10.7-1
2.10.7.8 Finite Element Stress Tables – 30-Foot Oblique Drop 2.10.7-2
2.10.8 Quarter-Scale Model Drop Test Program for the NAC-LWT Cask 2.10.8-1
2.10.8.1 Introduction 2.10.8-1
2.10.8.2 Purpose 2.10.8-1
2.10.8.3 Summary 2.10.8-1
2.10.8.4 Description of Quarter-Scale LWT Cask Model 2.10.8-4
2.10.8.5 Description of Test Procedures and Instrumentation 2.10.8-5
2.10.8.6 Detailed Test Results 2.10.8-7
2.10.8.7 Metrology Results 2.10.8-14
2.10.8.8 Discussion of Test Results 2.10.8-15
2.10.8.9 Post-Test Revisions 2.10.8-17
2.10.9 Bolts – Closure Lid (Stress Evaluations) 2.10.9-1
2.10.9.1 Analysis Approach 2.10.9-1
2.10.9.2 Closure Bolt Analyses – Analytics and Assumptions 2.10.9-2
2.10.10 Finite Element Stress Results for the 30-Foot Drop Accident Conditions 2.10.10-1
2.10.10.1 Discussion 2.10.10-1
2.10.10.2 Procedures 2.10.10-1
2.10.10.3 Analysis and Results 2.10.10-3
2.10.10.4 Conclusion 2.10.10-6
2.10.11 Hand Calculation for the 30-Foot Drop Accident Conditions 2.10.11-1
2.10.11.1 Top End Drop 2.10.11-1
2.10.11.2 Side Drop 2.10.11-2
2.10.12 Impact Limiter Force-Deflection Curves and Data 2.10.12-1
2.10.12.1 Potential Energy and Cask Drop Motion 2.10.12-1
2.10.12.2 Potential to Kinetic Energy Conversion 2.10.12-3
2.10.12.3 Deceleration Forces and Energy Absorption Calculation 2.10.12-4
2.10.12.4 RBCUBED Calculated Force-Deflection Graphs 2.10.12-7
2.10.12.5 Quarter-Scale Model Quasi-Static Force-Deflection Tests 2.10.12-7
2.10.13 Structural Evaluation of Failed Fuel Cans and Liners 2.10.13-1

Table of Contents (continued)

2.10.13.1 Discussion 2.10.13-1
2.10.13.2 Method of Analysis 2.10.13-1
2.10.13.3 Input Geometry & Data 2.10.13-2
2.10.13.4 Mechanical Properties of Material 2.10.13-3
2.10.13.5 Thermal Evaluation 2.10.13-3
2.10.13.6 Structural Evaluation 2.10.13-3
2.10.13.7 Results and Conclusion 2.10.13-11
2.10.13.8 Failed Fuel Shipment Component Drawings 2.10.13-12
2.10.14 Structural Evaluation of the NAC-LWT Cask Body with TPBAR Contents 2.10.14-1
2.10.14.1 Normal Conditions of Transport for Cask Body with TPBAR Contents 2.10.14-1
2.10.14.2 Hypothetical Accident Conditions for Cask Body with TPBAR Contents 2.10.14-3
2.10.14.3 Inner Shell Buckling 2.10.14-4
2.10.14.4 NAC-LWT Cask Closure Lid and Bolts 2.10.14-5
2.10.14.5 Conclusion 2.10.14-6
2.10.15 NAC-LWT Alternate B Port Cover 2.10.15-1
2.10.15.1 Alternate B Port Cover Bolt Analysis 2.10.15-1
2.10.16 Structural Evaluation of the NAC-LWT Cask Body with TPBARs in the PWR/BWR Rod Transport Canister 2.10.16-1
2.10.16.1 Normal Conditions of Transport for Cask Body and TPBARs in the PWR/BWR Rod Transport Canister 2.10.16-1
2.10.16.2 Hypothetical Accident Conditions for Cask Body with TPBARs and the PWR/BWR Rod Transport Canister 2.10.16-2
2.10.16.3 Inner Shell Buckling 2.10.16-3
2.10.16.4 NAC-LWT Cask Closure Lid and Bolts 2.10.16-4
2.10.16.5 Conclusion 2.10.16-5

List of Figures

Figure 2.1.3-1	Design Fatigue Curve for High Strength Steel Bolting	2.1.3-7
Figure 2.3.1-1	Static Stress-Strain Curve for Chemical Copper Lead	2.3.1-3
Figure 2.3.1-2	Dynamic Deformation Stress-Strain Curve for Chemical Copper Lead	2.3.1-4
Figure 2.5.1-1	Trunnion Cross-Section and Forging Shear Area	2.5.1-10
Figure 2.5.2-1	Front Support and Tiedown Geometry	2.5.2-13
Figure 2.5.2-2	Pressure Distribution of Horizontal Bearing Between Cask and Support Saddle	2.5.2-14
Figure 2.5.2-3	Free Body Diagram of Cask Subjected to Lateral Load	2.5.2-15
Figure 2.5.2-4	Rotation Trunnion Pocket	2.5.2-16
Figure 2.6.1-1	NAC-LWT Cask Critical Sections (Hot Case)	2.6.1-4
Figure 2.6.2-1	NAC-LWT Cask Critical Sections (Cold Case)	2.6.2-4
Figure 2.6.7-1	1-Foot Bottom End Drop with 130°F Ambient Temperature and Maximum Decay Heat Load	2.6.7-60
Figure 2.6.7-2	1-Foot Bottom End Drop with -40°F Ambient Temperature and Maximum Decay Heat Load	2.6.7-61
Figure 2.6.7-3	1-Foot Bottom End Drop with -40°F Ambient Temperature and No Decay Heat Load	2.6.7-62
Figure 2.6.7-4	1-Foot Top End Drop with 130°F Ambient Temperature and Maximum Decay Heat Load	2.6.7-63
Figure 2.6.7-5	1-Foot Top End Drop with -40°F Ambient Temperature and Maximum Decay Heat Load	2.6.7-64
Figure 2.6.7-6	NAC-LWT Cask Critical Sections (1-Foot Side Drop with 100°F Ambient Temperature)	2.6.7-65
Figure 2.6.7-7	1-Foot Top Corner Drop with 130°F Ambient Temperature and Maximum Decay Heat Load - Drop Orientation = 15.74 Degrees	2.6.7-66
Figure 2.6.7-8	1-Foot Bottom Corner Drop with 130°F Ambient Temperature and Maximum Decay Heat Load - Drop Orientation = 15.74 Degrees	2.6.7-67
Figure 2.6.7-9	1-Foot Top Corner Drop with -40°F Ambient Temperature and No Decay Heat Load - Drop Orientation = 15.74 Degrees	2.6.7-68
Figure 2.6.7-10	NAC-LWT Cask with Impact Limiters	2.6.7-69
Figure 2.6.7-11	Cross-Section of Top Impact Limiter	2.6.7-70
Figure 2.6.7-12	Load Versus Deflection Curve (Typical Aluminum Honeycomb)	2.6.7-71
Figure 2.6.7-13	Quarter-Scale Model Limiter End Drop Cross-Section	2.6.7-72
Figure 2.6.7-14	End Drop Impact Limiter Cross-Section	2.6.7-73
Figure 2.6.7-15	Impact Limiter Lug Detail	2.6.7-74
Figure 2.6.7-16	Cask Lug Detail	2.6.7-75
Figure 2.6.7-17	RBCUBED Output Summary – Center of Gravity Over Top Corner	2.6.7-76
Figure 2.6.7-18	Free Body Diagram - Top Impact Limiter - Center of Gravity Over Corner	2.6.7-77
Figure 2.6.7-19	Free Body Diagram - Top Impact Limiter - Cask Wedging Forces	2.6.7-78
Figure 2.6.7-20	Cask Lid Configuration	2.6.7-79
Figure 2.6.7-21	Closure Lid Free Body Diagram	2.6.7-80

List of Figures (continued)

Figure 2.6.7-22	NAC-LWT Cask Cross-Section	2.6.7-81
Figure 2.6.7-23	Component Parts of Shield Tank Structure	2.6.7-82
Figure 2.6.7-24	Shield Tank Cross-Section	2.6.7-83
Figure 2.6.7-25	Shield Tank Quarter-Section Geometry	2.6.7-84
Figure 2.6.7-26	Partial Bottom/Top End Plate Plan and Cross-Section	2.6.7-85
Figure 2.6.7-27	Shield Tank End Plate	2.6.7-86
Figure 2.6.7-28	Gusset Profile	2.6.7-87
Figure 2.6.7-29	End Plate Welds	2.6.7-88
Figure 2.6.7-30	Component Parts of the Expansion Tank Structure	2.6.7-89
Figure 2.6.7-31	Expansion Tank Top and Bottom End Plate	2.6.7-90
Figure 2.6.7-32	Expansion Tank Stiffener Load Geometry	2.6.7-91
Figure 2.6.7-33	Cask Upper Ring at Trunnion - ANSYS Model	2.6.7-92
Figure 2.6.7-34	Cask Upper Ring at Trunnion - Model Loads and Boundary Conditions	2.6.7-93
Figure 2.6.7-35	NACAC-LWT Cask Upper Ring at Trunnion - Critical Sections	2.6.7-94
Figure 2.6.10-1	Impact of Penetration Cylinder on Neutron Shield Tank and Expansion Tank – Points of Impact	2.6.10-12
Figure 2.6.10-2	Impact of Penetration Cylinder on Neutron Shield Tank and Expansion Tank – Details for Analysis	2.6.10-13
Figure 2.6.10-3	Impact of Penetration Cylinder on Port Cover	2.6.10-14
Figure 2.6.10-4	One-Sixth Model of the Alternate Port Cover – 60° Symmetry	2.6.10-15
Figure 2.6.12-1	Cask Side Drop Fuel Tube Loading – MTR Fuel Basket	2.6.12-23
Figure 2.6.12-2	Baseplate Supports for Cask End Drop Loads - MTR Fuel Basket	2.6.12-24
Figure 2.6.12-3	DIDO Fuel Basket Module Structural Model – Top View	2.6.12-56
Figure 2.6.12-4	DIDO Fuel Basket Module Structural Model – Bottom View	2.6.12-57
Figure 2.6.12-5	DIDO Fuel Basket Module Maximum Stress Locations for the Side Drop Orientation	2.6.12-58
Figure 2.6.12-6	DIDO Fuel Basket Module Maximum Stress Locations for the End Drop Orientation	2.6.12-59
Figure 2.6.12-7	Cross-Section of TPBAR Basket	2.6.12-82
Figure 2.6.12-8	TPBAR Spacer Schematic Triangular Top Plate and Tube	2.6.12-83
Figure 2.7.1-1	30-Foot Bottom End Drop with 130°F Ambient Temperature and Maximum Decay Heat Load	2.7.1-30
Figure 2.7.1-2	30-Foot Bottom End Drop with -40°F Ambient Temperature and Maximum Decay Heat Load	2.7.1-31
Figure 2.7.1-3	30-Foot Bottom End Drop with -40°F Ambient Temperature and No Decay Heat Load	2.7.1-32
Figure 2.7.1-4	30-Foot Top End Drop with 130°F Ambient Temperature and Maximum Decay Heat Load	2.7.1-33
Figure 2.7.1-5	30-Foot Top End Drop with -40°F Ambient Temperature and Maximum Decay Heat Load	2.7.1-34
Figure 2.7.1-6	Circumferential Load Distribution for Cask Side Drop Impact	2.7.1-35

List of Figures (continued)

Figure 2.7.1-7 Six Term Fourier Series Representation of Circumferential Load Distribution for Cask Side Drop Impact 2.7.1-36
Figure 2.7.1-8 NAC-LWT Cask Critical Sections (30-Foot Side Drop with 100°F Ambient Temperature) 2.7.1-37
Figure 2.7.1-9 Circumferential Load Distribution for Cask Oblique Drop Impact 2.7.1-38
Figure 2.7.1-10 30-Foot Top Corner Drop with 130°F Ambient Temperature - Drop Orientation = 15.74 Degrees 2.7.1-39
Figure 2.7.1-11 30-Foot Top Oblique Drop with 130°F Ambient Temperature - Drop Orientation = 30 Degrees 2.7.1-40
Figure 2.7.1-12 30-Foot Top Oblique Drop with 130°F Ambient Temperature - Drop Orientation = 45 Degrees 2.7.1-41
Figure 2.7.1-13 30-Foot Oblique Drop with 130°F Ambient Temperature - Drop Orientation = 60 Degrees 2.7.1-42
Figure 2.7.1-14 30-Foot Top Corner Drop with -40°F Ambient Temperature - Drop Orientation = 15.74 Degrees 2.7.1-43
Figure 2.7.1-15 30-Foot Top Oblique Drop with -40°F Ambient Temperature - Drop Orientation = 30 Degrees 2.7.1-44
Figure 2.7.1-16 30-Foot Top Oblique Drop with -40°F Ambient Temperature - Drop Orientation = 45 Degrees 2.7.1-45
Figure 2.7.1-17 30-Foot Top Oblique Drop with -40°F Ambient Temperature - Drop Orientation = 60 Degrees 2.7.1-46
Figure 2.7.1-18 30-Foot Bottom Oblique Drop with 130°F Ambient Temperature – Drop Orientation = 15.74 Degrees 2.7.1-47
Figure 2.7.1-19 30-Foot Bottom Oblique Drop with 130°F Ambient Temperature - Drop Orientation = 30 Degrees 2.7.1-48
Figure 2.7.1-20 30-Foot Bottom Oblique Drop with 130°F Ambient Temperature - Drop Orientation = 45 Degrees 2.7.1-49
Figure 2.7.1-21 30-Foot Bottom Oblique Drop with 130°F Ambient Temperature - Drop Orientation = 60 Degrees 2.7.1-50
Figure 2.7.1-22 Sectional Stress Plot - 30-Foot Bottom Oblique Drop with 130°F Ambient Temperature - Drop Orientation = 60 Degrees 2.7.1-51
Figure 2.7.1-23 Sectional Stress Plot (P_m) – 30-Foot Bottom Oblique Drop with 130°F Ambient Temperature - Drop Orientation = 60 Degrees 2.7.1-52
Figure 2.7.1-24 Sectional Stress Plot ($P_m + P_b$) - 30-Foot Bottom Oblique Drop with 130°F Ambient Temperature - Drop Orientation = 60 Degrees 2.7.1-53
Figure 2.7.1-25 Bottom Closure Plate - Section Cut Identification 2.7.1-54
Figure 2.7.1-26 Sectional Stress Plot - 30-Foot Bottom Oblique Drop with 130°F Ambient Temperature - Drop Orientation = 45 Degrees 2.7.1-55
Figure 2.7.1-27 Sectional Stress Plot - 30-Foot Bottom Oblique Drop with 130°F Ambient Temperature - Drop Orientation = 30 Degrees 2.7.1-56
Figure 2.7.2-1 NAC-LWT Cask Midpoint Section 2.7.2-18
Figure 2.7.2-2 Cask Lid Configuration 2.7.2-19
Figure 2.7.2-3 NAC-LWT Cask Bottom Design Configuration 2.7.2-20

List of Figures (continued)

Figure 2.7.2-4	Port Cover Geometry	2.7.2-21
Figure 2.7.2-5	Puncture of Cask at Valve Cover Region	2.7.2-22
Figure 2.7.2-6	Alternate Port Cover Thermal Analysis Geometry	2.7.2-23
Figure 2.7.7-1	PWR Spacer Geometry	2.7.7-22
Figure 2.10.2-1	ANSYS Finite Element Model – NAC-LWT Cask	2.10.2-5
Figure 2.10.2-2	Cask Bottom of Model	2.10.2-6
Figure 2.10.2-3	Inner, Lead and Outer Shells – Lower Region of Model	2.10.2-7
Figure 2.10.2-4	Inner, Lead and Outer Shells – Lower Middle Region of Model	2.10.2-8
Figure 2.10.2-5	Inner, Lead and Outer Shell – Upper Middle Region of Model	2.10.2-9
Figure 2.10.2-6	Inner, Lead and Outer Shells – Upper Region of Model	2.10.2-10
Figure 2.10.2-7	Upper Ring Forging on Model	2.10.2-11
Figure 2.10.2-8	Closure Lid on Model	2.10.2-12
Figure 2.10.2-9	ANSYS Finite Element Model – Component Identification	2.10.2-13
Figure 2.10.3-1	NAC-LWT Cask Isotherms (Hot Case)	2.10.3-3
Figure 2.10.3-2	NAC-LWT Cask Isotherms (Cold Case)	2.10.3-4
Figure 2.10.3-3	Stress Contour Plot – Hot Case	2.10.3-5
Figure 2.10.4-1	Cask Slapdown Geometry	2.10.4-6
Figure 2.10.4-2	Force Deflection Curve of Drop Tested Limiter – 0-Degree Impact	2.10.4-7
Figure 2.10.4-3	Force Deflection Curve of Drop Tested Limiter – 14-Degree Impact	2.10.4-8
Figure 2.10.4-4	Force Deflection Curve of Drop Tested Limiter – 90 Degree Impact	2.10.4-9
Figure 2.10.4-5	Oblique Drop	2.10.4-10
Figure 2.10.7-1	Representative Section Cut Diagram	2.10.7-3
Figure 2.10.8-1	Drawing of Quarter-Scale Model	2.10.8-19
Figure 2.10.8-2	Drawing of Model Body	2.10.8-20
Figure 2.10.8-3	Drawing of Model Lid	2.10.8-23
Figure 2.10.8-4	Drawing of Model Upper Impact Limiter	2.10.8-24
Figure 2.10.8-5	Drawing of Model Lower Impact Limiter	2.10.8-25
Figure 2.10.8-6	Drawing of Model Simulated Cask Contents	2.10.8-26
Figure 2.10.8-7	Quarter-Scale Model	2.10.8-27
Figure 2.10.8-8	Model Rigged for 30-Foot End Drop	2.10.8-28
Figure 2.10.8-9	Model Positioned for 30-Foot End Drop	2.10.8-29
Figure 2.10.8-10	Model Position Following 30-Foot End Drop	2.10.8-30
Figure 2.10.8-11	Top End Impact Limiter Following 30-Foot End Drop	2.10.8-31
Figure 2.10.8-12	Exterior of Top Impact Limiter Following 30-Foot End Drop	2.10.8-32
Figure 2.10.8-13	Model Rigged for 30-Foot Corner Drop	2.10.8-33
Figure 2.10.8-14	Model Positioned for 30-Foot Corner Drop	2.10.8-34
Figure 2.10.8-15	Model Following 30-Foot Corner Drop	2.10.8-35
Figure 2.10.8-16	Top Impact Limiter Following 30-Foot Corner Drop	2.10.8-36
Figure 2.10.8-17	Model Position Following 30-Foot Side Drop – View 1	2.10.8-37
Figure 2.10.8-18	Model Position Following 30-Foot Side Drop – View 2	2.10.8-38
Figure 2.10.8-19	Top Impact Limiter Following 30-Foot Side Drop	2.10.8-39
Figure 2.10.8-20	Bottom Impact Limiter Following 30-Foot Side Drop – View 1	2.10.8-40
Figure 2.10.8-21	Bottom Impact Limiter Following 30-Foot Side Drop – View 2	2.10.8-41

List of Figures (continued)

Figure 2.10.8-22 Model Rigged for 30-Foot Oblique Drop 2.10.8-42
Figure 2.10.8-23 Model Positioned for 30-Foot Oblique Drop 2.10.8-43
Figure 2.10.8-24 Model Position Following 30-Foot Oblique Drop 2.10.8-44
Figure 2.10.8-25 Bottom Impact Limiter Following 30-Foot Oblique Drop 2.10.8-45
Figure 2.10.8-26 Top Impact Limiter Following 30-Foot Oblique Drop 2.10.8-46
Figure 2.10.8-27 Model Rigged for Midpoint 40-Inch Pin Drop 2.10.8-47
Figure 2.10.8-28 Model Positioned for 40-Inch Pin Drop 2.10.8-48
Figure 2.10.8-29 Instant Before Midpoint 40-Inch Pin Drop 2.10.8-49
Figure 2.10.8-30 Model Position Following Midpoint 40-Inch Pin Drop 2.10.8-50
Figure 2.10.8-31 Impact Location – Midpoint 40-Inch Pin Drop 2.10.8-51
Figure 2.10.8-32 Angular Orientation of Instrumentation 2.10.8-52
Figure 2.10.8-33 Strain Gauge Time History for Channel 3 – End Drop 2.10.8-53
Figure 2.10.8-34 Strain Gauge Time History for Channel 4 – End Drop 2.10.8-54
Figure 2.10.8-35 Strain Gauge Time History for Channel 5 – End Drop 2.10.8-55
Figure 2.10.8-36 Strain Gauge Time History for Channel 3 – Side Drop 2.10.8-56
Figure 2.10.8-37 Strain Gauge Time History for Channel 4 – Side Drop 2.10.8-57
Figure 2.10.8-38 Strain Gauge Time History for Channel 5 – Side Drop 2.10.8-58
Figure 2.10.8-39 Location of Block Sets 2.10.8-59
Figure 2.10.10-1 Stress Point Locations 2.10.10-7
Figure 2.10.11-1 Mathmatical Model of NAC-LWT Cask (30-foot Top End Impact 2.10.11-8
Figure 2.10.12-1 Side Drop ($\theta = 90°$) 2.10.12-9
Figure 2.10.12-2 End Drop ($0° \leq \theta < 15°$) 2.10.12-10
Figure 2.10.12-3 Oblique Drop ($15° \leq \theta < 90°$) 2.10.12-11
Figure 2.10.12-4 Force Deflection Graph (0-Degree, Top End Drop) 2.10.12-12
Figure 2.10.12-5 Force-Deflection Graph (0-Degree, Bottom-End Drop) 2.10.12-13
Figure 2.10.12-6 Force-Deflection Graph (15.74-Degree, Top Corner Drop) 2.10.12-14
Figure 2.10.12-7 Force-Deflection Graph (14.5-Degree, Bottom Corner Drop) 2.10.12-15
Figure 2.10.12-8 Force-Deflection Graph (30-Degree, Top Oblique Drop) 2.10.12-16
Figure 2.10.12-9 Force-Deflection Graph (30-Degree, Bottom Oblique Drop) 2.10.12-17
Figure 2.10.12-10 Force-Deflection Graph (45-Degree, Top Oblique Drop) 2.10.12-18
Figure 2.10.12-11 Force-Deflection Graph (45-Degree, Bottom Oblique Drop) 2.10.12-19
Figure 2.10.12-12 Force-Deflection Graph (60-Degree, Top Oblique Drop) 2.10.12-20
Figure 2.10.12-13 Force-Deflection Graph (60-Degree, Bottom Oblique Drop) 2.10.12-21
Figure 2.10.12-14 Force-Deflection Graph (75-Degree, Top Oblique Drop) 2.10.12-22
Figure 2.10.12-15 Force-Deflection Graph (75-Degree, Bottom Oblique Drop) 2.10.12-23
Figure 2.10.12-16 Force-Deflection Graph (90-Degree, Top Side Drop) 2.10.12-24
Figure 2.10.12-17 Force-Deflection Graph (90-Degree, Bottom Side Drop) 2.10.12-25
Figure 2.10.12-18 Force-Deflection Curve (0-Degree Impact, Drop Tested Limiter) 2.10.12-26
Figure 2.10.12-19 Force-Deflection Curve (14-Degree Impact, Drop Tested Limiter) 2.10.12-27
Figure 2.10.12-20 Force-Deflection Curve (90-Degree Impact, Drop Tested Limiter) 2.10.12-28
Figure 2.10.12-21 End Drop Impact Limiter Cross Section 2.10.12-29
Figure 2.10.13-1 LWT Cask, Metal Fuel Basket Assembly Safety Analysis Report, NAC Drawing No. 315-40-12 ..... 2.10.13-13

List of Figures (continued)

Figure 2.10.13-2 Liner-Failed Fuel Can, 2.75 I.D., LWT Cask, Safety Analysis Report, NAC Drawing No. 315-040-43 ..... 2.10.13-14
Figure 2.10.13-3 Failed Fuel Rod Can – 4.00 I.D., Fuel Rod Containerization, NAC Drawing No. 340-108-D1 ..... 2.10.13-15
Figure 2.10.13-4 Failed Fuel Rod Can – 2.75 I.D., Fuel Rod Containerization, NAC Drawing No. 340-108-D2 ..... 2.10.13-16
Figure 2.10.13-5 Failed Fuel Filter, NAC Drawing No. 491-042 ..... 2.10.13-17
Figure 2.10.14-1 ANSYS Finite Element Model of the Cask Body 2.10.14-7
Figure 2.10.14-2 Detailed View of the Cask Body Finite Element Model Top 2.10.14-8
Figure 2.10.14-3 Detailed View of the Cask Body Finite Element Model Bottom 2.10.14-9
Figure 2.10.14-4 Location of Sections of the NAC-LWT Cask Body Model 2.10.14-10
Figure 2.10.15-1 Alternate B Port Cover Finite Element Model 2.10.15-10

List of Tables

Table 2.1.2-1	Allowable Stress Limits for Containment Structures	2.1.2-2
Table 2.1.2-2	Allowable Stress Limits for Noncontainment Structures	2.1.2-3
Table 2.1.3-1	Extreme Total Stress Intensities	2.1.3-8
Table 2.2.1-1	Weights of the NAC-LWT Cask Major Components	2.2.1-2
Table 2.2.1-2	Weights and Center of Gravity Locations for the NAC-LWT Cask Shipping Configurations	2.2.1-3
Table 2.3.1-1	Mechanical Properties of Type 304 Stainless Steel	2.3.1-5
Table 2.3.1-2	Mechanical Properties of Type XM-19 Stainless Steel	2.3.1-6
Table 2.3.1-3	Mechanical Properties of SA-705, Grade 630, Precipitation-Hardened Stainless Steel	2.3.1-7
Table 2.3.1-4	Mechanical Properties (6061-T6 and T651 per ASTM B-209)	2.3.1-8
Table 2.3.1-5	Mechanical Properties of SA-193, Grade B6 High Alloy, Steel Bolting Material	2.3.1-9
Table 2.3.1-6	Mechanical Properties of SA-453, Grade 660 High Alloy, Steel Bolting Material	2.3.1-10
Table 2.3.1-7	Static Mechanical Properties of Chemical Copper Lead	2.3.1-11
Table 2.3.1-8	Dynamic Mechanical Properties of Chemical Copper Lead	2.3.1-12
Table 2.3.1-9	Mechanical Properties of SB-637, Grade N07718, Nickel Alloy Steel Bolting Material	2.3.1-13
Table 2.5.1-1	Maximum Capacity of the Lifting Components	2.5.1-11
Table 2.5.2-1	Reactions Caused By Tiedown Devices	2.5.2-17
Table 2.6.1-1	Critical Stress Summary (Hot Case) - P_m	2.6.1-5
Table 2.6.1-2	Critical Stress Summary (Hot Case) - $P_m + P_b$	2.6.1-6
Table 2.6.1-3	Critical Stress Summary (Hot Case) – Total Range	2.6.1-7
Table 2.6.2-1	Critical Stress Summary (Cold Case) - P_m	2.6.2-5
Table 2.6.2-2	Critical Stress Summary (Cold Case) - $P_m + P_b$	2.6.2-6
Table 2.6.2-3	Critical Stress Summary (Cold Case) – Total Range	2.6.2-7
Table 2.6.7-1	Critical Stress Summary (1-Foot Bottom End Drop) – Loading Condition 1 – P_m	2.6.7-95
Table 2.6.7-2	Critical Stress Summary (1-Foot Bottom End Drop) – Loading Condition 1 - $P_m + P_b$	2.6.7-96
Table 2.6.7-3	Critical Stress Summary (1-Foot Bottom End Drop) – Loading Condition 1 - Total Range	2.6.7-97
Table 2.6.7-4	Critical Stress Summary (1-Foot Bottom End Drop) – Loading Condition 2 – P_m	2.6.7-98
Table 2.6.7-5	Critical Stress Summary (1-Foot Bottom End Drop) – Loading Condition 2 - $P_m + P_b$	2.6.7-99
Table 2.6.7-6	Critical Stress Summary (1-Foot Bottom End Drop) – Loading Condition 2 - Total Range	2.6.7-100
Table 2.6.7-7	Critical Stress Summary (1-Foot Bottom End Drop) – Loading Condition 3 – P_m	2.6.7-101
Table 2.6.7-8	Critical Stress Summary (1-Foot Bottom End Drop) – Loading Condition 3 - $P_m + P_b$	2.6.7-102

List of Tables (continued)

Table 2.6.7-9 Critical Stress Summary (1-Foot Bottom End Drop) – Loading Condition 3 - Total Range 2.6.7-103
Table 2.6.7-10 Critical Stress Summary (1-Foot Top End Drop) – Loading Condition 1 – P_m 2.6.7-104
Table 2.6.7-11 Critical Stress Summary (1-Foot Top End Drop) – Loading Condition 1 - $P_m + P_b$ 2.6.7-105
Table 2.6.7-12 Critical Stress Summary (1-Foot Top End Drop) – Loading Condition 1 - Total Range 2.6.7-106
Table 2.6.7-13 Critical Stress Summary (1-Foot Top End Drop) – Loading Condition 2 – P_m 2.6.7-107
Table 2.6.7-14 Critical Stress Summary (1-Foot Top End Drop) – Loading Condition 2 - $P_m + P_b$ 2.6.7-108
Table 2.6.7-15 Critical Stress Summary (1-Foot Top End Drop) – Loading Condition 2 - Total Range 2.6.7-109
Table 2.6.7-16 Critical Stress Summary (1-Foot Side Drop) – Loading Condition 1 – P_m 2.6.7-110
Table 2.6.7-17 Critical Stress Summary (1-Foot Side Drop) – Loading Condition 1 - $P_m + P_b$ 2.6.7-111
Table 2.6.7-18 Critical Stress Summary (1-Foot Side Drop) – Loading Condition 1 - S_n 2.6.7-112
Table 2.6.7-19 Critical Stress Summary (1-Foot Side Drop) – Loading Condition 1 - Total Range 2.6.7-113
Table 2.6.7-20 Critical Stress Summary (1-Foot Top Corner Drop) – Loading Condition 1 – P_m – Drop Orientation = 15.74 Degrees 2.6.7-114
Table 2.6.7-21 Critical Stress Summary (1-Foot Top Corner Drop) – Loading Condition 1 - $P_m + P_b$ – Drop Orientation = 15.74 Degrees 2.6.7-115
Table 2.6.7-22 Critical Stress Summary (1-Foot Top Corner Drop) – Loading Condition 1 - S_n – Drop Orientation = 15.74 Degrees 2.6.7-116
Table 2.6.7-23 Critical Stress Summary (1-Foot Top Corner Drop) – Loading Condition 1 - Total Range – Drop Orientation = 15.74 Degrees 2.6.7-117
Table 2.6.7-24 Critical Stress Summary (1-Foot Bottom Corner Drop) – Loading Condition 1 – P_m – Drop Orientation = 15.74 Degrees 2.6.7-118
Table 2.6.7-25 Critical Stress Summary (1-Foot Bottom Corner Drop) – Loading Condition 1 - $P_m + P_b$ – Drop Orientation = 15.74 Degrees 2.6.7-119
Table 2.6.7-26 Critical Stress Summary (1-Foot Bottom Corner Drop) – Loading Condition 1 - S_n – Drop Orientation = 15.74 Degrees 2.6.7-120
Table 2.6.7-27 Critical Stress Summary (1-Foot Bottom Corner Drop) – Loading Condition 1 - Total Range – Drop Orientation = 15.74 Degrees 2.6.7-121
Table 2.6.7-28 Critical Stress Summary (1-Foot Top Corner Drop) – Loading Condition 3 – P_m – Drop Orientation = 15.74 Degrees 2.6.7-122
Table 2.6.7-29 Critical Stress Summary (1-Foot Top Corner Drop) – Loading Condition 3 - $P_m + P_b$ – Drop Orientation = 15.74 Degrees 2.6.7-123

List of Tables (continued)

Table 2.6.7-30	Critical Stress Summary (1-Foot Top Corner Drop) – Loading Condition 3 - S_n – Drop Orientation = 15.74 Degrees	2.6.7-124
Table 2.6.7-31	Critical Stress Summary (1-Foot Top Corner Drop) – Loading Condition 3 - Total Range – Drop Orientation = 15.74 Degrees	2.6.7-125
Table 2.6.7-32	Summary of Results - Impact Limiter Analysis for 1-Foot Free Drop	2.6.7-126
Table 2.6.7-33	Summary of Results - Impact Limiter Analysis for 30-Foot Free Drop Subsequent to a 1-Foot Fall	2.6.7-128
Table 2.6.7-34	Summary of Cask Drop Equivalent G Load Factors	2.6.7-130
Table 2.6.7-35	NAC-LWT Cask Hot Bolt Analysis – Normal Conditions	2.6.7-131
Table 2.6.7-36	NAC-LWT Cask Cold Bolt Analysis – Normal Conditions	2.6.7-132
Table 2.6.7-37	Summary of Neutron Shield Tank Analysis	2.6.7-133
Table 2.6.7-38	Normal Transport Shield Tank Temperatures	2.6.7-134
Table 2.6.7-39	Normal Transport Shield Tank Pressures	2.6.7-135
Table 2.6.7-40	Summary of Expansion Tank Analysis	2.6.7-135
Table 2.6.7-41	Upper Ring – Cross-Section Principal Stresses	2.6.7-136
Table 2.6.12-1	Maximum Primary Membrane Stress for the 1-Foot Drop (DIDO Basket)	2.6.12-60
Table 2.6.12-2	Maximum Primary Membrane Plus Bending Stress for the 1-Foot Drop (DIDO Basket)	2.6.12-60
Table 2.7.1-1	Critical Stress Summary (30-Foot Bottom End Drop) – Loading Condition 1 – P_m	2.7.1-57
Table 2.7.1-2	Critical Stress Summary (30-Foot Bottom End Drop) – Loading Condition 1 - $P_m + P_b$	2.7.1-58
Table 2.7.1-3	Critical Stress Summary (30-Foot Bottom End Drop) – Loading Condition 1 - Total Range	2.7.1-59
Table 2.7.1-4	Critical Stress Summary (30-Foot Bottom End Drop) – Loading Condition 2 – P_m	2.7.1-60
Table 2.7.1-5	Critical Stress Summary (30-Foot Bottom End Drop) – Loading Condition 2 - $P_m + P_b$	2.7.1-61
Table 2.7.1-6	Critical Stress Summary (30-Foot Bottom End Drop) – Loading Condition 2 - Total Range	2.7.1-62
Table 2.7.1-7	Critical Stress Summary (30-Foot Bottom End Drop) – Loading Condition 3 – P_m	2.7.1-63
Table 2.7.1-8	Critical Stress Summary (30-Foot Bottom End Drop) – Loading Condition 3 - $P_m + P_b$	2.7.1-64
Table 2.7.1-9	Critical Stress Summary (30-Foot Bottom End Drop) – Loading Condition 3 - Total Range	2.7.1-65
Table 2.7.1-10	Critical Stress Summary (30-Foot Top End Drop) – Loading Condition 1 – P_m	2.7.1-66
Table 2.7.1-11	Critical Stress Summary (30-Foot Top End Drop) – Loading Condition 1 - $P_m + P_b$	2.7.1-67

List of Tables (continued)

Table 2.7.1-12 Critical Stress Summary (30-Foot Top End Drop) – Loading Condition 1 - Total Range 2.7.1-68
Table 2.7.1-13 Critical Stress Summary (30-Foot Top End Drop) – Loading Condition 2 – P_m 2.7.1-69
Table 2.7.1-14 Critical Stress Summary (30-Foot Top End Drop) – Loading Condition 2 - $P_m + P_b$ 2.7.1-70
Table 2.7.1-15 Critical Stress Summary (30-Foot Top End Drop) – Loading Condition 2 - Total Range 2.7.1-71
Table 2.7.1-16 Side Drop Load Analysis Description 2.7.1-72
Table 2.7.1-17 Critical Stress Summary (30-Foot Side Drop) – Loading Condition 1 - P_m 2.7.1-73
Table 2.7.1-18 Critical Stress Summary (30-Foot Side Drop) – Loading Condition 1 - $P_m + P_b$ 2.7.1-74
Table 2.7.1-19 Critical Stress Summary (30-Foot Side Drop) – Loading Condition 1 - Total Range 2.7.1-75
Table 2.7.1-20 G Loads – Oblique Drop 2.7.1-76
Table 2.7.1-21 Impact and Contents Pressures – Oblique Drop 2.7.1-77
Table 2.7.1-22 Fourier Series Modal Coefficients – Oblique Drop 2.7.1-78
Table 2.7.1-23 Oblique Drop Load Analysis Description 2.7.1-79
Table 2.7.1-24 Critical Stress Summary (30-Foot Top Corner Drop) – Loading Condition 1 - P_m – Drop Orientation = 15.74 Degrees 2.7.1-80
Table 2.7.1-25 Critical Stress Summary (30-Foot Top Corner Drop) – Loading Condition 1 - $P_m + P_b$ – Drop Orientation = 15.74 Degrees 2.7.1-81
Table 2.7.1-26 Critical Stress Summary (30-Foot Top Corner Drop) – Loading Condition 1 – Total Range – Drop Orientation = 15.74 Degrees 2.7.1-82
Table 2.7.1-27 Critical Stress Summary (30-Foot Top Oblique Drop) – Loading Condition 1 - P_m – Drop Orientation = 30 Degrees 2.7.1-83
Table 2.7.1-28 Critical Stress Summary (30-Foot Top Oblique Drop) – Loading Condition 1 - $P_m + P_b$ – Drop Orientation = 30 Degrees 2.7.1-84
Table 2.7.1-29 Critical Stress Summary (30-Foot Top Oblique Drop) – Loading Condition 1 – Total Range – Drop Orientation = 30 Degrees 2.7.1-85
Table 2.7.1-30 Critical Stress Summary (30-Foot Top Oblique Drop) – Loading Condition 1 - P_m – Drop Orientation = 45 Degrees 2.7.1-86
Table 2.7.1-31 Critical Stress Summary (30-Foot Top Oblique Drop) – Loading Condition 1 - $P_m + P_b$ – Drop Orientation = 45 Degrees 2.7.1-87
Table 2.7.1-32 Critical Stress Summary (30-Foot Top Oblique Drop) – Loading Condition 1 – Total Range – Drop Orientation = 45 Degrees 2.7.1-88
Table 2.7.1-33 Critical Stress Summary (30-Foot Top Oblique Drop) – Loading Condition 1 - P_m – Drop Orientation = 60 Degrees 2.7.1-89
Table 2.7.1-34 Critical Stress Summary (30-Foot Top Oblique Drop) – Loading Condition 1 - $P_m + P_b$ – Drop Orientation = 60 Degrees 2.7.1-90
Table 2.7.1-35 Critical Stress Summary (30-Foot Top Oblique Drop) – Loading Condition 1 – Total Range – Drop Orientation = 60 Degrees 2.7.1-91

List of Tables (continued)

Table 2.7.1-36 Critical Stress Summary (30-Foot Top Corner Drop) – Loading Condition 3 - P_m – Drop Orientation = 15.74 Degrees 2.7.1-92
Table 2.7.1-37 Critical Stress Summary (30-Foot Top Corner Drop) – Loading Condition 3 - $P_m + P_b$ – Drop Orientation = 15.74 Degrees 2.7.1-93
Table 2.7.1-38 Critical Stress Summary (30-Foot Top Corner Drop) – Loading Condition 3 – Total Range – Drop Orientation = 15.74 Degrees 2.7.1-94
Table 2.7.1-39 Critical Stress Summary (30-Foot Top Oblique Drop) – Loading Condition 3 - P_m – Drop Orientation = 30 Degrees 2.7.1-95
Table 2.7.1-40 Critical Stress Summary (30-Foot Top Oblique Drop) – Loading Condition 3 - $P_m + P_b$ – Drop Orientation = 30 Degrees 2.7.1-96
Table 2.7.1-41 Critical Stress Summary (30-Foot Top Oblique Drop) – Loading Condition 3 – Total Range – Drop Orientation = 30 Degrees 2.7.1-97
Table 2.7.1-42 Critical Stress Summary (30-Foot Top Oblique Drop) – Loading Condition 3 - P_m – Drop Orientation = 45 Degrees 2.7.1-98
Table 2.7.1-43 Critical Stress Summary (30-Foot Top Oblique Drop) – Loading Condition 3 - $P_m + P_b$ – Drop Orientation = 45 Degrees 2.7.1-99
Table 2.7.1-44 Critical Stress Summary (30-Foot Top Oblique Drop) – Loading Condition 3 – Total Range – Drop Orientation = 45 Degrees 2.7.1-100
Table 2.7.1-45 Critical Stress Summary (30-Foot Top Oblique Drop) – Loading Condition 3 - P_m – Drop Orientation = 60 Degrees 2.7.1-101
Table 2.7.1-46 Critical Stress Summary (30-Foot Top Oblique Drop) – Loading Condition 3 - $P_m + P_b$ – Drop Orientation = 60 Degrees 2.7.1-102
Table 2.7.1-47 Critical Stress Summary (30-Foot Top Oblique Drop) – Loading Condition 3 – Total Range – Drop Orientation = 60 Degrees 2.7.1-103
Table 2.7.1-48 Critical Stress Summary (30-Foot Bottom Oblique Drop) – Loading Condition 1 - P_m – Drop Orientation = 15.74 Degrees 2.7.1-104
Table 2.7.1-49 Critical Stress Summary (30-Foot Bottom Oblique Drop) – Loading Condition 1 - $P_m + P_b$ – Drop Orientation = 15.74 Degrees 2.7.1-105
Table 2.7.1-50 Critical Stress Summary (30-Foot Bottom Oblique Drop) – Loading Condition 1 – Total Range – Drop Orientation = 15.74 Degrees 2.7.1-106
Table 2.7.1-51 Critical Stress Summary (30-Foot Bottom Oblique Drop) – Loading Condition 1 - P_m – Drop Orientation = 30 Degrees 2.7.1-107
Table 2.7.1-52 Critical Stress Summary (30-Foot Bottom Oblique Drop) – Loading Condition 1 - $P_m + P_b$ – Drop Orientation = 30 Degrees 2.7.1-108
Table 2.7.1-53 Critical Stress Summary (30-Foot Bottom Oblique Drop) – Loading Condition 1 – Total Range – Drop Orientation = 30 Degrees 2.7.1-109
Table 2.7.1-54 Critical Stress Summary (30-Foot Bottom Oblique Drop) – Loading Condition 1 - P_m – Drop Orientation = 45 Degrees 2.7.1-110
Table 2.7.1-55 Critical Stress Summary (30-Foot Bottom Oblique Drop) – Loading Condition 1 - $P_m + P_b$ – Drop Orientation = 45 Degrees 2.7.1-111
Table 2.7.1-56 Critical Stress Summary (30-Foot Bottom Oblique Drop) – Loading Condition 1 – Total Range – Drop Orientation = 45 Degrees 2.7.1-112

List of Tables (continued)

Table 2.7.1-57	Critical Stress Summary (30-Foot Bottom Oblique Drop) – Loading Condition 1 - P_m – Drop Orientation = 60 Degrees	2.7.1-113
Table 2.7.1-58	Critical Stress Summary (30-Foot Bottom Oblique Drop) – Loading Condition 1 - $P_m + P_b$ – Drop Orientation = 60 Degrees	2.7.1-114
Table 2.7.1-59	Critical Stress Summary (30-Foot Bottom Oblique Drop) – Loading Condition 1 – Total Range – Drop Orientation = 60 Degrees	2.7.1-115
Table 2.7.1-60	NAC-LWT Cask Hot Bolt Analysis Hypothetical Accident Conditions	2.7.1-116
Table 2.7.1-61	NAC-LWT Cask Cold Bolt Analysis Hypothetical Accident Conditions	2.7.1-117
Table 2.7.6-1	Summary of Maximum Calculated Stresses – 30-Foot Drop	2.7.6-2
Table 2.7.6-2	Summary of Maximum Calculated Stresses – 40-Inch Free Drop	2.7.6-3
Table 2.7.6-3	Summary of Maximum Calculated Stresses - Fire	2.7.6-4
Table 2.7.7-1	Maximum Primary Membrane Stress for the 30-Foot Drop	2.7.7-50
Table 2.7.7-2	Maximum Primary Membrane Plus Bending Stress for the 30-Foot Drop	2.7.7-50
Table 2.10.2-1	Node Definitions	2.10.2-14
Table 2.10.2-2	Applied Impact Pressure Loadings – 30-Foot Hypothetical Accident Conditions	2.10.2-48
Table 2.10.3-1	P_m Stress Summary – Upper Ring Critical Section	2.10.3-6
Table 2.10.3-2	$P_m + P_b$ Stress Summary – Upper Ring Critical Section	2.10.3-11
Table 2.10.4-1	Determination of Maximum Energy for Secondary Impact – Full-Scale Impact Limiter	2.10.4-11
Table 2.10.6-1	Inner Shell Geometry Parameters	2.10.6-8
Table 2.10.6-2	Material Properties of Type XM-19 Stainless Steel for Buckling Analysis Input (ASME, Section III, Appendix I)	2.10.6-9
Table 2.10.6-3	Theoretical Elastic Buckling Stress Values (Temperature Independent Form)	2.10.6-10
Table 2.10.6-4	Theoretical Elastic Buckling Stresses for Selected Temperatures	2.10.6-11
Table 2.10.6-5	Capacity Reduction Factors for the Type XM-19 Stainless Steel Inner Shell	2.10.6-12
Table 2.10.6-6	Fabrication Tolerances for the NAC-LWT Cask Inner Shell	2.10.6-13
Table 2.10.6-7	Upper Bound Buckling Stresses	2.10.6-14
Table 2.10.6-8	Calculated Maximum Compressive Stresses in the Inner Shell	2.10.6-15
Table 2.10.6-9	Calculated Stresses with ASME Factors of Safety	2.10.6-17
Table 2.10.6-10	Results – Interaction Equations	2.10.6-18
Table 2.10.7-1	Section Cut Identification	2.10.7-4
Table 2.10.7-2	P_m Stress Summary (Hot Case)	2.10.7-5
Table 2.10.7-3	$P_m + P_b$ Stress Summary (Hot Case)	2.10.7-6
Table 2.10.7-4	P_m Stress Summary (Cold Case)	2.10.7-7
Table 2.10.7-5	$P_m + P_b$ Stress Summary (Cold Case)	2.10.7-8
Table 2.10.7-6	P_m Stress Summary (1-Foot Bottom End Drop) – Loading Condition 1	2.10.7-9

List of Tables (continued)

Table 2.10.7-7 $P_m + P_b$ Stress Summary (1-Foot Bottom End Drop) – Loading Condition 1 ..... 2.10.7-10
Table 2.10.7-8 P_m Stress Summary (1-Foot Bottom End Drop) – Loading Condition 2 ..... 2.10.7-11
Table 2.10.7-9 $P_m + P_b$ Stress Summary (1-Foot Bottom End Drop) – Loading Condition 2 ..... 2.10.7-12
Table 2.10.7-10 P_m Stress Summary (1-Foot Bottom End Drop) – Loading Condition 3 ..... 2.10.7-13
Table 2.10.7-11 $P_m + P_b$ Stress Summary (1-Foot Bottom End Drop) – Loading Condition 3 ..... 2.10.7-14
Table 2.10.7-12 P_m Stress Summary (1-Foot Top End Drop) – Loading Condition 1 .. 2.10.7-15
Table 2.10.7-13 $P_m + P_b$ Stress Summary (1-Foot Top End Drop) – Loading Condition 1 ..... 2.10.7-16
Table 2.10.7-14 P_m Stress Summary (1-Foot Top End Drop) – Loading Condition 2 .. 2.10.7-17
Table 2.10.7-15 $P_m + P_b$ Stress Summary (1-Foot Top End Drop) – Loading Condition 2 ..... 2.10.7-18
Table 2.10.7-16 P_m Stress Summary (1-Foot Side Drop) – Loading Condition 1 ..... 2.10.7-19
Table 2.10.7-17 $P_m + P_b$ Stress Summary (1-Foot Side Drop) – Loading Condition 1 . 2.10.7-20
Table 2.10.7-18 S_n Stress Summary (1-Foot Side Drop) – Loading Condition 1 ..... 2.10.7-21
Table 2.10.7-19 P_m Stress Summary (1-Foot Top Corner Drop) – Loading Condition 1 – Drop Orientation = 15.74 Degrees 2.10.7-22
Table 2.10.7-20 $P_m + P_b$ Stress Summary (1-Foot Top Corner Drop) – Loading Condition 1 – Drop Orientation = 15.74 Degrees 2.10.7-23
Table 2.10.7-21 S_n Stress Summary (1-Foot Top Corner Drop) – Loading Condition 1 – Drop Orientation = 15.74 Degrees 2.10.7-24
Table 2.10.7-22 P_m Stress Summary (1-Foot Bottom Corner Drop) – Loading Condition 1 – Drop Orientation = 15.74 Degrees 2.10.7-25
Table 2.10.7-23 $P_m + P_b$ Stress Summary (1-Foot Bottom Corner Drop) – Loading Condition 1 – Drop Orientation = 15.74 Degrees 2.10.7-26
Table 2.10.7-24 S_n Stress Summary (1-Foot Bottom Corner Drop) – Loading Condition 1 – Drop Orientation = 15.74 Degrees 2.10.7-27
Table 2.10.7-25 P_m Stress Summary (1-Foot Top Corner Drop) – Loading Condition 3 – Drop Orientation = 15.74 Degrees 2.10.7-28
Table 2.10.7-26 $P_m + P_b$ Stress Summary (1-Foot Top Corner Drop) – Loading Condition 3 – Drop Orientation = 15.74 Degrees 2.10.7-29
Table 2.10.7-27 S_n Stress Summary (1-Foot Top Corner Drop) – Loading Condition 3 – Drop Orientation = 15.74 Degrees 2.10.7-30
Table 2.10.7-28 P_m Stress Summary (30-Foot Bottom End Drop) – Loading Condition 1 ..... 2.10.7-31
Table 2.10.7-29 $P_m + P_b$ Stress Summary (30-Foot Bottom End Drop) – Loading Condition 1 ..... 2.10.7-32
Table 2.10.7-30 P_m Stress Summary (30-Foot Bottom End Drop) – Loading Condition 2 ..... 2.10.7-33

List of Tables (continued)

Table 2.10.7-31 $P_m + P_b$ Stress Summary (30-Foot Bottom End Drop) – Loading Condition 2 ..... 2.10.7-34
Table 2.10.7-32 P_m Stress Summary (30-Foot Bottom End Drop) – Loading Condition 3 ..... 2.10.7-35
Table 2.10.7-33 $P_m + P_b$ Stress Summary (30-Foot Bottom End Drop) – Loading Condition 3 ..... 2.10.7-36
Table 2.10.7-34 P_m Stress Summary (30-Foot Top End Drop) – Loading Condition 1 ..... 2.10.7-37
Table 2.10.7-35 $P_m + P_b$ Stress Summary (30-Foot Top End Drop) – Loading Condition 1 ..... 2.10.7-38
Table 2.10.7-36 P_m Stress Summary (30-Foot Top End Drop) – Loading Condition 2 ..... 2.10.7-39
Table 2.10.7-37 $P_m + P_b$ Stress Summary (30-Foot Top End Drop) – Loading Condition 2 ..... 2.10.7-40
Table 2.10.7-38 P_m Stress Summary (30-Foot Side Drop) – Loading Condition 1 ..... 2.10.7-41
Table 2.10.7-39 $P_m + P_b$ Stress Summary (30-Foot Side Drop) – Loading Condition 1 ..... 2.10.7-42
Table 2.10.7-40 P_m Stress Summary (30-Foot Top Corner Drop) – Loading Condition 1 – Drop Orientation = 15.74 Degrees 2.10.7-43
Table 2.10.7-41 $P_m + P_b$ Stress Summary (30-Foot Top Corner Drop) – Loading Condition 1 – Drop Orientation = 15.74 Degrees 2.10.7-44
Table 2.10.7-42 P_m Stress Summary (30-Foot Top Oblique Drop) – Loading Condition 1 – Drop Orientation = 30 Degrees 2.10.7-45
Table 2.10.7-43 $P_m + P_b$ Stress Summary (30-Foot Top Oblique Drop) – Loading Condition 1 – Drop Orientation = 30 Degrees 2.10.7-46
Table 2.10.7-44 P_m Stress Summary (30-Foot Top Oblique Drop) – Loading Condition 1 – Drop Orientation = 45 Degrees 2.10.7-47
Table 2.10.7-45 $P_m + P_b$ Stress Summary (30-Foot Top Oblique Drop) – Loading Condition 1 – Drop Orientation = 45 Degrees 2.10.7-48
Table 2.10.7-46 P_m Stress Summary (30-Foot Top Oblique Drop) – Loading Condition 1 – Drop Orientation = 60 Degrees 2.10.7-49
Table 2.10.7-47 $P_m + P_b$ Stress Summary (30-Foot Top Oblique Drop) – Loading Condition 1 – Drop Orientation = 60 Degrees 2.10.7-50
Table 2.10.7-48 P_m Stress Summary (30-Foot Top Corner Drop) – Loading Condition 3 – Drop Orientation = 15.74 Degrees 2.10.7-51
Table 2.10.7-49 $P_m + P_b$ Stress Summary (30-Foot Top Corner Drop) – Loading Condition 3 – Drop Orientation = 15.74 Degrees 2.10.7-52
Table 2.10.7-50 P_m Stress Summary (30-Foot Top Oblique Drop) – Loading Condition 3 – Drop Orientation = 30 Degrees 2.10.7-53
Table 2.10.7-51 $P_m + P_b$ Stress Summary (30-Foot Top Oblique Drop) – Loading Condition 3 – Drop Orientation = 30 Degrees 2.10.7-54
Table 2.10.7-52 P_m Stress Summary (30-Foot Top Oblique Drop) – Loading Condition 3 – Drop Orientation = 45 Degrees 2.10.7-55

List of Tables (continued)

Table 2.10.7-53 $P_m + P_b$ Stress Summary (30-Foot Top Oblique Drop) – Loading Condition 3 – Drop Orientation = 45 Degrees 2.10.7-56
Table 2.10.7-54 P_m Stress Summary (30-Foot Top Oblique Drop) – Loading Condition 3 – Drop Orientation = 60 Degrees 2.10.7-57
Table 2.10.7-55 $P_m + P_b$ Stress Summary (30-Foot Top Oblique Drop) – Loading Condition 3 – Drop Orientation = 60 Degrees 2.10.7-58
Table 2.10.7-56 P_m Stress Summary (30-Foot Bottom Corner Drop) – Loading Condition 1 – Drop Orientation = 15.74 Degrees 2.10.7-59
Table 2.10.7-57 $P_m + P_b$ Stress Summary (30-Foot Bottom Corner Drop) – Loading Condition 1 – Drop Orientation = 15.74 Degrees 2.10.7-60
Table 2.10.7-58 P_m Stress Summary (30-Foot Bottom Oblique Drop) – Loading Condition 1 – Drop Orientation = 30 Degrees 2.10.7-61
Table 2.10.7-59 $P_m + P_b$ Stress Summary (30-Foot Bottom Oblique Drop) – Loading Condition 1 – Drop Orientation = 30 Degrees 2.10.7-62
Table 2.10.7-60 P_m Stress Summary (30-Foot Bottom Oblique Drop) – Loading Condition 1 – Drop Orientation = 45 Degrees 2.10.7-63
Table 2.10.7-61 $P_m + P_b$ Stress Summary (30-Foot Bottom Oblique Drop) – Loading Condition 1 – Drop Orientation = 45 Degrees 2.10.7-64
Table 2.10.7-62 P_m Stress Summary (30-Foot Bottom Oblique Drop) – Loading Condition 1 – Drop Orientation = 60 Degrees 2.10.7-65
Table 2.10.7-63 $P_m + P_b$ Stress Summary (30-Foot Bottom Oblique Drop) – Loading Condition 1 – Drop Orientation = 60 Degrees 2.10.7-66
Table 2.10.8-1 Scaling Relations 2.10.8-60
Table 2.10.8-2 Metrology Results of Inner Diameter Measurements Before Drop 2.10.8-62
Table 2.10.8-3 Metrology Results of Outer Diameter Measurements Before Drop 2.10.8-63
Table 2.10.8-4 Metrology Results of External Length Measurements Before Drop 2.10.8-64
Table 2.10.8-5 Metrology Results of Inner Diameter Measurements After Drop 2.10.8-65
Table 2.10.8-6 Metrology Results of Outer Diameter Measurements After Drop 2.10.8-66
Table 2.10.8-7 Metrology Results of External Length Measurements After Drop 2.10.8-67
Table 2.10.9-1 NAC-LWT Cask Hot Bolt Analysis Hypothetical Accident Conditions 2.10.9-9
Table 2.10.10-1 Stress Point Locations 2.10.10-8
Table 2.10.10-2 Constraint Forces for the 30-Foot Top End Drop Condition ($\phi = 0°$) 2.10.10-12
Table 2.10.10-3 Constraint Forces for the 30-Foot Top Corner Drop Condition ($\phi = 15.74°$) 2.10.10-13
Table 2.10.10-4 Constraint Forces for the 30-Foot Top Oblique Drop Condition ($\phi = 60°$) 2.10.10-13
Table 2.10.10-5 Constraint Forces for the 30-Foot Side Drop Condition ($\phi = 90°$) 2.10.10-13
Table 2.10.10-6 Stress Components – Thermal; 130°F; 1.12-Inch Outer Shell Thickness 2.10.10-14
Table 2.10.10-7 Stress Components – Internal Pressure; 50 psi; 1.12-Inch Outer Shell Thickness 2.10.10-18

List of Tables (continued)

Table 2.10.10-8 Stress Components – Bolt Preload; 1.12-Inch Outer Shell Thickness 2.10.10-22
Table 2.10.10-9 Stress Components – Impact and Inertial Loads; 30-Foot Top End Drop; $\phi = 0°$; 1.12-Inch Outer Shell Thickness 2.10.10-26
Table 2.10.10-10 Stress Components – Impact and Inertial Loads; 30-Foot Top Corner Drop; $\phi = 15.74°$; 1.12-Inch Outer Shell Thickness 2.10.10-30
Table 2.10.10-11 Impact and Inertial Loads; 30-Foot Top Oblique Drop; $\phi = 60°$; 1.12-Inch Outer Shell Thickness 2.10.10-34
Table 2.10.10-12 Stress Components – Impact and Inertial Loads; 30-Foot Side Drop; $\phi = 90°$; 1.20-Inch Outer Shell Thickness; Circumferential Location = 0° 2.10.10-38
Table 2.10.10-13 Stress Components – Thermal; 130°F; 1.20-Inch Outer Shell Thickness 2.10.10-42
Table 2.10.10-14 Stress Components – 50 psi Internal Pressure and Bolt Preload; 1.20-Inch Outer Shell Thickness 2.10.10-46
Table 2.10.10-15 Primary Stresses; 30-Foot Top End Drop; $\phi = 0°$; 1.12-Inch Outer Shell Thickness 2.10.10-50
Table 2.10.10-16 Primary Plus Secondary Stresses; 30-Foot Top End Drop; $\phi = 0°$; 1.12-Inch Outer Shell Thickness 2.10.10-54
Table 2.10.10-17 Primary Membrane (P_m) Stresses; 30-Foot Top End Drop; $\phi = 0°$; 1.12-Inch Outer Shell Thickness 2.10.10-58
Table 2.10.10-18 Primary Membrane Plus Primary Bending ($P_m + P_b$) Stresses; 30-Foot Top End Drop; $\phi = 0°$; 1.12-Inch Outer Shell Thickness 2.10.10-59
Table 2.10.10-19 Primary Membrane (P_m) and Primary Membrane Plus Primary Bending ($P_m + P_b$) Stress Qualification; 30-Foot Top End Drop; $\phi = 0°$; 1.12-Inch Outer Shell Thickness 2.10.10-60
Table 2.10.10-20 Primary Stresses; 30-Foot Top Corner Drop; $\phi = 15.74°$; 1.12-Inch Outer Shell Thickness 2.10.10-61
Table 2.10.10-21 Primary Plus Secondary Stresses; 30-Foot Top Corner Drop; $\phi = 15.74°$; 1.12-Inch Outer Shell Thickness 2.10.10-65
Table 2.10.10-22 Primary Membrane (Pm) Stresses; 30-Foot Top Corner Drop; $\phi = 15.74°$; 1.12-Inch Outer Shell Thickness 2.10.10-69
Table 2.10.10-23 Primary Membrane Plus Primary Bending ($P_m + P_b$) Stresses; 30-Foot Top Corner Drop; $\phi = 15.74°$; 1.12-Inch Outer Shell Thickness 2.10.10-70
Table 2.10.10-24 Primary Membrane (P_m) and Primary Membrane Plus Primary Bending ($P_m + P_b$) Stresses; 30-Foot Top Corner Drop; $\phi = 15.74°$; 1.12-Inch Outer Shell Thickness 2.10.10-71
Table 2.10.10-25 Primary Stresses; 30-Foot Top Oblique Drop; $\phi = 60°$; 1.12-Inch Outer Shell Thickness 2.10.10-72
Table 2.10.10-26 Primary Plus Secondary Stresses; 30-Foot Top Oblique Drop; $\phi = 60°$; 1.12-Inch Outer Shell Thickness 2.10.10-76

List of Tables (continued)

Table 2.10.10-27 Primary Membrane (P_m) Stresses; 30-Foot Top Oblique Drop; ϕ = 60°; 1.12-Inch Outer Shell Thickness 2.10.10-80
Table 2.10.10-28 Primary Membrane Plus Primary Bending ($P_m + P_b$) Stresses; 30-Foot Top Oblique Drop; ϕ = 60°; 1.12-Inch Outer Shell Thickness 2.10.10-81
Table 2.10.10-29 Primary Membrane (P_m) and Primary Membrane Plus Primary Bending ($P_m + P_b$) Stresses; 30-Foot Top Oblique Drop; ϕ = 60°; 1.12-Inch Outer Shell Thickness 2.10.10-82
Table 2.10.10-30 Primary Stresses; 30-Foot Side Drop; ϕ = 90°; 1.20-Inch Outer Shell Thickness; Circumferential Location = 0° 2.10.10-83
Table 2.10.10-31 Primary Plus Secondary Stresses; 30-Foot Side Drop; ϕ = 90°; 1.20-Inch Outer Shell Thickness; Circumferential Location = 0° 2.10.10-87
Table 2.10.10-32 Primary Membrane (P_m) Stresses; 30-Foot Side Drop; ϕ = 90°; 1.20-Inch Outer Shell Thickness; Circumferential Location = 0° 2.10.10-91
Table 2.10.10-33 Primary Membrane Plus Primary Bending ($P_m + P_b$) Stresses; 30-Foot Side Drop; ϕ = 90°; 1.20-Inch Outer Shell Thickness; Circumferential Location = 0° 2.10.10-92
Table 2.10.10-34 Primary Membrane (P_m) Stresses; 30-Foot Side Drop; ϕ = 90°; 1.20-Inch Outer Shell Thickness; Circumferential Location = 90° 2.10.10-93
Table 2.10.10-35 Primary Membrane Plus Primary Bending ($P_m + P_b$) Stresses; 30-Foot Side Drop; ϕ = 90°; 1.20-Inch Outer Shell Thickness; Circumferential Location = 90° 2.10.10-94
Table 2.10.10-36 Primary Membrane (P_m) Stresses; 30-Foot Side Drop; ϕ = 90°; 1.20-Inch Outer Shell Thickness; Circumferential Location = 180° 2.10.10-95
Table 2.10.10-37 Primary Membrane Plus Primary Bending ($P_m + P_b$) Stresses; 30-Foot Side Drop; ϕ = 90°; 1.20-Inch Outer Shell Thickness; Circumferential Location = 180° 2.10.10-96
Table 2.10.10-38 Primary Membrane (P_m) and Primary Membrane Plus Primary Bending ($P_m + P_b$) Stress Qualification; 30-Foot Side Drop; ϕ = 90°; 1.20-Inch Outer Shell Thickness; Circumferential Location = 0° 2.10.10-97
Table 2.10.11-1 Geometric Dimensions of the Cask 2.10.11-9
Table 2.10.11-2 Comparison of the Hand-Calculated and Finite Element Results 2.10.11-10
Table 2.10.12-1 Determination of Maximum Energy Remaining for Secondary Impact – Full-Scale Impact Limiter 2.10.12-30
Table 2.10.12-2 Determination of Extreme Force During Cask Deceleration (First Limiter) – Quarter-Scale Impact Limiter 2.10.12-31
Table 2.10.14-1 Material Designations for Sections 2.10.14-11
Table 2.10.14-2 1-Foot Side Drop with Internal Pressure, P_m Stresses, ksi 2.10.14-12
Table 2.10.14-3 Side Drop with Internal Pressure, $P_m + P_b$ Stresses, ksi 2.10.14-13
Table 2.10.14-4 1-Foot Side Drop with Internal Pressure, P + Q Stresses, ksi 2.10.14-14
Table 2.10.14-5 1-Foot Top-End Drop with Normal Internal Pressure, P_m Stresses, ksi 2.10.14-15

List of Tables (continued)

Table 2.10.14-6 1-Foot Top-End Drop with Internal Pressure, $P_m + P_b$ Stresses, ksi.. 2.10.14-16
Table 2.10.14-7 1-Foot Top-End Drop with Internal Pressure, P + Q Stresses, ksi 2.10.14-17
Table 2.10.14-8 1-Foot Top-Corner Drop with Internal Pressure, P_m Stresses, ksi..... 2.10.14-18
Table 2.10.14-9 1-Foot Top-Corner Drop with Internal Pressure, $P_m + P_b$ Stresses, ksi..... 2.10.14-19
Table 2.10.14-10 1-Foot Top-Corner Drop with Internal Pressure, P + Q Stresses, ksi 2.10.14-20
Table 2.10.14-11 1-Foot Bottom-End Drop with Internal Pressure, P_m Stresses, ksi.... 2.10.14-21
Table 2.10.14-12 1-Foot Bottom-End Drop with Internal Pressure, $P_m + P_b$ Stresses, ksi..... 2.10.14-22
Table 2.10.14-13 1-Foot Bottom-End Drop with Internal Pressure, P + Q Stresses, ksi..... 2.10.14-23
Table 2.10.14-14 1-Foot Bottom-Corner Drop with Internal Pressure, P_m Stresses, ksi..... 2.10.14-24
Table 2.10.14-15 1-Foot Bottom-Corner Drop with Internal Pressure, $P_m + P_b$ Stresses, ksi..... 2.10.14-25
Table 2.10.14-16 1-Foot Bottom-Corner Drop with Internal Pressure, P + Q Stresses, ksi..... 2.10.14-26
Table 2.10.14-17 30-Foot Side Drop with Internal Pressure, P_m Stresses, ksi..... 2.10.14-27
Table 2.10.14-18 30-Foot Side Drop with Internal Pressure, $P_m + P_b$ Stresses, ksi..... 2.10.14-28
Table 2.10.14-19 30-Foot Top-End Drop with Internal Pressure, P_m Stresses, ksi 2.10.14-29
Table 2.10.14-20 30-Foot Top-End Drop with Internal Pressure, $P_m + P_b$ Stresses, ksi..... 2.10.14-30
Table 2.10.14-21 30-Foot Top-Corner Drop with Internal Pressure, P_m Stresses, ksi ... 2.10.14-31
Table 2.10.14-22 30-Foot Top-Corner Drop with Internal Pressure, $P_m + P_b$ Stresses, ksi..... 2.10.14-32
Table 2.10.14-23 30-Foot Bottom-End Drop with Internal Pressure, P_m Stresses, ksi.. 2.10.14-33
Table 2.10.14-24 30-Foot Bottom-End Drop with Internal Pressure, $P_m + P_b$ Stresses, ksi..... 2.10.14-34
Table 2.10.14-25 30-Foot Bottom-Corner Drop with Internal Pressure, P_m Stresses, ksi..... 2.10.14-35
Table 2.10.14-26 30-Foot Bottom-Corner Drop with Internal Pressure, $P_m + P_b$ Stresses, ksi..... 2.10.14-36
Table 2.10.14-27 Accident Internal Pressure with Inertia Load, P_m Stresses, ksi 2.10.14-37
Table 2.10.14-28 Accident Internal Pressure with Inertia Load , $P_m + P_b$ Stresses, ksi. 2.10.14-38

2.2 Weights and Centers of Gravity

2.2.1 Major Component Statistics

The weights of the major components of the NAC-LWT cask and their respective centers of gravity are presented in Table 2.2.1-1. The axial location of the center of gravity is measured from the bottom surface of the cask body. The center of gravity is always on the longitudinal centerline of the cask because the cask is essentially axisymmetric about that axis. The center of gravity location of the fuel is representative of typical fuel configurations.

The weights and centers of gravity of the cask package in eight different shipping configurations are presented in Table 2.2.1-2. In each case, the center of gravity is measured from the bottom surface of the cask body. The term "loaded" refers to the presence of fuel or other radioactive materials in the cask cavity; the term "empty" implies the absence of any fuel or other radioactive materials in the cask cavity. However, the fuel basket does remain in the cask cavity for the "empty" configuration. The weight of a lifting yoke is not included in the tabulated package weights.

All of the values tabulated in Table 2.2.1-1 and Table 2.2.1-2 are calculated to the nearest pound to obtain an accurate cask weight and center of gravity. The cask package weight and center of gravity used in the analyses of this report are the design values - 52,000 pounds and 98.93 inches. A design value of 4,000 pounds is conservatively used for the total weight of the cask contents (including the appropriate basket).

Table 2.2.1-1 Weights of the NAC-LWT Cask Major Components

Component	Weight (pounds)	Axial Center of Gravity Location (inches)
Cask Body	39,906	96.46
Closure Lid and Bolts	941	195.11
Impact Limiters Top Bottom	 1,535 1,320	 202.98 -3.18
Shield Tank Fluid	3,506	96.26
PWR Fuel Basket and Spacer	874	100.98
PWR High Burnup Rod Payload	1,620	95.33
PWR Fuel Payload (Maximum)	3,126	96.63
BWR Fuel Basket	1,124	97.88
BWR Fuel Payload	1,500	97.88
Metallic Fuel Basket	128	96.40
Metallic Fuel Payload	2,080	96.40
MTR Four Unit Basket MTR Four Unit Fuel Payload	982 840[1]	96.20 96.20
MTR Four Unit PULSTAR Fuel Payload	2,240[2]	96.20
MTR Five Unit Basket	1,015	96.20
MTR Five Unit Fuel Payload	1,050[1]	96.20
MTR Six Unit Basket	1,002	96.20
MTR Six Unit Fuel Payload	1,260[1]	96.20
GA IFM Basket and Spacer	818	98.06
GA IFM Fuel Payload	148	167.34
TPBAR Basket and Spacer	675	110.40
TPBAR Payload	978[3]	96.00
ANSTO Basket	911	100.95
ANSTO Payload	756	100.95
TPBAR Basket	575	97.43
TPBAR with Rod Transport Canister Payload	1,326[4]	102.26

[1] For conservatism, a design basis MTR fuel weight of 30 lbs/assy is used in the structural analysis. The maximum MTR element weight is 13.2 lbs for an intact element and 9.7 lbs for the cut elements in the 42-element configuration.

[2] For conservatism, a bounding weight of 80 pounds is considered for each of the 28 fuel cells for PULSTAR fuel

[3] TPBAR payload represents the combined weight of the TPBAR and consolidation canister. A conservative 1,000 lb weight is applied in the structural analysis.

[4] TPBAR with Rod Transport Canister payload represents the combined weight of the 25 TPBARs, the PWR/BWR Rod Transport Canister and the PWR insert.

Table 2.2.1-2 Weights and Center of Gravity Locations for the NAC-LWT Cask Shipping Configurations

Component	Weight (pounds)	Axial Center of Gravity Location (inches)
Package -Loaded for Shipment (PWR) Maximum Payload	51,208	98.96
Package – Loaded for Shipment PWR High Burnup Rods	49,702	99.0
Package - Empty for Shipment (PWR)	48,082	99.12
Package - Loaded for Shipment (BWR)	49,832	99.00
Package - Empty for Shipment (BWR)	48,332	99.07
Package - Loaded for Shipment* (Metallic Fuel)	45,910	98.88
Package - Empty for Shipment* (Metallic Fuel)	43,830	99.09
Package - Loaded for Shipment (PULSTAR Fuel, MTR Four Unit Basket)	50,430	99.1
Package - Loaded for Shipment (MTR Fuel, Four Unit Basket)	49,030	99.1
Package - Empty for Shipment (MTR Fuel, Four Unit Basket)	48,190	98.9
Package - Loaded for Shipment (MTR Fuel, Five Unit Basket)	49,273	99.1
Package - Empty for Shipment (MTR Fuel, Five Unit Basket)	48,223	98.9
Package - Loaded for Shipment (MTR Fuel, Six Unit Basket)	49,470	99.1
Package - Empty for Shipment (MTR Fuel, Six Unit Basket)	48,210	98.9
Package - Loaded for Shipment (GA IFM Fuel and Basket)	48,147	99.3
Package - Empty for Shipment (GA IFM Basket)	48,026	99.3
Package – Loaded for Shipment (TPBARs and Basket)	48,861	99.2
Package – Empty for Shipment (TPBAR Basket)	47, 883	99.2
Package - Loaded for Shipment (ANSTO Fuel and Basket)	48,875	99.2
Package - Empty for Shipment (ANSTO Basket)	48,119	99.1

* Neutron Shield Tank is empty.

Table 2.2.1-2 Weights and Center of Gravity Locations for the NAC-LWT Cask Shipping Configurations (cont'd)

Component	Weight (pounds)	Axial Center of Gravity Location (inches)
Package - Loaded for Shipment TPBARs in the PWR/BWR Rod Transport Canister	49,109	99.2
Package - Empty for Shipment (TPBAR Basket for PWR/BWR Rod Transport Canister)	47,783	99.1
Package - Design for Shipment	52,000	98.93

2.6.7 Free Drop (1 Foot)

The free drop scenario outlined by Subpart F of 10 CFR 71 requires the NAC-LWT cask to be structurally adequate for a 1-foot drop (normal transport conditions) onto a flat, essentially unyielding, horizontal surface in the orientation that inflicts the maximum damage to the cask. The following sub-sections evaluate the cask body; the impact limiters; the closure lid and bolts; the neutron shield shell; the expansion tank shell; and the upper ring components; for the end, side, and corner drop orientations.

2.6.7.1 End Drop (1 Foot)

2.6.7.1.1 Discussion

The NAC-LWT cask is analyzed for the effects of a normal operations end drop impact condition. The event scenario is that the NAC-LWT cask, equipped with an impact limiter, drops 1 foot onto a flat, unyielding, horizontal surface. The cask strikes the surface in a vertical position on either its bottom or its top end.

The 1-foot end drop analysis can be carried out in an identical fashion as was used in the 30-foot accident end drop analysis, Section 2.7.1.1. The general comments, analysis descriptions and the analysis method described in Section 2.7.1.1 also apply to this section.

The only difference between the 30-foot end drop analysis (Section 2.7.1.1) and this 1-foot end drop analysis is the magnitude of the impact force, i.e., impact load, which is expressed in terms of a g factor. The magnitude of the impact force varies with the different drop heights. As calculated in Section 2.6.7-4, the g loads for the 1-foot end drop condition and for the 30-foot end drop condition are 15.8 g and 60 g, respectively. These g loads are conservatively based on a maximum crush strength of 3850 psi for the aluminum honeycomb impact limiters, although the design maximum crush strength is 3675 psi. Also, these analyses conservatively use a 1.12-inch thick outer shell, although the actual outer shell thickness is 1.20 inches. Using the analysis results obtained in Section 2.7.1.1 to represent the structural response of the NAC-LWT cask for the 1-foot end drop condition is conservative and acceptable. Therefore, Tables 2.7-1 through 2.7-15 were used to compose Table 2.6.7-1 through Table 2.6.7-16, for the 1-foot drop analyses. The most critical sections for each component during a particular loading condition are shown in Figure 2.6.7-1 through Figure 2.6.7-5. The critical P_m, $P_m + P_b$, and total stresses for each component are documented in Table 2.6.7-1 through Table 2.6.7-16. The allowable stresses are those defined in Section 2.1.2 for the normal operations conditions based on 300°F. Note that the maximum cask component temperatures are below 300°F for all of the conditions that are considered. Additionally, the stresses at representative sections throughout the cask are

presented in the tables in Section 2.10.7. These tables document the maximum stress locations tabulated for each component.

The secondary stresses (thermal) are conservatively included in the primary stress categories and margin of safety calculations; therefore, the 3 S_m limit on the S_n stress intensity range is satisfied. This is because it is enveloped by the 1.5 S_m limit on $P_m + P_b$ stress intensity.

2.6.7.1.2 Results and Conclusions

Since the margins of safety are positive for all of the cask components, the NAC-LWT cask maintains its containment capability and satisfies the 10 CFR 71 requirements for the 1-foot normal operations end drop condition.

2.6.7.2 Side Drop (1 Foot)

2.6.7.2.1 Discussion

This section presents the evaluation of the structural adequacy of the NAC-LWT cask for the 1-foot side drop impact condition. In this event, the NAC-LWT cask with impact limiters attached over each end experiences a free drop through a distance of 1 foot onto a flat, unyielding surface, and strikes the surface in a horizontal position.

The 1-foot side drop analysis is performed in the same manner as was done for the 30-foot side drop analysis in Section 2.7.1.2. The general comments, analysis descriptions, and the analysis methods described in Section 2.7.1.2 also apply to this section.

The difference between the 30-foot side drop analysis and the 1-foot side drop analysis is the magnitude of the impact force, which varies because of the different drop heights. As determined in Section 2.6.7.4, the g loads for the 1-foot side drop condition and for the 30-foot side drop accident condition are 24.3 g and 49.7 g, respectively.

Analysis of the NAC-LWT cask for the normal operations conditions side drop follows the same methodology as used for the accident side drop analysis. Because all calculations for the accident side drop analysis are performed on a basis of linear elastic behavior, the stress components for the 1-foot side drop condition are calculated by multiplying the 30-foot side drop stress components (resulting from the effects of inertial and impact loads) by the ratio of the 1-foot side drop g load to the 30-foot side drop g load. These stress components are then combined with those induced by the thermal effects, internal pressure, and bolt preload.

2.6.7.2.2 Results and Conclusions

Since the material properties of the cask structure are temperature-dependent, varying environmental temperatures will produce changes in the calculated stresses in the cask for the thermal load cases. Environmental temperatures will not change the calculated stresses in the

cask produced by other types of loads. This is verified by comparing the finite element results for the NAC-LWT cask subjected to a gravity load for different temperature conditions. Also, the stress levels produced by the following thermal loading conditions were evaluated: (1) 100°F ambient temperature with maximum decay heat load, (2) -40°F ambient temperature with maximum decay heat load, and (3) -40°F ambient temperature with no decay heat load. The combination effect of the thermal loads with other load types (e.g., inertial body load) has also been studied. It is determined that the side drop event with 100°F ambient temperature represents the worst case for the normal operations 1-foot side drop condition. Therefore, only the stress results produced by a 1-foot side drop with 100°F ambient temperature are reported.

Stress components and stress intensities are calculated throughout the finite element model for the combined loads due to internal pressure, bolt preload, thermal, inertia, and impact. Table 2.6.7-16 through Table 2.6.7-19 report the P_m stress intensities, the $P_m + P_b$ stress intensities, the S_n stress intensities, and the total stress intensities for each cask component, which are obtained from the finite element side drop analysis. Additionally, the stresses at representative sections throughout the cask are presented in the tables in Section 2.10.7. These tables document the maximum stress locations tabulated for each component.

As mentioned previously, the finite element cask model conservatively ignores the effect of the neutron shield shell on the overall bending of the cask structure.

The margins of safety reported in Table 2.6.7-16 through Table 2.6.7-18 are positive for all cask components. It has been demonstrated that all margins of safety are positive for the normal operations 1-foot side drop condition.

The NAC-LWT cask maintains its containment capability and satisfies the 10 CFR 71 requirements for the normal operations 1-foot side drop condition.

2.6.7.3 Corner Drop (1 Foot)

2.6.7.3.1 Discussion

The analysis of the NAC-LWT cask for a 1-foot corner drop condition uses the same methods as those used for the hypothetical accident oblique drop analyses. The general comments, analysis descriptions, and analysis methods discussed in Section 2.7.1.3 also apply to this section. The difference between the hypothetical accident analysis and the normal operations conditions analysis in this section is the drop height. Refer to Section 2.6.7.4 for the calculation of the g loads induced by a normal operations conditions 1-foot corner drop and by an accident condition 30-foot corner drop. These g loads are conservatively based on a maximum crush strength of 3850 psi for the aluminum honeycomb impact limiters, although the design maximum crush strength is 3675 psi. The stress components for the 1-foot corner drop are calculated by multiplying the accident condition stress components (resulting from the effects of inertial and

impact loads) by the ratio of the 1-foot corner drop g load to the 30-foot corner drop g load. These stress components, then, are combined with those resulting from internal pressure, bolt preload, and thermal effects. These analyses conservatively use a 1.12-inch thick outer shell, although the actual outer shell thickness is 1.20 inches.

2.6.7.3.2 Results and Conclusions

The most critical sections for each component during a particular loading condition are shown in Figure 2.6.7-7 through Figure 2.6.7-9. Table 2.6.7-20 through Table 2.6.7-23 report the maximum P_m stress intensities, the maximum $P_m + P_b$ stress intensities, the maximum S_n stress intensities, and the maximum total stress intensities for each component resulting from the 1-foot top corner drop condition with a 130°F ambient temperature and maximum decay heat load. Similarly, Table 2.6.7-24 through Table 2.6.7-27 report those stress intensities resulting from the 1-foot bottom corner drop condition with a 130°F ambient temperature and maximum decay heat load. Also, Table 2.6.7-28 through Table 2.6.7-31 report the stress intensities for each component resulting from the 1-foot top corner drop condition with a -40°F ambient temperature. Additionally, the stresses at representative sections throughout the cask are presented in the tables in Section 2.10.7. These tables document the maximum stress locations for each component.

It has been demonstrated that all margins of safety are positive for the normal operations 1-foot corner drop condition. The NAC-LWT cask maintains its containment capability and satisfies the 10 CFR 71 requirements for the normal operations 1-foot corner drop condition.

2.6.7.4 Impact Limiters

2.6.7.4.1 Introduction

Removable impact limiters are supplied with the NAC-LWT cask to ensure that the design impact loads on the cask are not exceeded for any of the defined impact conditions. These defined conditions are:

1. The cask falls 1 foot and lands on: (a) its side, impacting both limiters simultaneously; (b) flat on one limiter at either end; or (c) oblique on either corner (the center of gravity is directly above the corner of the impact limiter).
2. The cask, having experienced a normal operating conditions 1-foot drop, is dropped through a distance of 30 feet and lands on its end, its side, or at any oblique angle. The impact limiter analysis considers a 31-foot drop (1 foot + 30 feet). This provides conservative impact loads, which are used in the cask analyses.

2.6.7.4.2 Assumptions

The following assumptions form the basis for the impact limiter analysis:

1. The cask impacts on an unyielding surface.
2. The impact limiter remains in position on the cask during all impact events. (The qualification of the impact limiter attachment is presented in Section 2.6.7.4.7.)

2.6.7.4.3 Load Conditions

The impact limiters described and analyzed in the following paragraphs decelerate the cask by applying a force in the direction opposite the motion of the cask. The deceleration force is generated by crushing the aluminum honeycomb material of the limiter between the cask and the unyielding surface. The energy absorbed during crushing is the net force, the vector sum of the cask weight (downward) and the deceleration force (upward), multiplied by the distance crushed. The amount of energy an impact limiter can absorb is calculated for various cask impact orientations, from vertical (0°) to horizontal (90°).

The specific loading conditions for the impact limiters are defined by 10 CFR 71.71(c)(7), 10 CFR 71.73(c)(1) and Regulatory Guide 7.8, as follows:

1. A 1-foot fall of the cask on one limiter, impacted at any angle from vertical (flat end) to corner (cask center of gravity is directly above the point of impact).
2. A 1-foot fall of the cask horizontally, so that the side surfaces of both limiters impact the unyielding surface simultaneously.
3. Any of the 1-foot falls can be followed by a 30-foot fall at an end, a side, or an oblique orientation.

Based on these loading conditions, the NAC-LWT cask impact limiters are designed for a 31-foot fall. Either of the first two conditions plus the third condition is equivalent to a single drop at the combined heights, as explained in Section 2.6.7.4.5. The maximum impact force and the maximum crush depth for the 1-foot falls are obtained from the computer output for the 31-foot fall analyses at the value of the energy dissipated in a 1-foot fall. This method is explained in Section 2.6.7.4.5.

2.6.7.4.4 Descriptions - Impact Limiters

Figure 2.6.7-10 shows the location on the cask and the primary dimensions of the impact limiters. A different impact limiter is used on the bottom of the cask to reduce weight. The top impact limiter diameter is larger because it is required to clear the cask lifting trunnions and to be of sufficient depth over the trunnions to prevent the limiter from behaving as a solid in the event of a side impact. The larger diameter provides greater distance from the point of impact to the cask body; however, the effective depth of the limiter is maintained at the trunnions and the same corner impact absorption capability is retained. Figure 2.6.7-11 shows a cross-section of the top impact limiter.

The bottom impact limiter does not have the cut-outs for the trunnions. It has a smaller outside diameter and larger bottom depth than the top impact limiter.

Each impact limiter consists of two different layers of aluminum honeycomb, which are enclosed in a thin outer aluminum shell. The layers of aluminum honeycomb are separated by a thin aluminum sheet. The honeycomb material absorbs the impact energy as it is crushed. A typical load versus deflection curve for aluminum honeycomb is presented in Figure 2.6.7-12. The force deflection curves and test data for the NAC-LWT cask impact limiters at the various drop angles are provided in Appendix 2.10.12. The nominal crush strength of the bottom layer of aluminum honeycomb is 250 psi axially, and is negligible radially. The nominal crush strength of the second layer is 3500 psi in both the axial and the radial directions. The tolerance on the crush strength is +5, -10 percent. The bottom, 250-psi crush strength, single-directional layer of honeycomb material absorbs the majority of the energy in a 1-foot flat impact on the end, and limits the impact force to a value acceptable for normal operations. The lower crush strength is necessary because the impact area is considerably greater in a flat bottom impact than in any other orientation. The second, 3500-psi crush strength, multi-directional layer of honeycomb material absorbs the majority of the energy in an impact on the corner of the impact limiter, and all of the energy in an impact on the side of the impact limiter. Both crushable aluminum honeycomb materials behave as a solid when compressed to 30 percent of their original depth.

The outside diameters of the impact limiters are 65.25 inches and 60.25 inches for the top and bottom impact limiters, respectively. The depth of the bottom aluminum honeycomb layer is 1.5 inches on each limiter. The second aluminum honeycomb layer is 14.0 inches deep for the top impact limiter and 14.5 inches for the bottom impact limiter. The top impact limiter has four recesses to provide clearance around the trunnions. This clearance is closed during the impact for a 30-foot side drop. Therefore, the trunnion provides a rigid foundation for the impact limiter in the region near the trunnion.

The impact limiter shells are positioned against the cask lid and bottom surfaces; the impact limiters overlap the cask cylinder by a length of 12 inches. The shells are mechanically attached to the cask as described in Section 2.6.7.4.7.

For each of the impact load conditions considered in this analysis, the impact limiters remain in position on the cask and absorb the energy of the impact; thus, they limit the impact load to the values calculated in this section.

2.6.7.4.5 Method of Analysis

The primary areas of analytical evaluation that are required in an impact limiter analysis are: (1) crush depth; (2) maximum crush force; and (3) attachment to the cask. The crush depth and

maximum crush force are dependent on the crush strength of the crushable material, the area engaged in crushing, the geometry of the impact limiter, and the energy to be dissipated.

Deceleration forces for constant crush strength aluminum honeycomb impact limiters are directly related to the area crushing. The area engaged in crushing can be best explained by examining the experimental results of a top end drop impact test. Figure 2.6.7-13 shows a quarter-scale model impact limiter just before crushing begins. The cask and the unyielding surface are rigid and undeformable compared to the honeycomb material. The 3.9 inches of honeycomb material are trapped in place between the cask and the impacted surface.

The 250-psi crush strength honeycomb is designed to absorb the potential energy of the cask in a 1-foot drop. The area of the 250-psi honeycomb covering the entire bottom of the impact limiter is 208.7 square inches. The higher crush strength honeycomb structurally supports or "backs" the lower crush strength honeycomb, even if just the cask backs the higher crush strength honeycomb. The force necessary to begin crushing the 250 psi crush strength material is 52,168 pounds. The quarter-scale model weighs approximately 800 pounds; therefore, the 52,168 pounds of force is equivalent to 65 g for the model (The normal operation g-load for the full-size cask is calculated to be 16.3 g).

The 3500-psi crush strength honeycomb absorbs the kinetic energy of the cask in a 30-foot drop. The area of the bottom of the scale model cask is 40.7 square inches. The force necessary to crush the 3500-psi crush strength honeycomb trapped between the model cask and the impacted surface is 142,500 pounds, or 178 g, based on the model weight of 800 pounds.

A force imbalance is immediately established between the lower and higher strength honeycombs at the onset of crushing. It requires 52,168 pounds to crush the lower strength honeycomb, which is 2.7 times smaller than the force required to crush the higher strength honeycomb. The lower strength honeycomb of constant crush strength will crush until lock-up occurs. When lock-up occurs, the crush strength of the lower strength honeycomb increases and exceeds that of the higher strength honeycomb. Crushing now begins beneath the cask because the force to crush the 16.3-inch diameter of the locked-up, lower strength honeycomb exceeds the 142,500 pounds necessary to crush the backed-up higher strength honeycomb.

The cask has kinetic energy gained while falling prior to the impact limiter contacting the unyielding surface. (Section 2.10.12 gives a more complete description of the kinetic energy gain.) Some kinetic energy was dissipated in crushing the lower strength honeycomb. The remaining energy will be absorbed by crushing the higher strength honeycomb between the cask and the impacted surface. The cask "backs" the higher crush strength honeycomb; therefore, the maximum force is easily compared with the average maximum force from the quasi-static test as adjusted to reflect the dynamic crush strength of the honeycomb (For an explanation of the term "dynamic" as applied to quasi-static tests, refer to Appendix 2.10.12).

Figure 2.6.7-14 is a photograph of a section of an end impact tested quarter-scale limiter. The average maximum force from the end drop quasi-static crush test is 158,400 pounds. If the backed and unbacked area were to crush, the required force would be 3500 psi x $\pi/4$ $(16.3)^2$ = 730,400 pounds of force. This is a factor of 4.6 times more than the actual measured force and shows that the unbacked area did not contribute to the limiter force. The calculated maximum force using the backed-up area of the limiter is approximately 11 percent lower than the test results. The scale model limiter crush test, therefore, demonstrates that the unbacked area did not crush and generate a force. One reason for the difference is the shearing of the high crush strength honeycomb, which is clearly visible in Figure 2.6.7-14. Shearing acts in a plane, surrounding the shear area. In an end impact crush, the plane is a thin ring with a diameter equal to the diameter of the cask. Since the crush force is proportional to the backed area, which depends on the square of the cask diameter, for the full-scale impact limiters, shearing becomes a much less significant part of the maximum force.

Figure 2.6.7-14 shows the sequence of crushing and the backed area as described above. The lower crush strength honeycomb is crushed to stack height completely to the outer edge of the cask. Higher crush strength honeycomb beneath the cask is crushed, while material on the "other side" of the shear plane is uncrushed.

The combination of the accurate prediction of measured impact limiter crush forces and the visual evidence in the sectioned limiter after the test shows that only the backed-up area crushes for aluminum honeycomb with a 3500-psi, multi-directional, dynamic crush strength.

The cask orientation for a corner impact is defined by the angle from vertical of the cask's longitudinal axis when the cask center of gravity is vertically aligned with the impact point on the limiter. This angle is 15.74 degrees for the top limiter and 14.52 degrees for the bottom limiter.

A proprietary computer program, RBCUBED, is used to analyze an impact limiter for an impact event, to determine the dynamics of the event, to determine the forces generated during that event, and to determine the depth of crush (Section 2.10.1.2).

The computer program, RBCUBED, is run for many combinations of crushable material strength until satisfactory results are obtained. Two runs are made for each impact orientation. One run is made using the maximum value of the aluminum honeycomb crush strength, 105 percent of the nominal crush strength, to determine the maximum force on the cask. A second run, using the minimum value for the aluminum honeycomb crush strength, 90 percent of the nominal crush strength, is also made to find the maximum crush depth of the crushable material.

A single RBCUBED run is necessary to determine the reaction force for a 1-foot fall and a subsequent 30-foot fall. The 1-foot fall crushes the limiter a distance (δ_1), and absorbs

12 inches × 52,000 lbs = 0.624×10^6 inch-pounds of energy. Then, the impact limiter must absorb the additional energy of 360 inches × 52,000 lbs = 18.72×10^6 inch-pounds by crushing an additional distance (δ_2) from a 30-foot drop. The total displacement is $\delta_1 + \delta_2$ and the total energy is $(18.72 + 0.624) \times 10^6 = 19.344 \times 10^6$ inch-pounds. Dividing this energy by the cask weight gives 372 inches (31 feet), which demonstrates that a 1-foot fall followed by a 30-foot fall can be evaluated from data for a 31-foot fall. The maximum impact force and the maximum crush depth for the 1-foot fall can be obtained from the RBCUBED output for the 31-foot fall analysis at the value of the energy dissipated in a 1-foot fall.

2.6.7.4.6 Results

The data in Table 2.6.7-32 and Table 2.6.7-33 give the results of the impact limiter design analyses for a 1-foot fall and a subsequent 30-foot fall, respectively. The calculated g loads for the 30-foot fall side impact are based on the 3675-psi design maximum crush strength of the multidirectional aluminum honeycomb. The calculated g loads for all of the other 1-foot and 30-foot fall impacts are conservatively based on an aluminum honeycomb maximum crush strength of 3850 psi. A design cask weight of 52,000 lbs is used.

The calculated (RBCUBED) and measured (quasi-static, adjusted for dynamic crush strength) force-deflection curves for the NAC-LWT cask impact limiters for all drop orientations are presented in Appendix 2.10.12. To verify the results, the area under the curves is calculated by the trapezoidal method. This area represents the energy dissipated for each of the cases, i.e., $E_{max} = 19.344 \times 10^6$ inch-pounds for the top limiter at maximum strength, and $E_{min} = 19.206 \times 10^6$ inch-pounds for the bottom limiter at minimum strength. The potential energy to be dissipated consists of the cask weight (52,000 lbs) multiplied by the distance the cask falls (372 inches), i.e., $E_p = 372 \times 52{,}000 = 19.344 \times 10^6$ inch-pounds. The calculated and actual values compare within 0.71 percent, which indicates that the proper amount of potential energy is dissipated in the RBCUBED analysis. Another check is to multiply the total crush area (the maximum area backed by the cask) by the crush strength of the impact limiters to determine the reacting force. This hand-calculated value of the reaction force for maximum impact limiter crush strength compares within 0.38 percent of the RBCUBED calculated value for the bottom impact limiter and within 1.88 percent for the top impact limiter. The hand-calculated value of the reaction force for minimum impact limiter crush strength compares within 0.46 percent of the RBCUBED calculated value for the bottom impact limiter and within 1.83 percent for the top impact limiter. These results verify both the energy absorption and the reaction force calculations of RBCUBED for the impact limiters.

A study of a side drop shows that the cask will come to rest at an angle of 0.76 degrees with the horizontal because the radius of the top limiter is 2.5 inches larger than that of the bottom limiter.

The RBCUBED analysis, analyzing the side drop as horizontal, is not affected by this small angle because the horizontal component of the forces is negligible.

With both impact limiters at their minimum allowable crush strength (maximum crush depth case), clearance is maintained between the neutron shield/expansion tank and the unyielding surface for the 1-foot side impact.

An evaluation of the displacements obtained from the RBCUBED runs is as follows:

1. The RBCUBED run for the 31-foot side drop assumes the cask is a rigid element and does not include the trunnions; therefore, the displacement from the 31-foot drop must be analyzed, by referring to Figure 2.6.7-11, as follows:

   The free distance of crushable material between the impact limiter and the trunnion equals 14.995 inches. The aluminum honeycomb compresses to 70 percent of its free height before exhibiting behavior as a solid (10.497 inches). The RBCUBED run for the 31-foot side drop with the crushable material at minimum strength calculates a crush depth of 10.00 inches; thus, 0.497 inch of crushable material remains before solid height occurs. Therefore, an impact directly on a trunnion does not change the energy absorbing characteristics of the impact limiter for this condition.

   The impact from a 31-foot side drop on the bottom impact limiter with the crushable material at minimum strength exhibits solid behavior at a displacement of 10.73 inches, which leaves 0.43 inch displacement before solid height occurs (crush depth = 10.30 inches).

2. The impact from a 31-foot flat end drop onto the top impact limiter with the crushable material at minimum strength exhibits solid behavior at a displacement of 10.85 inches, which leaves 0.61 inch displacement before solid height occurs. Similarly, for the bottom impact limiter, solid behavior occurs at 11.20 inches, which leaves 0.90 inch displacement before solid height occurs.

3. For a 31-foot corner drop on the top impact limiter with the crushable material at minimum crush strength, the crush distance of 12.72 inches is much less than the solid height displacement of 16.86 inches. Similarly, for the bottom impact limiter, the 12.70-inch crush distance is much less than the 15.83-inch solid height displacement.

The cask analysis for these impact conditions is based on the maximum deceleration (g) derived from the RBCUBED results. The critical condition for maximum lateral deceleration from both a 1-foot and a 31-foot drop is the side drop with the crushable material at its maximum strength. The critical condition for maximum longitudinal deceleration from a 1-foot drop is the flat bottom drop with the crushable material at its maximum strength, and from a 31-foot drop is the corner drop. The longitudinal component of the deceleration from the 31-foot corner drop was used as the longitudinal criteria; that is, 60.4 cos 15.74 degrees equals 58.1 g. Nevertheless, a 60.0 g (deceleration) is conservatively used as the maximum longitudinal deceleration. The design g load factors (deceleration values) for the NAC-LWT cask analyses are summarized in Table 2.6.7-34. The design g load for the 31-foot side drop is based on the 3675-psi design

maximum crush strength of the aluminum honeycomb impact limiters. The design g loads for all of the other 1-foot and 31-foot drops are conservatively based on an aluminum honeycomb maximum crush strength of 3850 psi.

2.6.7.4.7 Impact Limiter Attachment Analysis

A three-part design criteria applies to the method of attachment of the impact limiters to the cask body. These three criteria are as follows:

1. The impact limiters must remain attached to the cask body during normal handling and transport. Satisfaction of this criterion ensures that the limiters will be in a proper position to perform their impact limiting function in the event of a free drop (normal or accident).
2. In a free drop (normal or accident), the limiter(s) making initial contact with the unyielding surface must remain in position on the end(s) of the cask for the full duration of the initial impact. Satisfaction of this criterion ensures that the limiter(s) will be able to properly perform their impact limiting function.
3. In a free drop (normal or accident) involving an initial impact on a single impact limiter, the limiter on the opposite end of the cask must remain attached to the cask during the initial impact. Satisfaction of this criterion ensures that the limiter will be in a proper position to perform its impact limiting function in a subsequent secondary impact following the initial impact.

Section 2.6.7.4.7 demonstrates that each of the above criterion are satisfied.

Impact Limiter Attachment During Normal Handling and Transport

Attachment of the impact limiters to the cask body during normal handling and transport is ensured by demonstrating that the attachment hardware (pins, lugs and associated welds) does not yield under normal handling and transport conditions. The worst case loading associated with normal handling and transport is taken to be a 2.0-g load corresponding to the peak shock loading expected as the result of truck transport (per ANSI N14.23 for air ride suspensions). For this normal condition evaluation, it will be assumed that only two of the four attachment points for each limiter are effective. The load, P, per attachment point therefore becomes:

$$P = 2.0(1535)/2$$
$$= 1{,}535 \text{ lbs}$$

where 1,535 lbs is the weight of the heaviest (top) impact limiter.

Analysis of Impact Limiter Lug

The geometry of the impact limiter lug is as shown in Figure 2.6.7-15. As shown, the lug has an outer width of 2.0 inches, a hole diameter of 0.53 inch and an edge distance of 1.7 inches. The lug is made of 6061-T6 aluminum and is 0.5 inch thick. According to Table 2.3.1-5, the yield

strength of the aluminum at 150°F is 32,700 psi. Potential failure modes of tension across the net section and 40-degree shearout are considered as follows:

Tension Across the Net Section

$P = 1{,}535$ lbs

$A = 0.5(2.0 - 0.53)$

$= 0.735$ in^2

$S_t = 1535/0.735 = 2088$ psi ($S_y = 32{,}700$ psi)

$MS = 32{,}700/2088 - 1$

$= +$Large

40-Degree Shearout

$P = 1{,}535$ lbs

$e = 1.7 - (0.53/2) \cos 40°$

$= 1.497$ inches

$A_s = 2(0.5)(e)$

$= 1.497$ in^2

$S_s = 1535/1.497$

$= 1025$ psi ($0.6\ S_y = 19{,}620$ psi)

$MS = 19{,}620/1025 - 1$

$= +$Large

Analysis of Cask Lug

The geometry of the cask lug is a shown in Figure 2.6.7-16. As shown, the lug actually consists of two, 0.5-inch thick lugs, which are integral to a common base plate (the lugs and base plate are machined from one piece). Each of these two lugs is 2.0 inches wide, has a hole diameter of 0.53 inch and has a minimum edge distance of 0.72 inch. The base plate is 1.6 inches wide and 2.0 inches long. The material used is Type 304 stainless steel, which exhibits a yield strength at 150°F of 27,500 psi. Potential failure modes of 40-degree shearout and failure of the weld (3/8-inch bevel plus 3/8-inch fillet), which attaches the base plate to the cask body, are considered as follows:

40-Degree Shearout

$F = P/2 = 1535/2$

$= 768$ lbs

$e = 0.72 - (0.53/2) \cos 40°$

$= 0.517$ in

A_s = 2(0.5)(e)

= 0.517 in^2

S_s = 768/0.517

= 1485 psi (0.6 S_y = 16,500 psi)

MS = 16,500/1485 - 1 = +Large

Weld Stresses

The analysis of the weld will conservatively ignore the 3/8-inch bevel weld and only consider the 3/8-inch fillet weld around the perimeter of the base plate. Stresses in this weld resulting from the imposed bending moment and the imposed direct shear load will both be treated as shear stresses, combined using a square root sum of squares approach and compared against a shear allowable limit. The stress in the weld due to the applied moment is as follows:

$s_1 = 4.24M/(h[b^2 + 3L(b + h)])$

= 2006 psi

where:

M = 1.78(P) = 2732 in-lb

P = 1,535 lbs

h = 3/8 = 0.375 in

b = 2.0 inches

L = 1.6 inches

The stress in the weld due to the applied shear load is:

$s_2 = P/A_s$

= 804 psi

where:

P = 1,535 lbs

A_s = 2(1.6 + 2.0)(0.707)(0.375)

= 1.909 in^2

The combined stress is therefore:

$$s = (s_1^2 + s_2^2)^{0.5}$$

$$= 2161 \text{ psi } (0.6\ S_y = 16{,}500 \text{ psi})$$

$$MS = 16{,}500/2161 - 1$$

$$= +\underline{\text{Large}}$$

Analysis of Ball-Lock Pin

The 1/2-inch, AVIBANK 57459-1 ball-lock pins have a 36,800-pound capacity in double shear. With an applied load of 1,535 lbs, the margin of safety is very large.

Response of Impact Limiter(s) During Initial Impact of Package with Ground

The second criterion applicable to the impact limiters requires that the limiter(s) making initial contact with the unyielding surface must remain in position on the end(s) of the cask for the full duration of the initial impact. To satisfy this criterion, attachment hardware (pins, lugs and/or associated welds) may fail during an impact event as long as the limiter(s) being crushed remains in position on the end of the cask and does not separate from the cask. The ability of the limiter to remain in position during an impact is demonstrated with reference to a series of dynamic, free drop tests (end, center of gravity over corner, side and oblique), during which some attachment hardware failure occurred, and to several static crush tests, during which the only attachment mechanism was a strip of duct tape. All of the tests were performed using quarter-scale models of the limiters. Analytic evaluations are also presented to further justify that the limiters will remain in position during the impact.

Dynamic Free Drop Test Results

As presented in Appendix 2.10.8, a series of 30-foot free drop tests were performed on a quarter-scale model of the NAC-LWT cask. Drop orientations included an end drop, a center of gravity over struck corner drop, a side drop and an oblique drop with a subsequent secondary impact. A study of the drop test photographs presented in Appendix 2.10.8 indicates that although attachment hardware failed in some of the dynamic free drop tests, the limiters did not physically separate from the cask body and did completely perform their intended impact limiting function. In fact, the limiters wedged themselves even more securely onto the cask body.

At all times during the testing, the limiters remained in position on the ends of the cask. Notably, rebound from the drop pad due to the whipping action of the restraint cables, did not result in the limiters separating from the cask even though some attachment hardware failure had occurred. This observation demonstrates a tendency for the limiters to become wedged onto the cask body as the result of an impact.

Based on the above test observations, the conclusion reached is that the limiters will remain in position on the cask body during the full duration of the free drop impact event.

Static Crush Test Results

A series of quasi-static crush tests have been performed on quarter-scale models of the bottom impact limiter for the NAC-LWT cask. The limiter orientations tested were end (axial), side and center of gravity over corner (15.7 degrees from axial). The purpose of the quasi-static crush tests was to document the force-deflection and energy absorption characteristics of the honeycomb material used in the impact limiter. Additionally, the tests demonstrated that the limiters need not be mechanically attached to the cask body in order to remain in position to absorb the energy of crushing. No attachment between the model limiter and the test fixture was used for the end (axial) test. A strip of duct tape was adequate to retain the model limiters in position on the side (90-degree) and center of gravity over corner (15.7-degree) fixtures. Once crushing of the limiter is initiated, its cup-shaped geometry causes it to maintain its position on the fixture, which is identical to a quarter-scale model cask body. Thus, attachment of the impact limiter to the cask body is not necessary for maintaining proper position and energy absorption capability.

Analytic Evaluations

Although the results from the above discussed test programs are considered to be the primary proof that the limiters will remain in position during the impact event and properly perform their impact limiting function, analytic studies can also be used to confirm the test observations. Analytic assessments presented in this evaluation indicate that failure of the attachment hardware can be expected to occur for some drop orientations, but subsequent to such failure, the cask tends to wedge into the limiter and separation of the limiter from the cask does not occur. As shown, a significant resistance to the applied separation moment exists due to a combination of crushing of the limiter at the cask interface and due to frictional resistance that exists there. This total resistance is shown to be greater than the applied separation moment and is approximately 7.9 times greater than that provided by the attachment hardware alone.

Additionally, it is noted that the maximum applied separation moment occurs early in the impact when crush depths are small. As crush depths increase, the moment arm and the separation moment decrease to zero. The maximum separation moments occur early in the impact event when the package still possesses a significant downward velocity (87 percent of the initial impact velocity). Additionally, the duration of the impact is very short (approximately 0.04 to 0.06 seconds) and minimal rotation (approximately 1 degree) of the package occurs during the impact. Thus, the cask "drives" into the limiter and physically "traps" the limiter between the cask body and the ground.

The remainder of this section presents a detailed analytic study of the center of gravity over top corner impact event. This near vertical orientation, coupled with the fact that little energy will be converted into rotational energy of the entire package (that is, the center of gravity is over the impacted corner), makes this particular orientation a representative worst case regarding the development of significant separation moments. The available impact limiter analysis program results associated with the corner drop are summarized in Figure 2.6.7-17. The crush depths, crush forces and package velocities presented in the summary figure are directly available from the impact limiter analysis program, RBCUBED, and the separation moment is calculated based on the geometry (that is, the crush footprint) existing at the particular position of interest. Of note, the velocity of the package is still 466.2 inches/second (87 percent of the initial impact velocity) when the maximum separation moment of 7.67×10^6 inch-pounds has developed.

Capability of Attachment Hardware

Figure 2.6.7-18 presents a free body diagram for the top impact limiter during a top down center of gravity over corner impact. With point "A" being the pivot point of the impact limiter on the cask, taking moments about point "A" yields the following:

$$F_i x_i = 14.45\ F_2 + (14.45 + 16.1)\ F_1$$
$$= 14.45\ F_1 + 30.55\ F_1$$
$$= 45.0\ F_1 = \text{separation moment}$$

where:

F_1 = maximum force on a lug

$F_2 = 2(F_1/2) = F_1$

$F_3 = 0.0$ (approximately)

F_i = impact force at limiter to ground interface

x_i = moment arm for force F_i

According to the section titled "Response of Secondary Impact Limiter During Initial Impact of Package," the failure mode for the attachment hardware is tension on the net section of the impact limiter lug. Failure will occur at a load of 28,445 pounds, which corresponds to a stress equal to the ultimate strength of the aluminum lug. Substitution into the above separation moment equation indicates that a moment of 1.28×10^6 inch-pounds can be expected to fail the attachment hardware. As seen from Figure 2.6.7-17, this moment is exceeded prior to 2 inches of crush occurring for the limiter. Attachments may, therefore, fail in the center of gravity over top corner drop.

Resistance to Separation Following Attachment Hardware Failure

If attachments do fail, the cask tends to wedge itself into the limiter as shown in the free body diagram presented as Figure 2.6.7-19. From that figure:

f_{max} = force required to crush limiter honeycomb

= 28.9 S_c (projected area x crush strength) = 28.9(3850)

= 111,265 lb/in

where:

S_c = crush strength of honeycomb used in limiter

= 3850 psi (conservative upper bound crush strength, which was the case selected for Figure 2.6.7-17; the design upper bound crush strength is 3675 psi)

From moment equilibrium:

$F_i x_i = (6\ f_{max}) = 36\ f_{max}$

$= 4.006 \times 10^6$ in-lb

A significant frictional resistance to separation of the limiter also exists. Selecting a coefficient of friction of approximately 0.5 for aluminum on steel (Baumeister, pages 3-26), the frictional resistance to the separation moment is:

$M_f = F_f\ d$

$= 6.145 \times 10^6$ in-lb

where:

F_f = friction force

$0.5(6\ f_{max}) = 3\ f_{max} = 333{,}795$ lbs

and with the centroid of a 180-degree arc (that is, the arc over which f_{max} acts) being located at 63.7 percent of its radius:

$d = 0.637(28.9)$

= 18.41 inches

The total resistance to separation, therefore, becomes:

$M_t = 4.006 \times 10^6 + 6.145 \times 10^6$

$= 10.151 \times 10^6$ in-lb

This total resistance to separation exceeds the maximum applied separation moment of 7.67×10^6 inch-pounds (Figure 2.6.7-17). Separation of the limiter from the cask body will not occur. As discussed in the section titled "Dynamic Free Drop Test Results," this particular center of gravity over corner case was tested. Test results are consistent with the preceding

analysis in that attachment hardware did fail, that the cask did tend to wedge itself into the impact limiter, and that physical separation did not occur (Appendix 2.10.8, Figures 2.10.8-15 and 2.10.8-16).

Response of Secondary Impact Limiter During Initial Impact of Package

The final criterion to be satisfied is for a free drop (normal or accident) involving an initial impact on a single impact limiter, that the limiter on the opposite end of the cask (secondary limiter) must remain attached to the cask during the initial impact. This ensures that the secondary limiter will be in position to absorb the secondary impact and, as discussed in the section titled "Response of Impact Limiter(s) During Initial Impact of Package with Ground," it remains in position for the full duration of the secondary impact and performs its impact limiting function. Attachment is ensured by demonstrating that the attachment hardware (pins, lugs and associated welds) does not fail during the initial impact. For this evaluation, the worst case loading on the secondary impact limiter to separate it from the cask will conservatively be taken as the maximum accident condition acceleration experienced by the overall package on initial impact with the ground. This acceleration is 60.4 g, as shown in Table 2.6.7-34. With four attachment points, the load, P, per attachment point therefore becomes:

$$P = 60.4(1535)/4$$
$$= 23,179 \text{ lbs}$$

where 1,535 pounds is the weight of the heaviest (top) impact limiter.

Analysis of Impact Limiter Lug

The impact limiter lug is evaluated using the same approach as was used in the section titled "Analysis of Impact Limiter Lug," but the allowable limit is based on ultimate strength rather than yield strength. As shown in Table 2.3.1-5, the ultimate strength of 6061-T6 aluminum at 150°F is 38,700 psi. Potential failure modes of tension across the net section and 40-degree shearout are considered as follows:

Tension Across the Net Section

$$P = 23,179 \text{ lbs}$$
$$A = 0.5(2.0 - 0.53)$$
$$= 0.735 \text{ in}^2$$
$$S_t = 23,179/0.735$$
$$= 31,536 \text{ psi } (S_u = 38,700 \text{ psi})$$
$$MS = 38,700/31,536 - 1$$
$$= +0.23$$

40-Degree Shearout

$P = 23,179$ lbs

$e = 1.7 - (0.53/2) \cos 40°$

$= 1.497$ inches

$A_s = 2(0.5)(e)$

$= 1.497$ in^2

$S_s = 23,179/1.497$

$= 15,484$ psi ($0.6\ S_u = 23,220$ psi)

$MS = 23,220/15,484 - 1$

$= +0.50$

Analysis of Cask Lug

The cask lug is evaluated using the same approach as was used in the section titled "Analysis of Impact Limiter Lug," but the allowable limit is based on ultimate strength rather than yield strength. The ultimate strength of Type 304 stainless steel at 150°F is 73,000 psi. Potential failure modes of 40-degree shearout and failure of the weld (3/8-inch bevel plus 3/8-inch fillet), which attaches the base plate to the cask body, are considered as follows:

40-Degree Shearout

$F = P/2 = 23,179/2$

$= 11,590$ lbs

$e = 0.72 - (0.53/2) \cos 40°$

$= 0.517$ in

$A_s = 2(0.5)(e)$

$= 0.517$ in^2

$S_s = 11,590/0.517$

$= 22,418$ psi ($0.6\ S_u = 43,800$ psi)

$MS = 43,800/22,418 - 1$

$= +0.95$

Weld Stresses

The analysis will again conservatively ignore the 3/8-inch bevel weld and only consider the 3/8-inch fillet weld around the perimeter of the base plate.

The stress in the weld due to the applied moment is:

$s_1 = 4.24\ M/(h[b^2 + 3\ L(b + h)])$

$= 30{,}292$ psi

where:

$M = 1.78(P) = 41{,}259$ in-lb

$P = 23{,}179$ lbs

$h = 3/8 = 0.375$ in

$b = 2.0$ in

$L = 1.6$ in

The stress in the weld due to the applied shear load is:

$s_2 = P/A_s$

$= 12{,}142$ psi

where:

$P = 23{,}179$ lbs

$A_s = 2(1.6 + 2.0)(0.707)(0.375)$

$= 1.909$ in^2

The combined stress is therefore:

$s = (s_1^2 + s_2^2)^{0.5}$

$= 32{,}635$ psi ($0.6\ S_u = 43{,}800$ psi)

$MS = 43{,}800/32{,}635 - 1$

$= +0.34$

Analysis of Ball-Lock Pin

The 1/2-inch, AVIBANK 57459-1 ball-lock pins have a 36,800-pound capacity in double shear. With an applied load of 23,179 pounds, the margin of safety becomes:

$MS = 36{,}800/23{,}179 - 1$

$= +0.59$

2.6.7.5 Closure Lid

2.6.7.5.1 Discussion

The NAC-LWT cask closure lid is analyzed for structural adequacy in accordance with the requirements of 10 CFR 71.73(c)(1) free drop (hypothetical accident condition). The cask is assumed to be inverted, with the lid downward, when dropped through a distance of 30 feet onto

a flat, unyielding, horizontal surface. The structural evaluation is performed by classical elastic analysis methods.

2.6.7.5.2 Analysis Description

Geometry

The closure lid geometry is shown in Figure 2.6.7-20. The lid is bolted in position on the upper end of the cask. The lid material is Type 304 stainless steel. The temperature-dependent material properties for Type 304 stainless steel, which are presented in Section 2.3, are used in this analysis.

Loadings

During impact, the cask cavity contents are considered to apply an internal inertia pressure on the interior surface of the lid in the outward normal direction. The impact limiter applies an external inertia pressure on the exterior lid surface in the inward normal direction; however, this pressure is conservatively ignored in this analysis. Each bolt is torqued to a preload force of 21,000 pounds. The lid is also loaded with an assumed 50-psig internal pressure for the 130°F ambient temperature hot case.

Displacement Boundary Conditions

The closure lid is restrained from vertical and rotational deformation at the 17.875-inch bolt circle diameter by the preloaded lid bolts.

Detailed Analysis

For the loading and boundary conditions described, the structural behavior of the closure lid may be assessed by superposition of maximum stresses from Section 2.6.1, which includes consideration of thermal effects, bolt preload, and internal pressure, with the maximum stresses produced by the inertia loading. The maximum $P_m + P_b$ component stresses from Section 2.6.1 (Table 2.6.1-2) are:

S_x = -3060 psi; S_y = - 260 psi; S_z = 100 psi; S_{xy} = 180 psi

The free body diagram of Figure 2.6.7-21 can be evaluated by applying formulas from Case 6 (Roark, page 217) for a uniformly loaded circular plate.

The total deceleration force of the contents, F_D = 4000 lbf × 60 g deceleration = 240,000 lbf, creates a pressure, W, on the lid interior surface:

$$W = \frac{240,000}{\pi(8.938)^2} = 956 \text{ psi}$$

The maximum radial, tangential, and vertical stresses on the lid are:

$$S_r = \frac{3Wa^2}{4t^2}$$

$$= 895 \text{ psi}$$

$$S_t = \frac{3Wa^2\gamma}{4t^2}$$

$$= 246 \text{ psi}$$

$$S_v = -W$$

$$= -956 \text{ psi}$$

where:

a = 8.938 inches

γ = 0.275

t = 8.0 inches

Conservatively combining these stresses with $P_m + P_b$ stresses from Section 2.6.1 (Table 2.6.1-2), the total $P_m + P_b$ component stresses on the lid are:

S_x = -3955 psi; S_y = - 1216 psi; S_z = 346 psi; S_{xy} = 180 psi

For small S_{xy}, the stress intensity becomes S.I. = $S_z - S_x$ = 4301 psi. Since the maximum cask lid temperature is less than 300°F for the 130°F ambient temperature hot case (Section 3.4.2), the closure lid allowable $P_m + P_b$ stress is 72,000 psi (3.6 S_m). Therefore, the minimum margin of safety is +Large; thus, containment is maintained.

2.6.7.5.3 Conclusion

It is demonstrated by use of a conservative loading that the minimum margin of safety is +4.23 and containment is maintained. Therefore, the NAC-LWT cask lid satisfies the requirements of 10 CFR 71 for consideration of the closure lid impact in the 30-foot free drop accident.

2.6.7.6 Bolts - Closure Lid (Normal Conditions of Transport)

The NAC-LWT cask closure lid is bolted to the cask body top forging with twelve 1 - 8 UNC bolts fabricated from SA-453, Grade 660 high alloy steel. The threaded portion of the bolt engages the cask body a minimum of 1.875 inches. In accordance with the free drop provisions of the normal conditions of transport, 10 CFR 71.71(c)(7), this bolted closure has been carefully

evaluated for structural adequacy and found to satisfy all regulatory requirements and design criteria. Details of this analytic evaluation follow.

The simultaneous loads that may be imposed upon the cask closure bolts include: pressure loads, thermal differential expansion loads, pre-loads and inertial loads arising from impact responses. For a given set of initial conditions, the pressure loads, thermal loads and pre-loads all remain constant. Inertial impact loads, however, vary with impact orientation and bolt location. Lateral impact loads acting upon the lid are directly related to the mass of the lid and the lateral impact acceleration. Longitudinal impact loads acting on the lid are proportional to the longitudinal impact acceleration, as well as, the mass of the lid and the payload within the containment cavity.

In general, these lid impact loads impose unequal individual forces, or loadings, in the closure bolts. This NAC-LWT cask evaluation conservatively assumes a set of impact forces that induce maximum containment closure separation forces and bolt loadings. With this conservative assumption, the external impact force is presumed to be located at a point where it cannot restrain those forces that tend to separate the cask lid from the cask body. This assumption locates the external impact force at the lower corner of the lid-body interface. With this assumption the lower corner of the lid is assumed to be pinned (by the impact forces), and bolt tension forces are assumed to vary linearly from zero at this pinned lower corner to a maximum value at the opposite, or upper, corner of the lid.

A complete range of impact orientations is evaluated, from an end impact at 0 degrees to a flat side impact at 90 degrees, and at 5-degree increments in between. Loads are derived from the normal impact accelerations summarized within Table 2.6.7-34. Where necessary, impact accelerations have been interpolated at 5-degree increments from those values given in Table 2.6.7-34.

The details of this analytic evaluation are described and performed within Section 2.10.9 for both normal conditions of transport and hypothetical accident conditions. Normal conditions of transport results are summarized in Table 2.6.7-35 and Table 2.6.7-36, corresponding to a "hot" initial condition and a "cold" initial condition, respectively. The hot initial condition bolt temperature is taken at 227°F, as summarized in Table 3.4-2. The cold initial condition bolt temperature is assumed to be -20°F, per regulatory requirements. Physical properties for the SA-453, Grade 660 bolts are conservatively taken at 300°F and at room temperature (70°F) for hot and cold conditions, respectively. As defined within Table 2.1.2-1, the allowable bolt stress is taken as S_y, leading to allowable direct tension stresses of 81.9 and 85.0 ksi, at 300°F and 70°F, respectively. Based on this thorough evaluation, the closure bolts incur a maximum stress intensity of 61,012 psi, which results in a minimum margin of safety of 34 percent. See Table 2.6.7-35 (at 5°):

MS = 81.9/61.042 - 1

= +0.34

Bolt engagement may be evaluated by computing shear stresses within the SA-336, Type 304, end forging material. At 300°F, the allowable shear stress is 0.5 S_y, or 11.25 ksi, according to Tables 2.1.2-1 and 2.3.1-1. The maximum tensile load is found as the product of the maximum bolt stress intensity, noted above, and the bolt stress area; that is, (61,042 psi)(0.6051) = 36,937 pounds. The shear area per inch of engagement for a 1 - 8 UNC internal thread is 2.325 in^2/in ("Table Speeds Calculation of Strength of Threads," pp. 41-49). The resultant shear stress and margin of safety within the top body forging is:

$\tau = P/A = (36{,}937)/[(2.325)(1.875)]$

= 8473 psi

MS = 11.25/8.473 - 1

= +0.33

Using consistently conservative assumptions, the NAC-LWT cask lid bolted closure can be shown to satisfy the performance and structural integrity requirements of 10 CFR 71.71(c)(7) for normal conditions of transport.

2.6.7.7 Neutron Shield Tank

2.6.7.7.1 Introduction

The neutron shield tank is welded to, and concentric with, the NAC-LWT cask outer shell. The tank consists of eight cells. The neutron shield fluid flows freely through holes in the longitudinal stiffeners between these cells. During thermal expansion or contraction, fluid passes through the valve assembly into or out of the expansion tank, which is external to and concentric with, the shield tank. Table 2.6.7-37 summarizes the results of the structural analyses described below. The table shows positive margins of safety, demonstrating that each component of the neutron shield tank satisfies the requirements of the normal operations conditions 1-foot free drop as described in 10 CFR 71.71. Classical analysis techniques are used to demonstrate that each tank component withstands the hydrodynamic loads from a 1-foot side or end drop in combination with internal tank pressure. Similarly, classical analyses show that the shield/expansion tank does not rupture, nor does the check valve sustain damage during the penetration test.

The shield tank wall has a mean diameter of 39.04 inches, is located approximately 23 inches below the top edge of the upper end casting, and extends 164 inches longitudinally. Constructed entirely of Type 304 stainless steel, the tank external shell and eight longitudinal stiffeners are 0.24-inch thick plate. Each end of the tank is a 0.50-inch thick end plate. Equally spaced

between stiffeners are eight 0.24-inch thick gusset plates, which provide additional support to the end plates.

A 56 percent by volume ethylene glycol and water solution provides the neutron shielding. The shield tank fluid volume (excluding stiffeners) is 84,742 cubic inches or approximately 370 gallons (3,280 pounds) of fluid. At the upper end, concentric with the shield tank, is the expansion tank. The expansion tank is 46 inches long and is constructed from 0.32-inch thick stainless steel plate; there are eight cells divided by equally spaced plate stiffeners with holes in them, which enables the fluid to flow from chamber to chamber. The expansion tank empty volume is 13,245 cubic inches. It is filled with 11.5 gallons (103 pounds) of solution initially, leaving an expansion volume of 10,589 cubic inches. At the bottom of the expansion tank is a siphon tube, which goes around the shield tank and exits at its top. Volumetric expansion forces fluid through the siphon tube. During heating, the solution in the shield tank expands into the expansion tank avoiding uncontrolled pressurization of the shield/expansion tank. A pressure relief valve in the shield tank assures that the tank structure is protected against over pressurization. The pressure relief valve is set to begin relieving pressure at 165 psig. Initially, the expansion tank is filled with 11.5 gallons of fluid to assure that the shield tank remains filled at -40°F. A cross section of the upper end of the cask with pertinent dimensions is shown in Figure 2.6.7-22.

2.6.7.7.2 Structural Criteria

The neutron shield tank and expansion tank analyses use 10 CFR 71 and Regulatory Guide 7.8 to determine load/ambient conditions to bound other load conditions. In this way, the shield/expansion tank components are conservatively analyzed for the most severe structural loads at maximum temperatures; thus, the material properties and allowable stresses have minimum values.

The 10 CFR 71 requires that all transport packages weighing more than 30,000 pounds be evaluated to determine the consequences of a free fall through a distance of 1-foot onto a horizontal, unyielding surface for normal operation; cask orientation during the fall shall be such that maximum damage is inflicted upon the cask. End and side drop g loads are the most severe normal operating loads that the cask sustains; analyses of the shield and expansion tanks are based on the end and side drop loads. All other cask drop orientations produce less severe g loads.

Table 2 in Regulatory Guide 7.8 defines three initial ambient states that guide the analyses. The two extreme cases used to envelope analyses are:

1. 100°F ambient temperature, with maximum insolation, decay heat, internal pressure, weight, and minimum external pressure

2. 20°F ambient temperature, with no insolation or decay heat, minimum internal pressure, weight, and external pressure.

These conditions are used to evaluate the shield tank fluid temperatures (Actually, Sections 3.4.2 and 3.4.3 results, which are based on the more limiting ambient temperatures of 130°F and -40°F are used). With the fluid temperatures established, it is then possible to calculate the shield/expansion tank pressures for the extreme cases and the resulting amount of fluid flowing between the shield tank and the expansion tank (for expansion tank sizing). Table 2.6.7-38 summarizes the calculated shield tank fluid temperatures used in analyzing the shield tank structure.

Since the functional and structural adequacy of the neutron shield and expansion tanks depend on linear elastic evaluations, the allowable stress criteria is selected as the material yield strength. All calculated stresses are less than this criteria. From Table 2.6.7-38, the highest average fluid temperature is 227°F; therefore, material properties for 250°F are used in the analyses. The evaluation of the shield/expansion tank and the resulting conclusions are conservative.

2.6.7.7.3 Neutron Shield and Expansion Tank Loads

Structural, hydrostatic/hydraulic pressure and expansion pressure are the three components of shield tank loads. Structural loads result from decelerating the cask structure. Hydrostatic and hydraulic loads (water hammer) result from the shield tank fluid decelerating against the shield tank structure. Expansion pressure loads are generated when the fluid expands during heating. An explanation of how each type of load is calculated follows.

Structural loads are loads imposed on the structure by the weight of the structure itself. The stainless steel materials from which the cask is fabricated all have mass and are acted upon by gravity and the normal operations conditions 1-foot drop deceleration. Shield tank structural components weigh approximately 2,116 pounds. Expansion tank components weigh approximately 610 pounds. These loads are included in the analysis of the tanks.

Hydrostatic pressure is the pressure at a given depth within a fluid caused by the mass of the fluid being accelerated by gravity. Hydraulic pressure is the hydrostatic pressure acted upon by accelerations other than gravity. To determine the hydrostatic pressure of fluid acting on the plate, the following formula is used:

$$p = \rho g h$$

where:

ρ = mass density of fluid (lbm/in^3)

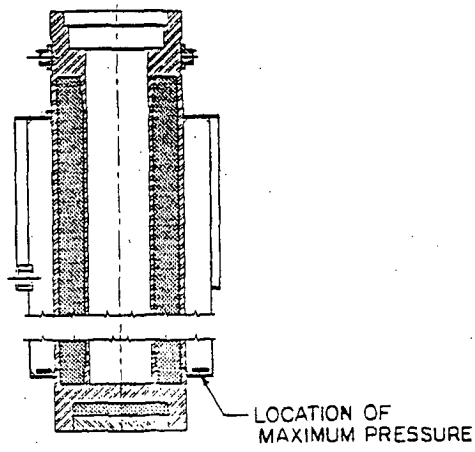
g = acceleration due to gravity (in/sec/sec)

h = height of fluid above point considered (in)

When the cask is vertical, the maximum fluid height in the shield tank is 164 inches, which is equivalent to 6.3 psig under the acceleration of gravity (1 g). When the cask is in the horizontal position, there is a 39-inch maximum fluid height (diameter of shield tank) or 1.56 psig (1 g). The presence of the expansion tank around the shield tank is conservatively neglected, because the fluid pressure acting on the exterior of the shield tank reduces the forces acting on the shield tank components. During a 1-foot end drop (normal operations conditions), the cask undergoes a 15.8 g deceleration (Section 2.6.7.4). This results in a hydraulic pressure of 100 psig (6.3 psig × 15.8 g) at the bottom of the shield tank. Similarly, during the side drop, the pressure at the lowest point on the shield tank is 38 psig (1.56 psig × 24.3 g). The maximum hydrostatic and hydraulic pressures for the end and side drops and the location of the maximum pressure for the shield tank analyses are shown in the following sketches.

1-Foot End Drop (15.8 g)

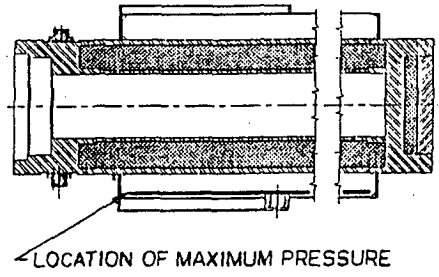
Maximum Hydrostatic Pressure	Maximum Hydraulic Pressure
6.3 psig	100 psig



Vertical Orientation

1-Foot Side Drop (24.3 g)

Maximum Hydrostatic Pressure	Maximum Hydraulic Pressure
1.56 psig	38 psig



Horizontal Orientation

The g loads for various drop orientations and how they were calculated are explained in Section 2.6.7.4.

Once the shield/expansion tank is filled, it is a sealed compartment, which will not permanently deform under normal transport conditions. The neutron shield tank solution expands or contracts when heated or cooled. During heating the liquid expansion causes fluid to flow into the expansion tank, compressing the air in the expansion tank and causing the pressure to increase. Similarly, as the cask fluid temperatures reach 40°F, there is sufficient fluid in the expansion tank to always keep the neutron shield tank completely filled.

The neutron shield tank is completely filled in the upright configuration, when the fluid and ambient conditions are at 68°F. The 56 percent by volume ethylene glycol and water solution has a density of 67.07 lbs/ft^3 at 68°F. After the neutron shield tank is filled, 11.5 gallons of solution are poured into the expansion tank. Both tanks are then sealed.

The normal transport condition of maximum decay heat load, 100°F ambient temperature and maximum insolation results in an average (natural and forced mixing of fluid is assumed) shield tank fluid temperature of 227°F. The volume of fluid that enters the expansion tank as the temperature increases from 68°F to 227°F is:

$$\Delta V = V_1\left(\frac{\rho_1}{\rho_2} - 1\right) = 5539 \text{ in}^3$$

where:

ρ_1 = 67.07 lb/ft^3 = density of 56 percent ethylene glycol and water solution at 68°F

ρ_2 = 63.07 lb/ft^3 = density of 56 percent ethylene glycol and water solution at 230°F

V_1 = 87,398 lb/in^3 = volume of fluid in the expansion and shield tank at 68°F

ΔV = volume of fluid entering the expansion tank

Then the increased uniform air pressure in the expansion tank at 230°F is:

$$P_2 = P_1\left(\frac{V_1 T_2}{T_1 V_2}\right) = 40.3 \text{ psia } (25.6 \text{ psig})$$

where:

P_1 = 14.7 psia

V_1 = 10,589 in^3 (expansion tank air volume at 68°F)

T_1 = 528°R = 68°F

T_2 = 690°R = 230°F

$V_2 = 10{,}589\ in^3 - 5539\ in^3 - 5050\ in^3$ (expansion tank air volume at 230°F)

The same analysis procedure was used to calculate the pressures at other significant normal operating states; these pressures are presented in Table 2.6.7-39. Properties for the 56 percent by volume ethylene glycol and water solution are presented in Table 3.2-5. Two normal operating conditions are presented in Table 2.6.7-39, and are helpful in understanding how the cask operates, but are all bounded by the pressure relief valve release pressure (PRVR) shown in Table 2.6.7-39. The PRVR pressure is used to establish the structural loads for shield and expansion tank analyses.

Thus, the magnitude of the expansion pressure is determined as discussed previously by the volume of fluid added to the expansion tank during the initial filling. It is assumed that 11.5 gallons of fluid are added to the expansion tank, 0.5 gallons more than specified. This results in a maximum expansion pressure of 26 psig.

In addition to the expansion pressure acting radially outward, 10 CFR 71, Subpart F, requires that the cask be able to sustain a reduced external pressure. The cask is initially filled and pressurized at atmospheric pressure (14.7 psia). When the external pressure is reduced to 3.5 psia, there is a relative increase in internal pressure of 11.5 psig (rounded to 12 psig). The reduced external pressure load has been included in the analysis as an increase in internal pressure.

The calculated pressures for the end drop load condition are as follows:

Reduced external pressure	12 psig
Hydraulic pressure	100 psig
Expansion pressure	26 psig
TOTAL	138 psig

The calculated pressures for the side drop load condition are as follows:

Reduced external pressure	12 psig
Hydraulic pressure	38 psig
Expansion pressure	26 psig
TOTAL	76 psig

These pressures are conservatively assumed to add algebraically and represent the highest pressure expected at a point on the shield/expansion tank structure. All other pressures within the shield/expansion tank are less because the hydraulic pressure is a function of fluid depth.

2.6.7.7.4 Neutron Shield Tank Structural Analyses

To simplify analysis of the shield tank structure, the use of symmetry, superposition and analysis of worst case loads are employed to reduce the number of calculations to be performed. Major shield tank structural components are shown in Figure 2.6.7-23. Analyses performed and resulting conclusions for one location of the shield tank are directly applicable to the same relative location elsewhere on the shield tank structure. For reasons stated earlier, the normal operating conditions 1-foot end drop loads envelope all other normal operations conditions drop orientations, and is the only loading condition that is considered in the following analyses. Moreover, the bottom end drop g load is more severe than the top end drop, and is used in both the top and bottom end drop analyses. The shield tank analysis is performed with the shield tank pressure equal to 180 psig, a pressure 42 psig higher than the calculated 138 psig for the end drop (which envelops the side drop condition).

The bottom end plate, shield tank shell, gussets, top end plate, and welds are the major components of interest in the shield tank evaluation for normal transport conditions.

To ensure a conservative analysis of the neutron shield and expansion tank structure, several simplifying assumptions are made for all analyses performed (other assumptions are stated with each analysis). The allowable stress is taken as the yield strength of Type 304 stainless steel at 250°F, which is 23,750 psi. This is conservative since the maximum calculated shield/expansion tank normal operating temperature is 227°F.

Finally, the edge restraint of the structural components analyzed is considered to be simply supported. The smallest welds are considered in the analyses; a larger weld assures a conservative analysis.

Weld Allowable Stresses

The shield and expansion tanks are constructed primarily from 0.24-inch thick Type 304 stainless steel plate. The plates are welded together using 0.188-inch fillet welds, using Type 308 weld material. From the Metals Handbook, 9th Edition, Volume 3, page 20, the ultimate tensile strength is 75.0 ksi. The allowable strength for shield tank fillet welds is:

$$S_{ALL} = (0.3)(75{,}000)$$
$$= 22{,}500 \text{ psi}$$

or:

$$f_{ALL} = (0.707)(22{,}500)\omega$$
$$= 15{,}900\omega \text{ lb/in}$$

where:

f_{ALL} = fillet allowable (lb/in)

ω = fillet weld size (in)

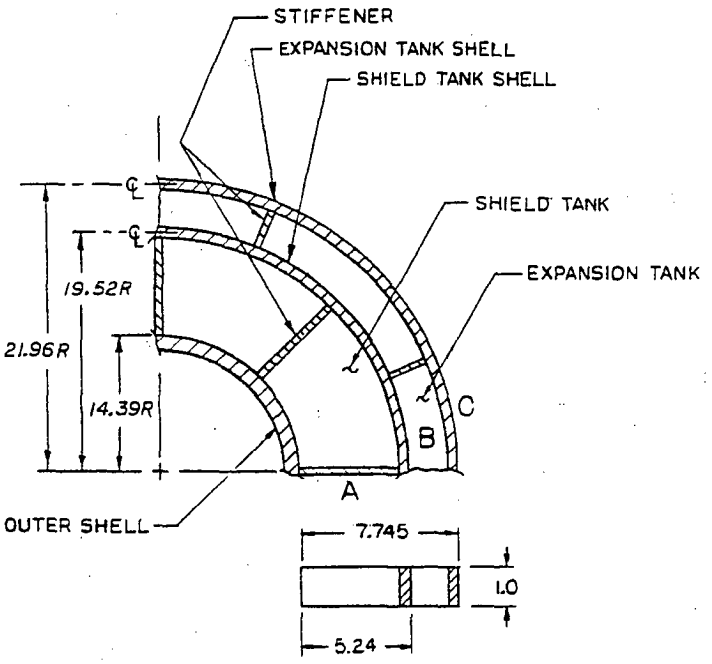
The only size fillet weld considered in the shield tank analysis is a 0.188-inch fillet. Therefore, the 0.188-inch fillet weld has an allowable strength of:

f_{ALL} = (15,900)(0.188 in)

= 2980 lb/in

Structural Loads

Shield tank and end plate loads are considered in the neutron shield tank analysis. The weight of a unit depth of the 0.24-inch thick shield tank plate material is considered to be located at the mass centroid of the plate assembly. The mass centroid is 6.13 inches from the outer shell, as shown in the following analysis:



Quarter Section - NAC LWT Cask

Two "A" plates weigh 1.051 pounds with a mass centroid at 3.87 inches from the outer shell.
Two "B" plates weigh 2.005 pounds with a mass centroid at 5.12 inches from the outer shell.
Two "C" plates weigh 3.032 pounds with a mass centroid at 7.59 inches from the outer shell.
The total weight of the plates is 6.09 pounds.

The mass centroid is located at:

$$\bar{x} = \frac{(1.051\ lb)(3.873\ in) + (2.005\ lb)(5.12\ in) + (3.032\ lb)(7.59\ in)}{5.643\ lb}$$

$$= 6.134\ in$$

The weight of the neutron shield tank structural plates is considered to act at 6.09 inches from the outer shell. The weight of one stiffener and shield/expansion tank shell section is 3.54 pounds.

The shield tank end plates are 0.5-inch thick stainless steel plate. To determine the structural load, the weight of the plate was divided by its area. The resulting structural load is 3 pounds/square inch.

Shield Tank Shell

The shield tank shell is analyzed as a thin-walled tube, taking no credit for the eight radial stiffeners, which run the length of the tank. Using Case 1 (Roark, page 298), the meridional and hoop stresses are calculated:

$$S_1 = \frac{pR}{2t} = 7414\ psi$$

where:

p = 180 psig

R = 19.44 inches

t = 0.24 in

and

$$S_2 = \frac{pR}{t} = 14,827\ psi$$

Von Mises yield criterion is used to calculate an equivalent stress, S_e, which is compared to the yield strength of stainless steel.

$$S_e = \frac{1}{\sqrt{2}}\left[(S_1 - S_2)^2 + (S_2 - S_3)^2 + (S_3 - S_1)^2\right]^{0.5}$$

$$= 12,841\ psi$$

where:

S_1 = 7414 psi

S_2 = 14,827 psi

S_3 = 0 psi

then

$$M.S. = \frac{S_{ALL}}{S_e} - 1 = \underline{+0.07}$$

where:

S_{ALL} = (0.577)(23,750 psi)
= 13,700 psi

Stiffener

A 1-inch longitudinal section of the neutron shield tank is analyzed. The total pressure load (180 psi) acts equally between stiffeners as shown in Figure 2.6.7-24. No credit is taken for support from the end plates or the expansion tank end plate. The load acting on the stiffener (L = 2772 pounds) is the area of the tank shell 15.4 square inches (15.4 inches × 1 inch) multiplied by the total end drop pressure, 180 psi. The cross sectional area, A_p, of a 1-inch section of the stiffener plate is 0.24 square inches (0.24 inch × 1.0 inch). The tensile stress acting on the stiffener is calculated:

$$S_T = \frac{L}{A_p} = 11,746 \text{ psi}$$

then

$$M.S. = \frac{S_{ALL}}{S_T} - 1 = \underline{+0.17}$$

where:

S_{ALL} = 13,700 psi (Section 2.6.7.7.4)

The stiffeners are the structural members locating the shield tank shell and providing support for the end plates (similar to the gussets) during end drops. This analysis demonstrates that the stiffeners have adequate strength to withstand the maximum pressure in the shield tank. The analysis in Section 2.6.7.7.4 shows that the shield tank shell has adequate strength to withstand the maximum pressure in the shield tank. All other drop orientations offer less severe structural loads on both the stiffeners and tank shell. Lightening holes in each stiffener do not affect the

structural integrity of the shield tank and stiffeners. Lightening holes are located away from the ends of the stiffeners where the hydraulic component of the pressure load is less severe.

Stiffener Weld

A unit section (1 inch longitudinal) of stiffener weld is analyzed. Two loads act on the weld attaching the stiffener to the cask outer shell. The drop pressure load acting on the stiffener is L = 2772 pounds (see section titled "Stiffener"). In addition to the pressure load, the structural load (L_s) is calculated concentrating the mass of the tank (stiffeners and shell) unit section (see section titled Structural Loads). The structural pressure loads and welds being examined are shown in Figure 2.6.7-25. Treating the two 1-inch welds as lines and determining the weld loading using methodology found in Design of Welded Structures (Blodgett, Section 7.4):

Tensile Load

$f_t = 2772/2$

$= 1{,}386$ lb/in

where:

$L = 2{,}772$ lbs

Shear Load

$f_s = 55.9/2$

$= 28.0$ lb/in

where:

$L_s = 3.54$ lb x 15.8 g

$= 55.9$ lbs

15.8 g = end drop g load
(Section 2.6.7.4)

The end drop structural load produces a bending moment on the weld group (Figure 2.6.7-25). The bending moment (M) is 343 inch-pounds (6.13 inches × 55.9 pounds). The section properties of the weld group are calculated from Blodgett, Table 5, page 7.4-7,

$$S_\omega = \frac{d^2}{3}$$

$$= 0.33 \text{ in}^2$$

where:

d = 1 in

Bending Load

$$f_b = \frac{M}{S_\omega}$$

$$= 343/0.33$$

$$= 1038 \text{ lb/in}$$

The resultant load on the weld group is calculated:

$$f_r = \sqrt{f_1^2 + f_2^2}$$

$$= 2424 \text{ lb/in}$$

where:

$f_1 = f_s = 28.0$ lb/in

$f_2 = f_t + f_b$

$= 2{,}424$ lb/in

The allowable weld load is $f_{ALL} = 2{,}980$ lb/in; therefore, the margin of safety is:

$$M.S. = \frac{f_{ALL}}{f_r} - 1 = \underline{+0.23}$$

Gusset Weld

It is assumed that the end drop load on the end plate is shared equally between the stiffeners and gussets (Figure 2.6.7-26). The fillet weld attaching the gusset to the cask outer shell and end plate is 0.188 inch and is on both sides of the gusset. Bending and shear stresses on the weld group A are calculated in the following analyses. Since the gussets and stiffeners share the end drop load, the end plate area, which the gusset must support, is calculated:

$$A = [\pi(R_o^2 - R_i^2) - (16)(T_{PLT})(R_o - R_i)]/16$$

$$= 33.95 \text{ in}^2$$

where:

$R_o = 19.6$ inches

$R_i = 14.3$ inches

$T_{PLT} = 0.25$ in

The distributed load is composed of the end drop pressure load (180 psig) and a structural load (3 psig) equivalent to the end plate weight. The concentrated load (L) is calculated by multiplying the area (A) by the sum of the distributed loads (183 psig): L = 6,213 pounds. Therefore, the moment acting on weld group A is:

$$M = L\left(\frac{5.1}{2}\right)$$

$$= 15{,}843 \text{ in-lb}$$

The section properties of the weld group are calculated from Blodgett, Table 5, page 7.4-7:

$$S_\omega = \frac{d^2}{3}$$

$$= 12 \text{ in}^2$$

where:

d = 6 inches

Bending Load

$$f_b = \frac{M}{S_\omega}$$

$$= 1320 \text{ lb/in}$$

Shear Load

$$f_s = \frac{L}{W_{LEN}}$$

$$= 518 \text{ lb/in}$$

where:

L = 6,213 lbs

$W_{LEN} = 2 \times 6$ inches

= 12 inches

The resultant load on the weld group is calculated by:

$$f_r = \sqrt{f_1^2 + f_2^2}$$

$$= 1418 \text{ lb/in}$$

where:

$f_1 = f_s = 518$ lb/in

$f_2 = f_b = 1320$ lb/in

The allowable weld load is $f_{ALL} = 2980$ lb/in; therefore, the margin of safety is:

$$M.S. = \frac{f_{ALL}}{f_r} - 1 = \underline{+1.10}$$

Bottom End Plate

It is assumed that the portions of the end plate between a gusset and the adjacent stiffener can be modeled by a rectangular plate of the appropriate dimensions. The width (b) of the plate is the difference between radii of the cask outer shell and the shield tank shell as shown in Figure 2.6.7-27. The length (a) of the plate is the average of the inner and outer arc lengths, 6.7 inches ((7.7 inches + 5.6 inches)/2). Using Case 36 (Roark, page 225), the maximum bending stress on the 0.5-inch thick end plate is:

$$S_b = \beta \frac{wb^2}{t^2}$$

$$= 8{,}525 \text{ psi}$$

where:

$\beta = 0.4146$

$w = 183$ psi (see section titled "Gusset Weld")

$b = 5.3$ inches

$t = 0.5$-in thick

The margin of safety is:

$$M.S. = \frac{S_{ALL}}{S_B} - 1 = \underline{+1.79}$$

where:

$S_{ALL} = S_{y_{250°F}}$

$= 23{,}750$ psi

Gusset Plate Cross Section

The plate was modeled as a large weld, with the throat in tension during an end drop. The end drop load (L) acting on the gusset is the load acting on the end plate between the gusset and adjacent stiffener. The gusset root cross section (R) is considered to be in tension (Figure 2.6.7-28). From the section titled "Gusset Weld," the load on the gusset root is L = 6213 pounds. The gusset root cross sectional area is calculated:

$$A_R = 0.707(h)(T_{PLT})$$
$$= 0.865 \text{ in}^2$$

where:

h = 5.1 in (shortest leg)

T_{PLT} = 0.24 in (thickness)

Calculating the tensile load:

$$S_T = \frac{L}{A_R}$$

$$= 7180 \text{ psi}$$

The margin of safety is:

$$M.S. = \frac{S_{ALL}}{S_T} - 1 = \underline{+LARGE}$$

where:

S_{ALL} = 23,750 psi

End Plate Welds

Peripheral weld group B (Figure 2.6.7-29) is considered to be in shear during an end drop. The end plate load is 6213 pounds, from the section titled "Gusset Weld." The area of weld material is:

$$A_W = 0.707\left(\frac{3}{16}[2(19.6 - 14.3) + 7.7] + \frac{3}{8}(5.6)\right)$$

$$= 3.9 \text{ in}^2$$

The tensile stress on weld group B is:

$$S_T = \frac{L}{A_W}$$

$$= 1593 \text{ psi}$$

The margin of safety is:

$$M.S. = \frac{S_{ALL}}{S_T} - 1 = \underline{+LARGE}$$

where:

$S_{ALL} = 23{,}750$ psi

Top End Plate - Normal Operations Conditions

In the analyses of the section titled "Bottom End Plate" and Section 2.6.7.8.2, the 0.5-inch thick bottom end plates are shown to be structurally adequate. This analysis shows that the top end plate, which is in effect equivalent to both bottom end plates welded together at the shield tank shell, is structurally adequate. Two bounding conditions are considered. The first condition considers the shield tank top end plate loaded with a pressure of 180 psig and the expansion tank top end plate unloaded. Using Case 38 (Roark, page 113), considering a unit strip of top end plate, where the two end points are considered pinned, the maximum bending stress is 10,272 psi, and the margin of safety equals +0.33. The second condition considers both the shield and expansion tank end plates loaded at 180 psig. Again using Case 38, the bending stress equals 11,172 psi, resulting in a margin of safety of +0.23. The maximum normal operations conditions pressure in the expansion tank is 162 psig; therefore, the top end plate is adequate for the normal operations conditions.

2.6.7.8 Expansion Tank

The expansion tank is located at the upper end of the cask and is concentric with the shield tank. As its name implies, the expansion tank provides a location for fluid to expand into during fluid heating; thus, protecting both the neutron shield tank and the expansion tank from over-pressurization during normal operations conditions. A description of the expansion tank, structural criteria, and structural loads is presented in Sections 2.6.7.7.1 through 2.6.7.7.3. Table 2.6.7-40 summarizes the results of the structural analyses described in the following sections. The table shows adequate margins of safety for each component of the expansion tank examined. Therefore, the normal operations conditions requirements of 10 CFR 71 are satisfied.

To simplify analysis of the expansion tank structure, the use of symmetry, superposition, and worst case loads are employed to reduce the number of calculations to be performed and yet provide a thorough analysis. Major expansion tank structural components are shown in Figure

2.6.7-30. Analysis of the expansion tank uses the same format and simplifying assumptions as were used in the neutron shield tank structural analysis.

2.6.7.8.1 Expansion Tank Shell

The expansion tank shell is analyzed as a thin-walled tube, taking no credit for the eight radial stiffeners, which run the length of the tank. Using Case 1 (Roark, page 298), the meridional and hoop stresses are calculated:

$$S_1 = \frac{pR}{2t}$$

$$= 6269 \text{ psi}$$

$$S_2 = \frac{pR}{t}$$

$$= 12,537 \text{ psi}$$

where:

p = 180 psig

R = 21.94 inches

t = 0.32 in

Von Mises yield criterion is used to calculate an equivalent stress (S_e), which is compared to the yield strength of Type 304 stainless steel.

$$S_e = \frac{1}{\sqrt{2}} \left[(S_1 - S_2)^2 + (S_2 - S_3)^2 + (S_3 - S_1)^2 \right]^{0.5}$$

$$= 10,857 \text{ psi}$$

where:

S_3 = 0 psi

then

$$M.S. = \frac{S_{ALL}}{S_e} - 1 = \underline{+0.26}$$

where:

S_{ALL} = 0.577 (23,750 psi)

= 13,700 psi

2.6.7.8.2 Bottom End Plate

It is assumed that the sections of end plate between stiffeners can be represented by a rectangular plate of appropriate dimensions. The width (b) of the plate is the difference between radii of the neutron shield tank and expansion tank shells, as shown in Figure 2.6.7-31. The length (a) of the plate is the average of the inner and outer arch lengths, a = 16.4 inches ((17.3 + 15.4)/2). Using Case 36 (Roark, page 225), the maximum bending stress on the 0.5-inch thick end plate is:

$$S_{max} = \beta \frac{wb^2}{t^2}$$

$$= 3375 \text{ psi}$$

where:

$\beta = 0.75$

$w = 180$ psig

$b = 2.5$ inches

$t = 0.5$ in

then

$$M.S. = \frac{S_{ALL}}{S_{max}} - 1 = \underline{+LARGE}$$

where:

$S_{ALL} = 23{,}750$ psi (S_y at 250°F)

2.6.7.8.3 Stiffener

The drop load is assumed to be distributed over all stiffeners equally. It is further assumed that the stiffener examined is in tension resulting from the drop load, as shown in Figure 2.6.7-32. The analysis shown below is for a 1-inch section (longitudinal) without credit for end plate welds. The drop pressure load is L = 3,114 pounds (17.3 in^2 x 180 psi). Additionally, the stiffener must support itself and the expansion tank shell during a drop, which adds an additional 45 pounds of structural load, bringing the total load (L) on the stiffener to 3,159 pounds. The cross sectional area of the 1-inch section analyzed is 132 in^2.

$$S_T = \frac{L}{A}$$

$$= 10{,}029 \text{ psi}$$

The margin of safety is:

$$M.S. = \frac{S_{ALL}}{S_T} - 1 = \underline{+0.37}$$

where:

$S_{ALL} = 0.577(23,750)$ psi
$= 13,700$ psi

2.6.7.8.4 Stiffener Weld

This analysis of a unit section (1-inch longitudinal) of expansion tank shell assumes that the drop load is equally distributed among all stiffeners. The load acting on the weld attaching the stiffener to the adjacent shield tank stiffener equals the load acting on the stiffener, L = 3,114 pounds (Section 2.6.7.8.3). The weld is a 0.188-inch fillet, both sides with a total throat area, $A_w = 0.265$ in^2. The tensile stress acting on the weld is:

$$S_T = \frac{L}{A_w}$$

$$= 11,750 \text{ psi}$$

The resulting margin of safety is:

$$M.S. = \frac{S_y}{S_T} - 1 = \underline{+0.17}$$

where:

$S_y = 0.577(23,750)$ psi
$= 13,700$ psi

2.6.7.9 Upper Ring/Outer Shell Intersection Analysis

Membrane and bending stresses are induced in the upper ring/outer shell intersection region of the cask body. These stresses are calculated using a detailed finite element model (Figure 2.6.7-33) and the ANSYS PC-Linear computer program.

The upper ring/outer shell intersection region is conservatively analyzed utilizing an axisymmetric model, axisymmetric loading and minimum ring cross section properties. The actual loading occurs only at the two lifting trunnions, and the minimum ring cross section occurs only at four 90-degree locations around the ring circumference. The model is restrained in the longitudinal direction by roller boundary conditions on the inner and outer shells (Figure 2.6.7-34) located 10 inches below the upper ring/outer shell intersection (attenuation length = 2.5 $(Rt)^{0.5} = 9.81$ inches). A fine mesh grid is used in the model in regions where peak stresses

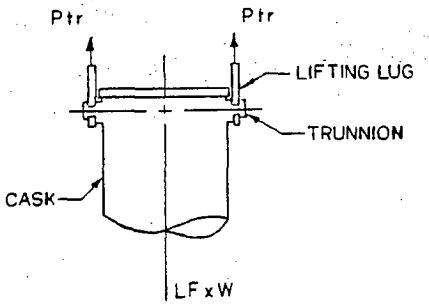
caused by concentration effects are expected. The following assumptions are made in this analysis:

1. The stiffness and support of the lead shell are not included.
2. The support/restraint of the upper ring provided by the closure lid and bolts is not included.
3. A uniform average temperature of 300°F is used in the analysis.
4. ANSYS STIF42 isoparametric quadrilateral elements adequately represent the cask geometry.

The sections analyzed as critical are shown in Figure 2.6.7-35. Section c-c is critical for P_m stress, and section a-a is critical for $P_m + P_b$ stress.

Applied Loads

The normal operations lifting trunnion loads used in this analysis are:

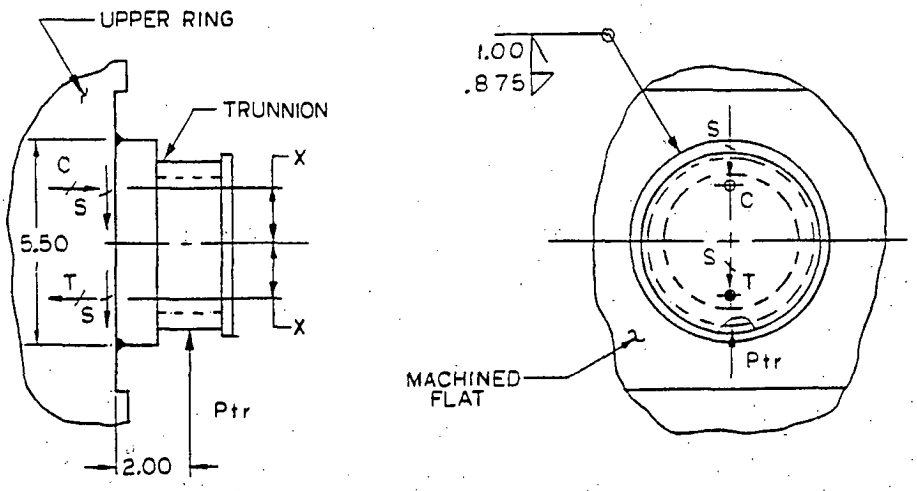


Lifting Load On Trunnions

Load Factor (LF) = 1.15

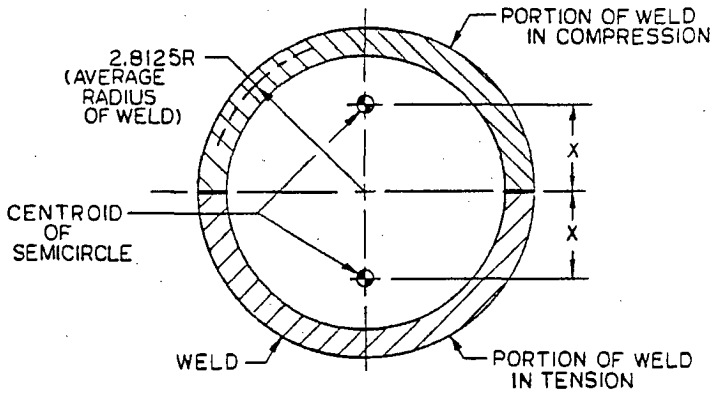
Cask Weight (W) = 52,000 lbs

$P_{tr} = (LF)(W/2) = (1.15)(52,000/2) = 29,900$ lbs



Lifting Trunnion Load Geometry

The concentrated loads were used to represent the distributed loads in the trunnion weld.



Trunnion Weld Group Centroid

To determine the trunnion weld group centroid:

$x = 0.6366\ R_{avg}$

$= 0.6366\ (2.8125)$

$= 1.790$ inches

$T = C = y\ (P_{tr}/2x)$

$= 2.00\ (29{,}900) / 2\ (2.8125)$

$= 16{,}704$ lbs

$S = P_{tr}/2$

$= 29,900/2$

$= 14,950$ lbs

Assume these loads are uniform over the trunnion weld diameter:

$T_u = C_u = 16,704/2(2.8125)$

$= 2969.6$ lb/in

$S_u = 14,950/2(2.8125)$

$= 2657.8$ lb/in

The ANSYS program requires that the loads for an axisymmetric model be input as load/radian:

Radians enclosed in 1 inch of circumference = 1/radius = 11/13.94 = 0.0717

$T_r = C_r = (2969.6)/0.0717$

$= 41,396.22$ lb/rad

$S = 2657.8/0.0717$

$= 37,049.73$ lb/rad

Calculated Stress Summary - Normal Operations Conditions

As anticipated, the maximum stresses occur at the upper ring/outer shell intersection, in the region of the machined flat and the internal radius of the outer shell. This analysis conservatively considers an outer shell thickness of 1.12 inches (actual shell thickness is 1.20 inches).

Stress peaking is present at the intersection of the outside surface of the outer shell with the upper ring because of stress concentration effects. The three sections through this region were investigated to determine the maximum stress intensity.

Section	Node	ANSYS Output Stress Summary			
		Radial S_x (ksi)	Axial S_y (ksi)	Hoop S_z (ksi)	Shear S_{xy} (ksi)
	66	1.6	7.3	2.9	-0.6
a-a	65	-0.1	4.9	1.9	-0.4
	64	-2.6	-0.4	-0.2	0.8
	66	1.6	7.3	2.9	-0.6
b-b	61	-0.7	5.1	1.6	0.5
	56	1.1	1.8	0.6	0.6
	66	1.6	7.3	2.9	-0.6
c-c	61	-0.7	5.1	1.6	0.5
	56	-0.2	4.5	0.6	0.6

The P_m and the $P_m + P_b$ stress components are determined by linearization of the ANSYS output stress components across sections a-a, b-b, and c-c. The principal stresses are calculated using the classical stress transformation law (Table 2.6.7-41).

The total normal operations lifting condition component stresses, principal stresses, and stress intensities at the critical section are calculated by combining the principal stresses from lifting, section b-b, with the internal pressure hot case (Table 2.6.1-1 and Table 2.6.2-2).

The P_m principal stress summary is:

Load Condition	Principal Stresses (ksi)		
	S_1	S_2	S_3
Lifting	5.5	-0.3	2.0
Internal Pressure	2.9	0.4	-0.4
Total	8.4	0.1	1.6

P_m stress differences are: S_{12} = 8.3 ksi, S_{23} = -1.5 ksi, and S_{31} = -6.8 ksi.

P_m stress intensity is S_i = 8.3 ksi.

Allowable stress intensity is S_a = 1.0 S_m = 20.0 ksi (Table 2.3.1-1).

$$M.S. = \frac{S_a}{S_i} - 1 = \underline{+1.41}$$

The $P_m + P_b$ principal stress summary is:

Load Condition	Principal Stresses (ksi)		
	S_1	S_2	S_3
Lifting	9.1	-2.7	4.0
Internal Pressure	4.2	1.5	0.2
Total	13.3	-1.2	4.2

The $P_m + P_b$ stress differences are: S_{12} = 14.5 ksi, S_{23} = -5.4 ksi, and S_{31} = -9.1 ksi.

The $P_m + P_b$ stress intensity is S_i = 14.5 ksi.

Allowable stress intensity is $S_a = 1.5\ S_m$ = 30.0 ksi.

$$M.S. = \frac{S_a}{S_i} - 1 = +1.07.$$

The maximum peak stress, S_y = 7.3 ksi, is less than 1.5 S_m; therefore, a fatigue evaluation is not required.

2.6.7.10 PWR/BWR Rod Transport Canister Assembly Analysis

2.6.7.10.1 Discussion

The NAC-LWT PWR/BWR Rod Transport Canister is analyzed for structural adequacy in accordance with the requirements of 10 CFR 71 for a 1-foot drop (normal transport condition). The structural evaluation is performed by classical elastic analysis methods. The components evaluated include the can weldment, internal spacer, 4×4 and 5×5 inserts (rod holder), PWR insert, BWR fuel assembly lattice spacer and can weldment spacer. In the 5×5 insert configuration, four of the tubes comprising the insert may be replaced with a single larger tube to accommodate an oversize nonfuel-bearing component (e.g., a single BWR water rod or a CE guide tube). Evaluations are performed for the inserts being comprised of 16 or 25 tubes to accommodate the fuel rods and these evaluations are considered to bound the insert configuration containing a single BWR water rod. The presence of the BWR water rod reduces the inertial loading due to contents, as well as employs a larger cross-section for the BWR water rod as compared to four smaller tubes containing fuel rods.

2.6.7.10.2 Analysis Description

Geometry

The geometry of the can assembly is shown in Drawing 315-40-098. Note that the tube component of the can assembly is fabricated from a 6-in.×6-in.×0.5-in.-thick tube that is machined to the final dimensions of 5.5-in.×5.5-in.×0.25-in.-thick. The can assembly is positioned within the basket during transport of the cask. If the cask is equipped with a PWR

basket, the PWR insert is required to provide correct positioning within the basket. The can assembly is constructed of Type 304 stainless steel with the exception of the PWR insert, which is constructed of 6061 Aluminum.

Loadings

The magnitude of the impact force varies according to the drop height and drop orientation. As calculated in Section 2.6.7.4, the g-loads for the 1-foot end and side drops are 15.8 and 24.3g, respectively.

Detailed Analysis

The maximum temperatures of the components are shown below. For the can weldment and components outside the can weldment, the temperatures are significantly below 700°F, which are within the 800°F design limits. For the tubes supporting the fuel pins, the maximum temperatures are determined to be 925°F. The tubes, which are only used with the insert for the high burnup pins, are shown to be acceptable using ASME Code, Section III, Division I, Subsection NH, which specifies allowable stresses above 800°F. The remaining components are shown to be acceptable using the stress allowable in ASME Code, Section III, Subsection NB.

Thermal Stresses

To evaluate effects of the calculated temperatures within the can assembly, the nominal dimensions of the can are used to calculate the resulting thermal expansions. The coefficient of thermal expansion for ASME SA 240 Type 304 stainless steel is 9.0×10^{-6} in./in.-°F. All components of the can assembly are constructed of Type 304 stainless steel, except for the PWR insert. The PWR insert is made of 6061 Aluminum with a coefficient of thermal expansion of 13.5E-6 in/in-°F. The following temperatures are used in the thermal expansion calculation and material property definitions.

Component Name	Maximum Operating Temperature (°F)	Temperature Used for Calculation (°F)
Aluminum PWR Insert	394	400
Can Weldment	538	575
5 × 5 Insert	885	925

Since the 5 × 5 insert is larger than the 4 × 4 insert, it is bounding for the thermal expansion calculations. The nominal gap between the insert and internal spacer is 3.56 – 3.44 = 0.12 inch. The growth of the insert is 3.44 × 9.0 E-6 in/in-°F × (925-70)°F = 0.027 inch. Since the growth of the insert is less than the nominal gap, no interference will occur.

The nominal gap between the can shell and PWR insert is 5.75 – 5.5 = 0.25 inch. The growth of the can shell is 5.5 × 9.0 E-6 in/in-°F × (575-70)°F = 0.025 inch. Since the growth of the can shell is less than the nominal gap, no interference will occur.

Because the differential thermal expansion causes no interference or binding, no further thermal stress evaluation is required.

Can Weldment

The can weldment is contained within the basket assembly and not subjected to bending stresses in the side-drop case.

For the end drop, the can weldment is loaded by its own weight. The can contents bear against the bottom or top of the can assembly, depending on drop orientation.

LWT Can Body Compressive Stress

Under normal operating conditions the tube is evaluated for a 15.8 g acceleration for the end drop. The compressive load (P) on the tube is the combined weight of the lid and tube times the appropriate g factor.

The compressive stress (S_c) in the tube body is:

$$S_c = \frac{P}{A} = \frac{4{,}898 \text{ lb}}{4.98 \text{ in}^2} \cong 984 \text{ psi}$$

where:

$A = \pi (0.75^2 - 0.5^2) + 4 \times 4.0 \times 0.25 = 4.98 \text{ in}^2$

P = 310 × 15.8 = 4,898 lbs (conservatively, the weigh of the tube, lid, and bottom plate is used)

The margin of safety (MS) is then:

$$MS = \frac{S_m}{S_c} - 1 = \frac{17{,}300 \text{ psi}}{984 \text{ psi}} - 1 = +16.6.$$

LWT Can Body Bearing Stress

For the bottom end drop, the can base feet are subjected to a bearing stress. The compressive load (P) on the base is the combined weight of the can assembly, fuel and insert, and the internal spacer times the appropriate g factor.

P = [310 (can weldment) + 350 (fuel) + 75 (tube insert) + 240 (internal spacer)] × 15.8 = 15,405 lbs

The compressive stress (S_c) in the feet is:

$$S_c = \frac{P}{A} = \frac{15{,}405}{2.8} \cong 5{,}502 \text{ psi}$$

where:

$$A = 4 \text{ x } 0.5 \text{ x } (2.0 - 0.6) = 2.8 \text{ in}^2$$

The margin of safety (MS) for bearing is then:

$$MS = \frac{S_m}{S_c} - 1 = \frac{17{,}300 \text{ psi}}{5{,}502 \text{ psi}} - 1 = +2.14$$

Can Internal Pressure

Can weldment internal pressure is considered insignificant in the end-drop and side-drop cases because it will tend to reduce the compressive loads on the can tube sides.

The effect of internal pressure is evaluated for the bending stress that the pressure imposes on the can weldment sides. Conservatively, a one-inch-wide section of the tube wall, equal in length to the outside dimension of the tube (L = 5.5 in.) is analyzed as a cantilevered beam with a uniform load.

The maximum moment (M) is determined by the following relation:

$$M = \frac{wL^2}{12} = \frac{(85 - 14.7)(5.5^2)}{12} \cong 177.2 \text{ in.-lb}$$

where w is the maximum differential pressure across the can wall due to the maximum normal temperature (assumes that the cask internal pressure is atmospheric). The 85 psia envelopes the pressure reported in Section 3.4.4.2.

The combined stress (σ) in the 0.25-inch thick tube wall is:

$$\sigma = \frac{Mc}{I} + \frac{wL}{t}$$

$$= \frac{(177.2)(0.125)}{0.0013} + \frac{(85 - 14.7)(5.5)}{0.25} \cong 18{,}600 \text{ psi}$$

The margin of safety (MS) is:

$$MS = \frac{1.5 S_m}{\sigma} - 1 = \frac{25.35 \text{ ksi}}{18.6 \text{ ksi}} - 1 = +0.36 \text{ for the normal condition}$$

Can Lid Bolt Analysis

The tensile force (F_p) on each lid bolt due to internal pressure is:

$$F_p = \frac{PA}{n} = \frac{(85-14.7)(3.75^2)}{8} \cong 123.6 \text{ lbs}$$

where

P = the pressure differential across the can wall at maximum normal temperature (assumes cask internal pressure is atmospheric)

A = 3.75 in × 3.75 in, the area of the can lid exposed to pressure

n = 8, number of bolts

The total tensile force on each lid bolt is F_p + the initial preload force, F_i = 635 lbs

The lid bolt tensile stress (σ) is:

$$\sigma = \frac{F_p + F_i}{A_t} = \frac{758.6}{0.049} = 15{,}480 \text{ psi}$$

where

A_t = 0.049 in.^{2}, the bolt tensile stress area $\frac{\pi}{4}(0.25^2)$

The margin of safety (MS) for the normal condition is:

$$MS = \frac{S_y}{\sigma} - 1 = \frac{18.8 \text{ ksi}}{15.48 \text{ ksi}} - 1 = +0.21$$

Can Tube Buckling

The tube is evaluated, using the Euler formula, to determine the critical buckling load (P_{cr}):

$$P_{cr} = \frac{K\pi^2 EI}{L^2} = \frac{3.26\pi^2(24.4\times10^6)(24.2)}{(165.5)^2} = 0.698 \times 10^6 \text{ lbs}$$

where:

E = 24.4×10^6 psi at 750°F

$$I = \frac{5.5^4 - 5.0^4}{12} = 24.2 \text{ in}^4$$

L = tube body length (165.5 inches)

Because the maximum compressive load (310 × 15.8 = 4,898 lbs) is much less than the critical buckling load (698×10^3 lbs), the tube has adequate resistance to buckling.

Internal Spacer

The internal spacer body is contained within the can assembly and not subjected to bending in the side drop condition.

The compressive stress in the internal spacer rails during the side drop is determined as follows:

$$\sigma_b = \frac{Wg}{A} = \frac{665 \times 24.3}{123.7} \cong 130.6 \text{ psi}$$

where:

W = total load = 350 (fuel) + 240 (internal spacer) + 75 (4x4 insert) = 665 lbs

g = 24.3 (normal condition side drop)

A = 123.7 in^2 cross-sectional area of spacer rails, $4 \times 0.188 \times (165.25 - 2 \times 0.38)$

The resulting margin of safety is large.

Internal Spacer Compressive Stress

For the end drop, the internal spacer shell is loaded by its own weight. The insert rail stiffness is conservatively neglected in the strength.

Under normal operating conditions, the spacer is evaluated for a 15.8 g acceleration. The compressive load (P) on the shell is due to the weight of the internal spacer. The entire weight of the internal spacer times the appropriate g factor will be used to calculate the compressive load.

$P = 240 \times 15.8 = 3{,}792$ lbs

The compressive stress (S_c) in the internal spacer body is:

$$S_c = \frac{P}{A} = \frac{3{,}792}{1.69} \cong 2{,}244 \text{ psi}$$

where:

A = $(3.936^2 - 3.56^2) - 12 \times 0.5 \times 0.188 = 1.69$ in^2

The margin of safety (MS) is then:

$$MS = \frac{S_m}{S_c} - 1 = \frac{17{,}300}{2{,}244} - 1 = +6.71$$

Internal Spacer Buckling

The shell is evaluated, using the Euler formula for an axially distributed load, to determine the critical buckling load (P_{cr}):

$$P_{cr} = \frac{K\pi^2 EI}{L^2} = \frac{3.26\pi^2 (24.4 \times 10^6)(6.615)}{(165.25)^2} = 0.19 \times 10^6 \text{ lbs}$$

where:

$E = 24.4 \times 10^6$ psi at 750°F

$I = \frac{3.936^4 - 3.56^4}{12} = 6.615 \text{ in}^4$

L = spacer body length (165.25 inches)

Because the maximum compressive load (240×15.8 = 3,792 lbs) is much less than the critical buckling load (190×10^3 lbs), the internal spacer has adequate resistance to buckling.

4×4 and 5×5 Inserts

The 4×4 and 5×5 inserts are contained within the internal spacer. The 4×4 inserts are supported by straps on 10-inch spacing. These straps provide a clearance of 0.31 inches and will allow bending of the tubes to occur. The 5×5 insert tubes are evaluated for a diametrically opposed load due to the weight of the adjacent tubes during the side drop.

The 4×4 insert lower tube will be evaluated as a fixed-fixed beam over a 10-inch span. The weight of the 3 tubes above (as well as lower tube self-weight) will be considered in the analysis. The stiffness of the tubes above the lower tube will conservatively be neglected. The combined weight (P) of the fuel pins and insert tubes are considered as a uniformly distributed load over the 10-inch span. In addition, the weights are scaled by the appropriate deceleration factor depending on the drop orientation and condition being evaluated.

The maximum bending stress (f_b) is determined as follows:

$$f_b = \frac{Wlg}{12Z} = \frac{5.8(10.0)24.3}{12x0.0092} \cong 12{,}766 \text{ psi}$$

where:

W = load on 10-inch section = (14 + 9.5) x 4 x 10/163.0 = 5.8 lbs

l = 10 inches (span of tube)

g = 24.3 (normal condition side drop)

Z = π/32 (0.6875^4-0.6315^4) / 0.6875 = 0.0092 in^3 (section modulus of the tube)

The margin of safety (MS) is:

$$MS = \frac{1.5S_m}{\sigma_{max}} - 1 = \frac{1.5(12{,}050)}{12{,}766} - 1 = +0.42$$

The bending moment due to the diametrically opposed line load on the 5×5 insert is calculated by the following:

$$M_b = \frac{WRg}{\pi} = \frac{70/163.0 \times 0.344 \times 24.3}{\pi} \cong 1.143 \text{ lb} - \text{in}$$

where:

W = total load = 14 × 4 + 70/5 = 70 lbs

g = 24.3 (normal condition side drop)

R = 0.6875/2 = 0.344 in (radius of insert tube)

The resulting bending stress is:

$$f_b = \frac{6M_b}{t^2} = \frac{6 \times 1.143}{0.028^2} \cong 8{,}745 \text{ psi}$$

The margin of safety (MS) is:

$$MS = \frac{1.5\ S_m}{\sigma_{max}} - 1 = \frac{1.5(12{,}050)}{8{,}745} - 1 = +1.07$$

4×4 and 5×5 Insert Tube Compressive Stress

Under normal operating conditions, the tube is evaluated for a 15.8 g acceleration. The compressive load (P) on the shell is due to the weight of the tube. The entire weight of the tube is calculated as:

$P = \pi/4\ (0.6875^2 - 0.6315^2) \times 163.0 \times 0.288 = 2.72$ lbs

The compressive stress (S_c) in the tube body is:

$$S_c = \frac{P}{A} = \frac{2.72 \times 15.8}{0.058} \cong 741 \text{ psi}$$

where:

$A = \pi/4\ (0.6875^2 - 0.6315^2) = 0.058 \text{ in}^2$

The margin of safety (MS) is then:

$$MS = \frac{S_m}{S_c} - 1 = \frac{14{,}100}{741} - 1 = +18.0$$

PWR Insert

The PWR insert contains the can assembly for insertion into the PWR basket. The PWR insert comprises a square box section with smooth sides. Therefore, no bending stresses will be introduced in the side drop condition.

PWR Insert Bearing Stress

The bearing load (P) on the PWR insert is due to the weight of the loaded can assembly. The entire weight of the assembly times the appropriate g factor will conservatively be used to calculate the bearing load.

W = bearing load = [350 (fuel) + 310 (can) + 240 (internal spacer) + 75 (4x4 insert)] x 24.3 = 23,693 lbs

The compressive stress (S_c) in the tube body is:

$$S_c = \frac{P}{A} = \frac{23,693}{921.3} \cong 26 \text{psi}$$

where:

$$A = 5.5 \times 167.5 = 921.3 \text{ in}^2$$

The margin of safety (MS) is then:

$$MS = \frac{S_y}{S_c} - 1 = \frac{23,500}{26} - 1 = +\text{Large}$$

PWR Insert Body Compressive Stress

Under normal operating conditions, the tube is evaluated for a 15.8 g acceleration. The compressive load (P) on the body is due to the weight of the PWR insert. The entire weight of the PWR insert, times the appropriate g factor, will conservatively be used to calculate the compressive load.

$$P = 650 \text{ lb} \times 15.8 = 10,270 \text{ lbs}$$

The compressive stress (S_c) in the tube body is:

$$S_c = \frac{P}{A} = \frac{10,270}{39.2} \cong 262 \text{ psi}$$

where:

$$A = (8.5^2 - 5.75^2) = 39.2 \text{ in}^2$$

The margin of safety (MS) is then:

$$MS = \frac{S_y}{S_c} - 1 = \frac{23,500}{262} - 1 = +\text{Large}$$

PWR Insert Tube Buckling

The tube is evaluated, using the Euler formula, to determine the critical buckling load (P_{cr}):

$$P_{cr} = \frac{K\pi^2 EI}{L^2} = \frac{3.26\pi^2 (8.8x10^6)(343.9)}{(167.0)^2} = 3.86\times10^6 \text{ lbs}$$

where:

E = 8.8×10^6 psi at 400°F

$$I = \frac{8.5^4 - 5.75^4}{12} = 343.9 \text{ in}^4$$

L = tube body length (167.0 inches)

Because the maximum compressive load (650 x 15.8 = 10,270 lbs) is much less than the critical buckling load (3.86×10^6 lbs), the PWR insert has adequate resistance to buckling.

PWR Insert Assembly Bolts

The PWR insert is comprised of four short and four long aluminum plates joined with ½-13 UNC × 1.5-in. long socket head cap screws to form a hollow box. Each plate is secured to each adjacent plate using three screws.

The screws joining the plates are loaded in shear when the two lift tabs are used to lift the PWR insert and its payload. The controlling load path is through the lift tab attached to the shorter side plate and the three screws connecting the shorter side plate to the adjacent long plate. The distance from the line of load application (centerline of the lift tab) to the centerline of the 3-screw pattern is approximately 3.6 inches. Any internal moment created by this eccentricity is reacted by the strong-direction section modulus of the side plates and is effectively countered by the stiffness inherent in the overall symmetry of the box section. The screw shear stress (τ) in each of the 3 screws is:

$$\tau = \frac{P/2}{A} = \frac{900}{3(0.130)} = 2{,}308 \text{ psi}$$

where:

P = [310 (can weldment)+350 (fuel rods)+240 (internal spacer)+70 (5×5 insert)+650 (PWR insert)]×1.1 = 1,782 lbs, use 1,800 lbs for analysis. (Total lift weight with 10% dynamic load factor.)

A = screw cross-sectional area = $(0.4069^2 \text{ x } \pi)/4 = 0.130 \text{ in}^2$ (Thread minor diameter)

The safety factor (FS) is calculated using a shear allowable of $0.6S_m$ at 750°F.

$$FS = \frac{0.6(15{,}600)}{2{,}308} = 4.06 > 3$$

where

S_m = 15,600 psi for commercial austenitic stainless steel.

Therefore the design condition that lifting stresses have a load factor of 3 on the basis of yield strength is met.

Can Weldment Spacer

The can weldment spacer prevents the PWR basket, PWR insert, fuel, and can weldment from shifting during transport. The spacer (Drawing 315-40-125, Item 10) is placed on the top of the can weldment. The spacer is bolted to the bottom side of the lid and the cruciform stiffener functions as the spacer between the lid and can weldment. The maximum load applied to the spacer occurs during the top end drop. To bound both normal and accident conditions, stresses are compared using accident load conditions and are compared to allowable stresses for normal operating conditions. The stress in the spacer is:

$$\sigma = \frac{P \times g}{A} = \frac{1{,}945 \times 60}{8.4} = 13{,}893 \text{ psi}$$

where:

P= Conservative weight of the PWR basket, PWR insert, fuel, and can weldment
= 1,945 lbs

g= Top end drop acceleration (60g)

A= Cross-sectional area of cruciform
$= 2 \times 7 \times 0.63 - 0.63^2 = 8.4 \text{ in}^2$

The margin of safety (MS) is:

$$MS = \frac{1.0 \times S_m}{\sigma} - 1 = \frac{17{,}500 \text{ psi}}{13{,}893 \text{ psi}} - 1 = +0.26$$

where:

S_m = The stress intensity of 304 stainless steel at 500°F

Because the height-to-diameter ratio (4.5/6.0 = 0.75) is less than one, the spacer has adequate resistance to buckling.

Using a bounding weight of 50.0 lbs for the spacer, the maximum shear stress on the 1/8-inch fillet weld corresponds to the hypothetical accident bottom end drop condition of 60g. The shear stress in the weld is computed as:

$$\tau = \frac{60 \times 50}{28.0 \times 0.707 \times 0.125} = 1{,}212 \text{psi}$$

where:

the perimeter of cruciform is 28.0 in $[(7\text{-}0.625) \times 4 + 0.625 \times 4]$

The margin of safety, based on the normal condition of transport allowable stress, is:

$$MS = \frac{0.6S_m}{\tau} - 1 = \frac{0.6 \times 17{,}500}{1{,}212} - 1 = +7.66$$

The can weldment spacer is, therefore, determined to be structurally adequate for normal and accident conditions for the NAC-LWT cask.

Fuel Assembly Lattice Spacer

The BWR fuel assembly lattice fits into the PWR insert in place of the can assembly. The fuel assembly lattice holds up to 25 intact BWR fuel rods. To accommodate the fuel assembly lattice, the bottom plate of the PWR insert is removed. This allows the fuel assembly lattice to rest on the bottom of the cask. To prevent the PWR basket from shifting during transport, a spacer (Drawing 315-40-125, Item 12) is placed at the top of the fuel assembly lattice. The spacer is bolted to the bottom side of the lid and eight 1-inch diameter posts function as the spacer between the lid and PWR basket. The maximum load applied to the spacer occurs during the top end drop. To bound both normal and accident conditions, accident stresses are compared to the normal allowable stress. The stress in the spacer is:

$$\sigma = \frac{P \times g}{A \times Np} = \frac{400 \times 60}{0.785 \times 8} = 3{,}822 \text{ psi}$$

where:

P= Conservative weight of the PWR basket

g= Top end drop acceleration (Table 2.6.7-34)

A= Cross-sectional area of a post

Np = Number of posts

The margin of safety is:

$$MS = \frac{1.0 \times S_m}{\sigma} - 1 = \frac{17{,}500 \text{ psi}}{3{,}822 \text{ psi}} - 1 = +3.58$$

where:

S_m = The stress intensity of 304 stainless steel at 500°F

Buckling of the post is evaluated using the Euler formula. The critical buckling load (P_{cr}) is:

$$P_{cr} = \frac{K\pi^2 EI}{L^2} = \frac{0.25\pi^2(25.8\times10^6)(0.0491)}{(13.4)^2} = 17{,}407 \text{ lbs}$$

where:

E = Modulus of elasticity = 25.8×10^6 psi at 500°F

I = Moment of inertia = $\frac{\pi \times d^4}{64} = 0.0491 \text{ in}^4$

d = Post diameter = 1 in

L = Post length = 13.38 inches

K = Euler buckling coefficient for fixed-free column = 0.25 (Marks, 9th Ed., p. 5-42)

Because the maximum compressive load (400/8 × 60 = 3,000 lbs) is less than the critical buckling load (17,407 lbs), the spacer has adequate resistance to buckling.

Figure 2.6.7-1 1-Foot Bottom End Drop with 130°F Ambient Temperature and Maximum Decay Heat Load

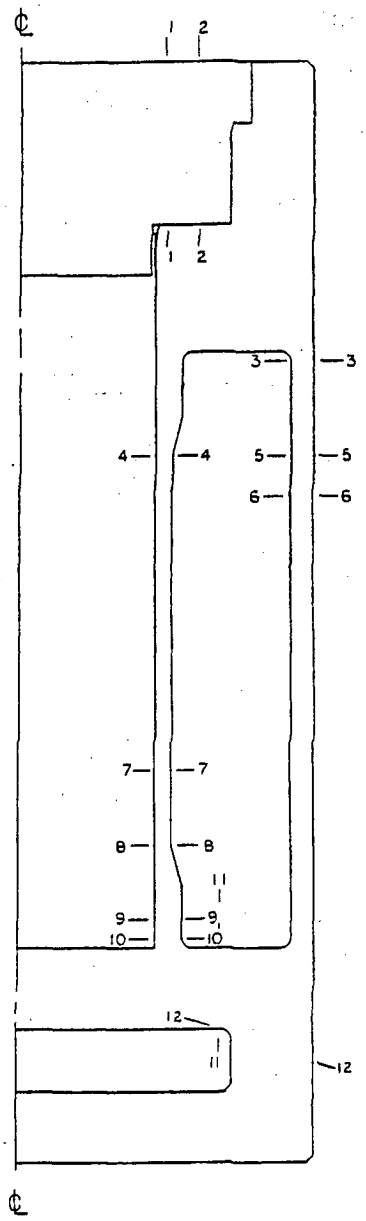


Figure 2.6.7-2 1-Foot Bottom End Drop with -40°F Ambient Temperature and Maximum Decay Heat Load

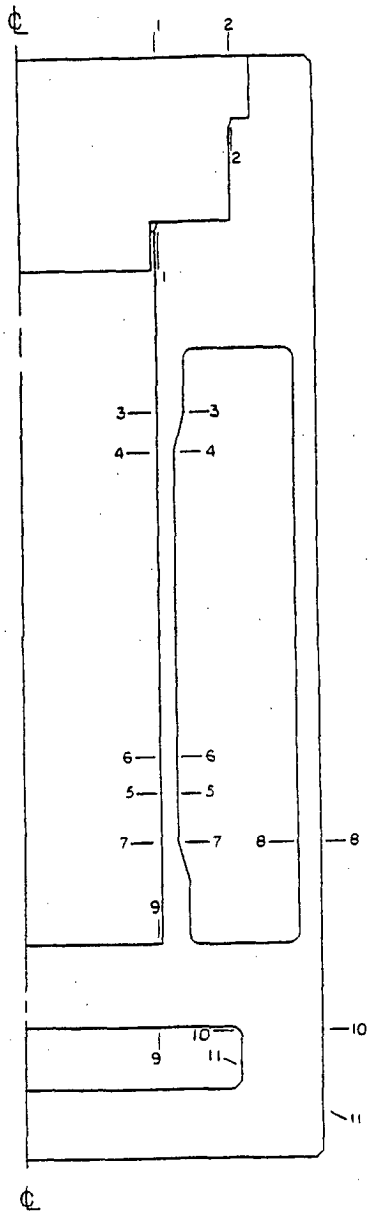


Figure 2.6.7-3 1-Foot Bottom End Drop with -40°F Ambient Temperature and No Decay Heat Load

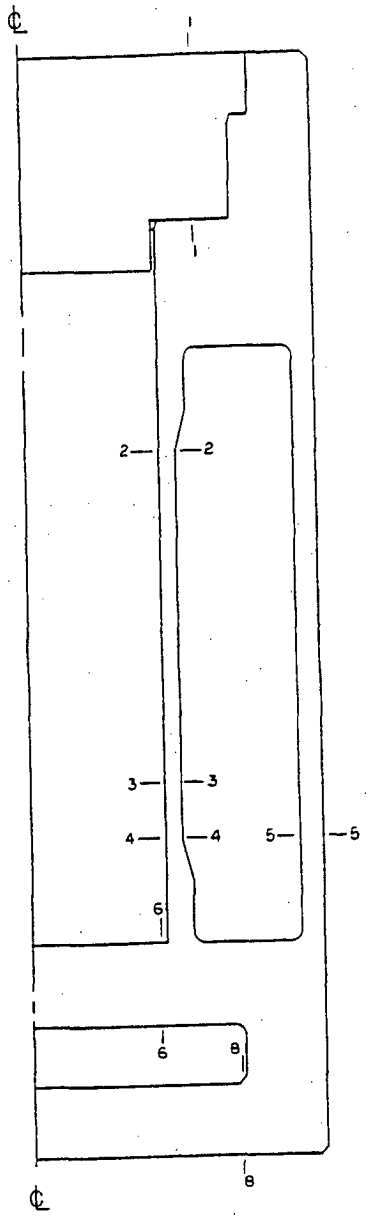


Figure 2.6.7-4 1-Foot Top End Drop with 130°F Ambient Temperature and Maximum Decay Heat Load

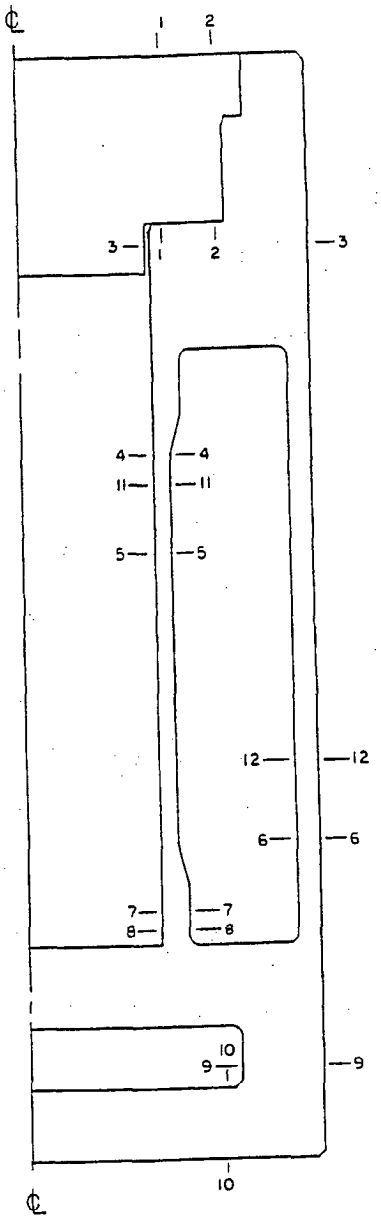


Figure 2.6.7-5 1-Foot Top End Drop with -40°F Ambient Temperature and Maximum Decay Heat Load

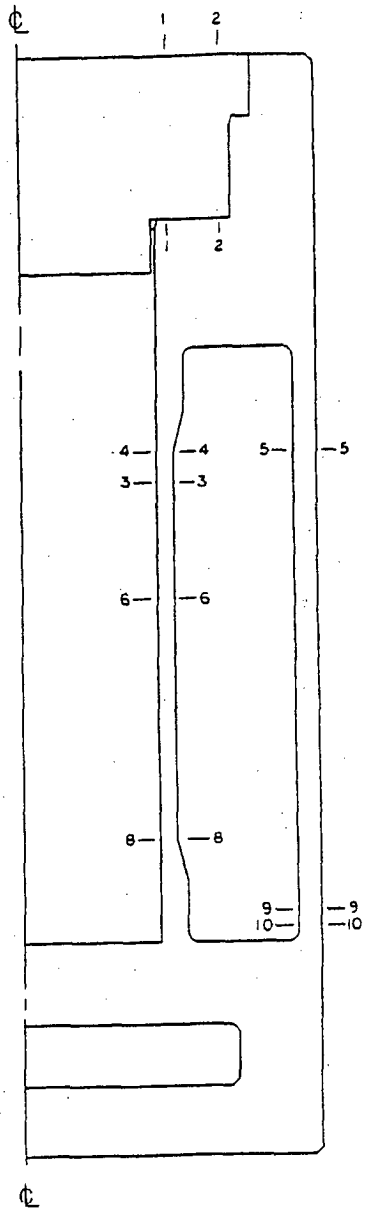


Figure 2.6.7-6 NAC-LWT Cask Critical Sections (1-Foot Side Drop with 100°F Ambient Temperature)

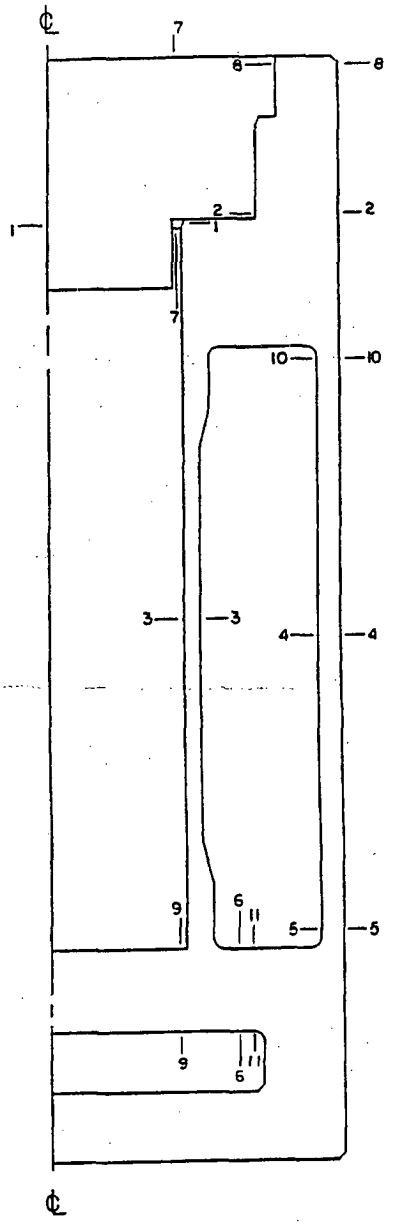


Figure 2.6.7-7 1-Foot Top Corner Drop with 130°F Ambient Temperature and Maximum Decay Heat Load - Drop Orientation = 15.74 Degrees

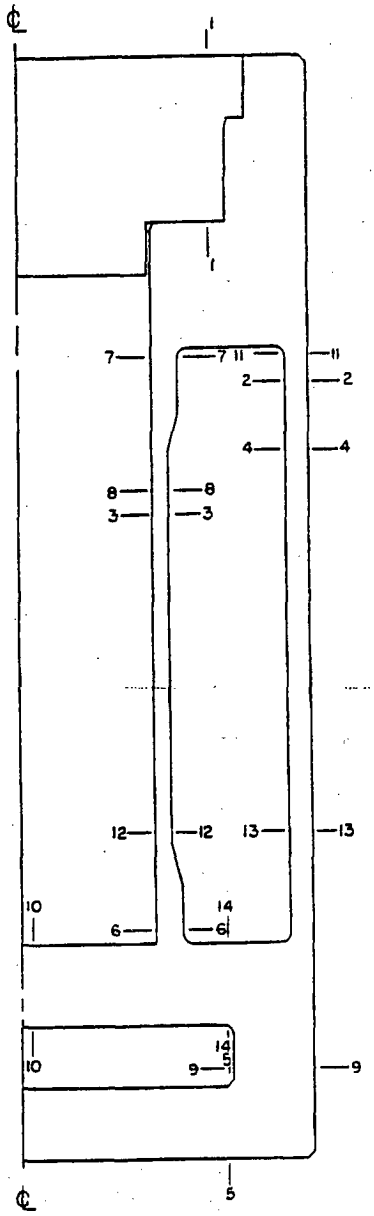


Figure 2.6.7-8 1-Foot Bottom Corner Drop with 130°F Ambient Temperature and Maximum Decay Heat Load - Drop Orientation = 15.74 Degrees

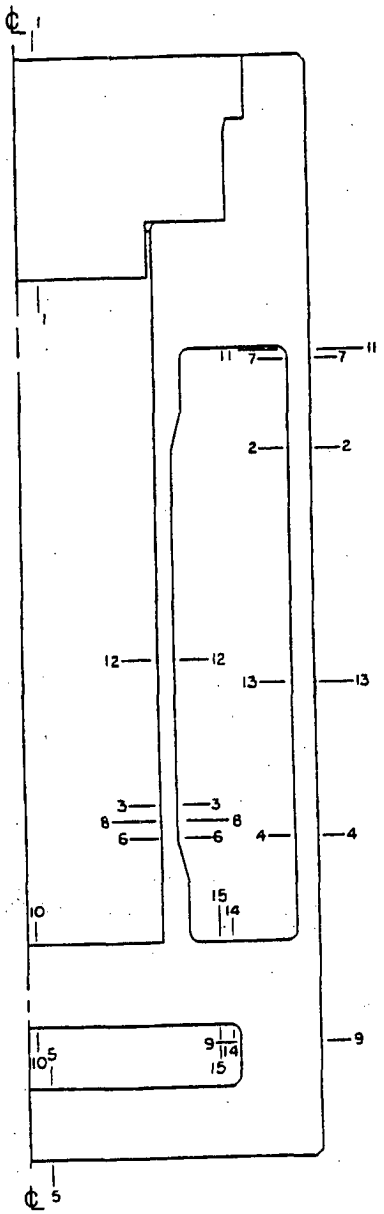


Figure 2.6.7-9 1-Foot Top Corner Drop with -40°F Ambient Temperature and No Decay Heat Load - Drop Orientation = 15.74 Degrees

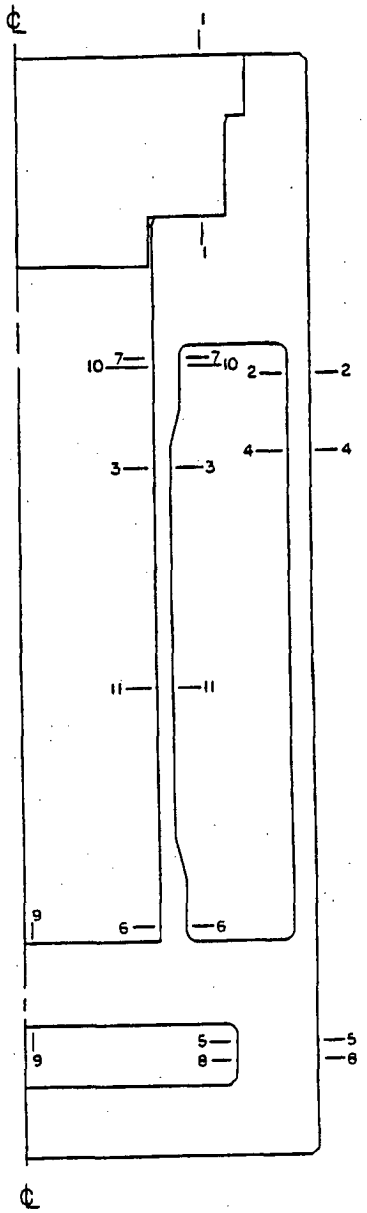


Figure 2.6.7-10 NAC-LWT Cask with Impact Limiters

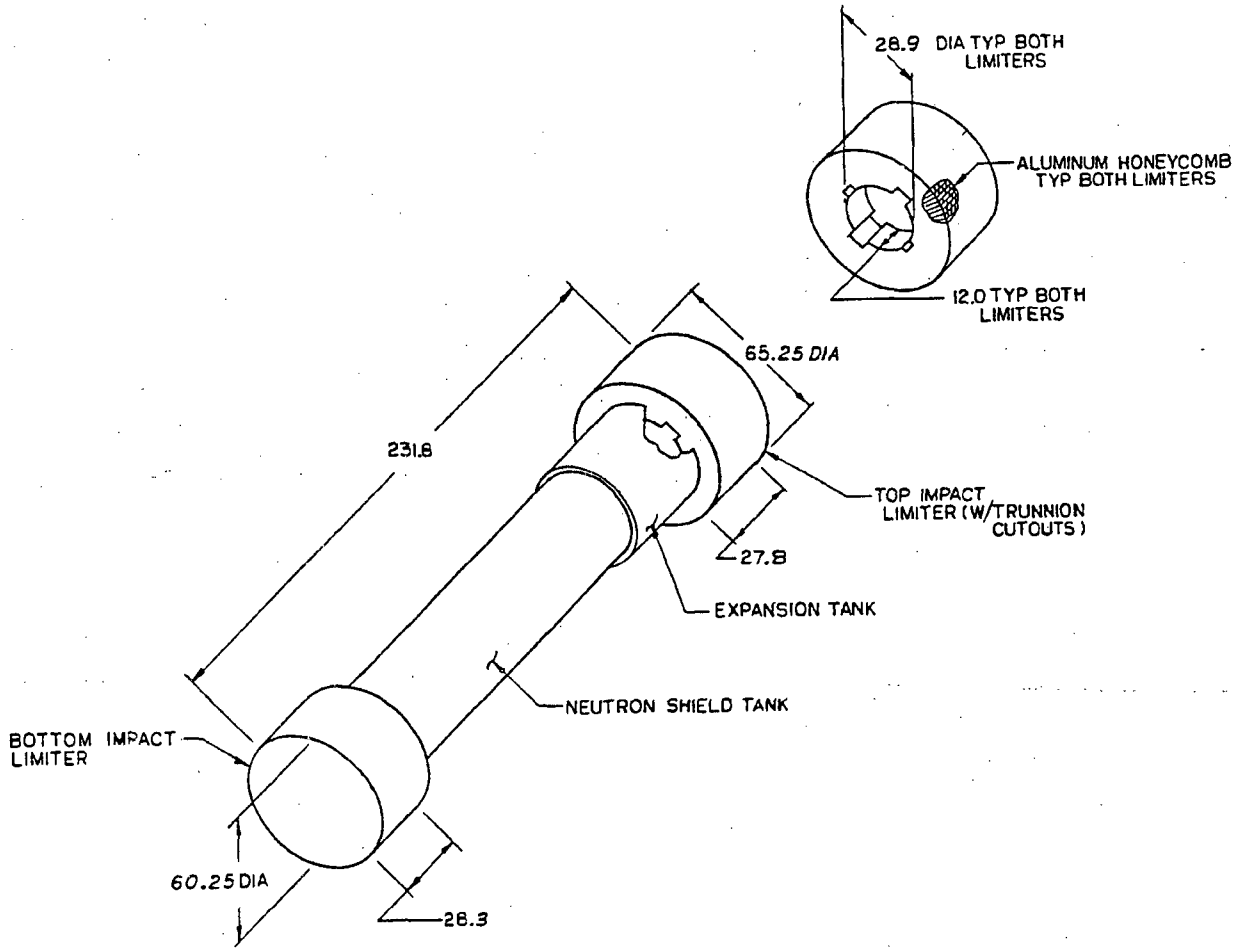


Figure 2.6.7-11 Cross-Section of Top Impact Limiter



Figure 2.6.7-12 Load Versus Deflection Curve (Typical Aluminum Honeycomb)

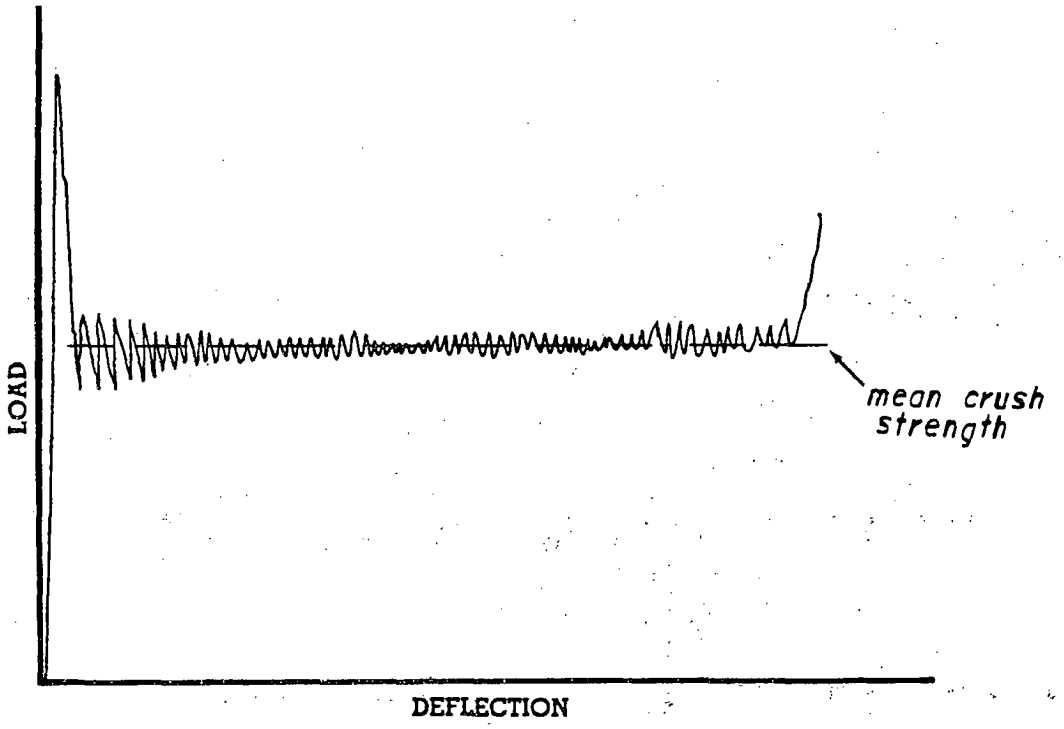


Figure 2.6.7-13 Quarter-Scale Model Limiter End Drop Cross-Section

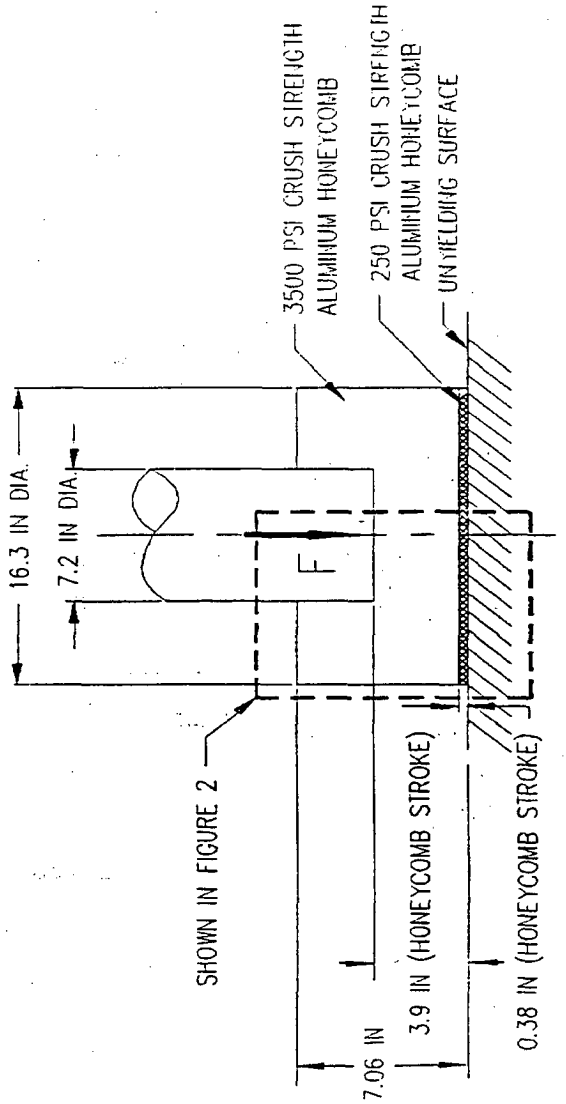


Figure 2.6.7-14 End Drop Impact Limiter Cross-Section

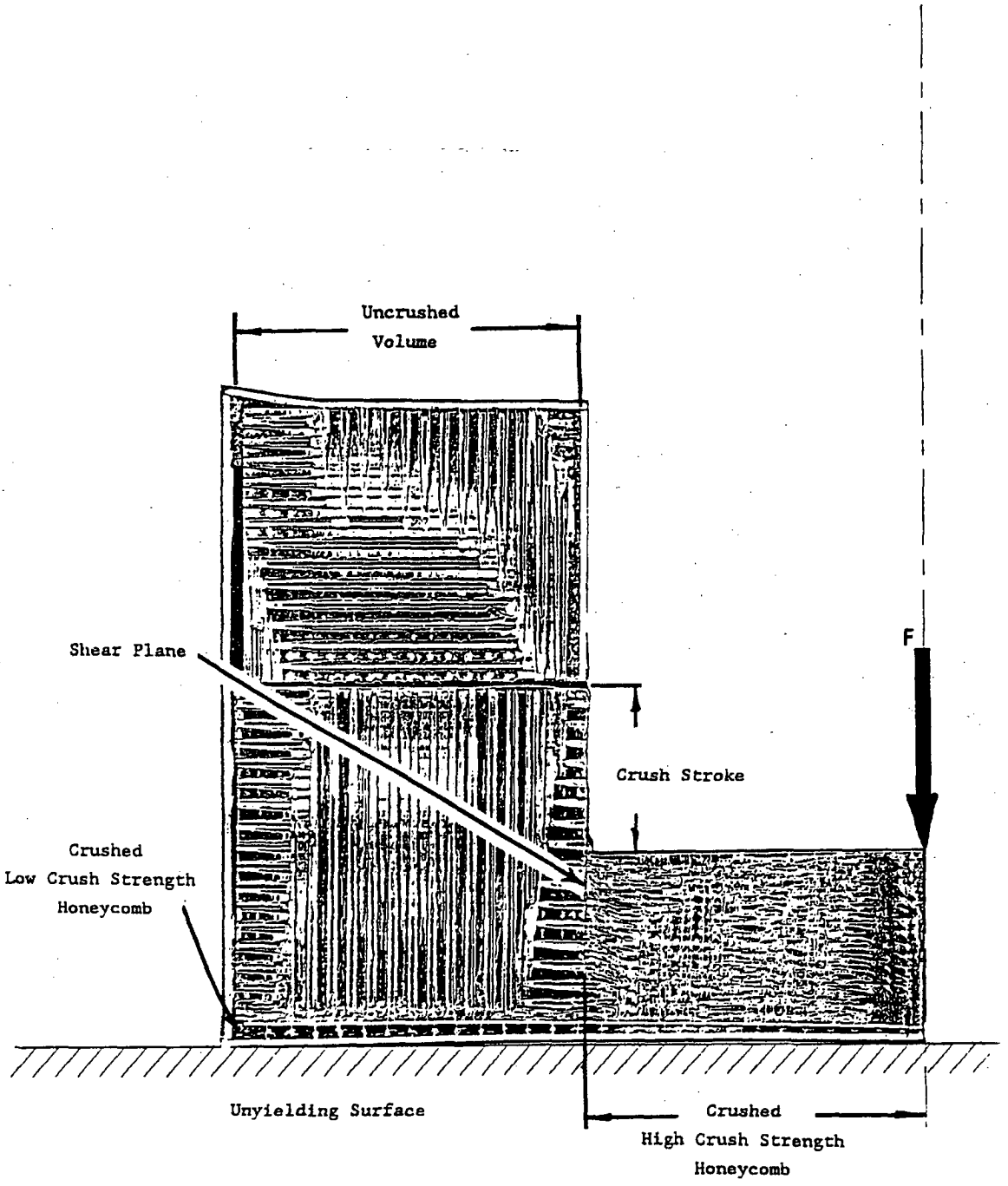


Figure 2.6.7-15 Impact Limiter Lug Detail



Figure 2.6.7-16 Cask Lug Detail



Figure 2.6.7-17 RBCUBED Output Summary – Center of Gravity Over Top Corner

Position	Crush Depth (in)	Crush Force, Fi (lb)	Package Velocity (in/sec)	Approximate Separation Moment (in-lb)
①	2	2.30×10^5	543.4	2.25×10^6
②	4	9.74×10^5	514.8	6.63×10^6
③	6	1.83×10^6	466.2	7.67×10^6
④	8	2.63×10^6	381.2	5.75×10^6

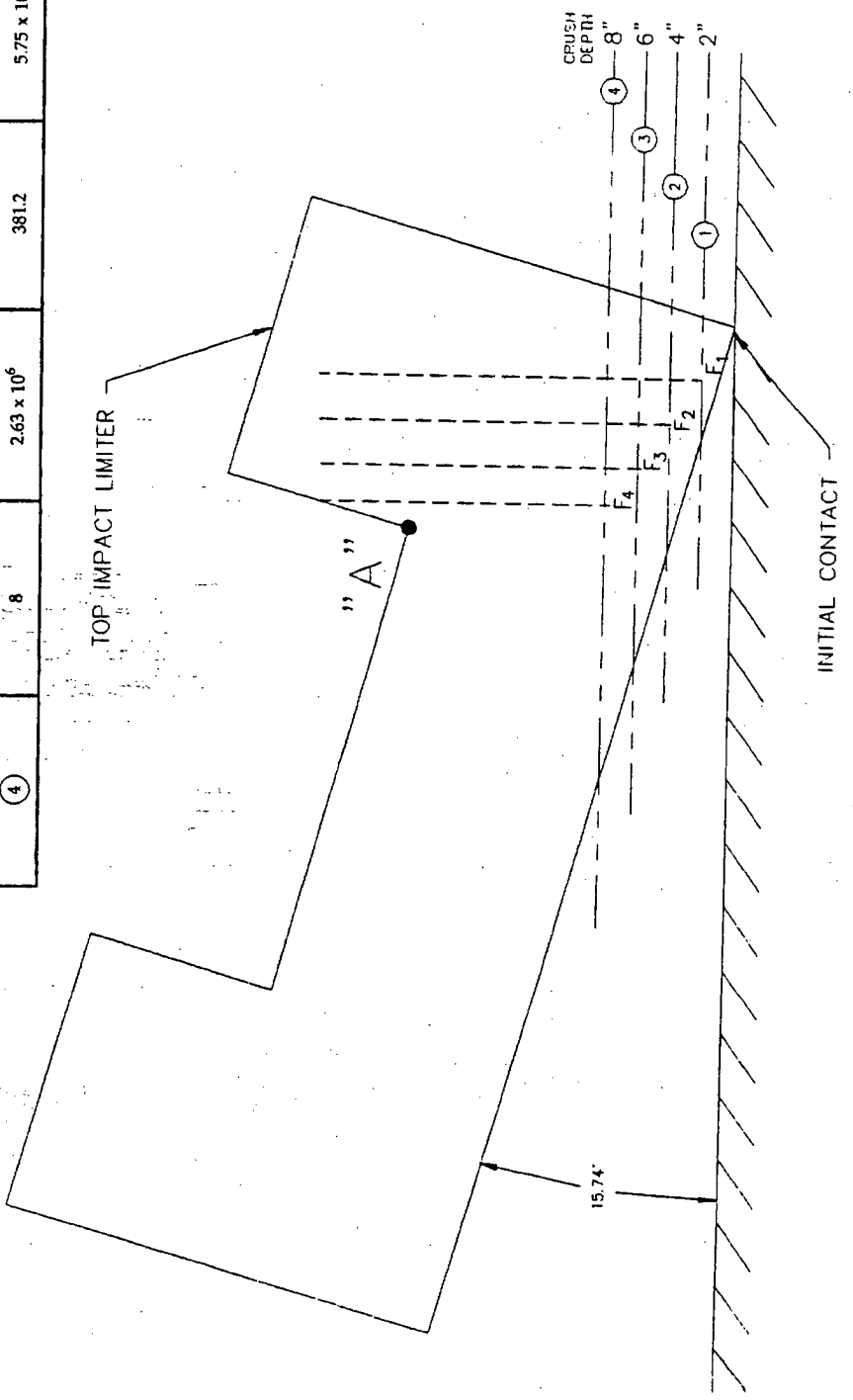


Figure 2.6.7-18 Free Body Diagram - Top Impact Limiter - Center of Gravity Over Corner

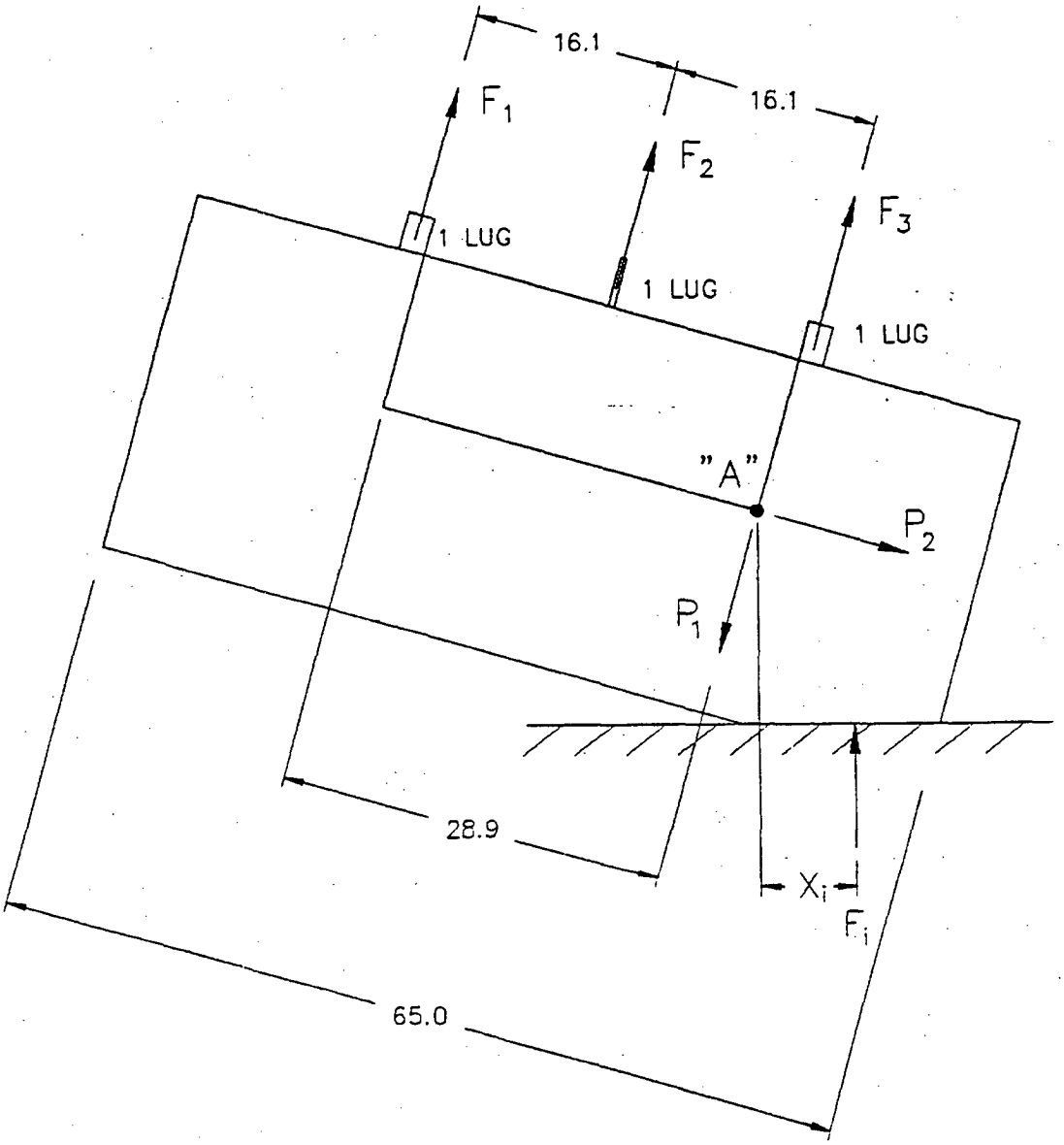


Figure 2.6.7-19 Free Body Diagram - Top Impact Limiter - Cask Wedging Forces

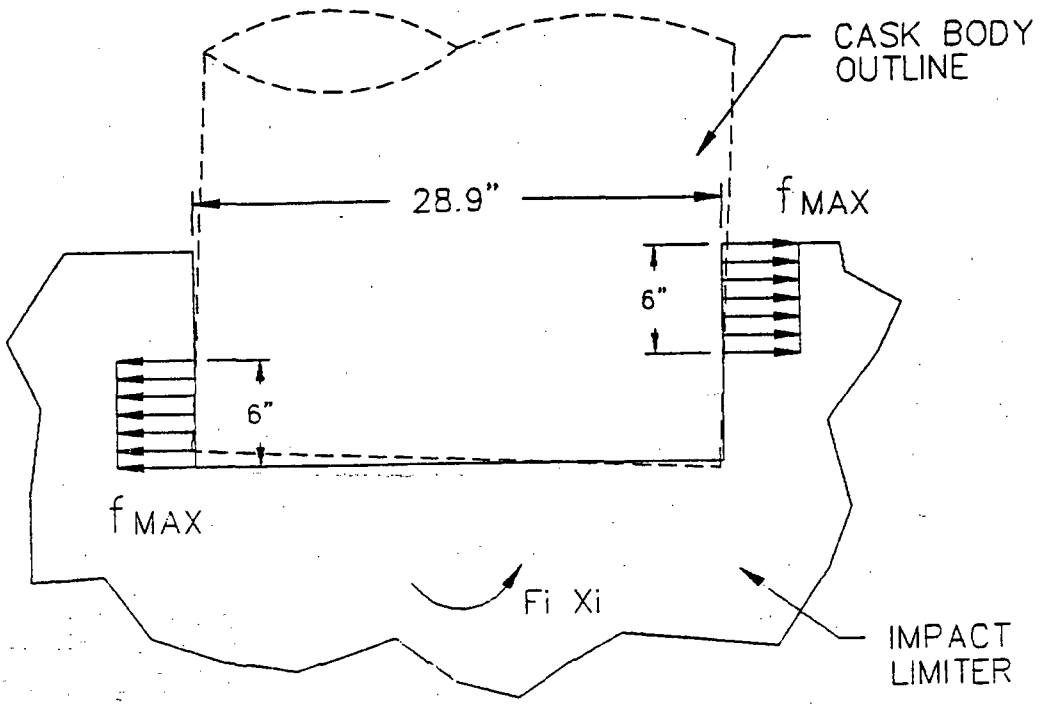


Figure 2.6.7-20 Cask Lid Configuration

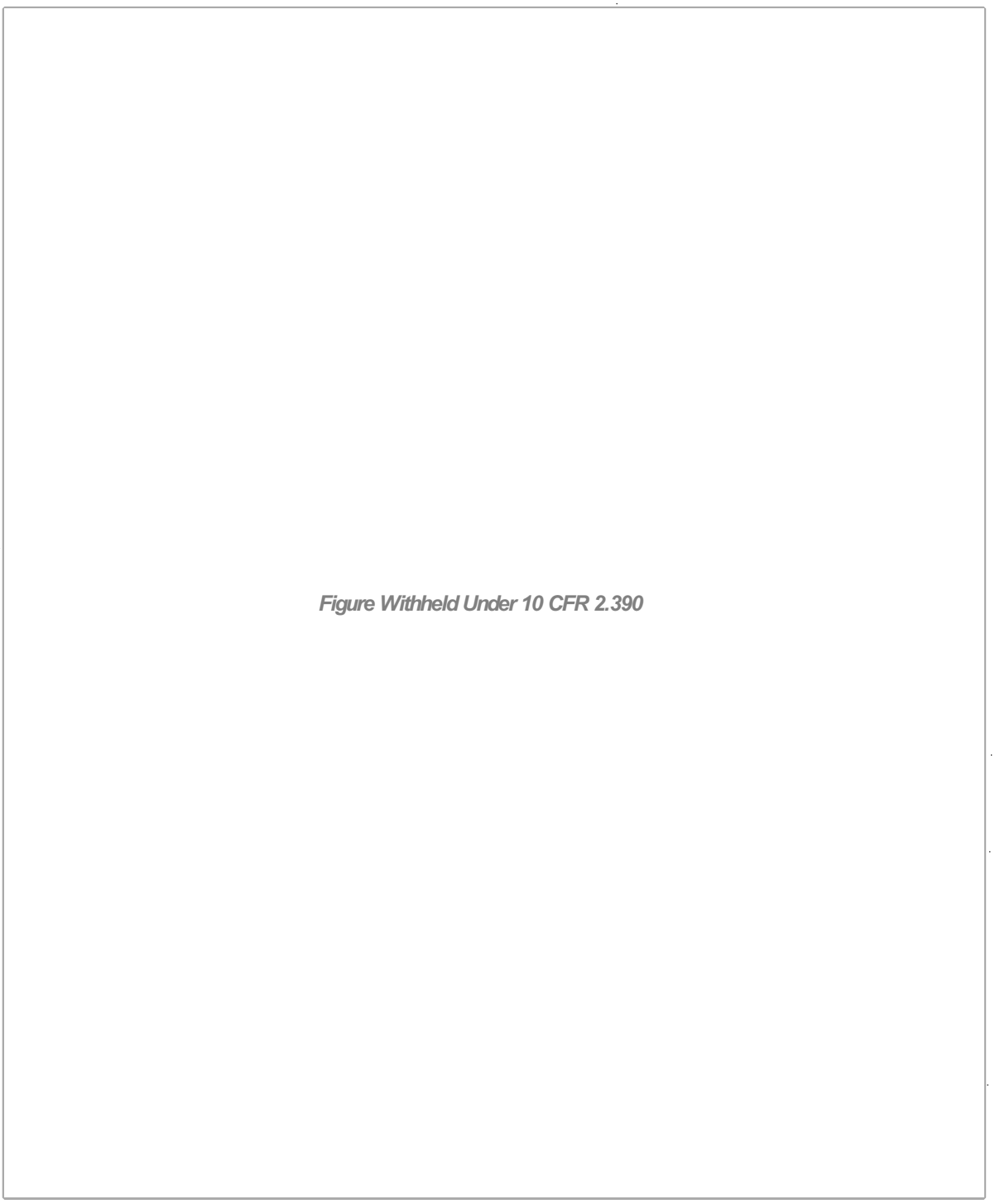


Figure 2.6.7-21 Closure Lid Free Body Diagram

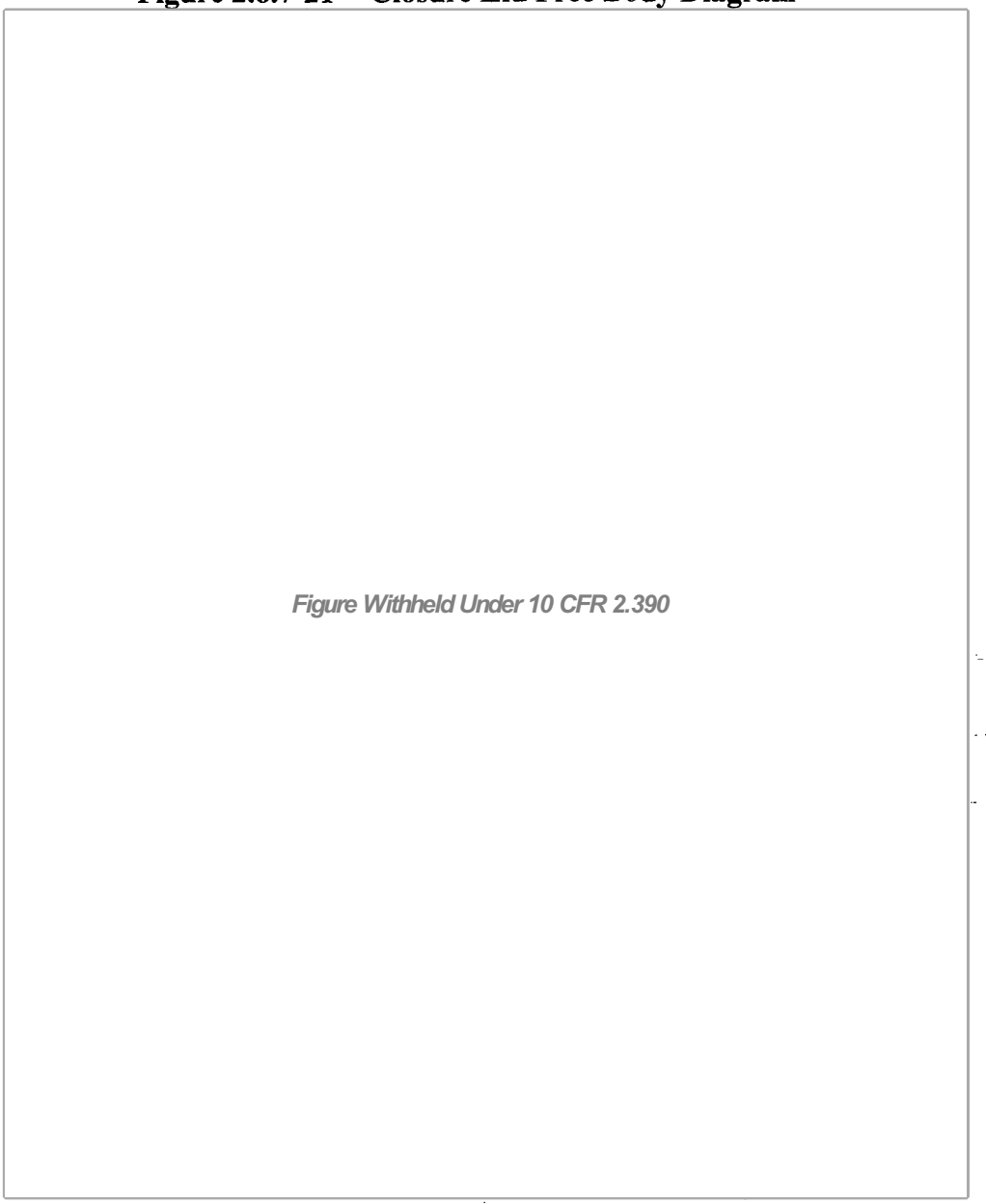


Figure 2.6.7-22 NAC-LWT Cask Cross-Section

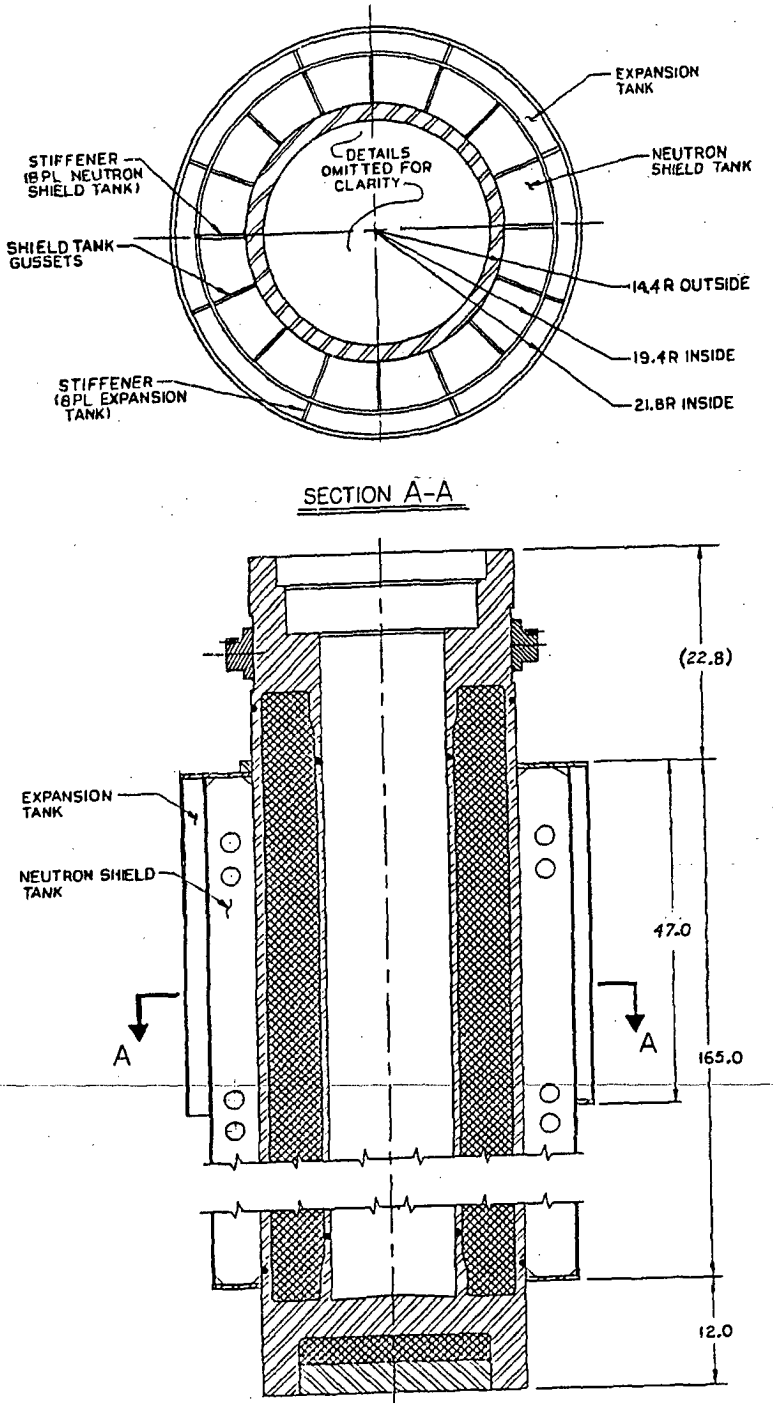


Figure 2.6.7-23 Component Parts of Shield Tank Structure

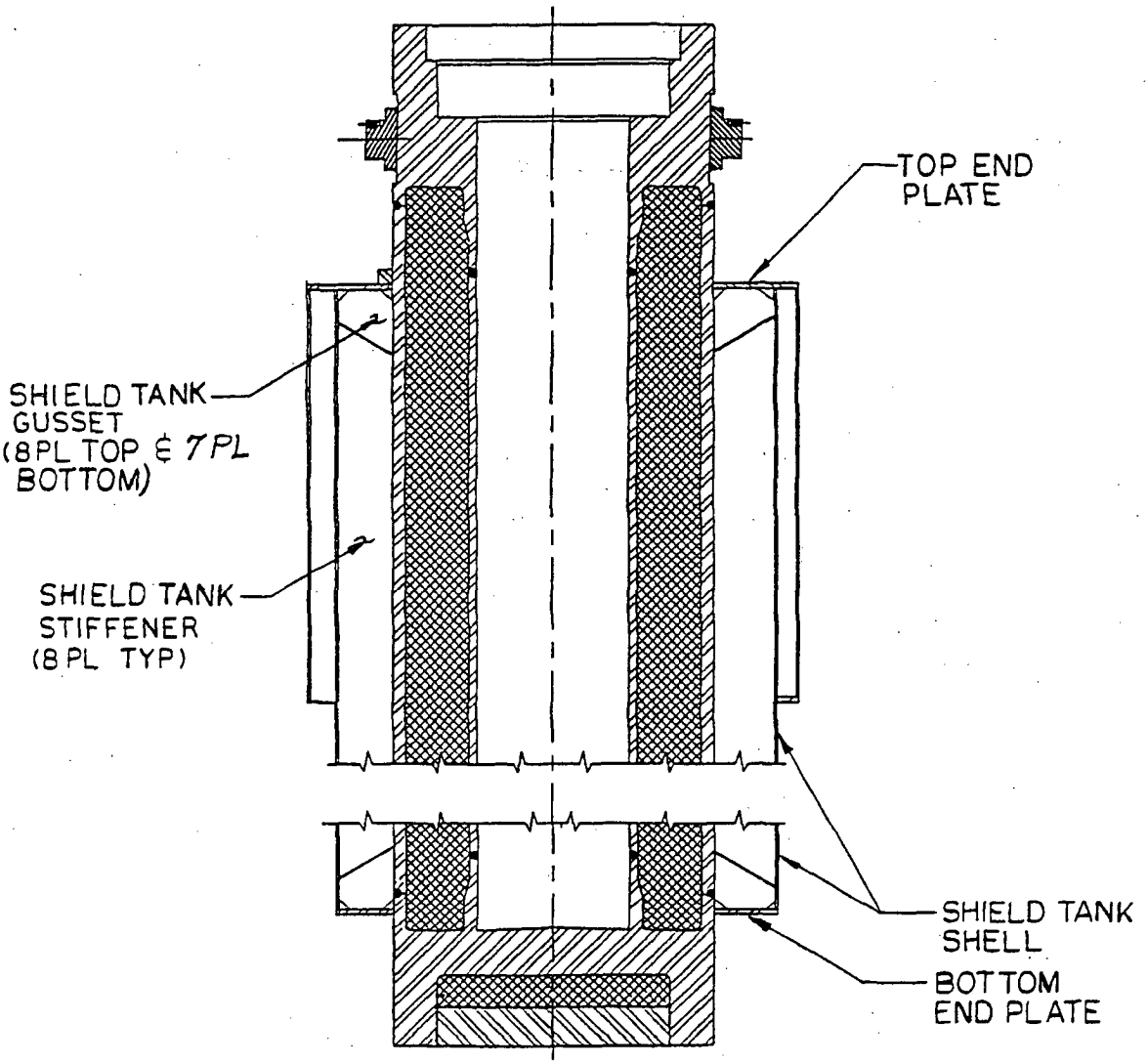


Figure 2.6.7-24 Shield Tank Cross-Section

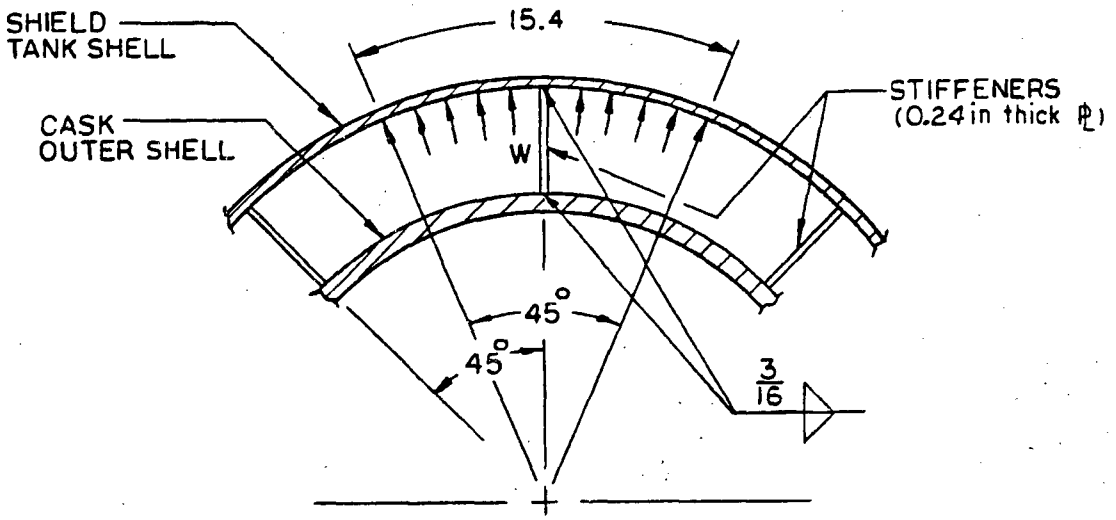
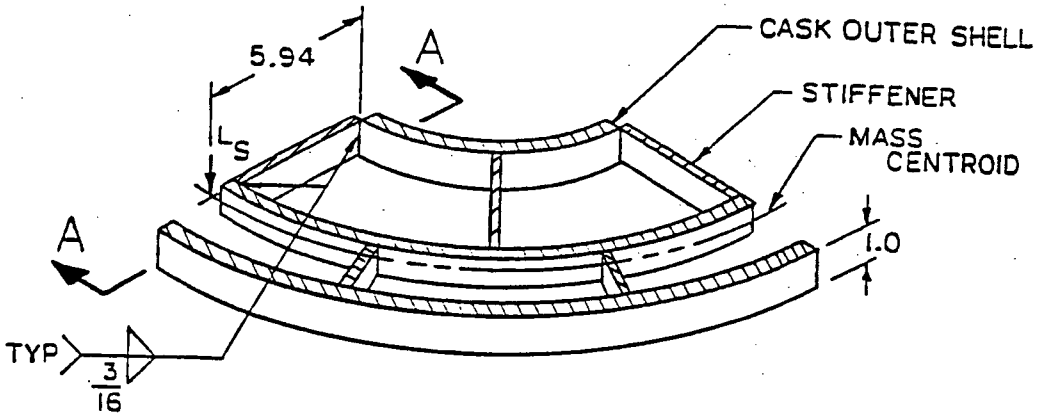
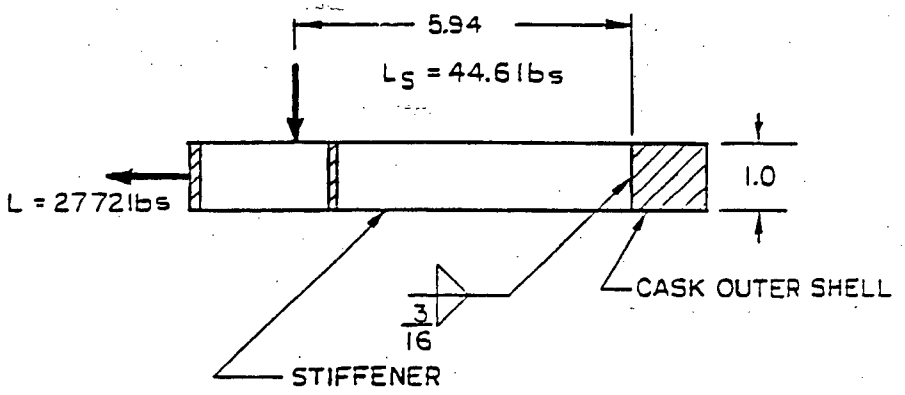


Figure 2.6.7-25 Shield Tank Quarter-Section Geometry



One Quarter of Tank Unit Section



Section A-A

Figure 2.6.7-26 Partial Bottom/Top End Plate Plan and Cross-Section

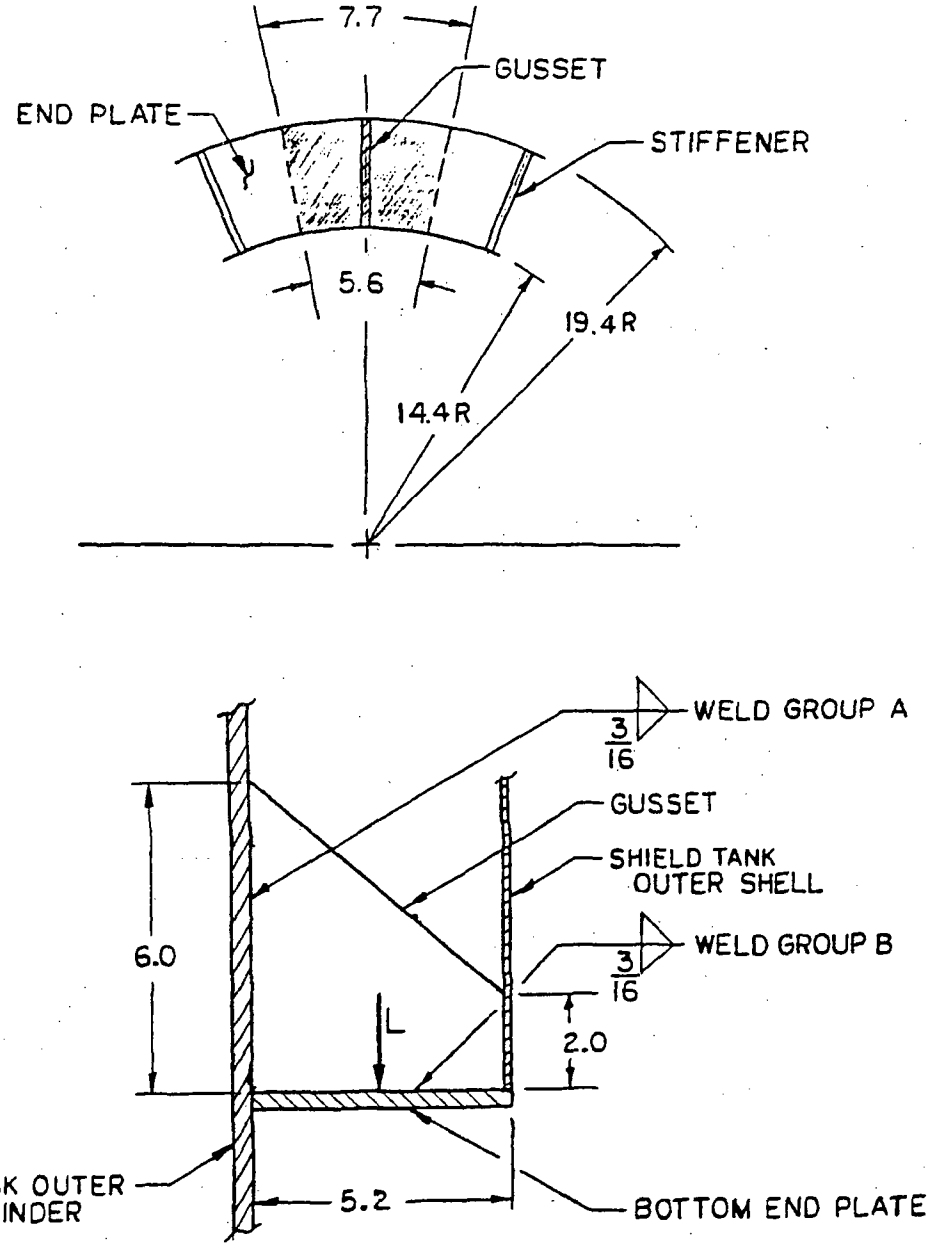


Figure 2.6.7-27 Shield Tank End Plate

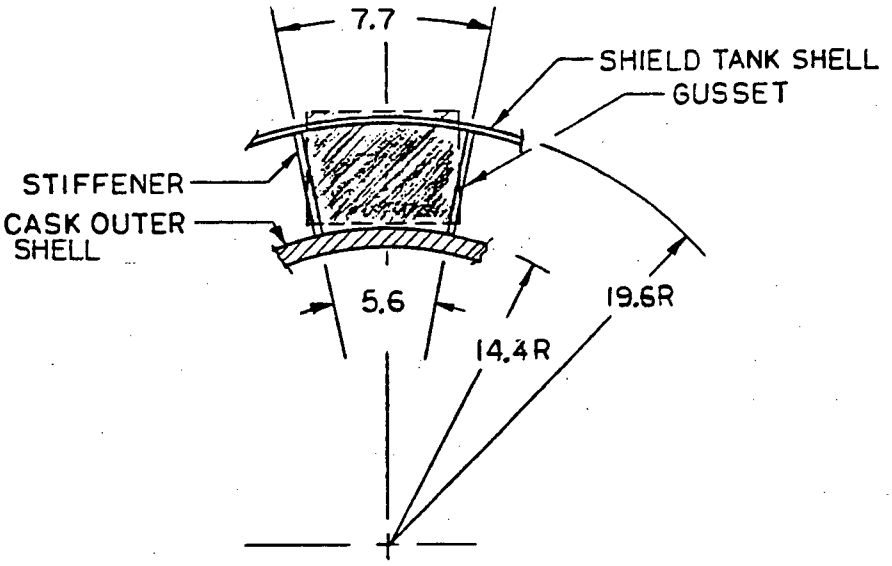


Figure 2.6.7-28 Gusset Profile

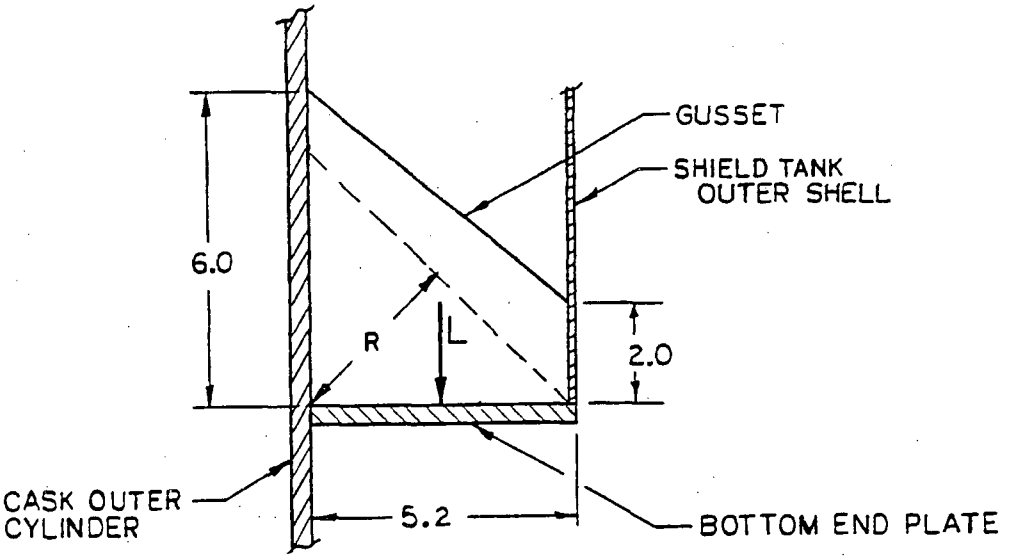


Figure 2.6.7-29 End Plate Welds

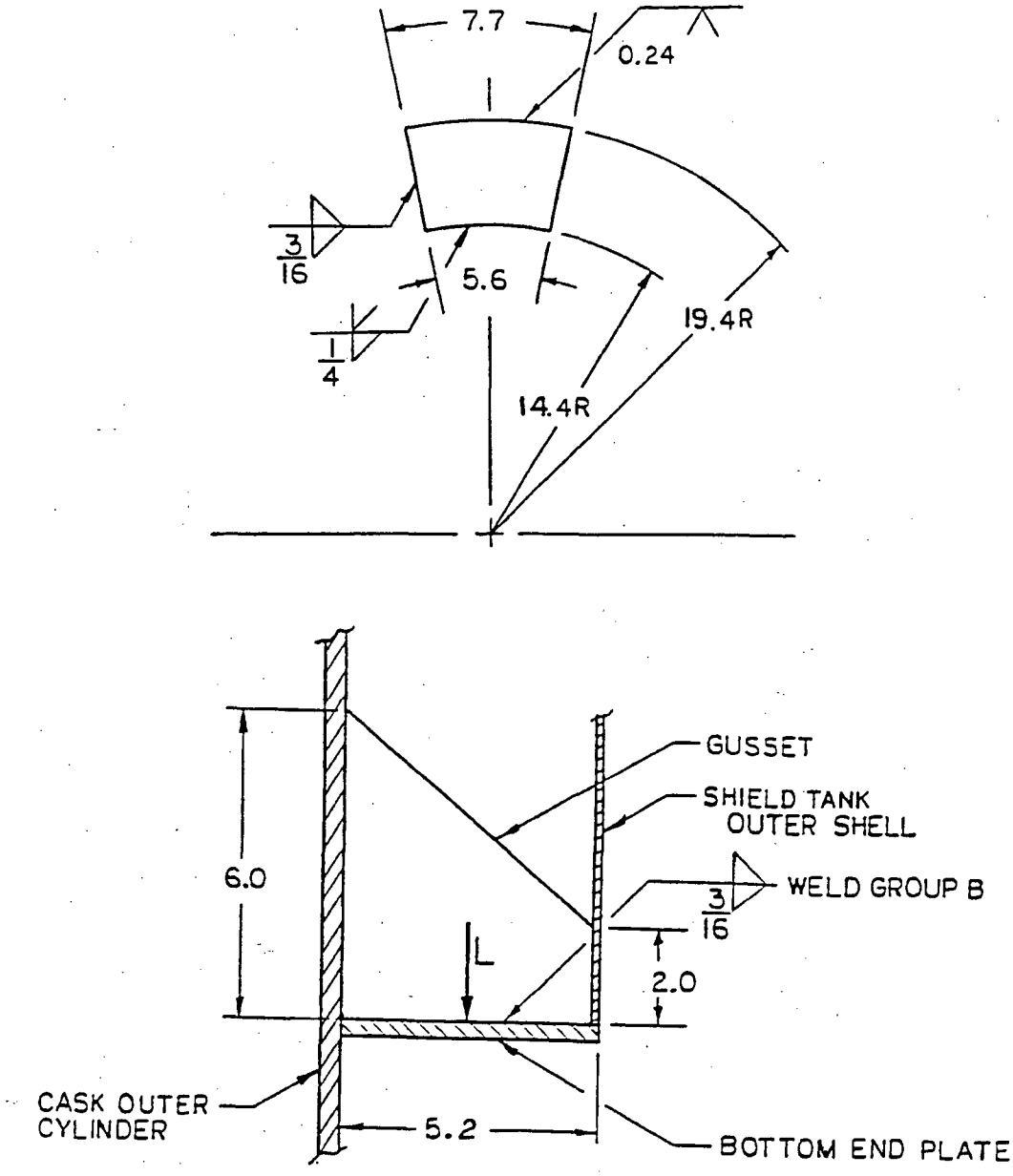


Figure 2.6.7-30 Component Parts of the Expansion Tank Structure

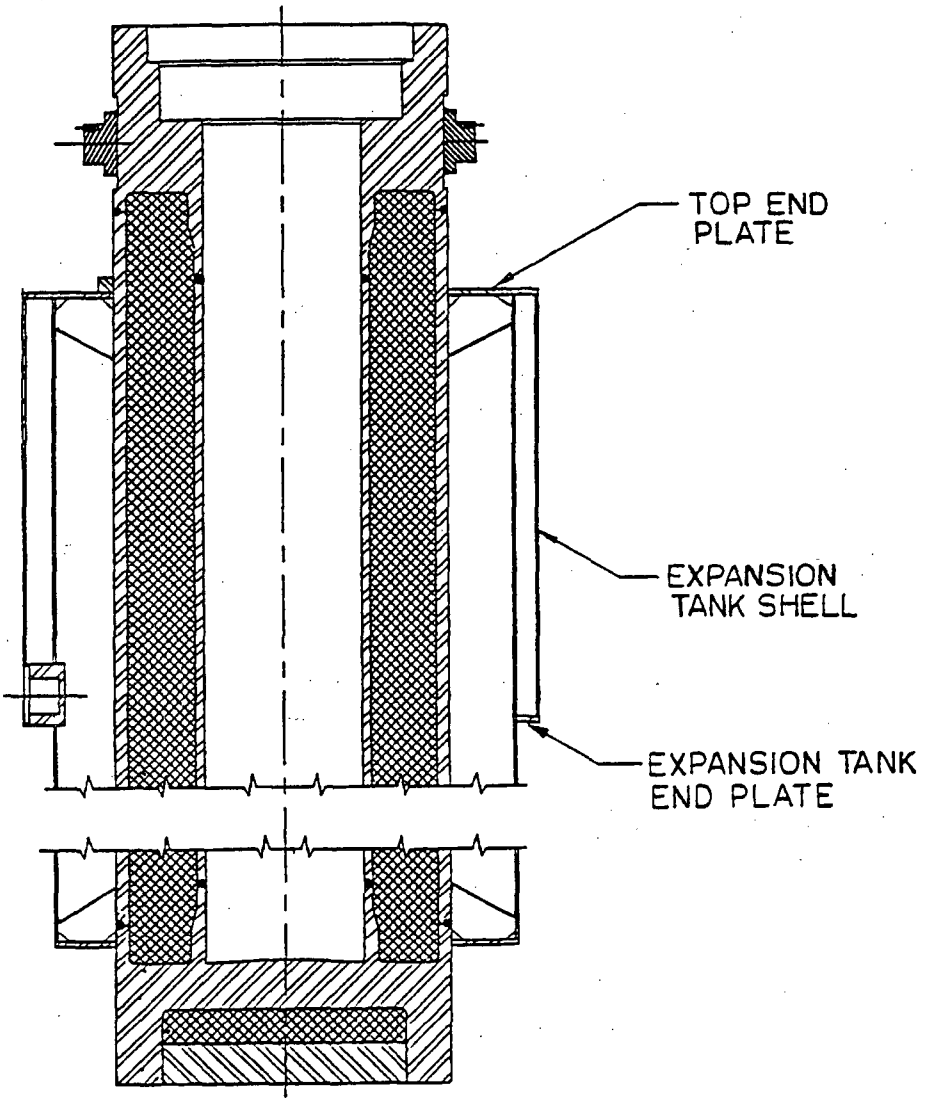


Figure 2.6.7-31 Expansion Tank Top and Bottom End Plate

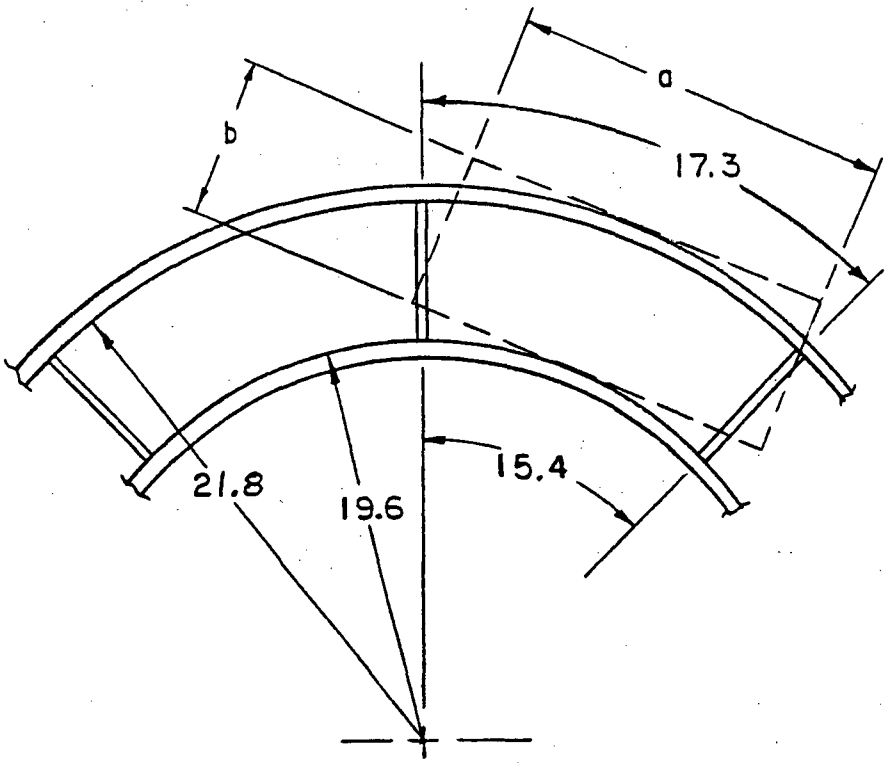


Figure 2.6.7-32 Expansion Tank Stiffener Load Geometry

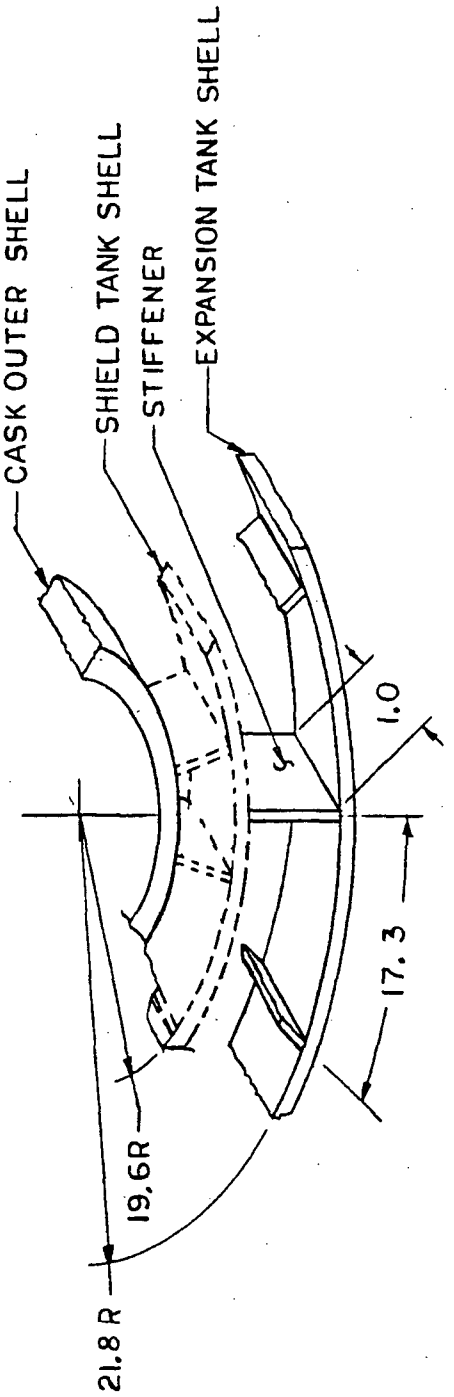


Figure 2.6.7-33 Cask Upper Ring at Trunnion - ANSYS Model

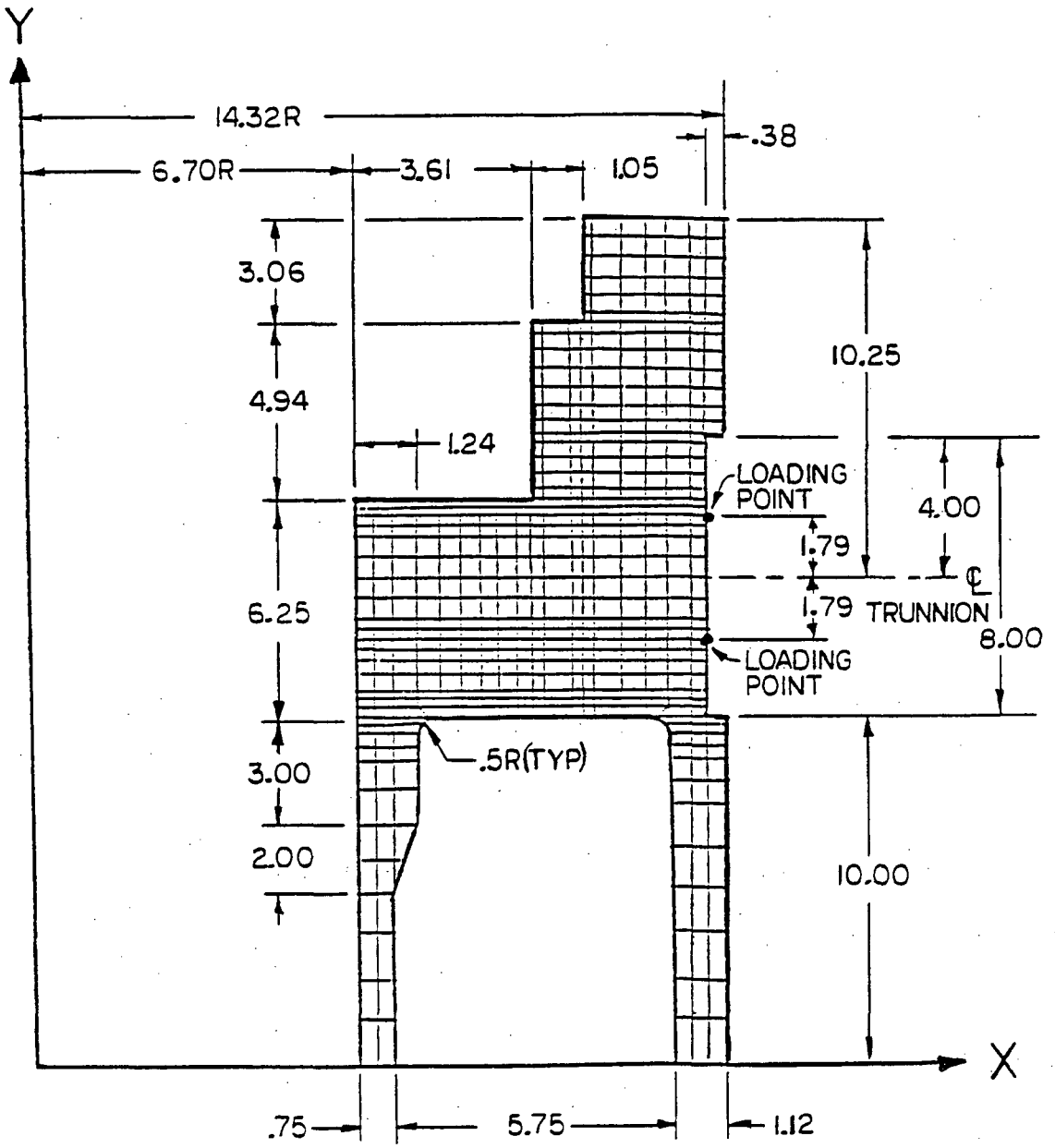


Figure 2.6.7-34 Cask Upper Ring at Trunnion - Model Loads and Boundary Conditions

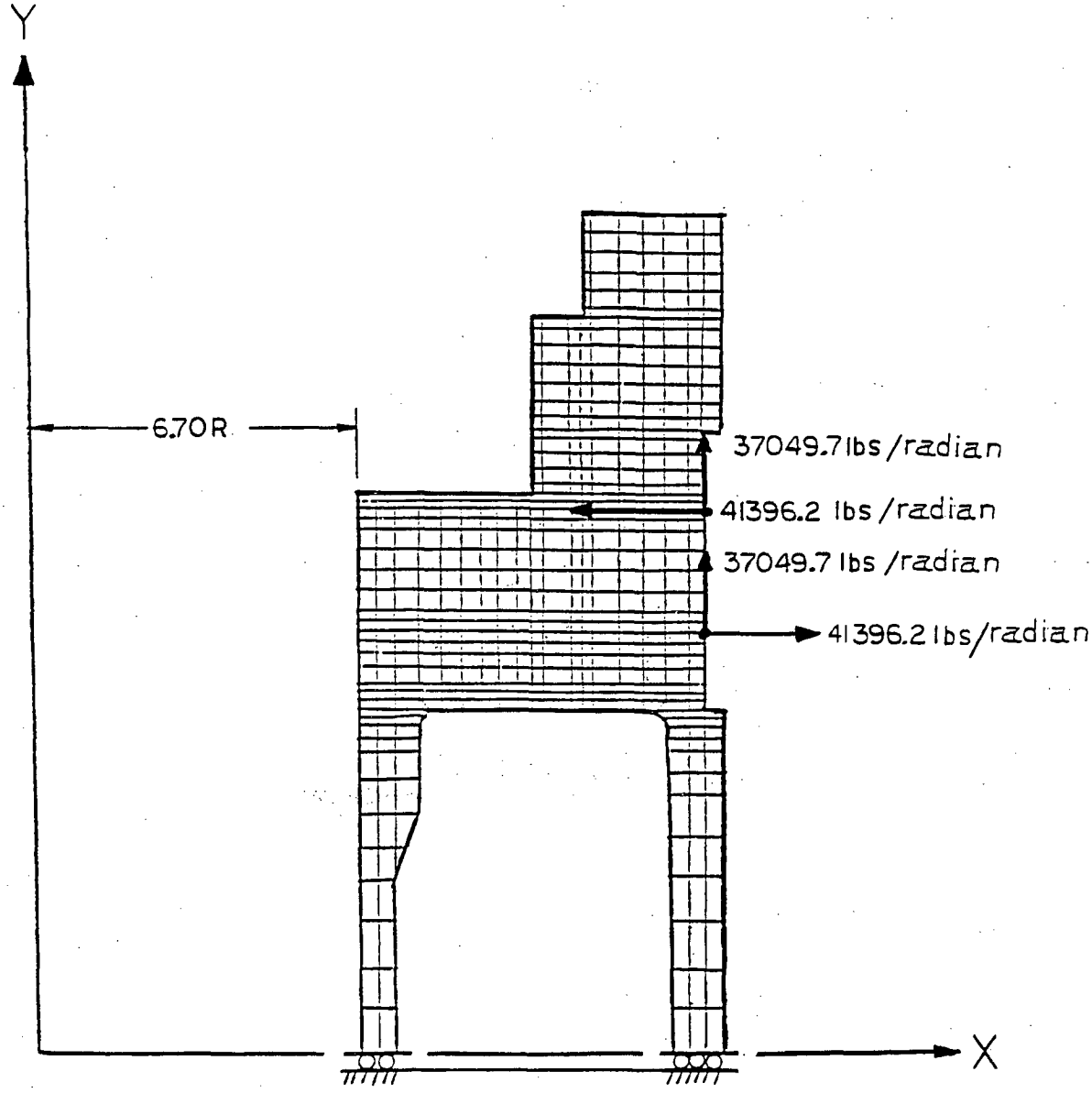


Figure 2.6.7-35 NAC-LWT Cask Upper Ring at Trunnion - Critical Sections

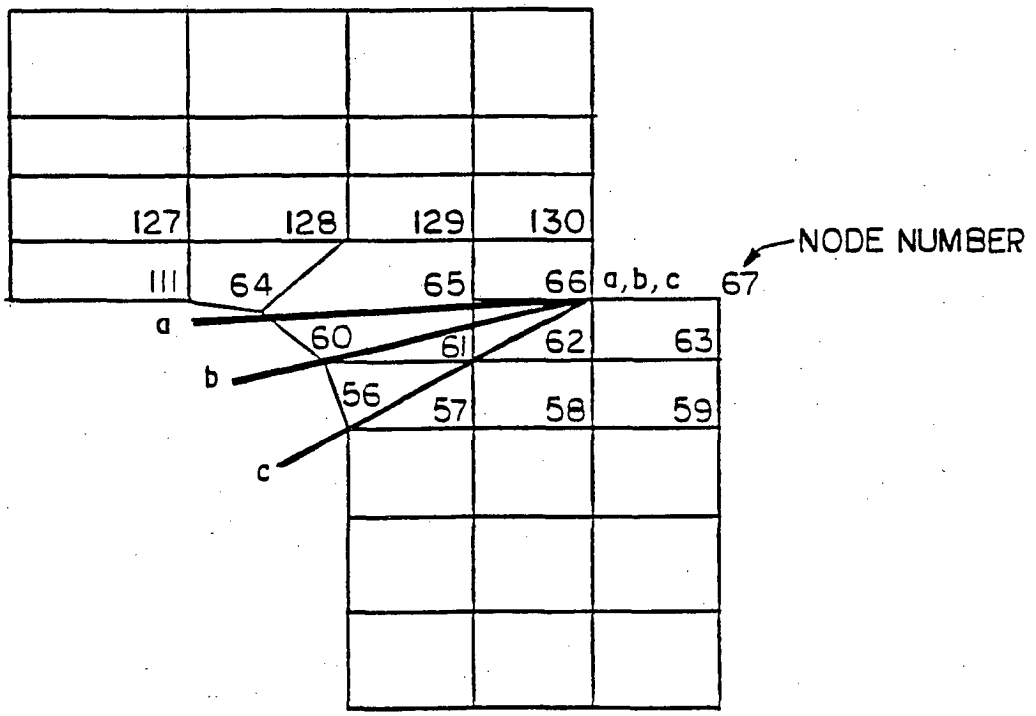


Table 2.6.7-1 Critical Stress Summary (1-Foot Bottom End Drop) – Loading Condition 1 – P_m

Loading Condition 1: 130°F Ambient Temperature and Maximum Decay Heat Load

		P_m Stresses[1] (ksi)				Principal Stresses					
Comp. No.[2]	Section Cut Node to Node	S_x	S_y	S_z	S_{xy}	S_1	S_2	S_3	S.I.	Allow. Stress 1.0 S_m	Margin of Safety
	2-2										
1	2375 to 2575	-0.17	-0.23	0.62	0.40	0.62	0.2	-0.6	1.22	20.0	Large
	4-4										
3	1581 to 1584	-0.1	-4.54	-0.16	-0.14	-0.1	-0.16	-4.55	4.45	20.0	+3.49
	7-7										
4	701 to 704	-0.03	-8.44	0.51	-0.02	0.51	-0.03	-8.44	8.94	31.4	+2.51
	6-6										
6	1515 to 1518	0.00	1.98	-0.16	-0.04	1.98	0.00	-0.16	2.14	31.4	Large
	11-11										
7	192 to 342	-6.50	1.18	1.28	1.69	1.54	1.28	-6.85	8.39	20.0	+1.38
	10-10										
8	361 to 365	0.77	-5.40	3.89	-0.99	3.89	0.92	-5.55	9.44	20.0	+1.19

[1] Conservatively based on a 1.12-inch thick outer shell and on a 3850-psi crush strength aluminum honeycomb impact limiter (Section 2.6.7.1.1).

[2] Refer to Figure 2.10.2-9 for component identification.

Table 2.6.7-2 Critical Stress Summary (1-Foot Bottom End Drop) – Loading Condition 1 - $P_m + P_b$

Loading Condition 1: 130°F Ambient Temperature and Maximum Decay Heat Load

		$P_m + P_b$ Stresses[1] (ksi)				Principal Stresses					
Comp. No.[2]	Section Cut Node to Node	S_x	S_y	S_z	S_{xy}	S_1	S_2	S_3	S.I.	Allow. Stress 1.5 S_m	Margin of Safety
	1-1										
1	2371 to 2571	-3.91	-0.35	0.11	0.00	0.11	-0.35	-3.91	4.01	30.0	+6.48
	3-3										
3	1835 to 1838	-0.1	4.66	2.25	0.29	4.68	2.25	-0.1	4.76	30.0	+5.30
	8-8										
4	621 to 624	0.15	-10.37	-1.16	0.28	0.16	-1.16	-10.38	10.54	47.1	+3.47
	5-5										
6	1595 to 1598	-0.01	3.03	0.57	0.00	3.03	0.57	-0.01	3.04	47.1	Large
	12-12										
7	150 to 193	9.25	-5.21	2.76	0.63	9.27	2.76	-5.24	14.51	30.0	+1.06
	9-9										
8	381 to 385	-0.21	-13.14	2.03	-1.07	2.03	-0.12	-13.23	15.26	30.0	+0.97

[1] Conservatively based on a 1.12-inch thick outer shell and on a 3850-psi crush strength aluminum honeycomb impact limiter (Section 2.6.7.1.1).

[2] Refer to Figure 2.10.2-9 for component identification.

Table 2.6.7-3 Critical Stress Summary (1-Foot Bottom End Drop) – Loading Condition 1 - Total Range

Loading Condition 1: 130°F Ambient Temperature and Maximum Decay Heat Load

		Total Stress Range[1] (ksi)				Principal Stresses			Stress Differences		
Comp. No.[2]	Node	S_x	S_y	S_z	S_{xy}	S_1	S_2	S_3	S_1-S_2	S_2-S_3	S_3-S_1
1	2376	0.80	-4.48	-0.22	-0.31	0.82	-0.22	-4.50	1.04	4.28	-5.32
3	1805	-0.19	-5.27	-2.19	-0.78	-0.07	-2.19	-5.39	2.12	3.20	-5.32
4	604	-0.69	-12.07	-1.65	0.61	-0.66	-1.65	-12.10	0.99	10.45	-11.44
6	1595	-0.02	2.93	0.48	0.00	2.93	0.48	-0.02	2.45	0.50	-2.95
7	192	12.54	-7.35	3.46	-3.90	13.28	3.46	-8.09	9.82	11.55	-21.37
8	361	-0.03	-16.44	0.82	-1.40	0.82	0.09	-16.57	0.73	16.65	-17.38

1 Conservatively based on a 1.12-inch thick outer shell and on a 3850-psi crush strength aluminum honeycomb impact limiter (Section 2.6.7.1.1).

2 Refer to Figure 2.10.2-9 for component identification.

Table 2.6.7-4 Critical Stress Summary (1-Foot Bottom End Drop) – Loading Condition 2 – P_m

Loading Condition 2: -40°F Ambient Temperature and Maximum Decay Heat Load

		P_m Stresses[1] (ksi)				Principal Stresses					
Comp. No.[2]	Section Cut Node to Node	S_x	S_y	S_z	S_{xy}	S_1	S_2	S_3	S.I.	Allow. Stress 1.0 S_m	Margin of Safety
	2-2										
1	2478 to 2578	0.03	-0.11	1.28	0.02	1.28	0.03	-0.11	1.39	20.0	Large
	4-4										
3	1581 to 1584	-0.15	-7.90	-0.93	-0.26	-0.14	-0.93	-7.91	7.77	20.0	+1.57
	6-6										
4	701 to 704	-0.02	-12.08	0.20	-0.03	0.20	-0.02	-12.08	12.28	31.4	+1.56
	8-8										
6	615 to 618	0.00	-2.85	0.80	0.00	0.80	0.00	-2.85	3.65	31.4	+7.60
	11-11										
7	100 to 143	-3.18	-4.19	2.15	2.18	2.15	-1.45	-5.93	8.07	20.0	+1.50
	7-7										
8	601 to 604	-0.23	-11.12	-1.21	0.46	-0.21	-1.21	-11.13	10.93	20.0	+0.83

1 Conservatively based on a 1.12-inch thick outer shell and on a 3850-psi crush strength aluminum honeycomb impact limiter (Section 2.6.7.1.1).

2 Refer to Figure 2.10.2-9 for component identification.

Table 2.6.7-5 Critical Stress Summary (1-Foot Bottom End Drop) – Loading Condition 2 - $P_m + P_b$

Loading Condition 2: -40°F Ambient Temperature and Maximum Decay Heat Load

		$P_m + P_b$ Stresses[1] (ksi)				Principal Stresses					
Comp. No.[2]	Section Cut Node to Node	S_x	S_y	S_z	S_{xy}	S_1	S_2	S_3	S.I.	Allow. Stress 1.5 S_m	Margin of Safety
	1-1										
1	2371 to 2571	-4.10	-0.43	0.14	0.00	0.14	-0.43	-4.10	4.24	30.0	+6.08
	3-3										
3	1701 to 1705	0.04	-8.08	-1.59	-0.34	0.05	-1.59	-8.10	8.15	30.0	+2.68
	5-5										
4	621 to 624	0.18	-13.91	-1.67	0.32	0.19	-1.67	-13.91	14.10	47.1	+2.34
	8-8										
6	615 to 618	0.03	-4.12	0.63	0.00	0.63	0.03	-4.12	4.75	47.1	+8.92
	10-10										
7	193 to 200	3.76	-9.04	1.83	-0.76	3.81	1.83	-9.09	12.89	30.0	+1.32
	9-9										
8	185 to 335	-12.66	-0.38	-0.11	1.93	-0.09	-0.11	-12.96	12.87	30.0	+1.33

1 Conservatively based on a 1.12-inch thick outer shell and on a 3850-psi crush strength aluminum honeycomb impact limiter (Section 2.6.7.1.1).

2 Refer to Figure 2.10.2-9 for component identification.

Table 2.6.7-6 Critical Stress Summary (1-Foot Bottom End Drop) – Loading Condition 2 - Total Range

Loading Condition 2: -40°F Ambient Temperature and Maximum Decay Heat Load

		Total Stress Range[1] (ksi)				Principal Stresses			Stress Differences		
Comp. No.[2]	Node	S_x	S_y	S_z	S_{xy}	S_1	S_2	S_3	S_1-S_2	S_2-S_3	S_3-S_1
1	2376	0.67	-4.03	0.05	-0.35	0.70	0.05	-4.06	0.65	4.11	-4.75
3	1805	-0.32	-9.36	-3.82	-1.34	-0.12	-3.82	-9.56	3.70	5.74	-9.44
4	604	-0.90	-15.99	-2.51	0.80	-0.86	-2.51	-16.03	1.65	13.52	-15.17
6	618	0.03	-4.20	0.57	0.00	0.57	0.03	-4.20	0.54	4.23	-4.77
7	143	-5.58	-14.56	-1.04	0.55	-1.04	-5.55	-14.59	4.51	9.05	-13.55
8	361	0.01	-14.97	-0.81	-1.62	0.18	-0.81	-15.14	0.99	14.33	-15.33

1 Conservatively based on a 1.12-inch thick outer shell and on a 3850-psi crush strength aluminum honeycomb impact limiter (Section 2.6.7.1.1).

2 Refer to Figure 2.10.2-9 for component identification.

Table 2.6.7-7 Critical Stress Summary (1-Foot Bottom End Drop) – Loading Condition 3 – P_m

Loading Condition 3: -40°F Ambient Temperature and No Decay Heat Load

Comp. No.[2]	Section Cut Node to Node	P_m Stresses[1] (ksi)				Principal Stresses			S.I.	Allow. Stress 1.0 S_m	Margin of Safety
		S_x	S_y	S_z	S_{xy}	S_1	S_2	S_3			
	1-1										
1	2375 to 2575	-0.21	0.00	-0.03	0.18	0.1	-0.03	-0.31	0.41	20.0	Large
	2-2										
3	1581 to 1584	-0.22	-3.78	-5.48	-0.28	-0.19	-3.80	-5.48	5.29	20.0	+2.78
	3-3										
4	621 to 624	0.04	-7.76	-1.05	0.24	0.04	-1.05	-7.77	7.81	31.4	+3.02
	5-5										
6	615 to 618	0.00	-6.85	-0.13	0.00	0.00	-0.13	-6.85	6.85	31.4	+3.58
	8-8										
7	18 to 118	-10.02	-0.60	-2.86	2.62	0.08	-2.86	-10.70	10.78	20.0	+0.86
	4-4										
8	601 to 604	-0.16	-7.07	-0.78	0.34	-0.14	-0.78	-7.09	6.95	20.0	+1.88

1 Conservatively based on a 1.12-inch thick outer shell and on a 3850-psi crush strength aluminum honeycomb impact limiter (Section 2.6.7.1.1).

2 Refer to Figure 2.10.2-9 for component identification.

Table 2.6.7-8 Critical Stress Summary (1-Foot Bottom End Drop) – Loading Condition 3 - $P_m + P_b$

Loading Condition 3: -40°F Ambient Temperature and No Decay Heat Load

		$P_m + P_b$ Stresses[1] (ksi)				Principal Stresses					
Comp. No.[2]	Section Cut Node to Node	S_x	S_y	S_z	S_{xy}	S_1	S_2	S_3	S.I.	Allow. Stress 1.5 S_m	Margin of Safety
	1-1										
1	2375 to 2575	-1.99	0.00	-0.03	0.18	0.01	-0.03	-2.01	2.02	30.0	Large
	2-2										
3	1581 to 1584	0.01	-3.30	-5.65	-0.28	0.03	-3.33	-5.65	5.68	30.0	+4.28
	3-3										
4	621 to 624	0.12	-8.99	-1.30	0.24	0.13	-1.30	-9.00	9.13	47.1	+4.16
	5-5										
6	615 to 618	0.00	-7.06	-0.19	0.00	0.00	-0.19	-7.06	7.06	47.1	+5.67
	8-8										
7	18 to 118	-20.14	-0.6	-2.86	2.62	-0.25	-2.86	-20.49	20.23	30.0	+0.48
	6-6										
8	185 to 335	-8.83	1.55	1.16	2.22	2.0	1.16	-9.29	11.29	30.0	+1.66

[1] Conservatively based on a 1.12-inch thick outer shell and on a 3850-psi crush strength aluminum honeycomb impact limiter (Section 2.6.7.1.1).

[2] Refer to Figure 2.10.2-9 for component identification.

Table 2.6.7-9 Critical Stress Summary (1-Foot Bottom End Drop) – Loading Condition 3 - Total Range

Loading Condition 3: -40°F Ambient Temperature and No Decay Heat Load

		Total Stress Range[1] (ksi)				Principal Stresses			Stress Differences		
Comp. No.[2]	Node	S_x	S_y	S_z	S_{xy}	S_1	S_2	S_3	S_1-S_2	S_2-S_3	S_3-S_1
1	2376	0.96	-3.75	-0.64	-0.11	0.96	-0.64	-3.75	1.60	3.11	-4.71
3	2176	3.74	-17.36	-1.84	-2.41	4.01	-1.84	-17.90	5.85	16.06	-21.91
4	604	-0.58	-10.47	-1.81	0.56	-0.55	-1.81	-10.50	1.26	8.69	-9.95
6	615	0.01	-7.05	-0.19	0.00	0.01	-0.19	-7.05	0.20	6.86	-7.06
7	143	0.08	-23.96	-3.03	-2.73	0.39	-3.03	-24.27	3.42	21.24	-24.66
8	361	-0.02	-10.55	0.26	-1.38	0.26	-0.16	-10.73	0.10	10.89	-10.99

1 Conservatively based on a 1.12-inch thick outer shell and on a 3850-psi crush strength aluminum honeycomb impact limiter (Section 2.6.7.1.1).

2 Refer to Figure 2.10.2-9 for component identification.

Table 2.6.7-10 Critical Stress Summary (1-Foot Top End Drop) – Loading Condition 1 – P_m

Loading Condition 1: 130°F Ambient Temperature and Maximum Decay Heat Load

		P_m Stresses[1] (ksi)				Principal Stresses					
Comp. No.[2]	Section Cut Node to Node	S_x	S_y	S_z	S_{xy}	S_1	S_2	S_3	S.I.	Allow. Stress 1.0 S_m	Margin of Safety
	2-2										
1	2377 to 2577	-7.46	-0.06	0.09	0.15	0.09	-0.05	-7.46	7.55	20.0	+1.65
	4-4										
3	1581 to 1584	-0.20	-7.58	-0.57	-0.33	-0.18	-0.57	-7.60	7.42	20.0	+1.70
	5-5										
4	1481 to 1484	-0.03	-8.19	0.52	0.02	0.52	-0.03	-8.19	8.71	31.4	+2.60
	12-12										
6	695 to 698	0.00	2.39	-0.10	0.04	2.40	0.00	-0.10	2.50	31.4	Large
	10-10										
7	17 to 117	-1.04	1.54	2.36	-2.84	3.37	2.36	-2.87	6.23	20.0	+2.21
	7-7										
8	401 to 405	-0.03	-2.63	1.89	-0.39	1.89	0.03	-2.69	4.58	20.0	+3.37

1 Conservatively based on a 1.12-inch thick outer shell and on a 3850-psi crush strength aluminum honeycomb impact limiter (Section 2.6.7.1.1).

2 Refer to Figure 2.10.2-9 for component identification.

Table 2.6.7-11 Critical Stress Summary (1-Foot Top End Drop) – Loading Condition 1 - $P_m + P_b$

Loading Condition 1: 130°F Ambient Temperature and Maximum Decay Heat Load

		$P_m + P_b$ Stresses[1] (ksi)				Principal Stresses					
Comp. No.[2]	Section Cut Node to Node	S_x	S_y	S_z	S_{xy}	S_1	S_2	S_3	S.I.	Allow. Stress 1.5 S_m	Margin of Safety
	1-1										
1	2371 to 2571	-12.69	-0.13	-0.22	-1.01	-0.05	-0.22	-12.77	12.72	30.0	+1.36
	3-3										
3	1941 to 1956	0.84	-10.28	-3.31	0.03	0.84	-3.31	-10.28	11.12	30.0	+1.70
	11-11										
4	1561 to 1564	0.12	-9.50	-0.89	-0.22	0.13	-0.89	-9.51	9.64	47.1	+3.89
	6-6										
6	615 to 618	-0.02	3.50	0.78	0.00	3.50	0.78	-0.02	3.52	47.1	Large
	9-9										
7	143 to 150	-7.68	6.60	1.37	1.33	6.72	1.37	-7.80	14.52	30.0	+1.07
	8-8										
8	381 to 385	-0.15	-6.77	0.67	-0.49	0.67	-0.12	-6.81	7.47	30.0	+3.02

1 Conservatively based on a 1.12-inch thick outer shell and on a 3850-psi crush strength aluminum honeycomb impact limiter (Section 2.6.7.1.1).

2 Refer to Figure 2.10.2-9 for component identification.

Table 2.6.7-12 Critical Stress Summary (1-Foot Top End Drop) – Loading Condition 1 - Total Range

Loading Condition 1: 130°F Ambient Temperature and Maximum Decay Heat Load

		Total Stress Range[1] (ksi)				Principal Stresses			Stress Differences		
Comp. No.[2]	Node	S_x	S_y	S_z	S_{xy}	S_1	S_2	S_3	S_1-S_2	S_2-S_3	S_3-S_1
1	2371	2.76	-10.30	0.04	3.56	3.67	0.04	-11.21	3.63	11.25	-14.88
3	1962	-1.54	-12.69	-5.46	-1.00	-1.45	-5.46	-12.78	4.01	7.32	-11.33
4	1584	-0.62	-10.96	-1.54	-0.54	-0.59	-1.54	-10.98	0.95	9.44	-10.39
6	615	-0.01	3.43	0.72	-0.01	3.43	0.72	-0.01	2.71	0.73	-3.44
7	143	-7.68	6.79	1.34	2.96	7.37	1.34	-8.26	6.03	9.60	-15.63
8	361	-0.07	-8.76	-0.09	-0.78	0.00	-0.09	-8.83	0.09	8.74	-8.83

1 Conservatively based on a 1.12-inch thick outer shell and on a 3850-psi crush strength aluminum honeycomb impact limiter (Section 2.6.7.1.1).

2 Refer to Figure 2.10.2-9 for component identification.

Table 2.6.7-13 Critical Stress Summary (1-Foot Top End Drop) – Loading Condition 2 – P_m

Loading Condition 2: -40°F Ambient Temperature and Maximum Decay Heat Load

		P_m Stresses[1] (ksi)				Principal Stresses					
Comp. No.[2]	Section Cut Node to Node	S_x	S_y	S_z	S_{xy}	S_1	S_2	S_3	S.I.	Allow. Stress 1.0 S_m	Margin of Safety
	2-2										
1	2377 to 2577	-7.42	-0.08	0.30	0.18	0.30	-0.08	-7.42	7.72	20.0	+1.59
	4-4										
3	1581 to 1584	-0.24	-10.89	-1.33	-0.44	-0.22	-1.33	-10.91	10.69	20.0	+0.87
	6-6										
4	1481 to 1484	-0.02	-11.77	0.24	0.04	0.24	-0.02	-11.77	12.01	31.4	+1.61
	5-5										
6	1595 to 1598	0.01	-2.37	1.0	0.02	1.0	0.01	-2.37	3.37	31.4	+8.32
	10-10										
7	375 to 378	-1.35	1.92	2.97	-0.61	2.97	2.03	-1.45	4.42	20.0	+3.52
	8-8										
8	601 to 604	-0.13	-7.55	-0.80	0.27	-0.12	-0.80	-7.56	7.44	20.0	+1.69

1 Conservatively based on a 1.12-inch thick outer shell and on a 3850-psi crush strength aluminum honeycomb impact limiter (Section 2.6.7.1.1).

2 Refer to Figure 2.10.2-9 for component identification.

Table 2.6.7-14 Critical Stress Summary (1-Foot Top End Drop) – Loading Condition 2 - $P_m + P_b$

Loading Condition 2: -40°F Ambient Temperature and Maximum Decay Heat Load

		$P_m + P_b$ Stresses[1] (ksi)				Principal Stresses					
Comp. No.[2]	Section Cut Node to Node	S_x	S_y	S_z	S_{xy}	S_1	S_2	S_3	S.I.	Allow. Stress 1.5 S_m	Margin of Safety
	1-1										
1	2371 to 2571	-12.88	-0.21	-0.19	-1.02	-0.13	-0.19	-12.96	12.84	30.0	+1.34
	4-4										
3	1581 to 1584	-0.52	-12.05	-1.44	-0.45	-0.51	-1.44	-12.07	11.56	30.0	+1.60
	3-3										
4	1561 to 1564	0.17	-13.22	-1.52	-0.30	0.17	-1.52	-13.23	13.40	47.1	+2.51
	5-5										
6	1595 to 1598	0.04	-3.78	0.86	0.02	0.86	0.04	-3.78	4.64	47.1	+9.15
	9-9										
7	395 to 398	-0.18	7.35	4.97	-0.78	7.42	4.97	-0.26	7.69	30.0	+2.90
	8-8										
8	601 to 604	-0.18	-7.94	-0.67	0.27	-0.18	-0.67	-7.95	7.78	30.0	+2.86

1 Conservatively based on a 1.12-inch thick outer shell and on a 3850-psi crush strength aluminum honeycomb impact limiter (Section 2.6.7.1.1).

2 Refer to Figure 2.10.2-9 for component identification.

Table 2.6.7-15 Critical Stress Summary (1-Foot Top End Drop) – Loading Condition 2 - Total Range

Loading Condition 2: -40°F Ambient Temperature and Maximum Decay Heat Load

		Total Stress Range[1] (ksi)				Principal Stresses			Stress Differences		
Comp. No.[2]	Node	S_x	S_y	S_z	S_{xy}	S_1	S_2	S_3	S_1-S_2	S_2-S_3	S_3-S_1
1	2371	2.56	-10.43	0.01	3.61	3.50	0.01	-11.37	3.49	11.38	-14.87
3	1962	-1.54	-12.88	-5.92	-1.05	-1.44	-5.92	-12.98	4.48	7.06	-11.54
4	1584	-0.85	-15.19	-2.48	-0.76	-0.81	-2.48	-15.23	1.67	12.75	-14.42
6	1598	0.02	-3.94	0.76	0.02	0.76	0.02	-3.94	0.74	3.96	-4.70
7	378	-0.19	7.42	4.95	-0.07	7.42	4.95	-0.19	2.47	5.14	-7.61
8	361	-0.02	-7.21	-1.70	-1.00	0.16	-1.70	-7.38	1.86	5.68	-7.54

1 Conservatively based on a 1.12-inch thick outer shell and on a 3850-psi crush strength aluminum honeycomb impact limiter (Section 2.6.7.1.1).
2 Refer to Figure 2.10.2-9 for component identification.

Table 2.6.7-16 Critical Stress Summary (1-Foot Side Drop) – Loading Condition 1 – P_m

Loading Condition 1: 100°F Ambient Temperature and Maximum Decay Heat Load

		P_m Stresses (ksi)				Principal Stresses					
Comp. No.[1]	Section Cut Node to Node	S_x	S_y	S_z	S_{xy}	S_1	S_2	S_3	S.I.	Allow. Stress 1.0 S_m	Margin of Safety
	1-1										
1	2361 to 2370	-3.39	-0.30	0.06	-0.26	0.06	-0.28	-3.42	3.48	20.0	+4.74
	2-2										
3	1969 to 1976	-10.14	1.89	-4.53	-1.65	2.11	-4.53	-10.37	12.47	20.0	+0.60
	3-3										
4	1141 to 1144	-0.11	15.43	0.25	0.00	15.43	0.25	-0.11	15.54	31.4	+1.02
	4-4										
6	1115 to 1118	-0.05	31.36	1.31	0.00	31.36	1.31	-0.05	31.4	31.4	+0.00
	5-5										
7	395 to 398	-2.17	4.06	-5.51	0.78	4.15	-2.27	-5.51	9.66	20.0	+1.07
	6-6										
8	192 to 342	-5.47	-0.35	-3.06	0.18	-0.35	-3.06	-5.48	5.13	20.0	+2.89

[1] Refer to Figure 2.10.2-9 for component identification.

Table 2.6.7-17 Critical Stress Summary (1-Foot Side Drop) – Loading Condition 1 - $P_m + P_b$

Loading Condition 1: 100°F Ambient Temperature and Maximum Decay Heat Load

		$P_m + P_b$ Stresses (ksi)				Principal Stresses					
Comp. No.[1]	Section Cut Node to Node	S_x	S_y	S_z	S_{xy}	S_1	S_2	S_3	S.I.	Allow. Stress 1.5 S_m	Margin of Safety
	7-7										
1	2301 to 2561	-0.78	0.06	0.82	3.96	3.62	0.82	-4.34	7.96	30.0	+2.77
	8-8										
3	2150 to 2156	-4.40	-0.08	-20.16	0.01	-0.08	-4.40	-20.16	20.08	30.0	+0.49
	3-3										
4	1141 to 1144	-0.07	16.41	0.86	0.00	16.41	0.86	-0.07	16.48	47.1	+1.86
	4-4										
6	1115 to 1118	0.01	33.37	1.50	0.00	33.37	1.50	0.01	33.36	47.1	+0.41
	5-5										
7	395 to 398	-1.11	16.09	-0.89	0.78	16.12	-0.89	-1.14	17.26	30.0	+0.74
	9-9										
8	177 to 327	-8.25	-1.80	0.27	-1.47	0.27	-1.48	-8.58	8.85	30.0	+2.39

[1] Refer to Figure 2.10.2-9 for component identification.

Table 2.6.7-18 Critical Stress Summary (1-Foot Side Drop) – Loading Condition 1 - S_n

Loading Condition 1: 100°F Ambient Temperature and Maximum Decay Heat Load

		S_n Stresses (ksi)				Principal Stresses					
Comp. No.[1]	Section Cut Node to Node	S_x	S_y	S_z	S_{xy}	S_1	S_2	S_3	S.I.	Allow. Stress 3.0 S_m	Margin of Safety
	1-1										
1	2361 to 2370	-9.54	-1.04	-1.24	-0.19	-1.04	-1.24	-9.55	8.51	60.0	+6.05
	10-10										
3	1815 to 1818	-0.09	22.64	2.62	-1.58	22.75	2.62	-0.20	22.95	60.0	+1.61
	3-3										
4	1141 to 1144	-0.07	17.55	0.98	0.00	17.55	0.98	-0.07	17.62	94.2	+4.34
	4-4										
6	1115 to 1118	0.01	38.01	1.65	0.00	38.01	1.65	0.01	38.00	94.2	+1.48
	11-11										
7	395 to 398	-1.10	19.46	0.52	0.51	19.47	0.52	-1.12	20.59	60.0	+1.91
	6-6										
8	177 to 327	-12.34	-1.86	-3.80	-1.48	-1.66	-3.80	-12.55	10.89	60.0	+4.51

[1] Refer to Figure 2.10.2-9 for component identification.

Table 2.6.7-19 Critical Stress Summary (1-Foot Side Drop) – Loading Condition 1 - Total Range

Loading Condition 1: 100°F Ambient Temperature and Maximum Decay Heat Load

		Total Stress Range (ksi)				Principal Stresses			Stress Differences		
Comp. No.[1]	Node	S_x	S_y	S_z	S_{xy}	S_1	S_2	S_3	S_1-S_2	S_2-S_3	S_3-S_1
1	2561	0.06	0.02	1.33	15.24	15.28	1.33	-15.19	13.95	16.52	-30.47
3	1815	1.72	24.87	3.61	7.38	27.05	3.61	-0.46	23.44	4.07	-27.51
4	1144	-0.07	17.55	0.96	0.00	17.55	0.96	-0.07	16.59	1.03	-17.62
6	1118	0.01	37.98	1.61	0.00	37.98	1.61	0.01	36.37	1.60	-37.97
7	395	-1.10	22.68	1.30	1.50	22.78	1.30	-1.20	21.48	2.50	-23.98
8	192	-22.96	-1.15	-9.18	-0.81	-1.10	-9.18	-23.00	8.08	13.82	-21.90

[1] Refer to Figure 2.10.2-9 for component identification.

Table 2.6.7-20 Critical Stress Summary (1-Foot Top Corner Drop) – Loading Condition 1 – P_m – Drop Orientation = 15.74 Degrees

Loading Condition 1: 130°F Ambient Temperature and Maximum Decay Heat Load

		P_m Stresses[1] (ksi)				Principal Stresses					
Comp. No.[2]	Section Cut Node to Node	S_x	S_y	S_z	S_{xy}	S_1	S_2	S_3	S.I.	Allow. Stress 1.0 S_m	Margin of Safety
	1-1										
1	2377 to 2577	-5.07	-0.37	-0.71	-0.29	-0.35	-0.71	-5.09	4.74	20.0	+3.22
	2-2										
3	1775 to 1778	-0.05	-4.39	0.55	0.01	0.55	-0.05	-4.39	4.95	20.0	+3.04
	3-3										
4	1501 to 1504	-0.03	-3.11	0.36	0.01	0.36	-0.03	-3.11	3.47	31.4	+8.05
	4-4										
6	1595 to 1598	-0.01	-3.94	0.52	0.03	0.52	-0.01	-3.94	4.46	31.4	+6.04
	5-5										
7	18 to 118	-1.72	2.83	0.47	-2.50	3.94	0.47	-2.83	6.76	20.0	+1.96
	6-6										
8	381 to 385	-1.83	-2.67	0.82	-0.32	0.82	-1.73	-2.77	3.60	20.0	+4.56

[1] Conservatively based on a 1.12-inch thick outer shell and on a 3850-psi crush strength aluminum honeycomb impact limiter (Section 2.6.7.3.1).

[2] Refer to Figure 2.10.2-9 for component identification.

Table 2.6.7-21 Critical Stress Summary (1-Foot Top Corner Drop) – Loading Condition 1 - $P_m + P_b$ – Drop Orientation = 15.74 Degrees

Loading Condition 1: 130°F Ambient Temperature and Maximum Decay Heat Load

		$P_m + P_b$ Stresses[1] (ksi)				Principal Stresses					
Comp. No.[2]	Section Cut Node to Node	S_x	S_y	S_z	S_{xy}	S_1	S_2	S_3	S.I.	Allow. Stress 1.5 S_m	Margin of Safety
	1-1										
1	2377 to 2577	-6.69	-0.37	-0.71	-0.29	-0.35	-0.71	-6.70	6.34	30.0	+3.73
	7-7										
3	1821 to 1825	-0.02	-4.40	1.73	0.32	1.73	0.00	-4.43	6.16	30.0	+3.87
	8-8										
4	1561 to 1564	0.06	-4.51	-0.67	-0.13	0.06	-0.67	-4.52	4.58	47.1	+9.28
	4-4										
6	1595 to 1598	0.01	-4.03	0.45	0.03	0.45	0.01	-4.03	4.47	47.1	+9.54
	9-9										
7	143 to 150	-7.82	11.71	1.04	1.55	11.83	1.04	-7.94	19.77	30.0	+0.52
	10-10										
8	176 to 326	-2.87	7.16	0.74	-0.96	0.74	-2.66	-7.37	8.10	30.0	+2.70

1 Conservatively based on a 1.12-inch thick outer shell and on a 3850-psi crush strength aluminum honeycomb impact limiter (Section 2.6.7.3.1).

2 Refer to Figure 2.10.2-9 for component identification.

Table 2.6.7-22 Critical Stress Summary (1-Foot Top Corner Drop) – Loading Condition 1 - S_n – Drop Orientation = 15.74 Degrees

Loading Condition 1: 130°F Ambient Temperature and Maximum Decay Heat Load

		S_n Stresses[1] (ksi)				Principal Stresses					
Comp. No.[2]	Section Cut Node to Node	S_x	S_y	S_z	S_{xy}	S_1	S_2	S_3	S.I.	Allow. Stress 3.0 S_m	Margin of Safety
	1-1										
1	2377 to 2577	-6.82	-0.40	0.32	-0.13	0.32	-0.40	-6.82	7.14	60.0	+7.40
	11-11										
3	1852 to 1856	-0.19	7.89	4.10	-0.42	7.91	4.10	-0.21	8.12	60.0	+6.39
	12-12										
4	601 to 604	0.09	-3.42	-0.54	-0.21	0.11	-0.54	-3.44	3.54	94.2	Large
	13-13										
6	615 to 618	-0.02	15.94	1.30	0.00	15.94	1.30	-0.02	15.95	94.2	+4.90
	14-14										
7	193 to 343	-7.81	12.82	1.50	1.46	12.93	1.50	-7.92	20.84	60.0	+1.88
	6-6										
8	381 to 385	-4.22	-7.18	-0.60	-0.96	-0.60	-3.93	-7.47	6.86	60.0	+7.74

1 Conservatively based on a 1.12-inch thick outer shell and on a 3850-psi crush strength aluminum honeycomb impact limiter (Section 2.6.7.3.1).
2 Refer to Figure 2.10.2-9 for component identification.

Table 2.6.7-23 Critical Stress Summary (1-Foot Top Corner Drop) – Loading Condition 1 - Total Range – Drop Orientation = 15.74 Degrees

Loading Condition 1: 130°F Ambient Temperature and Maximum Decay Heat Load

		Total Stress Range[1] (ksi)				Principal Stresses			Stress Differences		
Comp. No.[2]	Node	S_x	S_y	S_z	S_{xy}	S_1	S_2	S_3	S_1-S_2	S_2-S_3	S_3-S_1
1	2561	1.48	-1.26	0.20	43.95	44.08	0.20	-43.86	43.88	44.06	-87.94
3	1856	-0.19	7.24	3.70	0.08	7.24	3.70	-0.19	3.54	3.89	-7.43
4	1584	-0.13	-2.05	0.02	-0.11	0.02	0.12	-2.06	0.14	1.93	-2.08
6	1595	-0.05	7.09	0.97	0.01	7.09	0.97	-0.05	6.12	1.02	-7.14
7	192	-7.81	14.07	1.73	3.37	14.58	1.73	-8.32	12.85	10.05	-22.90
8	385	-7.64	-8.88	-3.12	-1.02	-3.12	-7.07	-9.46	3.95	2.39	-6.34

[1] Conservatively based on a 1.12-inch thick outer shell and on a 3850-psi crush strength aluminum honeycomb impact limiter (Section 2.6.7.3.1).

[2] Refer to Figure 2.10.2-9 for component identification.

Table 2.6.7-24 Critical Stress Summary (1-Foot Bottom Corner Drop) – Loading Condition 1 – P_m – Drop Orientation = 15.74 Degrees

Loading Condition 1: 130°F Ambient Temperature and Maximum Decay Heat Load

		P_m Stresses[1] (ksi)				Principal Stresses					
Comp. No.[2]	Section Cut Node to Node	S_x	S_y	S_z	S_{xy}	S_1	S_2	S_3	S.I.	Allow. Stress 1.0 S_m	Margin of Safety
	1-1										
1	2301 to 2561	-1.28	-0.32	0.62	0.30	0.62	-0.24	-1.37	1.99	20.0	Large
	2-2										
3	1595 to 1598	-3.44	-3.78	-1.65	-0.68	-1.65	-2.91	-4.31	2.66	20.0	+6.51
	3-3										
4	661 to 664	-0.04	-2.98	0.28	0.02	0.28	-0.04	-2.98	3.26	31.4	+8.63
	4-4										
6	615 to 618	-0.01	-4.93	0.28	-0.03	0.28	-0.01	-4.93	5.21	31.4	+5.03
	5-5										
7	2 to 102	-5.98	-3.63	-0.03	2.73	-0.03	-1.83	-7.78	7.76	20.0	+1.58
	6-6										
8	601 to 604	-0.10	-2.94	0.09	0.13	0.09	-0.09	-2.95	3.04	20.0	+5.58

1 Conservatively based on a 1.12-inch thick outer shell and on a 3850-psi crush strength aluminum honeycomb impact limiter (Section 2.6.7.3.1).

2 Refer to Figure 2.10.2-9 for component identification.

Table 2.6.7-25 Critical Stress Summary (1-Foot Bottom Corner Drop) – Loading Condition 1 - $P_m + P_b$ – Drop Orientation = 15.74 Degrees

Loading Condition 1: 130°F Ambient Temperature and Maximum Decay Heat Load

		$P_m + P_b$ Stresses[1] (ksi)				Principal Stresses					
Comp. No.[2]	Section Cut Node to Node	S_x	S_y	S_z	S_{xy}	S_1	S_2	S_3	S.I.	Allow. Stress 1.5 S_m	Margin of Safety
	1-1										
1	2301 to 2561	-4.05	-0.32	0.38	1.31	0.38	0.09	-4.46	4.84	30.0	+5.20
	7-7										
3	1815 to 1818	-1.55	4.49	-4.47	0.28	4.51	-1.56	-4.47	8.98	30.0	+2.34
	8-8										
4	621 to 624	0.04	-4.09	-0.52	0.09	0.04	-0.52	-4.10	4.14	47.1	Large
	4-4										
6	615 to 618	-0.02	-5.20	0.30	-0.03	0.30	-0.02	-5.20	5.49	47.1	+7.58
	9-9										
7	168 to 175	9.21	-3.47	-0.15	-0.29	9.22	-0.15	-3.48	12.70	30.0	+1.36
	10-10										
8	176 to 326	-6.65	0.00	-0.82	0.00	0.00	-0.82	-6.65	6.65	30.0	+3.51

1 Conservatively based on a 1.12-inch thick outer shell and on a 3850-psi crush strength aluminum honeycomb impact limiter (Section 2.6.7.3.1).

2 Refer to Figure 2.10.2-9 for component identification.

Table 2.6.7-26 Critical Stress Summary (1-Foot Bottom Corner Drop) – Loading Condition 1 - S_n – Drop Orientation = 15.74 Degrees

Loading Condition 1: 130°F Ambient Temperature and Maximum Decay Heat Load

		S_n Stresses[1] (ksi)				Principal Stresses					
Comp. No.[2]	Section Cut Node to Node	S_x	S_y	S_z	S_{xy}	S_1	S_2	S_3	S.I.	Allow. Stress 3.0 S_m	Margin of Safety
	1-1										
1	2301 to 2561	-6.94	-0.68	-0.30	-0.06	-0.30	-0.68	-6.94	6.64	60.0	+8.04
	11-11										
3	1852 to 1856	-0.13	11.99	3.05	-0.24	12.00	3.05	-0.13	12.13	60.0	+3.95
	12-12										
4	1301 to 1304	0.00	4.74	0.69	0.00	4.74	0.69	0.00	4.74	94.2	Large
	13-13										
6	1275 to 1278	-0.01	12.83	0.30	0.00	12.83	0.30	-0.01	12.84	94.2	+6.34
	14-14										
7	193 to 343	17.94	-0.43	1.20	2.27	18.22	1.20	-0.71	18.93	60.0	+2.17
	15-15										
8	192 to 342	-16.86	-0.12	-1.41	3.03	0.41	-1.41	-17.40	17.81	60.0	+2.37

1 Conservatively based on a 1.12-inch thick outer shell and on a 3850-psi crush strength aluminum honeycomb impact limiter (Section 2.6.7.3.1).
2 Refer to Figure 2.10.2-9 for component identification.

Table 2.6.7-27 Critical Stress Summary (1-Foot Bottom Corner Drop) – Loading Condition 1 - Total Range – Drop Orientation = 15.74 Degrees

Loading Condition 1: 130°F Ambient Temperature and Maximum Decay Heat Load

		Total Stress Range[1] (ksi)				Principal Stresses			Stress Differences		
Comp. No.[2]	Node	S_x	S_y	S_z	S_{xy}	S_1	S_2	S_3	S_1-S_2	S_2-S_3	S_3-S_1
1	2561	0.80	-4.34	0.23	4.73	3.61	0.23	-7.15	3.38	7.38	-10.76
3	1815	0.38	3.10	-0.93	1.68	3.90	-0.42	-0.93	4.32	0.51	-4.83
4	604	-0.19	-2.77	0.11	0.15	0.11	-0.18	-2.78	0.29	2.60	-2.89
6	615	-0.03	5.78	0.94	-0.03	5.78	0.94	-0.03	4.84	0.97	-5.81
7	1	3.73	-1.26	1.97	-43.45	44.76	1.97	-42.29	42.79	44.26	-87.04
8	192	0.11	-18.73	-9.11	2.58	0.46	-9.11	-19.08	9.57	9.97	-19.53

[1] Conservatively based on a 1.12-inch thick outer shell and on a 3850-psi crush strength aluminum honeycomb impact limiter (Section 2.6.7.3.1).

[2] Refer to Figure 2.10.2-9 for component identification.

Table 2.6.7-28 Critical Stress Summary (1-Foot Top Corner Drop) – Loading Condition 3 – P_m – Drop Orientation = 15.74 Degrees

Loading Condition 3: -40°F Ambient Temperature and No Decay Heat Load

		P_m Stresses[1] (ksi)				Principal Stresses					
Comp. No.[2]	Section Cut Node to Node	S_x	S_y	S_z	S_{xy}	S_1	S_2	S_3	S.I.	Allow. Stress 1.0 S_m	Margin of Safety
	1-1										
1	2377 to 2577	-4.89	-0.34	-0.78	-0.34	-0.32	-0.78	-4.91	4.59	20.0	+3.36
	2-2										
3	1775 to 1778	-0.06	-4.13	0.62	0.01	0.62	-0.06	-4.13	4.75	20.0	+3.21
	3-3										
4	1561 to 1564	0.02	-2.72	-0.33	-0.11	0.03	-0.33	-2.73	2.75	31.4	Large
	4-4										
6	1595 to 1598	-0.01	-3.71	0.53	0.03	0.53	-0.01	-3.71	4.23	31.4	+6.42
	5-5										
7	168 to 175	-2.03	3.20	1.06	-0.33	3.22	1.06	-2.05	5.27	20.0	+2.79
	6-6										
8	381 to 385	-1.93	-7.44	-1.79	0.32	-1.79	-1.91	-7.46	5.67	20.0	+2.53

1 Conservatively based on a 1.12-inch thick outer shell and on a 3850-psi crush strength aluminum honeycomb impact limiter (Section 2.6.7.3.1).

2 Refer to Figure 2.10.2-9 for component identification.

Table 2.6.7-29 Critical Stress Summary (1-Foot Top Corner Drop) – Loading Condition 3 - $P_m + P_b$ – Drop Orientation = 15.74 Degrees

Loading Condition 3: -40°F Ambient Temperature and No Decay Heat Load

		$P_m + P_b$ Stresses[1] (ksi)				Principal Stresses					
Comp. No.[2]	Section Cut Node to Node	S_x	S_y	S_z	S_{xy}	S_1	S_2	S_3	S.I.	Allow. Stress 1.5 S_m	Margin of Safety
	1-1										
1	2377 to 2577	-6.71	-0.34	-0.78	-0.34	-0.33	-0.78	-6.72	6.40	30.0	+3.69
	7-7										
3	1821 to 1825	0.03	-4.61	1.68	0.43	1.68	0.07	-4.65	6.33	30.0	+3.74
	3-3										
4	1561 to 1564	0.06	-3.75	-0.84	-0.11	0.06	-0.84	-3.75	3.81	94.2	Large
	4-4										
6	1595 to 1598	0.01	-3.81	0.45	0.03	0.45	0.01	-3.81	4.26	94.2	Large
	8-8										
7	143 to 150	-0.54	12.44	4.53	-0.50	12.46	4.53	-0.56	13.02	30.0	+1.30
	9-9										
8	176 to 326	-2.90	-8.30	-0.56	-0.22	-0.56	-2.89	-8.31	7.74	30.0	+2.87

1 Conservatively based on a 1.12-inch thick outer shell and on a 3850-psi crush strength aluminum honeycomb impact limiter (Section 2.6.7.3.1).

2 Refer to Figure 2.10.2-9 for component identification.

Table 2.6.7-30 Critical Stress Summary (1-Foot Top Corner Drop) – Loading Condition 3 - S_n – Drop Orientation = 15.74 Degrees

Loading Condition 3: -40°F Ambient Temperature and No Decay Heat Load

		S_n Stresses[1] (ksi)				Principal Stresses					
Comp. No.[2]	Section Cut Node to Node	S_x	S_y	S_z	S_{xy}	S_1	S_2	S_3	S.I.	Allow. Stress 3.0 S_m	Margin of Safety
	1-1										
1	2377 to 2577	-6.95	-0.47	-1.07	-0.53	-0.43	-1.07	-6.99	6.56	60.0	+8.15
	10-10										
3	1801 to 1805	0.47	14.21	7.54	1.89	14.46	7.54	0.22	14.25	60.0	+3.21
	11-11										
4	661 to 664	0.14	-7.03	-1.15	-0.29	0.15	-1.15	-7.04	7.20	94.2	Large
	4-4										
6	1595 to 1598	0.02	-7.43	0.70	0.05	0.70	0.02	-7.43	8.13	94.2	Large
	8-8										
7	143 to 150	-0.54	13.55	4.99	-0.59	13.58	4.99	-0.56	14.14	60.0	+3.24
	6-6										
8	381 to 385	-4.25	-8.32	-1.90	-0.23	-1.90	-4.23	-8.33	6.42	60.0	+8.34

1 Conservatively based on a 1.12-inch thick outer shell and on a 3850-psi crush strength aluminum honeycomb impact limiter (Section 2.6.7.3.1).

2 Refer to Figure 2.10.2-9 for component identification.

Table 2.6.7-31 Critical Stress Summary (1-Foot Top Corner Drop) – Loading Condition 3 - Total Range – Drop Orientation = 15.74 Degrees

Loading Condition 3: -40°F Ambient Temperature and Maximum Decay Heat Load

		Total Stress Range[1] (ksi)				Principal Stresses			Stress Differences		
Comp. No.[2]	Node	S_x	S_y	S_z	S_{xy}	S_1	S_2	S_3	S_1-S_2	S_2-S_3	S_3-S_1
1	2561	0.05	-1.17	-1.15	40.01	39.49	-1.15	-40.61	40.64	39.46	-80.10
3	1805	0.47	16.81	8.08	2.75	17.26	8.08	0.02	9.18	8.06	-17.24
4	1584	-0.04	4.04	-3.61	-0.44	4.09	-0.09	-3.61	4.17	3.52	-7.70
6	1598	-0.02	-7.58	0.65	0.03	0.65	-0.02	-7.58	0.67	7.56	-8.23
7	2	-0.55	14.68	5.23	0.43	14.69	5.23	-0.56	9.46	5.79	-15.25
8	385	-7.60	-7.37	-4.68	-1.24	-4.68	-6.24	-8.73	1.56	2.48	-4.05

1 Conservatively based on a 1.12-inch thick outer shell and on a 3850-psi crush strength aluminum honeycomb impact limiter (Section 2.6.7.3.1).

2 Refer to Figure 2.10.2-9 for component identification.

Table 2.6.7-32 Summary of Results - Impact Limiter Analysis for 1-Foot Free Drop

Analysis Description	Displacement (in)	Force (lb)	Equivalent[1] G Load Factor
Flat End Impact			
Bottom Limiter with Max Crush Strength	0.76	8.22×10^5	15.8
Bottom Limiter with Min Crush Strength	0.94	6.60×10^5	12.7
Top Limiter with Max Crush Strength	0.82	8.22×10^5	15.8
Top Limiter with Min Crush Strength	0.96	6.71×10^5	12.9
Corner Impact			
Bottom Limiter with Max Crush Strength	3.16	6.29×10^5	12.1
Bottom Limiter with Min Crush Strength	3.40	6.29×10^5	12.1
Top Limiter with Max Crush Strength	3.18	6.40×10^5	12.3
Top Limiter with Min Crush Strength	3.42	5.98×10^5	11.5

[1] Equivalent g load factor = Force/52,000.

Table 2.6.7-32 Summary of Results - Impact Limiter Analysis for 1-Foot Free Drop (continued)

Analysis Description	Displacement (in)	Force (lb)	Equivalent[1] G Load Factor
Flat Side Impact			
Bottom Limiter with Max Crush Strength	0.83	1.21×10^6	23.3
Bottom Limiter with Min Crush Strength	0.95	1.03×10^6	19.8
Top Limiter with Max Crush Strength	0.83	1.26×10^6	24.3
Top Limiter with Min Crush Strength	0.94	1.07×10^6	20.6

[1] Equivalent g load factor = Force/52,000.

Table 2.6.7-33 Summary of Results - Impact Limiter Analysis for 30-Foot Free Drop Subsequent to a 1-Foot Fall

Analysis Description	Displacement (in)	Force (lb)	Equivalent[1] G Load Factor
Flat End Impact			
Bottom Limiter with Max Crush Strength	8.50	2.50×10^6	48.1
Bottom Limiter with Min Crush Strength	10.30	2.03×10^6	39.0
Top Limiter with Max Crush Strength	8.47	2.51×10^6	48.3
Top Limiter with Min Crush Strength	10.24	2.04×10^6	39.2
Corner Impact			
Bottom Limiter with Max Crush Strength	11.30	3.08×10^6	59.2
Bottom Limiter with Min Crush Strength	12.70	2.58×10^6	49.6
Top Limiter with Max Crush Strength	11.38	3.14×10^6	60.4
Top Limiter with Min Crush Strength	12.72	2.98×10^6	57.3

[1] Equivalent g load factor = Force/52,000.

Table 2.6.7-33 Summary of Results - Impact Limiter Analysis for 30-Foot Free Drop Subsequent to a 1-Foot Fall (continued)

Analysis Description	Displacement (in)	Force (lb)	Equivalent[1] G Load Factor
Flat Side Impact			
Bottom Limiter with Max Crush Strength	8.60	2.65×10^6	48.7
Bottom Limiter with Min Crush Strength	10.30	2.17×10^6	41.8
Top Limiter with Max Crush Strength	8.42	2.71×10^6	49.7
Top Limiter with Min Crush Strength	10.00	2.22×10^6	42.7

[1] Equivalent g load factor = Force/52,000.

Table 2.6.7-34 Summary of Cask Drop Equivalent G Load Factors

Direction	Equivalent G Load Factor[1]			
	1-Foot Drop	31-Foot Drop		
		Total	Axial[2] Comp.	Lateral[3] Comp.
Lateral (Side)	24.3	49.7	—	49.7
Longitudinal	15.8	60.0	60.0	—
Corner (15.74°)	12.3	60.4	58.2	16.4
Oblique (30°)	—	54.4	47.1	27.2
Oblique (45°)	—	43.8	31.0	31.0
Oblique (60°)	—	44.4	22.2	38.5

[1] Equivalent g load factor = Force/52,000.
[2] Axial Component = total x cosθ where θ = 15.74°, 30°, 45°, or 60°
[3] Lateral Component = total x sinθ where θ = 15.74°, 30°, 45°, or 60°

Table 2.6.7-35 NAC-LWT Cask Hot Bolt Analysis – Normal Conditions

Nominal Diameter (in):	1.00	
Number of Bolts:	12	
Service Stress, Sy (ksi):	81.9	at a 300 degree-F Service Temperature
Bolt Expansion (in/in):	9E-06	
Bolt Modulus (ksi):	26700	
Lid Expansion (in/in):	9E-06	
Lid Modulus (ksi):	27000	
Stress Area (in2):	0.6051	
Grip Length (in):	7.99	
Maximum Pressure (psi):	50	
Seal Diameter (in):	15.750	
Preload Torque (ft-lbs):	260	at RT
Nominal Room Temp, RT:	70	deg-F
Bolt Circle Diameter (in):	17.88	
Lid Diameter (in):	22.50	

(a) Longitudinal Weight (lbs):	4941
(b) Lateral Weight (lbs):	941
Service DT (degrees):	157
[default value =]	230
CALCULATED LOADS & STIFFNESS	
(c) Bolt Thermal Load (lbs):	1423
(d) Bolt Preload (lbs):	34770
(e) Bolt Pressure Load (lbs):	812
(f) Bolt Stiffness (lbs/in):	1.9E+06
(g) Lid Stiffness (lbs/in):	2.1E+07

Angle wrt Vert. (Deg)	Impact Accel. (g)	<**** LOADS (lbs.) Impact Tension	Impact Shear	Bolt Tension Applied	Bolt Tension Net ****	<**** STRESSES (psi) Direct Tension	Direct Shear	Principal Sig-1	Principal Sig-2	Stress Intens. ****	Margin of Safety
	(h)		(k)	(l)	(m)	(n)	(o)		(p)	(q)	(r)
0 End	60.00	24705[(i)]	0	25517	38292	63282	0	0	63282	63282	0.29
5 (+)	60.13	33641[(j)]	411	34453	39027	64497	679	-7	64504	64511	0.27
10 (+)	60.25	33327	820	34138	39001	64454	1356	-29	64483	64511	0.27
15.7 Corner	60.40	32657	1282	33469	38946	64363	2118	-70	64433	64503	0.27
20 (+)	58.60	30924	1572	31736	38804	64128	2597	-105	64233	64338	0.27
25 (+)	56.50	28758	1872	29570	38626	63833	3094	-150	63983	64133	0.28
30 (calc)	54.40	26459	2133	27271	38436	63521	3525	-195	63716	63911	0.28
35 (+)	50.87	23402	2288	24213	38185	63105	3781	-226	63331	63557	0.29
40 (+)	47.33	20364	2386	21176	37935	62692	3943	-247	62939	63186	0.30
45 (calc)	43.80	17394	2429	18206	37691	62289	4014	-258	62546	62804	0.30
50 (+)	44.00	15884	2643	16696	37567	62083	4368	-306	62389	62695	0.31
55 (+)	44.20	14238	2839	15050	37431	61860	4692	-354	62213	62567	0.31
60 (calc)	44.40	12468	3015	13280	37286	61619	4983	-400	62019	62420	0.31
65 (+)	45.68	10843	3247	11655	37152	61398	5366	-465	61863	62329	0.31
70 (+)	46.97	9022	3461	9834	37002	61150	5719	-530	61681	62211	0.32
75 (+)	48.25	7014	3655	7825	36837	60877	6040	-593	61471	62064	0.32
80 (+)	49.53	4831	3825	5643	36657	60581	6322	-653	61233	61886	0.32
85 (+)	50.82	2487	3970	3299	36465	60262	6560	-706	60968	61674	0.33
90 Side	52.10	0	4086	812	36260	59924	6752	-751	60675	61427	0.33

Minimum Margin of Safety: 0.27

Table 2.6.7-36 NAC-LWT Cask Cold Bolt Analysis – Normal Conditions

Nominal Diameter (in):	1.00		
Number of Bolts:	12		
Service Stress, Sy (ksi):	85	at a 70	
Bolt Expansion (in/in):	8E-06	degree-F	
Bolt Modulus (ksi):	27800	Service	
Lid Expansion (in/in):	8E-06	Temperature	
Lid Modulus (ksi):	28300		
Stress Area (in2):	0.6051		
Grip Length (in):	7.99		
Maximum Pressure (psi):	50		
Seal Diameter (in):	15.750		
Preload Torque (ft-lbs):	260	at RT	
Nominal Room Temp, RT:	70	deg-F	
Bolt Circle Diameter (in):	17.88		
Lid Diameter (in):	22.50		

Longitudinal Weight (lbs):	4941
Lateral Weight (lbs):	941
Service DT (degrees):	-90
[default value =]	0
CALCULATED LOADS & STIFFNESS	
Bolt Thermal Load (lbs):	-594
Bolt Preload (lbs):	34770
Bolt Pressure Load (lbs):	812
Bolt Stiffness (lbs/in):	2.0E+06
Lid Stiffness (lbs/in):	2.2E+07

Angle wrt Vert. (Deg)	Impact Accel. (g)	<***** LOADS (lbs.) Impact Tension	Impact Shear	Bolt Tension Applied	Bolt Tension Net ****>	<***** STRESSES (psi) Direct Tension	Direct Shear	Principal Sig-1	Principal Sig-2	Stress Intens. ****>	Margin of Safety
0 End	60.00	24705	0	25517	36262	59928	0	0	59928	59928	0.42
5 (+)	60.13	33641	411	34453	36993	61135	679	-8	61143	61150	0.39
10 (+)	60.25	33327	820	34138	36967	61093	1356	-30	61123	61153	0.39
15.7 Corner	60.40	32657	1282	33469	36912	61002	2118	-73	61076	61149	0.39
20 (+)	58.60	30924	1572	31736	36771	60768	2597	-111	60879	60990	0.39
25 (+)	56.50	28758	1872	29570	36594	60475	3094	-158	60633	60791	0.40
30 (calc)	54.40	26459	2133	27271	36406	60165	3525	-206	60371	60577	0.40
35 (+)	50.87	23402	2288	24213	36156	59752	3781	-238	59990	60228	0.41
40 (+)	47.33	20364	2386	21176	35908	59341	3943	-261	59602	59863	0.42
45 (calc)	43.80	17394	2429	18206	35665	58940	4014	-272	59212	59484	0.43
50 (+)	44.00	15884	2643	16696	35541	58736	4368	-323	59059	59382	0.43
55 (+)	44.20	14238	2839	15050	35407	58514	4692	-374	58888	59262	0.43
60 (calc)	44.40	12468	3015	13280	35262	58275	4983	-423	58698	59121	0.44
65 (+)	45.68	10843	3247	11655	35129	58055	5366	-492	58547	59039	0.44
70 (+)	46.97	9022	3461	9834	34980	57809	5719	-560	58369	58930	0.44
75 (+)	48.25	7014	3655	7825	34816	57538	6040	-627	58165	58792	0.45
80 (+)	49.53	4831	3825	5643	34638	57243	6322	-690	57933	58622	0.45
85 (+)	50.82	2487	3970	3299	34446	56926	6560	-746	57672	58419	0.46
90 Side	52.10	0	4086	812	34243	56590	6752	-794	57384	58179	0.46

Minimum Margin of Safety: 0.39

Table 2.6.7-37 Summary of Neutron Shield Tank Analysis

Load Condition: 1-Foot End Drop and 1-Foot Side Drop

Description	Stress Magnitude (psi)	Margin of Safety[1]
Tank Shell	12,841	+0.07
Stiffener	11,746	+0.17
Stiffener Weld	2,424 lb/in	+0.23
Gusset Weld	1,418 lb/in	+1.10
Bottom End Plate	8,525	+1.79
Gusset Plate Cross Section	7,180	+LARGE
End Plate Welds	1,593	+LARGE
Top End Plate	11,172	+0.23

This table summarizes the stresses and margins for a design condition of 180 psig (Section 2.6.7.7.4), which envelops both the end drop and side drop conditions.

[1] Based on an allowable stress equal to the yield strength of Type 304 stainless steel at 250°F.

Table 2.6.7-38 Normal Transport Shield Tank Temperatures

Transport Condition	Average Fluid Temperature
100°F/Full Heat Load	227°F
68°F/No Heat Load	68°F
-20°F/Full Heat Load	99°F
-20°F/No Heat Load	-20°F

Table 2.6.7-39 Normal Transport Shield Tank Pressures

Transport Condition	Calculated Tank Pressure
PRVR	165 psig
100°F/Full Heat Load	25.6 psig
68°F/No Heat Load	0 psig

Table 2.6.7-40 Summary of Expansion Tank Analysis

Load Condition: 1-Foot End Drop and 1-Foot Side Drop

Description	Stress Magnitude (psi)	Margin of Safety[1]
Bottom/Top End Plate	3,375	+LARGE
Tank Shell	10,857	+0.26
Tank Stiffener	9,997	+0.37
Shell Weld	11,750	+0.17

This table summarizes the stresses and margins for a design condition of 180 psig (Sections 2.6.7.8 and 2.6.7.7.4), which envelops both the end drop and side drop conditions.

[1] Based on an allowable stress equal to the yield strength of Type 304 stainless steel at 250°F.

Table 2.6.7-41 Upper Ring – Cross-Section Principal Stresses

Section	P_m Stresses							$P_m + P_b$ Stresses						
	Component (ksi)				Principal (ksi)			Component (ksi)				Principal (ksi)		
	S_x	S_y	S_z	S_{xy}	S_1	S_2	S_3	S_x	S_y	S_z	S_{xy}	S_1	S_2	S_3
a-a	-0.8	4.7	1.9	-0.1	4.7	-0.8	1.9	-2.6	9.0	4.0	-1.0	9.1	-2.7	4.0
b-b	0.1	4.9	1.9	-0.2	4.9	0.1	1.9	1.2	8.0	2.9	-1.0	8.1	1.1	2.9
c-c	-0.1	5.5	2.0	0.5	5.5	-0.3	2.0	-0.2	6.5	2.6	1.0	6.6	-0.3	2.6

2.6.12.9 General Atomics IFM Basket Construction

The General Atomics Irradiated Fuel Material (IFM) basket consists of a top module assembly designed to carry two IFM Fuel Handling Units (FHUs). Each IFM FHU is associated with RERTR or HTGR fuel materials. A spacer assembly is used to permit the top module assembly to be positioned next to the transport cask lid.

The top module is 43.7 inches long and is made up of two fuel tubes and three support plates. All components are made from ASME SA240 Type 304 stainless steel. The fuel tubes have a 6.0-inch outer diameter and a 0.25-inch wall thickness. Two of the support plates are 0.50-inch thick and the third, center plate, is 1.0-inch thick. The support plates are welded to the fuel tubes with 1/8-inch bevel welds.

Two types of IFM FHU are carried by the top module. One FHU carries irradiated HTGR fuel material and is 5.25 inches in diameter (0.12-inch thick wall) and 39.0 inches long. The other FHU contains irradiated RERTR fuel material, is 4.75 inches in diameter (0.12-inch thick wall), and is 37.25 inches long.

Each end of the FHU is comprised of a 0.25-inch thick plate welded to the container shell. The weld connecting the end plate to the container shell is labeled as a full-penetration butt weld. The dimensions of the end plate and the container shell provide a minimal gap (2 mils when considering maximum tolerances) to permit the end plate to be inserted into the container end. The close tolerances ensure that the two components are effectively in contact along the 0.5-inch common interface length of the end plate and the container. Once the end plate is inserted, a fusion weld procedure is employed to weld the lip of the end plate to the wall of the container. The depth of the weld along the interface between the end plate and the container is equal to approximately 70% of the thickness of the end plate lip or the container lip.

Due to the location of the weld for the end plate, the weld does not transfer any load for the drop conditions. Additionally, since the heat loads are insignificant (13w) and the backfill for the FHU and the cask cavity are limited to atmospheric pressure, the pressure differential across the welded plates is insignificant. Each of these FHUs also has an additional smaller container, which holds the fuel. In these evaluations, the inner container is neglected.

The spacer assembly is 133.0 inches in length, excluding guide pins. The assembly is comprised of one spacer tube and five support plates. The spacer tube consists of a Type 304 stainless steel 8-inch Schedule 80S pipe. The tube has an outside diameter of 8.63 inches and a wall thickness of 0.50 inch. The spacer plates are 1.0-inch thick and are welded to the tube with 1/8-inch bevel welds. Two guide pins are located at the top of the spacer assembly to facilitate alignment with the top module.

2.6.12.9.1 General Atomics IFM Basket Interface Analysis

The structural evaluation of the top module assembly is performed using classical hand calculations. The weight of the top module is bounded by 200 lbs, and the maximum weight of one FHU and its fuel contents is 76 lbs. Therefore, the total weight of a loaded top module system is 200 + 2(76) or 352 lbs. The weight of the spacer assembly is 760 lbs. The total loaded system weight is 1,112 lbs, and this weight is bounded by the design basis contents weight for the LWT system. Therefore, no analysis of the LWT cask body is required.

2.6.12.9.2 General Atomics Top Module Structural Analysis

Structural analyses for the top module for the 1-foot end drop and 1-foot side drop are performed using classical hand calculations.

General Atomics 1-Foot Side Drop Analysis

Top Module:

During a 1-foot side drop, the distributed load on one fuel tube is:

$$W = \frac{\left(76 + 0.291 \times \frac{\pi\left(6.0^2 - 5.5^2\right)}{4} \times 43.7\right)}{43.7} = 3.1 \text{ lb/in}$$

where:

weight of fuel = 76 lbs
length of tube = 43.7 inches
outer diameter = 6.0 inches
inner diameter = 5.5 inches

The maximum bending moment in tube is:

$$M = \frac{3.1 \times 20.35^2}{8} = 160 \text{ in - lbs}$$

The maximum bending stress in the fuel tube for 1g loading is:

$$I = \frac{\pi\left(6.0^4 - 5.5^4\right)}{64} = 18.7 \text{ in}^4$$

$$S_b = \frac{160 \times 3}{18.7} = 26 \text{ psi}$$

The margin of safety for tube bending for a 1-foot side drop (25g) is:

$$MS = \frac{1.5S_m}{S_b} - 1 = \frac{1.5 \times 19350}{25 \times 26} - 1 = +\underline{\text{Large}}$$

During a 1-foot side drop, the support plates bear up against the inner shell of the LWT cask. The center plate will carry the maximum weight. The bearing load on the center plate is:

$$W = \frac{10 \times \frac{[(2 \times 76) + 200]}{40.7} \times 20.35}{8} = 220 \text{ lbs}$$ (Page 2-299, #12, Manual of Steel Construction)

The bearing stress is maximum for the center disk.

The bearing stress is (Item 2c, Table 33, Young):

LWT cask cavity diameter, D1 = 13.375 inches

Support plate diameter, D2 = 13.265 inches

$$K_D = \frac{D_1 D_2}{D_1 - D_2} = 1{,}613$$

$$C_E = \frac{1 - 0.31^2}{26.75e6} + \frac{1 - 0.31^2}{8.29e6} = 1.42e-7$$

$$S_c = 0.798\sqrt{\frac{p}{K_D C_E}} = 0.798\sqrt{\frac{220}{1613 \times 1.42e\text{-}7}} = 782 \text{ psi, 1g loading}$$

where:

p = 220/(1.0) = 220 lbs/in

E = 26.75e6 psi @ 350°F

Effective 'E' of LWT shells with lead:

$$E = \frac{0.75 \times 26.75e6 + 1.25 \times 26.75e6 + 5.75 \times 1.87e6}{7.75} = 8.29e6 \text{ psi}$$

The margin of safety for bearing for a 1-foot side drop (25g) is:

$$MS = \frac{S_y}{25 \times S_c} = \frac{21600}{25 \times 782} - 1 = +0.10$$

During a side drop, the top and bottom support plate welds are in shear. The load on the weld due to 1g is:

$$W = \frac{3 \times \frac{[(2 \times 76) + 200]}{40.7} \times 20.35}{8} = 66 \text{ lbs}$$ (Page 2-299, #12, Manual of Steel Construction)

The weld length is:

$$L = 2(\pi d_{tube} - r_{tube}\theta)$$
$$= 2(\pi \times 6.0 - 3.0 \times 1.57) = 28.3 \text{ inches}$$
$$\theta = \text{non welded arc length} = 90 \text{ deg} = 1.57 \text{ radians}$$

The support disk/ tube weld is a 1/8-inch bevel weld. The stress in the weld for 1g is:

$$S = \frac{66}{(28.3 \times 0.125 \times 0.7071)} = 26.4 \text{ psi, 1g loading}$$

For visual inspection, the weld factor is 0.25 per ASME Section III, Subsection NG-3352. The margin of safety for shear is:

$$MS = \frac{0.25 \times 0.6S_m}{25S} - 1 = \frac{0.25 \times 0.6 \times 19350}{25 \times 26.4} - 1 = +3.4$$

Spacer Assembly:

During a 1-foot side drop, the distributed load on the tube is:

$$W = \frac{760}{129.5} = 5.9 \text{ lb/in, use } 6.0 \text{ lb/in}$$

The maximum bending moment in tube, conservatively assuming a simply supported beam, is:

$$M = \frac{6 \times 32.0^2}{8} = 768 \text{ in - lbs}$$

The bending stress in tube for a 1g loading is:

$$I = \frac{\pi(8.63^4 - 7.63^4)}{64} = 106 \text{ in}^4$$
$$S_b = \frac{768 \times (8.63/2)}{106} = 31 \text{ psi}$$

The margin of safety for bending in the 1-foot side drop (25g) is:

$$MS = \frac{1.5S_m}{S_b} - 1 = \frac{1.5 \times 19350}{25 \times 31} - 1 = + \underline{\text{Large}}$$

During a 1-foot side drop, the support plates bear up against the inner shell of the LWT cask. The maximum load on a support plate during a side drop is:

$$W = 1.143 \times \frac{760}{128.0} \times 32.0 = 217 \text{ lbs}$$ (Page 2-309, #39, Manual of Steel Construction)

The bearing stress is (Item 2c, Table 33, Young):

LWT cask cavity diameter $D_1 = 13.375$ inches

Support plate diameter $D_2 = 13.265$ inches

$$K_D = \frac{D_1 D_2}{D_1 - D_2} = 1{,}613$$

$$C_E = \frac{1-0.31^2}{26.75e6} + \frac{1-0.31^2}{8.29e6} = 1.42e-7$$

$$S_c = 0.798\sqrt{\frac{p}{K_D C_E}} = 0.798\sqrt{\frac{217}{1613 \times 1.42e-7}} = 777 \text{ psi}$$

where:

$p = 217 / 1.0 = 217$ lb/in

$E = 26.75e6$ psi @ 350°F

Effective 'E' of LWT shells with lead:

$$E = \frac{0.75 \times 26.75e6 + 1.25 \times 26.75e6 + 5.75 \times 1.87e6}{7.75} = 8.29e6 \text{ psi}$$

The margin of safety for bearing is:

$$MS = \frac{S_y}{25 \times S_c} = \frac{21600}{25 \times 777} - 1 = +0.11$$

During a side drop, the top and support plate weld is in shear. The load on the weld is:

$$W = 0.393 \times \frac{760}{128.0} 32.0 = 75 \text{ lbs}$$ (Page 2-309, #39, Manual of Steel Construction)

The weld length is:

$$L = \pi \times 8.63 = 27.1 \text{ inches}$$

The weld between the support disk and tube is a 1/8-inch bevel weld. The stress in the weld for 1g is:

$$S = \frac{75}{(27.1 \times 0.125 \times 0.7071)} = 31 \text{ psi, 1g loading}$$

For visual inspection, the weld factor is 0.25 per ASME Section III, Subsection NG-3352. The margin of safety for shear is:

$$MS = \frac{0.25 \times 0.6 S_m}{25S} - 1 = \frac{0.25 \times 0.6 \times 19350}{25 \times 31} - 1 = 2.7$$

Fuel Handling Units (FHU)

The FHUs are analyzed in accordance with ASME Section III, Subsection NG. The bounding weight of a loaded fuel container is 76 lbs.

The side drop is analyzed assuming a circular ring under an external compressive load using Roarks Table 17, Item 1 (Young). The stress in the container shell is:

$$\alpha = \frac{I}{AR^2} = \frac{\pi(2.125^3) \times (0.12)}{\pi(2.125^2 - 2.0^2) \times 2.125^2} = 0.49$$

$$k_2 = 1 - \alpha = 1 - 0.49 = 0.51$$

$$M = (0.5 - 0.3183 k_2) WR = [0.5 - 0.3183(0.51)] \frac{76}{35.5} 2.125 = 1.5 \text{ in - lb}$$

$$S = \frac{6(1.5)}{0.12^2} = 0.63 \text{ ksi}$$

The margin of safety is:

$$MS = \frac{1.5 S_m}{25S} - 1 = \frac{1.5 \times 19.35}{25 \times 0.63} - 1 = +0.84$$

General Atomics 1-Foot End Drop Analysis

Top Module:

During an end drop, the stress in the fuel tubes is calculated as follows.

The cross-sectional area of a tube is:

$$A = \frac{\pi(6.0^2 - 5.5^2)}{4} = 4.52 \text{ in}^2$$

Using a top module weight of 200 lbs, fuel weight not included, the stress in the two fuel tubes is:

$$S = \frac{200}{2 \times 4.52} = 22 \text{ psi}$$

The margin of safety is:

$$MS = \frac{S_m}{20S} - 1 = \frac{19350}{20 \times 22} - 1 = +\underline{\text{Large}}$$

Since the axial compression stress in the tubes is minimal, no buckling evaluation is required.

The top end drop is the bounding end drop because the top end has significantly less bearing area than the bottom end, and the weight of the spacer is included.

The bearing area for the top end is assumed to be the two fuel tubes, conservatively neglecting the lifting components. The cross-sectional area is:

$$A = 2\left[\frac{\pi(6.0^2 - 5.5^2)}{4} - 3.22 \times 0.25\right] = 7.42 \text{ in}^2$$

where:

outer diameter = 6.0 inches

inner diameter = 5.5 inches

cut out arc length = 3.22 inches

$$S = r\theta = 2.875 \times 1.12 = 3.22 \text{ inches}$$

$$\theta = 2 \times \tan^{-1}\left(\frac{1.72}{2.75}\right) = 64.05^\circ = 1.12 \text{ radians}$$

The bearing stress, fuel weight not included, in the module for a 1g loading is:

$$S_{brg} = \frac{200 + 760}{7.42} = 129 \text{ psi}$$

The margin of safety is:

$$S_{brg} = 20 \times 129 = 2.58 \text{ ksi}$$

$$MS = \frac{S_y}{S_{brg}} - 1 = \frac{21.6}{2.58} - 1 = +7.37$$

During an end drop, the self-weight of the center support plate has to be carried by the welds. The weight of the center support plate is:

$$W = 0.291\left\{1.0\left[\frac{\pi \times 13.265^2}{4} - 2\left(\frac{\pi \times 6.0^2}{4}\right)\right]\right\} = 24 \text{ lbs (use 30 lbs)}$$

where:

0.291 lbs/in^3 is the density of 304 stainless steel

1.0 inch is the disk thickness

13.265 inches is the disk diameter

6.0 inches is the cutout diameter

The weld length is:

$$L = 2(\pi d_{tube} - r_{tube}\theta)$$
$$= 2(\pi \times 6.0 - 3.0 \times 1.57) = 28.3 \text{ in.}$$
$$\theta = \text{nonwelded arc length} = 90 \text{ deg} = 1.57 \text{ radians}$$

The welds are 1/8-inch bevel welds on both sides of the disk. The stress in the weld for 1g is:

$$S = \frac{30}{2(28.3 \times 0.125 \times 0.7071)} = 6.0 \text{ psi}$$

For visual inspection, the weld factor is 0.25 per ASME Section III, Subsection NG-3352. The margin of safety for normal conditions is:

$$MS = \frac{0.25 \times 0.6 S_m}{20S} - 1 = \frac{0.25 \times 0.6 \times 19350}{20 \times 6} - 1 = +\underline{\text{Large}}$$

Spacer Assembly:

During an end drop, the stress in the tube is calculated as follows.

The cross-sectional area of a tube is:

$$A = \frac{\pi(8.63^2 - 7.63^2)}{4} = 12.77 \text{ in}^2$$

The stress in the tube is:

$$S = \frac{760 + 200 + 2 \times 76}{12.77} = 87 \text{ psi}$$

The margin of safety is:

$$MS = \frac{S_m}{20S} - 1 = \frac{19350}{20 \times 87} - 1 = +\underline{\text{Large}}$$

Since the axial stress in the tube is minimal, no buckling evaluation is required.

For a top and bottom end drop, the bearing stresses for 1g are:

$$A_{top} = 2(9.9 \times 0.3125) = 6.19 \text{ in}^2$$

$$S_{brg} = \frac{760}{6.19} = 123 \text{ psi}$$

$$A_{bot} = \frac{\pi(8.63^2 - 7.63^2)}{4} - (4 \times 1.0 \times 0.5) = 10.77 \text{ in}^2$$

$$S_{brg} = \frac{760 + 200 + 2 \times 76}{10.77} = 103 \text{ psi}$$

The margin of safety is:

$$S_{brg} = 20 \times 123 = 2.46 \text{ ksi}$$

$$MS = \frac{S_y}{S_{brg}} - 1 = \frac{21.6}{2.46} - 1 = +7.78$$

During an end drop, the weight of a support plate has to be carried by the welds to the tube.

The weight of the support plate is:

$$W = 0.291\left(\frac{\pi\left(13.265^2 - 8.63^2\right)}{4} \times 1.0\right) \approx 25 \text{ lbs}$$

The weld length is:

$$L = \pi \times 8.63 = 27.1 \text{ inches}$$

$$S = \frac{25}{2(27.1 \times 0.125 \times 0.7071)} = 5.2 \text{ psi}$$

Since the weld stress is less than the weld stress in the support disks in the top module, no additional analysis is required.

Fuel Handling Unit:

The maximum bearing stress occurs in the top end drop orientation. The bearing area for the handle supports is:

$$A = 2 \times 0.5^2 = 0.5 \text{ in}^2$$

The bearing stress is:

$$S_{brg} = \frac{76}{0.5} = 152 \text{ psi}$$

$$S_{brg} = 20 \times 152 = 3.0 \text{ ksi}$$

The margin of safety is

$$MS = \frac{S_y}{S_{brg}} - 1 = \frac{21.6}{3.0} - 1 = +6.2$$

The top lid and bottom plates sit on a lip in the container shell. The cross-sectional area of the lip is:

$$A = \frac{\pi\left(4.124^2 - 4.0^2\right)}{4} = 0.79 \text{ in}^2$$

Since the area is greater than the handle support area above, no additional analysis is required.

The cross-sectional area of the tube is:

$$A = \frac{\pi\left(4.25^2 - 4.0^2\right)}{4} = 1.62\,in^2$$

For a 20g end drop, normal conditions, the stress in the tube is:

$$S = \frac{20 \times 76}{1.62} = 0.94\,ksi$$

$$MS = \frac{S_m}{S} - 1 = \frac{19.35}{0.94} - 1 = +\underline{Large}$$

Since the axial compression stresses in the tube are minimal, no buckling evaluation is required.

2.6.12.10 TPBAR Basket Analysis

The TPBAR basket is a modified NAC-LWT PWR basket with increased free volume that is fabricated from 6061-T651 aluminum alloy. Figure 2.6.12-7 shows the cross-section of the TPBAR basket. A 13.25-inch outside diameter, 8.25-inch long stainless steel alternate upper fitting is bolted to the top of the basket body. This fitting provides lifting points for removing the basket from the cask. Additionally, this alternate upper fitting prevents the basket from applying load to the TPBAR contents during the top-end drop. A stainless steel lower fitting is bolted to the bottom of the basket body. The lower fitting assembly supports the fuel basket and contents longitudinally. An additional spacer assembly is bolted to the cask lid to prevent the TPBAR contents from shifting axially and rotationally within the basket. A groove on the periphery of the basket body provides for the cask drain tube. The drain tube is connected to a fitting on the cask body for draining or filling the cask during wet cask loading or unloading operations.

The TPBAR basket accommodates two TPBAR content configurations. The first TPBAR content configuration is the shipment of up to 300 production TPBARs (of which two can be prefailed) contained in an open consolidation canister with optional top insert. The consolidation canister body is fabricated from Type 304 stainless steel and the bail is fabricated from Type 7-4 precipitation hardened stainless steel. The consolidation canister is used to load and unload the TPBARs into and from the NAC-LWT cask configured with a TPBAR basket assembly.

The second TPBAR content configuration is the shipment of up to 55 segmented TPBARs, following post-irradiation examinations (PIE), contained in a welded sealed waste container. The waste container is welded to an extension weldment to provide the identical length as the consolidation canister to assure fit-up in the TPBAR basket assembly. The waste container and extension are fabricated from Type 316L stainless steel.

Following placement of the consolidation canister or the waste container with extension in the TPBAR basket, and installation and bolting of the lid, the TPBAR basket and contents are evaluated without consideration of the strength of the consolidation canister or waste container. The TPBAR basket provides a boundary for support on all sides of the consolidation canister and TPBARs for the full length of the canister. The cylindrical TPBAR waste container (external diameter 8.6 inches) is sized to fit within the square cross-section (8.8 inches) of the TPBAR basket. The TPBAR upper end-fitting spacer guides do not permit the consolidation canister to be loaded by the TPBAR basket in any drop orientation. The TPBAR spacer assembly attached to the bottom of the cask lid restricts the movement of the TPBARs in the axial direction and prevents rotation of the TPBAR waste container. Therefore, no additional evaluations are required for the TPBAR consolidation canister or TPBAR waste container and extension weldment.

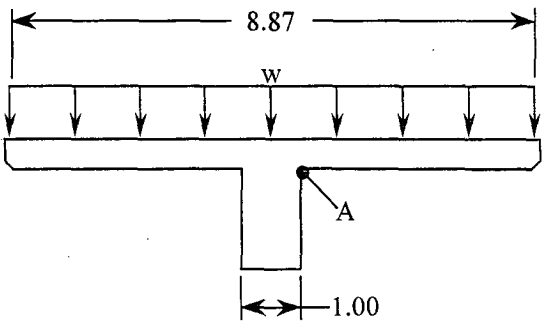
2.6.12.10.1 TPBAR Basket Body

Structural analyses of the TPBAR basket for 1-foot side and end drops are performed using classical hand calculations. The analyzed weight of the loaded TPBAR consolidation canister is 1,000 lbs, which bounds the loaded weight of the TPBAR waste container and extension of 700 lbs. Therefore, the analyses provided for the consolidation canister are bounding.

TPBAR Basket Body 1-Foot Side Drop Analysis

The TPBAR basket body is constructed of four machined segments held together with aluminum bands at five locations along the axial length of the basket; as well as the top and bottom fittings, which are bolted to the aluminum basket. During a side drop, the TPBAR basket is subjected to bending and bearing stresses. The maximum bending stress occurs at Location 'A' as shown in the following sketch and is due to the content weight. The maximum bending stress is calculated using a cantilevered beam. This is conservative, since it neglects any support of the load due to the edges of the basket being supported by the cask inner shell. The maximum bending stress is:

$$S_b = \frac{6M}{t^2} = \frac{6 \times 152}{0.5^2} = 3.6 \text{ ksi}$$



where:

$$w = \frac{W_c \times g}{L \times b} = \frac{1000 \times 25}{144 \times 8.87} = 19.6 \text{ psi}$$

(distributed load of the TPBAR consolidation canister)

W_c = 1,000 lbs, bounding TPBAR canister weight (with TPBARs)

L = 144 inches, length of consolidation canister

b = 8.87 inches, TPBAR basket opening width

g = 25g, bounding side drop acceleration

$$M = w\times\left(\frac{b}{2}-\frac{1}{2}\right)\times\frac{1}{2}\left(\frac{b}{2}-\frac{1}{2}\right)$$

$$= 19.6\times\left(\frac{8.87}{2}-\frac{1}{2}\right)\times\frac{1}{2}\left(\frac{8.87}{2}-\frac{1}{2}\right) = 152 \text{ in-lb/in, the maximum bending moment}$$

t = 0.5 in, thickness of the flange

The margin of safety is:

$$MS = \frac{1.5S_m}{S_b}-1 = \frac{1.5\times 8.4}{3.6}-1 = +2.5$$

where:

S_m = 8.4 ksi, stress intensity of 6061-T651 aluminum @300°F

The bearing stress in the basket is:

$$S_{brg} = \frac{P}{A} = \frac{47{,}500}{1.00\times 161.5} = 294 \text{ psi} \approx 0.3 \text{ ksi}$$

where:

P = $g \times (W_c + W_b)$ = 25 × (1,000 lbs + 900 lbs) = 47,500 lbs, total side drop load

W_b = 900 lbs, the bounding weight of the TPBAR basket

A = is the minimum bearing area of the basket

The margin of safety is:

$$MS = \frac{S_y}{S_{brg}} = \frac{26.9}{0.3}-1 = +\underline{\text{Large}}$$

where:

S_y = 26.9 ksi, yield strength of 6061-T651 aluminum @300°F

TPBAR Basket 1-Foot End-Drop Analysis

During an end drop, the maximum compressive stress on the minimum cross-section of the basket body is:

$$S_{comp} = \frac{g\times W_b}{A} = \frac{20\times 900}{32.26} = 558 \text{ psi} \approx 0.6 \text{ ksi}$$

where:

$A = 9.87^2 - 8.87^2 + 4(1.00 \times (13.25 - 9.87)) = 32.26\,in^2$, the minimum cross-sectional area of the basket (see Figure 2.6.12-7)

g = 20g, bounding end drop acceleration

W_b = 900 lbs, bounding weight of the TPBAR basket

The margin of safety is:

$$MS = \frac{S_y}{S_{comp}} - 1 = \frac{26.9}{0.6} - 1 = +\underline{Large}$$

where:

S_y = 26.9 ksi, yield strength of 6061-T651 aluminum @300°F

2.6.12.10.2 TPBAR Basket Upper Fitting

The upper fitting prevents the basket from loading the consolidation canister and TPBARs during a top-end drop. Four (4) spacer guides of the upper fitting are provided for this purpose. The spacer guides have a length of 7.63 inches, a width of 2.0 inches, and a thickness of 1.00 inch with a 45° × 0.25-inch chamfer. A bounding weight of 900 lbs is used for the TPBAR basket analysis. The temperature of the lid and upper region of the NAC-LWT cask body during TPBAR shipment is conservatively assumed to be 300°F. From Chapter 3, a temperature of 300°F bounds the maximum temperature of the upper LWT region for a maximum heat load of 1.05 kW. Since the maximum heat load for the TPBAR shipment is less than 1.0 kW, using 300°F for the analysis of the TPBAR upper fitting is conservative.

TPBAR Basket Upper Fitting 1-Foot Side Drop

During a side drop, the welds that hold the spacer guides to the top fitting are in shear and bending. The shear load on the welds is:

$$P = (b \times t \times L) \times \rho \times g = (2.0 \times 1.0 \times 7.63) \times 0.288 \times 25 = 110\,lbs$$

where:

b = 2.0 inches, spacer guide width

t = 1.0 in, spacer guide thickness

L = 7.63 inches, spacer guide length

ρ = 0.288 lb/in^3, density of Type 304 stainless steel

g = 25g, side drop acceleration

The welds for the spacer are ⅛-inch fillet welds on three sides. The shear stress in the welds is:

$$\tau = \frac{P}{A} = \frac{110}{0.354} = 311\,\text{psi} = 0.3\,\text{ksi}$$

where:

$A = 0.125 \times 0.707 \times (2.0 + 2 \times 1.0) = 0.354\ \text{in}^2$, weld area

The bending moment is:

$$M = \frac{wL^2}{2} = \frac{(b \times t \times \rho \times g) \times L^2}{2} = \frac{(2 \times 1 \times 0.288 \times 25) \times 7.63^2}{2} = 419\ \text{in-lb}$$

The stress in the weld due to bending is:

$$S = \frac{M}{t \times S_w} = \frac{419}{(0.125 \times 0.707) \times 0.56} = 8.5\,\text{ksi}$$

where:

$$S_w = \frac{d^2(2b + d^2)}{3(b + d)} = \frac{1^2(2 \times 2 + 1^2)}{3(2 + 1)} = 0.56\ \text{in}^2, \text{ section modulus of weld (Blodgett)}$$

The maximum shear stress, τ_{max}, in the weld which, is equivalent to the stress intensity divided by two is:

$$\tau_{max} = \frac{\sqrt{S^2 + 4\tau^2}}{2} = \frac{\sqrt{8.5^2 + 4 \times 0.3^2}}{2} = 4.26\,\text{ksi}$$

The margin of safety is:

$$MS = \frac{0.6S_y}{\tau_{max}} - 1 = \frac{0.6 \times 22.5}{4.26} - 1 = +2.17$$

where:

S_y = 22.5 ksi, yield strength of Type 304 stainless steel @300°F

TPBAR Basket Upper Fitting 1-Foot Top-End Drop

For a top-end drop the weight of the TPBAR basket will load the four spacer guides. The membrane stress in the spacer guide is:

$$S = \frac{W_b \times g}{A} = \frac{900 \times 20}{(2.0 \times 1.0) \times 4} = 2.3\,\text{ksi}$$

where:

W_b = 900 lbs, bounding TPBAR basket weight

$A = (2.0 \times 1.0) \times 4 = 8\ \text{in}^2$, cross sectional area of the spacer guide

g = 20g, bounding end drop acceleration

The margin of safety is:

$$MS = \frac{S_y}{S} - 1 = \frac{22.5}{2.3} - 1 = +8.8$$

where:

S_y = 22.5 ksi, yield strength of Type 304 stainless steel @300°F

The bearing stress is:

$$S = \frac{W_b \times g}{A} = \frac{900 \times 20}{6} = 3.0 \text{ ksi}$$

where:

A = $(2.0 \times 0.75) \times 4 = 6$ in^2, bearing area of the spacer guide

The margin of safety is:

$$MS = \frac{S_y}{S} - 1 = \frac{22.5}{3.0} - 1 = +6.5$$

The critical buckling load for the spacer is determined by using Euler's buckling equation. The critical buckling load is:

$$W_{cr} = K_c \frac{EI}{L^2} = 2.47 \frac{27 \times 10^6 (0.1667)}{7.63^2} \approx 190.9 \text{ kip}$$

where:

E = 27×10^6 psi, modulus of elasticity of Type 304 stainless steel @ 300°F

K_c = 2.47, buckling constant (Blake, Table 10.3)

I = $\frac{bt^3}{12}$ = 0.1667 in^4, minimum moment of inertia for cross section

b = 2.0 inches, spacer guide width

t = 1.0 in, spacer guide thickness

L = 7.63 inches, length of spacer guide

The margin of safety against buckling of the four spacer guides is:

$$MS = \frac{190{,}900}{20 \times 900/4} - 1 = + \underline{\text{Large}}$$

2.6.12.10.3 TPBAR Basket Lower Fitting

The TPBAR basket lower fitting is identical to the lower fitting of the PWR basket. The weight of the loaded TPBAR basket is less than the weight of the loaded PWR basket. Therefore, no further analysis is required.

2.6.12.10.4 TPBAR Spacer

The TPBAR Spacer is designed to limit the movement of the TPBAR contents during transport and to prevent the consolidation canister from loading the TPBARs during a top-end drop. The spacer is constructed of a circular base plate, two triangular spacer bases, two tubes, and two triangular top plates. The circular base plate forms the attachment of the spacer to the lower surface of the NAC-LWT cask closure lid. The circular base plate is attached with Type 304 stainless steel bolts. The two triangular spacer bases are bolted to the circular base plate. The tubes, constructed of 3-inch schedule 80 pipes, are welded to the spacer base and the triangular top plates that provide the interface with the TPBAR contents. The triangular top plates are arranged to form a square with a gap that fits over the consolidation canister or waste container bail and above the consolidation canister contents or the welded top of the waste container. Figure 2.6.12-8 shows the top view of the triangular top plate and tube. The calculated weight of the spacer assembly is 115 lbs. The analyzed loaded weight of the consolidation canister is 1,000 lbs, which bounds the loaded weight of the waste container (700 lbs). During the top-end drop condition, the weight of the consolidation canister is supported by the bail and directly transmitted into the NAC-LWT cask lid. Therefore, only the weight of the TPBARs is supported by the spacer for top-end drop conditions. The temperature of the lid and upper region of the NAC-LWT cask body during TPBAR transport is conservatively assumed to be 300°F. From Chapter 3, a temperature of 300°F bounds the maximum temperature of the upper LWT region for a maximum heat load of 1.05 kW. Since the maximum heat load for the transport of the TPBAR consolidation canister shipment is less than 0.7 kW, using 300°F for the analysis of the TPBAR spacer is conservative. The heat load of the TPBAR waste container is 0.127 kW and, therefore, the evaluated temperatures for the consolidation canister are bounding.

TPBAR Spacer 1-Foot Side Drop

Bolts

During 1-foot side-drop conditions, the weight of the spacer applies a shearing and tensile load to the bolts. The tensile load is due to the moment generated by the cantilever action of the spacer.

The shear stress is:

$$\tau = \frac{P}{A_t} = \frac{719}{0.1419} = 5.1\,\text{ksi}$$

where:

$P = \frac{W \times g}{4} = \frac{115 \times 25}{4} = 719$ lbs

W = 115 lb, spacer assembly weight abbreviations

g = 25g, side-drop acceleration

$A_t = 0.7854\left(D - \frac{0.9743}{n}\right)^2 = 0.7854\left(0.5 - \frac{0.9743}{13}\right)^2 = 0.1419\,in^2$, tensile area of screw thread with ultimate strength up to 100 ksi

For ½-13UNC bolts (Machinery's Handbook)

n = 13, number of threads per inch

D = 0.50 in, bolt diameter

Kn_{max} = 0.434 in, maximum minor diameter of internal thread

Es_{min} = 0.4435 in, minimum major diameter of external thread

En_{max} =0.4565 in, maximum pitch diameter of internal thread

Ds_{min} =0.4876 in, minimum major diameter of external thread

L_e = 1.0 in, Thread engagement

$P = \frac{M}{d} = \frac{16,891}{2 \times 4.95} = 1,706$ lbs, the tensile load

d = 9.9 in, maximum distance between bolts

$M = \frac{wL^2}{2} \times g = \frac{\left(\frac{115}{11.75}\right)(11.75^2)}{2} \times 25 = 16,891\,in\text{-}lb$, the prying moment generated by the cantilever action of the spacer

The bolt tensile stress due to the moment, M, is:

$S = \frac{P}{A_t} = \frac{1706}{0.1419} = 12.0$ ksi

The membrane stress intensity on the fastener is:

$SI = \sqrt{S^2 + 4\tau^2} = \sqrt{12.0^2 + 4 \times 5.1^2} = 15.7$ ksi

The margin of safety is:

$MS = \frac{S_y}{SI} - 1 = \frac{22.5}{15.7} - 1 = +0.43$

where:

S_y = 22.5 ksi, yield strength of Type 304 stainless steel @300°F

The shear stress on the external threads is:

$$\tau = \frac{P}{A_S} = \frac{1706}{0.7789} = 2.2 \text{ ksi}$$

where:

$$A_s = 3.1416 n L_e Kn_{max}\left[\frac{1}{2n} + 0.57735(Es_{min} - Kn_{max})\right]$$

$$= 3.1416(13)(1.00)(0.434)\left[\frac{1}{2(13)} + 0.57735(0.4435 - 0.434)\right]$$

= 0.7789 in^2, shear area of the bolt threads

The margin of safety is:

$$MS = \frac{0.6S_y}{\tau} - 1 = \frac{0.6 \times 22.5}{2.2} - 1 = +6.14$$

Spacer Welds

Using a bounding weight (W) of 25 pounds for the tube and triangular plates, the shear load on the welds is:

$$P = W \times g = 25 \times 25 = 625 \text{ lbs}$$

where:

g = 25 g, side-drop acceleration

The welds for the spacer are ¼-inch fillet weld. The shear stress in the weld is:

$$\tau = \frac{P}{t_w 0.707 \pi d} = \frac{625}{0.25 \times 0.707 \times (\pi \times 3.5)} = 322 \text{ psi}$$

where:

t_w = 0.25 in, weld size

d = 3.5 inches, outside diameter of 3-inch schedule-80 pipe

The stress in the weld due to bending is:

$$S = \frac{M}{t \times S_w} = \frac{5{,}263}{(0.25 \times 0.707)9.62} = 3.1 \text{ ksi}$$

where:

$M = wL = 25 \times 25 \times 8.42 = 5{,}263 \text{ in - lb}$, the bending moment

$S_w = \frac{\pi d^2}{4} = \frac{\pi \times 3.5^2}{4} = 9.62 \text{ in}^2$, section modulus of the weld (Blodgett)

The maximum shear stress (τ_{max}) in the weld, which is equivalent to the stress intensity divided by two, is:

$$\tau_{max} = \frac{\sqrt{S^2 + 4\tau^2}}{2} = \frac{\sqrt{3.1^2 + 4 \times 0.3^2}}{2} = 1.6 \text{ ksi}$$

The margin of safety is:

$$MS = \frac{0.6S_y}{\tau_{max}} - 1 = \frac{0.6 \times 22.5}{1.6} - 1 = +7.4$$

where:

S_y = 22.5 ksi, yield strength of Type 304 stainless steel @300°F

TPBAR Spacer 1-Foot Top-End Drop

When loaded in the consolidation canister, the TPBARs (held in the shape of a square) load the spacer tubes via the triangular top plates during top-end drop conditions. The compressive load applied to the tubes during the top-end drop is the weight of the TPBARs, 795 lbs (300 TPBARs at a bounding weight of 2.65 lbs per TPBAR), times the bounding acceleration of 20g (actual 15.8 g). For this analysis, W=1,000 lbs, is conservatively used.

Tube

The compressive stress in the tubes is:

$$S = \frac{W \times g}{A} = \frac{1000 \times 20}{2 \times \left(\frac{\pi}{4} \left(3.5^2 - 2.9^2 \right) \right)} = 3.3 \text{ ksi}$$

where:

A = the cross sectional area of a 3-inch schedule-80 pipe with an outer diameter of 3.5 inches and a thickness of 0.3 inch

The margin of safety is:

$$MS = \frac{S_y}{S} - 1 = \frac{22.5}{3.3} - 1 = +5.8$$

where:

S_y = 22.5 ksi, yield strength of Type 304 stainless steel @300°F

Triangular Top Plate

Referring to the dimensions provided in Figure 2.6.12-8, the pressure applied to a triangular plate is

$$P_{TP} = \frac{1}{2} \times \frac{1000}{0.5 \times 7.43 \times 7.43} \times 20 = 362 \text{ psi}$$

The bending moment in the top plate is (see Line A in Figure 2.6.12-6)

$$M = 362 \times \left(0.5 \times 4.18^2\right) \times \left(\frac{1}{3} \times 4.18\right) = 4406 \text{ in-lb}$$

The bending stress in the plate is:

$$S = \frac{6M}{bt^2} = \frac{6 \times 4{,}406}{4.18 \times 0.75^2} = 11.2 \text{ ksi}$$

The margin of safety is:

$$MS = \frac{1.5S_m}{S} - 1 = \frac{1.5 \times 20.0}{11.2} - 1 = +1.68$$

where:

S_m = 20.0 ksi, stress intensity of Type 304 stainless steel @300°F

TPBAR Spacer 1-Foot Bottom-End Drop

During the one-foot bottom-end drop, the inertial load of the spacer is applied to the bolts that affix the spacer to the NAC-LWT cask lid and the welds used to fabricate the spacer assembly. The maximum bottom-end drop acceleration is 20g.

Bolts

Four bolts (½-13UNC, Type 304 stainless steel) hold the spacer assembly to the bottom of the NAC-LWT cask lid and six bolts hold the spacer base to the circular base plate. For this evaluation, only the four spacer assembly bolts are considered since the individual bolt load is higher and the thread engagement length is shorter. The Internal lid thread evaluation is not required since high strength Helicoil inserts are utilized. Using the spacer assembly weight of 115 lbs and an acceleration of 20g, the critical bolt load is:

$$P = \frac{115 \times 20}{4} = 575 \text{ lbs}$$

The tensile stress is:

$$S = \frac{P}{A_t} = \frac{575}{0.1419} = 4.1\,\text{ksi}$$

The margin of safety is:

$$MS = \frac{S_y}{S} - 1 = \frac{22.5}{4.1} - 1 = +4.49$$

where:

S_y = 22.5 ksi, yield strength of Type 304 stainless steel @300°F

The shear stress in the bolt thread is:

$$\tau = \frac{P}{A_S} = \frac{575}{0.7789} = 0.74\,\text{ksi}$$

The margin of safety is:

$$MS = \frac{0.6S_y}{\tau} - 1 = \frac{0.6(22.5)}{0.74} - 1 = +\underline{\text{Large}}$$

Spacer Welds

During a 1-foot bottom-end drop (20g), the spacer weld is loaded by the inertial load of the spacer tube and the triangular top plate (25 lbs bounding). The weld is a ¼-inch fillet weld. The weld stress is:

$$S_w = \frac{W \times g}{t(0.707)(\pi d)} = \frac{25 \times 20}{0.25 \times 0.707 \times (\pi \times 3.5)} = 257\ \text{psi} = 0.3\ \text{ksi}$$

where:

d = 3.5 in, outside diameter of 3-inch schedule 80 pipe
t = 0.25 in, weld size

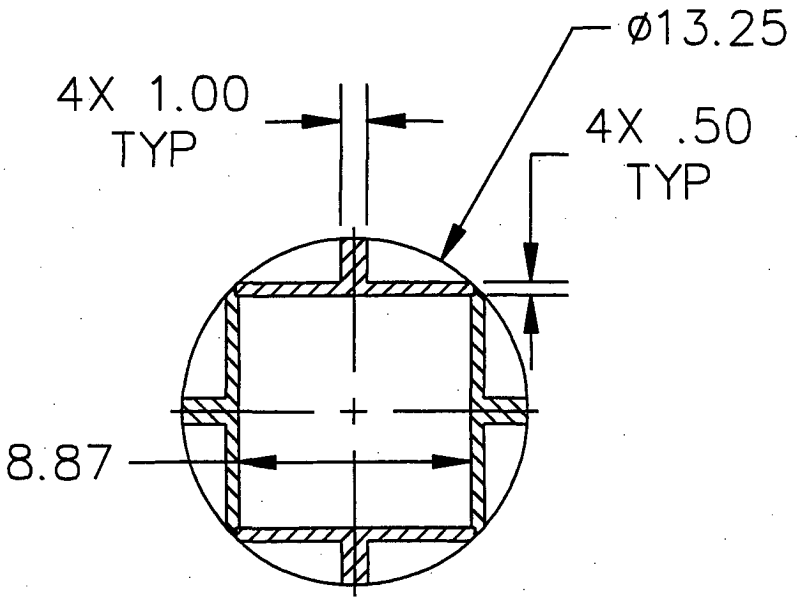
The margin of safety is:

$$MS = \frac{0.6S_y}{S_w} - 1 = \frac{0.6(22.5)}{0.3} - 1 = +\underline{\text{Large}}$$

where:

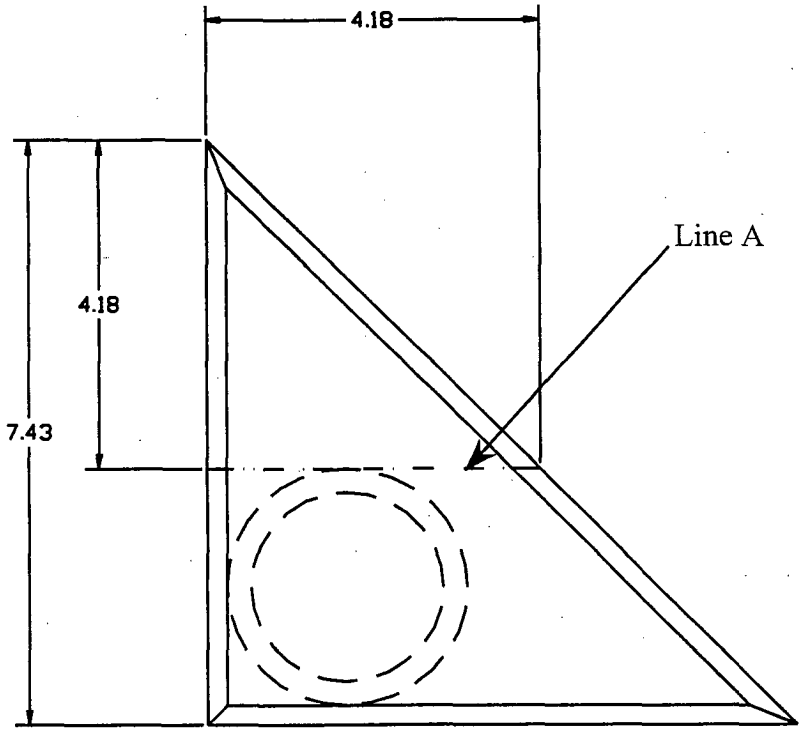
S_y = 22.5 ksi, yield strength of Type 304 stainless steel @300°F

Figure 2.6.12-7 Cross-Section of TPBAR Basket



(Unit = inches)

Figure 2.6.12-8 TPBAR Spacer Schematic Triangular Top Plate and Tube



(Unit = inches)

2.6.12.11 ANSTO Basket Analysis

The ANSTO modular basket assembly consists of a top module, four intermediate modules, and a base module. The top and base modules are each 29.8 inches long; each of the four intermediate modules is 29.3 inches long (not including guide pins); and all six modules have an outer diameter of 13.27 inches. Each module is capable of holding up to seven spiral fuel assemblies or MOATA plate bundles. Each module is a weldment made up of a 13.27-inch-diameter, 1/2-inch-thick base plate and six 13.27-inch-diameter, 1/2-inch-thick support plates scalloped on the inner diameter to fit around six peripheral fuel tubes. The weldment structure, fuel tubes, and base and support plates are fabricated from Type 304 stainless steel. Each of the seven fuel tubes in each module has an outer diameter of 4.375 inches and a wall thickness of 0.125 inch. The bottom of each fuel tube is welded to the 1/2-inch-thick base plate. At the bottom of each fuel tube, where it is welded to the base plate, there is a 0.3-inch slot to permit water to drain from the tube. The base plate supports the fuel assembly/bundle in the end drop orientation. The base module sits on a 0.5-inch-high, 10-inch-diameter ring that is welded in segments to the base plate. The total weight of the ANSTO basket assembly bears directly on the bottom forging of the cask through the ring. The six scalloped 1/2-inch-thick support plates and the base plate of each basket module provide lateral support and maintain the fuel configuration in the side drop orientation.

2.6.12.11.1 ANSTO Basket Body 1-Foot Side Drop Analysis

Structural analyses of the ANSTO basket for 1-foot side and end drops are performed using classical hand calculations.

The inertia load of the LWT cask for a 1-foot side drop is 25g. A conservative loading condition of a diametrically loaded ring (Table 17, Case 1, Roark) is considered, which neglects any load distribution. Also, it is conservative to assume that there are three loaded fuel tubes acting on the top of a fuel tube since, in reality, there are only two of them. The stresses in the circumferential direction and in the longitudinal direction are added without regard to their signs. Since the circumferential direction and the longitudinal direction also correspond to the direction of the principal stresses, the addition of the two magnitudes reflects the possibility of the principal stresses being of opposite signs.

The maximum applied load to a fuel tube for the circumferential bending stress is:

$$P_s = (3W_{FT} + 3W) \times 25 = 2{,}415 \text{ lbs}$$

where:

W_{FT} = 14.2 lbs, maximum fuel tube weight

W = 18.0 lbs, maximum average fuel assembly weight

The bending moment in the fuel tube is:

$$M = \frac{wRk_2}{\pi} = \frac{84 \times 2.13 \times 1.00}{\pi} = 57 \text{ in-lb/in}$$ (Table 17, Case 1, Roark)

where:

$$w = \frac{P_s}{L_t} = 84 \text{ lb/in}$$

L_t = 28.81 inches, shortest fuel tube length

R = 2.13 inches, mean radius of fuel tube

$k_2 = 1-\alpha = 1.00$

$$\alpha = \frac{I}{A \times R^2} = \frac{bt^3/12}{b \times t \times R^2} = 2.87 \times 10^{-4}$$

b = 1.0 in, unit length

t= 0.125 in, tube wall thickness

The circumferential bending stress in the fuel tube is:

$$\sigma c = \frac{6M}{bt^2} = \frac{6 \times 57}{1 \times 0.125^2} = 21.9 \text{ ksi}$$

The stress in the fuel tube in the longitudinal direction is calculated assuming the fuel tube acts like a beam. The maximum bending moment occurs at the top of the basket where the fuel tube acts like a cantilever beam. (The maximum moment for a cantilevered beam with a uniform loading of w (lb/in) and length (l) is $wl^2/2$, as compared to the maximum moment $wl^2/8$ for a simply supported beam.) The bending moment in the tube is:

$$M = \frac{wl^2}{2} = \frac{84 \times 4.0^2}{2} = 672 \text{ in-lb}$$

where:

l = 4.0 inches, the length of the tube extending beyond the support plates

The bending stress is:

$$\sigma_l = F\frac{Mc}{I} = \frac{672 \times 2.19}{3.77} \approx 1.1 \text{ ksi}$$

where:

c = 2.19 inches, distance to extreme outer fiber of tube from centroid of tube

I = 3.77 in^4, tube moment of inertia

F = 2.725, factor to account for the effect of the small diameter-to-length ratio on bending for a cantilevered tube. This is obtained for a uniformly loaded beam in Article 7.10 in Roark.

The maximum stress in the tube is:

$$\sigma_b = 21.9 + 1.1 = 23.0 \text{ ksi}$$

The margin of safety is:

$$MS = \frac{1.5S_m}{\sigma_b} - 1 = +0.26$$

where:

S_m = 19.4 ksi, design stress intensity, Type 304 stainless steel, 350°F

The bearing stress on the support plate is calculated using Table 33, Case 2c from Roark.

The maximum weight of a loaded module is the weight of the base module, W_{BM} = 280 lbs. The weight of the loaded basket is supported by the six support plates and the base plate (i.e., total of seven). The bearing stress on a support plate is:

$$\sigma_{brg} = 0.591\sqrt{\frac{pE}{K_D}} = 3.6 \text{ ksi}$$

where:

$$p = \frac{W}{7t_d}g = \frac{280}{7 \times 0.5} \times 25 = 2{,}000 \text{ lb/in, bearing load for 25g side drop}$$

t_d = 0.5 in, support disk thickness

g = 25g, side drop inertia load

$$K_D = \frac{D_1 D_2}{D_1 - D_2} = 1{,}366.81$$

D_1 = 13.395 inches, LWT cask inner diameter

D_2 = 13.265 inches, support disk diameter

E = 25.7×10^6 psi, modulus of elasticity, Type 304 stainless steel, 350°F

The margin of safety is:

$$MS = \frac{S_y}{\sigma_{brg}} - 1 = +5.06$$

where:

S_y = 21.8 ksi, yield strength, Type 304 stainless steel, 350°F

2.6.12.11.2 ANSTO 1-Foot End Drop Evaluation

The inertia load for the LWT for a 1-foot end drop is 20g. The applied load to the ANSTO basket is:

$$P = W_{total} \times 20 = 35{,}400 \text{ lbs}$$

where:

W_{total} = 1,770 lbs, total weight of loaded basket, which bounds the calculated weight of 1,667 lbs

The minimum cross-sectional area is at the base of the fuel tubes where the cutouts for water drainage are located. The cross-sectional area is:

$$A = \frac{\left[\frac{\pi}{4}\left(D_o^2 - D_i^2\right) \times 6\right]}{2} + \left[\frac{\pi}{4}\left(D_o^2 - D_i^2\right) - 6 \times l_c \times t_t\right] = 5.93 \text{ in}^2$$

where:

D_o = 4.375 inches, tube outer diameter

D_i = 4.125 inches, tube inner diameter

l_c = 1.00 in, cutout length in center tube

t_t = 0.125 in, tube wall thickness

The membrane stress in the basket is:

$$\sigma = \frac{P}{A} = \frac{35{,}400}{5.93} = 5.97 \text{ ksi}$$

The margin of safety is:

$$MS = \frac{S_m}{\sigma} - 1 = +2.2$$

where:

S_m = 19.4 ksi, design stress intensity, Type 304 stainless steel, 350°F

The support plates are welded to the fuel tube with 1/16-inch bevel welds on both sides of the plate. The area of the weld is:

$$A_W = \frac{6(\pi D_o)}{2} \times 2t_w = 5.15 \text{ in}^2$$

where:

D_o = 4.375 inches, outer diameter of tube

t_w = 1/16 in, weld thickness

The bounding weight of the support plates is 20.1 lbs; and the bounding g-load factor is 60. A weld quality factor of 0.25 for a surface visual examination is divided into the calculated stress. This factor corresponds to the largest stress reduction factor in Table NG-3352-1 of the ASME Code. Therefore, the stress in the weld is:

$$\sigma_w = \frac{20.1 \times 60}{A_w (0.25)} = 936 \text{ psi}$$

The margin of safety using normal conditions allowable is:

$$MS = \frac{0.6S_m}{\sigma_w} - 1 = +\underline{\text{Large}}$$

where:

S_m = 19.4 ksi, design stress intensity, Type 304 stainless steel, 350°F

2.6.12.11.3 ANSTO Thermal Stress Evaluation

Thermal stress caused by a temperature gradient in the basket is calculated in this section. The thermal stress is minimal since the basket is free to expand. The thermal stress occurs as the hotter tubes expand radially against the basket support plates, which are at a lower temperature.

The maximum thermal stress of the fuel tube is back-calculated from the displacement computed using equations for circular rings from Table 17, Case 1, Roark.

The diametrical displacements caused by the thermal expansions for the center tube (Δ_1) and the tube adjacent to it (Δ_2) are calculated as:

$$\Delta_1 = \alpha \times \Delta T \times R_t = 4.58 \times 10^{-3} \text{ in}$$

where:

$\alpha = 9.1 \times 10^{-6}$ /°F, coefficient of thermal expansion, Type 304 stainless steel, 350°F

ΔT= 230°F (300-70), T_{max} of the basket is conservatively considered to be 300°F

70°F is room temperature

R_t = 2.19 inches (4.375/2), radius of the fuel tube outer surface

$$\Delta_2 = \alpha \times \Delta T \times D_t = 9.17 \times 10^{-3} \text{ in}$$

where,

$\alpha = 9.1 \times 10^{-6}$ /°F, coefficient of thermal expansion, Type 304 stainless steel, 350°F

ΔT= 230°F (300-70), T_{max} of the basket is conservatively considered to be 300°F

70°F is room temperature

D_t = 4.375, diameter of the fuel tube

The displacement caused by the thermal expansions for the outer surface of the support plate (Δ_S) is calculated as:

$$\Delta_S = \alpha \times \Delta T \times R_S = 8.58 \times 10^{-3} \text{ in}$$

where,

$\alpha = 9.1 \times 10^{-6}$ /°F, coefficient of thermal expansion, Type 304 stainless steel, 350°F

ΔT= 144°F (214-70), T_{max} of the inner shell

70°F is room temperature

R_S = 6.55 inches (13.1/2), radius of the support plate

Note: 214°F is conservatively used to result in a minimum Δ_S in order to maximize the thermal stress.

The deformation that results in thermal stress is -5.17×10^{-3} inch ($\Delta_S - \Delta_1 - \Delta_2$). Therefore, the fuel tube will experience a reduction in diameter due to the differential thermal expansion of the fuel tubes and support plates. It is conservative to assume that all deformation occurs at the center tube. Using Case 1 in Table 17 of Roark, the change in the diameter of the circular ring, D_V, and the moment, M_A, are given by:

$$D_V = 0.1488\times\frac{WR^3}{EI} \quad \text{and} \quad M_A = \frac{WR\times k_2}{\pi}$$

therefore:

$$M_A = \frac{D_V\times EI}{0.1488\times R^2}\times\frac{k_2}{\pi}$$

where:

W is the load due to differential thermal expansion

$D_V = 5.17\times10^{-3}$ inch, change in the diameter due to thermal stress

R = 2.13 inches, mean radius of fuel tube

$E = 25.7 \times 10^6$ psi, modulus of elasticity, Type 304 stainless steel, 350°F

$I = bt^3/12$, inertial of the cross-section

b = 1.0 in, unit length

t = 0.125 in, tube wall thickness

$k_2 = 1-\alpha = 1.00$

$$\alpha = \frac{I}{A\times R^2} = \frac{bt^3/12}{b\times t\times R^2} = 2.87\times10^{-4}$$

The thermal stress is:

$$\sigma = \frac{6M_A}{bt^2} = \frac{D_V E t k_2}{0.2976\pi R^2} = \frac{5.17\times10^{-3}\times25.7\times10^6\times0.125\times1.0}{0.2976\times\pi\times2.13^2} = 3{,}916 \text{ psi}$$

The maximum P+Q stress in the basket is conservatively calculated by combining the bending stress and thermal stress in the basket. The P+Q stress is:

$$\sigma_{pq} = \sigma_b + \sigma_{th} = 23.0 + 3.9 = 26.9 \text{ ksi}$$

The margin of safety is:

$$MS = \frac{3S_m}{\sigma_{pq}} - 1 = +1.16$$

where:

S_m = 19.4 ksi, design stress intensity, Type 304 stainless steel, 350°F

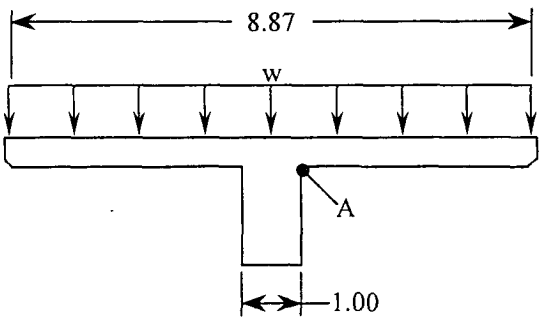
2.6.12.12 TPBAR Basket with the PWR/BWR Rod Transport Canister

This section provides the structural analysis for the shipment of up to 25 individual TPBARs in the PWR/BWR Rod Transport Canister, the PWR insert and the TPBAR basket. Section 2.6.12.10 provides the structural evaluation of the TPBAR basket, with 300 TPBARs, considering a slightly lower contents weight (1800 lbs) than the TPBARs in the PWR/BWR Rod Transport Canister configuration (1901 lbs). The effects of the increased weight loading for the TPBAR basket are addressed in this section. The structural evaluation of the PWR/BWR Rod Transport Canister and the PWR insert is performed in Section 2.6.7.10.

TPBAR Basket Body 1-Foot Side Drop Analysis – Normal Condition

The TPBAR basket body is constructed of four machined segments that are held together with aluminum bands at five locations along the axial length of the basket, as well as the top and bottom fittings, which are bolted to the aluminum basket. During a side drop, the TPBAR basket is subjected to bending and bearing stresses. The maximum bending stress occurs at Location 'A' in the following figure and is due to the content weight. The maximum bending stress is calculated using a cantilevered beam. This is conservative since it neglects any support of the load due to the edges of the basket being supported by the cask inner shell. The maximum bending stress is:

$$S_b = \frac{6M}{t^2} = \frac{6 \times 226}{0.5^2} = 5.42 \text{ ksi}$$



where:

$w = \frac{W_c \times g}{L \times b} = \frac{1{,}650 \times 25}{159.5 \times 8.87} = 29.2 \text{ psi}$, the distributed load transfer by the PWR insert on the TPBAR basket

W_c = 1,650 lb, bounding TPBAR contents weight (with TPBARs, PWR/BWR Rod Transport Canister and the PWR insert)

L = 159.5 in, loadable length of the TPBAR basket
b = 8.87 in, TPBAR basket opening width
g = 25g, bounding side drop acceleration

$$M = w\times\left(\frac{b}{2}-\frac{1}{2}\right)\times\frac{1}{2}\left(\frac{b}{2}-\frac{1}{2}\right)$$

$$= 29.2\times\left(\frac{8.87}{2}-\frac{1}{2}\right)\times\frac{1}{2}\left(\frac{8.87}{2}-\frac{1}{2}\right)=226 \text{ in-lb/in, the maximum bending moment}$$

t = 0.5 in, thickness of the flange

The margin of safety is

$$MS = \frac{1.5S_m}{S_b}-1=\frac{1.5\times8.4}{5.42}-1=+1.32$$

where:

S_m = 8.4 ksi, stress intensity of 6061-T6 aluminum @ 300°F

The bearing stress in the basket is

$$S_{brg} = \frac{P}{A}=\frac{63{,}750}{1.00\times161.5}=395 \text{ psi}=0.4 \text{ ksi}$$

where:

P = $g \times (W_c + W_b) = 25 \times (1{,}650 \text{ lb} + 900 \text{ lb}) = 63{,}750$ lb, total side drop load
W_b = 900 lb, the bounding weight of the TPBAR basket
A = is the minimum bearing area of the basket

The margin of safety is

$$MS = \frac{S_y}{S_{brg}}=\frac{26.9}{0.4}-1=+\text{large}$$

where:

S_y = 26.6 ksi, yield strength of 6061-T6 aluminum @ 300°F

TPBAR Basket – End Drop

In an end drop scenario, the basket is only loaded by its own weight. The TPBAR basket weight is bounded by what was considered for the end drop analysis of the TPBAR basket in Section 2.6.12.10. Additionally, the assumed component temperatures remain conservative. Therefore, the results of section 2.6.12.10 are bounding and no further analysis is required.

TPBAR Basket Upper Fitting

The TPBAR basket upper fitting is identical to what was analyzed for the TPBAR basket in Section 2.6.12.10. The TPBAR basket weight and component temperatures considered in Section 2.6.12.10 are conservative. Therefore, the results of the Section 2.6.12.10 are bounding and no further analysis is required.

TPBAR Basket Lower Fitting

The TPBAR basket lower fitting is identical to the lower fitting of the PWR basket. The weight of the loaded TPBAR basket is less than the weight of the loaded PWR basket. Therefore, no further analysis is required.

PWR Insert

The PWR insert contains the PWR/BWR Rod Transport Canister assembly for insertion into the TPBAR basket. The PWR insert is not a structural component and, therefore, an analysis of its performance under normal conditions is not required.

PWR/BWR Rod Transport Canister Assembly Analysis

The PWR/BWR Rod Transport Canister is identical to the configuration analyzed in Section 2.6.7.10. The fuel weight considered in the Section 2.6.7.10 analysis for the PWR/BWR fuel (350 lbs) bounds the fuel weight of 25 TPBARs in the PWR/BWR Rod Transport Canister (66 lbs). Therefore, no further analysis is required for the canister.

Internal Spacer

The internal spacer for the PWR/BWR Rod Transport Canister is identical to what was analyzed in Section 2.6.7.10. The fuel weight considered in the Section 2.7.1.7 analysis for the PWR/BWR fuel (350 lbs) bounds the fuel weight of 25 TPBARs in the PWR/BWR Rod Transport Canister (66 lbs). Therefore, no further analysis is required for the internal spacer.

4×4 and 5×5 Inserts

The 4×4 and 5×5 inserts for the PWR/BWR Rod Transport Canister are identical to what was analyzed in Section 2.6.7.10. The fuel weight considered in the Section 2.7.1.7 analysis for the PWR/BWR fuel (350 lbs) bounds the fuel weight of 25 TPBARs in the PWR/BWR Rod Transport Canister (66 lbs). Therefore, no further analysis is required for the 4×4 and 5×5 inserts.

2.6.12.13 Conclusion

Loads generated during normal operations conditions for each basket assembly design result in total equivalent stresses, which each basket body can adequately sustain. Analyses show that all

basket-bearing stresses during a side drop are much less than the material yield strength. Column analyses demonstrate that each basket assembly is self-supporting during an end drop. The minimum Margin of Safety, for all basket designs, is +0.10 as reported in Section 2.6.12.7.4 for the TRIGA basket; +0.003 as shown in Table 2.6.12-2 for the DIDO basket; +0.10 as reported in Section 2.6.12.9.2 for the GA fuel basket; and +0.26 as reported in Section 2.6.12.11.1 for the ANSTO basket. Therefore, it can be concluded that all basket designs have sufficient structural integrity for adequate service during normal conditions of transport.

2.7.7.11 General Atomics IFM Basket Construction

The General Atomics IFM basket consists of a top module assembly designed to carry two IFM FHU. Each fuel container is associated with a RERTR fuel element or HTGR fuel materials. A spacer assembly is used to permit the top module assembly to be positioned next to the transport cask lid.

The top module is 43.7 inches long and is made up of two fuel tubes and three support plates. All components are made from ASME SA240 Type 304 stainless steel. The fuel tubes have a 6.0-inch outer diameter and a 0.25-inch wall thickness. Two of the support plates are 0.50-inch thick and the third, center plate, is 1.0-inch thick. The support plates are welded to the fuel tubes with 1/8-inch bevel welds.

Two types of IFM FHU are carried by the basket. One FHU carries irradiated HTGR fuel material and is 5.25 inches in diameter (0.12-inch thick wall) and is 39.0 inches long. The other FHU contains irradiated RERTR fuel material and is 4.75 inches in diameter (0.12-inch thick wall) and is 37.25 inches long.

Each end of the FHU is comprised of a 0.25-inch thick plate welded to the container shell. The weld connecting the end plate to the container shell is labeled as a full penetration butt weld. The dimensions of the end plate and the container shell provide a minimal gap (2 mils when considering maximum tolerances) to permit the end plate to be inserted into the container end. The close tolerances ensure that the two components are effectively in contact along the 0.5-inch common interface length of the end plate and the container. Once the end plate is inserted, a fusion weld procedure is employed to weld the lip of the end plate to the wall of the container. The depth of the weld along the interface between the end plate and the container is equal to approximately 70% of the thickness of the end plate lip or the container lip.

Due to the location of the weld for the end plate, the weld does not transfer any load for the drop conditions. Additionally, since the heat loads are insignificant (13w) and the backfill for the FHU and the cask cavity is limited to atmospheric pressure, the pressure differential across the welded plates is insignificant. Each of these FHUs also has an additional smaller container, which holds the fuel. In these evaluations, the inner container is neglected.

The spacer assembly is 133.0 inches in length, excluding guide pins. The assembly is made up of one spacer tube and five support plates. The spacer tube consists of a Type 304 stainless steel 8-inch Schedule 80S pipe. The tube has an outside diameter of 8.63 inches and a wall thickness of 0.50 inch. The spacer plates are 1.0-inch thick and are welded to the tube with 1/8-inch bevel welds. Two guide pins are located at the top of the spacer assembly to facilitate alignment with the top module.

2.7.7.11.1 General Atomics IFM Basket Interface Analysis

The structural evaluation of the fuel basket assembly is performed using classical hand calculations. The weight of the top module is bounded by 200 lbs, and the maximum weight of one FHU is 76 lbs (General Atomics, April 2002). Therefore, the total weight of a loaded top module system is 200 + 2(76) or 352 lbs. The weight of the spacer assembly is 760 lbs. The total loaded system weight is 1,112 lbs, and this weight is bounded by the design basis contents weight for the LWT system. Therefore, no analysis of the LWT cask is required.

2.7.7.11.2 General Atomics IFM Basket Structural Analysis

Structural analyses for the General Atomics basket for the 30-foot end drop and 30-foot side drop are performed using classical hand calculations.

General Atomics 30-Foot Side Drop Analysis

Top Module:

Using the 1 g bending stress, 26 psi, calculated in the subsection titled "General Atomics Top Module Structural Analysis," the margin of safety for a 30-foot side drop is:

$$MS = \frac{S_u}{S_b} - 1 = \frac{65200}{55 \times 26} - 1 = +\underline{\text{Large}}$$

During a side drop, the top and bottom support plate welds are in shear. Using the stress in the weld for 1g, 26.4 psi, calculated in the subsection titled "General Atomics Top Module Structural Analysis," and the visual inspection weld factor, the margin of safety for shear, 30-foot side drop (55 g), is:

$$MS = \frac{0.25 \times 0.42 S_u}{55S} - 1 = \frac{0.25 \times 0.42 \times 65{,}200}{55 \times 26.4} - 1 = +3.71$$

Spacer Assembly:

Using the 1g bending stress, 31 psi, calculated in the subsection titled "General Atomics Top Module Structural Analysis," the margin of safety for bending during a 30-foot side drop is:

$$MS = \frac{S_u}{S_b} - 1 = \frac{65{,}200}{55 \times 31} - 1 = +\underline{\text{Large}}$$

During a side drop, the top support plate weld is in shear. From the subsection titled "General Atomics Top Module Structural Analysis," the weld shear stress for a 1 g loading is 31 psi. Using a 0.25-inch weld quality factor, the margin of safety for a 30-foot side drop is:

$$MS = \frac{0.25 \times 0.42 S_u}{55S} - 1 = \frac{0.25 \times 0.42 \times 65{,}200}{55 \times 31} - 1 = +3.0$$

Fuel Handling Unit (FHU):

The FHUs are analyzed in accordance with ASME Section III, Subsection NG. From the subsection titled General Atomics Top Module Structural Analysis, the stress in the FHU for a 1g side drop is 0.63 ksi. For a 30-foot side drop, the margin of safety is

$$MS = \frac{S_u}{55S} - 1 = \frac{65.2}{55 \times 0.63} - 1 = +0.88$$

Because the internal and external pressures on the container are essentially identical, no additional ASME Section III, Subsection NG analysis is required.

General Atomics 30-Foot End Drop Analysis

Top Module:

During an end drop, the stress in the fuel tubes is 22 psi for a 1 g end drop (see subsection titled General Atomics 1-Foot End Drop Analysis). The margin of safety for a 30-foot end drop is:

$$MS = \frac{0.7 S_u}{60S} - 1 = \frac{0.7 \times 65{,}200}{60 \times 22} - 1 = +\underline{\text{Large}}$$

Since the stress in the tubes is significantly below yield, no buckling evaluation is required.

During an end drop, the stress in the support plate weld for a 1g end drop is 6.0 psi (see subsection titled "General Atomics 1-Foot End Drop Analysis"). For a 30-foot end drop, the margin of safety in the weld is:

$$MS = \frac{0.25 \times 0.6 S_m}{20S} - 1 = \frac{0.25 \times 0.6 \times 19{,}350}{20 \times 6} - 1 = +\underline{\text{Large}}$$

Spacer Assembly:

During an end drop, the stress in the tube for a 1 g end drop is 87 psi. For a 30-foot end drop, the margin of safety is:

$$MS = \frac{0.7 S_u}{60S} - 1 = \frac{0.7 \times 65{,}200}{60 \times 87} - 1 = +\underline{\text{Large}}$$

Since the stress in the tube is significantly below yield, no buckling evaluation is required.

During a 1 g end drop, the stress in the support disk weld is 5.2 psi. Since the weld stress is less than the weld stress in the top module support disk, no additional analysis is required.

Fuel Handling Unit:

During a 30-foot end drop, the stress in the tube is:

$$S = \frac{60 \times 76}{1.62} = 2.8 \text{ ksi}$$

$$MS = \frac{0.7S_u}{S} - 1 = \frac{0.7 \times 65.2}{2.8} - 1 = +\underline{\text{Large}}$$

Since the stresses in the tube are significantly below the yield stress allowable, no buckling evaluation is required.

2.7.7.12 TPBAR Basket Analysis

The TPBAR basket is a modified NAC-LWT PWR basket that has had material removed to increase free volume in the cask cavity. The cylindrical basket is fabricated from 6061-T651 aluminum alloy. A central opening, 8.82 inches square, extends the length of the basket and provides lateral support for the two TPBAR content conditions: the TPBAR consolidation canister; and the TPBAR waste canister. A 13.25-inch outside diameter, 8.25-inch long stainless steel upper fitting is bolted to the top of the basket body. This fitting provides lifting points for installation and removal of the basket from the cask. Additionally, this fitting prevents the basket from applying load to the TPBAR consolidation canister or waste container during the top-end drop. The lifting bail for both the consolidation canister and the waste container are fabricated from Type 17-4 precipitation hardened stainless steel. A second stainless steel fitting is bolted to the bottom of the basket body. The lower fitting assembly supports the fuel basket and contents longitudinally and limits movement within the cask. A TPBAR spacer assembly is bolted to the underside of the cask lid to prevent the TPBAR contents from shifting axially within the basket, and maintains the waste container rotational orientation. A groove on the periphery of the basket body provides for the cask drain tube. The drain tube is connected to a fitting on the cask body and is used to drain or fill the cask during cask loading or unloading operations.

The first TPBAR content condition is for the transport of up to 300 production TPBARs in an open (unsealed), Type 304 stainless steel consolidation canister with optional top insert. The canister is considered a nonstructural component and is only used to position the TPBARs within the basket and to handle the TPBARs during loading and unloading operations. The second content condition is for the transport of up to 55 TPBARs, which have been segmented from PIE, in a welded, Type 316L stainless steel waste container. The container is also considered a nonstructural component only used for handling the TPBAR segments and debris during cask

loading and unloading operations. Therefore, for purposes of the basket structural analyses, the canister and container are both considered to fail and to not protect the contents from damage. The effects of damage to the TPBARs are evaluated in other sections of the SAR.

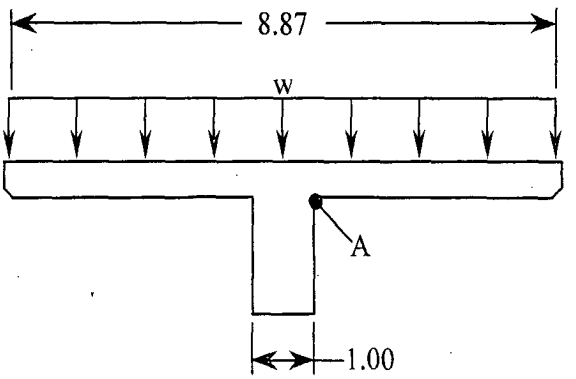
Once the cask lid is bolted to the cask body, the configuration of the TPBAR contents (i.e., consolidation canister or waste container) are maintained by the TPBAR basket without consideration of the strength of the canister or container. The TPBAR basket provides a boundary for support on all sides and for the full length of the contents. The TPBAR basket upper end-fitting spacer guides carry the weight of the basket and prevent the contents from being loaded by the TPBAR basket in any drop orientation. The TPBAR spacer assembly attached to the bottom of the cask lid restricts the axial movement of the contents. Therefore, no additional evaluation is required for either the TPBAR consolidation canister or the TPBAR waste container and extension. The analyses for the loaded consolidation canister weight of 1,000 lbs bounds the loaded weight of the TPBAR waste container (700 lbs).

2.7.7.12.1 TPBAR Basket Body

Structural analyses of the TPBAR basket for 30-foot end and side drops are performed using classical hand calculations.

TPBAR Basket Body 30-Foot Side-drop Analysis

The TPBAR basket body is constructed of four machined segments held together with aluminum bands at five locations along the axial length of the basket, as well as the upper and lower fittings, which are bolted to the aluminum basket. During a side drop, the TPBAR basket is subjected to bending and bearing stresses. The maximum bending stress occurs at Location 'A' shown in the following sketch and is due to the content weight. The maximum bending stress is calculated using a cantilevered beam. This is conservative since it neglects any support of the load due to the edges of the basket being supported by the cask inner shell. The maximum bending stress is:



$$S_b = \frac{6M}{t^2} = \frac{6 \times 364}{0.5^2} = 8.7 \text{ ksi}$$

where:

$$M = w \times \left(\frac{b}{2} - \frac{1}{2}\right) \times \frac{1}{2}\left(\frac{b}{2} - \frac{1}{2}\right)$$

$$= 47 \times \left(\frac{8.87}{2} - \frac{1}{2}\right) \times \frac{1}{2}\left(\frac{8.87}{2} - \frac{1}{2}\right) = 364 \text{ in-lb/in, the maximum bending moment}$$

$$w = \frac{W_c \times g}{L \times b} = \frac{1000 \times 60}{144 \times 8.87} = 47 \text{ psi}$$, the distributed load of the TPBAR consolidation canister

W_c = 1,000 lbs, bounding TPBAR canister weight (with TPBAR rods)

L = 144 inches, length of consolidation canister

b = 8.87 inches, TPBAR basket opening width

g = 60 g, side-drop acceleration

t = 0.5 in, thickness of the flange

The margin of safety is:

$$MS = \frac{S_u}{S_b} - 1 = \frac{31.5}{8.7} - 1 = +2.6$$

where:

S_u = 31.5 ksi, ultimate strength of 6061-T651 aluminum @300°F

TPBAR Basket Body 30-Foot End Drop Analysis

During end drops, the maximum compressive stress on the minimum cross- section of the basket body is:

$$S_{comp} = \frac{g \times W_b}{A} = \frac{60 \times 900}{32.26} = 1.7 \text{ ksi}$$

where:

W_b = 900 lbs, the bounding weight of the TPBAR basket

g = 60 g, accident end drop acceleration

A = $9.87^2 - 8.87^2 + 4(1.00 \times (13.25 - 9.87)) = 32.26 \text{ in}^2$, the minimum cross-sectional area of the basket

The margin of safety is:

$$MS = \frac{0.7S_u}{S_{comp}} - 1 = \frac{0.7 \times 31.5}{1.7} - 1 = +\underline{\text{Large}}$$

where:

S_u = 31.5 ksi, ultimate strength of 6061-T651 aluminum @ 300°F

2.7.7.12.2 TPBAR Basket Upper Fitting

The upper fitting of the TPBAR basket prevents the basket from loading the TPBAR contents during a top-end drop. Four spacer guides of the upper fitting fabricated from Type 304 stainless steel are provided for this purpose. The spacer guides have a length of 7.63 inches, a width of 2.0 inches, and a thickness of 1.00 inch with a 45° × 0.25-inch chamfer. A bounding weight of 900 pounds is used for the TPBAR basket. The temperature of the lid and upper region of the NAC-LWT cask body during TPBAR shipment is conservatively assumed to be 300°F. From Chapter 3, a temperature of 300°F bounds the maximum temperature of the upper NAC-LWT region for a maximum heat load of 1.05 kW. Since the maximum heat load for the TPBAR shipment is less than 1.0 kW, using 300°F for the analysis of the TPBAR upper fitting is conservative.

TPBAR Basket Upper Fitting 30-foot Side Drop

During a side drop, the welds that hold the spacer guides to the top fitting are in shear and bending. The shear load on the welds is:

$$P = (b \times t \times L) \times \rho \times g = (2.0 \times 1.0 \times 7.63) \times 0.288 \times 60 = 264 \text{ lbs}$$

where:

b = 2.0 inches, spacer guide width
t = 1.0 in, spacer guide thickness
L = 7.63 inches, spacer guide length
ρ = 0.288 lb/in^3, density of Type 304 stainless steel
g = 60 g, side-drop acceleration

The welds for the spacer are ⅛-inch fillet welds on three sides. The shear stress in the welds is:

$$\tau = \frac{P}{A} = \frac{264}{0.354} = 747 \text{ psi} \approx 0.8 \text{ ksi}$$

where:

$$A = 0.125 \times 0.707 \times (2.0 + 2 \times 1.0) = 0.354 \text{ in}^2, \text{ weld area}$$

The bending moment is:

$$M = \frac{wL^2}{2} = \frac{(b \times t \times \rho \times g) \times L^2}{2} = \frac{(2 \times 1 \times 0.288 \times 60) \times 7.63^2}{2} = 1{,}006 \text{ in-lb}$$

The stress in the weld due to bending is:

$$S = \frac{M}{t \times S_w} = \frac{1{,}006}{(0.125 \times 0.707)0.56} = 20.3 \text{ ksi}$$

where:

t = weld throat

$S_w = \frac{d^2(2b+d^2)}{3(b+d)} = \frac{1^2(2\times 2+1^2)}{3(2+1)} = 0.56 \text{ in}^2$, section modulus of weld (Blodgett)

The maximum shear stress, τ_{max}, in the weld that is equivalent to the stress intensity divided by two is:

$$\tau_{max} = \frac{\sqrt{S^2+4\tau^2}}{2} = \frac{\sqrt{20.3^2+4\times 0.8^2}}{2} = 10.2 \text{ ksi}$$

The margin of safety is:

$$MS = \frac{0.5 \times S_u}{SI} - 1 = \frac{0.5 \times 66.0}{10.2} - 1 = +2.2$$

where:

S_u = 66.0 ksi, ultimate strength of Type 304 stainless steel @ 300°F

TPBAR Basket Upper Fitting 30-Foot Top-End Drop

For a top-end drop, the weight of the TPBAR basket will load the four spacer guides. The membrane stress in the spacer guide is:

$$S = \frac{W_b \times g}{A} = \frac{900 \times 60}{(2.0 \times 1.0) \times 4} = 6.8 \text{ ksi}$$

where:

W_b = 900 lbs, bounding TPBAR basket weight

A = $(2.0 \times 1.0) \times 4 = 8 \text{ in}^2$, cross-sectional area of the spacer guide

g = 60 g, end-drop acceleration

The margin of safety is:

$$MS = \frac{0.7 \times S_u}{S} - 1 = \frac{46.2}{6.8} - 1 = +5.8$$

where:

S_u = 66.0 ksi, ultimate strength of Type 304 stainless steel @300°F

The critical buckling load for the spacer is determined by using Euler's buckling equation. The critical buckling load is:

$$W_{cr} = K_c \frac{EI}{L^2} = 2.47 \frac{27 \times 10^6 (0.1667)}{7.63^2} \approx 190.9 \text{ kip}$$

where:

E = 27×10^6 psi, modulus of elasticity of Type 304 stainless steel @ 300°F

K_c = 2.47, buckling constant (Blake, Table 10.3)

$I = \frac{bt^3}{12} = 0.1667$ in^4, minimum moment of inertia for cross-section

b = 2.0 inches, spacer guide width

t = 1.0 in, spacer guide thickness

L = 7.63 inches, length of spacer guide

The margin of safety against buckling of the four spacer guides is:

$$MS = \frac{190{,}900}{60 \times 900/4} - 1 = +\underline{\text{Large}}$$

2.7.7.12.3 TPBAR Basket Lower Fitting

The TPBAR basket lower fitting is identical to the bottom fitting of the PWR basket. The weight of the loaded TPBAR basket is less than the weight of the loaded PWR basket. Therefore, additional analyses are not required.

2.7.7.12.4 TPBAR Spacer

The TPBAR spacer is designed to maintain the location of the TPBARs during transport and to prevent the consolidation canister from loading the TPBAR contents during a top-end drop. The spacer is constructed of a circular base plate, two triangular spacer bases, two tubes, and two triangular top plates. The circular base plate is used to attach the spacer to the lower surface of the NAC-LWT cask closure lid. The circular base plate is attached with Type 304 stainless steel bolts. The two triangular spacer bases are bolted to the circular base plate. The tubes, constructed of 3-inch schedule 80 pipes, are welded to the spacer base and the triangular top plates that provide the interface with the TPBARs. The triangular top plates are arranged to form a square that fits inside the consolidation canister. A gap between the triangular top plates provides a recess to accommodate the lifting bail of the canister and container. The weight of the spacer assembly is bounded by 115 lbs. The bounding weight of the consolidation canister is 184 lbs (978 lbs when loaded with 300 TPBARs). During top-end drop conditions, the weight of the consolidation canister is carried by the bail and directly transmitted into the NAC-LWT cask

lid. Therefore, only the weight of the TPBARs is supported by the spacer for top-end drop conditions. The temperature of the lid and upper region of the NAC-LWT cask body during TPBAR shipment is conservatively assumed to be 300°F. From Chapter 3, a temperature of 300°F bounds the maximum temperature of the upper LWT region for a maximum heat load of 1.05 kW. Since the maximum heat load for the TPBAR shipment is less than 1.0 kW, using 300°F for the analysis of the TPBAR spacer is conservative. In the case of the TPBAR waste container, the entire loaded weight of the container of 700 lbs is conservatively assumed to be supported by the spacer. This loading condition is bounded by the loading of the 794-pound maximum TPBAR weight in the consolidation canister.

TPBAR Spacer 30-foot Side Drop

Bolts

During 30-foot side-drop conditions, the weight of the spacer applies a shearing and tensile load to the bolts. The tensile load is due to the couple reacting out the moment generated by the cantilever action of the spacer. The shear stress is:

$$\tau = \frac{P}{A_t} = \frac{1{,}725}{0.1419} = 12.2 \text{ ksi}$$

where:

$$P = \frac{W \times g}{4} = \frac{115 \times 60}{4} = 1{,}725 \text{ lbs}$$

W = 115 lbs, spacer assembly weight

g = 60 g, side-drop acceleration

$A_t = 0.7854\left(D - \frac{0.9743}{n}\right)^2 = 0.7854\left(0.5 - \frac{0.9743}{13}\right)^2 = 0.1419 \text{ in}^2$, tensile area of bolt thread with ultimate strength up to 100 ksi

For ½-13UNC bolts (Machinery's Handbook):

n = 13, number of threads per inch

D = 0.50 in, bolt diameter

Kn_{max} = 0.434 in, maximum minor diameter of internal thread

Es_{min} = 0.4435 in, minimum major diameter of external thread

En_{max} = 0.4565 in, maximum pitch diameter of internal thread

Ds_{min} = 0.4876 in, minimum major diameter of external thread

L_e = 1.0 in, thread engagement

The bolt tensile load is:

$$P = \frac{M}{d} = \frac{40{,}538}{2 \times 4.95} = 4{,}095 \text{ lbs}$$

d = 9.9 inches, maximum distance between bolts

$$M = \frac{wL^2}{2} \times g = \frac{\left(\frac{115}{11.75}\right)(11.75^2)}{2} \times 60 = 40{,}538 \text{ in - lb}$$, the prying moment generated by the cantilever action of the spacer

The bolt tensile stress due to the moment, M, is:

$$S = \frac{P}{A_t} = \frac{4{,}095}{0.1419} = 28.9 \text{ ksi}$$

The membrane stress intensity on the bolt is:

$$SI = \sqrt{S^2 + 4\tau^2} = \sqrt{28.9^2 + 4 \times 12.2^2} = 37.8 \text{ ksi}$$

The margin of safety is:

$$MS = \frac{0.7\,S_u}{SI} - 1 = \frac{0.7(66.0)}{37.8} - 1 = +0.22$$

where:

S_u = 66.0 ksi, yield strength of Type 304 stainless steel @ 300°F

The shear stress on the external threads is:

$$\tau = \frac{P}{A_S} = \frac{4{,}095}{0.7789} = 5.3 \text{ ksi}$$

where:

$$A_s = 3.1416 n L_e Kn_{max}\left[\frac{1}{2n} + 0.57735(Es_{min} - Kn_{max})\right]$$

$$= 3.1416(13)(1.00)(0.434)\left[\frac{1}{2(13)} + 0.57735(0.4435 - 0.434)\right]$$

$$= 0.7789 \text{ in}^2$$, shear area of the bolt threads

The margin of safety is:

$$MS = \frac{0.5S_u}{\tau} - 1 = \frac{0.5(66.0)}{5.3} - 1 = +5.23$$

where:

S_u = 66.0 ksi, ultimate strength of Type 304 stainless steel @ 300°F

Spacer Welds

Using a bounding weight (W) of 25 pounds for the tube and triangular plates, the shear load on the welds is:

$$P = W \times g = 25 \times 60 = 1{,}500 \text{ lbs}$$

where:

g = 60 g, side-drop acceleration

The welds for the spacer are ¼-inch fillet weld. The shear stress in the weld is:

$$\tau = \frac{P}{t_w 0.707 \pi d} = \frac{1{,}500}{0.25 \times 0.707 \times (\pi \times 3.5)} = 772 \text{ psi} = 0.77 \text{ ksi}$$

where:

t_w = 0.25 in, weld size

d = 3.5 inches, outside diameter of 3 inch schedule 80 pipe

The stress in the weld due to bending is:

$$S = \frac{M}{t \times S_w} = \frac{12{,}630}{(0.25 \times 0.707)9.62} = 7.4 \text{ ksi}$$

where:

$M = wL = 25 \times 60 \times 8.42 = 12{,}630$ in - lb, the bending moment

$S_w = \frac{\pi d^2}{4} = \frac{\pi \times 3.5^2}{4} = 9.62 \text{ in}^2$, section modulus of the weld (Blodgett)

The maximum shear stress (τ_{max}) in the weld, which is equivalent to the stress intensity divided by two, is:

$$\tau_{max} = \frac{\sqrt{S^2 + 4\tau^2}}{2} = \frac{\sqrt{7.4^2 + 4 \times 0.77^2}}{2} = 3.8 \text{ ksi}$$

The margin of safety is:

$$MS = \frac{0.5 S_u}{SI} - 1 = \frac{0.5 \times 66.0}{3.8} - 1 = +7.7$$

where:

S_u== 66 ksi, ultimate strength of Type 304 stainless steel @ 300°F

TPBAR Spacer 30-Foot Top-End Drop

The maximum content of 300 TPBARs is retained in the consolidation canister in the shape of a square and this configuration loads the spacer tubes via the triangular top plates during top-end drop conditions. The compressive load applied to the tubes during the top-end drop is the weight of the TPBARs, 794 lbs (300 × 2.65 lb/TPBAR), times the bounding acceleration of 60 g. For this analysis, W_c = 1,000 lbs, is conservatively used. This conservatively bounds the loaded weight of the TPBAR waste container of 700 lbs.

Tube

The compressive stress in the tubes is:

$$S = \frac{W_c \times g}{A} = \frac{1000 \times 60}{2 \times \left(\frac{\pi}{4}\left(3.5^2 - 2.9^2\right)\right)} = 9.9 \text{ ksi}$$

where:

A = the cross-sectional area of a 3-inch schedule 80 pipe with an outer diameter of 3.5 inches and a thickness of 0.3 inch

The margin of safety is:

$$MS = \frac{0.7S_u}{S} - 1 = \frac{46.2}{9.9} - 1 = +3.7$$

where:

S_u = 66.0 ksi, ultimate strength of Type 304 stainless steel @ 300°F

Triangular Top Plate

Referring to the dimensions provided in Figure 2.6.12-6, the pressure applied to a triangular plate is:

$$p_{TP} = \frac{1}{2} \times \frac{1000}{0.5 \times 7.43 \times 7.43} \times 60 = 1{,}087 \text{ psi}$$

The bending moment in the top plate is (see Line A in Figure 2.6.12-6):

$$M = 1{,}087 \times \left(0.5 \times 4.18^2\right) \times \left(\frac{1}{3} \times 4.18\right) = 13{,}231 \text{ in-lbs}$$

The bending stress in the plate is:

$$S = \frac{6M}{bt^2} = \frac{6 \times 13{,}231}{4.18 \times 0.75^2} = 33.8 \text{ ksi}$$

The margin of safety is:

$$MS = \frac{S_u}{S} - 1 = \frac{66.0}{11.2} - 1 = +0.95$$

where:

S_u = 66.0 ksi, ultimate strength of Type 304 stainless steel @300°F

TPBAR Spacer 30-Foot Bottom-End Drop

During the 30-foot bottom-end drop, the inertial load of the spacer is applied to the bolts that affix the spacer to the NAC-LWT cask lid and the welds used to fabricate the spacer assembly. The maximum bottom-end drop acceleration is 60 g.

Bolts

Four bolts (½-13UNC, Type 304 stainless steel bolts) hold the spacer assembly to the bottom of the NAC-LWT cask lid and six fasteners hold the two spacer bases to the circular base plate. For this evaluation, only the four spacer assembly bolts are considered since the individual bolt load is higher and the thread engagement length is shorter. Internal lid threads are not required since high- strength Helicoils are utilized. Using the spacer assembly weight of 115 lbs and an acceleration of 60 g, the critical bolt load is:

$$P = \frac{115 \times 60}{4} = 1{,}725 \text{ lbs}$$

The tensile stress is:

$$S = \frac{P}{A_t} = \frac{1{,}725}{0.1419} = 12.2 \text{ ksi}$$

The margin of safety is:

$$MS = \frac{0.7\,S_u}{S} - 1 = \frac{0.7(66.0)}{12.2} - 1 = +2.79$$

where:

S_u = 66.0 ksi, ultimate strength of Type 304 stainless steel @300°F

The shear stress in the bolt thread is:

$$\tau = \frac{P}{A_S} = \frac{1{,}725}{0.7789} = 2.2 \text{ ksi}$$

The margin of safety is:

$$MS = \frac{0.5S_u}{\tau} - 1 = \frac{0.5(66.0)}{2.2} - 1 = +\underline{\text{Large}}$$

where:

S_u = 66.0 ksi, ultimate strength of Type 304 stainless steel @ 300°F

Spacer Welds

During a 30-foot bottom-end drop (60 g), the spacer weld is loaded by the inertial load of the spacer tube and the triangular top plate (25 lbs bounding). The weld is a ¼-inch fillet weld. The weld stress is:

$$S_w = \frac{W \times g}{t(0.707)(\pi d)} = \frac{25 \times 60}{0.25 \times 0.707 \times (\pi \times 3.5)} \approx 772 \text{ psi} \approx 0.8 \text{ ksi}$$

where:

d = 3.5 inches, outside diameter of 3-inch schedule 80 pipe

t = 0.25 in, weld size

The margin of safety is:

$$MS = \frac{0.5S_u}{S_w} - 1 = \frac{0.5(66.0)}{0.8} - 1 = +\underline{\text{Large}}$$

where:

S_u = 66.0 ksi, ultimate strength of Type 304 stainless steel @ 300°F

2.7.7.13 ANSTO Basket Analysis

The ANSTO modular basket assembly consists of a top module, four intermediate modules, and a base module. The top and base modules are each 29.8 inches long; each of the four intermediate modules is 29.3 inches long; and all six modules have an outer diameter of 13.27 inches. Each module is capable of holding up to seven spiral fuel assemblies or MOATA plate bundles. Each module is a weldment made up of a 13.27-inch-diameter 1/2-inch-thick base plate and six 13.27-inch-diameter, 1/2-inch-thick support plates scalloped on the inner diameter to fit around six peripheral fuel tubes. The weldment structure, fuel tubes, and base and support plates are fabricated from Type 304 stainless steel. Each of the seven fuel tubes in each module has an outer diameter of 4.375 inches and a wall thickness of 0.125 inch. The bottom of each fuel tube is welded to the 1/2-inch-thick base plate. At the bottom of each fuel tube, where it is welded to the base plate, there is a 0.3-inch slot to permit water to drain from the tube. The base plate supports the fuel in the end drop orientation. The base module sits on a 0.5-inch-long, 10-inch-diameter ring that is welded to the base plate. The total weight of the ANSTO basket assembly bears directly on the bottom forging of the cask through the ring. The six scalloped 1/2-inch-thick support plates and the base plate of each basket module provide lateral support and maintain the fuel configuration in the side drop orientation.

2.7.7.13.1 ANSTO Basket Body 30-Foot Side Drop Analysis

Structural analyses of the ANSTO basket for 30-foot side and end drops are performed using classical hand calculations.

The inertia load for the LWT for a 30-foot side drop is 60 g. A conservative loading condition (Table 17, Case 1, Roark) is considered, which neglects any load distribution. Also, it is conservative to assume that there are three loaded fuel tubes acting on the top of a fuel tube since, in reality, there are only two of them. The stresses in the circumferential direction and in the longitudinal direction are added without regard to their signs. Since the circumferential direction and the longitudinal direction also correspond to the direction of the principal stresses, the addition of the two magnitudes reflects the possibility of the principal stresses being of opposite signs.

The maximum applied load to a fuel tube for the circumferential bending stress is:

$$P_s = (3W_{FT} + 3W) \times 60 = 5{,}796 \text{ lbs}$$

where:

W_{FT} = 14.2 lbs, maximum fuel tube weight

W = 18.0 lbs, maximum fuel assembly weight

The bending moment in the fuel tube is:

$$M = \frac{wRk_2}{\pi} = \frac{201 \times 2.13 \times 1.0}{\pi} = 136 \text{ in-lb/in} \quad \text{(Table 17 Case 1, Roark)}$$

where:

$w = \frac{P_s}{L_t} = 201$ lb/in

L_t = 28.81 inches, shortest fuel tube length

R = 2.13 inches, mean radius of fuel tube

$k_2 = 1-\alpha = 1.00$

$$\alpha = \frac{I}{A \times R^2} = \frac{bt^3/12}{b \times t \times R^2} = 2.87 \times 10^{-4}$$

b = 1.0 in, unit length

t = 0.125 in, tube wall thickness

The circumferential bending stress in the fuel tube is:

$$\sigma_c = \frac{6M}{bt^2} = \frac{6 \times 136}{1 \times 0.125^2} = 52.2 \text{ ksi}$$

where:

b = 1.0 in, unit length

t = 0.125 in, tube wall thickness

The stress in the fuel tube in the longitudinal direction is calculated assuming the fuel tube acts like a beam. The maximum bending moment occurs at the top of the basket where the fuel tube acts like a cantilever beam. (The maximum moment for a cantilevered beam with a uniform loading of w (lb/in) and length (l) is $wl^2/2$, as compared to the maximum moment $wl^2/8$ for a simply supported beam.) The bending moment in the tube is:

$$M = \frac{wl^2}{2} = \frac{201 \times 4.^2}{2} = 1{,}608 \text{ in-lb}$$

where:

l = 4.0 inches, the length of the tube extending beyond the support plates

The bending stress is:

$$\sigma_l = F\frac{Mc}{I} = \frac{1{,}608 \times 2.19}{3.77} = 2.5 \text{ ksi}$$

where:

c = 2.19 inches, distance to extreme outer fiber of tube from centroid of tube

I = 3.77 in^4, tube moment of inertia

F = 2.725, factor to account for the effect of the small diameter to length ratio on bending for a cantilevered tube. This is obtained for a uniformly loaded beam in Article 7.10 in Roark.

The maximum stress in the tube is:

$$\sigma_b = 52.2 + 2.5 = 54.7 \text{ ksi}$$

The margin of safety is:

$$MS = \frac{S_u}{\sigma_b} - 1 = +0.20$$

where:

S_u = 65.6 ksi, ultimate strength, Type 304 stainless steel, 350°F

2.7.7.13.2 ANSTO Basket Body 30-Foot End Drop Analysis

The inertia load for the LWT for a 30-foot end drop is 60g. The applied load to the ANSTO basket is:

$$P = W \times 60 = 106{,}200 \text{ lbs}$$

where:

W = 1,770 lbs, total weight of the loaded basket, which bounds the calculated value of 1,667 lbs

The minimum cross-sectional area is at the base of the fuel tubes where the cutouts for water drainage are located. The cross-sectional area is:

$$A = \frac{\left[\frac{\pi}{4}\left(D_o^2 - D_i^2\right) \times 6\right]}{2} + \left[\frac{\pi}{4}\left(D_o^2 - D_i^2\right) - 6 \times l_c \times t_t\right] = 5.93 \text{ in}^2$$

where:

D_o = 4.375 inches, tube outer diameter

D_i = 4.125 inches, tube inner diameter

l_c = 1.00 in, cutout length in center tube

t_t = 0.125 in, tube wall thickness

The membrane stress in the basket is:

$$\sigma = \frac{P}{A} = \frac{106{,}200}{5.93} = 17.9 \text{ ksi}$$

The margin of safety is:

$$MS = \frac{0.7S_u}{\sigma} - 1 = +1.5$$

where:

S_u = 65.6 ksi, ultimate strength, Type 304 stainless steel, 350°F

The welds between the support plates and the fuel tube, and the welds between the base plate and the fuel tube for the accident condition are qualified in Section 2.6.12.11.2

Localized buckling of a fuel tube is evaluated using the methodology presented in Blake. The critical stress is:

$$S_{CR} = E\frac{0.605 - 10^{-7}m^2}{m(1+0.004\phi)} = 160.0 \text{ ksi}$$

where:

E = 25.7×10^6 psi, modulus of elasticity, Type 304 stainless steel, 350°F

$$m = \frac{r_m}{t} = \frac{2.125}{0.125} = 17$$

r_m = 2.125 inches, mean radius of fuel tube

t = 0.125 in, fuel tube thickness

$$\phi = \frac{E}{S_y} = \frac{25.7\times10^6}{21{,}800} = 1{,}179$$

S_y = 21.8 ksi, yield strength, Type 304 stainless steel, 350°F

This critical stress, which is required to result in tube buckling, is much larger than the stress of 17.9 ksi for the fuel tube during the 30-foot end drop condition. Therefore, the fuel tube remains stable during the drop.

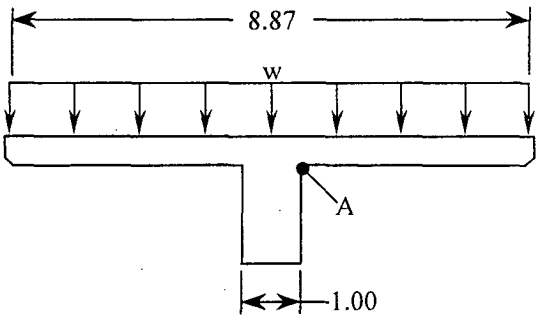
2.7.7.14 TPBAR Basket with the PWR/BWR Rod Transport Canister

This section provides the structural analysis for the shipment of up to 25 individual TPBARs in the PWR/BWR Rod Transport Canister, the PWR insert and the TPBAR basket under accident conditions. Section 2.7.7.12 provides the structural evaluation of the TPBAR basket with 300 TPBARs, considering a slightly lower content weight (1800 lbs) than the TPBARs in the PWR/BWR Rod Transport Canister configuration (1901 lbs). The effects of the increased weight loading for the TPBAR basket are addressed in this section. The structural evaluation of the PWR/BWR Rod Transport Canister and the PWR insert is presented in Section 2.7.1.7.

TPBAR Basket Body 30-Foot Side Drop Analysis – Accident Condition

The TPBAR basket body is constructed of four machined segments that are held together with aluminum bands at five locations along the axial length of the basket, as well as the top and bottom fittings, which are bolted to the aluminum basket. During a side drop, the TPBAR basket is subjected to bending and bearing stresses. The maximum bending stress occurs at Location 'A' in the following figure and is due to the content weight. The maximum bending stress is calculated using a cantilevered beam. This is conservative since it neglects any support of the load due to the edges of the basket being supported by the cask inner shell. The maximum bending stress is:

$$S_b = \frac{6M}{t^2} = \frac{6 \times 542}{0.5^2} = 13 \text{ ksi}$$



where:

$w = \frac{W_c \times g}{L \times b} = \frac{1{,}650 \times 60}{159.5 \times 8.87} = 70$ psi, the distributed load of the TPBAR consolidation canister

W_c = 1,650 lb, bounding TPBAR contents weight (with TPBARs, PWR/BWR Rod Transport Canister assembly and the PWR insert)

L = 159.5 in, loadable length of the TPBAR basket

b = 8.87 in, TPBAR basket opening width

g = 60g, side drop acceleration

$$M = w \times \left(\frac{b}{2} - \frac{1}{2}\right) \times \frac{1}{2}\left(\frac{b}{2} - \frac{1}{2}\right)$$

$$= 70\times\left(\frac{8.87}{2}-\frac{1}{2}\right)\times\frac{1}{2}\left(\frac{8.87}{2}-\frac{1}{2}\right)=542 \text{ in-lb/in, the maximum bending moment}$$

t = 0.5 in, thickness of the flange

The margin of safety is

$$MS=\frac{S_u}{S_b}-1=\frac{31.5}{13}-1=+1.42$$

where:

S_u = 31.5 ksi, ultimate strength of 6061-T6 aluminum @300°F

TPBAR Basket – End Drop

In an end drop scenario, the basket is only loaded by its own weight. The TPBAR basket weight is bounded by what was considered for the end drop analysis of the TPBAR basket in Section 2.7.7.12.1. Therefore, the results of the previous analysis are bounding and no further analysis is required.

TPBAR Basket Upper Fitting

The TPBAR basket upper fitting is identical to what was analyzed for the TPBAR basket in Section 2.7.7.12. The TPBAR basket weight and component temperatures considered in Section 2.7.7.12 are conservative. Therefore, the results of the 2.7.7.12 are bounding and no further analysis is required.

TPBAR Basket Lower Fitting

The TPBAR basket lower fitting is identical to the lower fitting of the PWR basket. The weight of the loaded TPBAR basket is less than the weight of the loaded PWR basket. Therefore, no further analysis is required.

PWR Insert

The PWR insert contains the PWR/BWR Rod Transport Canister assembly for insertion into the TPBAR basket. The PWR insert is not a structural component and, therefore, an analysis for accident conditions is not required.

PWR/BWR Rod Transport Canister Assembly Analysis

The PWR/BWR Rod Transport Canister is identical to what was analyzed in Section 2.7.1.7. The fuel weight considered in the Section 2.7.1.7 analysis for the PWR/BWR fuel (350 lbs) bounds the weight of 25 TPBARs in the PWR/BWR Rod Transport Canister (66 lbs). Therefore, no further analysis is required for the PWR/BWR Rod Transport Canister.

Internal Spacer

The internal spacer for the PWR/BWR Rod Transport Canister is identical to what was analyzed in Section 2.7.1.7. The fuel weight considered in the Section 2.7.1.7 analysis for the PWR/BWR fuel (350 lbs) bounds the fuel weight of 25 TPBARs in the PWR/BWR Rod Transport Canister (66 lbs). Therefore, no further analysis is required for the internal spacer.

4×4 and 5×5 Inserts

The 4×4 and 5×5 inserts for the PWR/BWR Rod Transport Canister are identical to what was analyzed in Section 2.7.1.7. The fuel weight considered in the Section 2.7.1.7 analysis for the PWR/BWR fuel (350 lbs) bounds the weight of up to 25 TPBARs in the PWR/BWR Rod Transport Canister (66 lbs max.). Therefore, no further analysis is required for 4×4 and 5×5 inserts.

2.9 Spent Fuel Contents

2.9.1 PWR and BWR Fuel Rods

Regulatory Guide 7.9 requires that analysis or test data be provided showing that the fuel rod cladding has structural integrity, justifying the amount of integrity claimed. This section is not applicable to the NAC-LWT cask, since no fuel rod structural integrity is claimed. However, it is noted that according to "Dynamic Impact Effects on Spent Fuel Assemblies" (Chun), damage is not likely to occur to the Westinghouse 17 × 17 fuel assembly for a 63 g side drop or an 82 g end drop load. (Of the fuel assemblies examined, the Westinghouse 17 × 17 had the "weakest" structural parameters.) Fuel rod resistance to impact load is dependent on clad temperature and cool time. The NAC-LWT cask impact limiter analyses (Section 2.6.7.4) demonstrate that the maximum design side drop and end drop are 49.7 g and 60 g, respectively. Since the cask g loads are less than the g loads reported in the reference noted above, damage to the fuel rods in the NAC-LWT cask is not likely to occur.

2.9.2 TRIGA Fuel Elements

This section shows that the TRIGA fuel cladding remains intact when hypothetical accident deceleration loads (end and side drops) are applied to the NAC-LWT cask. Hand calculations are used to analyze the TRIGA fuel cladding. All analyses are performed using temperature dependent material properties and a bounding temperature value of 600°F. The following table summarizes the properties used to evaluate the aluminum cladding (1100-0 alloy) and stainless steel cladding (Type 304).

	Aluminum	Steel
Ultimate tensile strength, S_u	2,900 psi	63,500 psi
Tensile yield strength, S_y	2,000 psi	18,200 psi
Modulus of Elasticity, E	7.0×10^6 psi	25.3×10^6 psi 28.3×10^6 psi @70°F (conservative value for bearing)
Poisson's ratio, ν	0.3	0.275
Density, ρ	0.1	0.288 lb/in^3

ASME Code Section III, Subsection NG stress allowables are used for this evaluation. As stated in the previous section, design g values are 60.0 g and 49.7 g for the end and side drops, respectively.

The weight of the standard stainless steel fuel element is 4 kg (8.82 lbs) and the weight of the fuel follower control elements is 6 kg (13.2 lbs). There are a maximum of four (4) elements in any fuel can resulting in a maximum weight of 53 lbs. The aluminum (0.03-inches thick) and stainless steel (0.02-inches thick) cladding are described in TRIGA fuel characterization reports (Tomsio). The bounding weight of the cladding is:

$$W_{cladding} = \frac{\pi}{4}(D_o^2 - D_i^2) \times L \times \rho = 2 \text{ lbs}$$

where:

Do = 1.47 inches, outside diameter of cladding
Di = 1.41 inches, inside diameter of cladding
L = 45 inches, length of cladding (fuel follower rod)
ρ = 0.288 lb/in^3, density of steel

2.9.2.1 End Drop

The end drop evaluation determines if the cladding is structurally stable under its own weight with dynamic load factors to account for cask drop deceleration. Because it is longer and heavier, the fuel follower control element is investigated for buckling. For conservatism, the thinnest cladding is used in conjunction with stainless steel density and aluminum properties. The fuel is taken as self supporting. The buckling load is the weight of the cladding times the end drop design g value of 60g.

$$P_c = 60 \times 2 = 120 \text{ lbs}$$

The critical buckling load is:

$$P_{cr} = \frac{\pi^2 EI}{(2L)^2} = 205 \text{ lbs}$$

where:

I = 0.0491 × (1.47^4-1.43^4) = 0.024 in^4
E = 7.0 × 10^6 psi
L = 45 inches, length of the fuel follower control element

The effective length factor is taken as 2.

The margin of safety is:

$$MS = \frac{P_{cr}}{P_c} - 1 = +0.71$$

Therefore, the cladding will not buckle under its own weight due to the cask end drop.

2.9.2.2 Side Drop

In the side drop, two fuel elements can bear on each other and two elements (one on top of the other) can bear on the flat surface of the module cell wall.

Because of aluminum's lower strength, the bearing stress in the aluminum clad fuel element is the governing case.

For the aluminum clad fuel elements, the bearing stresses will cause local cladding deformation in the radial direction along the line of contact. The deformation will be limited to the distance producing an area, A, sufficient to limit bearing stress to the yield stress of the aluminum cladding.

$$A = \frac{p}{S_y} = \frac{0.51(49.7)}{2{,}000} = 0.0127 in^2$$

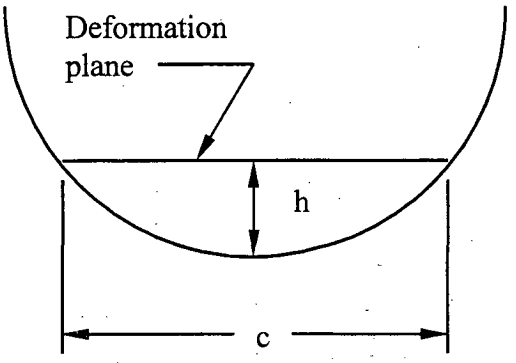
where:

$$p = \frac{W}{L} = \frac{15.2\ lb}{30} = 0.51 lb / in.$$

W = ss clad fuel element, 8.8 lbs (4 kg) + aluminum clad fuel element, 6.4 lbs (2.9 kg) = 15.2 lbs. (Tomsio)

L= fuel element length = 30 inches (Tomsio)

Acceleration from side drop = 49.7 g



The area, A, of the deformation plane is:

$A = c \times \text{unit length} = 0.0127 \text{ in}^2$, therefore,

$c = 0.0127$ inches

The deformation depth, h, is then:

$$h = r - \frac{1}{2}\sqrt{4r^2 - c^2} = 0.735 - \frac{1}{2}\sqrt{4(0.735)^2 - 0.0127^2} = 2.7 \times 10^{-5} \text{ inches}$$

This deformation is insignificant when compared to the 0.030-inch wall thickness of the aluminum cladding.

The slight local deformation (0.000027 in) along the line of contact between fuel elements reduces the bearing stress in the aluminum cladding at this point to the yield strength of the cladding. The small linear deformation of the cladding has no adverse effect on its ability to contain the fuel and does not impede its insertion into or removal from the fuel basket cell.

Therefore, the integrity and function of the fuel element cladding is not impaired.

2.9.3 PULSTAR Intact Fuel Elements

There are two configurations for the PULSTAR intact fuel elements:

1. Intact PULSTAR fuel assemblies that are comprised of a 5 × 5 array of fuel elements. Elements in the assembly are spaced by a tie plate at each end and by periodic spacer tabs on each fuel element (see Figure 1.2-13).
2. Intact PULSTAR fuel elements that are loaded into the TRIGA fuel rod insert (Drawing 315-40-096).

In the item a) configuration, the PULSTAR fuel assembly is inserted in a cell of a MTR basket module that provides full-length support of the fuel assembly. The tabs connecting the individual fuel elements are separated by 6.37 inches and each fuel element has a 0.47-inch outer diameter. The span between PULSTAR fuel element supports is bounded by a standard PWR fuel assembly, while the outer diameter of 0.47 inch bounds a standard PWR rod diameter of 0.37 inch. As the PULSTAR fuel assembly is fully supported, similar to a PWR assembly in the LWT basket, it is concluded that the PULSTAR fuel assembly will remain intact during normal and accident conditions, as is presented for a PWR assembly in the LWT SAR.

In the item b) configuration, the individual elements are supported for the full length of the fuel element. The stresses being developed in the fuel element for the normal and accident conditions for either the end drop or the side drop are considered to be minimal since the fuel element is supported for the full length of the element. The tube has been evaluated in Section 2.6.12.7.9 for the normal transport condition 1-foot drops and in Section 2.7.7.9.8 for the hypothetical accident condition 30-foot drops. The evaluations concluded that in either of the configurations described, the fuel assembly, or the individual fuel elements, will remain intact for the normal transport and hypothetical accident conditions.

2.9.4 ANSTO Fuels

The structural integrity of the MARK III spiral fuel assemblies and the MOATA plate bundles is evaluated in this section for normal and accident conditions of transport. Table 1.1-1 defines the condition of the ANSTO degraded fuel (and for undamaged aluminum clad fuel elements) as fuel with a maximum damaged or degraded area of 5% of the total cross-sectional area. The calculations presented in this section on ANSTO fuel integrity use methodologies that evaluate the overall cross-section of the fuel. This is based on the requirement that localized stresses are not required to be evaluated under accident conditions. Localized damage or degradation is defined as being limited to 5% or less, which can only result in stresses in the structure of a localized nature. Small through holes in the active fuel region (for removed PIE samples) would represent the bounding condition of damage/degradation, and these would generate stress concentrations only locally around the hole. These local stresses would not affect the overall performance of the cross-section in consideration of primary stresses, which are the stresses that would challenge the integrity of the fuel.

2.9.4.1 MARK III Spiral Fuel Assemblies

The Mark III spiral fuel assembly is comprised of a center tube, an outer tube and 10 fuel plates that are 25 inches long (see Figure 1.2.3-14). The fuel plates are curved and are positioned between the center tube and the outer tube in a spiral configuration, as opposed to forming a radial type "spoke" between the center and the outer tubes. Evaluations are performed for the center tube and the outer tube since they are the components that must transfer the weight of the plates during normal and accident conditions. Aluminum 1100 properties, which are considered to provide minimal values for the stress allowables, are used in the plates and tubes.

Center Tube

A structural evaluation of the center tube of the MARK III spiral fuel is performed. Two loads are considered: the tube self-weight and 50% of the weight of the fuel plates. Five out of 10 of the fuel plates can transfer their weight to the inner tube; therefore, 50% of the weight of the fuel plates is considered. The weight of the center tube is increased to account for 50% of the fuel plate weight. The formula for the circular rings from Case 15 (ring supported at the base at a single point and loaded by their own weight per unit length of circumference w) of Table 17 in Roark is used for this evaluation. It is conservatively assumed that the tube weight and 50% of the fuel plate weight are supported at a single point.

There are 10 fuel plates in a fuel assembly. A fuel plate of MARK III spiral fuel weighs 0.4431 lb (201 g). The weight of the five fuel plates (2.22 lbs) contributes to the load and pushes the

tube down during the basket side drop. The weight of the five plates, converted to its own weight per unit length of circumference, w_p, is (before considering the g load factor):

$$w_p = \frac{m_p}{L \times 2\pi R} = 0.0121 \text{ lb/in}$$

where:

m_p = 2.22 lbs, the weight of five plates

L = 25 inches, the length of the plate

R = 1.1678, median radius of the fuel inner tube

The tube weight per unit length of circumference, w_t, is (before considering the g load factor):

$$w_t = \frac{m_t}{2\pi R} = 0.0058 \text{ lb/in.}$$

where:

m_t = 1.0582/25 = 0.0423 lb, the weight of tube (480 g) per inch

R = 1.1678, median radius of the fuel inner tube

Normal Condition

The maximum bending moment at the support point for the normal condition is:

$$M_c = \frac{3}{2} \times f_{GN} \times (w_p + w_t) \times R^2 = 0.9154 \text{ lb-in}$$

where:

f_{GN} = 25, the side drop g load for the normal condition

The circumferential bending stress in the tube for the normal condition is:

$$\sigma_c = \frac{6M_c}{bt^2} = \frac{6 \times 0.9154}{1 \times 0.0443^2} = 2{,}799 \text{ psi}$$

where:

t = 0.0443 inch, tube thickness

b = 1 inch, unit length of tube

The margin of safety corresponding to the allowable for the normal condition is:

$$MS = \frac{1.5S_m}{\sigma_c} - 1 = +0.58$$

where:

Sm = 2.95 ksi, Design Stress Intensity, Aluminum 1100, 250°F (Table 2.2, "Aluminum Standards and Data," The Aluminum Association)
(S_m is the lesser of $S_u/3$ and $2S_y/3$)

Accident Condition

The maximum bending moment at the support point for the accident condition is:

$$M_c = \frac{3}{2} \times f_{GA} \times (w_p + w_t) \times R^2 = 2.197 \text{ lb} - \text{in}$$

where:

f_{GA} = 60, the side drop g load for the accident condition

The circumferential bending stress in the fuel tube for the accident condition is:

$$\sigma_c = \frac{6M_c}{bt^2} = \frac{6 \times 2.197}{1 \times 0.0443^2} = 6{,}717 \text{ psi}$$

The margin of safety corresponding to the allowable for the accident condition is:

$$MS = \frac{S_u}{\sigma_c} - 1 = +0.36$$

where:

Su = 9.14 ksi, ultimate stress of Aluminum 1100 at 250°F (Table 2.2, "Aluminum Standards and Data," The Aluminum Association)

Outer Tube

A structural evaluation of the outer tube of the MARK III spiral fuel is performed. Three loads are considered: the tube self-weight, the weight of the fuel plates, and the weight of the inner tube. The weight of the outer tube is increased to account for the fuel plate weight and the weight of the inner tube. The formula for a curved beam (pinned arch under uniform load) from Blake is used for this evaluation. Since the diametrical gap between the MARK III spiral fuel and the basket tube inner surface is 0.125 inch, the use of the pin-pin configuration is adequate.

There are 10 fuel plates in a fuel assembly. A fuel plate of MARK III spiral fuel weighs 0.4431 pound (201 g). The weight of the inner tube (1.0582 lbs) and the 10 fuel plates (4.431 lbs) contributes to the load and pulls the tube down during the basket side drop. The weight of the inner tube and the fuel plates, converted to its own weight per unit length of circumference, q_c, is (before considering the g load factor):

$$q_c = \frac{m_p + m_i}{Lp \times 2\pi R} = 0.0177 \text{ lb/in}$$

where:

m_p = 4.431 lbs, the weight of 10 plates

m_i = 1.0582 lbs, the weight of inner tube (480 g)

Lp = 25 inches, the length of the plate

R = 1.9695, median radius of the fuel outer tube

The outer tube weight per unit length of circumference, q_t, is (before considering the g load factor):

$$q_t = \frac{m_t}{2\pi R} = 0.0078 \text{ lb/in.}$$

where:

m_t = 2.4251/25 = 0.0970 lb, the weight of outer tube (1,100 g) per inch

R = 1.9695, median radius of the fuel outer tube

The combined load factor, q_{total}, is 1.53 lb/in [$60 \times (q_c + q_t)$, 60 is the side drop g load factor] for the accident condition of the side drop case.

The maximum moment (Equation 27.63, Blake) for the accident conditions is:

$$M = q_{total} \times R^2 \times B = 0.5460 \text{ lb-in for accident condition}$$

where:

R = 1.9695, median radius of the fuel outer tube

B = 0.092, the maximum absolute value of the bending moment factor
(B is from Figure 27.17 in Blake)

Based on Equation 28.1 from Blake, the stress due to this bending is:

$$S = \frac{M}{A \times R}\left[1 + \frac{c}{\lambda(R + c)}\right] = 879 \text{ psi for accident condition}$$

where:

A = 0.061 in^2, the cross-section area (thickness of the outer tube is 0.061 in)

R = 1.9695, median radius of the fuel outer tube

c = 0.03 in, half of the thickness of the outer tube

λ = 7.8×10^{-5}, the Winkler's factor for rectangular cross-section, as calculated:
(Table 28.1, Blake)

$$\lambda = \frac{1}{3}\left(\frac{c}{R}\right)^2 + \frac{1}{5}\left(\frac{c}{R}\right)^4 + \frac{1}{7}\left(\frac{c}{R}\right)^6 + \cdots = 7.8\times10^{-5}$$

Conservatively, the allowable for the normal condition is used for calculating the margin of safety in the accident condition. The margin of safety corresponding to the allowable for the normal condition is:

$$MS = \frac{1.5S_m}{S} - 1 = +4.0$$

where:

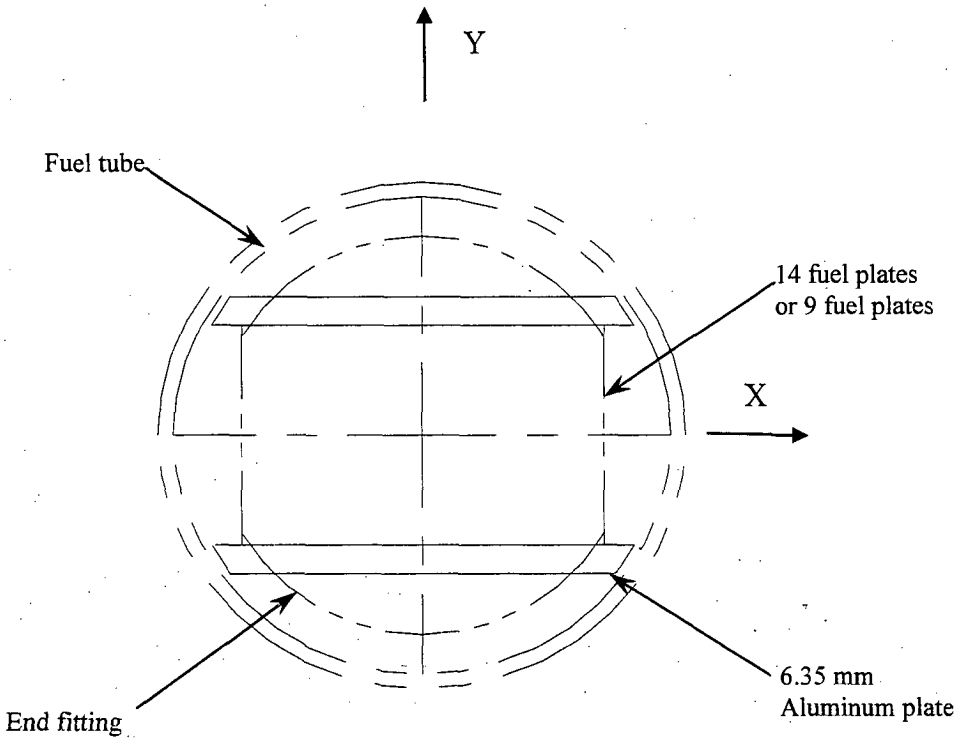
S_m = 2.95 ksi, Design Stress Intensity, Aluminum 1100, 250°F

Therefore, the Mark III spiral fuel remains intact for the normal and accident conditions of transport.

2.9.4.2 MOATA Plate Bundles

Two 6.35-mm aluminum plates are required to carry the weight of the MOATA plate bundle during transport. The aluminum plates sandwich the 14 or the 9 aluminum fuel plates (see the following illustration). At each end of the plate bundle is an end fitting that permits handling. Each end fitting also contains a bolt assembly that threads into the walls of the end fitting. The outer diameter of the end fitting is 3.449 inches. The diametrical gap between the end fitting and the inner diameter of the basket tube is 4.125 – 3.449 or 0.68 inch. During transport, it is not possible for the bolt to become disengaged from the end fitting due to the 0.68-inch gap. Therefore, the configuration of the fuel plates and the aluminum plates will not be altered during transport. The bolt assembly is considered to experience negligible loading stress due to its own weight. Likewise, the stresses occurring in the end fittings are expected to be minimal and are bounded by stresses occurring in the aluminum plates.

For the stress evaluation of the aluminum plates, the bounding condition is the side drop. To compute the minimum margin for both the normal condition and the accident condition, the stress is computed using the accident loading case, but the margin of safety is computed using the stress allowable for the normal condition.



For a 30-foot side drop in the direction aligned with the Y axis, the maximum stress in the aluminum plate is calculated by representing the plate as a uniformly loaded, simply supported beam. Since the plate is supported at the edges along the 26-inch length of the plate, the length of the beam in this calculation is its width, or 3.7 inches. The bending moment on the center of the plate is:

$$M = \frac{Pw^2}{8} = \frac{36.5 \times 3.7^2}{8} = 62.5 \text{ in-lb}$$

where:

$$P = \frac{Wg}{L} = \frac{15.8 \times 60}{26} = 36.5 \text{ lb/in}$$

W =18-2.2 = 15.8 lbs, since the top aluminum plate is significantly stiffer than the fuel elements below the top aluminum plate and does not load the bottom plate

w = 3.7 inches (94 mm), maximum plate width

L = 26 inches, length of the aluminum plate

The bending stress in the plate (0.25-in thick) is:

$$\sigma = \frac{6M}{bt^2} = \frac{6 \times 62.5}{1 \times 0.25^2} = 6.0 \text{ ksi}$$

Conservatively using the membrane plus bending allowable for normal conditions, the margin of safety is:

$$MS = \frac{1.5S_m}{\sigma} - 1 = +1.9$$

where:

S_u = 34.6, ultimate strength, 6061-T6, 250°F

(design stress intensity, S_m, is the lesser of $S_u/3$ and $2 \times S_y/3$)

For a 30-foot side drop of the fuel aligned with the X axis, the fuel plates are not supported by the 6.35-mm aluminum plates. The maximum stress in the fuel plate (Aluminum 1100) is calculated by representing the plate (26 inches long) as a uniformly loaded, simply supported beam. The bending moment on the center of the plate is:

$$M = \frac{PL^2}{8} = \frac{1.53 \times 26^2}{8} = 129.3 \text{ in-lb}$$

where:

$$P = \frac{Wg}{L} = \frac{0.66 \times 60}{26} = 1.53 \text{ lb/in}$$

W = 0.66 lb (300 g);

L = 26 inches, length of the fuel plate

The bending stress in the plate (0.08-in thick) is:

$$\sigma = \frac{6M}{bt^2} = \frac{6 \times 129.3}{0.08 \times 3^2} = 1.1 \text{ ksi}$$

Conservatively using the allowable for normal conditions, the margin of safety is:

$$MS = \frac{1.5S_m}{\sigma} - 1 = +3.0$$

where:

S_m = 2.95 ksi, Design Stress Intensity, Aluminum 1100, 250°F

(design stress intensity, S_m, is the lesser of $S_u/3$ and $2 \times S_y/3$)

During an end drop, a compressive load is developed in the aluminum plates and in the fuel elements. Due to the proximity of the end of the fuel elements to the lifting bracket or to the

bottom of the basket, the axial load of the fuel elements will be transmitted directly into the lifting bracket or the bottom of the basket. The compressive load on the aluminum plates is the weight of the end fittings and the self-weight of the aluminum plates. However, the inertial load in the end drop of the aluminum plates is not uniform, but rather is at a maximum at the bottom of the plate nearest the plane of impact. The maximum compressive stress is the product of the 26-inch length, the density of 0.098 lb/in^3, and the acceleration of 60g's or 153 psi. This compressive stress is considered to be minimal and only occurs at the base. The load that is considered to be uniform over the length of the aluminum plate is the weight of the end fitting, or 4.34 lbs. Since there are two plates of equal stiffness, the load is considered to be distributed equally to the two plates.

For a 60g end drop, the load on one plate is:

$$P = W_a g = \left(\frac{4.34}{2}\right) \times 60 = 130.2 \text{ lbs}$$

The stress in the aluminum plate is:

$$\sigma = \frac{P}{bt} = \frac{130.2}{3.38 \times 0.25} = 154 \text{ psi}$$

Using the Euler buckling methodology from the "Manual of Steel Construction," the critical buckling stress, for $KL/r > C_c$ is:

$$F_a = \frac{12\pi^2 E}{23(KL/r)^2} = 371 \text{ psi}$$

where:

b = 3.38 inches, plate width

t = 0.25 in (6.35 mm), plate thickness

L = 26.0 inches, plate length between bolt supports

K = 1.0, buckling end fixity constant – simply supported at each end due to the retaining pin

E = 9.1×10^6 psi, modulus of elasticity, 6061-T6, 250°F

F_y = 29.8 ksi, yield strength, 6061-T6, 250°F

$$r = \sqrt{\frac{I}{A}} = 0.072$$

$$I = \frac{bt^3}{12} = 0.0044 \text{ in}^4$$

$$A = bt = 0.84 \text{ in}^2$$

$KL/r = 361$

$$C_c = \sqrt{\frac{2\pi^2 E}{F_y}} = 79$$

The safety factor against the plate buckling is calculated to be larger than unity, as shown in the following equation. Therefore, aluminum plates will not buckle.

$$FS = \frac{F_a}{\sigma} = \frac{371}{154} = 2.4$$

Since the aluminum plates do not buckle, the fuel elements will only be loaded by their own self-weight. The compressive loading on the fuel elements also varies uniformly from zero at the top of the fuel element to the base. This stress is the ratio of the total compressive load (0.66 lb × 60g's) to the cross-sectional area (7.6 cm × 0.203 cm or 0.24 in^2), or 166 psi. This is considered to be a minimal compressive stress that would not result in damage to the fuel element. Since the aluminum plates do not buckle and are further restrained by the fuel basket tubes, the buckling of the fuel elements cannot occur during the end drop. Therefore, the fuel is not damaged.

2.10.14 Structural Evaluation of the NAC-LWT Cask Body with TPBAR Contents

This section presents a structural evaluation of the NAC-LWT cask system with TPBAR contents under normal conditions of transport and hypothetical accident conditions. The NAC-LWT cask system with TPBARs is comprised of four primary components: NAC-LWT cask body, TPBAR basket, basket spacers, and TPBAR contents. The NAC-LWT cask system is structurally evaluated for two TPBAR content conditions: up to 300 production TPBARs loaded into an open (i.e., unsealed) consolidation canister; and up to 55 segmented TPBARs loaded into a welded closed waste container.

The NAC-LWT cask system containing TPBAR contents is required to have the Alternate B port covers installed and tested on the vent and drain ports to assure a leaktight containment boundary during transport. Section 2.10.15 presents the structural evaluation of the Alternate B port cover. Sections 2.6.12.10 and 2.7.7.12 present the structural evaluation for the TPBAR basket and basket spacers for the transport of the TPBAR content conditions under normal conditions of transport and hypothetical accident conditions, respectively.

2.10.14.1 Normal Conditions of Transport for Cask Body with TPBAR Contents

This section provides the cask body structural evaluation for normal conditions of transport. The following sections discuss the governing conditions of hot, cold, and drop conditions for normal transport.

2.10.14.1.1 Hot and Cold Conditions

Hot and cold conditions, as defined in 10CFR 71.71 (c) (1) and (2), are evaluated as part of the normal conditions of transport for a 1-foot free-drop evaluation (see Section 2.10.14.1.2). Since the 1-foot drop evaluations include the inertial loads and a bounding thermal load, the 1-foot drop evaluation bounds the evaluation for hot and cold conditions.

2.10.14.1.2 Free Drop (1 Foot)

The normal conditions drop orientations considered are: side drop, top-end drop, bottom-end drop, top-end CG-over-corner drop, and bottom-end CG-over-corner drop. Corner drops are defined as the CG of the cask over the impact limiter corner (15.74° from vertical).

Finite Element Model Description

A three-dimensional half-symmetry model of the LWT cask body is constructed using ANSYS solid elements (SOLID45). The finite element model contains the top and bottom forgings, cask sidewalls, lead shielding, cask lid and bolts. The cask shells are modeled using SA-240 Type

XM-19 stainless steel material properties. The cask top and bottom forgings and cask lid are modeled using SA182 Type 304 stainless steel forging material properties. The model is shown in Figure 2.10.14-1 through Figure 2.10.14-3.

The neutron shield tank and water inside the neutron shield tanks are represented with ANSYS MASS21 elements (approximately 5,600 lbs for entire cask, 2,000 lbs for tanks, and 3,600 lbs for the water). For the end drops, the MASS21 elements are applied around the outer circumference (0°–180°) of the LWT cask. For the side and corner drops, the MASS21 elements are applied to the lower half of the outer circumference (0°–90°) of the outer shell. As a modeling convenience, a small hole is modeled in the center of the lid and bottom of the cask. Symmetry boundary conditions are applied to the plane of symmetry of the cask body model. The lid bolts are modeled using beam elements (BEAM4). The preload of 35,000 lbs per bolt is modeled by applying an initial strain to the beam elements. The applied strain is 0.00273 in/in.

The lead is considered a soft material when compared with the stainless steel shells. To simulate the interface between lead and the stainless steel shells, a small gap of 0.015 inch is modeled using ANSYS CONTAC52 gap elements. Gap elements are also modeled between the lid and top forging and between the cask and the impact limiters. The interface between the cask and impact limiters simulates the pressure applied by the impact limiters during drop conditions. The gap stiffness is modeled as a cosine distribution from a maximum value of 1.0×10^6 lb/in at the line of impact to a value of 1.31×10^5 lb/in at an angle of 82.5° from the line of impact. A minimal value of 100 lb/in is used from 90° to 180°.

Inertia loads of 25 g for side drop and 20 g for the end and corner drops are used in the cask body evaluation for normal conditions. For all drop cases, a conservative internal pressure of 300 psig is applied on the cask cavity and lid interior surfaces in the outward normal direction. The pressure bounds the MNOP of 289 psig for normal conditions of transport (Section 3.4.4.4). The weight of the contents (basket, consolidation canister, and TPBARs) is also applied as a concentrated pressure loading over a single row of elements (7.5°) for side and corner drops. For end drops, the contents weight is applied to either the cask lid or bottom forging as appropriate. For other drop orientations, pressure is applied on the appropriate surface, depending on the drop angle.

To calculate the thermal stresses in the cask, the temperature results from the design basis PWR fuel configuration are used to derive a conservative temperature gradient for the calculation of thermal stresses. The heat load for the design basis PWR fuel of 2.5 kW is greater than the heat load for the TPBAR configuration (< 0.7 kW) and, therefore, the analysis is conservative. A temperature of 227°F is applied to the cask lid and top forging regions. At the axial center of the inner and outer shells, a temperature of 274°F and 229°F is applied, respectively. For the bottom of the cask and interface with the inner and outer shells, a temperature of 239°F is used. Using

these temperatures as input, a thermal conduction solution is obtained using the finite element model described in this section, with the exception that the ANSYS SOLID45 structural elements are replaced with the equivalent SOLID70 thermal elements. Once calculated, the temperatures from the thermal conduction solution are applied as a boundary condition to the cask body structural model to calculate thermal stresses.

Finite Element Analysis Result Summary

The most crucial sections for each cask component are shown in Figure 2.10.14-4. Table 2.10.14-1 shows the material designation at each section location. The maximum P_m, $P_m + P_b$, and P+Q stresses for each component are reported in Table 2.10.14-2 through 2.10.14-16 for the different drop orientations. Allowable stresses are conservatively reported at a temperature of 250°F. Margins of Safety greater than +10 are reported as "+Large."

The minimum margin of safety is +0.13, which occurs at section 2 for the condition of P_m stress for 1-foot side-drop conditions. This section is located at the axial center of the cask outer shell. The minimum margins of safety for each stress category for 1-foot drop conditions are as follows.

Stress Category	Section	Drop Orientation	Stress Intensity, ksi	Stress Allowable, ksi	Margin of Safety
P_m	2	Side	28.57	32.3	+0.13
$P_m + P_b$	2	Side	32.87	48.45	+0.47
P+Q	18	Side	31.3	60.0	+0.93

2.10.14.2 Hypothetical Accident Conditions for Cask Body with TPBAR Contents

This section provides the cask body structural evaluation for hypothetical accident conditions. The following sections discuss drop conditions and inner shell buckling.

2.10.14.2.1 Free Drop (30-Foot)

The hypothetical accident conditions drop orientations considered are: side drop, top-end drop, bottom-end drop, top-end CG-over-corner drop, and bottom-end CG-over-corner drop. Corner drops are defined as the CG of the cask over the impact limiter corner (15.74° from vertical).

Finite Element Model Description

The finite element model is described in Section 2.10.14.1.2. For accident conditions, an acceleration of 60 g is applied to all drop orientations. The temperature-dependent material properties presented in Section 2.3 are used in the analysis.

Finite Element Analysis Result Summary

The most critical sections for each cask component are shown in Figure 2.10.14-4. Table 2.10.14-1 shows the material at each section location. The maximum P_m and $P_m + P_b$ stresses for each component are reported in Tables 2.10.14-17 through 2.10.14-26 through for different drop conditions. Allowable stresses are reported at a temperature of 250°F. Margins of Safety greater than +10.0 are reported as "+Large."

The minimum margin of safety is +0.02, which occurs at section 2 for the condition of P_m stress, for 30-foot drop conditions. This section is located at the axial center of the cask outer shell. The minimum Margins of Safety for each stress category for 30-foot drop conditions are as follows.

Stress Category	Section	Drop Orientation	Stress Intensity, Ksi	Stress Allowable, ksi	Margin of Safety
P_m	2	Side	66.5	67.83	+0.02
P_m+P_b	2	Side	74.14	96.9	+0.31

2.10.14.2.2 Fire Accident

A finite element analysis is performed using the three-dimensional model as described in Section 2.10.14.1.2 for the evaluation of the fire accident conditions. The maximum calculated internal pressure for the fire accident is 337 psig (Section 3.5.4.4). A bounding internal pressure of 600 psig is conservatively used in combination with the inertial load in the model. The maximum P_m and P_m+P_b stresses for each cask component are presented in Table 2.10.14-27 and Table 2.10.14-28. The minimum Margin of Safety is +7.38 and +8.32 for the P_m and P_m+P_b stresses, respectively.

2.10.14.3 Inner Shell Buckling

Section 2.10.6 presents a buckling evaluation of the cask inner shell per ASME Code Case N-284 for the design basis cask configuration. The evaluation presented in Section 2.10.6 bounds the TPBAR contents based on the following.

- The maximum weight of the TPBAR contents of 1,000 lbs is enveloped by the weight of the design basis contents, which would reduce the compressive stresses in the cask shells due to less inertia loading for the drop conditions.
- The cask internal pressure for the TPBAR contents is significantly higher than the cask internal pressure for the design basis contents. The increase in the pressure would increase the tensile stresses in the shell that result in stiffening of the inner shell and, consequently, in reducing the compressive stresses associated with buckling.

The interaction summary presented in Table 2.10.6-10, associated with the design basis weight and the design basis pressure, is bounding for the TPBAR content conditions. Therefore, it is

concluded that the cask inner shell will not buckle with the TPBAR contents in the NAC-LWT cask.

2.10.14.4 NAC-LWT Cask Closure Lid and Bolts

The NAC-LWT cask closure lid is bolted to the cask body top forging with twelve 1-8 UNC bolts fabricated from SA-453, Grade 660 high-alloy steel. The threaded portion of the bolt engages the cask body a minimum of 1.875 inches. From Section 2.1.3.2.2, the torque on the cask lid bolts is 260 ± 20 ft-lb and the bolt preload is specified as 34,843 lbs. For the LWT cask configured to ship TPBARs, the maximum internal pressure of 600 psig is conservatively used in the closure lid evaluation. This pressure bounds the maximum pressure during the fire accident contained in Section 3.5.4.4. To ensure that the seal is not unloaded during accident conditions, the preload is calculated to account for the weight of the lid, internal weight of the cask contents, force resulting from internal pressure, force resulting from compression of the TFE O-ring, and force resulting from compression of the metallic O-ring. The load resulting from the weight of the LWT cask contents is

$$F_2 = W_c a = 1{,}800 \times 60g = 108{,}000 \text{ lbs}$$

where:

W_c = 1,800 lbs (bounding weight of TPBAR basket and contents)

a = 60 g (maximum accident acceleration)

The load resulting from accident pressure (fire accident) is:

$$F_{ip} = P_{ip} A = 600 \times 171.36 = 102{,}816 \text{ lbs}$$

where:

P_{ip} = 600 psig (accident internal pressure)

$$A = \frac{\pi}{4} \times 14.771^2 = 171.36 \text{ in}^2$$

The total required bolt preload force (12 bolts) is:

$$FT = F_1 + F_2 + F_{tr} + F_{mr} + F_{ip}$$

$$= 56{,}460 + 108{,}000 + 2{,}474 + 79{,}470 + 102{,}816 = 349{,}220 \text{ lbs}$$

where:

F_{tr} = 2,474 lbs, TFE O-ring load (Section 2.1.3.2.2)

F_{mr} = 79,470 lbs, Metallic O-ring load (Section 2.1.3.2.2)

F_1 = 56,460 lbs, Lid load (Section 2.1.3.2.2)

The required bolt preload per bolt is:

$$F_{bolt} = \frac{F_T}{12} = \frac{349{,}220}{12} = 29{,}102 \text{ lbs} \quad < 34{,}843 \text{ lbs} \quad \text{(Section 2.1.3.2.2)}$$

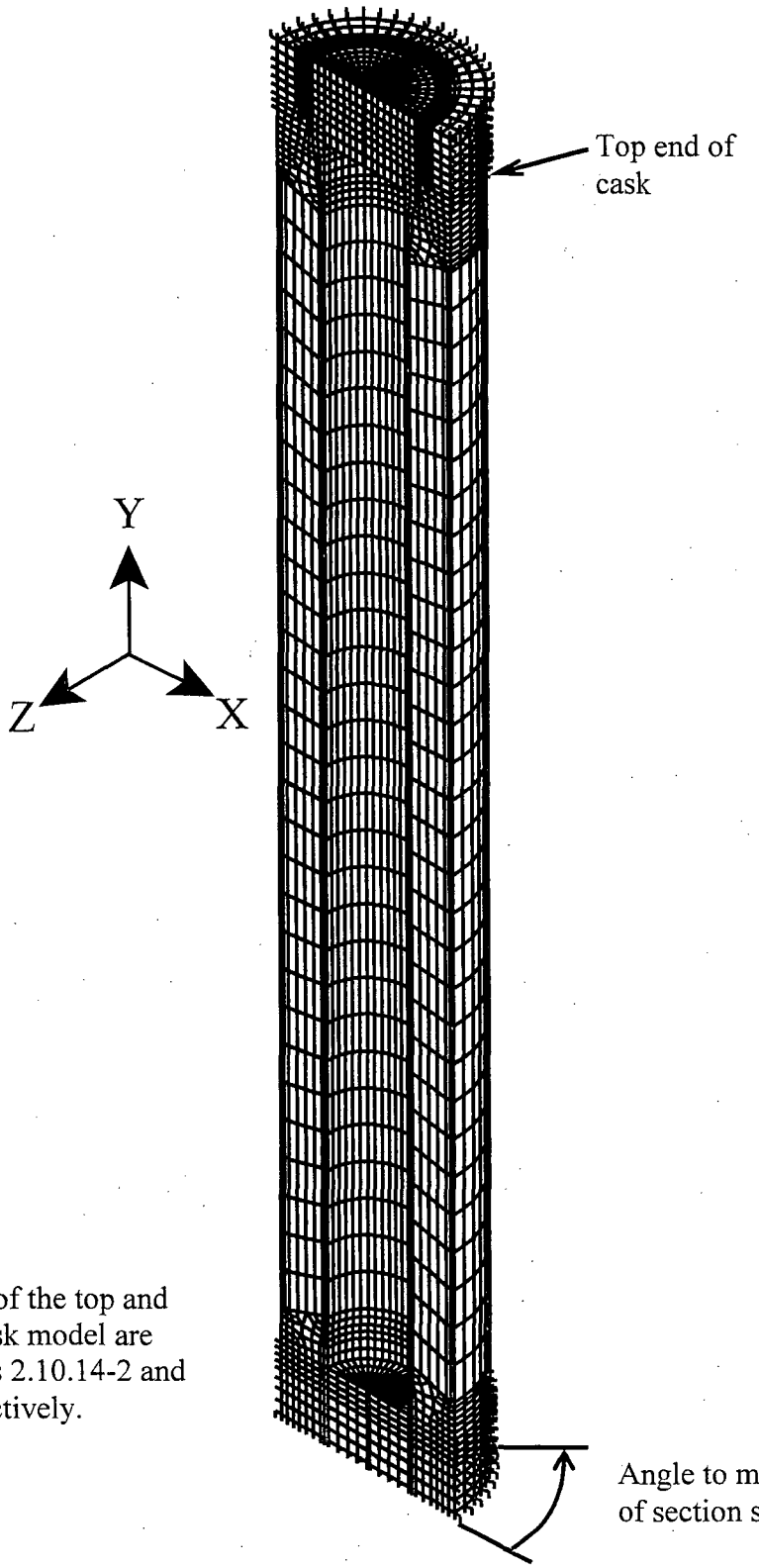
Since the bolt preload presented in Section 2.1.3.2.2 of the NAC-LWT is bounding, no further analysis of the LWT lid bolts is required.

The preload applied to the cask lid bolts is due to the load applied to the lid. The load applied to the lid for the design basis weight and pressure for the PWR fuel bounds the load applied to the lid for the TPBAR contents. Therefore, the stresses in the cask lid due to the design basis weight and pressure also bound the stresses in the cask lid due to the TPBAR content weight and pressure.

2.10.14.5 Conclusion

Based on the evaluations presented in Sections 2.10.14.1 through 2.10.14.4, the NAC-LWT cask with TPBAR contents satisfies the requirements of 10 CFR 71 for the normal conditions of transport and for hypothetical accidents.

Figure 2.10.14-1 ANSYS Finite Element Model of the Cask Body



Note:
A detailed view of the top and bottom of the cask model are shown in Figures 2.10.14-2 and 2.10.14-3, respectively.

Figure 2.10.14-2 Detailed View of the Cask Body Finite Element Model Top

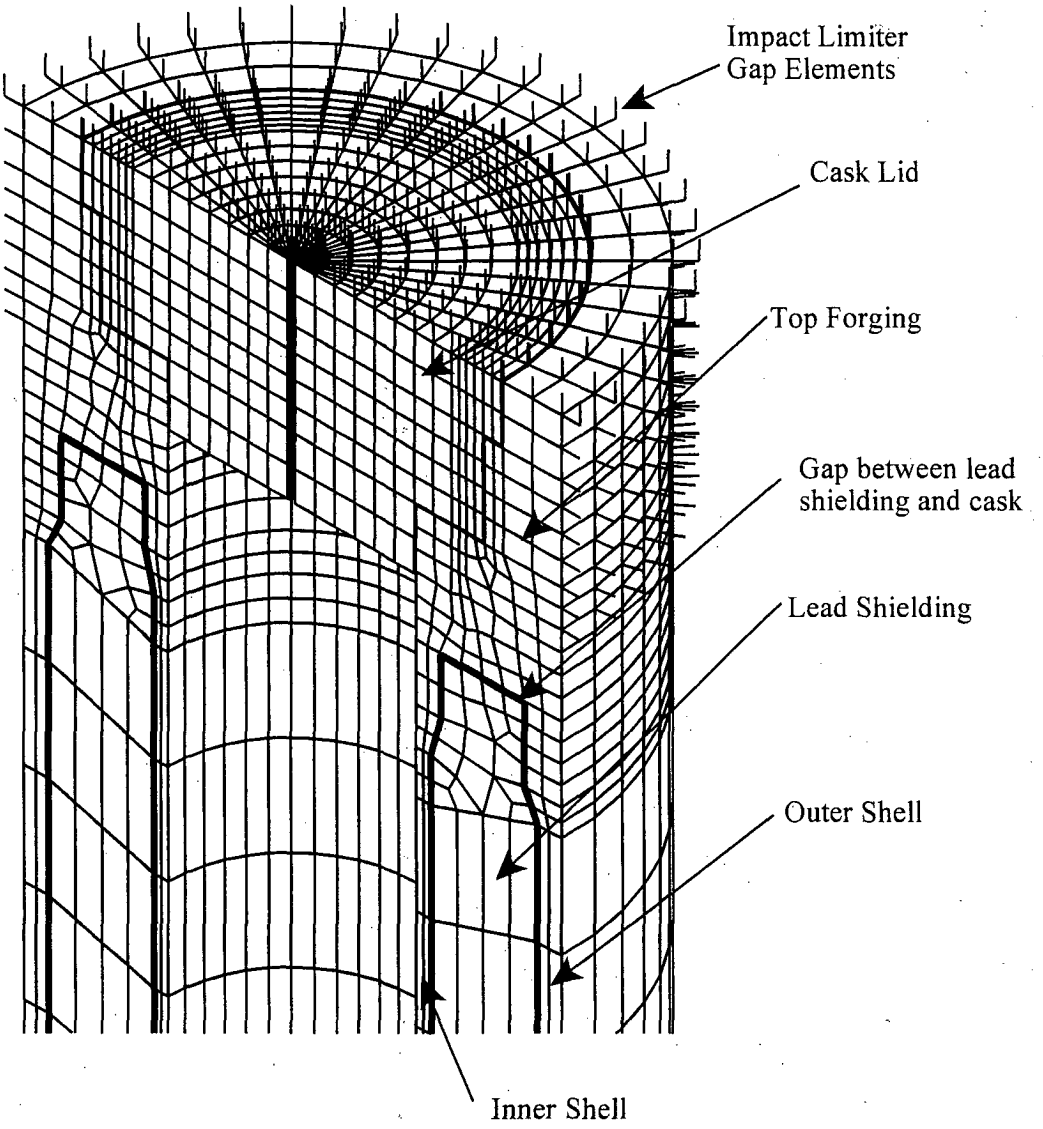


Figure 2.10.14-3 Detailed View of the Cask Body Finite Element Model Bottom

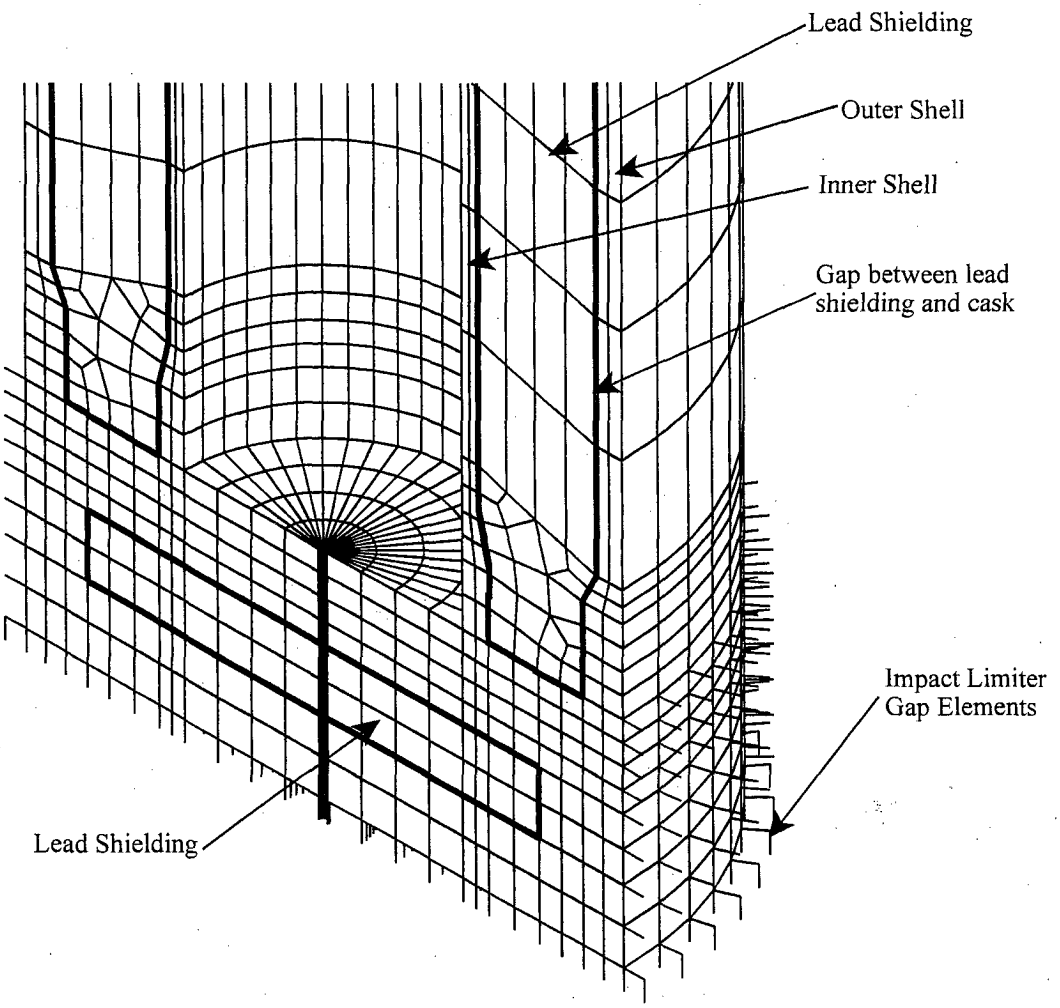


Figure 2.10.14-4 Location of Sections of the NAC-LWT Cask Body Model

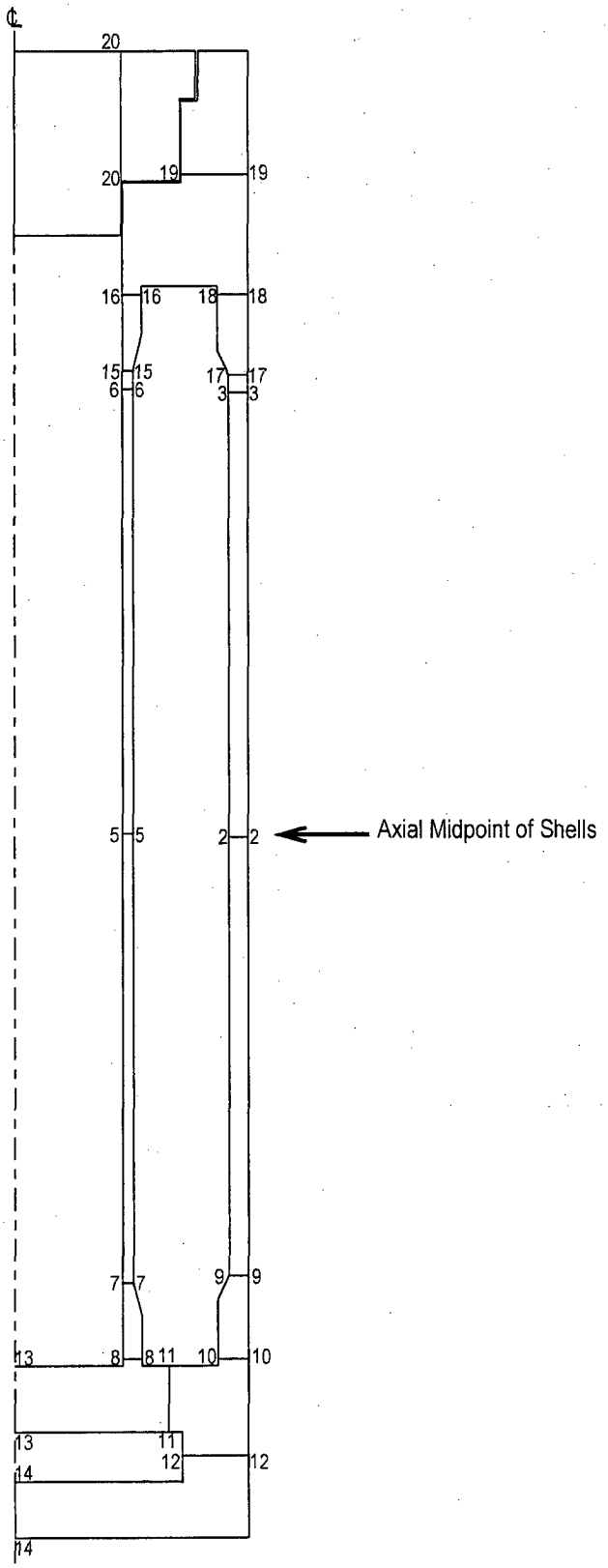


Table 2.10.14-1 Material Designations for Sections

Location	Material	Sections[14]
Outer Shell	SA240 Type XM-19	1-3
Inner Shell	SA240 Type XM-19	4-6
Bottom Forging	SA182 Type 304	7-14
Top Forging	SA182 Type 304	15-19
Lid	SA182 Type 304	20

[14] Sections are shown on Figure 2.10.14-4

Table 2.10.14-2 1-Foot Side Drop with Internal Pressure, P_m Stresses, ksi

Sec[1]	Location (deg)[2]	S_x[3]	S_y[3]	S_z[3]	S_{xy}[3]	S_{yz}[3]	S_{xz}[3]	Stress Intensity	Stress Allow.	MS
1	75	0.03	0.28	2.66	0.08	-6.74	-0.03	13.69	32.30	1.36
2	0	-0.14	1.71	28.41	-0.18	-0.01	0.00	28.57	32.30	0.13
3	67.5	0.04	0.39	3.97	0.05	6.06	0.00	12.64	32.30	1.56
4	97.5	-0.21	2.30	1.31	0.10	-4.21	0.01	8.48	32.30	2.81
5	180	-0.17	2.54	-16.05	0.18	0.00	0.00	18.61	32.30	0.74
6	97.5	-0.22	2.26	1.16	0.10	4.14	-0.01	8.36	32.30	2.86
7	112.5	-0.25	1.92	1.95	0.01	-5.75	-0.01	11.50	20.00	0.74
8	180	-1.99	1.79	6.11	0.06	-0.30	-1.98	9.04	20.00	1.21
9	67.5	0.02	-0.43	2.97	-0.34	-6.56	0.06	13.57	20.00	0.47
10	0	1.78	-4.55	1.05	0.74	-0.43	3.56	9.81	20.00	1.04
11	0	-4.87	-4.05	-0.46	0.11	0.06	0.28	4.45	20.00	3.49
12	0	-0.02	-1.51	-0.31	0.12	0.03	-0.54	1.92	20.00	9.42
13	90	-0.73	-3.26	-0.41	-0.08	0.36	0.04	2.94	20.00	5.80
14	0	-0.26	0.85	-0.41	0.00	-0.18	-0.33	1.56	20.00	+Large
15	112.5	-0.26	1.58	1.55	-0.03	5.90	0.00	11.81	20.00	0.69
16	127.5	-0.18	0.66	1.86	0.03	4.05	0.06	8.18	20.00	1.44
17	67.5	0.04	0.22	3.39	-0.30	6.07	-0.05	12.56	20.00	0.59
18	60	0.04	-0.27	2.57	0.05	4.11	-0.18	8.70	20.00	1.30
19	0	-2.82	-3.44	-1.15	0.41	0.06	1.74	4.04	20.00	3.95
20	105	0.12	-0.10	-0.78	-0.14	0.08	-0.43	1.30	20.00	+Large

Notes:
1. See Figure 2.10.14-4 for locations of sections.
2. The location specifies the angle at which the maximum stress intensity occurs. See Figure 2.10.14-1 for definition of angular location.
3. Stress components correspond to a cylindrical coordinate system.

Table 2.10.14-3 Side Drop with Internal Pressure, $P_m + P_b$ Stresses, ksi

Sec[1]	Location (deg)[2]	S_x[3]	S_y[3]	S_z[3]	S_{xy}[3]	S_{yz}[3]	S_{xz}[3]	Stress Intensity	Stress Allow.	MS
1	67.5	0.06	1.96	3.85	0.10	-7.45	-0.02	15.03	48.45	2.22
2	180	-0.06	5.49	-27.35	0.40	-0.01	0.00	32.87	48.45	0.47
3	67.5	0.07	2.32	4.74	0.08	6.85	-0.01	13.91	48.45	2.48
4	105	-0.38	-2.18	-0.40	0.07	-4.49	0.00	9.17	48.45	4.28
5	180	-0.10	3.68	-16.56	0.25	0.00	0.00	20.25	48.45	1.39
6	105	-0.10	6.74	2.59	0.03	3.79	-0.01	9.08	48.45	4.34
7	120	-0.31	-2.74	-0.38	-0.08	-6.52	-0.03	13.25	30.00	1.26
8	180	-3.38	1.06	11.77	0.00	0.00	-2.00	15.66	30.00	0.92
9	60	-0.07	0.46	3.44	-0.65	-7.78	0.24	15.90	30.00	0.89
10	0	4.60	-8.34	-11.23	0.64	-0.03	3.96	17.74	30.00	0.69
11	0	-8.51	-6.19	-0.09	0.09	0.09	0.82	8.59	30.00	2.49
12	0	0.19	-1.60	0.64	0.08	-0.06	-0.26	2.37	30.00	+Large
13	90	-1.43	-4.34	-0.43	-0.03	0.22	0.02	3.93	30.00	6.63
14	0	0.16	1.78	-1.80	0.02	-0.64	-0.30	3.84	30.00	6.81
15	120	-0.31	-3.50	-0.84	-0.15	6.59	0.01	13.45	30.00	1.23
16	180	-1.05	2.38	12.50	0.23	0.12	2.22	14.27	30.00	1.10
17	60	-0.08	1.62	4.85	-0.61	7.18	-0.31	14.78	30.00	1.03
18	37.5	-0.28	-0.47	6.66	0.12	5.17	-1.38	12.88	30.00	1.33
19	0	-1.16	-0.70	2.61	0.02	0.20	1.43	4.74	30.00	5.33
20	15	-2.43	-1.21	-1.48	0.08	-0.17	1.79	3.73	30.00	7.04

Notes:
1. See Figure 2.10.14-4 for locations of sections.
2. The location specifies the angle at which the maximum stress intensity occurs. See Figure 2.10.14-1 for definition of angular location.
3. Stress components correspond to a cylindrical coordinate system.

Table 2.10.14-4 1-Foot Side Drop with Internal Pressure, P + Q Stresses, ksi

Sec[1]	Location (deg)[2]	S_x[3]	S_y[3]	S_z[3]	S_{xy}[3]	S_{yz}[3]	S_{xz}[3]	Stress Intensity	Stress Allow.	MS
1	0	-0.55	15.41	23.96	-1.59	-0.42	0.12	24.70	96.90	2.92
2	0	-0.71	19.69	44.57	-1.80	-0.01	0.00	45.44	96.90	1.13
3	0	-0.54	13.83	26.27	-1.43	0.36	-0.13	26.97	96.90	2.59
4	105	-0.36	-2.17	3.28	0.07	-4.50	0.01	10.53	96.90	8.20
5	0	-0.18	6.18	23.65	-0.50	0.00	0.00	23.86	96.90	3.06
6	105	-0.38	-2.53	2.98	0.06	4.39	0.01	10.37	96.90	8.34
7	127.5	-0.28	-1.89	5.19	-0.29	-6.44	-0.03	14.72	60.00	3.08
8	180	-3.32	7.25	20.14	0.56	-0.01	-3.12	24.31	60.00	1.47
9	60	-0.93	8.89	16.68	-0.64	-7.74	1.26	22.56	60.00	1.66
10	0	0.34	6.19	26.82	0.50	-0.65	3.58	27.50	60.00	1.18
11	180	4.69	4.56	-9.20	0.03	-0.55	-3.99	16.06	60.00	2.74
12	180	-9.18	5.30	19.13	0.72	-0.15	1.68	28.54	60.00	1.10
13	90	-5.07	-10.02	0.47	-0.13	0.49	0.28	10.56	60.00	4.68
14	0	13.71	21.20	-4.61	-0.29	-0.83	-0.40	25.89	60.00	1.32
15	120	-0.32	-3.25	1.66	-0.15	6.60	0.17	14.09	60.00	3.26
16	180	-6.25	-4.80	8.34	-0.53	0.72	5.04	17.92	60.00	2.35
17	52.5	-0.81	9.24	19.43	-0.69	6.98	-1.50	24.02	60.00	1.50
18	0	-10.55	1.90	17.33	-1.49	-0.70	-6.67	31.10	60.00	0.93
19	0	-4.67	-5.23	-4.44	0.73	-0.11	2.00	4.31	60.00	+Large
20	45	-0.64	0.39	-1.81	0.39	-0.15	-3.41	7.01	60.00	7.56

Notes:
1. See Figure 2.10.14-4 for locations of sections.
2. The location specifies the angle at which the maximum stress intensity occurs. See Figure 2.10.14-1 for definition of angular location.
3. Stress components correspond to a cylindrical coordinate system.

Table 2.10.14-5 1-Foot Top-End Drop with Normal Internal Pressure, P_m Stresses, ksi

Sec[1]	S_x^2	S_y^2	S_z^2	S_{xy}^2	S_{yz}^2	S_{xz}^2	Stress Intensity	Stress Allow.	MS
1	0.00	-0.01	0.02	0.00	0.00	0.00	0.03	32.30	+Large
2	0.00	0.00	-0.42	0.00	0.00	0.00	0.42	32.30	+Large
3	0.00	-0.05	-0.95	0.00	0.00	0.00	0.96	32.30	+Large
4	-0.13	2.65	0.80	-0.18	0.00	0.00	2.81	32.30	+Large
5	-0.13	2.66	0.36	-0.18	0.00	0.00	2.82	32.30	+Large
6	-0.13	2.69	-0.15	-0.19	0.00	0.00	2.85	32.30	+Large
7	-0.14	2.75	0.82	-0.19	0.00	-0.05	2.92	20.00	5.85
8	-0.18	0.63	0.50	-0.05	0.01	0.14	0.84	20.00	+Large
9	0.00	-0.01	0.04	0.00	0.00	0.00	0.05	20.00	+Large
10	0.00	0.01	0.04	0.00	0.00	0.00	0.04	20.00	+Large
11	-0.04	0.01	-0.02	0.00	0.00	0.02	0.06	20.00	+Large
12	0.00	0.02	0.01	0.00	0.00	0.02	0.04	20.00	+Large
13	0.02	0.02	-0.21	0.00	0.00	0.03	0.24	20.00	+Large
14	0.04	0.05	-0.02	0.00	0.00	0.01	0.07	20.00	+Large
15	-0.15	2.63	-0.25	-0.18	0.01	0.04	2.91	20.00	5.87
16	-2.27	-1.66	-1.13	-0.24	0.10	0.88	2.16	20.00	8.26
17	0.02	0.35	-0.94	0.00	0.00	0.02	1.29	20.00	+Large
18	-2.14	0.67	-1.27	0.34	0.14	-0.50	3.12	20.00	5.41
19	-0.25	0.73	-1.44	0.10	-0.06	0.34	2.27	20.00	7.81
20	-0.27	-0.52	-2.01	-0.01	-0.01	0.31	1.85	20.00	9.81

Notes: 1. See Figure 2.10.14-4 for locations of sections.

2. Stress components correspond to a cylindrical coordinate system.

Table 2.10.14-6 1-Foot Top-End Drop with Internal Pressure, $P_m + P_b$ Stresses, ksi

Sec[15]	S_x[16]	S_y[2]	S_z[2]	S_{xy}[2]	S_{yz}[2]	S_{xz}[2]	Stress Intensity	Stress Allow.	MS
1	0.00	-0.01	0.03	0.00	0.00	0.00	0.03	48.45	+Large
2	0.00	0.00	-0.42	0.00	0.00	0.00	0.43	48.45	+Large
3	0.00	-0.11	-1.10	0.01	0.00	0.00	1.10	48.45	+Large
4	-0.21	2.84	0.84	-0.20	0.00	0.00	3.07	48.45	+Large
5	-0.20	2.85	0.39	-0.20	0.00	0.00	3.07	48.45	+Large
6	-0.21	2.94	-0.09	-0.21	0.01	0.01	3.18	48.45	+Large
7	-0.20	2.80	0.36	-0.20	0.00	-0.05	3.02	30.00	8.93
8	-0.33	0.92	1.28	-0.08	0.01	0.16	1.65	30.00	+Large
9	0.00	0.00	0.06	0.00	0.00	0.01	0.06	30.00	+Large
10	0.00	0.01	0.04	0.00	0.00	0.00	0.04	30.00	+Large
11	-0.06	0.02	-0.04	0.00	0.00	0.00	0.08	30.00	+Large
12	-0.01	0.02	0.00	0.00	0.00	0.02	0.05	30.00	+Large
13	0.33	0.48	-0.15	-0.01	0.00	0.03	0.63	30.00	+Large
14	0.08	0.13	-0.02	0.00	0.00	0.01	0.16	30.00	+Large
15	-0.19	2.70	-0.94	-0.19	0.01	0.05	3.65	30.00	7.22
16	-3.18	-3.36	-4.31	0.43	-0.36	1.53	3.42	30.00	7.77
17	0.00	0.22	-1.23	-0.02	0.01	0.02	1.45	30.00	+Large
18	-3.50	-0.35	-3.43	-0.47	-0.39	-1.04	4.34	30.00	5.91
19	-0.49	0.68	-1.77	0.14	-0.13	0.47	2.64	30.00	+Large
20	0.13	-0.14	-1.72	0.00	-0.01	1.83	4.10	30.00	6.32

[15] See Figure 2.10.14-4 for locations of sections.
[16] Stress components correspond to a cylindrical coordinate system.

Table 2.10.14-7 1-Foot Top-End Drop with Internal Pressure, P + Q Stresses, ksi

Sec[17]	S_x[18]	S_y[2]	S_z[2]	S_{xy}[2]	S_{yz}[2]	S_{xz}[2]	Stress Intensity	Stress Allow.	MS
1	-0.52	12.95	15.18	-1.32	0.04	0.04	15.83	96.90	5.12
2	-0.64	15.83	13.76	-1.49	0.00	0.00	16.74	96.90	4.79
3	-0.52	10.70	13.97	-1.14	-0.10	-0.08	14.61	96.90	5.63
4	-0.20	3.10	4.88	0.00	-0.21	0.02	5.10	96.90	+Large
5	-0.20	2.83	3.76	-0.20	0.00	0.00	3.97	96.90	+Large
6	-0.21	3.31	4.56	0.02	0.48	-0.01	4.93	96.90	+Large
7	-0.28	5.22	5.61	-0.18	-1.18	-0.12	6.91	60.00	7.68
8	-0.81	6.85	8.05	-0.38	-0.88	-0.76	9.45	60.00	5.35
9	-0.51	7.65	14.92	-0.65	0.20	0.33	15.50	60.00	2.87
10	2.39	4.05	20.04	1.25	-0.57	2.66	19.10	60.00	2.14
11	-2.18	-14.93	-8.39	2.15	0.03	-3.63	15.09	60.00	2.98
12	-11.68	-3.17	20.44	0.95	0.25	0.86	32.27	60.00	0.86
13	-12.94	-27.36	-3.27	2.41	1.70	0.18	24.72	60.00	1.43
14	14.78	25.68	0.00	0.43	2.99	0.07	26.38	60.00	1.27
15	-0.51	6.64	6.70	-0.24	1.89	0.26	9.09	60.00	5.60
16	-2.24	-10.97	2.01	-0.21	3.30	0.34	14.59	60.00	3.11
17	-1.28	7.78	13.30	-0.79	0.05	-1.06	14.80	60.00	3.05
18	-13.49	2.32	3.59	1.97	1.52	-5.23	20.64	60.00	1.91
19	-0.33	-21.42	-6.90	1.77	2.11	-0.54	21.71	60.00	1.76
20	-4.38	-1.14	-3.50	-0.08	-0.46	6.65	13.37	60.00	3.49

[17] See Figure 2.10.14-4 for locations of sections.
[18] Stress components correspond to a cylindrical coordinate system.

Table 2.10.14-8 1-Foot Top-Corner Drop with Internal Pressure, P_m Stresses, ksi

Sec[19]	Location (deg)[20]	S_x[21]	S_y[3]	S_z[3]	S_{xy}[3]	S_{yz}[3]	S_{xz}[3]	Stress Intensity	Stress Allow.	MS
1	180	0.00	0.10	-1.84	0.00	-0.03	-0.01	1.95	32.30	+Large
2	180	-0.03	-0.13	-3.67	0.00	0.02	0.00	3.65	32.30	7.85
3	0	0.02	0.11	-2.83	0.00	0.07	0.00	2.94	32.30	9.99
4	90	-0.14	2.66	0.59	0.04	-0.87	0.01	3.12	32.30	9.35
5	180	-0.15	2.63	-2.37	0.17	0.01	0.00	5.01	32.30	5.45
6	0	-0.14	2.80	-2.49	-0.22	0.05	0.00	5.31	32.30	5.08
7	120	-0.17	2.54	1.01	0.03	-1.26	-0.02	3.42	20.00	4.85
8	180	-0.75	1.14	2.00	0.05	-0.09	-0.55	2.97	20.00	5.73
9	60	0.00	-0.06	0.42	-0.04	-0.95	-0.01	1.96	20.00	9.20
10	0	0.10	-0.78	-0.21	0.09	-0.07	0.72	1.58	20.00	+Large
11	180	0.18	0.23	0.19	-0.01	0.04	-0.42	0.85	20.00	+Large
12	0	0.00	-0.23	-0.17	0.02	0.02	-0.19	0.43	20.00	+Large
13	82.5	-0.04	-0.25	0.00	0.02	0.07	0.00	0.30	20.00	+Large
14	90	0.03	-0.30	0.00	-0.01	0.08	-0.01	0.36	20.00	+Large
15	0	-0.13	2.29	-3.27	-0.17	0.05	-0.05	5.57	20.00	2.59
16	180	-2.14	-1.54	0.38	-0.23	0.09	0.87	3.12	20.00	5.41
17	0	0.03	0.55	-3.01	-0.03	0.07	0.07	3.57	20.00	4.60
18	0	-2.92	0.34	-3.47	-0.43	-0.12	-0.68	4.35	20.00	3.60
19	0	-1.02	-0.31	-3.45	0.01	0.12	0.47	3.24	20.00	5.17
20	0	-0.56	-0.65	-2.69	0.03	0.04	0.38	2.27	20.00	7.81

[19] See Figure 2.10.14-4 for locations of sections.
[20] The location specifies the angle at which the maximum stress intensity occurs. See Figure 2.10.14-1 for definition of angular location.
[21] Stress components correspond to a cylindrical coordinate system.

Table 2.10.14-9 1-Foot Top-Corner Drop with Internal Pressure, $P_m + P_b$ Stresses, ksi

Sec[22]	Location (deg)[23]	S_x[24]	S_y[3]	S_z[3]	S_{xy}[3]	S_{yz}[3]	S_{xz}[3]	Stress Intensity	Stress Allow.	MS
1	52.5	0.02	0.75	0.68	0.02	-1.19	-0.01	2.38	48.45	+Large
2	180	-0.02	1.88	-3.16	0.14	0.02	0.00	5.06	48.45	8.58
3	0	0.03	0.19	-2.96	-0.01	0.07	0.00	3.15	48.45	+Large
4	180	-0.21	5.36	1.54	0.29	-0.06	0.00	5.60	48.45	7.65
5	180	-0.22	2.93	-2.17	0.19	0.01	0.00	5.11	48.45	8.48
6	0	-0.04	3.07	-2.44	-0.23	0.04	-0.01	5.53	48.45	7.76
7	180	-0.30	4.86	3.07	0.23	-0.18	-0.03	5.20	30.00	4.77
8	180	-1.05	0.29	3.37	-0.02	0.08	-0.57	4.56	30.00	5.58
9	45	-0.02	0.29	0.44	-0.12	-1.30	0.03	2.62	30.00	+Large
10	0	0.63	-1.09	-2.46	0.08	0.07	0.74	3.44	30.00	7.72
11	180	0.85	0.60	0.02	-0.01	0.05	-0.55	1.37	30.00	+Large
12	180	0.06	0.13	0.24	0.00	0.01	-0.25	0.54	30.00	+Large
13	90	-0.13	-0.39	0.03	-0.02	0.10	0.01	0.47	30.00	+Large
14	105	-0.05	-0.48	0.02	-0.13	0.07	0.00	0.56	30.00	+Large
15	15	-0.16	2.38	-3.36	-0.02	0.29	-0.04	5.77	30.00	4.20
16	7.5	-1.53	-2.80	-6.23	0.11	-0.21	0.48	4.81	30.00	5.24
17	0	-0.03	0.52	-3.23	-0.03	0.06	-0.02	3.75	30.00	7.00
18	0	-4.71	-0.82	-5.65	-0.61	-0.44	-1.37	6.00	30.00	4.00
19	7.5	-0.55	-0.93	-4.50	0.09	0.07	0.29	4.02	30.00	6.46
20	15	0.53	-0.15	-1.96	0.03	0.01	1.82	4.41	30.00	5.80

[22] See Figure 2.10.14-4 for locations of sections.
[23] The location specifies the angle at which the maximum stress intensity occurs. See Figure 2.10.14-1 for definition of angular location.
[24] Stress components correspond to a cylindrical coordinate system.

Table 2.10.14-10 1-Foot Top-Corner Drop with Internal Pressure, P + Q Stresses, ksi

Sec[25]	Location (deg)[26]	S_x[27]	S_y[3]	S_z[3]	S_{xy}[3]	S_{yz}[3]	S_{xz}[3]	Stress Intensity	Stress Allow.	MS
1	0	-0.61	13.84	16.03	-1.45	0.00	0.09	16.78	96.90	4.77
2	0	-0.68	17.69	17.49	-1.62	0.02	0.00	18.65	96.90	4.20
3	180	-0.58	10.62	13.95	1.13	0.13	-0.09	14.65	96.90	5.61
4	180	-0.20	5.24	5.22	0.28	-0.07	0.01	5.52	96.90	+Large
5	0	-0.08	3.13	6.51	-0.23	0.01	0.00	6.61	96.90	+Large
6	180	-0.23	2.64	5.39	0.20	0.04	0.00	5.63	96.90	+Large
7	180	-0.31	5.20	7.56	0.25	-0.19	0.00	7.90	60.00	6.59
8	180	-1.00	6.47	11.74	0.54	0.07	-1.69	13.22	60.00	3.54
9	30	-0.89	8.92	13.67	-0.16	-1.38	1.06	15.09	60.00	2.98
10	0	0.94	6.46	15.53	-0.24	-0.04	1.11	14.77	60.00	3.06
11	7.5	5.44	-0.93	-7.47	0.03	-0.02	-3.90	15.09	60.00	2.98
12	180	-9.30	4.39	18.60	0.70	-0.13	1.85	28.18	60.00	1.13
13	75	7.18	10.40	-0.43	-0.01	0.04	-0.03	10.83	60.00	4.54
14	0	13.27	19.46	-2.77	-0.31	-0.19	-0.14	22.25	60.00	1.70
15	180	-0.25	3.87	8.31	0.26	0.03	0.26	8.59	60.00	5.98
16	165	-2.03	-4.30	7.35	-0.10	0.25	0.62	11.71	60.00	4.12
17	180	-1.17	7.04	14.41	0.73	0.03	-1.36	15.88	60.00	2.78
18	180	-12.10	2.59	6.12	1.79	1.42	-4.91	21.15	60.00	1.84
19	0	-1.40	0.01	-4.32	0.09	-0.01	0.22	4.36	60.00	+Large
20	15	1.69	0.13	-2.70	0.02	0.00	3.18	7.73	60.00	6.76

[25] See Figure 2.10.14-4 for locations of sections.
[26] The location specifies the angle at which the maximum stress intensity occurs. See Figure 2.10.14-1 for definition of angular location.
[27] Stress components correspond to a cylindrical coordinate system.

Table 2.10.14-11 1-Foot Bottom-End Drop with Internal Pressure, P_m Stresses, ksi

Sec[28]	S_x[29]	S_y[2]	S_z[2]	S_{xy}[2]	S_{yz}[2]	S_{xz}[2]	Stress Intensity	Stress Allow.	MS
1	0.01	0.08	-1.34	0.00	0.00	-0.01	1.42	32.30	+Large
2	0.00	0.00	-0.78	0.00	0.00	0.00	0.78	32.30	+Large
3	0.00	0.02	-0.34	0.00	0.00	0.00	0.36	32.30	+Large
4	-0.13	2.69	-0.49	-0.18	0.00	0.00	3.19	32.30	9.13
5	-0.13	2.66	0.00	-0.18	0.00	0.00	2.82	32.30	+Large
6	-0.13	2.67	0.43	-0.18	0.00	0.00	2.82	32.30	+Large
7	-0.12	2.58	-0.57	-0.18	0.00	0.00	3.16	20.00	5.33
8	0.07	1.33	-0.38	-0.01	-0.01	0.04	1.71	20.00	+Large
9	0.01	0.09	-1.30	-0.01	0.00	-0.03	1.39	20.00	+Large
10	0.09	0.29	-0.98	0.01	0.00	-0.08	1.28	20.00	+Large
11	0.62	0.06	-3.56	-0.04	-0.22	0.14	4.20	20.00	3.76
12	-0.35	0.34	-1.66	0.04	0.03	-0.17	2.03	20.00	8.85
13	0.69	0.93	-0.79	0.02	0.00	-0.13	1.73	20.00	+Large
14	-0.40	-0.68	-4.05	0.02	-0.05	-0.60	3.85	20.00	4.19
15	-0.14	2.68	0.45	-0.18	0.00	0.03	2.84	20.00	6.04
16	-0.08	1.08	0.29	-0.08	0.00	-0.06	1.18	20.00	+Large
17	0.00	0.02	-0.29	0.00	0.00	0.01	0.32	20.00	+Large
18	0.00	0.06	-0.18	0.00	0.00	0.02	0.25	20.00	+Large
19	-0.04	0.22	-0.22	0.00	0.00	0.03	0.45	20.00	+Large
20	-0.15	0.08	-0.90	0.00	0.00	-0.25	1.06	20.00	+Large

[28] See Figure 2.10.14-4 for locations of sections.
[29] Stress components correspond to a cylindrical coordinate system.

Table 2.10.14-12 1-Foot Bottom-End Drop with Internal Pressure, $P_m + P_b$ Stresses, ksi

Sec[30]	S_x[31]	S_y[2]	S_z[2]	S_{xy}[2]	S_{yz}[2]	S_{xz}[2]	Stress Intensity	Stress Allow.	MS
1	0.01	0.12	-1.35	-0.01	0.00	-0.01	1.47	48.45	+Large
2	0.00	0.01	-0.78	0.00	0.00	0.00	0.79	48.45	+Large
3	0.00	0.02	-0.34	0.00	0.00	0.00	0.36	48.45	+Large
4	-0.20	2.92	-0.45	-0.20	0.00	0.00	3.38	48.45	+Large
5	-0.20	2.85	0.03	-0.20	0.00	0.00	3.07	48.45	+Large
6	-0.21	2.85	0.47	-0.20	0.00	0.00	3.09	48.45	+Large
7	-0.19	2.75	-0.71	-0.19	0.00	0.00	3.47	30.00	7.65
8	-0.08	1.45	-0.52	0.10	-0.01	0.01	1.98	30.00	+Large
9	0.03	0.11	-1.36	-0.01	-0.01	-0.07	1.47	30.00	+Large
10	0.07	0.21	-1.16	-0.03	-0.03	-0.06	1.38	30.00	+Large
11	-0.32	-1.37	-7.60	-0.07	-0.62	0.23	7.37	30.00	3.07
12	-0.63	-0.07	-3.13	0.04	0.03	-0.26	3.09	30.00	8.71
13	1.89	2.83	-0.47	0.01	-0.01	-0.11	3.31	30.00	8.06
14	1.41	3.02	-2.90	0.00	0.05	-0.70	6.03	30.00	3.98
15	-0.20	2.77	0.13	-0.19	0.00	0.03	2.99	30.00	9.03
16	-0.18	1.29	0.63	-0.10	-0.01	-0.06	1.49	30.00	+Large
17	0.01	0.02	-0.31	0.00	0.00	0.02	0.34	30.00	+Large
18	0.01	0.07	-0.18	0.00	0.00	0.02	0.26	30.00	+Large
19	-0.06	0.22	-0.45	0.00	0.01	0.02	0.67	30.00	+Large
20	-0.31	0.33	-0.88	0.01	0.00	-1.66	3.37	30.00	7.90

[30] See Figure 2.10.14-4 for locations of sections.
[31] Stress components correspond to a cylindrical coordinate system.

Table 2.10.14-13 1-Foot Bottom-End Drop with Internal Pressure, P + Q Stresses, ksi

Sec[32]	S_x[33]	S_y[2]	S_z[2]	S_{xy}[2]	S_{yz}[2]	S_{xz}[2]	Stress Intensity	Stress Allow.	MS
1	-0.51	12.99	13.84	-1.32	0.03	0.04	14.48	96.90	5.69
2	-0.64	15.83	13.40	-1.49	0.00	0.00	16.74	96.90	4.79
3	-0.53	10.82	14.75	-1.15	-0.10	-0.07	15.40	96.90	5.29
4	-0.16	3.34	3.35	-0.07	-0.56	-0.01	4.06	96.90	+Large
5	-0.20	2.83	3.40	-0.20	0.00	0.00	3.61	96.90	+Large
6	-0.21	3.26	5.02	0.02	0.46	-0.01	5.34	96.90	+Large
7	-0.28	5.08	4.11	-0.19	-1.24	-0.08	6.22	60.00	8.65
8	-0.61	7.94	8.34	-0.39	-0.92	-0.87	9.81	60.00	5.12
9	-0.52	7.71	13.65	-0.66	0.20	0.36	14.24	60.00	3.21
10	2.70	4.55	19.44	1.26	-0.54	2.56	18.13	60.00	2.31
11	1.52	0.70	-16.74	-0.02	-1.30	-1.91	18.76	60.00	2.20
12	-12.30	-3.34	17.50	0.96	0.22	0.72	29.94	60.00	1.00
13	-13.81	-28.99	-4.35	2.43	1.73	0.00	25.26	60.00	1.38
14	11.85	19.76	-7.14	0.45	1.90	-0.81	27.22	60.00	1.20
15	-0.46	6.38	6.77	-0.23	1.81	0.24	8.88	60.00	5.76
16	-1.29	-7.82	1.82	-0.45	3.42	0.31	11.86	60.00	4.06
17	-1.31	7.38	13.67	-0.76	0.05	-1.07	15.20	60.00	2.95
18	-10.04	2.68	6.68	1.51	1.13	-4.19	19.03	60.00	2.15
19	-0.21	-22.47	-6.98	1.67	2.23	-0.70	22.88	60.00	1.62
20	-5.62	-2.02	-2.52	-0.04	-0.44	5.39	11.25	60.00	4.33

[32] See Figure 2.10.14-4 for locations of sections.
[33] Stress components correspond to a cylindrical coordinate system.

Table 2.10.14-14 1-Foot Bottom-Corner Drop with Internal Pressure, P_m Stresses, ksi

Sec[34]	Location (deg)[35]	S_x[36]	S_y[3]	S_z[3]	S_{xy}[3]	S_{yz}[3]	S_{xz}[3]	Stress Intensity	Stress Allow.	MS
1	0	0.03	0.29	-3.53	-0.01	-0.09	-0.02	3.83	32.30	7.43
2	180	-0.03	-0.13	-3.65	0.00	-0.02	0.00	3.62	32.30	7.92
3	180	0.00	0.13	-2.21	0.01	0.03	0.01	2.34	32.30	+Large
4	0	-0.14	2.80	-2.63	-0.21	-0.05	0.00	5.44	32.30	4.94
5	180	-0.15	2.63	-2.35	0.17	-0.01	0.00	4.99	32.30	5.47
6	82.5	-0.14	2.69	0.54	0.04	0.82	0.00	3.11	32.30	9.39
7	0	-0.11	2.28	-3.40	-0.17	-0.05	0.08	5.70	20.00	2.51
8	7.5	0.17	0.97	-2.24	-0.02	-0.04	0.23	3.23	20.00	5.19
9	0	0.02	0.09	-3.75	0.00	-0.08	-0.07	3.84	20.00	4.21
10	0	0.50	-0.14	-2.88	0.07	-0.06	0.08	3.39	20.00	4.90
11	0	-0.04	-0.24	-4.08	0.05	0.26	0.53	4.22	20.00	3.74
12	0	-0.96	-0.25	-3.79	0.03	-0.07	-0.25	3.56	20.00	4.62
13	180	0.12	0.71	-0.73	0.01	0.00	-0.24	1.51	20.00	+Large
14	180	-0.38	-0.52	-3.79	-0.02	0.06	-0.75	3.73	20.00	4.36
15	112.5	-0.16	2.56	0.76	0.04	1.25	0.01	3.36	20.00	4.95
16	165	-0.16	1.58	1.85	-0.01	0.53	0.46	2.59	20.00	6.72
17	180	0.00	0.16	-1.95	-0.01	0.02	0.05	2.12	20.00	8.43
18	180	-0.01	0.04	-1.25	0.00	0.01	0.08	1.29	20.00	+Large
19	180	-0.09	0.20	-0.32	0.02	-0.03	0.17	0.61	20.00	+Large
20	82.5	0.02	-0.38	-0.99	0.10	0.02	-0.16	1.08	20.00	+Large

[34] See Figure 2.10.14-4 for locations of sections.
[35] The location specifies the angle at which the maximum stress intensity occurs. See Figure 2.10.14-1 for definition of angular location.
[36] Stress components correspond to a cylindrical coordinate system.

Table 2.10.14-15 1-Foot Bottom-Corner Drop with Internal Pressure, $P_m + P_b$ Stresses, ksi

Sec[37]	Location (deg)[38]	S_x[39]	S_y[3]	S_z[3]	S_{xy}[3]	S_{yz}[3]	S_{xz}[3]	Stress Intensity	Stress Allow.	MS
1	0	0.04	0.39	-3.44	-0.02	-0.08	0.00	3.84	48.45	+Large
2	180	-0.02	1.88	-3.13	0.14	-0.03	0.00	5.03	48.45	8.63
3	180	0.01	0.38	-2.18	0.02	0.04	0.00	2.56	48.45	+Large
4	0	-0.05	3.09	-2.58	-0.23	-0.04	0.01	5.69	48.45	7.51
5	180	-0.22	2.87	-2.17	0.19	-0.01	0.00	5.06	48.45	8.58
6	180	-0.21	5.48	1.33	0.30	0.06	0.00	5.72	48.45	7.47
7	0	-0.03	2.32	-3.59	-0.17	-0.03	0.08	5.92	30.00	4.07
8	7.5	0.41	0.83	-2.60	-0.03	0.02	0.22	3.45	30.00	7.70
9	0	0.09	0.04	-3.99	0.00	-0.11	-0.22	4.11	30.00	6.30
10	0	0.50	-0.74	-4.57	0.03	-0.07	0.18	5.08	30.00	4.91
11	0	-0.70	-1.66	-8.28	0.10	0.70	0.77	7.82	30.00	2.84
12	0	-0.96	-0.45	-4.83	-0.01	-0.06	-0.34	4.41	30.00	5.80
13	7.5	1.23	2.32	-0.47	0.06	0.00	-0.02	2.79	30.00	9.75
14	7.5	1.46	2.91	-2.86	0.01	-0.01	-0.44	5.81	30.00	4.16
15	180	-0.28	4.86	3.14	0.23	0.18	-0.02	5.19	30.00	4.78
16	180	-0.09	1.16	4.05	0.13	-0.08	0.62	4.34	30.00	5.91
17	37.5	-0.01	0.54	0.81	-0.14	1.21	-0.06	2.45	30.00	+Large
18	22.5	-0.07	0.01	1.28	0.02	1.01	-0.28	2.46	30.00	+Large
19	180	-0.21	0.31	-0.27	0.05	-0.08	0.25	0.83	30.00	+Large
20	45	-0.23	0.33	-0.87	0.11	-0.03	-1.67	3.41	30.00	7.80

[37] Figure 2.10.14-4 for locations of sections.
[38] The location specifies the angle at which the maximum stress intensity occurs. See Figure 2.10.14-1 for definition of angular location.
[39] Stress components correspond to a cylindrical coordinate system.

Table 2.10.14-16 1-Foot Bottom-Corner Drop with Internal Pressure, P + Q Stresses, ksi

Sec[40]	Location (deg)[41]	S_x[42]	S_y[3]	S_z[3]	S_{xy}[3]	S_{yz}[3]	S_{xz}[3]	Stress Intensity	Stress Allow.	MS
1	180	-0.62	12.07	14.85	1.27	-0.13	0.07	15.60	96.90	5.21
2	0	-0.68	17.69	17.35	-1.62	-0.02	0.00	18.65	96.90	4.20
3	0	-0.57	12.42	16.02	-1.31	-0.01	-0.10	16.72	96.90	4.80
4	180	-0.08	2.46	5.51	0.17	-0.04	0.00	5.60	96.90	+Large
5	0	-0.09	3.16	6.42	-0.23	-0.01	0.00	6.52	96.90	+Large
6	180	-0.22	5.33	5.05	0.30	0.06	0.00	5.59	96.90	+Large
7	180	-0.22	3.33	6.15	0.24	-0.04	-0.04	6.39	60.00	8.39
8	0	0.29	4.73	-5.70	-0.27	-0.09	-0.99	10.61	60.00	4.66
9	180	-1.36	7.51	13.74	0.81	0.02	1.25	15.38	60.00	2.90
10	180	1.51	7.41	13.95	0.36	-0.24	0.37	12.49	60.00	3.80
11	0	1.43	0.66	-17.49	0.04	1.40	-1.33	19.21	60.00	2.12
12	180	-9.62	4.51	17.43	0.73	-0.17	2.15	27.43	60.00	1.19
13	7.5	8.54	12.54	-0.89	0.03	0.00	-0.04	13.43	60.00	3.47
14	0	11.05	15.72	-8.54	-0.22	-0.32	-0.43	24.29	60.00	1.47
15	127.5	-0.23	4.70	7.10	0.00	1.04	0.17	7.72	60.00	6.77
16	180	-5.29	-6.02	-0.11	-0.63	0.52	3.45	9.07	60.00	5.62
17	30	-0.79	8.41	14.78	-0.16	1.26	-1.19	15.99	60.00	2.75
18	0	-10.18	2.24	9.24	-1.50	-0.97	-4.88	21.99	60.00	1.73
19	165	-0.10	1.23	-1.27	-0.02	-0.02	-0.22	2.54	60.00	+Large
20	75	-0.96	0.43	-1.89	0.03	-0.01	-3.39	6.84	60.00	7.77

[40] See Figure 2.10.14-4 for locations of sections.
[41] The location specifies the angle at which the maximum stress intensity occurs. See Figure 2.10.14-1 for definition of angular location.
[42] Stress components correspond to a cylindrical coordinate system.

Table 2.10.14-17 30-Foot Side Drop with Internal Pressure, P_m Stresses, ksi

Sec[43]	Location (deg)[44]	S_x[45]	S_y[3]	S_z[3]	S_{xy}[3]	S_{yz}[3]	S_{xz}[3]	Stress Intensity	Stress Allow.	MS
1	75	0.04	0.89	5.89	0.11	-15.69	-0.04	31.78	67.83	1.13
2	0	-0.30	4.10	66.15	-0.43	-0.03	0.00	66.50	67.83	0.02
3	75	0.08	0.97	6.23	0.07	14.38	0.01	29.24	67.83	1.32
4	97.5	-0.31	1.59	1.21	0.02	-9.10	0.02	18.20	67.83	2.73
5	180	-0.12	2.40	-36.71	0.12	-0.01	0.00	39.12	67.83	0.73
6	97.5	-0.31	1.50	0.66	-0.02	9.07	-0.01	18.16	67.83	2.74
7	112.5	-0.37	0.56	2.52	-0.23	-12.30	-0.04	24.67	48.00	0.95
8	180	-3.13	3.13	10.63	0.08	-0.56	-3.64	15.61	48.00	2.07
9	75	0.02	-0.55	5.28	-0.81	-15.37	0.09	31.32	48.00	0.53
10	0	4.62	-9.90	3.03	1.72	-0.95	7.57	21.90	48.00	1.19
11	0	-11.37	-9.00	-0.92	0.29	0.10	0.26	10.50	48.00	3.57
12	0	-0.01	-3.58	-0.50	0.28	0.02	-1.20	4.59	48.00	9.46
13	90	-1.53	-7.84	-0.72	-0.20	0.73	0.06	7.28	48.00	5.59
14	127.5	0.31	-0.09	-0.05	-1.20	0.67	0.35	2.83	48.00	+Large
15	112.5	-0.29	-0.22	1.50	-0.43	12.67	0.02	25.41	48.00	0.89
16	120	-0.16	-0.93	1.93	-0.02	8.29	-0.07	16.83	48.00	1.85
17	75	0.05	0.84	5.35	-0.73	14.28	-0.05	28.95	48.00	0.66
18	67.5	0.05	-0.15	4.57	0.03	9.72	-0.32	20.02	48.00	1.40
19	0	-6.41	-8.47	-2.13	1.01	0.16	3.99	9.76	48.00	3.92
20	15	-2.56	-0.62	-1.27	0.41	-0.29	0.45	2.32	48.00	+Large

[43] See Figure 2.10.14-4 for locations of sections.
[44] The location specifies the angle at which the maximum stress intensity occurs. See Figure 2.10.14-1 for definition of angular location.
[45] Stress components correspond to a cylindrical coordinate system.

Table 2.10.14-18 30-Foot Side Drop with Internal Pressure, $P_m + P_b$ Stresses, ksi

Sec[46]	Location (deg)[47]	S_x[48]	S_y[3]	S_z[3]	S_{xy}[3]	S_{yz}[3]	S_{xz}[3]	Stress Intensity	Stress Allow.	MS
1	75	0.07	3.30	6.47	0.19	-17.17	-0.04	34.49	96.90	1.81
2	180	-0.09	8.89	-65.21	0.65	-0.03	0.00	74.14	96.90	0.31
3	75	0.13	3.98	7.54	0.14	15.84	0.00	31.88	96.90	2.04
4	97.5	-0.50	-6.43	-1.73	0.03	-9.93	0.01	20.41	96.90	3.75
5	0	-0.26	3.65	40.86	-0.45	-0.01	0.00	41.17	96.90	1.35
6	97.5	-0.46	-6.87	-2.30	-0.02	9.80	0.01	20.13	96.90	3.81
7	112.5	-0.37	-6.53	-2.00	-0.19	-13.83	-0.04	28.04	68.50	1.44
8	180	-5.70	2.96	22.06	0.07	-0.15	-3.64	28.71	68.50	1.39
9	67.5	-0.15	0.45	6.24	-1.51	-17.91	0.42	36.41	68.50	0.88
10	0	10.64	-18.81	-23.45	1.44	-0.18	8.60	38.28	68.50	0.79
11	0	-19.75	-13.55	-0.19	0.25	0.16	1.39	19.77	68.50	2.46
12	0	0.45	-3.78	1.86	0.18	-0.19	-0.51	5.83	68.50	+Large
13	90	-2.66	-9.71	-0.67	-0.11	0.43	0.01	9.08	68.50	6.54
14	0	0.61	3.47	-1.97	0.02	-0.65	-0.53	5.69	68.50	+Large
15	112.5	-0.33	-7.35	-2.50	-0.44	13.99	0.02	28.41	68.50	1.41
16	127.5	-0.11	-2.45	-0.26	0.04	12.99	0.54	26.10	68.50	1.62
17	67.5	-0.07	2.89	8.46	-1.40	16.45	-0.51	33.50	68.50	1.04
18	52.5	-0.37	-0.58	10.45	0.23	12.54	-1.93	27.69	68.50	1.47
19	22.5	-0.91	-4.63	6.48	0.55	0.46	1.91	11.68	68.50	4.86
20	15	-5.76	-2.35	-2.16	0.25	-0.35	2.61	6.40	68.50	9.70

[46] See Figure 2.10.14-4 for locations of sections.
[47] The location specifies the angle at which the maximum stress intensity occurs. See Figure 2.10.14-1 for definition of angular location.
[48] Stress components correspond to a cylindrical coordinate system.

Table 2.10.14-19 30-Foot Top-End Drop with Internal Pressure, P_m Stresses, ksi

Sec[49]	S_x[50]	S_y[2]	S_z[2]	S_{xy}[2]	S_{yz}[2]	S_{xz}[2]	Stress Intensity	Stress Allow.	MS
1	0.00	0.00	-0.16	0.00	0.00	0.00	0.16	67.83	+Large
2	0.00	0.00	-1.49	0.00	0.00	0.00	1.50	67.83	+Large
3	0.02	-0.11	-3.07	0.01	0.00	-0.01	3.08	67.83	+Large
4	-0.13	2.65	0.60	-0.18	0.00	0.00	2.81	67.83	+Large
5	-0.13	2.66	-0.71	-0.18	0.00	0.00	3.39	67.83	+Large
6	-0.12	2.76	-2.20	-0.19	0.01	0.00	4.97	67.83	+Large
7	-0.14	2.74	0.68	-0.19	0.00	-0.04	2.90	48.00	+Large
8	-0.18	0.67	0.42	0.06	-0.01	0.13	0.89	48.00	+Large
9	0.00	0.01	-0.09	0.00	0.00	0.00	0.09	48.00	+Large
10	0.00	0.02	-0.04	0.00	0.00	-0.01	0.07	48.00	+Large
11	-0.02	0.03	-0.03	0.00	0.00	0.00	0.07	48.00	+Large
12	-0.01	0.01	-0.01	0.00	0.00	-0.01	0.03	48.00	+Large
13	0.04	0.06	-0.22	0.00	0.00	0.02	0.28	48.00	+Large
14	0.01	0.01	-0.02	0.00	0.00	0.00	0.03	48.00	+Large
15	-0.17	2.42	-2.51	0.01	0.08	0.05	4.94	48.00	8.72
16	-6.61	-6.94	-4.45	-0.87	0.30	2.74	6.31	48.00	6.61
17	0.05	1.10	-3.01	0.00	0.05	0.07	4.11	48.00	+Large
18	-6.44	1.95	-3.98	1.02	0.41	-1.48	9.35	48.00	4.13
19	-0.66	1.84	-3.89	0.26	-0.17	0.99	6.04	48.00	6.95
20	-1.11	-1.22	-4.78	-0.08	-0.11	1.01	4.23	48.00	+Large

[49] See Figure 2.10.14-4 for locations of sections.
[50] Stress components correspond to a cylindrical coordinate system.

Table 2.10.14-20 30-Foot Top-End Drop with Internal Pressure, $P_m + P_b$ Stresses, ksi

Sec[51]	S_x[52]	S_y[2]	S_z[2]	S_{xy}[2]	S_{yz}[2]	S_{xz}[2]	Stress Intensity	Stress Allow.	MS
1	0.00	0.00	-0.16	0.00	0.00	0.00	0.16	96.90	+Large
2	0.00	0.01	-1.50	0.00	0.00	0.00	1.51	96.90	+Large
3	0.02	-0.30	-3.47	0.02	0.01	0.00	3.49	96.90	+Large
4	-0.21	2.84	0.64	-0.20	0.00	0.00	3.07	96.90	+Large
5	-0.20	2.84	-0.68	-0.20	0.00	0.00	3.53	96.90	+Large
6	-0.22	3.12	-2.13	-0.22	0.01	0.01	5.26	96.90	+Large
7	-0.20	2.78	0.25	-0.19	0.00	-0.04	3.01	68.50	+Large
8	-0.33	0.94	1.15	-0.08	0.01	0.16	1.52	68.50	+Large
9	0.00	0.01	-0.09	0.00	0.00	0.00	0.10	68.50	+Large
10	0.00	0.02	-0.07	0.00	0.00	-0.01	0.09	68.50	+Large
11	-0.04	0.01	-0.07	0.00	0.00	-0.03	0.10	68.50	+Large
12	-0.01	0.01	-0.02	0.00	0.00	-0.01	0.04	68.50	+Large
13	0.27	0.40	-0.17	-0.01	0.00	0.03	0.57	68.50	+Large
14	0.02	0.02	-0.03	0.00	0.00	0.01	0.05	68.50	+Large
15	-0.18	2.46	-3.79	-0.17	0.01	0.06	6.25	68.50	9.96
16	-9.52	-11.56	-13.10	1.37	-1.07	4.69	10.62	68.50	5.45
17	0.00	0.75	-3.79	-0.06	0.02	0.06	4.54	68.50	+Large
18	-10.51	-1.13	-10.56	-1.41	-1.16	-3.09	13.02	68.50	4.26
19	-1.35	1.80	-4.42	0.40	-0.31	1.41	6.85	68.50	9.00
20	0.31	-0.29	-3.55	0.00	-0.02	3.23	7.52	68.50	8.11

[51] See Figure 2.10.14-4 for locations of sections.
[52] Stress components correspond to a cylindrical coordinate system.

Table 2.10.14-21 30-Foot Top-Corner Drop with Internal Pressure, P_m Stresses, ksi

Sec[53]	Location (deg)[54]	S_x[55]	S_y[3]	S_z[3]	S_{xy}[3]	S_{yz}[3]	S_{xz}[3]	Stress Intensity	Stress Allow.	MS
1	67.5	0.02	0.20	0.80	0.04	-2.72	-0.02	5.48	67.83	+Large
2	180	-0.04	-0.28	-10.37	0.00	0.04	0.00	10.33	67.83	5.57
3	52.5	0.07	0.30	-5.70	0.02	3.53	0.00	9.26	67.83	6.33
4	120	-0.19	2.32	-0.33	-0.06	-1.41	0.00	3.87	67.83	+Large
5	180	-0.08	2.48	-6.10	0.14	0.02	0.00	8.59	67.83	6.90
6	0	-0.17	2.59	-5.85	-0.24	0.04	0.02	8.46	67.83	7.02
7	120	-0.19	1.96	-0.08	0.00	-2.50	0.03	5.40	48.00	7.89
8	180	-1.22	1.17	2.55	0.05	-0.18	-1.09	4.37	48.00	9.98
9	60	0.01	-0.12	0.86	-0.14	-2.70	0.00	5.50	48.00	7.73
10	0	0.44	-1.90	-0.39	0.26	-0.20	1.58	3.77	48.00	+Large
11	0	-1.54	-1.53	-0.01	0.05	-0.02	-0.23	1.63	48.00	+Large
12	0	0.03	-0.75	-0.27	0.07	0.01	-0.48	1.16	48.00	+Large
13	90	-0.17	-1.05	-0.06	-0.03	0.10	0.00	1.01	48.00	+Large
14	97.5	0.11	-0.49	-0.02	-0.10	0.11	-0.01	0.66	48.00	+Large
15	0	-0.22	1.61	-6.24	-0.20	-0.02	-0.04	7.88	48.00	5.09
16	180	-6.31	-7.41	-1.56	-0.90	0.29	2.61	7.97	48.00	5.02
17	30	0.08	1.49	-7.98	-0.13	2.34	0.18	10.58	48.00	3.54
18	0	-7.62	0.50	-10.26	-1.09	-0.25	-1.78	11.84	48.00	3.05
19	0	-2.63	-1.19	-8.95	0.04	0.32	1.43	8.09	48.00	4.93
20	0	-1.82	-1.55	-6.33	0.14	0.20	1.14	5.25	48.00	8.14

[53] See Figure 2.10.14-4 for locations of sections.
[54] The location specifies the angle at which the maximum stress intensity occurs. See Figure 2.10.14-1 for definition of angular location.
[55] Stress components correspond to a cylindrical coordinate system.

Table 2.10.14-22 30-Foot Top-Corner Drop with Internal Pressure, $P_m + P_b$ Stresses, ksi

Sec[56]	Location (deg)[57]	S_x[58]	S_y[3]	S_z[3]	S_{xy}[3]	S_{yz}[3]	S_{xz}[3]	Stress Intensity	Stress Allow.	MS
1	60	0.04	1.44	1.37	0.04	-3.16	-0.02	6.33	96.90	+Large
2	180	-0.03	3.04	-9.78	0.22	0.04	0.00	12.83	96.90	6.55
3	60	0.04	0.53	-4.64	0.05	4.17	0.01	9.82	96.90	8.87
4	180	-0.16	6.38	0.28	0.33	-0.14	-0.02	6.58	96.90	+Large
5	180	-0.12	7.50	-4.28	0.48	0.02	0.00	11.80	96.90	7.21
6	0	-0.27	4.85	-5.03	-0.40	0.01	0.04	9.91	96.90	8.78
7	127.5	-0.25	-0.78	-1.40	-0.07	-3.30	0.01	6.64	68.50	9.32
8	180	-1.96	0.27	5.70	-0.03	0.07	-1.09	7.97	68.50	7.59
9	52.5	-0.03	0.56	0.96	-0.30	-3.42	0.05	6.88	68.50	8.96
10	0	1.66	-3.19	-5.62	0.24	0.03	1.68	8.03	68.50	7.53
11	180	1.34	1.11	0.01	-0.01	0.08	-0.94	2.30	68.50	+Large
12	0	-0.10	-0.60	-0.13	0.09	0.02	-0.67	1.36	68.50	+Large
13	105	-0.03	-0.98	-0.06	-0.26	0.03	0.01	1.09	68.50	+Large
14	105	0.08	-0.63	-0.01	-0.23	0.09	0.00	0.86	68.50	+Large
15	15	-0.02	2.92	-6.20	0.08	-0.25	-0.03	9.13	68.50	6.50
16	0	-9.28	-10.03	-13.27	1.18	-0.98	4.68	10.55	68.50	5.49
17	45	0.17	1.62	-6.23	-0.33	3.87	0.37	11.06	68.50	5.19
18	0	-12.28	-2.39	-15.48	-1.58	-1.06	-3.57	15.87	68.50	3.32
19	7.5	-1.31	-2.99	-12.42	0.24	0.21	0.86	11.28	68.50	5.07
20	15	1.26	-0.32	-4.05	0.08	0.04	3.14	8.23	68.50	7.32

[56] See Figure 2.10.14-4 for locations of sections.
[57] The location specifies the angle at which the maximum stress intensity occurs. See Figure 2.10.14-1 for definition of angular location.
[58] Stress components correspond to a cylindrical coordinate system.

Table 2.10.14-23 30-Foot Bottom-End Drop with Internal Pressure, P_m Stresses, ksi

Sec[59]	S_x[60]	S_y[2]	S_z[2]	S_{xy}[2]	S_{yz}[2]	S_{xz}[2]	Stress Intensity	Stress Allow.	MS
1	0.02	0.24	-4.22	-0.01	-0.01	-0.02	4.46	67.83	+Large
2	0.00	0.00	-2.55	0.00	0.00	0.00	2.55	67.83	+Large
3	0.00	0.09	-1.21	0.00	0.00	0.01	1.30	67.83	+Large
4	-0.12	2.77	-3.26	-0.18	-0.01	0.00	6.04	67.83	+Large
5	-0.13	2.66	-1.79	-0.18	0.00	0.00	4.47	67.83	+Large
6	-0.13	2.68	-0.49	-0.18	0.00	0.00	3.19	67.83	+Large
7	-0.10	2.23	-3.48	-0.15	0.00	0.10	5.72	48.00	7.39
8	0.80	2.85	-2.23	-0.01	-0.02	-0.17	5.09	48.00	8.43
9	0.03	0.34	-4.10	-0.03	-0.01	-0.08	4.45	48.00	9.79
10	0.34	1.15	-3.10	0.03	-0.01	-0.29	4.27	48.00	+Large
11	2.86	1.32	-7.84	-0.10	-0.48	0.34	10.75	48.00	+Large
12	-1.00	0.93	-5.08	0.12	0.10	-0.67	6.13	48.00	6.83
13	2.20	2.97	-1.94	0.05	0.01	-0.46	4.96	48.00	8.68
14	-1.32	-2.22	-11.77	0.07	-0.15	-1.74	11.02	48.00	3.36
15	-0.13	2.58	-0.39	-0.18	0.00	0.00	2.98	48.00	+Large
16	-0.08	1.10	-0.16	-0.08	0.00	-0.09	1.33	48.00	+Large
17	0.00	0.10	-1.08	0.00	0.00	0.03	1.18	48.00	+Large
18	-0.01	0.07	-0.68	0.00	0.00	0.06	0.76	48.00	+Large
19	-0.05	0.22	-0.32	0.00	0.00	0.06	0.56	48.00	+Large
20	-0.18	0.05	-0.93	0.00	0.00	-0.20	1.03	48.00	+Large

[59] See Figure 2.10.14-4 for locations of sections.
[60] Stress components correspond to a cylindrical coordinate system.

Table 2.10.14-24 30-Foot Bottom-End Drop with Internal Pressure, $P_m + P_b$ Stresses, ksi

Sec[61]	S_x[62]	S_y[2]	S_z[2]	S_{xy}[2]	S_{yz}[2]	S_{xz}[2]	Stress Intensity	Stress Allow.	MS
1	0.02	0.36	-4.25	-0.02	-0.01	-0.04	4.61	96.90	+Large
2	0.00	0.01	-2.55	0.00	0.00	0.00	2.56	96.90	+Large
3	0.00	0.08	-1.26	0.00	0.00	0.01	1.34	96.90	+Large
4	-0.20	3.09	-3.22	-0.21	-0.01	-0.01	6.33	96.90	+Large
5	-0.20	2.84	-1.76	-0.20	0.00	0.00	4.62	96.90	+Large
6	-0.21	2.87	-0.46	-0.20	0.00	0.00	3.35	96.90	+Large
7	-0.01	1.77	-4.01	-0.12	-0.01	0.10	5.79	68.50	+Large
8	0.68	2.56	-4.53	0.12	-0.02	-0.29	7.12	68.50	8.62
9	0.10	0.42	-4.24	-0.03	-0.02	-0.24	4.68	68.50	+Large
10	0.64	1.84	-2.82	0.01	-0.04	-0.35	4.69	68.50	+Large
11	2.16	-1.09	-16.04	-0.20	-1.32	0.68	18.38	68.50	2.73
12	-1.81	-0.19	-9.08	0.10	0.11	-1.00	9.03	68.50	6.59
13	6.29	9.44	-0.86	0.02	-0.04	-0.38	10.32	68.50	5.64
14	4.12	8.84	-8.49	0.01	0.15	-2.03	17.65	68.50	2.88
15	-0.19	2.69	-0.63	-0.19	0.00	0.00	3.33	68.50	+Large
16	-0.19	1.32	0.18	-0.10	-0.01	-0.09	1.54	68.50	+Large
17	0.01	0.06	-1.24	0.00	0.00	0.09	1.30	68.50	+Large
18	0.01	0.07	-0.73	0.00	0.01	0.07	0.80	68.50	+Large
19	-0.08	0.24	-0.49	0.00	0.01	0.06	0.74	68.50	+Large
20	-0.36	0.25	-0.89	0.01	0.00	-1.65	3.34	68.50	+Large

[61] See Figure 2.10.14-4 for locations of sections.
[62] Stress components correspond to a cylindrical coordinate system.

Table 2.10.14-25 30-Foot Bottom-Corner Drop with Internal Pressure, P_m Stresses, ksi

Sec[63]	Location (deg)[64]	S_x[65]	S_y[3]	S_z[3]	S_{xy}[3]	S_{yz}[3]	S_{xz}[3]	Stress Intensity	Stress Allow.	MS
1	0	-0.04	1.75	-10.25	-0.18	-0.35	-0.03	12.04	67.83	4.63
2	180	-0.04	-0.28	-10.82	0.00	-0.05	0.00	10.78	67.83	5.29
3	180	-0.01	0.31	-5.34	0.01	0.09	0.03	5.66	67.83	+Large
4	0	-0.17	2.59	-6.85	-0.23	-0.03	-0.02	9.46	67.83	6.17
5	180	-0.08	2.48	-6.68	0.14	-0.02	0.00	9.17	67.83	6.40
6	142.5	-0.18	2.20	-1.87	-0.20	1.02	0.03	4.57	67.83	+Large
7	0	-0.16	1.50	-7.19	-0.19	0.02	0.15	8.71	48.00	4.51
8	15	0.95	2.55	-4.19	-0.02	0.02	-0.09	6.74	48.00	6.12
9	0	0.13	0.48	-11.26	0.00	-0.34	-0.18	11.76	48.00	3.08
10	0	1.33	-0.73	-9.11	0.22	-0.24	0.19	10.47	48.00	3.58
11	0	1.26	0.32	-8.62	0.15	0.51	0.82	10.09	48.00	3.76
12	0	-2.47	-1.01	-10.59	0.09	-0.23	-1.08	9.73	48.00	3.93
13	180	0.74	2.35	-1.83	0.03	-0.01	-0.80	4.41	48.00	9.88
14	180	-1.31	-1.79	-11.13	-0.07	0.15	-2.16	10.74	48.00	3.47
15	112.5	-0.18	1.91	-1.13	0.04	2.48	-0.07	5.83	48.00	7.23
16	127.5	-0.06	0.49	-0.50	0.07	2.06	-0.26	4.26	48.00	+Large
17	180	0.01	0.40	-4.57	-0.01	0.08	0.14	4.97	48.00	8.66
18	60	0.02	0.09	0.45	0.02	1.74	0.07	3.50	48.00	+Large
19	0	-1.44	-1.46	-0.82	0.18	0.05	0.74	1.66	48.00	+Large
20	97.5	0.07	-0.46	-1.01	-0.13	0.00	-0.15	1.15	48.00	+Large

[63] See Figure 2.10.14-4 for locations of sections.
[64] The location specifies the angle at which the maximum stress intensity occurs. See Figure 2.10.14-1 for definition of angular location.
[65] Stress components correspond to a cylindrical coordinate system.

Table 2.10.14-26 30-Foot Bottom-Corner Drop with Internal Pressure, $P_m + P_b$ Stresses, ksi

Sec[66]	Location (deg)[67]	S_x[68]	S_y[3]	S_z[3]	S_{xy}[3]	S_{yz}[3]	S_{xz}[3]	Stress Intensity	Stress Allow.	MS
1	15	-0.01	1.27	-10.61	0.02	-1.51	-0.06	12.27	96.90	6.90
2	180	-0.03	3.04	-10.21	0.22	-0.05	0.00	13.27	96.90	6.30
3	180	0.01	0.82	-5.25	0.05	0.11	0.01	6.08	96.90	+Large
4	0	-0.26	4.74	-6.06	-0.38	-0.01	-0.03	10.83	96.90	7.95
5	180	-0.12	7.49	-4.87	0.48	-0.02	0.00	12.39	96.90	6.82
6	180	-0.17	6.47	-0.89	0.35	0.13	0.03	7.38	96.90	+Large
7	37.5	0.01	1.65	-7.51	0.03	-0.35	0.19	9.20	68.50	6.45
8	0	0.63	2.19	-7.06	-0.18	0.06	-0.14	9.27	68.50	6.39
9	52.5	0.22	0.18	-8.01	-0.42	-4.78	-0.44	12.63	68.50	4.42
10	0	1.30	-2.45	-14.17	0.11	-0.25	0.46	15.51	68.50	3.42
11	0	1.99	-1.54	-16.99	0.28	1.42	1.39	19.35	68.50	2.54
12	0	-2.54	-1.43	-12.80	0.00	-0.22	-1.52	11.59	68.50	4.91
13	7.5	4.62	8.13	-0.86	0.17	-0.01	-0.10	9.00	68.50	6.61
14	7.5	4.26	8.58	-8.38	0.03	0.00	-1.33	17.10	68.50	3.01
15	127.5	-0.25	-1.48	-2.34	-0.11	3.37	-0.04	6.79	68.50	9.09
16	142.5	-0.17	0.45	-0.67	0.06	4.05	0.17	8.19	68.50	7.36
17	52.5	-0.04	1.06	0.90	-0.28	3.14	-0.03	6.31	68.50	9.86
18	37.5	-0.10	0.08	1.60	0.06	2.68	-0.36	5.63	68.50	+Large
19	0	-0.66	-0.19	1.04	-0.02	0.15	0.74	2.28	68.50	+Large
20	45	-0.20	0.21	-0.85	0.23	-0.06	-1.66	3.42	68.50	+Large

[66] See Figure 2.10.14-4 for locations of sections.
[67] The location specifies the angle at which the maximum stress intensity occurs. See Figure 2.10.14-1 for definition of angular location.
[68] Stress components correspond to a cylindrical coordinate system.

Table 2.10.14-27 Accident Internal Pressure with Inertia Load, P_m Stresses, ksi

Sec[69]	Location (deg)[70]	S_x[71]	S_y[3]	S_z[3]	S_{xy}[3]	S_{yz}[3]	S_{xz}[3]	Stress Intensity	Stress Allow.	MS
1	0	0.01	0.07	-1.22	0.00	0.00	-0.01	1.29	67.83	+Large
2	30	0.00	0.00	-0.67	0.00	0.00	0.00	0.67	67.83	+Large
3	180	0.00	0.00	-0.23	0.00	0.00	0.00	0.23	67.83	+Large
4	0	-0.26	5.34	0.37	-0.37	0.00	0.00	5.65	67.83	+Large
5	0	-0.26	5.33	0.86	-0.37	0.00	0.00	5.63	67.83	+Large
6	0	-0.26	5.32	1.29	-0.37	0.00	0.00	5.63	67.83	+Large
7	0	-0.26	5.33	0.29	-0.36	-0.01	-0.04	5.64	48.00	7.51
8	97.5	-0.16	2.06	0.30	-0.01	-0.07	0.16	2.27	48.00	+Large
9	0	0.01	0.08	-1.19	-0.01	0.00	-0.02	1.27	48.00	+Large
10	7.5	0.09	0.31	-0.90	0.01	0.00	-0.07	1.22	48.00	+Large
11	180	0.58	0.06	-3.57	-0.04	-0.22	0.16	4.18	48.00	+Large
12	180	-0.35	0.37	-1.64	0.05	0.03	-0.15	2.03	48.00	+Large
13	180	0.71	0.95	-0.99	0.02	0.01	-0.10	1.95	48.00	+Large
14	0	-0.36	-0.63	-4.17	0.02	-0.06	-0.61	4.00	48.00	+Large
15	0	-0.27	5.41	1.31	-0.37	0.00	0.06	5.73	48.00	7.38
16	0	-0.17	2.25	0.80	-0.16	0.00	-0.09	2.45	48.00	+Large
17	157.5	0.00	0.05	-0.19	0.00	0.00	0.00	0.24	48.00	+Large
18	180	0.01	0.20	-0.11	0.01	0.00	0.04	0.33	48.00	+Large
19	105	-0.03	0.20	-0.20	0.00	0.00	0.04	0.41	48.00	+Large
20	105	-0.15	0.13	-0.88	0.00	0.00	-0.33	1.14	48.00	+Large

[69] See Figure 2.10.14-4 for locations of sections.
[70] The location specifies the angle at which the maximum stress intensity occurs. See Figure 2.10.14-1 for definition of angular location.
[71] Stress components correspond to a cylindrical coordinate system.

Table 2.10.14-28 Accident Internal Pressure with Inertia Load , $P_m + P_b$ Stresses, ksi

Sec[72]	Location (deg)[73]	S_x[74]	S_y[3]	S_z[3]	S_{xy}[3]	S_{yz}[3]	S_{xz}[3]	Stress Intensity	Stress Allow.	MS
1	0	0.01	0.11	-1.23	0.00	0.00	-0.01	1.34	96.90	+Large
2	0	0.00	0.01	-0.66	0.00	0.00	0.00	0.67	96.90	+Large
3	0	0.00	-0.01	-0.24	0.00	0.00	0.00	0.24	96.90	+Large
4	0	-0.41	5.76	0.46	-0.41	0.00	0.00	6.22	96.90	+Large
5	0	-0.41	5.69	0.93	-0.40	0.00	0.00	6.15	96.90	+Large
6	0	-0.41	5.69	1.38	-0.40	0.00	0.00	6.16	96.90	+Large
7	0	-0.39	5.55	-0.31	-0.39	-0.01	-0.05	6.01	68.50	+Large
8	105	-0.47	2.39	0.87	0.00	-0.09	0.19	2.89	68.50	+Large
9	0	0.03	0.11	-1.22	-0.01	-0.01	-0.06	1.33	68.50	+Large
10	0	0.07	0.22	-1.09	-0.03	-0.03	-0.06	1.33	68.50	+Large
11	180	-0.34	-1.37	-7.60	-0.07	-0.62	0.27	7.35	68.50	8.32
12	180	-0.63	-0.04	-3.13	0.04	0.03	-0.22	3.11	68.50	+Large
13	172.5	1.58	2.37	-0.74	0.01	-0.01	-0.09	3.11	68.50	+Large
14	7.5	1.42	3.06	-2.98	0.00	0.05	-0.71	6.15	68.50	+Large
15	0	-0.39	5.57	0.65	-0.39	0.00	0.06	6.02	68.50	+Large
16	0	-0.36	2.64	1.34	-0.20	-0.01	-0.09	3.03	68.50	+Large
17	150	0.00	0.03	-0.22	0.00	0.00	0.00	0.26	68.50	+Large
18	0	0.03	0.17	-0.26	-0.01	0.00	0.05	0.44	68.50	+Large
19	105	-0.05	0.22	-0.33	0.00	0.01	0.03	0.55	68.50	+Large
20	45	-0.25	0.42	-0.89	0.01	0.00	-1.68	3.42	68.50	+Large

[72] See Figure 2.10.14-4 for locations of sections.
[73] The location specifies the angle at which the maximum stress intensity occurs. See Figure 2.10.14-1 for definition of angular location.
[74] Stress components correspond to a cylindrical coordinate system.

2.10.16 Structural Evaluation of the NAC-LWT Cask Body with TPBARs in the PWR/BWR Rod Transport Canister

This section presents a structural evaluation of the NAC-LWT cask system for the shipment of up to 25 individual TPBARs in the PWR/BWR Rod Transport Canister, the PWR insert and the TPBAR basket under normal conditions of transport and hypothetical accident conditions. Section 2.10.14 presents the structural evaluation of the NAC-LWT cask system for two TPBAR content conditions: up to 300 production TPBARs loaded into an open (i.e., unsealed) consolidation canister; and up to 55 segmented TPBARs loaded into a welded closed waste container. Although the analysis provided in Section 2.10.14 uses a slightly lower contents weight than the TPBARs in the PWR/BWR Rod Transport Canister configuration, the applied contents load is comparable as conservative accelerations are used. As such, the evaluation of TPBARs in the PWR/BWR Rod Transport Canister uses the results of Section 2.10.14, appropriately scaled to account for any increase in total applied contents load.

2.10.16.1 Normal Conditions of Transport for Cask Body and TPBARs in the PWR/BWR Rod Transport Canister

This section provides the cask body structural evaluation for normal conditions of transport for the shipment of TPBARs in the PWR/BWR Rod Transport Cansister, the PWR insert and the TPBAR basket. Section 2.10.14 provides the critical stress intensity results of the NAC-LWT cask system for two TPBAR content conditions: up to 300 production TPBARs loaded into an open (i.e., unsealed) consolidation canister; and up to 55 segmented TPBARs loaded into a welded closed waste container. The Section 2.10.14 analysis used a three-dimensional half-symmetry model of the LWT cask body constructed using ANSYS. A detailed description of the implemented finite element model can be found in Section 2.10.14.1.2. Both the pressure and component temperatures considered in Section 2.10.14 bound the TPBARs in the PWR/BWR Rod Transport Canister configuration.

For the side drop, the cask is loaded by both the contents weight and the weight of the cask body surrounding the cask cavity. The weight of the cask body surrounding the cavity is 34,400 lbs, which includes the lead for shielding, the inner and outer shells, as well as portions of the top and bottom forgings. The evaluation in Section 2.10.14 uses a cask contents weight of 1800 lbs, which is 101 lbs less than the TPBAR in the PWR/BWR Rod Transport Canister contents weight of 1901 lbs. The normal conditions evaluation of Section 2.10.14 uses a conservative inertial load of 25 g for the side drop, which is 0.7 g greater than the required inertial load of 24.3 g (Table 2.6.7-34). Section 2.10.14 provides the minimum margins of safety for each stress category for 1-foot drop conditions. For the analysis of the TPBARs in the PWR/BWR Rod

Transport Canister configuration, the stress-intensity results of critical sections, listed Section 2.10.14, are scaled by the ratio of the contents weight and cask body weight surrounding the cavity, using the following scale factor.

$$SF_{sd} = \frac{W_{TPBAR\,/\,PWR} + W_{cavity\ cask\ body}}{W_{TPBAR} + W_{cavity\ cask\ body}} = \frac{1{,}901 + 34{,}400}{1{,}800 + 34{,}400} = 1.003$$

where:

SF_{sd} = side drop stress intensity scale factor

$W_{TPBAR/PWR}$ = the contents weight for the 25 TPBARs in the PWR/BWR Rod Transport Canister

W_{TPBAR} = the contents weight analyzed in Section 2.10.14

$W_{cavity\ cask\ body}$ = the weight of the cask body radially surrounding the cask cavity

The minimum margin of safety is +0.13, which occurs at section 2 for the condition of P_m stress for 1-foot side-drop condition. This section is located at the axial center of the cask outer shell. The minimum margins of safety for each stress category for 1-foot drop conditions are as follows.

Stress Category	Section	Drop Orientation	Stress Intensity, ksi	Stress Allowable, ksi	Margin of Safety
P_m	2	Side	28.66	32.3	+0.13
$P_m + P_b$	2	Side	32.97	48.45	+0.47
P+Q	18	Side	31.39	60.0	+0.91

2.10.16.2 Hypothetical Accident Conditions for Cask Body with TPABARs and the PWR/BWR Rod Transport Canister

This section provides the cask body structural evaluation for hypothetical accident conditions. The following sections discuss drop conditions and inner shell buckling.

2.10.16.2.1 Free Drop (30-Foot)

This section provides the cask body structural evaluation for the 30-foot drop accident conditions of transport for the shipment of TPBARs in the PWR/BWR Rod Transport Cansister, the PWR insert and the TPBAR basket. Section 2.10.14 provides the critical stress intensity results of the NAC-LWT cask system for two TPBAR content conditions: up to 300 production TPBARs loaded into an open (i.e., unsealed) consolidation canister; and up to 55 segmented TPBARs loaded into a welded closed waste container. The Section 2.10.14 analysis used a three-dimensional half-symmetry model of the LWT cask body constructed using ANSYS. A detailed description of the implemented finite element model can be found in Section 2.10.14.1.2. Both

the pressure and component temperatures considered in Section 2.10.14 bound the TPBARs in the PWR/BWR Rod Transport Canister configuration.

Section 2.10.14.2.1 provides the results of the critical section stresses for the 30-foot drop accident conditions. As listed in Section 2.10.14.2.1, the minimum margins of safety resulted from the 30-foot side drop condition. The evaluation of Section 2.10.14 uses a cask contents weight of 1800 lbs, which is 101 lbs less than the TPBAR in the PWR/BWR Rod Transport Canister contents weight of 1901 lbs. The accident conditions evaluation of Section 2.10.14 uses a conservative inertial load of 60 g for side drop, which is 10.3 g greater than the required inertial load of 49.7 g (Table 2.6.7-34). As a result, the 30-foot drop evaluation of Section 2.10.14.2 uses a contents inertial load of 108,000 lb (1800 lbs × 60 g). Assuming a conservative acceleration of 55 g for the side drop inertial load, the contents inertial load for the TPBARs in the PWR/BWR Rod Transport Canister is calculated as 104,555 lbs (1901 lbs × 55 g). The total applied contents load for the critical stresses of Section 2.10.14.2.1 is greater than that for the TPBARs in the PWR/BWR Rod Transport Canister. Therefore, it is concluded that the NAC-LWT cask is structurally adequate for the shipment of TPBARs in the PWR/BWR Rod Transport Canister under the 30-foot drop accident conditions of transport.

2.10.16.2.2 Fire Accident

The pressure and component temperatures for the TPBARs in the PWR/BWR Rod Transport Canister for the fire accident conditions are bounded by the fire accident evaluation of the NAC-LWT cask body with TPBARs in a consolidation canister in Section 2.10.14.2.2. Therefore, based on the results of Section 2.10.14.2.2, presented in Table 2.10.14-27 and Table 2.10.14-28, the NAC-LWT cask is structurally adequate for the shipment of TPBARs in the PWR/BWR Rod Transport Canister under fire accident conditions.

2.10.16.3 Inner Shell Buckling

Section 2.10.6 presents a buckling evaluation of the cask inner shell per ASME Code Case N-284 for the design basis cask configuration. The evaluation presented in Section 2.10.6 bounds the TPBAR contents (up to 25 TPBARs in a rod holder in the PWR/BWR Rod Transport Canister) based on the following.

- The maximum weight of the TPBAR contents (up to 25 TPBARs in a rod holder) in the PWR/BWR Rod Transport Canister of 1901 lbs is enveloped by the weight of the design basis contents, which would reduce the compressive stresses in the cask shells due to less inertia loading for the drop conditions.
- The cask internal pressure for the TPBAR contents (up to 25 TPBARs in a rod holder in the PWR/BWR Rod Transport Canister) is significantly higher than the cask internal pressure for the design basis contents. The increase in the pressure would increase the

tensile stresses in the shell that result in stiffening of the inner shell and, consequently, in reducing the compressive stresses associated with buckling.

The interaction summary presented in Table 2.10.6-10, associated with the design basis weight and the design basis pressure, is bounding for the TPBAR content (up to 25 TPBARs in a rod holder in the PWR/BWR Rod Transport Canister) conditions. Therefore, it is concluded that the cask inner shell will not buckle with the TPBAR contents (up to 25 TPBARs in a rod holder in the PWR/BWR Rod Transport Canister) in the NAC-LWT cask.

2.10.16.4 NAC-LWT Cask Closure Lid and Bolts

The NAC-LWT cask closure lid is bolted to the cask body top forging with twelve 1-8 UNC bolts fabricated from SA-453, Grade 660 high-alloy steel. The threaded portion of the bolt engages the cask body a minimum of 1.875 inches. From Section 2.1.3.2.2, the torque on the cask lid bolts is 260 ± 20 ft-lb and the bolt preload is specified as 34,843 lbs. For the LWT cask configured to ship TPBARs in the PWR/BWR Rod Transport Canister, the maximum internal pressure of 600 psig is conservatively used in the closure lid evaluation. This pressure bounds the maximum pressure during the fire accident contained in Section 3.5.4.4. To ensure that the seal is not unloaded during accident conditions, the preload is calculated to account for the weight of the lid, internal weight of the cask contents, force resulting from internal pressure, force resulting from compression of the TFE O-ring, and force resulting from compression of the metallic O-ring. The load resulting from the weight of the LWT cask contents is:

$$F_2 = W_c a = 1{,}901 \times 60g = 114{,}060 \text{ lbs}$$

where:

W_c = 1,901 lbs (weight of TPBAR basket and contents for TPBARs in the PWR/BWR rod transport canister)

a = 60 g (maximum accident acceleration)

The load resulting from accident pressure (fire accident) is:

$$F_{ip} = P_{ip} A = 600 \times 171.36 = 102{,}816 \text{ lbs}$$

where:

P_{ip} = 600 psig (accident internal pressure)

$$A = \frac{\pi}{4} \times 14.771^2 = 171.36 \text{ in}^2$$

The total required bolt preload force (12 bolts) is:

$$FT = F_1 + F_2 + F_{tr} + F_{mr} + F_{ip}$$

$$= 56{,}460 + 114{,}060 + 2{,}474 + 79{,}470 + 102{,}816 = 355{,}280 \text{ lbs}$$

where:

F_{tr} = 2,474 lbs, TFE O-ring load (Section 2.1.3.2.2)

F_{mr} = 79,470 lbs, Metallic O-ring load (Section 2.1.3.2.2)

F_l = 56,460 lbs, Lid load (Section 2.1.3.2.2)

The required bolt preload per bolt is:

$$F_{bolt} = \frac{F_T}{12} = \frac{355{,}280}{12} = 29{,}607 \text{ lbs} \qquad < 34{,}843 \text{ lbs} \quad \text{(Section 2.1.3.2.2)}$$

Since the bolt preload presented in Section 2.1.3.2.2 of the NAC-LWT is bounding, no further analysis of the LWT lid bolts is required.

The preload applied to the cask lid bolts is due to the load applied to the lid. The load applied to the lid for the design basis weight and pressure for the PWR fuel bounds the load applied to the lid for the TPBARs in the PWR/BWR Rod Transport Canister contents. Therefore, the stresses in the cask lid due to the design basis weight and pressure also bound the stresses in the cask lid due to the TPBARs in the PWR/BWR Rod Transport Canister content weight and pressure.

2.10.16.5 Conclusion

Based on the evaluations presented in Sections 2.10.14.1 through 2.10.14.4, the NAC-LWT cask with TPBAR contents in the PWR/BWR Rod Transport Canister satisfies the requirements of 10 CFR 71 for the normal conditions of transport and for hypothetical accident conditions.

Chapter 3

Table of Contents

3.0 THERMAL EVALUATION 3.1-1
3.1 Discussion 3.1-1
3.2 Thermal Properties of Materials 3.2-1
3.2.1 Conductive Properties 3.2-1
3.2.2 Radiative Properties 3.2-2
3.2.3 Convective Properties 3.2-3
3.3 Technical Specifications of Components 3.3-1
3.4 Thermal Evaluation for Normal Conditions of Transport 3.4-1
3.4.1 Thermal Model 3.4-1
3.4.2 Maximum Temperatures 3.4-34
3.4.3 Minimum Temperatures 3.4-34
3.4.4 Maximum Internal Pressures 3.4-35
3.4.5 Maximum Thermal Stresses 3.4-50
3.4.6 Evaluation of Package Performance for Normal Conditions of Transport 3.4-50
3.5 Hypothetical Accident Thermal Evaluation 3.5-1
3.5.1 Finite Element Models 3.5-1
3.5.2 Package Conditions and Environment 3.5-4
3.5.3 Package Temperatures 3.5-5
3.5.4 Maximum Internal Pressure 3.5-13
3.5.5 Maximum Thermal Stresses 3.5-17
3.5.6 Evaluation of Package Performance for Hypothetical Accident Thermal Conditions 3.5-17
3.5.7 Assessment of the Effects of the Fission Gas Release in the Fire Accident Condition 3.5-18
3.6 Failed Metallic Fuel Basket – SCOPE Evaluations 3.6-1

List of Figures

Figure 3.4-1 HEATING5 Normal Transport Conditions Thermal Model 3.4-51
Figure 3.4-2 Design Basis PWR Fuel Assembly Axial Flux Distribution 3.4-52
Figure 3.4-3 ANSYS MTR Fuel Design Basis Heat Load Thermal Model (Uniform 30-Watt/Element Configuration Heat Load) 3.4-53
Figure 3.4-4 MTR Fuel Variable Decay Heat ANSYS Thermal Model 3.4-54
Figure 3.4-5 Thermal Resistance Model for TRIGA Fuel Elements 3.4-55
Figure 3.4-6 Modeling Details for the MTR Fuel Assembly Resting on the Surface of the NAC-LWT MTR Basket 3.4-56
Figure 3.4-7 Finite Element Thermal Model for TRIGA Fuel Cluster Rods 3.4-57
Figure 3.4-8 Details of the TRIGA Fuel Cluster Rods in the Finite Element Model 3.4-58
Figure 3.4-9 Individual TRIGA Fuel Cluster Rod Finite Element Model Details 3.4-59
Figure 3.4-10 PWR and BWR High Burnup Fuel Rods Normal Condition ANSYS Thermal Model (Condition 1) 3.4-60
Figure 3.4-11 Close-up of PWR and BWR High Burnup Fuel Rods Normal Condition ANSYS Thermal Model 3.4-61
Figure 3.4-12 PWR and BWR High Burnup Fuel Rods Normal Condition ANSYS Thermal Model (Condition 2) 3.4-62
Figure 3.4-13 Finite Element Thermal Model for MTR Fuel Element 3.4-63
Figure 3.4-14 Detailed DIDO Basket Module Finite Element Model 3.4-64
Figure 3.4-15 Detailed DIDO Fuel Assembly Model 3.4-65
Figure 3.4-16 ANSYS Model for BWR 7 × 7 Fuel Lattice with 25 High Burnup Fuel Rods 3.4-66
Figure 3.4-17 Fuel Rod Locations in the Thermal Model for Damaged Fuel 3.4-67
Figure 3.4-18 Finite Element Model for TPBARs 3.4-68
Figure 3.4-19 Finite Element Model for MOATA Plate Fuel – ANSTO 3.4-69
Figure 3.4-20 Finite Element Model for Mark III Spiral Fuel - ANSTO 3.4-70
Figure 3.5-1 Transient Thermal Analysis Finite Element Model of the NAC-LWT 3.5-19
Figure 3.5-2 Top Region of the ANSYS Model 3.5-20
Figure 3.5-3 Bottom Region of the ANSYS Model 3.5-21
Figure 3.5-4 Temperature History of NAC-LWT O-Rings and Valves in the Hypothetical Fire Event 3.5-22
Figure 3.5-5 Temperature History of NAC-LWT Components in the Hypothetical Fire Event 3.5-23
Figure 3.5-6 MTR Fuel Design Basis Heat Load Fire Accident ANSYS Thermal Model (Uniform 30-Watt/Element Configuration Heat Load) 3.5-24
Figure 3.5-7 MTR Fuel Variable Heat Load Fire Accident ANSYS Thermal Model (120-Watt/70-Watt/20-Watt Configuration Heat Load) 3.5-25
Figure 3.5-8 Temperature History in the MTR Fuel Variable Heat Load Fire Accident Analysis 3.5-26
Figure 3.5-9 Location of the Maximum Temperature in the MTR Fuel Variable Heat Load 3.5-27
Figure 3.5-10 Temperature History for the TRIGA Fuel Cluster Rods Design Basis Heat Load Fire Accident Analysis 3.5-28

List of Figures (continued)

Figure 3.5-11 Temperature History of NAC-LWT Cask Components with PWR and BWR High Burnup Fuel Rods in the Hypothetical Fire Event 3.5-29
Figure 3.5-12 End of Fire Temperatures of the Alternate Port Cover Components 3.5-30
Figure 3.5-13 Transient Temperatures of the Alternate Port Cover Components 3.5-31
Figure 3.6-1 Failed Fuel Basket SCOPE Input 3.6-2
Figure 3.6-2 Failed Fuel Basket SCOPE Output 3.6-3
Figure 3.6-3 Nine Failed Metallic Fuel Rods SCOPE Input 3.6-7
Figure 3.6-4 Nine Failed Metallic Fuel Rods SCOPE Output 3.6-8

List of Tables

Table 3.2-1 Thermal Properties of Type 304 Stainless Steel 3.2-7
Table 3.2-2 Thermal Properties of 6061-T6 Aluminum Alloy 3.2-7
Table 3.2-3 Thermal Properties of Dry Air 3.2-8
Table 3.2-4 Thermal Properties of Chemical Copper Lead 3.2-8
Table 3.2-5 Thermal Properties of 56 Percent Ethylene Glycol Solution 3.2-9
Table 3.2-6 Thermal Properties of BISCO FPC (Fireblock Silicone Foam) 3.2-10
Table 3.2-7 Thermal Properties of Helium 3.2-10
Table 3.2-8 Fiberfrax Ceramic Fiber Paper, Grades 550, 880, and 970 ..... 3.2-11
Table 3.4-1 Temperatures for Metallic Fuel Transport 3.4-71
Table 3.4-2 Maximum Component Temperatures – Design Basis PWR Fuel 3.4-72
Table 3.4-3 Limiting Cold Case Component Temperatures – Design Basis PWR Fuel 3.4-73
Table 3.4-4 Fission Product Gas Inventories and Pressures for Design Basis PWR Fuel Assembly 3.4-74
Table 3.4-5 NAC-LWT Cask Thermal Performance Summary 3.4-74
Table 3.4-6 MTR Fuel Maximum Component Temperatures – Normal Transport Condition 3.4-75
Table 3.4-7 PWR Rods (25 Total) Maximum Component Temperatures – Normal Transport Condition 3.4-76
Table 3.4-8 TRIGA Fuel Element Maximum Component Temperatures - Normal Conditions of Transport 3.4-77
Table 3.4-9 TRIGA Fuel Cluster Rod Temperatures – Normal Conditions of Transport 3.4-78
Table 3.4-10 PWR and BWR High Burnup Fuel Rods Maximum Component Temperatures – Normal Transport Condition 3.4-79
Table 3.4-11 Fission Product Gas Inventories and Pressures for the Exxon 7 × 7 BWR Fuel Assembly 3.4-80
Table 3.4-12 DIDO Fuel Maximum Component Temperatures – Normal Transport Condition 3.4-81
Table 3.4-13 General Atomics IFM Maximum Component Temperatures – Normal Transport Condition 3.4-82
Table 3.4-14 PWR and BWR High Burnup Fuel Rods in a Fuel Assembly Lattice Maximum Component Temperatures—Normal Transport Condition 3.4-83
Table 3.4-15 Maximum Component Temperatures for High Burnup Fuel Rods with Damaged Fuel Rods in a Rod Holder 3.4-83
Table 3.4-16 Maximum Component Temperatures for TPBAR Shipment – Normal Conditions of Transport 3.4-84
Table 3.4-17 Maximum Component Temperatures - PULSTAR Fuel in MTR Basket 3.4-85
Table 3.4-18 PULSTAR Fuel Dimensions 3.4-86
Table 3.4-19 PULSTAR Payload Volume Summary 3.4-86
Table 3.4-20 PULSTAR Fuel Assembly Fission Product Gas Inventory 3.4-87
Table 3.4-21 PULSTAR Fuel Element Normal Condition Internal Pressure Summary 3.4-87

List of Tables (continued)

Table 3.4-22 Maximum Component Temperatures – MOATA Plate Fuel and Mark III Spiral Fuel in ANSTO Basket 3.4-88
Table 3.5-1 Maximum Component Temperatures (°F) During the Fire Accident Design Basis PWR Fuel, 2.5 kW Heat Load) 3.5-32
Table 3.5-2 MTR Fuel Fire Accident Maximum Temperatures (°F), 10 Fuel Plate/ 120W Element Case (Bounding Configuration) 3.5-33
Table 3.5-3 TRIGA Fuel Fire Accident Maximum Temperatures (°F) 3.5-33
Table 3.5-4 PWR and BWR High Burnup Fuel Rods Fire Accident Maximum Temperatures (°F) 3.5-34
Table 3.5-5 Maximum Component Temperatures for High Burnup Fuel Rods in a Rod Holder with Damaged Fuel Rods for the Fire Accident 3.5-34
Table 3.5-6 TPBAR Fire Accident Maximum Temperatures 3.5-35

3.4 Thermal Evaluation for Normal Conditions of Transport

The temperatures of each of the components of the NAC LWT cask must be evaluated during normal transport conditions. The NAC-LWT cask must prevent components from exceeding their allowable temperatures by rejecting sufficient decay heat to the environment when the design basis, 2-year cooled, Westinghouse 15 × 15 fuel assembly is being transported. Since the neutron shield may be empty when metallic fuel is being transported, cask temperatures are also evaluated for this configuration. Components important to safety, identified in Section 3.3, must be maintained within their safe operating ranges. Also, the thermally induced stresses, in combination with pressure and mechanical load stresses, must be maintained below allowable stress levels.

3.4.1 Thermal Model

The temperatures of the NAC-LWT cask are evaluated for normal transport conditions. The cask is analyzed for two different cases referred to as the Heat Case and the Cold Case.

The Heat Case consists of an ambient temperature of 130°F, still air, and direct solar heating of 737 Btu/ft^2 on the vertical flat surfaces and 1,475 Btu/ft^2 on the curved surfaces for a period of 12 out of every 24 hours.

The Cold Case uses an ambient temperature of –40°F, still air, and shade (no solar heat load). This case requires no thermal analysis when a 0.0 kW decay heat load is considered because a uniform cask temperature of –40°F results. The more limiting decay heat load, from a thermal stress standpoint, is the design fuel assembly maximum decay heat load of 2.5 kW.

3.4.1.1 PWR Analytical Model

The temperatures of the NAC-LWT cask were evaluated using the HEATING5 computer code (Turner). The model used to evaluate the temperature distribution is shown in Figure 3.4-1. The model consists of the fuel basket section and the cask body.

The fuel basket section consists of several regions. These are the active fuel region, the non-power producing portion of the fuel region, the end-fittings, the spacer, an air region above the upper end-fitting, an air gap surrounding the fuel region, and an aluminum annulus (the basket wall) surrounding the gap. The fuel region is modeled as a cylinder 9.5 inches in diameter. (This diameter is actually an effective diameter for an 8.426-inch square fuel assembly.) The active fuel region is broken up into six regions of varying heat generation to closely approximate the axial power distribution shown in Figure 3.4-2. The effective diameter of the air gap is determined based on the 8.875-inch square cavity area minus the 8.426-inch

square fuel assembly area. The effective diameter of the aluminum annulus is obtained by taking the area of the basket and subtracting the area of the cavity. The cask cavity is modeled axially with an active fuel length of 144 inches, 6 inches on either side of the active fuel length as the non-power producing portion of the fuel region, a 4-inch end-fitting on the top and a 3-inch endfitting on the bottom, a 7-inch spacer at the bottom and an 8-inch air gap at the top.

The cask body is modeled based on the nominal dimensions of the license drawings in Section 1.4 with the exception of the radial lead region. The method used to obtain the dimensions of the lead region is described in Section 3.2. Because the calculation of the gap is conservative, the effect of the thermal insulator can be ignored during normal transport conditions. The resulting temperatures will still be conservative.

For ease of designing the analytical model, some of the methods of heat transfer within the NAC-LWT cask are not modeled. The effect of this simplification is an additional conservative small overestimation of overall temperatures within the cask. The heat generated by the fuel rods is transferred within the fuel assembly by conduction and to the air gap surrounding the assembly by convection. Conduction is the only axial means of heat transfer from the fuel assembly to the stainless steel at the top and bottom of the fuel basket. Heat is conducted through the aluminum surrounding the fuel assembly and then transferred by means of convection through the air gap between the fuel basket and the cask body. Heat is then conducted through the inner stainless steel wall, the air gap assumed in the lead region, the lead itself, and the outside stainless steel wall. In the liquid neutron shield, heat is transferred by both convection and conduction. It is then conducted through the stainless steel to the surface of the cask where it is transferred to the environment by means of convection and radiation. The solar heat load is evaluated using a steady-state HEATING5 analysis based on one-half of the maximum hourly solar heat load. The factor of one-half is based on the maximum insolance being applied to all cask surfaces for a period of 12 out of every 24 hours. For this report, this steady-state value for the solar heat load is referred to as full insolation.

3.4.1.2 Metallic Fuel Analytical Model

A HEATING5 computer analysis is performed for the NAC-LWT cask containing metallic fuel. When loaded with this fuel, the neutron shield tank (which is not required for neutron shielding of metallic fuel) is empty. This configuration reduces the heat transfer through the neutron shield region requiring further evaluation. The analysis is performed on the NAC-LWT cask containing the design basis metallic fuel producing 540 watts of decay heat.

This thermal analysis shows that the design basis PWR is the more limiting fuel. The results of the metallic fuel thermal analysis are presented in Table 3.4-1 and show that the temperatures are

lower at all locations (except the neutron shield region) than the corresponding temperatures for the design basis PWR fuel presented in Table 3.4-2.

3.4.1.3 MTR Fuel Analytical Models

Heat transfer analysis of the NAC-LWT containing MTR fuel is performed using two separate two-dimensional planar finite element models and the general purpose ANSYS computer code. The first model represents the entire cask and uses a nominal, effective thermal conductivity to represent the fuel element in each basket location. This cask model is used to determine the maximum temperatures throughout the cask, including the temperature of the fuel element side plates. The second model represents the detailed construction of the fuel element itself. The detailed fuel model uses the results from the cask model to specify the boundary condition temperature of the fuel element side plate. This model is used to determine the maximum fuel temperature for each case. Note that the loose fuel plate configuration in the MTR canister is bounded by the assembled fuel element because the stacked loose plates have a much greater contact area for heat transfer to the basket walls. Therefore, the loose fuel plate configuration is not evaluated. Two transport conditions are evaluated:

Condition 1:

The NAC-LWT is supported in an ISO container with solar insolance applied on the surface of the ISO container, and the NAC-LWT is considered to be insulated from the environment (only for normal conditions of transport steady state conditions). The gas inside the ISO container is air. The cavity of the NAC-LWT is backfilled with helium as required by operational procedures.

Condition 2:

The NAC-LWT is not located in an ISO container and solar insolance is applied to the NAC-LWT cask surface. For the purpose of performing the thermal analyses, the cavity of the NAC-LWT is considered to be filled with air.

Of these two conditions, Condition 2 (air in cavity case) produces the higher temperatures as shown in Table 3.4-6. Therefore, the detailed fuel model is used to evaluate Condition 2 only. For each of the two conditions listed above, two different fuel configurations are considered for evaluation for steady-state normal transport conditions.

(1) Uniform design basis heat load of 30 watts per MTR fuel assembly:

This configuration consists of seven MTR fuel elements with design basis heat loads (30 watts per element) corresponding to a total MTR package contents heat load of 1.26 kilowatts (42 fuel elements).

(2) MTR fuel with variable decay heat:

As described in Section 5.3.4, MTR fuel may also be shipped in a variable decay heat configuration. In this case, a basket module may be loaded with only three elements, each having a maximum decay heat of 70 watts, or with three elements with maximum decay heats of 120 watts, 70 watts, and 20 watts. The total decay heat load for the basket must not exceed 210 watts. The same detailed heat transfer model described in Section 3.4.1.3.1 is also used for this analysis.

The fuel decay heat is modeled using uniform volumetric heat generation terms defined by administrative controls from Section 7.1.5. The administrative controls define bounding basket loading configurations that:

- Limit the combined basket heat load to 210 watts per basket module.
- Exclude MTR elements having decay heat loads in excess of 120 watts.
- Require MTR elements having decay heat loads between 120 watts and 70 watts to be loaded into the center basket module position.
- Require MTR elements with decay heat loads between 30 watts and 70 watts to be loaded in the center in-line row of the basket module.
- Limit decay heat loads of MTR elements placed in peripheral basket tubes, not on the center line, to a 30-watt decay heat load (per element).

These constraints result in two bounding loading configurations of MTR fuel elements. Assuming that individual elements have maximum decay heats of 70 watts and 120 watts, the two bounding configurations are:

1. Three 70-watt fuel elements
2. One 120-watt fuel element, one 70-watt fuel element, and one 20-watt fuel element

These combinations are depicted in Figure 3.5-7. Of these two configurations, the second configuration will produce the highest temperatures, as the center assembly contains a 120-watt MTR fuel element. This is the fuel configuration, which is analyzed for the variable decay heat loading. The thermally limiting configuration is also depicted in Figure 3.4-4, which conservatively bounds any fuel loading configuration permitted by the operating procedure presented in Section 7.1.5.

3.4.1.3.1 MTR Fuel Thermal Model of the NAC-LWT (Transported in an ISO Container)

For Condition 1, the detailed fuel model is not used because this condition is bounded by Condition 2, as shown in Section 3.4.1.3.2. Thermal analyses of the NAC-LWT cask for Condition 1 are performed using a half-symmetry, cross-sectional model of the cask in an ISO container positioned along the container centerline. Heat transfer to the environment is limited to surface convection and radiation on both horizontal and vertical surfaces of the ISO container with an emissivity of 0.36. Solar insolance is applied to the vertical surfaces and the top horizontal surface of the ISO container. Heat transfer from the cask to the ISO container is modeled as conduction, convection and radiation. Convective and conductive heat transfer are modeled in the liquid neutron shield, while heat transfer in the cask cavity is limited to conduction and radiation. Axial heat transfer is conservatively ignored in the model. The MTR fuel elements are represented in the model with homogenized fuel elements. The conductive heat flow path from the cask through the saddle support to the bottom surface of the ISO container is conservatively ignored.

Thermal conductivity for 6061-T6 aluminum alloy is based on ASME Code, Section II, Part D, Table TCD. The finite element model for the uniform 30 watts per MTR fuel element is shown in Figure 3.4-3, while the finite element model for the variable decay heat of 120 watts, 70 watts and 20 watts is shown in Figure 3.4-4. For the basket slots, which are empty for the variable decay heat, only conduction through the cavity gas is modeled. In each of these fuel models, the fuel is considered to rest on the surface of each basket slot. The details of this modeling are shown in Figure 3.4-6. While the MTR fuel assemblies are considered to rest on the surface of the basket, the basket is conservatively modeled as being in the center of the cask cavity. Conduction (through helium) and radiation (using emissivity of stainless steel for both surfaces) are modeled from the inner shell of the cask to the basket.

The heat transfer analysis model represents the cask cavity free space using the conductivity of helium. (see Table 3.2-7). The properties for the remaining materials are contained in Table 3.2-1 through Table 3.2-6.

The air space between the NAC-LWT cask and the ISO container is modeled using air with an effective conductivity. This effective conductivity (Incropera) is:

$$\frac{k_{eff}}{k} = 0.386\left(\frac{Pr}{0.861+Pr}\right)^{1/4}\left(Ra_c^{*}\right)^{1/4}$$

$$Ra_c^* = \frac{[\ln(D_0/D_i)]^4}{L^3 (D_i^{-3/5} + D_0^{-3/5})^5} Ra_L$$

$$Ra_L = \frac{g\beta(T_i - T_o)L^3}{\alpha\nu}$$

where:

Pr = Prandtl number (Krieth)

ν = kinematic viscosity (Krieth)

α = thermal diffusivity (Krieth)

$\beta = 1/T_f$

$T_f = (T_i + T_o)/2$

T_i = inner surface temperature

T_o = outer surface temperature

D_i = inner diameter (cask surface)

D_o = outer diameter (height of the ISO container)

$L = (D_o - D_i)/2$

The effective conductivity for the neutron shield and expansion tank as well as the convection from the surface of the ISO container to an ambient temperature of 100°F are presented in Section 3.2.3.

Decay heat for the different MTR package configurations is conservatively enveloped for the heat transfer analysis. Each fuel element of the maximum capacity MTR package configuration, 42 elements, is modeled with a heat generation of 30 watts. Total MTR package contents heat load is 1.26 kilowatts, approximately half of the NAC-LWT cask maximum decay heat load of 2.5 kilowatts. The decay heat is modeled as uniformly generated within the homogenized fuel regions.

The Condition 1 models of the NAC-LWT cask with uniform and variable decay heat MTR fuel element loadings are shown in Figure 3.4-3 and Figure 3.4-4, respectively.

3.4.1.3.2 MTR Fuel Thermal Model of the NAC-LWT (Transported via Truck Trailer)

Thermal analyses of the NAC-LWT cask for Condition 2 are performed using two separate models. The first is a half-symmetry cross-sectional model of the cask in which the outer surface of the expansion tank is the boundary of the model. This model is used to determine the temperatures throughout the cask up to and including the maximum fuel element side plate temperatures. The second is a half-symmetry cross-sectional model of the fuel element. This model is used to determine the maximum fuel temperature within the element for the worst-case fuel plate dimensions. The worst case dimensions are based on the limiting design dimensions combined with the limiting manufacturing tolerances that result in the maximum resistance to heat transfer from the fuel to the side plates.

Cask Model

The modeling of the normal steady state condition of the NAC-LWT from the center of the cask to the outer surface of the expansion tank is identical to the model described in Section 3.4.1.3.1 with the following exceptions:

1. The gas in the NAC-LWT cask cavity is considered to be air.
2. The MTR basket is shifted downward towards the inner shell leaving a minimum gap of 0.07 inch between the outer diameter of the basket end plate and the cask inner shell surface. This is an effective representation of the normal condition of transport (i.e. cask horizontal).
3. The solar insolance and convection to the ambient temperature of 100°F is applied to the outer shell of the expansion tank.

The Condition 2 models of the NAC-LWT cask with uniform and with variable decay heat MTR fuel element loadings are shown in Figure 3.5-6 and Figure 3.5-7, respectively. These same models are used to calculate both normal and accident condition temperatures for the cask.

Fuel Element Model

The fuel element model includes the side plate, the fuel, cladding, and the air between the plates and surrounding the side plate. The total element heat load is uniformly distributed throughout the fuel. Based on symmetry, only one-half of the fuel element assembly is modeled. Figure 3.4-13 shows the model for both the minimum 10-plate and maximum 23-plate cases. These two configurations bound fuel elements with any intermediate number of plates. The boundary condition for this model is the applied side plate temperature at the lower right corner of the model. This assumes that the basket is oriented such that only the ends of the element side plates are in contact with the basket. The lateral surfaces of the side plates are assumed to be adiabatic, which results in a conservative calculation of the maximum temperature of the fuel.

	K, BTU/hr-in-°F		
Temperature, °F	Aluminum	UO_2	Fuel Matrix 75% UO_2
100	8.08	0.42	2.33
200	8.25	0.37	2.34
300	8.38	0.33	2.35
400	8.49	0.30	2.35

The worst-case fuel effective thermal conductivity occurs for the maximum UO_2 percentage of 75% and corresponds to the LEU fuel plates.

The fuel in the center of each fuel plate is a matrix of aluminum and uranium or aluminum and uranium oxide (UO_2) combined in various ratios. The effective thermal conductivity is calculated using a mass-weighted average of the conductivity of the individual materials. The fuel plates are modeled using worst-case dimensions as shown:

1. Fuel plate thickness = 0.045 inch (< 0.05 inch)
2. Cladding thickness = 0.008 inch (< 0.015 inch)

A sensitivity analysis shows that variation of the active fuel width within the fuel plate has a negligible effect. A constant value of 6.6 cm is used in the analysis. This corresponds to the worst case for reactivity considerations. Note that the case of the loose fuel plates in the MTR canister is bounded by that of the assembled fuel element and, therefore, is not evaluated.

3.4.1.3.3 MTR Fuel Heat Transfer Analyses Results

The thermal analysis is performed to demonstrate that the temperature of the MTR fuel is maintained within acceptable limits. A conservative temperature of 400°F is established as the maximum allowable MTR fuel cladding temperature for normal conditions of transport. The aluminum retains its capability to function as a mechanical component in this temperature range, and it is not close to the 1,220°F melting temperature of aluminum (Table 6.4.1, pg. 6-60, Marks' Standard Handbook for Mechanical Engineers). The material properties presented in MIL-HDBK-5F indicate that 6061-T6 aluminum alloy retains over 40% of its room temperature yield and ultimate strengths at a long-term temperature of 400°F.

Maximum temperatures for package components with the NAC-LWT configured for MTR fuel are summarized in Table 3.4-6. The reported temperatures are lower at all locations than the corresponding temperatures for the design basis PWR fuel presented in Table 3.4-2. Temperatures of the MTR fuel element cladding are maintained below 400°F for both the design basis uniform decay heat loading and the variable heat loading.

3.4.1.4 PWR Rod

Heat transfer of the NAC-LWT containing 25 PWR rods with a total heat load of 1.41 kW configured in the PWR/BWR aluminum basket in the NAC-LWT cask enclosed in an International Shipping Organization (ISO) container was evaluated using ANSYS. The model presented in Figure 3.4-3 was revised to include the PWR/BWR aluminum basket and 25 PWR rods. Results from this evaluation are summarized in Table 3.4-7.

These results show that the temperatures are lower at all locations (except the neutron shield region) than the corresponding temperatures for the design basis PWR fuel presented in Table 3.4-2. Similar to the discussion presented in Section 3.4.1.3.3 for the MTR heat transfer analysis, temperature results from the two dimensional heat transfer analysis are conservative based on the imposed limitations of the model and can be used to evaluate acceptability of component temperatures outside the modeled section. Temperature of components in the lid closure region is less than the hottest basket temperature which is directly influenced by the decay heat of the fuel. It is concluded that the temperature of the safety related O-ring seals is within the allowable range of temperature of -40°F to +735°F. The maximum temperature of the lead gamma shield in the base of the LWT cask is less than the cask inner shell and much lower than the maximum of +600°F.

3.4.1.5 Thermal Evaluation for TRIGA Fuel

The thermal evaluation for TRIGA fuel is performed using classical analysis employing a thermal resistance model. The TRIGA fuel is transported in a basket assembly consisting of five modules - a base module, a top module, and three intermediate modules. During transport all 5 modules must be installed in the cask. The three intermediate modules are interchangeable, but the top and base modules are not. Each module contains 7 cells, and each open cell holds up to 4 TRIGA fuel elements. The top module is sized to accept fuel follower control elements, which are longer than the typical element. The center cell of each module is blocked with an 11-gage stainless steel plate so that fuel cannot be loaded in the center cell. The thermal evaluation conservatively assumes that the center cell also contains 4 fuel elements, so although only 120 fuel elements may be loaded into the cask, the thermal evaluation assumes 140 elements. Consequently, the total heat load in the thermal evaluation is conservatively considered to be 1.05 kW (7.5 watt/fuel element × 140 = 1.05 kW).

TRIGA fuel elements may be transported directly in a basket module cell, in a screened failed fuel can, or in a sealed failed fuel can. The fuel cans fit in either a top or base module cell. The screened failed fuel cans hold up to four (4) TRIGA fuel elements, while the sealed failed fuel can holds up to two (2) damaged elements or equivalent fuel debris.

As described in Section 1.2.3.1, TRIGA fuel elements with minor cladding defects are loaded into screened failed fuel cans (screened cans). The screened can precludes gross particulate material from escaping the cell. The screened failed fuel cans are provided in two lengths. The screened failed fuel can is a square tube of 14-gage, Type 304 stainless steel, that holds four fuel elements. It is provided with a closure lid and an end plate that is screened to allow water draining.

TRIGA fuel debris and damaged fuel elements, which do not have structural integrity, are loaded into sealed failed fuel cans (sealed cans). The sealed cans are used to containerize the TRIGA fuel debris. The cans are provided in two lengths. The shorter can may be used in the base or top basket modules. The longer can may only be used in the top module. The cans are vacuum dried and leak tested prior to loading into a TRIGA fuel basket.

The TRIGA fuel thermal evaluation determines the maximum fuel cladding temperatures based on the maximum basket temperatures determined for the design basis heat load MTR thermal analysis presented in Section 3.4.1.3.1. An intermediate basket module with the shortest TRIGA fuel, which provides the highest heat load density, is used to obtain a bounding evaluation. Based on the maximum basket temperature and heat load density, the maximum fuel cladding temperatures are determined using a thermal resistance model.

The cross-section of the TRIGA and MTR fuel baskets are identical. As shown in Section 1.2.3 and Table 1.2-4, the maximum decay heat load for MTR fuel is 1.26 kW per cask. The maximum decay heat load for TRIGA fuel is 1.05 kW per cask. Therefore, it is conservative to use the maximum basket temperature for MTR fuel as a boundary condition for the thermal resistance model for TRIGA fuel.

Since the total decay heat load for MTR fuel bounds that for TRIGA fuel, the temperatures for cask components for the MTR fuel also bound those for the TRIGA fuel. The cask body temperatures for the MTR fuel are shown in Table 3.4-6.

3.4.1.5.1 TRIGA Model Description

The heat generated from the TRIGA fuel in the basket is transferred to the basket module by thermal conduction and radiation, and then transferred to the cask inner shell from the basket surface by the same heat transfer modes. The heat is finally transferred through the cask and International Shipping Organization (ISO) container to ambient. The thermal resistance model and thermal analysis of TRIGA fuel considers the regions inside a single basket opening of the TRIGA fuel basket. This analysis bounds transport in the cask without an ISO container.

The thermal resistance model is shown in Figure 3.4-5. The maximum temperature of the basket (T_{basket}) is taken from the MTR design basis heat loading thermal analysis. The temperatures for

the TRIGA fuel are determined by stepping through each of the resistors in the thermal circuit, from the basket to the fuel cladding. All temperatures calculated are maximums, based on the basket temperature. Each successive maximum temperature calculated is then applied uniformly over the next surface in the resistance model. Fuel may be shipped directly in a basket cell, in a screened failed fuel can, or in a sealed failed fuel can. Since the model assumes the presence of the can, the model is conservative for configurations in which a can is not used.

The gas in the cask cavity is considered to be air in the thermal resistance model. Thermal conductivities of air and stainless steel are obtained from "Fundamentals of Heat and Mass Transfer" (Incropera). Emissivities of stainless steel (basket) and aluminum (fuel clad) are obtained from the Nuclear Systems Material Handbook and from "Scoping Design Analyses for Optimized Shipping Casks Containing 1-, 2-, 3-, 5-, or 10-Year-Old PWR Spent Fuel" (Bucholz), respectively.

Assuming the maximum temperature of the basket (T_{basket}) occurs at all inside surfaces of the webs forming the central cell in the basket module, the temperature of the can (T_{can}) is then determined by considering heat conduction and radiation between the can surface and the inside surface of the basket central cell. Convection in the gap between these surfaces is conservatively ignored.

The heat transfer rate across the gap per unit length (q_{gap}) between the can surface and the inside surface of the basket central cell wall can be represented as follows:

$$q_{gap} = q_{cond} + q_{rad}$$

$$q_{gap} = \frac{A(k_{cond})(T1 - T2)}{L_{gap}} + \frac{A(\sigma)(T1^4 - T2^4)}{\left(\frac{1}{\varepsilon 1} + \frac{1}{\varepsilon 2} - 1\right)}$$

where:

q_{gap} = 7.5 watt × 4/14 = 2.14 watt = 7.302 Btu/hr

A = Can surface area = 3.33 × 4 = 13.32 inch^2

K_{cond} = Air conductivity @ 260°F (400°K) = 1.628 × 10^{-3} Btu/hr-in-°F

L_{gap} = Gap size between can and basket = (3.44-3.33)/2 = 0.055 inch

T1 = temperature at can surface (T_{can})

T2 = temperature at inside surface of the basket central cell (T_{basket}) = 267°F

σ = 1.19 × 10^{-11} Btu/hr-in^2-°R

$\varepsilon 1$ = emissivity of web of basket central cell (stainless steel) = 0.36

$\varepsilon 2$ = emissivity of can (stainless steel) = 0.36

The temperature at the can (T_{can}) is calculated to be 287°F.

The maximum temperature of the can (T_{can}) is then applied to all can surfaces for determining the cladding temperature of the fuel. It is assumed that there are four (4) fuel elements inside the can surrounded by air. In the equivalent resistor analogy, the fuel elements do not contact each other, neglecting heat conduction between fuel elements. For a specific fuel element, an assumed circular region equivalent to 1/4 of the area inside the can, is developed to contain a fuel element, which results in a uniform air gap. The fuel cladding temperature is determined using the formula representing a hollow cylinder. Note that convective heat transfer in the gap between the fuel clad and the can is conservatively ignored.

Heat transfer rate per unit length of the basket (Q_{leng}) can be represented as:

$$Q_{leng} = q_{cond} + q_{rad}$$

$$Q_{leng} = \frac{2\pi(k_{cond})(T1 - T2)}{\ln\left(\frac{r2}{r1}\right)} + \frac{\sigma(2\pi r1)(T1^4 - T2^4)}{\left(\frac{1}{\varepsilon 1}\right) + \left(\frac{1-\varepsilon 2}{\varepsilon 2}\right)\left(\frac{r1}{r2}\right)}$$

where:

r1 = fuel cladding outer radius = 0.675-inch

r2 = radius of equivalent circular region representing ¼ of the area inside a can
= 0.93 inch.

K_{cond} = Air conductivity @ 260°F (400°K) = 1.628×10^{-3} Btu/hr-in-°F

σ = 1.19×10^{-11} Btu/hr-in^2-°R

$\varepsilon 1$ = emissivity of fuel cladding (aluminum) = 0.22

$\varepsilon 2$ = emissivity of the can (stainless steel) = 0.36

T1 = fuel cladding temperature (T_{clad})

T2 = can temperature (T_{can}) = 287°F

The fuel cladding temperature (T_{clad}) is solved to be 326°F.

3.4.1.5.2 TRIGA Fuel Thermal Evaluation Results

Using the model described above, and the assumed boundary condition of 267°F for the maximum basket temperature (from Table 3.4-6), the maximum normal transport conditions temperature of the TRIGA fuel is determined as shown in Table 3.4-8.

A conservative temperature of 400°F is established as the maximum allowable temperature for aluminum-clad TRIGA fuel, as described in Section 3.4.1.3.3 for MTR fuel. Stainless steel clad TRIGA fuel is allowed a significantly higher cladding temperature, since the melting temperature of stainless steel is 2,600°F (Mark's) and stainless steel retains its capability to function as a mechanical component at temperatures up to the 800°F range. Therefore, the temperatures calculated for the TRIGA fuel cladding are acceptable.

3.4.1.6 TRIGA Fuel Cluster Rods

The TRIGA fuel cluster rods are 0.542 inches OD with 0.016-inch thick Incoloy 800 cladding. Each rod is inserted into a 6061-T6 aluminum tube (0.75 inch OD, 0.62 inch ID) that is part of the fuel rod insert. Up to sixteen rods and a fuel rod insert are placed into a single cell of the seven cell basket. This TRIGA basket has the same cross sectional dimensions and basket material as the MTR basket presented in Section 3.4.1.3. The thermal evaluation for the TRIGA fuel cluster rods is performed using two-dimensional planar finite element analyses and the general purpose ANSYS computer code. Two transport conditions are evaluated:

Condition 1:

The NAC-LWT is supported in an ISO container with solar insolance applied on the surface of the ISO container, and the NAC-LWT is considered to be insulated from the environment (only for the normal conditions of transport steady state conditions). The gas inside the ISO container is air. The cavity of the NAC-LWT is actually backfilled with helium as required by operational procedures.

Condition 2:

The NAC-LWT is not located in an ISO container and solar insolation is applied to the NAC-LWT cask surface.

For the purpose of performing these thermal analyses, the cavity of the NAC-LWT is considered to be filled with air.

For each of the two conditions listed above, only a single fuel configuration is evaluated: 16 rods in a fuel rod insert in each of the seven cells comprising a basket section. This corresponds to a total heat load of 210 watts for each basket section (30 watts per cell of a basket section which

corresponds to 30/16 or 1.875 watts per rod). Therefore, the heat load in the cask cavity corresponding to five basket sections is 5 times 210 watts or 1.05 kW.

Since the finite element model corresponds to a one inch axial length, the heat generation applied to each rod in the model was 1.875 watts divided by the length of the rod or 22 inches. Although the aluminum inserts will conduct heat in the axial direction, this was conservatively ignored.

3.4.1.6.1 Condition 1 Analysis of TRIGA Fuel Cluster Rods

Thermal analyses of the NAC-LWT cask for Condition 1 are performed using a half symmetry cross sectional model of the cask in an ISO container positioned along the container centerline. The model employed for the ISO container, cask body and the seven-celled basket is the same finite element model used in Section 3.4.1.3.1 for the MTR fuel thermal model (Condition 1). The similarity in modeling includes the finite element mesh and the material properties for conduction, convection and radiation. The 16 rods and fuel rod inserts are modeled in each of the seven cells, as shown in Figure 3.4-7. Figure 3.4-8 and Figure 3.4-9 show details of the fuel region model. The TRIGA fuel cluster rods were conservatively modeled in the center of the aluminum fuel tube, and the fuel rod inserts were modeled without any contact with the sides of the basket. The 0.13 inch aluminum shell, which surrounds the TRIGA fuel cluster, provides a heat transfer path from the rods to the basket surface. This aluminum shell was conservatively not considered in the analysis. The space between the aluminum tubes and the stainless steel basket surface was modeled with the cavity gas, and the modes of heat transfer from fuel rod insert to the basket surface included conduction through the gas and radiation from the surface of the insert to the basket surface.

3.4.1.6.2 Condition 2 Analysis of TRIGA Fuel Cluster Rods

Thermal analyses of the NAC-LWT cask for Condition 2 are performed using a half symmetry cross sectional model of the cask in which the outer surface of the expansion tank is the boundary of the model. The modeling of the normal steady state conditions of the NAC-LWT from the center of the cask to the outer surface of the expansion tank is identical to the model described in Section 3.4.1.3.1 with the following exceptions:

1. The gas in the NAC-LWT cask cavity is considered to be air.
2. The solar insolance and convection to the ambient temperature of 100°F is applied to the outer shell of the expansion tank.

3.4.1.6.3 TRIGA Fuel Cluster Rods Heat Transfer Results

The thermal analysis is performed to demonstrate that the temperature of the TRIGA fuel cluster rod is maintained within acceptable limits. A conservative temperature of 800°F is established as

the maximum allowable TRIGA fuel cladding temperature for normal conditions of transport. For aluminum 6061-T6 aluminum alloy, the allowable temperature is considered to be 400°F.

Temperatures for package components with the NAC-LWT configured for the TRIGA fuel are summarized in Table 3.4-9. In this table, the maximum fuel clad temperature is 295°F, which is significantly below the 800°F value. For the aluminum, the maximum reported temperature is 292°F, which is also well below the 400°F limit.

3.4.1.7 High Burnup PWR or BWR Rods in a PWR/BWR Rod Transport Canister

The high burnup rods may be either BWR rods or PWR rods. The decay heat for the PWR fuel rod contents is 2.3 kW with a corresponding peaking factor of 1.1. The decay heat for the BWR fuel rod contents is 2.1 kW with a peaking factor of 1.22. The thermal evaluation employs a two-dimensional planar model to ensure that the peaking factor is conservatively included and the heat load applied to the finite element model is the total heat load factored by the peaking factor. The bounding product of the heat load and the peaking factor corresponds to the BWR. The evaluation of the BWR rod is considered to bound the temperatures corresponding to the PWR rod configuration. All of the fuel rods are considered to be intact for this evaluation. The evaluation of damaged fuel rods is provided in Section 3.4.1.11. An additional configuration is also considered in which four tubes of the 5×5 insert are replaced by a single tube to accommodate a BWR water rod, which has negligible heat load. The single water rod occupies a position near the center of the matrix. However, the thermal response associated with the configuration with the water rod is bounded by the evaluation of the 5×5 matrix due to the reduced heat load and the removal of the heat generation at the center of the matrix.

The PWR/BWR Rod Transport Canister for the high burnup rod transport can accommodate three configurations: a 4×4 matrix of pin tubes containing up to 16 rods, a 5×5 matrix of pin tubes containing up to 25 rods, and an alternative 5×5 rod holder designed to contain an oversize nonfuel-bearing component (e.g., CE guide tube or BWR water rod) and up to 21 rods. Since the decay heat per rod is considered to be the same, the maximum heat load is bounded by the 25-rod configuration. For the 4×4 matrix of pin tubes, an additional 31-inch-thick stainless steel insert is placed in the can weldment. This permits the can weldment to be employed for the 16-rod transport or the 25-rod transport configuration. For the can weldment, the aluminum basket and the remainder of the cask, the additional insert has a negligible affect on their temperatures. Therefore, the bounding configuration is the 25-rod configuration, since it produces 56% more heat load in the cask basket than the 16-rod configuration. The bounding configuration for the clad temperatures and the pin tubes supporting the fuel rods is also the 25-rod configuration due

to the 56% additional heat load. While the additional insert increases the thermal resistance, this is significantly offset by the additional 56% additional decay heat.

Heat transfer analysis of the NAC-LWT containing high burnup rods is performed using two-dimensional planar finite element analyses and the general purpose ANSYS computer code. Two transport conditions are evaluated:

Condition 1:

The NAC-LWT is supported in an ISO container with solar insolance applied on the surface of the ISO container, and the NAC-LWT is considered to be insulated from the environment (only for normal conditions of transport steady state conditions). The gas inside the ISO container is air.

The cavity of the NAC-LWT is backfilled with helium as required by operational procedures.

Condition 2:

The NAC-LWT is not located in an ISO container and solar insolance is applied to the NAC-LWT cask surface.

For the purpose of performing the thermal analyses, the cavity of the NAC-LWT is considered to be filled with air.

3.4.1.7.1 High Burnup PWR and BWR Fuel Rods Thermal Model of the NAC-LWT (Transported in an ISO Container)

Thermal analyses of the NAC-LWT cask for Condition 1 are performed using a half-symmetry, cross-sectional model of the cask in an ISO container. Heat transfer to the environment is limited to surface convection and radiation on both horizontal and vertical surfaces of the ISO container with an emissivity of 0.36. Solar insolance is applied to the vertical surfaces and the top horizontal surface. Heat transfer from the cask to the ISO container is modeled as conduction, convection and radiation. Convective and conductive heat transfer are modeled in the liquid neutron shield, while heat transfer in the cask cavity is limited to conduction and radiation. Axial heat transfer is conservatively ignored in the model.

Bounding configuration of BWR fuels used in analyses is based on U.S. Department of Energy, Office of Civilian Radioactive Waste Management, "Characteristics of Spent Fuel, High-Level Waste, and Other Radioactive Wastes Which May Require Long -Term Isolation," Appendix 2A, December 1987. Thermal properties of UO_2 and zirconium alloy cladding are from 1) Hagrman, D.L., Reymann, G.A., "Matpro-Version 11, A Handbook of Material Properties for Use in the Analysis of Light Water Reactor Rod Behavior," Idaho Falls, ID, EG&G Idaho, Inc., 1997; 2) Rust, J.H., "Nuclear Power Plant Engineering," Atlanta, GA, S.W., Holland Company, 1979.

Thermal conductivity for 6061-T651 aluminum alloy is based on ASME Code, Section II, Part D, Table TCD.

The finite element model for the condition 1 is shown in Figure 3.4-10. The fuel cladding and the inner surface of the pin tube are considered to be in point-to-point contact. The outer surface of the fuel cladding only contacts the pin tube in one point in the model. The pin tubes are conservatively considered separated and a gap of 0.0005 inch between pin tubes is modeled. This condition neglects any pin tube contact due to dead weight loading of the contents. One of the can weldment sides is modeled in contact with the aluminum insert. For the other three sides, a gap 0.042/0.084/0.042 inch between the aluminum insert and the tube of the can weldment is modeled. The details of this modeling are shown in Figure 3.4-11. Likewise, only one surface between the PWR aluminum insert and the PWR basket is considered to be in contact.

Conduction (through helium) and radiation (using emissivity of stainless steel for both surfaces) are modeled from the inner shell of the cask to the basket.

The heat transfer analysis model uses conduction in the remaining volume of the cask cavity. The conductivity of this material corresponds to helium. (see Table 3.2-7). The properties for the remaining materials are contained in Table 3.2-1 through Table 3.2-8.

The air space between the NAC-LWT cask and the ISO container is modeled using air with an effective conductivity. This effective conductivity (Incropera) is:

$$\frac{k_{eff}}{k} = 0.386\left(\frac{Pr}{0.861+Pr}\right)^{1/4}\left(Ra_c^{*}\right)^{1/4}$$

$$Ra_c^{*} = \frac{[\ln(D_0/D_i]^4}{L^3\left(D_i^{-3/5}+D_0^{-3/5}\right)^5}\,Ra_L$$

$$Ra_L = \frac{g\beta(T_i-T_o)L^3}{\alpha\nu}$$

where:

Pr = Prandtl number (Krieth)

ν = kinematic viscosity (Krieth)

α = thermal diffusivity (Krieth)

β = $1/T_f$

T_f = $(T_i+T_o)/2$

T_i = inner surface temperature

T_o = outer surface temperature

D_i = inner diameter (cask surface)

D_o = outer diameter (height of the ISO container)

$L = (D_o - D_i)/2$

3.4.1.7.2 High Burnup PWR and BWR Fuel Rods Thermal Model of the NAC-LWT (Transported via Truck Trailer)

Thermal analyses of the NAC-LWT cask for Condition 2 are performed using a half-symmetry planar cross-sectional model of the cask in which the inner surface of the inner shell is the boundary of the model. The maximum temperature of 274°F (PWR design basis fuel with 2.5 kW heat load and a peaking factor of 1.2 under normal transport condition [Table 3.4-2]) is applied to the boundary of the model. The modeling of the normal steady state condition of the NAC-LWT from the center of the cask to the inner surface of the inner shell is identical to the model described in Section 3.4.1.7.1 with the following exceptions:

1. The gas in the NAC-LWT cask cavity is considered to be air.
2. The constant temperature of 274°F is applied to the outer surface of the model, which corresponds to the inner surface of the cask inner shell. This temperature corresponds to the condition, which imposes solar insolance and convection/radiation boundary at the outer shell of the expansion tank. This is also described in Section 3.4.1.1.

The Condition 2 model of the NAC-LWT cask with high burnup PWR and BWR fuel rods is shown in Figure 3.4-12. This model is also used to calculate both normal and accident condition temperatures for the cask.

3.4.1.7.3 High Burnup PWR and BWR Fuel Rods Heat Transfer Analyses Results

The thermal analysis is performed to demonstrate that the component temperature of NAC-LWT cask loaded with high burnup PWR and BWR rods is maintained within acceptable limits.

Maximum temperatures for package components with the NAC-LWT configured for high burnup PWR and BWR rods are summarized in Table 3.4-10. As shown in Table 3.4-10, component temperatures are all maintained within their allowable temperatures.

3.4.1.8 Thermal Evaluation for DIDO Fuel

3.4.1.8.1 Analytical Models for the DIDO Fuel Contents

Heat transfer analysis of the NAC-LWT containing DIDO fuel is performed using a two-dimensional planar finite element analysis and the general purpose ANSYS computer code. Two transport conditions are evaluated:

Condition 1:

The NAC-LWT is supported in an ISO container with solar insolance on the surface of the ISO container, and the NAC-LWT is considered to be insulated from the environment (only for the normal conditions of transport steady state conditions). The gas inside the ISO container is air. The cavity of the NAC-LWT is backfilled with helium as required by operational procedures.

Condition 2:

The NAC-LWT is not located in an ISO container and solar insolation is applied to the NAC-LWT cask surface. For the purpose of performing the thermal analysis, the cavity of the NAC-LWT is considered to be filled with air.

A single fuel configuration is considered for this evaluation. Each DIDO fuel assembly is limited to having a heat load of 25 W per assembly. The total contents of the NAC-LWT for the DIDO fuel are limited to having six basket modules and each module is limited to having seven DIDO fuel assemblies. This limits the heat load of a basket module to 175 W, and a total NAC-LWT heat load of 1.05 kW. The 1.05 kW total heat load is enveloped by the 1.26 kW total heat load for the NAC-LWT MTR fuel contents contained in Section 3.4.1.3. Since the NAC-LWT cask ambient conditions are the same for the DIDO fuel as for the MTR fuel, the maximum temperature of all cask body components for the DIDO contents are enveloped by the maximum temperatures for the MTR fuel contents. Therefore, the cask inner shell temperature for the MTR fuel contents bounds the maximum cask inner shell temperature for the DIDO fuel contents. The maximum cask inner shell temperature is used as the boundary condition for the finite element model for the DIDO thermal evaluation. For Condition 1 and Condition 2, the maximum inner shell temperatures are 214°F and 181°F, respectively. These values correspond to the design basis heat load values obtained from Table 3.4-6.

Two finite element models are used in the evaluation of the DIDO fuel basket and the DIDO fuel assemblies.

The evaluation of the maximum basket component temperatures for these conditions is performed using a finite element model, which is shown in Figure 3.4-14. This model is used to evaluate both conditions. This model corresponds to the 4.01-inch inside diameter stainless steel tubes, the 1/2-inch thick plates, the 3/4-inch × 3/8-inch aluminum bars (thermal shunts) and the 0.19-inch thick aluminum sheet (heat transfer shell) on the outside of the tubes. The SOLID70, eight-noded brick element is used to represent stainless steel components, the heat transfer shell and the cavity gas between the surfaces of the circular plates and the heat transfer shell and the inner shell of the cask body. To account for the axial conductance of the thermal shunts, they are modeled as conduction elements using an area corresponding to the dimensions of the aluminum bars. Radiation is conservatively neglected from the outer surface of the heat transfer shell and the inner surface of the cask inner shell. The center tube is assumed not to be in contact with any of the six outer tubes. During transport, the NAC-LWT is in a horizontal position in which the basket modules are in contact with the inner shell of the cask. To represent the contact of the basket module with the cask inner shell, the inner shell temperature was applied to two nodes of the circular plates and the remaining nodes corresponding to the inner surface of the inner shell of the cask body. The 25 W per assembly heat load is represented by applying the heat flux along a concentrated area at the inner tube surface, which would correspond to the contact of the fuel assembly with the 4.01-inch inside diameter stainless steel tube.

For Condition 1, the elements representing the cavity gas between the basket and the inner shell correspond to helium, whereas for Condition 2, these elements use properties for air.

To determine the maximum temperature for the fuel, a separate detailed model of a DIDO fuel assembly is constructed. This model is shown in Figure 3.4-15, which consists of four circular cylinders in contact at a corresponding single point to be transported in the horizontal position. Each cylinder is comprised of a layer of fuel of 0.64 mm (0.025 in.) thickness between two aluminum shells, each being 0.46 mm (0.018 in.) thick. The boundary condition of this model is the maximum basket temperature determined from the detailed basket model and the volumetric heat generation corresponding to 25 W per assembly.

3.4.1.8.2 DIDO Fuel Heat Transfer Analyses Results

The thermal analysis is performed to demonstrate that the temperature of the DIDO fuel is maintained within acceptable limits. A conservative temperature of 400°F is established as the maximum allowable DIDO fuel cladding temperature for normal conditions of transport. The aluminum retains it capability to function as a mechanical component in this temperature range and it is not close to the 1,220°F melting temperature of aluminum (Table 6.4.1, p. 6-60, Marks' Mechanical Handbook for Mechanical Engineers). The material properties presented in

MIL-HDBK-5F indicate that 2000 series aluminum retains over 40% of its room temperature yield and ultimate strengths at a long-term temperature of 300°F.

Maximum temperatures for package components with the NAC-LWT configured for DIDO fuel are summarized in Table 3.4-12. The reported temperatures are lower at all locations than the corresponding temperatures for the design basis PWR fuel presented in Table 3.4-2. The DIDO fuel assembly cladding temperatures are maintained below 400°F.

3.4.1.9 Thermal Evaluation for General Atomics IFM

The heat generated from the General Atomics IFM in the Fuel Handling Unit (FHU) is transferred to the basket by thermal conduction and radiation, and is then transferred to the cask inner shell from the basket surface by the same heat transfer modes. The heat is finally transferred through the cask and International Shipping Organization (ISO) container to ambient. The thermal resistance model and thermal analysis of General Atomics IFM consider a single FHU of the fuel. The maximum temperature from the resistor model corresponds to the FHU's stainless steel shell, while the minimum temperature corresponds to the inner surface of the transport cask inner shell. The fuel is actually stored in two FHUs, but the evaluation conservatively considers the total heat load of 13 W to be placed into a container at the center of the cask cavity. The evaluation does not consider the reduction in thermal resistance due to the contact of the FHU with the basket or of the basket with the inner shell of the transport cask. Additional conservatism is included by ignoring heat transfer by radiation across any of the gaps in the system. To ensure that a bounding temperature for the basket is calculated, air properties are used in the analysis for the gas in the cavity. Also, conservatism is included by using the inner shell temperature corresponding to the 1.26 kW condition for the cask body as opposed to 13 W. This analysis, therefore, bounds transport in the cask with and without an ISO container.

A thermal evaluation of the top module is performed by considering a heat load of 13 W in the center of the basket with only one 6.0-inch diameter top module tube. This is conservative because it maximizes the gap between the tube and the cask inner shell. Air is used as the cavity gas as an additional conservatism. The maximum temperature is computed using the resistor analogy.

For concentric cylinders, the thermal resistance (R) for the heat flow through the cylinders is taken from Krieth as:

$$R = \frac{\ln\left(\frac{r_2}{r_1}\right)}{2\pi K L}$$

where:

r_2 = outer radius of cylinder (inch)

r_1 = inner radius of cylinder (inch)

K = thermal conductivity (BTU/hr/in/°F)

The effective resistance from the secondary enclosure can be expressed as to the cask inner shell:

$$R_T = R_1 + R_2 + R_3 + \frac{1}{\frac{1}{R_4} + \frac{1}{R_5}}$$

where:

R_1 = resistor of the outer canister

R_2 = resistor of the gap between outer canister and the basket shell

R_3 = resistor basket shell

R_4 = resistor of the air from the basket shell to inner shell surface (outside of the basket disks)

R_5 = resistor of stainless steel disks supporting the basket shell in series with the air gap between the basket disks and the inner shell

The maximum temperature of the secondary enclosure can be determined by the following equation:

$$T_i = R_t Q + T_{cask}$$

where:

Q = total heat load

T_{cask} = temperature of cask inner shell

The following parameters will be used for this evaluation:

Q = 13 Watts

L = 37.0 inches – length of shortest secondary fuel closure

r1 = 2.255 inches – minimum inner radius of secondary closure

r2 = 2.375 inches – minimum outer radius of secondary closure

r3 = 2.75 inches – inner radius of module fuel cell

r4 = 3.00 inches – outer radius of module fuel cell

r5 = 6.688 inches – inner radius of LWT

r6 = 6.6325 inches – outer radius of the basket disks

K_{ss} = 0.7143 Btu/hr/in/F at 70°F for stainless steel

K_{air} = 0.00161 Btu/hr/in/F at 300°F for air

From Table 3.4-6, the maximum temperature of the LWT inner shell for a 1.26 kW heat load is 214°F, with 100°F ambient temperature with solar insolance. This is used as a bounding temperature for the cask inner shell (T_{cask}) for this evaluation.

$$R_{eff} = \frac{1}{\frac{1}{R_4} + \frac{1}{R_5}} \qquad R_4 = \frac{\ln(6.688/3.0)}{2\pi(0.00161)(37.0-2)}$$

$$R_4 = 2.264$$

$$R_5 = \frac{\ln(6.8125/3.0)}{2\pi(0.7143)(2)} + \frac{\ln(6.688/6.6325)}{2\pi(0.00161)(2)}$$

(Stainless steel disk in series with the air between the basket disk and the inner shell)

$$R_5 = 0.503$$

$$R_{eff} = \frac{1}{\frac{1}{R_4} + \frac{1}{R_5}}$$

$$R_{eff} = 0.412$$

$$R_T = R_1 + R_2 + R_3 + R_{eff}$$

$$R_T = \frac{\ln(2.375/2.255)}{2\pi(0.7143)(37.0)} + \frac{\ln(2.75/2.375)}{2\pi(0.00161)(37.0)} + \frac{\ln(3.0/2.75)}{2\pi(0.7143)(37.0)} + 0.412$$

$$R_T = 0.0003 + 0.392 + 0.0005 + .412 = 0.805$$

The maximum temperature of the secondary enclosure (T_i) is:

$$T_i = 0.805(13 \times 3.415) + 214 = 250^\circ F$$

The maximum temperature of the basket is conservatively considered to be the same as the temperature of the secondary enclosure (250°F). Temperatures of individual components are summarized in Table 3.4-13.

The maximum content temperature for the GA IFM shipment is considered to be bounded by the TRIGA maximum fuel cladding temperature of 326°F contained in Table 3.4-8, which corresponds to a bounding heat load of 1.05 kW (as compared to the approximately 13 watts for the GA IFM).

A conservative temperature of 800°F is established as the maximum allowable temperature for the stainless steel basket and the contents, which is comprised of the steel-clad TRIGA fuel and the HTGR pellets. The steel cladding of the TRIGA fuel is actually an inconel alloy. Mil HDBK-5G (1 November 1994), Section 6.3.2, identifies that alloys of inconel are used for parts requiring strength for temperatures exceeding 1,000°F, which significantly exceeds 800°F. The HTGR pellets were designed for operational exposure to reactor core temperatures exceeding 1,000°F, which also exceeds 800°F. Therefore, the maximum temperatures for the contents for the GA IFM are acceptable.

3.4.1.10 High Burnup PWR or BWR Fuel Rods in a Fuel Assembly Lattice

The NAC-LWT cask may transport up to 25 intact high burnup PWR or BWR fuel rods that are in a fuel assembly lattice. The decay heat for the PWR rods is 2.3 kW with a corresponding peaking factor of 1.1, and the decay heat for the BWR rods is 2.1 kW with a corresponding peaking factor of 1.22.

The thermal evaluation employs two-dimensional planar half-symmetry models of the fuel lattice with 25 fuel rods, fuel channel (for BWR fuel), PWR insert (for BWR fuel), fuel basket, and the gas inside the cask cavity. The model extends to the inner surface of the cask inner shell. The model for a 7 × 7 BWR fuel lattice with 25 fuel rods is shown in Figure 3.4-16. BWR arrays of 7 × 7, 8 × 8, 9 × 9, and 10 × 10 are analyzed. PWR arrays of 14 × 14, 15 × 15, 16 × 16, and 7 × 17 are analyzed. The BWR model includes a fuel channel and insert, which are absent from the PWR model.

To determine the worst-case fuel rod arrangement, the 25 fuel rods are analyzed in five different arrangements:

1. Centered (top and bottom) in the two-dimensional model (as shown in Figure 3.4-16).
2. Centered horizontally and concentrated at the bottom of the lattice cross-section.
3. Spread out horizontally and concentrated at the bottom of the lattice cross-section.
4. Centered horizontally and concentrated at the top of the lattice cross-section.
5. Spread out horizontally and concentrated at the top of the lattice cross-section.

For the even numbered fuel arrays (i.e., 8 × 8, 10 × 10, 14 × 14, and 16 × 16), only 24 fuel rods are modeled due to the use of the half-symmetry models. For these cases, a higher heat generation rate is applied at each fuel rod so that the total heat load of 2.3 kW for PWR and 2.1 kW for BWR is maintained. The empty fuel rod locations in the lattice are modeled as air. The maximum inner shell temperature (274°F) for the PWR design basis fuel with 2.5 kW heat load (Table 3.4-2) is applied to the boundary of the model.

For each fuel array and fuel rod location configuration, a steady-state thermal analysis is performed using the general purpose ANSYS computer code. The Condition 2 transport case, with the NAC-LWT not located in an ISO container is evaluated. As shown in Table 3.4-10, this results in higher maximum temperatures for the fuel cladding than transport Condition 1 where the cask is assumed to be inside of the ISO container. Transport Conditions 1 and 2 are described in Section 3.4.1.3.

3.4.1.11 High Burnup PWR and BWR Fuel Rods in a Rod Holder with Damaged Fuel Rods

The NAC-LWT may transport up to 25 PWR or BWR high burnup fuel rods in a rod holder, with up to 14 of the fuel rods classified as damaged. The maximum decay heat for these configurations is 2.3 kW for PWR and 2.1 kW for BWR. The finite element model for the evaluation of the 25 intact fuel rods in a rod holder is described in Section 3.4.1.7. This section provides the thermal evaluation for the configuration containing damaged fuel rods. The analysis conservatively assumes 15 damaged fuel rods, with the remainder of the rod holder containing intact fuel. The model used for this analysis is based on the two-dimensional half-symmetry model described in Section 3.4.1.7 (Condition 2 configuration), as shown in Figure 3.4-12. Modifications were made to the fuel regions to simulate the damaged fuel rods.

The basket design for the high burnup fuel rod transport can accommodate three configurations: a 4×4 matrix of fuel tubes containing up to 16 rods, a 5×5 matrix of fuel tubes containing up to 25 rods, and an alternate 5×5 rod holder designed to contain an oversize nonfuel-bearing component (e.g., CE guide tube or BWR water rod) and up to 21 rods. Since the decay heat per rod is considered the same, the maximum heat load occurs with the 5×5 matrix and is the configuration evaluated. Thermal analysis is performed for three cases with different locations of the 15 damaged fuel rods. The fuel rod locations are shown in Figure 3.4-17, which shows the matrix region of the thermal model shown in Figure 3.4-12. The nine locations in the half-symmetry model correspond to 15 actual fuel rod locations. The three cases evaluated are:

Case 1: Damaged fuel rods in locations 4 through 12
Case 2: Damaged fuel rods in locations 7 through 15

Case 3: Damaged fuel rods in locations 1 through 9

The inner surface of the inner shell is the boundary of the model. From Table 3.4-2, the maximum inner shell temperature of 274°F for PWR design basis fuel with 2.5 kW heat load for normal transport conditions is applied to the boundary of the model. The maximum temperature of 274°F results from the condition of solar insolation and convection/radiation to surroundings.

To simulate the damaged fuel rods, a 50% compaction of the fuel material in the fuel tubes is considered. It is assumed that the interior region of the fuel rod tube consists of 50% fuel debris and 50% gas. One half of the heat generation rate for the intact fuel rod is conservatively applied to the entire interior region of the fuel rod tube. Since the volume of the interior of the fuel rod tube is four times that of the volume of an intact fuel rod, the applied heat load for the damaged fuel is two times that of the heat load for an intact fuel rod. In addition, the heat generation rate is multiplied by a peaking factor of 1.22. The material properties in the entire interior of the fuel rod tubes for the damaged fuel are conservatively considered to be the thermal properties of the fuel (rather than 50% fuel and 50% gas), since this results in higher temperatures in the fuel rod tube walls and the surrounding components.

3.4.1.12 Thermal Evaluation for TPBARs

Heat transfer analysis of the NAC-LWT containing TPBARs is performed using a two-dimensional planar finite element analysis and the general purpose ANSYS computer code. The NAC-LWT is transported in an ISO container with solar insolance on the surface of the ISO container during normal conditions of transport. The gas inside the ISO container is air. The cavity of the NAC-LWT is backfilled with helium as required by operational procedures.

There are two TPBAR content conditions requested for certification: the first is for the transport of up to 300 production TPBARs (of which two can be prefailed) in an open consolidation canister; the second is for the transport of up to 55 segmented TPBARs in a welded closed waste container. The 55 segmented TPBARs and debris resulting from PIE are limited to a total heat load of 127 W, based on a minimum of 90 days of cooling (2.31 watts/rod). Therefore, the loaded TPBAR consolidation canister with 300 rods is considered the bounding content condition for this thermal evaluation with each TPBAR limited to a heat load of 2.31 W, which corresponds to a 90-day cooling period (see Appendix 1-C of Chapter 1). This limits the maximum heat load of the NAC-LWT with TPBAR contents to 0.693 kW. The 0.693 kW total heat load is enveloped by the 1.05 kW total heat load for the NAC-LWT TRIGA fuel contents as described in Section 3.4.1.6. Since the NAC-LWT cask ambient conditions are the same for the TPBAR contents as for the TRIGA fuel contents, the maximum temperature of all cask body components for the TPBAR contents are enveloped by the maximum temperatures for the

TRIGA fuel contents. Therefore, the cask inner shell temperature of 222°F (Table 3.4-9) for the TRIGA fuel contents bounds the cask inner shell temperature for the TPBAR contents and is used as the bounding condition for the TPBAR thermal evaluation.

The evaluation of the maximum component temperatures for TPBARs is performed using a finite element model as shown in Figure 3.4-18. This model corresponds to the aluminum basket, the consolidation canister containing 300 TPBARs, and the helium inside the cask. The loaded TPBAR consolidation canister bounds the maximum decay heat of the TPBAR waste container containing 55 segmented TPBARs and, therefore, the thermal evaluation bounds all TPBAR content conditions.

Any axial conductance of the contents is conservatively neglected in this two dimensional planar model. The ANSYS PLANE55 and MATRIX50 elements are used. Radiation is considered using radiation matrix elements while convection is conservatively ignored in the following regions.

- Between the outer surfaces of TPBARs.
- Between the inner surface of the consolidation canister and the adjacent TPBARs.
- Between the outer surface of the consolidation canister and the inner surface of the basket.
- Between the outer surface of the basket and the inner surface of the cask inner shell.

A constant temperature of 222°F (Table 3.4-9, Condition 1) was applied to the outer surface of the model, which corresponds to the inner surface of the cask inner shell. During transport, the NAC-LWT is in a horizontal position in which the TPBAR contents are in contact with the inner surface of the basket, while the basket plates are in contact with the inner shell of the cask.

The heat generated by the 300 TPBARs is applied via a heat generation rate to the stainless steel cladding of the TPBARs. A peaking factor of 1.15 is used in the heat generation rate calculation based on a heat load of 2.31 W for each TPBAR.

The thermal analysis demonstrates that the temperature of the TPBARs is maintained within a conservative limit of 300°F for normal conditions of transport. At 300°F, the aluminum retains its capability as a mechanical component.

Maximum component temperatures for the NAC-LWT containing TPBAR contents are summarized in Table 3.4-16. Maximum cask component temperatures for normal conditions are conservatively obtained from the analysis results corresponding to the TRIGA fuel contents, as shown in Table 3.4-9 (Condition 1).

3.4.1.13 PULSTAR Fuel Elements in 28 MTR Basket

Three loading patterns for PULSTAR fuel elements are postulated for the 28 MTR basket configuration.

- Intact fuel assemblies will be directly loaded into 28 MTR basket;
- Intact fuel elements (rods) will be loaded in the fuel rod insert or the PULSTAR cans;
- Damaged fuel elements (rods) or debris will be loaded in the PULSTAR cans.

The heat load in each basket cell is limited to 30 watts. This corresponds to a maximum heat load of 210 watts for each of the four basket modules. The cask cavity is back-filled with helium.

The thermal analysis for the PULSTAR fuel contents in the 28 MTR basket is bounded by the thermal analysis for the TRIGA fuel cluster rods as presented in Section 3.4.1.6. The MTR basket (Section 3.4.1.3) has the same cross-sectional dimensions and basket material as the basket for TRIGA fuel cluster rods. The maximum modular heat load for TRIGA fuel cluster rods is identical to the maximum modular heat load of the PULSTAR fuel contents (210 watts). The bounding condition for the thermal evaluation for the TRIGA fuel cluster rods is "Condition 2" as described in Section 3.4.1.6.2. In the two-dimensional planar model for the TRIGA fuel cluster, the cask cavity is modeled as air. The model conservatively includes an air gap between the fuel cladding and the aluminum tube and between fuel tube assembly and the inner surface of the basket cell, as shown in Figure 3.4-8 and Figure 3.4-9. This is conservative since there is contact between these components, which provides a significant heat transfer path from the fuel to the basket. Note that the aluminum tubes have an insignificant effect on heat transfer, since the air gap controls the heat conduction in the in-plane direction and the model is a two-dimensional planar model, which neglects any heat transfer in axial direction. Since the PULSTAR fuel rod insert is identical to the TRIGA rod insert, the thermal analysis results for TRIGA fuel cluster rods, Condition 2, as presented in Table 3.4-9, are used as the temperature results for the PULSTAR fuel. These temperatures are summarized in Table 3.4-17 for the PULSTAR fuel. The cask body component maximum temperatures with the NAC-LWT configured for the PULSTAR fuel conservatively use the temperatures from Condition 1 and Condition 2 in Table 3.4-17. The maximum temperatures for the cask body and basket are 222°F and 278°F, respectively, which are significantly below the allowable for stainless steel. For the configuration with intact rods or failed rods loaded in a PULSTAR can, the maximum fuel cladding temperature from Table 3.4-17 is conservatively used as the maximum temperature of the fuel can. The maximum fuel cladding temperature is 295°F, which is significantly below the allowable temperature limit of 1,058°F during transport.

3.4.1.14 Thermal Evaluation for ANSTO Fuel

Two types of ANSTO fuel may be loaded in the ANSTO basket in the NAC-LWT cask:

- MOATA plate fuel elements
- Mark III spiral fuel elements

The ANSTO basket consists of six modules with seven fuel tubes in each module. Each fuel tube may be loaded with a MOATA plate bundle or a Mark III spiral fuel assembly. The maximum heat load for a MOATA plate bundle is 0.4 watt (3 watts per assembly is conservatively considered in the thermal evaluation in this section). The maximum heat load is 18 watts per assembly for the Mark III spiral fuel. The corresponding maximum heat load per cask is 0.126 kW for the MOATA plate bundles and 0.756 kW for the Mark III spiral fuel.

The NAC-LWT is supported in an ISO container with solar insolance applied on the surface of the ISO container. The gas inside the ISO container is air. The cavity of the NAC-LWT is actually backfilled with helium as required by operational procedures.

The thermal evaluation for the MOATA plate fuel elements and Mark III spiral fuel is performed using finite element analysis with the ANSYS program. The finite element models for the MOATA plate bundles and Mark III spiral fuel are shown in Figure 3.4-19 and Figure 3.4-20, respectively. Each model corresponds to a quarter-symmetry cross-section of the fuel, the basket and the helium inside the cask cavity. The models are constructed using ANSYS PLANE55 two-dimensional planar elements. The maximum cask inner shell temperature of 222°F for the LWT cask loaded with the TRIGA fuel cluster rods (see Table 3.4-9) is conservatively used as the boundary condition for both models. The heat load used in the evaluation of the TRIGA fuel cluster rods is 1.05 kW per cask (see Section 3.4.1.6), which is significantly higher than the heat load for the MOATA fuel and Mark III spiral fuel. The MOATA plate fuel elements are explicitly modeled with aluminum cladding on both sides of the fuel meat. A volumetric heat generation rate corresponding to 3 watts per assembly is applied to the elements for fuel meat for the MOATA plate fuel.

The MARK III spiral fuel assemblies are modeled as straight plates with effective orthotropic properties. The longitudinal (radial) properties are decreased to reflect the reduction of the length (from the actual curved plates to the straight plates in the model). The material properties for the fuel meat are conservatively used in the transverse (circumferential) direction of the fuel elements in the model (conductivity of the aluminum clad is higher than that for the fuel meat). A volumetric heat generation rate corresponding to 18 watts per assembly is applied to the fuel elements for the Mark III spiral fuel.

The thermal conductivities of the fuel matrix for MTR fuel from Section 3.4.1.3 are used as the conductivities for the fuel meat for the MOATA plate and MARK III spiral fuel elements in the thermal models. These thermal conductivities are conservative since the fuel meat for the MOATA plate fuel and Mark III spiral fuel is composed of uranium and aluminum alloy, which are significantly more conductive than the fuel matrix material for the MTR fuel. Radiation between the basket tube and the cask inner shell is conservatively not considered in the models. For the MOATA fuel, radiation is only considered between fuel plates. For the Mark III spiral fuel, radiation is modeled across the helium gap between the fuel outer tube and the basket tube.

Steady-state thermal analysis is performed to demonstrate that the temperature of the MOATA plate fuel and Mark III spiral fuel is maintained within acceptable limits. A conservative temperature of 400°F is established as the maximum allowable temperature for these aluminum-clad fuel elements, as discussed in Section 3.4.1.3.3 for the MTR fuel.

3.4.1.15 High Burnup PWR MOX Rods in a PWR/BWR Rod Transport Canister

A maximum of 16 PWR MOX fuel rods (or a combination of PWR MOX and standard PWR fuel rods) may be placed in the PWR/BWR Rod Transport Canister, including a 5 × 5 insert. Along with the maximum 16 PWR MOX rod contents, the remaining tubes may be loaded with burnable poison rods or other zirconium alloy-based hardware components with negligible activation and heat load. The maximum decay heat for the PWR MOX rods is 2.3 kW (or 143 W/rod), with a corresponding peaking factor of 1.1.

The thermal evaluation described in Section 3.4.1.7 for the high burnup PWR and BWR rods is a two-dimensional planar model in which the heat load applied to the model is based on the BWR rod decay heat load factored by the peaking factor. The bounding product of the heat load and the peaking factor for the PWR MOX rods is (2.3)(1.1) or 2.53 kW, as compared to (2.1)(1.22) or 2.56 kW for the BWR high burnup rods. The evaluation performed in Section 3.4.1.7 using the BWR high burnup rods is considered to bound the heat load for the 16 PWR MOX rods.

As described in Section 3.4.1.7, the model for the 25-rod configuration (in a 5 × 5 insert) uses a heat load of (25/16) times the product of the BWR rod decay heat and associated peaking factor. With this bounding heat load, it is, therefore, not necessary to evaluate the 16-rod configuration in the Rod Transport Canister with a 5 × 5 insert.

The thermal conductivities of the UO_2 and MOX from MATPRO-Version 11 at 600°F are 0.26 Btu/hr-in-°F and 0.22 Btu/hr-in-°F, respectively. The thermal resistance to the heat rejection of the rod canister is due to the thin tube walls and the gaps modeled between the tubes and rods and the basket insert. The reduction in the conductivity of the rod material has an insignificant effect on the thermal resistance incorporated in the gaps and thin tube walls in the model. The

thermal resistance internal to each rod does not affect the rejection of the heat from other rods in the basket. Since the maximum number of PWR MOX rods is limited to 16, there are nine or more other vacant positions in the basket without the heat generation of the PWR MOX rods. The evaluation of any arbitrary configuration of tubes, with and without the PWR MOX rods, is bounded by an evaluation of the model having all tubes containing the design basis heat load of 143 W for each PWR MOX rod.

The evaluation using BWR rods in Section 3.4.1.7 is considered to bound all configurations of PWR MOX rods.

Maximum temperatures for package components with the NAC-LWT cask configured for high burnup PWR and BWR fuel rods are summarized in Table 3.4-10. As the analyzed BWR fuel rod content condition is bounding, the temperatures presented in Table 3.4-10, Condition 1 (helium cavity gas backfill) provide bounding temperatures for the PWR MOX fuel rod content configuration. As shown in Table 3.4-10, maximum calculated component temperatures for all critical safety components including the fuel rod cladding, the lid metallic containment seal, the Alternate B port cover metallic containment seals, the lead gamma shield and the liquid neutron shield are maintained within their allowable temperature limits as further defined in Section 3.3. Note that for the transport of PWR MOX fuel rods, metallic containment seals will be installed on the lid and Alternate B port cover in accordance with the NAC-LWT cask leaktight transport configuration specified for the PWR MOX fuel rod contents.

3.4.1.16 Thermal Evaluation for TPBARs in the PWR/BWR Rod Transport Canister

The thermal evaluation of the NAC-LWT transport cask loaded with up to 25 TPBARs, the PWR/BWR Rod Transport Canister, the PWR insert and the TPBAR basket is conducted for the normal conditions of transport. The evaluation relies on the results of analyses for the shipment of 300 TPBARs in the TPBAR basket (see Section 3.4.1.12), and the shipment of high burnup PWR or BWR rods in a rod holder (see Section3.4.1.7), in which bounding total heat loads and temperatures were considered. For this analysis, each TPBAR rod is limited to a heat load of 2.31 W, which corresponds to a 90-day cooling period.

The PWR/BWR Rod Transport Canisters can accommodate three configurations: a 4×4 matrix of pin tubes containing up to 16 rods, a 5×5 matrix of pin tubes containing up to 25 rods, and an alternate 5×5 rod holder designed to contain an oversize nonfuel-bearing component (e.g., CE guide tube or BWR water rod) and up to 21 rods. Since the maximum decay heat per TPBAR is 2.31 W, the maximum heat load of the NAC-LWT cask with TPBAR fuel rods and the

PWR/BWR Rod Transport Canisters is 25 × 2.31 W or 58 W. A conservative maximum total heat load of 100 W is used for this evaluation.

The maximum contents temperature for the TPBARs in the PWR/BWR Rod Transport Canister is determined by first computing the temperature difference from the center of the basket, which is the location of the maximum contents temperature, to the inner surface of the cask's inner shell. This temperature difference is added to the inner shell temperature to determine the maximum contents temperature.

The computation of the center to inner shell temperature difference is divided into two separate calculations: first, the temperature difference from the basket center to the inner surface of the basket (ΔT_a); second, the temperature difference across the TPBAR basket (ΔT_b). The first segment of the temperature difference includes the PWR/BWR canister and PWR insert, which was analyzed for the evaluation of high burnup PWR or BWR rods in a Rod Transport Canister. The second segment of the temperature difference across the TPBAR basket was analyzed for the evaluation of TPBAR fuel in a TPBAR basket. Both the TPBAR and PWR analyses use a greater total heat load than what is associated with the 25 TPBARs in the PWR/BWR Rod Transport Canister configuration. The calculated temperature difference from each segment is scaled by the ratio of the total heat load for the 25 TPBARs in the PWR/BWR Rod Transport Canister configuration to that of the corresponding analysis, or

$$\Delta T_a = \Delta T_{PWR} \frac{Q_{TPBAR/PWR} P_{TPBAR}}{Q_{PWR/BWR} P_{PWR/BWR}}$$

$$\Delta T_b = \Delta T_{TPBAR} \frac{Q_{TPBAR/PWR} P_{TPBAR}}{Q_{TPBAR} P_{TPBAR}} = \Delta T_{TPBAR} \frac{Q_{TPBAR/PWR}}{Q_{TPBAR}}$$

where:

$Q_{TPBAR/PWR}$ = the heat load for the shipment of 25 TPBARs in a PWR/BWR Rod Transport Canister.

Q_{TPBAR} = the heat load of the TPBAR analysis for the shipment of 300 TPBARs in the TPBAR basket (Section 3.4.1.12).

$Q_{PWR/BWR}$ = the heat load of the PWR/BWR analysis for the shipment of high burnup PWR (2.3 kW) or BWR (2.1 kW) rods in a PWR/BWR Rod Transport Canister (Section 3.4.1.7).

P_{TPBAR} = the TPBAR peaking factor = 1.15 (Section 3.4.1.12).

$P_{PWR/BWR}$ = the peaking factor used in the analysis of the high burnup PWR (1.1) or BWR (1.22) rods in a PWR/BWR Rod Transport Canister (Section 3.4.1.7).

The scaled temperature difference provides an appropriate value for the 25 TPBARs in the PWR/BWR Rod Transport Canister configuration. This scaling method is conservative since 100 W bounds the actual heat load of 58 W.

The analysis for the 300 TPBARs in the TPBAR basket, for normal conditions of transport, used a maximum inner shell temperature of 222°F and a design heat load of 690 W with a peaking factor of 1.15, which resulted in a maximum TPBAR basket temperature of 228°F and a maximum contents temperature of 290°F (Section 3.4.1.12). The analysis for the high burnup PWR/BWR fuel in a rod holder for normal conditions of transport used a maximum inner shell temperature of 385°F and a head load of 2.1 kW with a peaking factor of 1.22, which resulted in a maximum PWR basket temperature of 387°F and a maximum fuel temperature of 671°F (Section 3.4.1.7).

The segmented temperature differences and total temperature difference are calculated as follows.

$$\Delta T_a = (671°F - 387°F)\frac{0.1kW \times 1.15}{2.1kW \times 1.22} = 12.75°F$$

$$\Delta T_b = (228°F - 222°F)\frac{0.1kW}{0.69kW} = 0.87°F$$

$$\Delta T_{total} = \Delta T_a + \Delta T_b = 14°F$$

where:

ΔT_a: is the temperature difference between the maximum contents temperature and PWR insert for the TPBARs in the PWR/BWR Rod Transport Canister configuration.

ΔT_b: is the temperature difference across the TPBAR basket to the inner surface of the inner shell for the TPBARs in the PWR/BWR Rod Transport Canister configuration.

ΔT_{total}: is the temperature difference from the inner surface of the inner shell to the maximum contents temperature.

The maximum contents temperature for the TPBARs in the PWR/BWR Rod Transport Canister configuration is calculated as follows for the normal conditions of transport.

$$T_{max\ contents} = Tis_{max} + \Delta T_{total} = 222°F + 14°F = 236°F$$

where:

Tis_{max}: is the assumed maximum inner shell temperature for the TPBARs in the PWR/BWR Rod Transport Canister configuration

The maximum contents temperature for the NAC-LWT transport cask loaded with TPBAR fuel, the PWR/BWR Rod Transport Canisters, the PWR insert and the TPBAR basket is lower than the maximum temperature for the 300 TPBARs in the TPBAR basket analysis of Section 3.4.1.12 (236°F versus 290°F). Therefore, the component temperatures for the 25 TPBARs in the Rod Transport Canister configuration are bounded by the results of Section 3.4.1.12, which are summarized in Table 3.4-16

3.4.2 Maximum Temperatures

Using the models described, temperatures for the cask body and fuel rod cladding are determined for maximum normal operation conditions (2.5 kW decay heat load, 130°F ambient temperature, still air, full insolation). The maximum cask component and fuel rod cladding temperatures for PWR fuel (2.5 kW) are listed in Table 3.4-2. Not all of the cask components are explicitly modeled; their temperatures are obtained by evaluating the analytical model at the component location. Maximum normal operating temperatures for the 1.26 kW MTR fuel and the 1.05 kW TRIGA fuel configurations are shown in Table 3.4-6 and Table 3.4-8, respectively. Maximum normal operating temperatures for high burnup PWR and BWR fuel rods in a rod holder are shown in Table 3.4-10. The maximum component temperatures for DIDO fuel and General Atomics IFM for normal conditions of transport are shown in Table 3.4-12 and Table 3.4-13, respectively. The maximum component temperatures for 25 high burnup PWR and BWR fuel rods in a fuel assembly lattice are shown in Table 3.4-14. The maximum component temperatures for high burnup PWR or BWR fuel with up to 14 damaged fuel rods in a rod holder are shown in Table 3.4-15. Maximum operating component temperatures for the NAC-LWT containing TPBARs are shown in Table 3.4-16. The maximum operating temperatures for the PULSTAR fuel contents in the MTR basket are shown in Table 3.4-17. The maximum component temperatures for the NAC-LWT containing MOATA plate fuel and Mark III spiral fuel are presented in Table 3.4-22.

3.4.3 Minimum Temperatures

As stated in Section 3.4.1, the minimum temperatures in the cask occur with a 0.0 kW decay heat load and the minimum ambient conditions. Under these conditions, a uniform temperature of -40°F will exist in the cask. The maximum thermal stresses in the cask, during normal operations conditions, occur when the design basis decay heat load of 2.5 kW exists in the cask along with the minimum ambient conditions (-40°F ambient temperature and no insolance). The cask component and fuel rod clad temperatures for the 2.5 kW decay heat load with minimum ambient conditions are listed in Table 3.4-3.

3.4.4 Maximum Internal Pressures

3.4.4.1 Maximum Internal Pressure for Design Basis Fuel in Normal Conditions

The NAC-LWT cask is filled to one atmosphere (14.7 psia) upon loading. It is necessary to evaluate the internal pressure of the cask after thermal equilibrium has been attained. Assuming a maximum normal fuel cladding temperature of 472°F (932°R) from Table 3.4-2, 3 percent fuel rods rupture, and 30 percent of the fission gas and 100 percent of the rod backfill gas escape from the ruptured fuel rods, the cask internal pressure is calculated. Table 3.4-4 reports the fission gas inventories for the design basis PWR fuel assembly. Table 5.1-2 reports the design parameters of the design basis PWR fuel. Using information from Table 5.1-2, the void volume of a single fuel rod is calculated as 2.43 in^3 (39.82 cm^3) by subtracting the volume of the fuel pellets from the volume of an empty fuel rod (the plenum spring volume is disregarded). The total fuel assembly void volume is calculated as 495.16 in^3 (8,123.28 cm^3) by multiplying the single fuel rod volume by 204, the number of fuel rods in the fuel assembly. The total fuel assembly void volume, the fission gas inventory information in Table 3.4-4, and the maximum normal transport temperature (472°F) are applied to the ideal gas law (PV = nRT) to obtain the pressure in the unruptured fuel rods due to the fission gases. This fission gas pressure, 1,771.5 psia, is also reported in Table 3.4-4, based on 100% availability of fission gases, later adjusted to 30%. The releasable fission gas pressure and rod backfill pressure (assumed 565 psia) are summed to obtain the total fuel rod pressure.

The cask pressure is obtained using Dalton's Law of Partial Pressures:

$$P = P_A + P_B$$

where:

P = total pressure

P_A = partial pressure of gas A (cask cavity helium gas backfill)

P_B = partial pressure of gas B (fuel rod backfill and fission gas)

The reported cask and fuel rod backfill pressures are at standard temperature (72°F) and must be corrected to the normal transport temperature. Given that the internal volumes of the NAC-LWT Cask and the fuel rods remain constant, the resultant pressure is proportional to the temperature change according to the ideal gas law:

$$P_2 = P_1\left(\frac{T_2}{T_1}\right)$$

where:

P_1 = 14.7 psia (cask backfill pressure)

T_1 = 72°F (532°R) (cask backfill temperature)

T_2 = 472°F (932°R) (maximum normal operating condition cavity gas temperature)

Thus, the cask backfill pressure at normal operating temperature equals:

$$P_2 = 14.7 \text{ psia}\left(\frac{932°R}{532°R}\right)$$

$$P_2 = 25.8 \text{ psia}$$

For the fuel rod backfill pressure at normal operating temperature:

P_1 = 565 psia (fuel rod backfill pressure)

T_1 = 72°F (532°R) (fuel rod backfill temperature)

T_2 = 472°F (932°R) (maximum normal operating condition cavity gas temperature)

and:

$$P_2 = 565 \text{ psia}\left(\frac{932°R}{532°R}\right)$$

$$P_2 = 989.8 \text{ psia}$$

The partial pressure of the cask backfill distributed over the cask free volume (including 3% failed rods) is calculated by:

$$P_{\text{cask backfill}} = P_{\text{initial}}\left(\frac{V_{\text{cask}}}{V_{\text{total}}}\right)$$

where:

$P_{initial}$ = 25.8 psia (temperature adjusted cask backfill pressure)

V_{cask} = 5.196 ft^3 (147,134 cm^3)

$V_{rod\ void}$ = 244 cm^3 (volume of 3% failed fuel rods)

$V_{total} = V_{cask} + V_{rod\ void}$

$V_{total} = 147{,}378\ cm^3$

Thus, the cask backfill partial pressure at normal operating temperature, including the volume of failed fuel rods equals:

$$P_{cask\ backfill} = 25.8\ psia \left(\frac{147{,}134 cm^3}{147{,}378 cm^3} \right)$$

$$P_{cask\ backfill} = 25.8\ psia$$

The partial pressure of the failed fuel rod gases in the cask cavity is calculated by:

$$P_{fuelrods} = P_{initial} \left(\frac{V_{rodvoid}}{V_{total}} \right)$$

P

where:

$P_{initial}$ = 1,521.3 psia (fission gas pressure (0.30 x 1,771.5 psia) plus rod backfill pressure (989.8 psia))

$V_{rod\ void}$ = 244 cm^3

Vtotal = 147,378 cm3

Thus, the failed fuel rod partial pressure at normal operating temperature, including fission gases and the volume of cask cavity void equals:

$$P_{fuel\ rods} = 1{,}521.3\ psia \left(\frac{243.7 cm^3}{147{,}378 cm^3} \right)$$

$$P_{fuel\ rods} = 2.5\ psia$$

Summing the two partial pressures yields the total cask pressure.

$$P_{Total} = P_{cask\ backfill} + P_{fuel\ rods}$$

$$P_{Total} = 25.8\ psia + 2.5\ psia$$

$$P_{Total} = 28.3\ psia$$

3.4.4.2 High Burnup Fuel Rod Canister Maximum Normal Conditions Internal Pressure

The high burnup fuel sealed canister is filled to one atmosphere (14.7 psia) upon loading. The canister internal pressure is calculated assuming that the average helium backfill gas temperature is 600°F (1060 R) and that 3 percent of the fuel rods fail in normal conditions of transport. The temperature of the canister gas is selected to conservatively bound the temperatures given in Table 3.4-10, Table 3.4-14 and Table 3.4-15. On failure, the fuel rods are assumed to release 30% of the fission gas and 100% of the rod backfill gas. To bound both the PWR and BWR analysis, the fuel type with the highest fission source, on a per rod basis, and smallest free gas volume inside the sealed canister is selected. This fuel type is the Exxon 7 × 7 BWR fuel. The fission gas inventory for this fuel is shown in Table 3.4-11, which reports the fission gas inventory for the assembly, and on a per rod basis. The design parameters for the Exxon 7 × 7 fuel rod are:

Parameter	Value
Number of Rods	49
Rod Diameter (in)	0.570
Clad Thickness (in)	0.036
Pellet Diameter (in)	0.4900
Active Fuel Length (in)	150
Rod Length (in)	170

From the values shown, the void volume of a single fuel rod is calculated as 4.82 in^3 (78.99 cm^3) by subtracting the volume of the fuel pellets from the volume of an empty fuel rod (the plenum spring volume is disregarded). For the analysis, 3% of 25 rods is taken to fail, which is 0.75 rods. Conservatively, the number of failed rods is defined as one, which is equal to a 4% fuel rod failure. The equivalent void volume is then equal to one rod, or 4.82 in^3. The fission gas inventory, provided in Table 3.4-11, and the maximum normal transport temperature (600°F) are applied to the ideal gas law (PV = nRT) to obtain the pressure in the unruptured fuel rods due to the fission gases. This fission gas pressure, 4,251 psia (Table 3.4-11), is based on 100% availability of fission gases, which is adjusted to account for the 30 percent release of the fission gas. The releasable fission gas and rod backfill pressures are summed to obtain the total fuel rod pressure.

The ideal gas law is used to analyze the effects of pressure, temperature, volume, and gas inside the cask the ideal gas law states:

$$pV = nRT$$

where:

p = pressure (atm)
V = volume (liters)
n = gram-moles of material
R = gas constant (0.0831 atm-liters/K g-mole)
T = temperature (K)

After the rods rupture, the resultant internal cask pressure is impacted by three sources: the 1-atm inert gas backfill of the canister, the fission product gas escaping from the fuel rods, and the fuel rod inert gas backfill escaping from the ruptured fuel rods. To calculate the resultant internal cask pressure after the fuel rods rupture, partial pressures are calculated using Dalton's law:

$$P = P_a + P_b$$

where:

P = total pressure

P_a = partial pressure of gas A

P_b = partial pressure of gas B

The void volume of the fuel rod is simply the volume contained within the cladding less the fuel volume. The rod is modeled as a cylinder with a 0.570-in outside diameter, a 0.036-in. wall thickness, and a 150-in. active fuel length. The volume of the plenum spring is disregarded. The void volume, which includes the plenum volume, is 4.82 in^3 per rod.

The partial pressure of the canister is calculated by:

$$P_{canister} = P_{initial}\left(\frac{V_{canister}}{V_{total}}\right)$$

where:

$$P_{initial} = P_{atm} * \frac{T_{norm}}{T_{stand}} = 14.7 \text{ psia} * \frac{588.7 \text{ K}}{295.35 \text{ K}} = 29.3 \text{ psia}$$

Pinitial = 29.3 psia

The minimum free gas volume is calculated as:

$$V_{canister} = 2{,}800\,in^3 - \pi * r_{OD}^2 * L_{rod} * 25\,rods = 2{,}800\,in^3 - \pi * \left(\frac{0.57\,in}{2}\right)^2 * 170\,in. * 25\,rods$$

$$= 2{,}800\,in^3 - 1085\,in^3 = 1715\,in^3$$

Vcanister = 28.1 liters

$$V_{void} = 4.82\,in^3 * (2.54\,cm/in)^3 * 0.001\,liters/cc = 0.079\,liters$$

$$V_{total} = V_{canister} + 25 * 0.04 * V_{void} = 28.1\,liters + 0.04 * 25 * 0.079 = \sim 28.2\,liters$$

Vtotal = ~28.2 liters

This results in a $P_{canister}$ of 29.3 psia.

Fission product gas inventories were obtained from Table 3.4-11. Using the ideal gas law, the initial pressure of each fission product gas is calculated based upon these inventories, the normal condition temperature (600°F), and the calculated void volume of the fuel (25 rods). The partial pressure of the fuel rod volume is calculated by:

$$P_{fuel\ rods} = P_{initial}\left(\frac{V_{fuel\ rods}}{V_{total}}\right)$$

where:

$$P_{initial} = 0.3 * P_{fission} + P_{backfill}$$

$$P_{fission} = 4251\,psia$$

$$P_{backfill} = P_{initial}^{backfill} * \frac{T_{norm}}{T_{stand}} = 75\,psia * \frac{588.7\,K}{295.35\,K} = 150\,psia$$

$P_{initial}$ = ~1,425 psia

$V_{fuel\ rods}$= ~0.079 liters (at 4% of the total fuel rod volume)

V_{total} = 28.2 liters = $V_{canister}$ + 25*0.04(V_{void})

$$P_{fuel\ rods} = 1425\,psia\left(\frac{0.079\,liters}{28.2\,liters}\right) = \sim 4.00\,psia$$

then:

$$P_{total} = P_{canister} + P_{fuel\ rods} = 29.3\,psia + \sim 4.00\,psia = \sim 33.3\,psia\ (2.3\,atm)$$

An additional analysis was performed for BWR high burnup rods (>45 GWd/MTU) with a 56% failure fraction to envelope damaged fuel rod shipments. This evaluation is conservative since damaged rods are likely to have released their gas inventory prior to shipment.

Following the methodology used for calculating the pressure given above and the calculated canister free gas volume of 29.2 liters, the resulting internal canister pressure from a 56% failed fuel fraction is 82.3 psia (~ 5.6 atm). The calculation follows.

$P_{canister} = P_{initial} * V_{canister} / V_{total}$

$P_{initial} = 29.3$ psia

$V_{canister} = 28.1$ liters

$V_{total} = V_{canister} + 14 * V_{void} = (28.1 \text{ liters}) + 14 * (0.079 \text{ liters}) = 29.2$ liters

$P_{canister} = (29.3 \text{ psia}) * (28.1 \text{ liters}) / (29.2 \text{ liters}) = 28.2$ psia

$P_{fuelrods} = P_{initial} * V_{fuelrods} / V_{total}$

$P_{initial} = 1{,}425$ psia

$V_{fuelrods} = 14 * V_{void} = 1.108$ liters

$P_{fuelrods} = (1{,}425 \text{ psia}) * (1.108 \text{ liters}) / (29.2 \text{ liters}) = 54.1$ psia

$P_{total} = P_{canister} + P_{fuelrods} = 28.2 \text{ psia} + 54.1 \text{ psia} = 82.3 \text{ psia} = 5.6$ atm

3.4.4.3 25-Rod Maximum Cask Cavity Internal Pressure-Normal Conditions

Following the methodology used for calculating pressure in Section 3.4.4.2, the cask free gas volume is calculated as:

$$V_{cask} = 6{,}534 \text{ in}^3 - \pi * r_{OD}^2 * L_{rod} * 25 \text{ rods} = 6{,}534 \text{ in}^3 - \pi * \left(\frac{0.57 \text{ in}}{2}\right)^2 * 170 \text{ in.} * 25 \text{ rods}$$

$$= 6{,}534 \text{ in}^3 - 1{,}085 \text{ in}^3$$

$$= 5{,}449 \text{ in}^3$$

$V_{cask} = 89.32$ liters

Using this free gas volume in place of $V_{canister}$ and the temperatures in Section 3.4.4.2, the cask cavity pressure resulting from a 3% fuel rod failure is 31 psia (~2.1 atm). This pressure is based on the assumption that the gases in the canister are released to the cask cavity. There are no design basis events that could result in the release of the gas in the canister to the cask cavity.

An additional analysis was performed for a bounding 25 BWR high burnup rod configuration (>45 GWd/MTU) containing up to 14 damaged rods. The damaged fuel rods are conservatively assumed to release the rod gas inventory during transport.

Following the methodology used for calculating the pressures given above and the cask free gas volume of 90.4 liters, the resulting internal cask pressure from a 56% failed fuel fraction is 46.4 psia (~ 3.2 atm). The calculation is outlined below.

$P_{cask} = P_{initial}*V_{cask}/V_{total}$

$P_{initial} = 29.3$ psia

$V_{cask} = 89.3$ liters

$V_{total} = V_{cask} + 14*V_{void} = (89.3 \text{ liters}) + 14*(0.079 \text{ liters}) = 90.4$ liters

$P_{cask} = (29.3 \text{ psia})*(89.3 \text{ liters})/(90.4 \text{ liters}) = 28.9$ psia

$P_{fuelrods} = P_{initial}*V_{fuelrods}/V_{total}$

$P_{initial} = 1{,}425$ psia

$V_{fuelrods} = 14*V_{void} = 1.108$ liters

$P_{fuelrods} = (1{,}425 \text{ psia})*(1.108 \text{ liters})/(90.4 \text{ liters}) = 17.5$ psia

$P_{total} = P_{cask} + P_{fuelrods} = 28.9 \text{ psia} + 17.5 \text{ psia} = 46.4 \text{ psia} = 3.2$ atm

PWR rods may contain Integral Fuel Burnable Absorbers (with rods referred to as IFBA rods). These rods may contain integral neutron absorber comprised of gadolinium, erbium, or boron. Only boron has the potential to impact pressure calculations as the ^{10}B isotope alpha decays upon neutron activation, thereby adding gas to the system. Activation of erbium and gadolinium does not produce additional gases. The effect on system pressure of the additional gas was evaluated based on a 2.4 g ^{10}B/in coating level [ORNL/TM-200/321], considering 100% conversion to gas, and conservatively applying the fixed absorber level to the full active fuel length. A normal condition failure of 3% of the rods (1 rod, rounded to 4%) increases the cask pressurizing gas quantity by less than 0.04 mole, which translates to a pressure change of 0.3 psi. When considering a conservative in-cask failure of 14 rods, the potential increase in pressure rises to 4 psi for the IFBA rods. Given the conservative cask free volume and fission gas generation (both based on significantly larger BWR rods), in combination with a conservative (rounded up) system temperature applied in the analysis, there is no significant effect on system pressure with the inclusion of IFBA rods.

3.4.4.4 Maximum Cask Cavity Internal Pressure for the General Atomics IFM

The combined heat load of the two GA IFM FHUs is 13 watts. This heat load is distributed between two separate canisters, which have a length of approximately 40 inches. As a result, the

heat generation, which would result in a temperature differential between the cavity and ambient, is insignificant.

The internal pressure in the LWT cask cavity is due to the fission gas release from the TRIGA fuel or HTGR fuel pellets in conjunction with the cavity being heated by solar insolance. No credit is taken for the pressure retention capability of the FHUs. The internal pressure that may result from the 20 TRIGA fuel rods in the GA IFM is significantly enveloped by that of the 120 TRIGA fuel rods, which are authorized for transport in the NAC-LWT cask. Likewise, the fission gas release by the HTGR elements is considered to be bounded by the current design basis PWR fuel. Since the free volume for the GA IFM shipment is significantly larger than for the design basis PWR fuel assembly with the PWR basket, the pressure increase in the cavity gas due to the GA IFM shipment is considered to be significantly bounded by the design basis condition in the current NAC-LWT cask. Therefore, the current design pressure of 50 psig for the cask cavity envelopes the cask cavity pressure for the GA IFM contents.

3.4.4.5 TPBAR Shipment Cask Cavity Internal Pressure-Normal Conditions

The method employed in the TPBAR (Tritium Producing Burnable Absorber Rod) shipment evaluation is similar to that employed in the fuel rod evaluations where the cask cavity free volume and molar gas quantities are combined with the ideal gas law (PV=nRT) to determine system pressure. The bounding TPBAR content condition consists of up to 300 production TPBARs (of which two can be prefailed) placed in a consolidation canister and loaded into a NAC-LWT with a TPBAR basket installed in the cavity.

A typical TPBAR is composed of a steel clad rod 0.381 inch in diameter, with a maximum length of 154.15 inches, and a minimum internal free volume of 5.727 inch^3. The TPBARs are located in a consolidation canister composed of three primary pieces: canister body, top insert, and bail. A spacer, attached to the NAC-LWT cask lid, assures that rods remain within the canister envelope and provides support to both the basket and canister under end-drop conditions. The TPBAR basket is a modified NAC-LWT PWR basket that increases the cavity free volume from that provided by a standard PWR basket design.

For conservatism in determining the cask internal pressure, the 298 TPBARs that are not prefailed at loading are assumed to undergo cladding failure during normal transport conditions. Prefailed rods have cladding damage that allows reactor coolant or spent fuel pool water to enter the rod cavity. Cladding failure during transport results in the release of the rod helium backfill gas, helium gas generated during the tritium production, and a portion of the tritium gas produced. For rods not prefailed, the majority of the tritium is locked in the TPBAR structure and is not released during normal or accident conditions of cask transport. Tritium release from

intact or in-cask prefailed rods is limited to 55 Ci/rod (0.0019 mole – See Chapter 1, Appendix 1-B) versus a helium release of 0.42 mole per rod after the 90-day cool-down period. A conservative tritium release of 100 Ci per rod is applied in this calculation. After the 90-day cool-down period, the helium release increases according to the decay of tritium.

$$^{3}\mathrm{He[moles]}(t) = 0.398 \times \left(1 - \exp\left(\frac{-\ln(2)t}{12.33}\right)\right)$$

The remaining two rods in the 300 TPBAR shipment are assumed to be prefailed and waterlogged. These rods contain a maximum of 7.5 moles of H_2O and 0.199 moles of T_2O (1.2 grams H_2), 2% of which dissociate into their constituent gases due to elevated temperatures in the cask cavity (see Chapter 1 appendices). The NAC-LWT is vacuum dried prior to transport, removing water from the cask cavity. This process is expected to remove water from the prefailed rod. The water content is conservatively assumed to remain in the rods for the pressure calculated. After dissociation, the total gaseous inventory in each prefailed TPBAR is 7.78 moles.

Cask cavity gases after rod failure are therefore comprised of the cask helium backfill (one atmosphere at loading); the combined helium rod backfill, helium generated during the tritium production, helium production from tritium decay, and the tritium release itself (298 rods); and the molar inventory of the two prefailed, waterlogged rods. The total free volume available for the gas is the cask cavity volume plus the internal free volume of the failed rods, minus the canister, spacer, basket, and rod volumes.

Description (Based on 300 Rods Failing)	Volume [cm³]
Cavity (Empty)	4.10E+05
TPBAR Rod (Based on Exterior Rod Dimension)	-8.64E+04
TPBAR Minimum Free Interior	2.82E+04
TPBAR Consolidation Canister	-1.40E+04
TPBAR Basket	-8.49E+04
Cask Cavity Spacer	-5.55E+03
Cask Free volume (300 Rods Failed)	2.47E+05

The free volume in the cask cavity for intact rods is 2.19×10^{5} cm^3. Applying a conservative volume 2.4×10^{5} cm^3 to calculate the cask backfill molar quantity yields 9.98 moles of helium. The backfill conditions at sealing used in the calculation are one atmosphere pressure and a

temperature of 68°F. The backfill pressure is specified in the operating procedure, while 68°F is conservative for the cask with a heat-generating payload.

Again employing the ideal gas law with a total 152 moles of gas (298 rods releasing 0.42 moles of helium and 0.003 mole of tritium, two waterlogged rods releasing 7.78 moles each, plus the 10.27 moles cask backfill), a conservative free volume of 2.47×10^5 cm^3, and the normal condition average gas temperature of 246°F, yields an operating pressure of 276 psig at the end of a 90-day cooldown. For a period of one year following the 90-day cooldown and considering a fixed gas temperature of 246°F, the pressure increases to 289 psig (MNOP). System pressure at cool times greater than 90 days will be lower due to the decreased heat loads associated with the radioactive decay of the payload.

The TPBAR content condition of up to 25 TPBARs contained in a 5×5 rod holder is bounded by the pressure analysis performed for the fully loaded TPBAR consolidation canister. Approximately 80% of the free volume in the consolidation canister analysis is the space associated with the volume between radial extent of the consolidation canister and cask shell (i.e., void volume within the radial cross-section of the TPBAR basket). This volume is available regardless of TPBAR basket payload. Combining the 25 TPBAR reduced releasable gases (20% of the 300 TPBAR payload for 23 intact and two prefailed TPBARs) with a similar free volume assures lower pressure in the 25 TPBAR shipment configuration.

The TPBAR content condition of 55 segmented TPBARs contained in a sealed waste container is bounded by the pressure analyses performed for the fully loaded TPBAR consolidation canister. The contents include segments, debris and vented shrouds, all placed in a vented inner storage container within the welded waste container. Due to the condition of the TPBAR segments and the cooling period since irradiation, the heat load of the waste container is 0.127 kW, significantly less than the 0.693 kW analyzed for the production TPBAR content condition of 300 TPBARs in an open consolidation canister.

Each of the 55 TPBARs is assumed to contain a maximum of 1.2 grams of tritium at the time of sealing the waste container, and all backfill gases have been vented. For the purpose of the maximum pressure analysis, all of the contained tritium is assumed to decay to He^3, resulting in a total of 66 grams of He^3. Note that the confinement boundary of the welded waste container is assumed to fail during normal transport conditions. Due to the state of the TPBAR segments and the loading of the materials in dry loading conditions, no water will be present in the waste container. Conservatively assuming that the cask free volume and gas temperature for the transport of the waste container is the same as that for the production TPBAR contents listed previously (2.47×10^5 cm^3), the calculated maximum normal operating pressure (MNOP) for the 55 segmented TPBARS in the waste container is less than 65 psia. Therefore, the MNOP for the

55 segmented TPBAR content condition is conservatively bounded by the MNOP of the 300 production TPBARs in the consolidation canister of 289 psig.

Combustible Hazard Assessment

Hydrogen may be released by prefailed, waterlogged TPBARs (TPBARs damaged during in-core use or in-pool storage) primarily in the form of water, tritiated water, and potentially some tritiated methane. Each prefailed TPBAR has the potential to release the tritium assumed to dissociate from tritiated water (0.004 moles) as well as up to 0.15 moles hydrogen gas dissociated from 7.5 moles of H_2O. Both the hydrogen and the tritium gas, as well as the water and tritiated water, will be removed from the cask during vacuum drying prior to helium backfill.

The flammability/ignitability characteristics of tritium (T_2) in the presence of oxygen are substantially the same as for hydrogen (H_2). Hydrogen in air reaches a lower flammability limit at 4% volume.

Tritium escapes intact TPBARs in the form of molecular tritium gas at a rate of less than 0.12 mCi/hr/TPBAR. For a one-year transport period and a 300 TPBAR payload this rate results in a release of less than 0.01 moles of T_2 gas. Given a helium gas back-fill of approximately 10 moles helium (1 atmosphere) no flammability hazard exists for intact TPBARs.

Tritium may be released by event-failed (in-cask failed) TPBARs in the form of tritiated methane (CH_4) or tritiated water. Event-failed TPBARs may release up to 55 Ci of tritium. This translates to approximately 0.002 mole of tritium that may be released from a TPBAR in conjunction with 0.42 mole of helium.

The reduced available hydrogen content of the 25 TPBAR payload, including two prefailed TPBARs, in combination with a similar free volume to the consolidation canister configuration, and cask helium backfill quantity, produces a lower maximum hydrogen concentration in the up to 25 TPBAR configuration than that of the 300 TPBAR consolidation canister configuration. No flammability hazard exists for the up to 25 TPBAR shipment configuration.

The 55 equivalent TPBARs, in segments and debris, may release up to 100% of the tritium contained in the pellets during transport. The pellets contain approximately 40% of the tritium quantity in the TPBAR. At NAC-LWT normal and accident conditions temperatures, the TPBAR components release tritium primarily as tritiated water with only a small fraction (maximum 2%) as gaseous tritium (see Appendix 1-B of Chapter 1). During a one-year transport, an additional maximum 1% of the tritiated water may undergo radiolysis and dissociate. Conservatively applying a maximum 3% release rate to the 55 equivalent TPBAR total inventory of 66 grams (1.2 grams per rod) yields an inventory of 0.33 moles T_2. Based on an inert gas cask backfill in excess of 10.3 moles, a bounding estimated maximum hydrogen (T_2)

volume fraction of 3.1% is calculated. Therefore, no flammability hazard will exist for the 55 segmented TPBAR content condition.

3.4.4.6 Maximum Internal Pressure for PULSTAR Fuel Element Payload

Based on the allowable loading configurations for PULSTAR fuel elements, cask internal pressures are calculated for a payload of 28 intact assemblies and a mixed payload of 14 intact assemblies and the equivalent of 14 canned assemblies. A payload of 28 4×4 intact rod inserts is bounded by either of these evaluated payloads.

The ideal gas law and Dalton's law of partial pressures are used to calculate internal pressures. Cask, can, and element backfill initial conditions are taken as a pressure of 1 atm and a temperature of 68°F.

PULSTAR fuel element and fuel assembly dimensions are summarized in Table 3.4-18. Elements are UO_2 pellets clad with zirconium alloy. A PULSTAR fuel assembly is a 5×5 rectangular array of elements with aluminum upper and lower fittings.

Based on the PULSTAR fuel element, PULSTAR failed fuel can, MTR basket stack, and NAC-LWT cavity dimensions, volumes are calculated and summarized in Table 3.4-19.

The remaining two inputs to the pressure calculation are the temperature and fission gas inventory. For conservatism, the average gas temperature applied is the maximum TRIGA fuel clad temperature of 295°F. The TRIGA temperatures are applicable to the PULSTAR fuel element evaluation as discussed in Section 3.4.1.13. The fission gas inventory is taken from the SAS2H results discussed in Chapter 5 and is shown in Table 3.4-20.

For a payload of 28 intact PULSTAR fuel assemblies, the partial pressures of the cask, element (rod) backfill, and fission gases are summed. The cask free volume is 217 liters and is calculated by subtracting the basket stack volume and the assembly envelope volume (multiplied by 28) from the cavity volume. The partial pressure of the cask, P_{Cask}, is simply the initial backfill pressure multiplied by the temperature ratio:

$$P_{Cask} = 1\,\text{atm}\frac{419.26\,\text{K}}{293.15\,\text{K}} = 1.430\,\text{atm}$$

The cask partial pressure due to a 100% release of element backfill, $P_{RodBackfill}$, is the initial backfill pressure multiplied by the temperature ratio and the backfill-to-cask volume ratio:

$$P_{RodBackfill} = 1\,\text{atm}\frac{419.26\,\text{K}}{293.15\,\text{K}}\frac{2.7\,\text{liters}}{217.0\,\text{liters}} = 0.018\,\text{atm}$$

Only 3% of this pressure contributes to the total pressure under normal conditions.

The cask partial pressure due to a 100% release of the element fission gases, $P_{FissionGas}$, is calculated using the Ideal Gas Law:

$$P_{FissionGas} = \frac{28 \cdot 0.448 \cdot 0.08205 \cdot 419.26}{217} = 1.989 \text{ atm}$$

Only 30% of the fission gases are released, and only 3% of the resultant pressure contributes to the total pressure under normal conditions.

The total cask pressure is the sum of the partial pressures, adjusted by the relevant release fractions:

$$P_{Total} = P_{Cask} + 0.03 \cdot P_{RodBackfill} + 0.03 \cdot 0.30 \cdot P_{FissionGas}$$

$$P_{Total} = 1.430 + 0.03 \cdot 0.018 + 0.03 \cdot 0.30 \cdot 1.989 = 1.449 \text{ atm}$$

Cask internal pressure for a mixed payload is calculated in a similar fashion, with a smaller cask free volume due to the difference in can and assembly envelope volume, and an assumed 100% failure rate of PULSTAR elements in either the screened or sealed can. The calculated maximum cavity pressure is 1.8 atm. Pressure in the sealed can is based on a 100% failure rate, the can cavity volume, and a payload equivalent in volume to 25 intact PULSTAR fuel elements. Normal condition pressure in the sealed can is 4.4 atm.

A summary of the pressure calculations is given in Table 3.4-21.

3.4.4.7 Maximum Internal Pressure for 16 PWR MOX/UO_2 Fuel Rods in a Rod Holder

Based on the allowable loading of up to 16 PWR MOX/UO_2 fuel rods, cask internal pressures are calculated. Bounding cask free volume, gas temperatures, and rod backfill pressure are directly obtained from the BWR high burnup rod evaluations in Section 3.4.4.3.

Variable	Unit	Value
Cask Free Volume (PWR Basket with Insert/Canister/Rod Holder)	in^3	5908
Normal Condition Cask Average Gas Temperature	°F	600
Normal Condition Cask Backfill Partial Pressure (at temperature)	psia	29.3
PWR Fuel Rod Backfill Pressure	psia	565

These values are combined with a conservative 2.9 in^3 fuel rod free volume and SAS2H calculated fission and actinide gas inventories to determine system pressure. The 2.9 in^3 free rod volume applied here is larger than the UO_2 rod volume previously employed (2.5 in^3) to account

for additional volume designed into the MOX rods to counter any potential increase in fission gas release from the PuO_2 / UO_2 MOX fuel mixture.

The ideal gas law and Dalton's law of partial pressures are used to calculate internal pressures by combining cask backfill, rod backfill, and fission/actinide gases. Fill temperature applied to the rod gases is 22°C (standard temperature). Maximum fission and actinide gas inventories were obtained from 80 GWd/MTHM fuel rod, 3% enriched ^{235}U or 3 wt % fissile Pu, SAS2H output sets. The fuel rod corresponds to the maximum fissile mass defined in the shielding source term calculations. SAS2H runs produced a total gas inventory of 0.29 moles per rod (99+% fission gas), with bounding values obtained from the UO_2 rods (MOX rods produce approximately 98% of the UO_2 rod fission gas). Gas inventories increase as a function of reduced initial fissile material content. A 3% enrichment and/or 3% fissile Pu content is significantly below levels required to reach an 80 GWd/MTHM burnup level.

The resulting normal condition pressure for a failure fraction of 1/16 (bounds the 3% normal condition PWR rod failure fraction in the Standard Review Plan, NUREG-1617, Supplement 1) and 30% fission gas release is 17.2 psig (31.9 psia, or 2.2 atm).

Parametric studies are performed on the number of rods failing and the release fraction under normal conditions with an applied limit of 50 psig (normal condition structural analysis input value). Normal condition failure of up to 13 rods, at 100% gas release, remains below 50 psig. A similar analysis results in a maximum normal condition pressure of 48.5 psig for a normal condition failure of all 16 rods at a 75% fission gas release fraction (100% of backfill gas is released). Given that each of the rods is individually located within a support tube, no normal condition rod failures are expected during transport.

UO_2 or MOX rods included in the payload may be IFBA rods. As presented in Section 3.4.4.3, IFBA rods are expected to contribute in the range of 0.04 mole per rod to system pressure, assuming the absorber material is boron. As the MOX/UO_2 pressure calculations assumed a conservative 100% fission gas release of 0.29 mole per rod, a rod backfill of 0.075 mole, and a cask backfill of approximately 3.6 moles, the release of IFBA boron-generated gases would not significantly affect system pressure.

3.4.5 Maximum Thermal Stresses

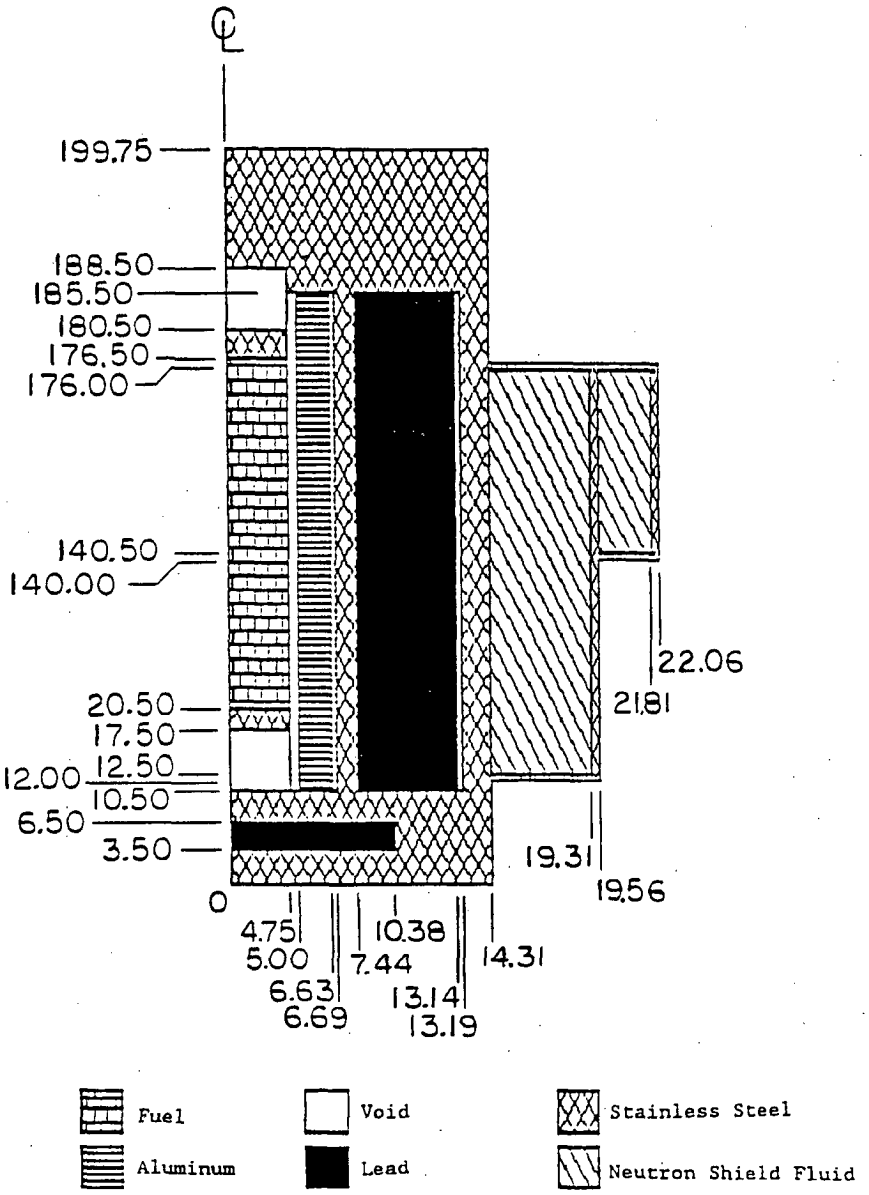
The conditions within the range of normal transport conditions and fabrication that result in the limiting combination of thermal gradient and isothermal stresses have been evaluated. The analyses are performed in Sections 2.5 through 2.7. The resulting isothermal temperature plots are presented in Section 2.10.3.

3.4.6 Evaluation of Package Performance for Normal Conditions of Transport

Section 3.4 provides analyses of the NAC-LWT cask thermal performance for normal transport conditions. The analyses demonstrate that the NAC-LWT cask thermal performance meets the criteria of 10 CFR 71 for normal transport conditions.

The maximum fuel rod cladding temperature under normal transport conditions is 472°F. This is well below the temperatures that can cause fuel rod cladding deterioration. Components important to safety remain within their safe operating ranges (Section 3.3) during normal transport conditions. Thermally induced stresses (in combination with pressure and mechanical load stresses) are less than allowable stresses as shown in Section 2.6. Thus, the analyses of Section 3.4 demonstrate that the NAC-LWT cask fulfills the heat rejection criteria established in Section 3.1 for normal transport conditions.

Figure 3.4-1 HEATING5 Normal Transport Conditions Thermal Model



(Dimensions in inches)

Figure 3.4-2 Design Basis PWR Fuel Assembly Axial Flux Distribution

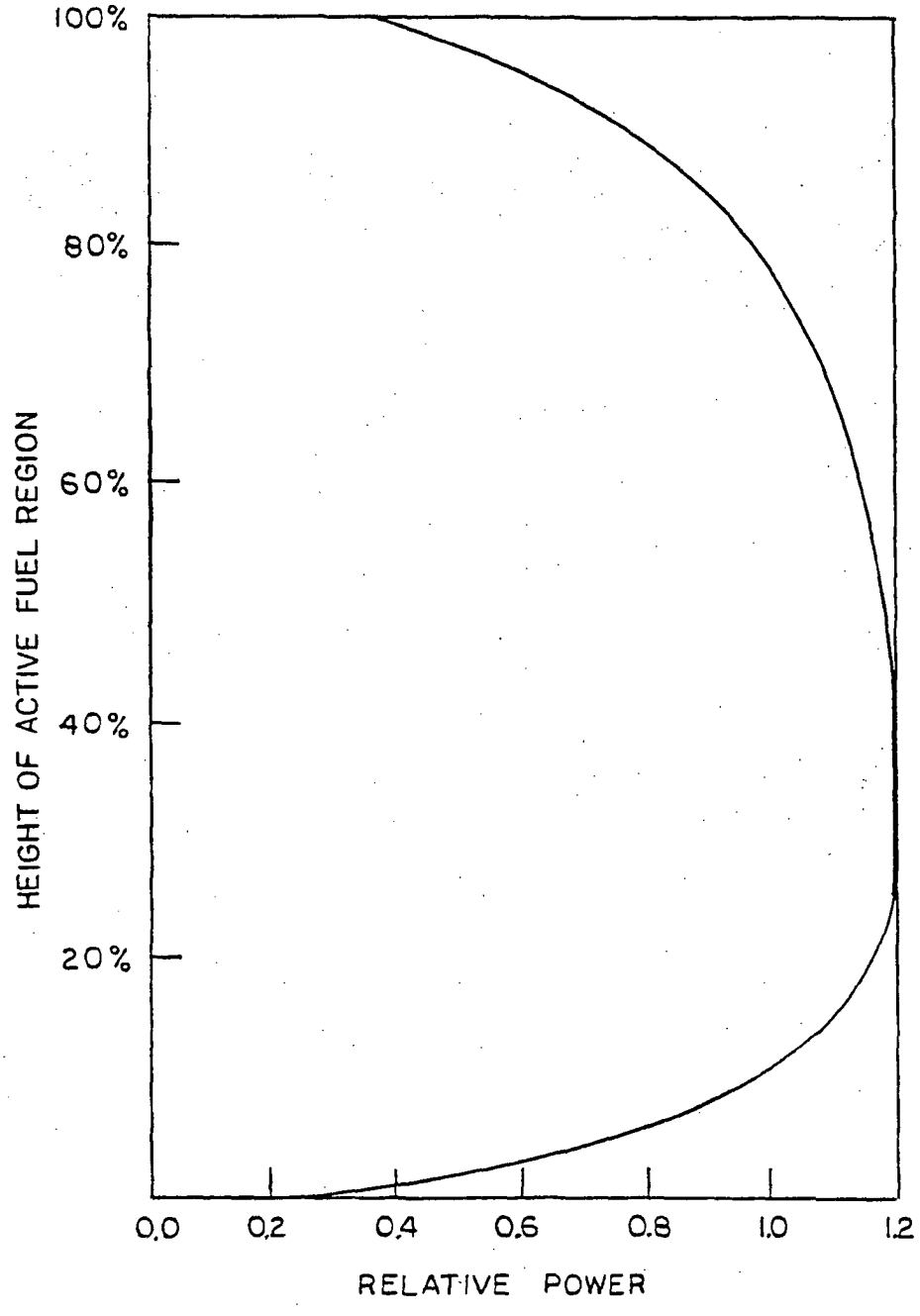


Figure 3.4-3 ANSYS MTR Fuel Design Basis Heat Load Thermal Model (Uniform 30-Watt/Element Configuration Heat Load)

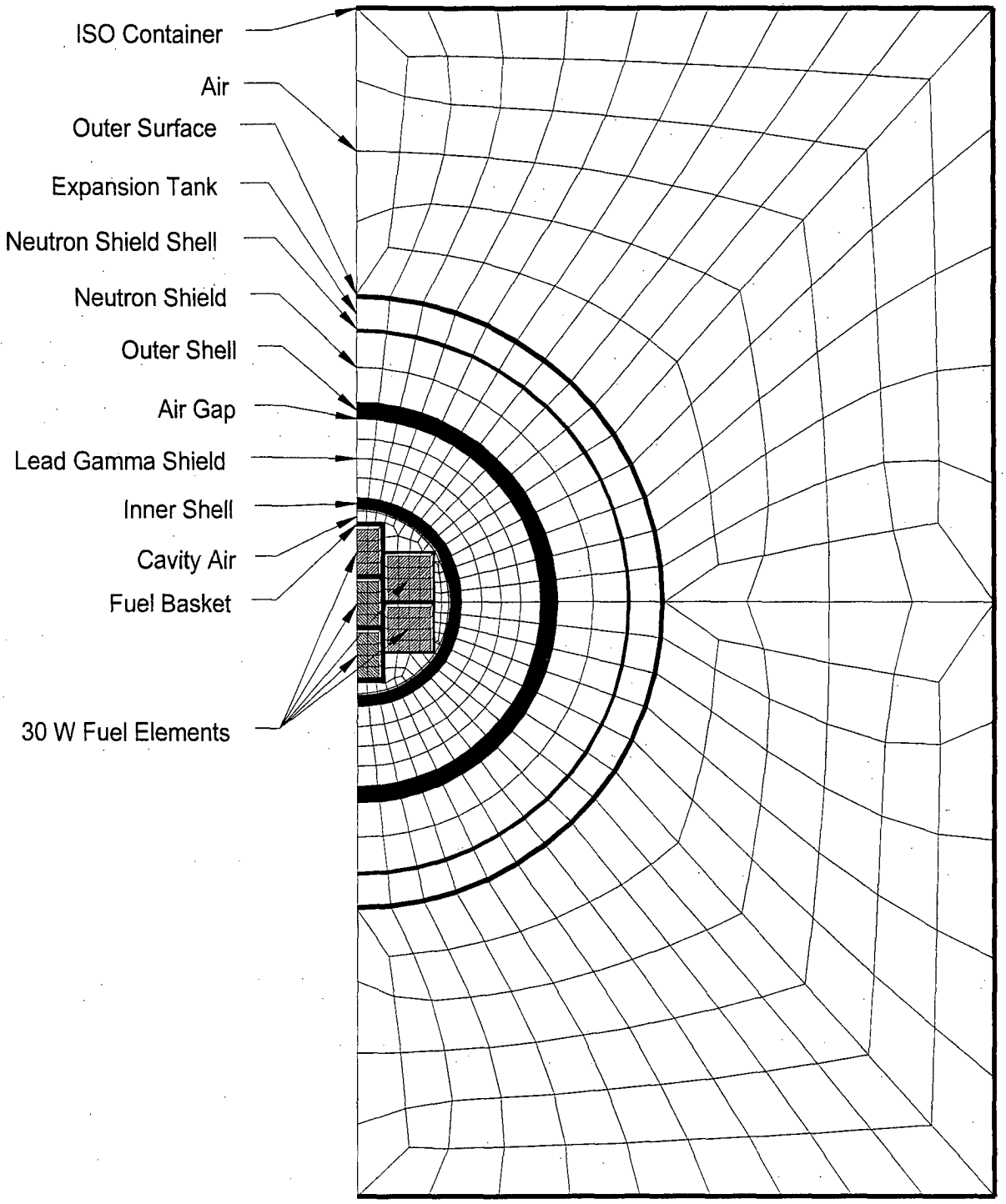


Figure 3.4-4 MTR Fuel Variable Decay Heat ANSYS Thermal Model

(120-Watt / 70-Watt / 20-Watt Configuration Heat Load)

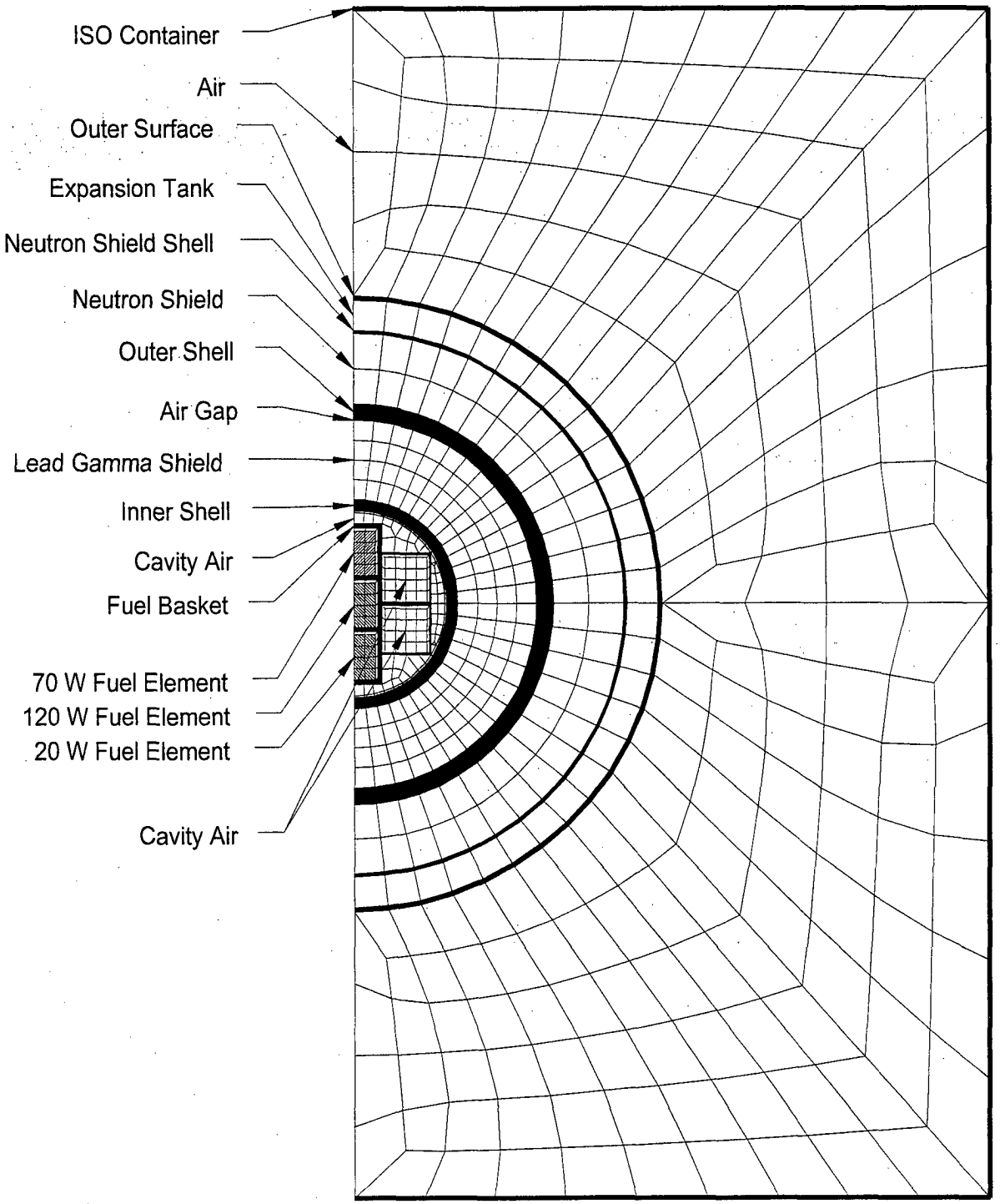
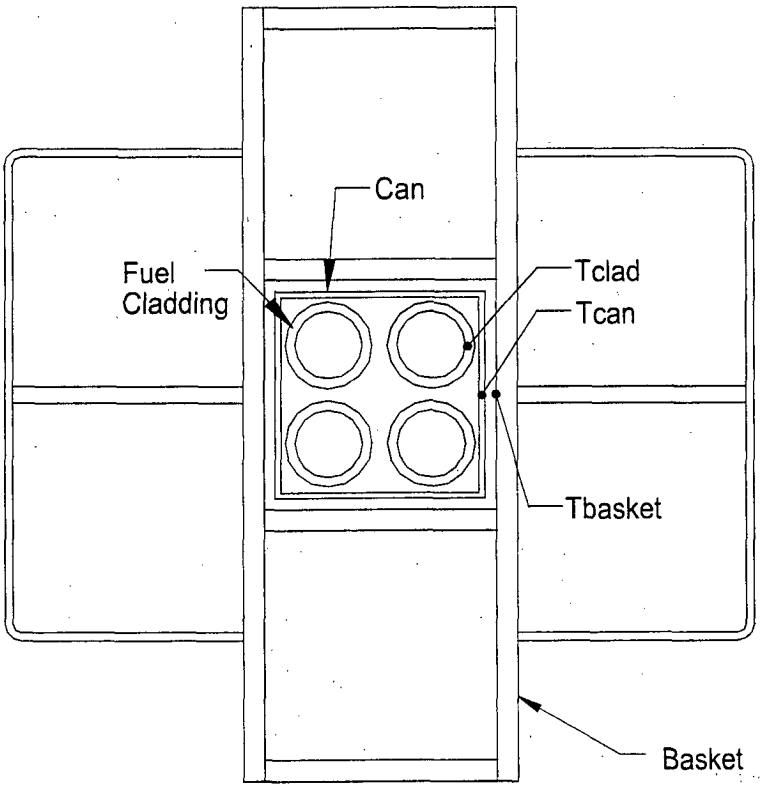
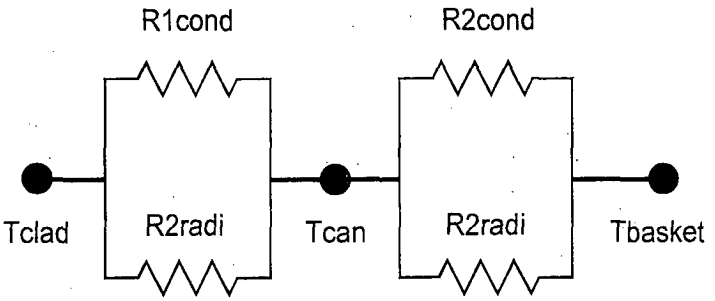


Figure 3.4-5 Thermal Resistance Model for TRIGA Fuel Elements





Where:

Rcond =	Thermal resistance for conduction	Tclad =	Maximum fuel cladding temperature
Rradi =	Thermal resistance for radiation		
Tbasket =	Maximum basket temperature		
Tcan =	Maximum can temperature		

Figure 3.4-6 Modeling Details for the MTR Fuel Assembly Resting on the Surface of the NAC-LWT MTR Basket

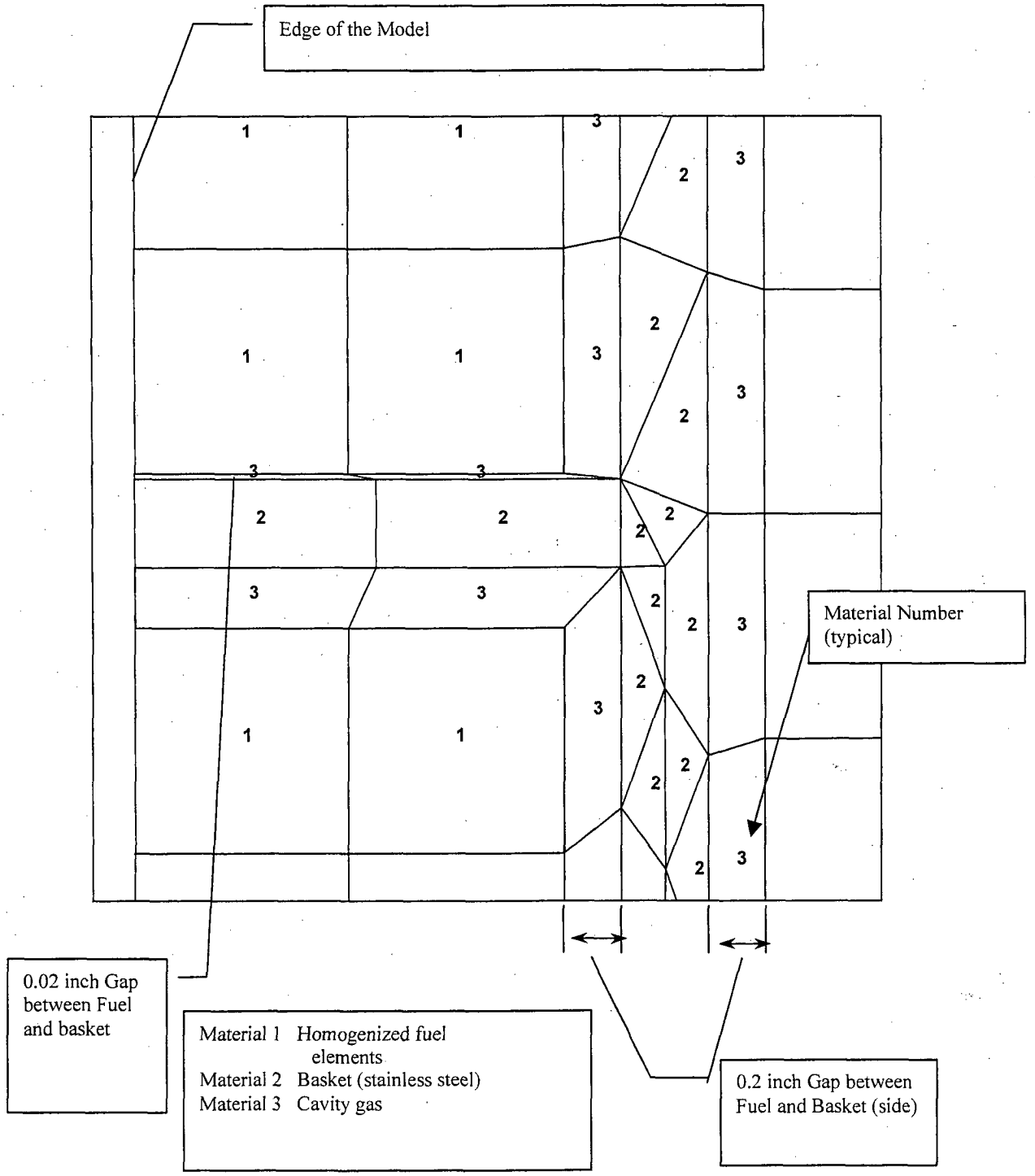


Figure 3.4-7 Finite Element Thermal Model for TRIGA Fuel Cluster Rods

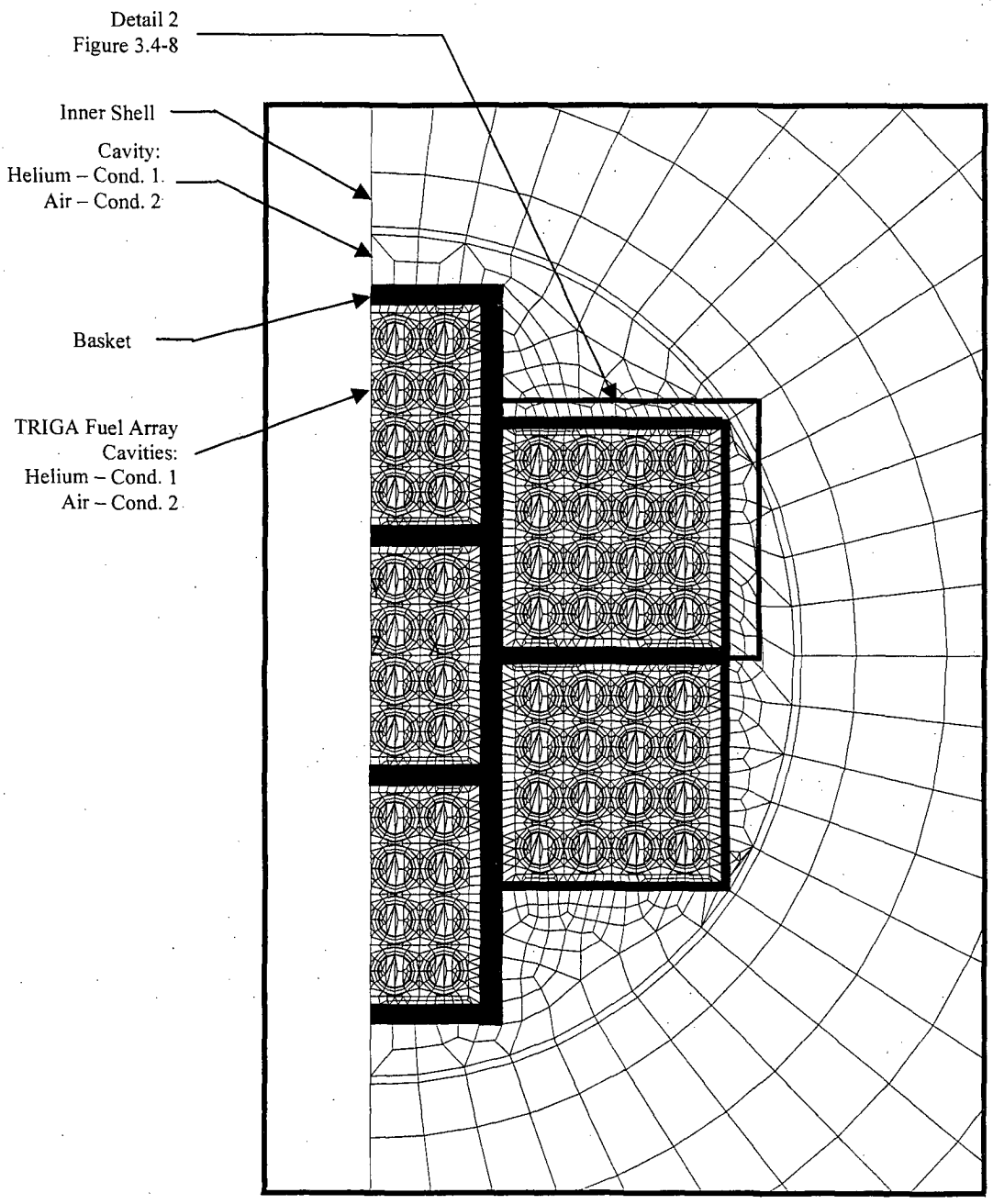


Figure 3.4-8 Details of the TRIGA Fuel Cluster Rods in the Finite Element Model

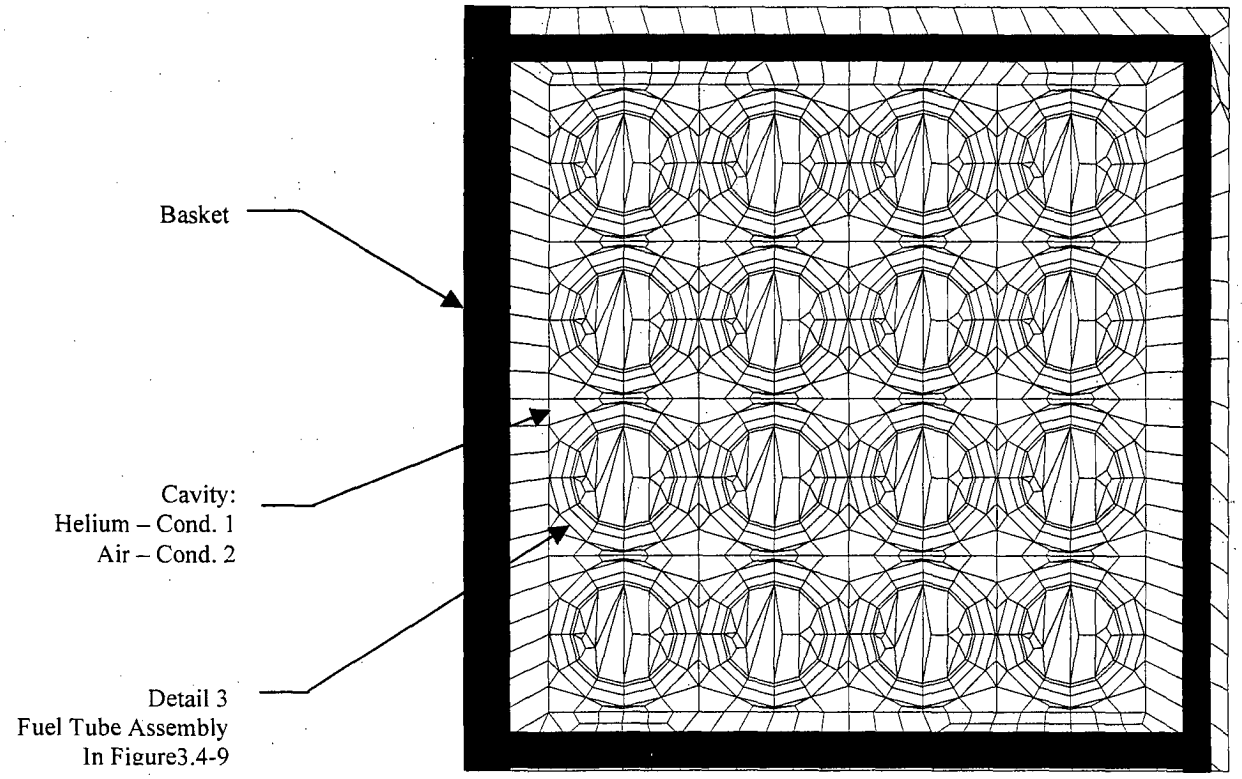


Figure 3.4-9 Individual TRIGA Fuel Cluster Rod Finite Element Model Details

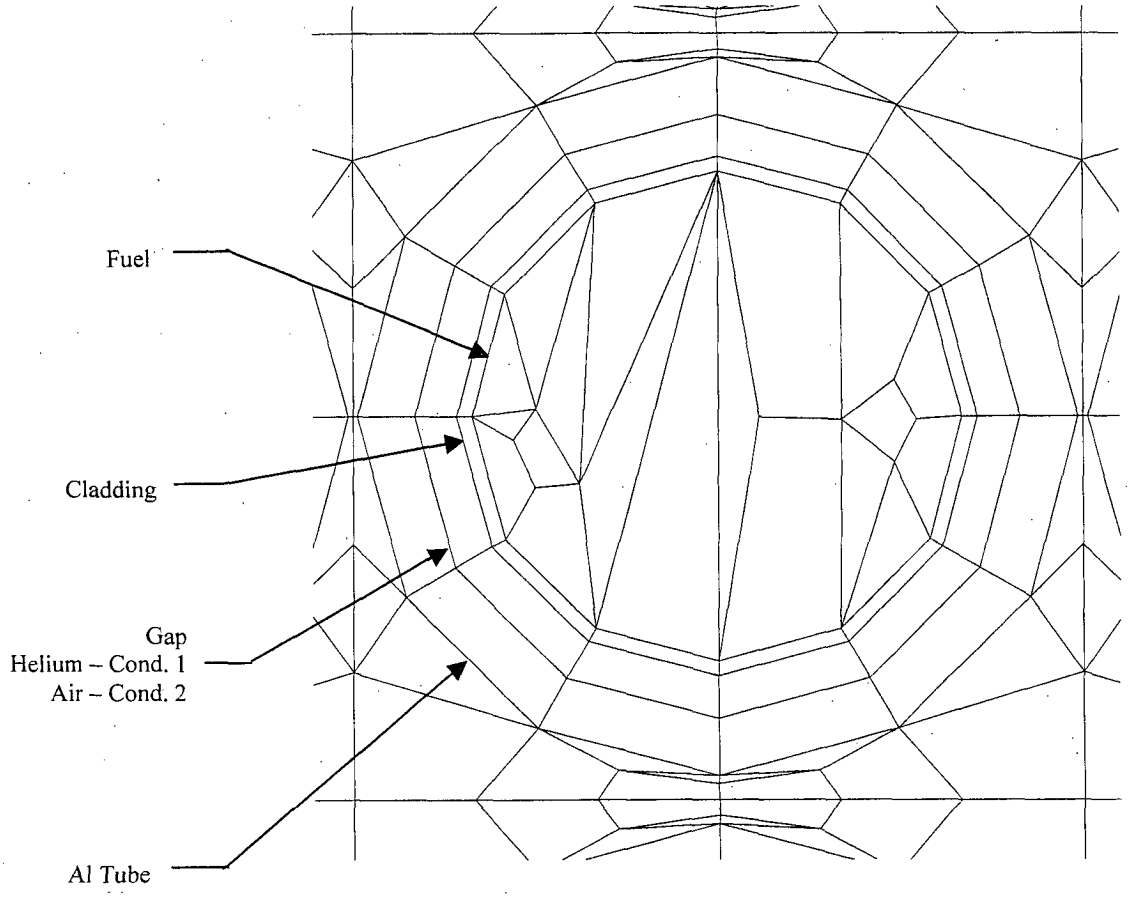


Figure 3.4-10 PWR and BWR High Burnup Fuel Rods Normal Condition ANSYS Thermal Model (Condition 1)

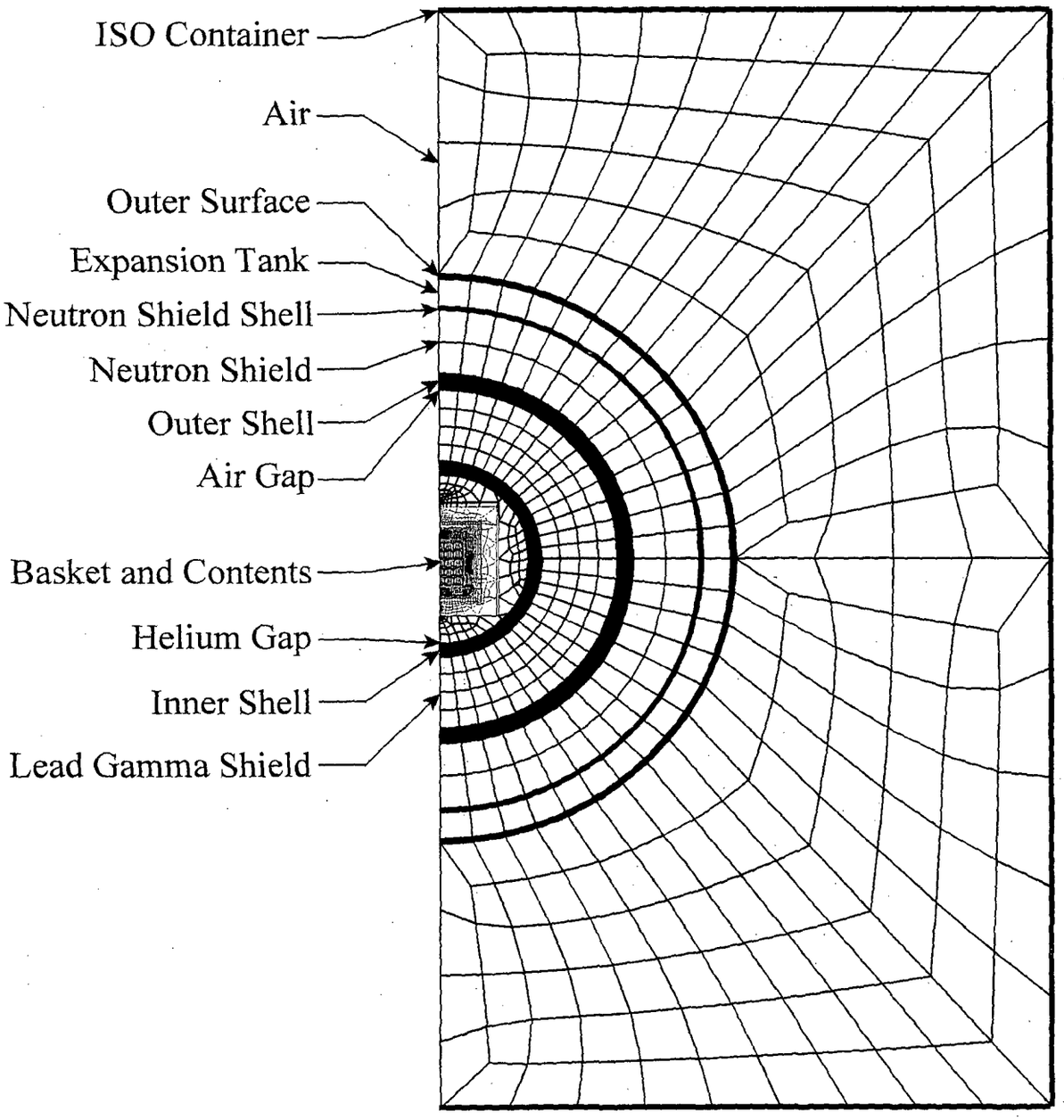
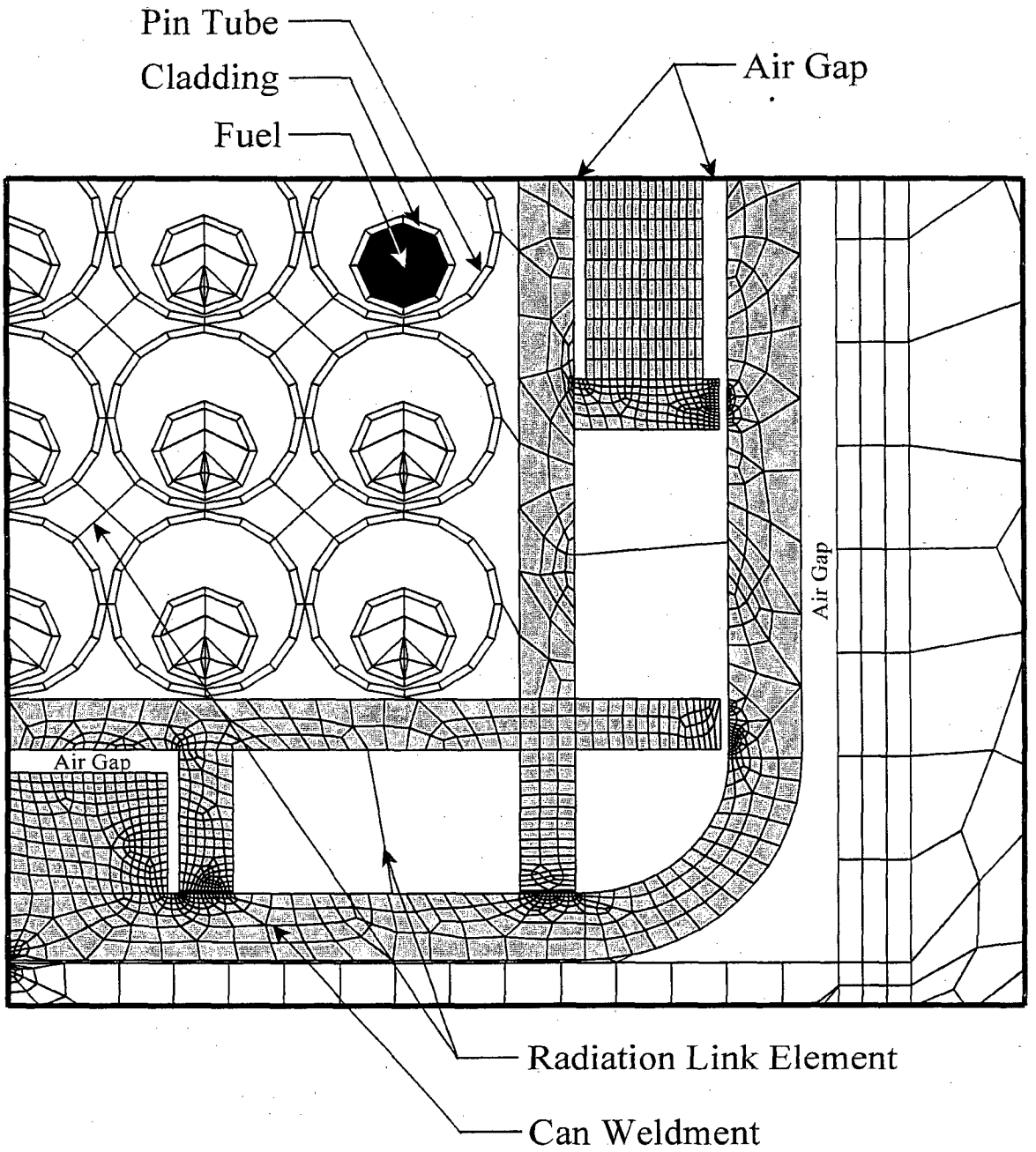


Figure 3.4-11 Close-up of PWR and BWR High Burnup Fuel Rods Normal Condition ANSYS Thermal Model



Note: air elements are not shown for clarity.

Figure 3.4-12 PWR and BWR High Burnup Fuel Rods Normal Condition ANSYS Thermal Model (Condition 2)

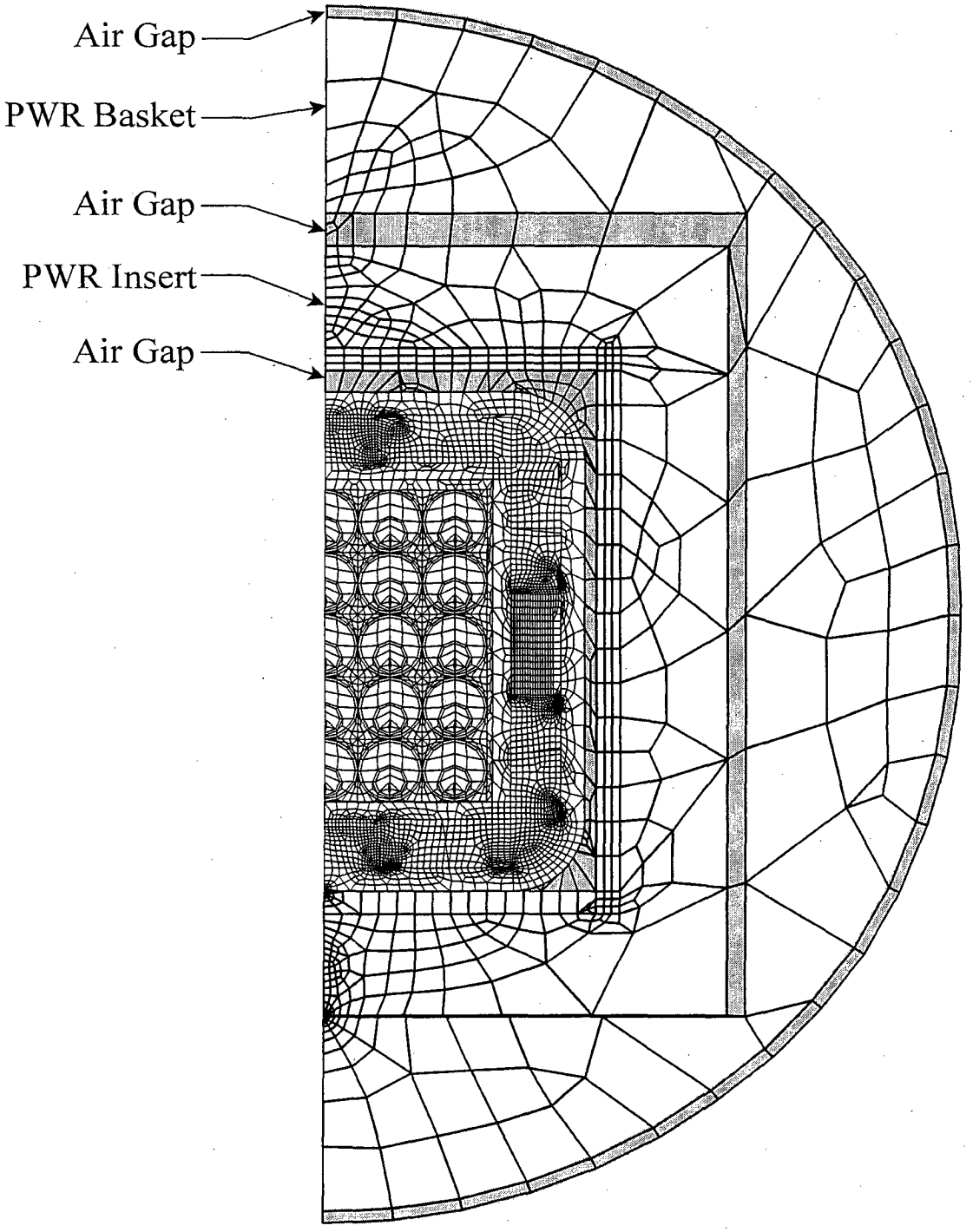
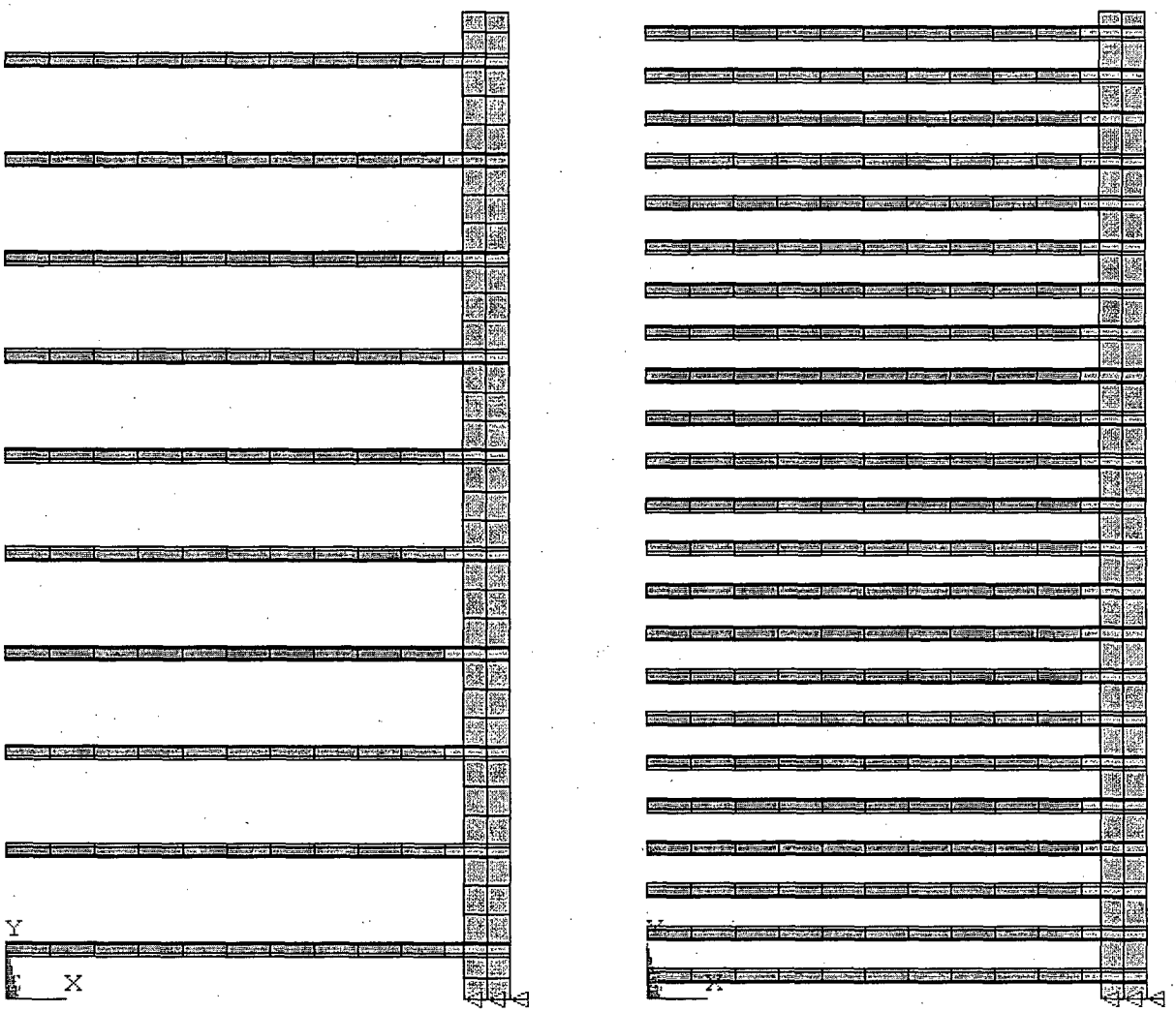


Figure 3.4-13 Finite Element Thermal Model for MTR Fuel Element



(Air elements omitted for clarity)

Figure 3.4-14 Detailed DIDO Basket Module Finite Element Model

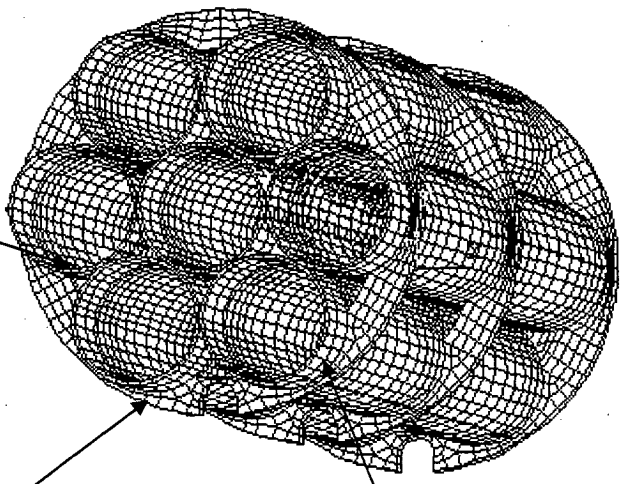


Figure 3.4-15 Detailed DIDO Fuel Assembly Model

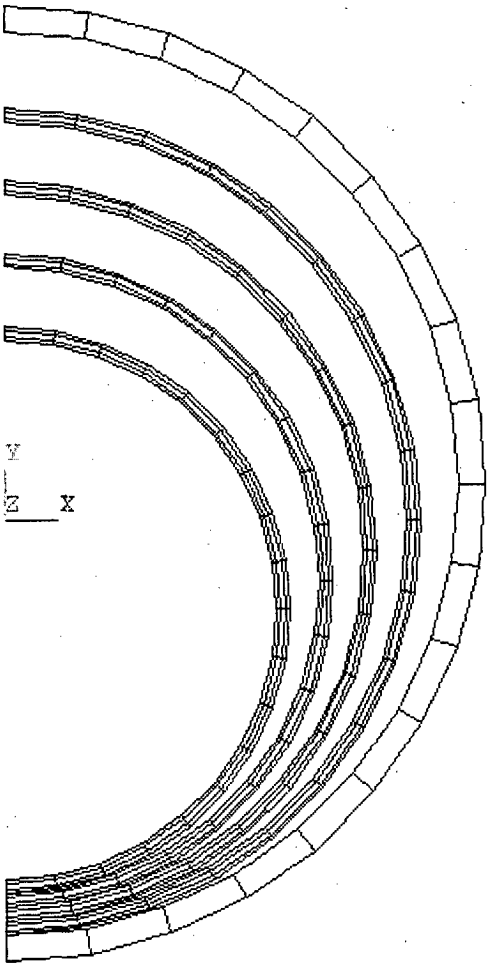


Figure 3.4-16 ANSYS Model for BWR 7 × 7 Fuel Lattice with 25 High Burnup Fuel Rods

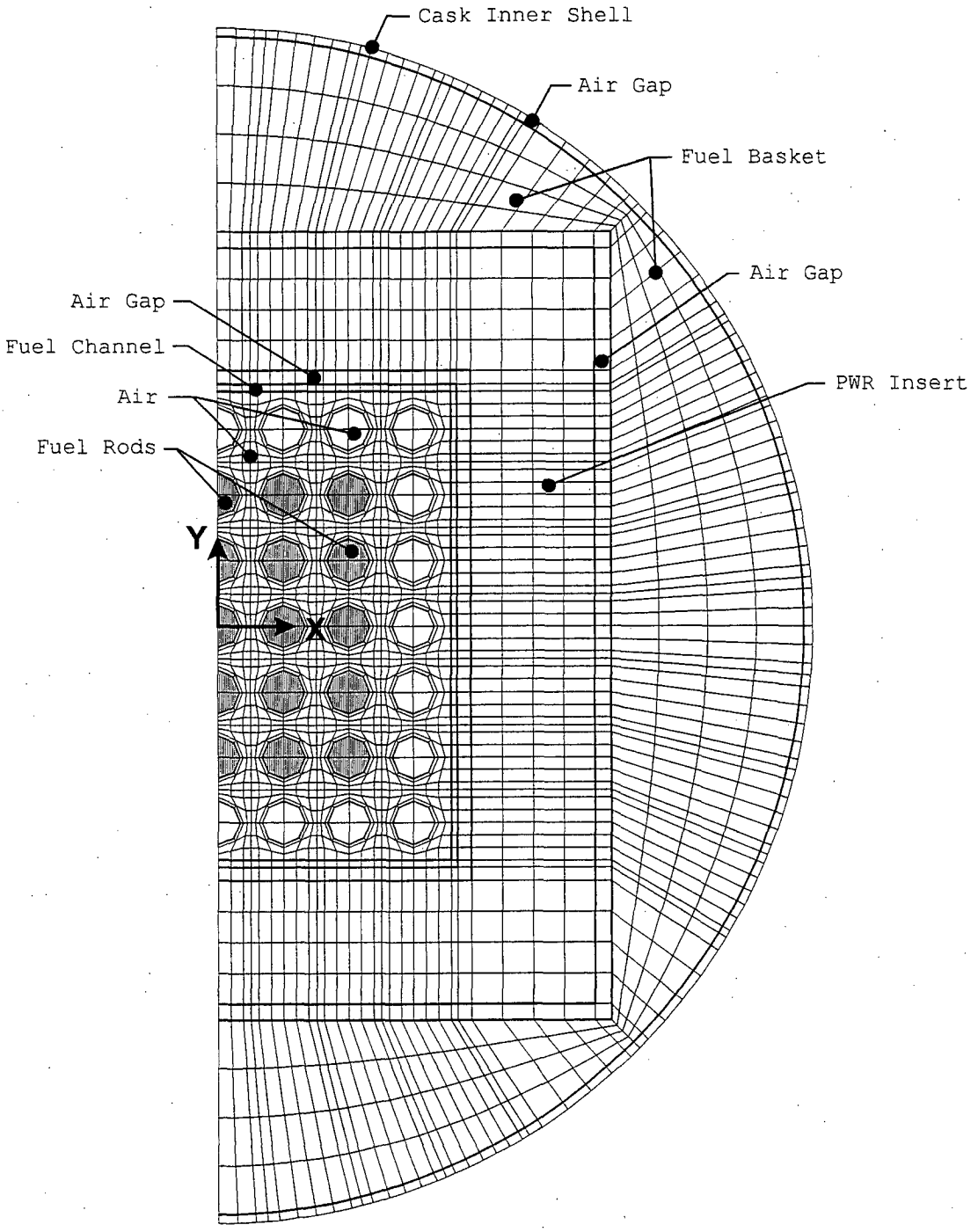


Figure 3.4-17 Fuel Rod Locations in the Thermal Model for Damaged Fuel

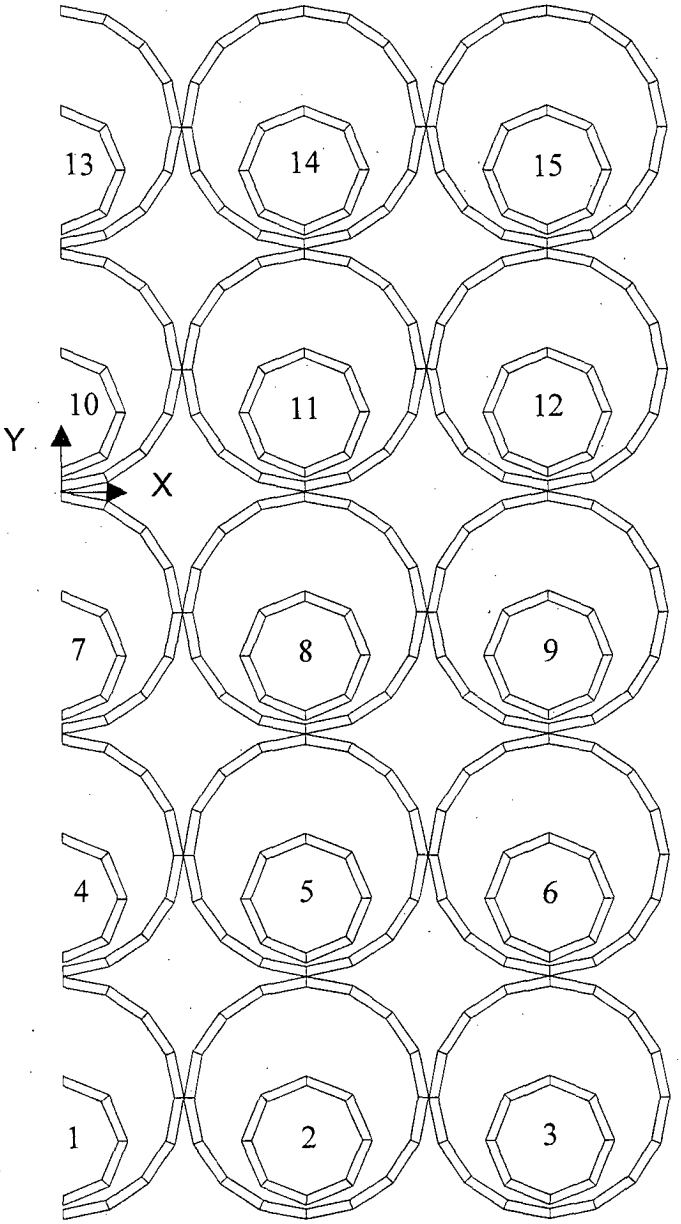
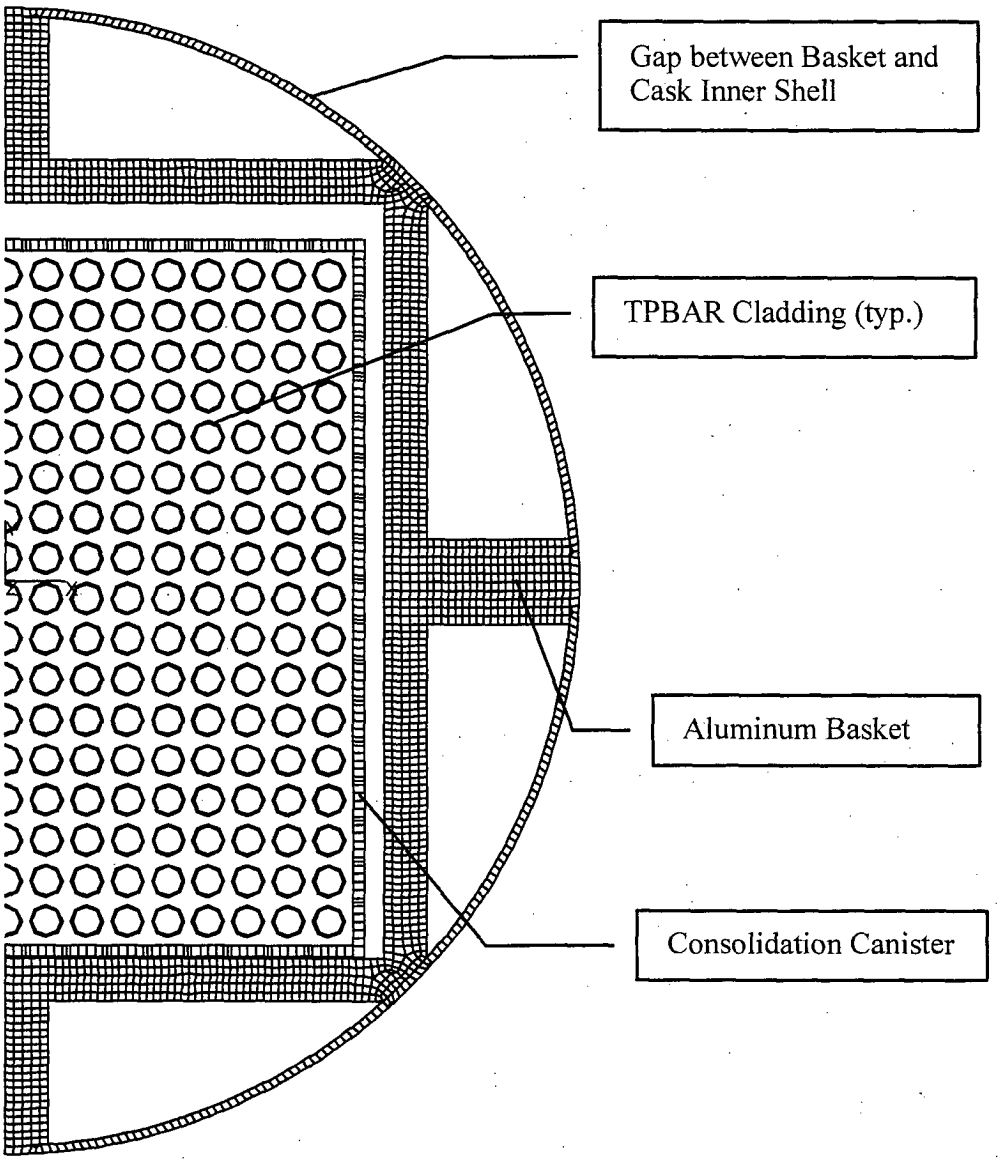


Figure 3.4-18 Finite Element Model for TPBARs



Note: Helium elements, except the gap between the basket and cask inner shell, are not shown for clarity.

Figure 3.4-19 Finite Element Model for MOATA Plate Fuel – ANSTO

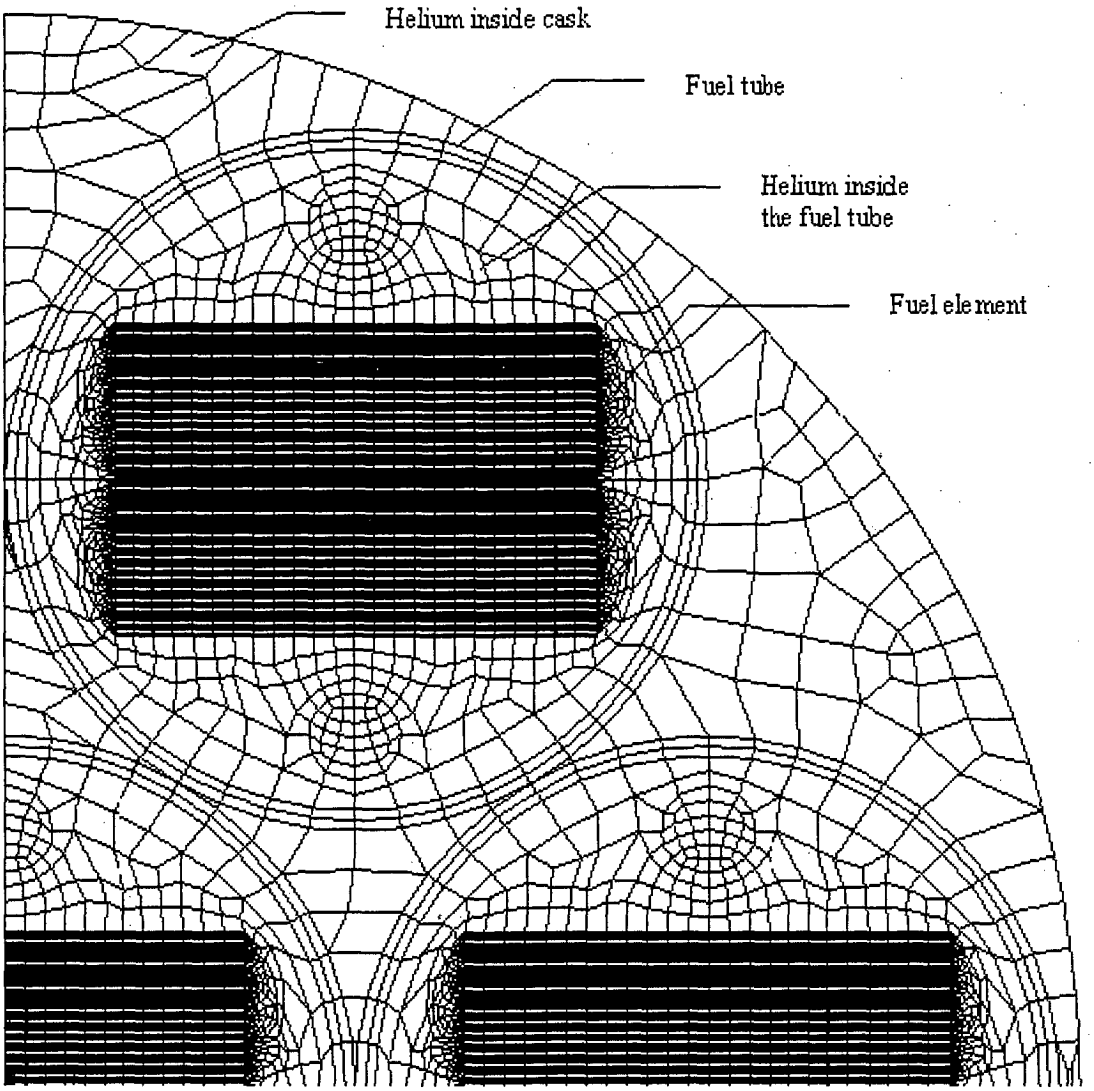


Figure 3.4-20 Finite Element Model for Mark III Spiral Fuel - ANSTO

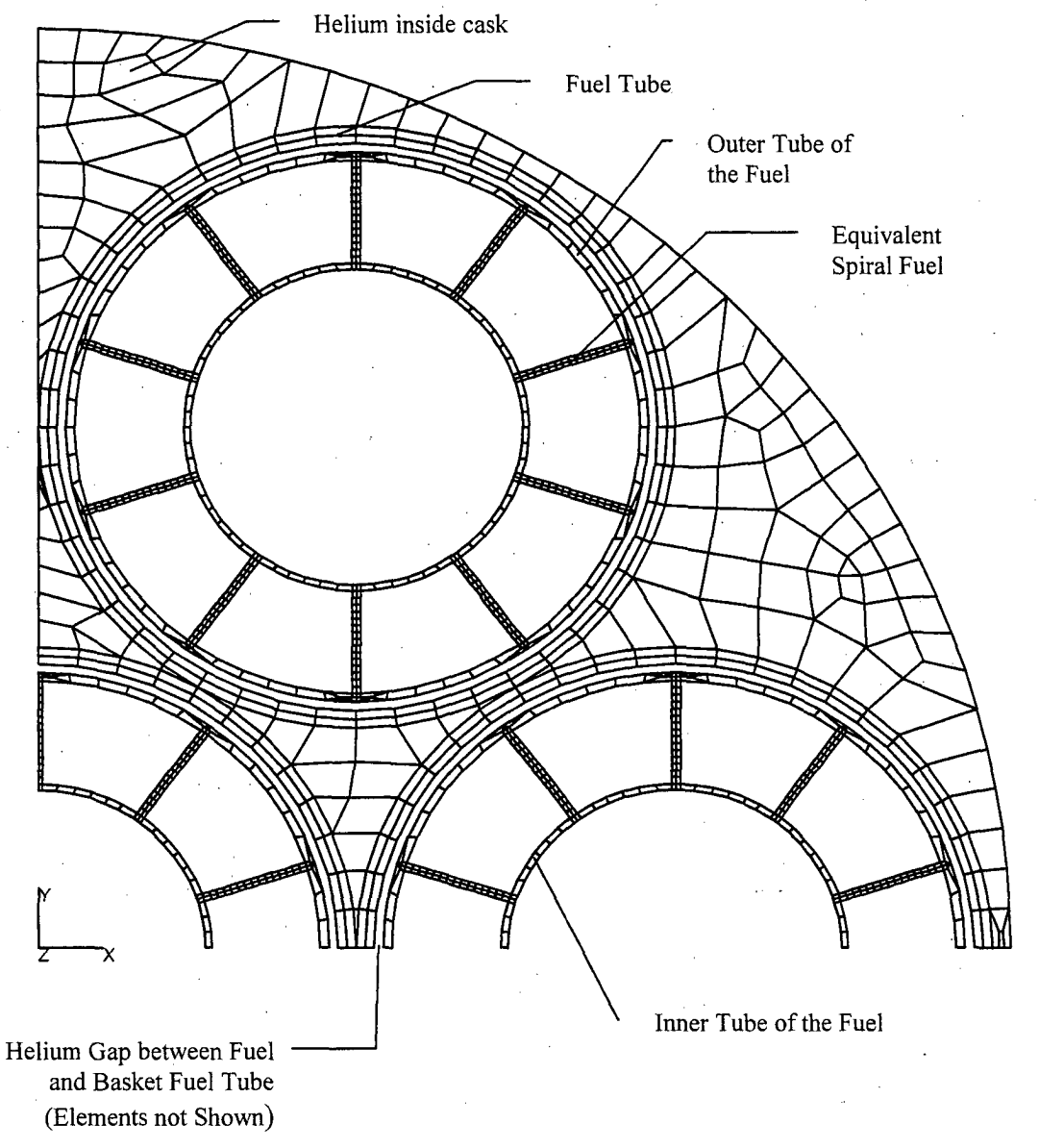


Table 3.4-1 Temperatures for Metallic Fuel Transport

Normal Transport Conditions

Component	Temperature (°F)
O-rings	200
Valves	201
Cask Radial Outer Surface	173
Neutron Shield	252
Radial Lead Gamma Shield	254
Bottom Lead Gamma Shield	210
Inner Stainless Steel Shell	255
Fuel Basket Outer Wall	255
Maximum Fuel Rod Cladding	270

Table 3.4-2 Maximum Component Temperatures – Design Basis PWR Fuel

Normal Transport Conditions

Component	Temperature (°F)
O-rings	227
Valves	231
Cask Radial Outer Surface	229
Neutron Shield	238
Radial Lead Gamma Shield	273
Bottom Lead Gamma Shield	239
Inner Stainless Steel Shell	274
Fuel Basket Outer Wall	276
Maximum Fuel Rod Cladding	472

Table 3.4-3 Limiting Cold Case Component Temperatures – Design Basis PWR Fuel

Normal Transport Conditions

Maximum Decay Heat Load, Minimum Ambient

Component	Temperature (°F)
O-rings	124
Valves	129
Cask Radial Outer Surface	128
Neutron Shield	110
Radial Lead Gamma Shield	167
Bottom Lead Gamma Shield	150
Inner Stainless Steel Shell	167
Fuel Basket Outer Wall	170
Maximum Fuel Rod Cladding	336

Table 3.4-4 Fission Product Gas Inventories and Pressures for Design Basis PWR Fuel Assembly

Fission Product	Inventory per Fuel Assembly (moles)	Initial Pressure (psia)
H-3	0.008	0.615
Kr-80	0.000	0.000
Kr-81	0.000	0.000
Kr-82	0.004	0.308
Kr-83	0.234	17.989
Kr-84	0.687	52.814
Kr-85	0.129	9.917
Kr-86	1.060	81.489
I-127	0.167	12.838
Xe-128	0.010	0.769
I-129	0.704	54.121
Xe-129	0.000	0.000
Xe-130	0.032	2.460
Xe-131	1.641	126.154
Xe-132	4.159	319.728
Xe-134	5.679	436.580
Xe-136	8.529	655.678
Total	**23.044**	**1771.5**

Table 3.4-5 NAC-LWT Cask Thermal Performance Summary

Normal Transport Conditions

Component	Minimum Temperature °F	Maximum Temperature °F	Safe Operating Range °F
TFE O-rings	-40	227	-40 to +735[1]
Metallic O-rings	-40	227	-40 to +800
Viton® O-rings	-40	227[2]	-40 to +550[3]
Lead gamma shield	-40	273	-40 to +600
Liquid neutron shield	-40	238	-40 to +350

[1] Verified through testing (Certified Test Report D9-3362-1, Applied Technical Services, Inc., Marietta, GA, February 8, 1989)

[2] Normal Transport Condition maximum O-ring temperatures were not calculated. The Viton® O-rings are located in close proximity to the TFE O-rings and there is substantial thermal margin, a new O-ring temperature is not calculated

[3] Verified through testing (Certified Test Report 43939-01, Wyle Laboratories, Inc., Huntsville, AL, February 21, 2000).

Table 3.4-6 MTR Fuel Maximum Component Temperatures – Normal Transport Condition

Conditions: 100°F Ambient Temperature
Solar Insolation
1.26 Kilowatts Decay Heat Load

Condition 1: NAC-LWT (Transported in an ISO Container)
Cavity gas: Helium

Component	Temperature (°F)	
	Design Basis Decay Heat Load [1]	Variable Decay Heat Load [2]
Liquid Neutron Shield	198	198
Outer Shell	199	199
Lead Gamma Shield	212	214
Inner Shell	214	215
Basket (maximum)	256	292
Fuel (maximum)	< 363 [3]	< 363 [3]

Condition 2: NAC-LWT (Transported via Truck Trailer)
Cavity gas: Air

Component	Temperature (°F)	
	Design Basis Decay Heat Load [1]	Variable Decay Heat Load [2]
Liquid Neutron Shield	160	160
Outer Shell	161	160
Lead Gamma Shield	180	180
Inner Shell	181	180
Basket (maximum)	267	312
Fuel (maximum)	< 363 [3]	363

[1] Uniform 30-Watt/Element Configuration Heat Load.
[2] 120-Watt / 70-Watt / 20-Watt Configuration Heat Load.
[3] Fuel not modeled for this condition. Fuel temperature is bounded by the variable decay heat load in air case.

Table 3.4-7 PWR Rods (25 Total) Maximum Component Temperatures – Normal Transport Condition

Conditions: 100°F Ambient Temperature
Cask Inside ISO Container
Solar Insolation
1.41 Kilowatts Decay Heat Load

Component	Temperature (°F)
O-rings	< 249
Valves	< 249
Cask Radial Outer Surface	185
Lead Gamma Shield	248
Inner Shell	249
Outer Shell	235
Basket	252
Liquid Neutron Shield	235
Maximum Cladding Temperature	358

Table 3.4-8 TRIGA Fuel Element Maximum Component Temperatures - Normal Conditions of Transport

Conditions: 100°F Ambient Temperature
Solar Insolation
1.05 Kilowatts Decay Heat Load

Condition 2: NAC-LWT (Transported via Truck Trailer)
Cavity Gas: Air

Component	Temperature (°F)
Liquid Neutron Shield	< 160
Outer Shell	< 161
Lead Gamma Shield	< 180
Inner Shell	< 181
Basket (maximum)	267[1]
Cladding (maximum)	326[1]

[1] As shown in Table 3.4-6, the Condition 2 analysis produces higher basket temperatures than Condition 1. Therefore, the Condition 2 analysis for TRIGA fuel bounds transport of the cask in an ISO container.

Table 3.4-9 TRIGA Fuel Cluster Rod Temperatures – Normal Conditions of Transport

Conditions: 100°F Ambient Temperature
Solar Insolation
1.05 Kilowatts Decay Heat Load

Condition 1: NAC-LWT (Transported in an ISO Container)
Cavity gas: Helium

Component	Temperature (°F)
Liquid Neutron Shield	207
Outer shell	207
Lead Gamma shield	221
Inner shell	222
Basket (maximum)	263
Aluminum insert tube	265
Cladding (maximum)	266

Condition 2: NAC-LWT (Transported via Truck Trailer)
Cavity gas: Air

Component	Temperature (°F)
Liquid Neutron Shield	159
Outer shell	160
Lead Gamma shield	177
Inner shell	178
Basket (maximum)	278
Aluminum insert tube	292
Cladding (maximum)	295

Table 3.4-10 PWR and BWR High Burnup Fuel Rods Maximum Component Temperatures – Normal Transport Condition

Conditions: 100°F Ambient Temperature Solar Insolation
2.1 Kilowatts Decay Heat Load
Condition 1: NAC-LWT (Transported in an ISO Container)
Cavity Gas: Helium

Component	Component Temperature (°F)	Allowable Temperature (°F)
Liquid Neutron Shield	306	N/A
Outer Shell	308	800
Lead Gamma Shield	375	600
Inner Shell	385	800
Lid Metallic Containment Shell	385	800
Port Cover Containment Shell	385	550
Basket (maximum)	387	800(1)
Cladding (maximum)	671	752(2)
Aluminum PWR Insert	394	700(3)
Stainless Steel Can Weldment	500	800(2)
Average Cavity Gas	506	N/A

(1) Allowable temperatures greater than 800°F for stainless steel can e used provided stress limits in ASME III, Subsection NH, are employed in the stress evaluations.

(2) The maximum allowable temperature under NCT for PWR, BWR and PWR MOX fuel rod cladding is 752°F (400°C) per ISG-11, Revision 3.

(3) The aluminum insert is not a structural component. The primary consideration in establishing the safe operating range of the aluminum is maintaining the integrity of the aluminum. According to MIL-HDBK-5F, it can be shown that aluminum at 700°F retains component performance.

Condition 2: NAC-LWT (Transported via Truck Trailer)
Cavity Gas: Air

Component	Temperature (°F)
Inner Shell	274
Basket (maximum)	280
Aluminum PWR Insert	286
Stainless Steel Can Weldment	538
Cladding (maximum)	896
Average Cavity Gas	541

Table 3.4-11 Fission Product Gas Inventories and Pressures for the Exxon 7 × 7 BWR Fuel Assembly

Fission Product	Inventory per Fuel Assembly (moles)	Initial Partial Pressure per Rod (psia)
H-3	7.670E-03	1.408E+00
Kr-80	0.000E+00	0.000E+00
Kr-81	0.000E+00	0.000E+00
Kr-82	8.110E-03	1.489E+00
Kr-83	1.270E-01	2.331E+01
Kr-84	7.060E-01	1.296E+02
Kr-85	9.590E-02	1.760E+01
Kr-86	9.330E-01	1.713E+02
I-127	1.770E-01	3.249E+01
Xe-128	3.000E-02	5.507E+00
I-129	7.030E-01	1.290E+02
Xe-129	4.260E-04	7.819E-02
Xe-130	9.040E-02	1.659E+01
Xe-131	9.710E-01	1.782E+02
Xe-132	5.030E+00	9.233E+02
Xe-134	5.690E+00	1.044E+03
Xe-136	8.590E+00	1.577E+03
Total	2.32E+01	4.251E+03

Table 3.4-12 DIDO Fuel Maximum Component Temperatures – Normal Transport Condition

Conditions: 100°F Ambient Temperature
Solar Insolation
1.05 Kilowatts Decay Heat Load

Condition 1: NAC-LWT (Transported in an ISO Container)
Cavity gas: Helium

Component	Temperature (°F)
	Design Basis Decay Heat Load
Liquid Neutron Shield	198[1,2]
Outer Shell	199[1,2]
Lead Gamma Shield	212[1,2]
Inner Shell	214[1,2]
Basket (maximum)	299[3]
Fuel (maximum)	306[3]

1 Uniform 30-Watt/Assembly Configuration Heat Load for MTR fuel.
2 Bounding values obtained from Table 3.4-6 for MTR fuel.
3 Uniform 25-Watt/Assembly Configuration Heat Load for DIDO fuel.

Condition 2: NAC-LWT (Transported via Truck Trailer)
Cavity gas: Air

Component	Temperature (°F)
	Design Basis Decay Heat Load
Liquid Neutron Shield	160[1,2]
Outer Shell	161[1,2]
Lead Gamma Shield	180[1,2]
Inner Shell	181[1,2]
Basket (maximum)	327[3]
Fuel (maximum)	338[3]

1 Uniform 30-Watt/Assembly Configuration Heat Load for MTR fuel.
2 Bounding values obtained from Table 3.4-6 for MTR fuel.
3 Uniform 25-Watt/Assembly Configuration Heat Load for DIDO fuel.

Table 3.4-13 General Atomics IFM Maximum Component Temperatures – Normal Transport Condition

Conditions: 100°F Ambient Temperature
Solar Insolation
13 W Decay Heat Load

NAC-LWT (Transported in an ISO Container)

Component	Temperature (°F)
	Design Basis Decay Heat Load
Liquid Neutron Shield	198[1]
Outer Shell	199[1]
Lead Gamma Shield	212[1]
Inner Shell	214[1]
Basket (maximum)	250[2]
FHU contents (maximum)	326[3]

[1] Bounding values obtained from Table 3.4-6 for MTR fuel.
[2] 13-Watt Configuration Heat Load for General Atomics fuel.
[3] Bounding value obtained from Table 3.4-8 for the 1.05 kW TRIGA fuel.

Table 3.4-14 PWR and BWR High Burnup Fuel Rods in a Fuel Assembly Lattice Maximum Component Temperatures—Normal Transport Condition

Conditions: 100°F Ambient Temperature
Solar Insolation
2.1 Kilowatts Decay Heat Load (BWR)
2.3 Kilowatts Decay Heat Load (PWR)
Transport Condition 2 (no ISO container) with air in the cavity

Component	Temperature (°F)
Inner Shell	274
Basket (maximum)	276
Aluminum PWR Insert	336
Cladding (maximum)	664
Average Cavity Gas	430

Table 3.4-15 Maximum Component Temperatures for High Burnup Fuel Rods with Damaged Fuel Rods in a Rod Holder

	Maximum Temperatures (°F)					
Case[1]	Basket	Aluminum Insert	Rod Holder Weldment	Fuel Rod Tube[2]	Fuel Cladding[3]	Cavity Gas Average
Damaged Rods at Locations #4, 5, 6, 7, 8, 9, 10, 11, 12	280	285	523	835	809	479
Damaged Rods at Locations #7, 8, 9, 10, 11, 12, 13, 14, 15	280	286	567	866	653	482
Damaged Rods at Locations #1, 2, 3, 4, 5, 6, 7, 8, 9	280	284	474	743	749	465

[1] See Figure 3.4-17 for fuel rod locations. The nine locations in the half-symmetry model correspond to fifteen actual fuel rod locations.
[2] The structural analysis of the fuel tubes in Section 2.6.7.10.2.3 uses a maximum temperature of 925°F.
[3] Maximum temperatures are reported for intact fuel rods only.

Table 3.4-16 Maximum Component Temperatures for TPBAR Shipment – Normal Conditions of Transport

Component	Temperature (°F)
Liquid Neutron Shield	207[1]
Outer Shell	207[1]
Lead Gamma Shield	221[1]
Inner Shell	222[1]
TPBARs	290
Aluminum Basket	228
Consolidation Canister	245
Gas (average)	246

[1] Cask component temperature conservatively obtained from Table 3.4-9, Condition 1 for TRIGA Fuel Cluster Rod.

Table 3.4-17 Maximum Component Temperatures - PULSTAR Fuel in MTR Basket

Conditions: 100°F Ambient Temperature
Solar Insolation
840 watts Decay Heat Load
(30 watts in Each Basket Cell)

Condition 1: NAC-LWT (Transported in an ISO Container)
Cavity gas: Helium

Component	Temperature (°F)
Liquid Neutron Shield	207
Outer shell	207
Lead Gamma shield	221
Inner shell	222
Basket (maximum)	263
Aluminum insert tube	265
Cladding (maximum)	266

Condition 2: NAC-LWT (Transported via Truck Trailer)
Cavity gas: Air

Component	Temperature (°F)
Liquid Neutron Shield	159
Outer shell	160
Lead Gamma shield	177
Inner shell	178
Basket (maximum)	278
Aluminum insert tube	292
Cladding (maximum)	295

Notes:
1. The temperatures in this table correspond to the temperatures in Table 3.4-9.
2. PULSTAR fuel can (if used) = 295°F (assume same as fuel cladding temperature).

Table 3.4-18 PULSTAR Fuel Dimensions

Description	Value
Fuel Assembly Height (inch)	38
Fuel Assembly Width (inch)	3.15 × 2.74
Active Fuel Region Height (inch)	24.1
Fuel Rod Diameter (inch)	0.47
Fuel Clad Thickness (inch)	0.0185
Fuel Pellet Diameter (inch)	0.423
Rod Length (inch)	26.2
Plenum Length (inch)	0.5
Number of Fuel Rods	25

Table 3.4-19 PULSTAR Payload Volume Summary

Description	Dimension[cm^3]
Fuel Volume (25 Elements)	1,860
Pellet to Clad Volume (25 Elements)	97
PULSTAR Can Free Volume	1,440
PULSTAR Can Total Volume	4,230
Assembly Envelope Volume	5,370
LWT Cavity Volume	409,300
MTR Basket Stack Volume	41,900

Table 3.4-20 PULSTAR Fuel Assembly Fission Product Gas Inventory

Isotope	Moles
^{4}He	2.28E-03
^{3}H	1.30E-04
^{82}Kr	6.32E-05
^{83}Kr	7.03E-03
^{84}Kr	1.66E-02
^{85}Kr	2.41E-03
^{86}Kr	2.81E-02
^{127}I	2.87E-03
^{128}Xe	1.27E-04
^{129}I	1.42E-02
^{130}Xe	3.11E-04
^{131}Xe	3.91E-02
^{132}Xe	8.49E-02
^{134}Xe	1.27E-01
^{136}Xe	1.23E-01
Total	4.48E-01

Table 3.4-21 PULSTAR Fuel Element Normal Condition Internal Pressure Summary

Description	Free Volume (liters)	Pressure (atm)	Pressure (psia)	Pressure (psig)
Cask Pressure -28 Intact Assemblies	217.0	1.4	21.3	6.6
Cask Pressure -14 Intact Assemblies and 14 Cans	233.0	1.8	27.2	12.5
Can Pressure - PULSTAR Failed Fuel Can	1.53	4.4	65.4	50.7

Table 3.4-22 Maximum Component Temperatures – MOATA Plate Fuel and Mark III Spiral Fuel in ANSTO Basket

Conditions: 100°F Ambient Temperature
Solar Insolation
Heat Load: 126 Watts – MOATA Plate Fuel; 756 Watts – Mark III Spiral Fuel

Component	Temperature (°F)
Liquid Neutron Shield[1]	207
Outer Shell[1]	207
Lead Gamma Shield[1]	221
Inner Shell[1]	222
Basket - MOATA Plate Fuel	230
Fuel Cladding – MOATA Plate Fuel	233
Basket – Mark III Spiral Fuel	248
Fuel Cladding – Mark III Spiral Fuel	250

[1] The cask component temperatures are conservatively obtain from Table 3.4-9 for the TRIGA Fuel Cluster Rod.

3.5 Hypothetical Accident Thermal Evaluation

The hypothetical accident scenario is a series of accidents that occur in a specified order as described in 10 CFR 71.73. The only thermal consequence as a result of the drop and puncture portions of the hypothetical accident is the assumption that the neutron shield is lost prior to the start of the fire. The remainder of the thermal analysis in this section consists of an evaluation of the thermal consequences of the fire portion of the hypothetical accident.

3.5.1 Finite Element Models

There are two finite element models used to evaluate the hypothetical fire accident condition. The axisymmetric thermal model, as described in Section 3.5.1.1, is used to evaluate all configurations except for the PWR and BWR high burnup fuel rod configuration. For the PWR and BWR high burnup fuel rod configuration, two-dimensional planar finite element model is used. The planar model is described in Section 3.5.1.2.

3.5.1.1 Axisymmetric Thermal Model

The finite element code ANSYS (Revision 5.5) is used to generate a two-dimensional (2-D) axisymmetric finite element model and to perform thermal analyses for the pre-fire, fire and post-fire (cool down) conditions. The ANSYS finite element model is shown in Figure 3.5-1. Figure 3.5-2 and Figure 3.5-3 show the detail of the model at the locations where the thermal insulator is installed in the top and bottom regions. The ANSYS model uses thermal conductivity values for the thermal insulators that are conservative in that they are higher than the values shown in Table 3.2-6 and Table 3.2-8. The thermal insulator protects the lead gamma shield against localized melting during the fire event. As shown, the main components in the radial direction consist of the inner shell, the radial lead, the outer shell, the neutron shield tank and the expansion tank.

The model is constructed using the ANSYS thermal PLANE55 element. Thermal radiation and convection heat transfer at the cask surface is modeled using the PLANE55 and SURF19 elements. Radiation heat transfer across the neutron shield tank and neutron shield expansion tank is modeled using the ANSYS radiation LINK31 element.

The pre-fire condition is defined as the normal transport condition, and a steady-state analysis is performed to determine the temperature field of the cask body. This temperature field is used as the initial condition for the 30 minute fire transient analysis (fire condition), which is followed by a 50-hour cool down period (post-fire condition). Analysis of the 50-hour cool down period ensures that the maximum component temperatures are determined.

The pre-fire analysis considers the convection heat transfer of the liquid neutron shielding inside the shell, but convection heat transfer of the air inside the expansion tank is conservatively neglected. During the fire and post-fire conditions, the liquid neutron shielding is considered to be lost, due to either the pin puncture accident or the failure of the relief valve in the neutron shield tank resulting from high pressure steam produced by the fire. The convection heat transfer of the air in the tank is negligible compared to the radiation heat transfer. The radiation heat transfer across the air-filled tank, and expansion tank, is explicitly modeled using the ANSYS radiation LINK31 element. An emissivity of 0.36 is used for all inner surfaces of the stainless steel neutron shield tank and the expansion tank.

The impact limiters are not discretely modeled, but are represented as thermal boundary conditions. Before the fire accident, adiabatic thermal boundary conditions are conservatively applied to the interface regions between the cask and the impact limiters so that no heat is transferred out of the cask through the impact limiters. During the fire and post-fire periods, the impact limiters are assumed to be removed. In this time period, heat transfer by convection and radiation are modeled in the regions previously covered by the impact limiters. Solar insolation is considered in the model during the pre-fire and post-fire conditions, but neglected during the fire.

The heat input from the fire considers thermal radiation and convection heat transfer. A convection heat transfer coefficient of 0.02446 Btu/hr-in2-°F is applied to account for heat transfer to the cask surface. This value is twice the theoretical value (Wix) to account for uncertainties in the fire accident condition and the data from which the recommended value is derived. These assumptions lead to maximizing the material temperatures and are conservative.

The cask contents (basket and fuel) are not directly modeled. The decay heat generated from the fuel region inside the cask is simulated using an equivalent non-uniform heat flux applied to the inner surface of the cask cavity inner shell, corresponding to the height of the active fuel region. The analysis considers the bounding fuel heat load, 2.5 kW for PWR fuel, and applies the power distribution curve shown in Figure 3.4-2 with a peaking factor of 1.2.

ANSYS 5.5 was used to calculate the maximum post-fire accident temperatures at four new locations for the alternate port cover design. Temperatures calculated for comparable locations on the port cover body vary from those temperatures presented in Table 3.5-1. Changes in the ANSYS 5.5 version and computational solvers account for the differences in calculated results. The transient temperature analysis results are presented in Figure 3.5-12 and Figure 3.5-13.

Exactly the same model described above was rerun using ANSYS 5.5 for the alternate port cover to determine the bolt head and thread temperatures and the temperatures at both O-ring locations. The output is post-processed to determine the maximum average temperatures at specific locations of interest. The temperatures calculated are presented in Table 3.5-1.

3.5.1.2 Two-Dimensional Planar Thermal Model

Thermal analysis of the NAC-LWT cask loaded with PWR and BWR high burnup fuel rods is performed using a two-dimensional planar thermal model. The thermal model is identical to the model utilized to perform the steady state analysis (condition 2, Section 3.4.1.7) for the NAC-LWT cask loaded with PWR and BWR high burnup fuel rods. The detailed model description is contained in Section 3.4.1.7.2.

The Condition 2 model was selected since it initiates the thermal transient with clad temperatures 225°F higher (from Table 3.4-10, 896°F-671°F) than the Condition 1 model steady-state condition. This increase in the initial condition temperature for the cask cavity air-filled condition overcompensates for the higher conductivity of helium as the cavity gas. The effect of the higher helium conductivity heat input during the period of fire exposure is significantly less due to the influence of the parallel heat transfer paths by conduction through the metal contents and by radiation across the gas-filled space. This influence is seen in the transient maximum temperature difference from the higher steady-state temperature of 896°F to the maximum transient temperature of 1014°F (a change of 118°F), which is significantly bounded by the steady-state temperature condition difference of 225°F, as stated previously. In addition to the conservative modeling introduced by the initial steady-state temperature, during the cooldown portion of the transient, the use of air thermal conductivity in the cavity retards the heat removal from the fuel (as compared to helium conductivity). This also results in a maximum transient temperature higher than when modeling helium as the cavity gas.

A thermal transient analysis for the design basis fuel is performed using the two-dimensional planar thermal model (see Figure 3.4-12). To impose the fire accident condition on this model, a temperature time history was applied to the outer surface of the model, which corresponds to the inner surface of the inner shell. This temperature time history at the inner shell inner surface near the axial midplane is obtained from the fire accident analysis (heat load of 2.5 kW and a peaking factor of 1.2, as described in Section 3.5.2) using the axisymmetric two-dimensional model described in Section 3.5.1.1.

Using a two-dimensional planar model of the cross-section, a 50.5-hour transient analysis is performed with a heat load of 2.1 kW with a peaking factor of 1.22. This represents the bounding heat load for the high burnup PWR and BWR fuel rods.

3.5.2 Package Conditions and Environment

The fire accident is preceded by the cask drop and cask puncture portions of the hypothetical accident. The only damage that occurs as a result of the drop and puncture accident events that are of importance to the cask thermal performance is the damage to the NAC-LWT cask neutron shield. As a result of these events, it is assumed that the integrity of the neutron shield has been damaged to such an extent that the entire contents of the neutron shield are no longer present.

The fuel heat load of 2.5 kW is applied using a nonuniform heat flux with a peaking factor of 1.2. Solar insolation is applied to the outer surfaces of the cask, including the area covered by the impact limiters, during the post-fire conditions, and neglected during the fire condition. The value of solar insolation, based on a 24-hour average to curved surfaces, is:

$$Q_{sun}=1475/(24\times144) = 0.4268 \text{ BTU/hr-in}^2$$

Convection and radiation heat transfer at the outer surfaces of the cask were considered in the analysis. During the pre-fire (normal) and post-fire periods, the ambient temperature assumed is 100°F, and the cask outer surface emissivity is 0.36. During the fire, the ambient temperature is 1,475°F, and the cask surface emissivity is 0.9. The convection coefficient applied is 0.02446 Btu/hr-in^2-°F.

Using a decay heat of 2.5 kW, the conditions for the hypothetical fire accident are:

Analysis Condition	Loads and Boundary Conditions
Initial steady-state (pre-fire)	• Solar Insolation • Combined convection (using the film coefficent for the cask surface, $0.00125\Delta T^{0.33}$ Btu/hr-in^2-°F) and radiation heat transfer (as defined in Section 3.2.3) between the cask exterior (ε=0.36) and the ambient (100°F) • The surface of the cask in contact with the impact limiter is adiabatic
Fire transient (during fire)	• Ambient temperature 1,475°F with no solar insolation • Combined convective (additional coefficient of 0.02446 Btu/hr-in^2-°F) and radiative heat transfer using a film coefficient (as defined in Section 3.2.3) between the cask exterior (ε=0.9), including the area normally covered by impact limiters, and the fire • Neutron shield fluid lost
Cool down (post-fire)	• Ambient temperature 100°F with solar insolation • Combined convection (using the film coefficent for the cask surface, $0.00125\Delta T^{0.33}$ Btu/hr-in^2-°F) and radiation heat transfer (as defined in Section 3.2.3) between the cask exterior (ε=0.36), including the area covered by the impact limiters, and ambient • Neutron shield fluid lost

3.5.3 Package Temperatures

The temperatures of the cask body resulting from the fire are determined using ANSYS. The heat load used in the transient thermal analysis corresponds to the PWR fuel, since its heat load envelopes all other fuel types that can be transported in the NAC-LWT cask.

The maximum temperatures of the basket and fuel for the different fuel types are determined using the results of the fire transient analysis of the cask body and the maximum temperature differences between the basket and fuel and the inner shell of the cask body as computed in the steady state thermal evaluations.

3.5.3.1 Evaluation for PWR Fuel Contents

The maximum temperatures of the cask body and principal components are evaluated using the ANSYS model described in Section 3.5.1.1. A radial temperature profile is obtained during the postulated 30-minute fire and for a cooldown period of 50 hours. The maximum cask component temperatures for the hypothetical accident are presented in Table 3.5-1.

Maximum time dependent temperatures of different cask components, before, during and after the fire, are shown in Figure 3.5-4 and Figure 3.5-5. The temperatures of the components show a sharp increase during the fire and a sharp decrease that begins right after the fire. After the 50 hour cooling period, the temperatures of the components do not return to the normal conditions of transport values. This is attributed to the loss of the liquid neutron shield during the accident, which results in the loss of the (liquid) convection heat transfer across the tank.

As noted above, the fuel and the fuel basket were not directly modeled in the ANSYS analysis. To determine the maximum temperature of the components inside the basket, the following method is applied:

$$T_{max} = Tis_{max} + \Delta T_{comp}$$

where:

Tis_{max} is the maximum temperature of the inner shell, obtained in the ANSYS transient thermal analysis.

ΔT_{comp} is the difference in maximum temperatures from Table 3.4-2 between the inner shell and the fuel basket outer wall or the fuel rod cladding during normal transport.

The maximum temperatures of fuel cladding and basket wall are:

Component	ΔT_{comp} (°F) [1]	Tis_{max} (°F) [2]	T_{max} (°F)
Fuel basket outer wall	2 (276-274)	505	507
Fuel cladding	198 (472-274)	505	703

[1] Temperatures from Table 3.4-2.

[2] Temperatures obtained in the ANSYS evaluation.

As a result, the maximum average cavity gas temperature can be taken as the average of the maximum basket wall and maximum fuel cladding temperatures. This produces an average cavity gas temperature of 605°F.

As shown in Table 3.5-1, all of the cask component temperatures are within the allowable temperature limit during the fire accident event.

3.5.3.2 Evaluation of MTR Fuel Contents

The temperatures in the MTR fuel basket and MTR fuel plates produced during the fire accident were determined using the two ANSYS finite element models of the NAC-LWT cask for MTR fuel element discussed in Section 3.4.1.3.2. The gas in the NAC-LWT cask cavity is considered to be air. Other conditions applied to the model are the same as those described in Sections 3.5.1 and 3.5.2 for the axisymmetric fire transient model with respect to the liquid neutron shield and outer surface boundary conditions. The accident thermal models for MTR fuel are shown in Figure 3.5-6 and Figure 3.5-7, for the design basis decay heat loading and the variable decay heat loading, respectively. The type, form, design or enrichment of the MTR fuel assemblies has no effect as long as the decay heat load and other fuel characteristics are in compliance with the requirements of Table 1.2-4. The presence and/or use of axial fuel spacers and spacer plates to position the fuel assemblies for ease of handling have no effect on the thermal analyses of the MTR basket assembly.

The transient calculation is performed to determine the maximum temperatures in the MTR fuel elements only for the variable decay heat loading because this is the worst-case condition. The cask model is used to determine the temperature history of the cask components, including the basket. The fuel element model is used to determine the temperature rise between the basket and the hottest point in the fuel element. The capacitance of the fuel element is negligible compared to the very large capacitance of the cask assembly. Therefore, a constant ΔT between basket and fuel is used. The temperature history for the MTR fuel variable heat load fire accident analysis is

shown Figure 3.5-8. The temperature profile within the cask model at the time of the maximum fuel temperature is shown in Figure 3.5-9. The bounding case is an element with 10 fuel plates, a decay heat of 120W and with worst-case dimensions. The maximum temperatures of the components are presented in Table 3.5-2. These results demonstrate that the maximum MTR fuel plate temperature for the variable decay heat loading is 473°F. The MIL-HDBK-5F Specification for 6061-T6 aluminum alloy indicates that the material retains more than 35% of its room temperature yield and ultimate strengths during transient exposure to temperatures as high as 500°F. Therefore, the reduction in strength for the fuel cladding as a result of the fire transient is minor when compared to the values presented in Section 3.4.1.3.3 for aluminum at 400°F. Since the fuel cladding temperatures are maintained significantly below 500°F, it is concluded that the structural integrity of the fuel cladding is maintained. Furthermore, the aluminum cladding of the MTR fuel elements is heated to a temperature of approximately 900°F during the fabrication process and it is clear that the cladding integrity is maintained during that process.

3.5.3.3 Evaluation of TRIGA Fuel Contents

The accident condition temperatures are obtained by applying the temperature differential calculated for the MTR fuel configuration to the TRIGA fuel configuration. To determine the TRIGA accident condition maximum cladding temperature, the temperature difference between the maximum basket temperatures for the normal and accident component temperatures calculated for MTR fuel in Section 3.5.3.2, is added to the maximum cladding temperature calculated for TRIGA fuel in Section 3.4.1.5.

The maximum basket temperature for the MTR fuel design basis heat load fire accident analysis is 374°F, as reported in Table 3.5-2. This temperature is 107°F higher than the normal condition maximum temperature (267°F) reported in Table 3.4-6. The corresponding maximum TRIGA fuel cladding temperature for the fire accident condition is reported in Table 3.5-3 to be 433°F. The MIL-HDBK-5F Specification for 6061-T6 aluminum alloy indicates that the material retains more than 35% of its room temperature yield and ultimate strengths during transient exposure to temperatures as high as 500°F. Therefore, the reduction in strength for the aluminum-clad TRIGA fuel cladding as a result of the fire transient is minor when compared to the values presented in Section 3.4.1.3.3 for aluminum at 400°F. Since the fuel cladding temperatures are maintained significantly below 500°F, it is concluded that the structural integrity of the aluminum-clad TRIGA fuel is maintained. The allowable temperature for stainless steel-clad TRIGA fuel is significantly higher.

The TRIGA fuel generates small amounts of fission gases during reactor operations, but it contains no initial charge of helium gas. Consequently, the internal pressure developed in the accident condition is less for TRIGA fuel than for the design basis PWR fuel.

3.5.3.4 Evaluation of TRIGA Fuel Cluster Rod Contents

The temperatures in the TRIGA fuel cluster rod basket and cladding produced during the fire accident were determined using the ANSYS finite element model of the NAC-LWT for the TRIGA fuel discussed in Section 3.4.1.6 for Condition 2 (air in the cavity and without the ISO container). The gas in the NAC-LWT cask cavity is considered to be air. Other conditions applied to the model are the same as those described in Sections 3.5.1 and 3.5.2 for the axisymmetric fire transient model with respect to the liquid neutron shield and outer boundary conditions.

The temperatures in the basket are bounded by the maximum temperatures of the fuel region. The temperature time history for the fuel region is shown in Figure 3.5-10. The maximum temperature of the clad was determined to be 394°F. This value is below the 800°F limit for the clad or the 400°F limit for the aluminum specified in Section 3.4.1.6. Therefore, the components are determined to be acceptable for the fire accident condition.

3.5.3.5 Evaluation for PWR and BWR High Burnup Fuel Rod Contents in a Rod Holder

The maximum temperatures of the principal components are evaluated using the ANSYS model described in Section 3.5.1.2. The maximum cask component temperatures for the hypothetical accident are identical to those presented in Table 3.5-1 since the bounding temperature history from the analysis of NAC-LWT PWR contents is used as a boundary condition for the analysis for PWR and BWR high burnup fuel rod contents.

Maximum time dependent temperatures of different components, before, during and after the fire, are shown in Figure 3.5-11. For the maximum time dependent temperatures of cask components see Figure 3.5-4 and Figure 3.5-5.

As a result, the maximum average cavity gas temperature for fire accident is calculated as the average of the air contained inside the basket. This produces an average cavity gas temperature of 695°F.

Table 3.5-4 shows the can weldment and fuel rod cladding temperatures during the fire accident event.

3.5.3.6 Evaluation of DIDO Fuel Contents

The DIDO fuel maximum heat load is bounded by the maximum heat load of the MTR fuel. Therefore, in the accident condition, the maximum temperatures of the cask components for the MTR contents will bound the maximum temperatures for the cask components for the DIDO

contents. It is conservative to use the results of the fire transient evaluated in Section 3.5.3.2 for the cask inner shell temperature. The maximum basket and fuel temperatures (T_{max}) for the DIDO fuel for the accident conditions are determined by adding the increase in steady state temperature from the cask inner shell to the maximum temperature of the component ($\Delta T_{component}$) to the maximum cask inner shell temperature ($T_{inner\ shell}$) obtained from the MTR evaluation. The maximum temperatures of the fuel cladding and basket wall are:

Component	$\Delta T_{component}$ (°F)	$T_{inner\ shell}$[1] (°F)	T_{max} (°F)
Fuel basket	146 = 327[2]-181	334	480
Fuel cladding	157 = 338[2]-181	334	491

[1] Obtained from Table 3.5-2 for the uniform heat distribution.
[2] Obtained from Table 3.4-12, Condition 2.

The fuel cladding temperature previously listed is bounded by those determined for the MTR contents. It is concluded that the structural integrity of the fuel cladding is maintained for the fire accident condition.

3.5.3.7 Evaluation for General Atomics Fuel Contents

The General Atomics fuel maximum heat load is bounded by the maximum heat load of the DIDO and MTR fuels. Therefore, in the accident condition, the maximum temperatures of the cask components for the MTR contents will bound the maximum temperatures for the cask components with General Atomics fuel. It is conservative to use the results of the fire transient calculation evaluated in Section 3.5.3.2 for the cask inner shell temperature. The maximum basket temperature (T_{max}) for the General Atomics fuel for accident conditions is determined by adding the increase in steady-state temperature from the cask inner shell to the maximum temperature of the component ($\Delta T_{component}$) to the maximum cask inner shell temperature ($T_{inner\ shell}$) obtained from the MTR evaluation. The maximum temperature of the basket is:

$$T_{max} = (250 - 214) + 334 = 370^{\circ}F$$

where:

334°F is the maximum temperature of the LWT inner shell during a fire accident

This temperature is bounded by those determined for the MTR contents. It is concluded that the structural integrity of the General Atomics basket and contents is maintained for the fire accident condition.

3.5.3.8 Evaluation of PWR and BWR High Burnup Fuel Rods in Fuel Assembly Lattice

The total heat load of the PWR and BWR high burnup fuel rods (up to 25 rods) in a fuel assembly lattice is bounded by that for the PWR and BWR high burnup fuel in a rod holder as evaluated in Section 3.5.3.5. Therefore, in the accident condition, the maximum temperatures of the cask components for the design basis PWR configuration bound the maximum temperatures for the PWR or BWR high burnup fuel rods in the fuel assembly lattice. The fuel cladding is expected to have the same difference in temperature between normal conditions and the accident fire conditions as determined in Section 3.5.3.5. The temperature difference for the fuel cladding between normal and accident conditions for the high burnup fuel in a rod holder is 118°F (1,014°F – 896°F). The maximum fuel cladding temperature is 664°F for high burnup fuel rods in a fuel assembly lattice for normal conditions of transport as evaluated in Section 3.4.1.10 (Table 3.4-14). Therefore, the maximum temperature of the fuel cladding for the 25 fuel rods in the fuel assembly lattice for accident conditions is 782°F (664°F + 118°F).

3.5.3.9 Evaluation of PWR and BWR High Burnup Fuel in a Rod Holder with Damaged Rods

The damaged fuel maximum heat load is equal to the maximum heat load of the PWR and BWR high burnup fuel rods. To determine maximum temperatures of the fuel configuration with damaged fuel rods in the fire accident condition, temperatures from the normal and accident conditions for the PWR and BWR high burnup intact fuel rods (Table 3.4-10 and Table 3.5-4) are used to determine the temperature differentials that are caused by the fire accident. The increase in temperatures is added to the maximum normal conditions temperature for the fuel rods in a rod holder with damaged rods (Table 3.4-15) to compute the maximum fire temperatures. The maximum temperatures of the fuel cladding and stainless steel rod holder are shown in Table 3.5-5. The maximum temperatures for the cask components are bounded by those for the design basis PWR fuel assembly configuration.

3.5.3.10 Evaluation of TPBAR Contents

The maximum heat load of TPBARs is bounded by the maximum heat load of the MTR fuel. Therefore, in the accident condition, the maximum temperatures of the cask components for the MTR contents will bound the maximum temperatures for the cask components for the TPBAR contents. It is conservative to use the results of the fire transient evaluated in Section 3.5.3.2 for the cask inner shell temperature. The maximum component temperatures (T_{max}) for the TPBARs for the accident conditions are determined by adding the temperature difference ($\Delta T_{component}$)

between the cask inner shell and the maximum component temperature for normal conditions to the maximum accident cask inner shell temperature ($T_{inner\ shell}$) obtained from the MTR evaluation. The maximum component temperatures are computed as follows.

Component	$\Delta T_{component}$ (°F)	$T_{inner\ shell}$[2] (°F)	T_{max} (°F)
TPBAR	68 (290[1]-222[1])	334	402
Aluminum Basket	6 (228[1]-222[1])	334	340
Consolidation Canister	23 (245[1]-222[1])	334	357
Gas (average)	24 (246[1]-222[1])	334	358

[1] See Table 3.4-16
[2] See Table 3.5-2

The maximum temperatures of the components are presented in Table 3.5-6.

3.5.3.11 Evaluation of PULSTAR Fuel Elements in 28 MTR Basket

As described in Section 3.4.1.13, the thermal performance of the configuration of PULSTAR fuel elements in the 28 MTR basket is bounded by the thermal performance of the TRIGA fuel cluster rods, condition 2. The temperatures in the TRIGA fuel cluster rod basket and cladding produced during the fire accident were determined and described in Section 3.5.3.4. The temperatures in the basket are bounded by the maximum temperatures of the fuel region. The temperature time history for the fuel region is shown in Figure 3.5-11. The maximum temperature of the cladding was determined to be 394°F. This value is below the 1,058°F limit for the fuel cladding. Therefore, the components for PULSTAR fuel elements in the 28 MTR basket are determined to be acceptable for the fire accident condition.

3.5.3.12 Evaluation of ANSTO Fuels

The maximum heat load of the spiral fuel assemblies (0.756 kW per cask) is bounded by the maximum heat load of the MTR fuel (1.05 kW per cask). Therefore, in the accident condition, the maximum temperatures of the cask components for the MTR contents will bound the maximum temperatures for the cask components for the ANSTO basket contents. It is conservative to use the results of the fire transient evaluated in Section 3.5.3.2 for the cask inner shell temperature. The maximum basket and fuel temperatures (T_{max}) for the ANSTO fuel contents for the accident condition are determined by adding the temperature difference ($\Delta T_{component}$) between the maximum temperature of the cask inner shell and the component (basket or fuel) for the normal condition to the maximum cask inner shell temperature ($T_{innershell}$)

for the accident condition obtained from the MTR evaluation. The maximum temperatures of the fuel cladding and basket are computed as follows.

Component	$\Delta T_{component}$ (°F)	$T_{innershell}$[1] (°F)	T_{max} (°F)
Fuel basket – MOATA Plate Fuel	8 = 230[2]-222[2]	334	342
Fuel cladding – MOATA Plate Fuel	11 = 233[2]-222[2]	334	345
Fuel basket – Mark III Spiral Fuel	26 = 248[2]-222[2]	334	360
Fuel cladding – Mark III Spiral Fuel	28 = 250[2]-222[2]	334	362

[1] Obtained from Table 3.5-2 for the uniform heat distribution
[2] Obtained from Table 3.4-22

3.5.3.13 Evaluation of 16 PWR MOX High Burnup Rods

The PWR/BWR Rod Transport Canister and 5 × 5 insert used for the transport of 16 PWR MOX high burnup rods is the same design as the one used for the BWR and PWR high burnup rods. The heat load used in the evaluation of the BWR high burnup rods, which includes the effect of the peaking factor, bounds that of the PWR MOX high burnup rods (see Section 3.4.1.15). As presented in Section 3.4.1.15, the reduced conductivity of the PWR MOX fuel rods does not affect the heat transfer through the canister or insert or, in the case of the transient, it does not affect the ability to absorb and retain heat. The initial temperatures of the fuel rods are conservative since the heat load used in the steady-state evaluation is for 25 rods of the design basis heat load (see Section 3.4.1.7), rather than the 16 PWR MOX high burnup rods. Therefore, the maximum component temperatures under the hypothetical accident condition (HAC) are identical to the results reported in Table 3.5-1 for the PWR assembly contents, which were used as the boundary condition for the analysis for PWR and BWR high burnup fuel rod contents and, therefore, are applicable to the PWR MOX fuel rod contents. Table 3.5-1 shows that the lid metallic seal, Alternate B port cover metallic face seal and lead gamma shield are below their respective temperature limits. In addition, the bounding temperatures for the PWR and BWR rod contents reported in Table 3.5-4, which are bounding for the PWR MOX fuel rod contents, show that the can weldment and fuel rod cladding temperatures under the HAC are below their respective limits.

3.5.3.14 Evaluation for TPBARs in the PWR/BWR Rod Transport Canister

Similar to Section 3.5.3.10, the maximum heat load of TPBARs in the Rod Transport Canister is bounded by the maximum heat load of the MTR fuel. Therefore, in the accident condition, the

maximum temperatures of the cask components for the MTR contents will bound the maximum temperatures for the cask components for the TPBAR contents. It is conservative to use the results of the fire transient evaluated in Section 3.5.3.2 for the cask inner shell temperature. The maximum content temperature (T_{max}) for the TPBARs in a Rod Transport Canister for the accident conditions are determined by adding the temperature difference ($\Delta T_{component}$) between the cask inner shell and the maximum component temperature for normal conditions to the maximum accident cask inner shell temperature ($T_{inner\ shell}$) obtained from the MTR evaluation. The maximum component temperature is computed as follows.

Component	$\Delta T_{component}$ [1] (°F)	$T_{inner\ shell}$ [2] (°F)	T_{max} (°F)
TPBAR	14	334	348

[1] See Section 3.4.1.17
[2] See Table 3.5-2

The computed maximum contents temperature is less than for the TPBAR analysis of Section 3.5.3.10. Therefore, the component temperatures, namely, the aluminum basket and TPBARs, for the fire accident condition are bounded by the results of Section 3.5.3.10.

3.5.4 Maximum Internal Pressure

3.5.4.1 Maximum Internal Pressure for Design Basis Fuel in Accident Conditions

The accident internal pressure is calculated assuming an accident with 100 percent fuel rod failure combined with the design basis fire described in 10 CFR 71. The fuel rod failure assumes 30 percent of the fission gas and 100 percent of the backfill gas escapes the ruptured fuel rods.

The internal pressure due to the 100 percent fuel rod rupture is calculated using the method described in Section 3.4.4. The total cask pressure of the cask backfill and failed fuel rods is calculated by a two step procedure. First, the pressures documented under normal conditions in Section 3.4.4 are adjusted to include the increased total free volume associated with 100% fuel rod failure. Then, the revised cask pressure at normal operating temperature is adjusted to accident condition temperatures.

Adjusting the partial pressure of the cask backfill:

$$P_{cask} = P_{initial}\left(\frac{V_{cask}}{V_{total}}\right)$$

where:

$P_{initial}$ = 25.8 psia (normal condition temperature adjusted cask backfill pressure)

V_{cask} = 5.196 ft^3 (147,134 cm^3) [Section 3.4.4]

$V_{rod\ void}$ = 8,123 cm^3 [Section 3.4.4]

V_{total} = 155,257 cm^3 ($V_{cask} + V_{rod\ void}$)

$$P_{cask} = 25.8\ \text{psia}\left(\frac{147{,}134\text{cm}^3}{155{,}257\text{cm}^3}\right)$$

$$P_{cask} = 24.4\ \text{psia}$$

Adjusting the partial pressure of the fuel rod backfill and fission gases:

$$P_{fuel\,rods} = P_{initial}\left(\frac{V_{rod\,void}}{V_{total}}\right)$$

where:

$P_{initial}$ = 1,521.3 psia (fuel rod backfill pressure of 989.8 psia plus fission gas pressure of 0.30 x 1771.5 psia)

$V_{rod\ void}$ = 8,123 cm^3

V_{total} = 155,257 cm^3

$$P_{fuel\,rods} = 1{,}521.3\ \text{psia}\left(\frac{8{,}123.28\text{cm}^3}{155{,}257\text{cm}^3}\right)$$

$$P_{fuel\,rods} = 79.6\ \text{psia}$$

Summing the two partial pressures yields the total cask pressure at normal operating condition temperature:

$$P_{Total} = P_{cask} + P_{fuel\,rods}$$

$$P_{Total} = 24.4\ \text{psia} + 79.6\ \text{psia}$$

$$P_{Total} = 104.0\ \text{psia}$$

The fuel cladding has the highest temperature of any barrier with which the gas comes in contact during a design basis fire. As shown in Section 3.5.3.1, the maximum average cavity gas temperature is 605°F during the fire accident condition. For conservatism, a temperature of

667°F is used in the calculation of the maximum accident condition internal pressure. Given that the internal volume of the NAC-LWT Cask remains constant during the fire, the resultant pressure is proportional to the temperature change according to the ideal gas law:

$$P_2 = P_1\left(\frac{T_2}{T_1}\right)$$

Thus, for the design basis fire:

$$P_{fire} = 104.0 \text{ psia}\left(\frac{1127^\circ R}{932^\circ R}\right)$$

$$P_{fire} = 125.8 \text{ psia}$$

3.5.4.2 High Burnup Fuel Rod Canister Maximum Internal Pressure

The high burnup fuel rod canister maximum internal pressure in the accident conditions is calculated assuming 100 percent fuel rod failure combined with the design basis fire maximum temperature. The fuel rod failure assumes release of 30 percent of the fission gas and 100 percent of the backfill gas.

The canister internal pressure is calculated using the method described in Section 3.4.4.2, with the BWR used as the bounding fuel type for the analysis. The total canister pressure is calculated in two steps. First, the pressures documented under normal conditions in Section 3.4.4.2 are adjusted to include the increased total free volume associated with 100 percent fuel rod failure. Then, the canister pressure is adjusted to account for the accident condition temperature.

The partial pressure of the canister volume is calculated by:

$$P_{canister} = P_{initial}\left(\frac{V_{canister}}{V_{total}}\right)$$

where:

P_{inital} = 29.3 psia (from earlier)

$V_{canister}$ = 28.2 liters (from earlier)

V_{void} = 0.079 liters (from earlier)

V_{void} = $25*V_{void} + V_{canister} = 30.2$ liters

V_{total} = 30.2 liters

Therefore, $P_{canister}$ is equal to 27.4 psia. The partial pressure of the fuel rods is calculated by:

$$P_{\text{fuel rods}} = P_{\text{initial}}\left(\frac{V_{\text{fuel rods}}}{V_{\text{total}}}\right)$$

where:

$P_{initial}$ = 1,425 psia (earlier from Section 3.4.4.2)

$V_{\text{fuel rods}}$= $25*V_{void}$

$V_{\text{fuel rods}}$ = ~1.97 liters (at 100% of the total fuel rod volume)

V_{total} = 30.2 liters ($V_{canister}$ + ($25*V_{void}$))

then:

$$P_{\text{fuel rods}} = 1{,}425 \text{ psia}\left(\frac{1.97 \text{ liters}}{30.2 \text{ liters}}\right) = \sim 94 \text{ psia}$$

and

$$P_{\text{total}} = P_{\text{canister}} + P_{\text{fuel rods}} = 27.4 \text{ psia} + \sim 94 \text{ psia} = \sim 121 \text{ psia } (\sim 8.2 \text{ atm})$$

For the 100% fuel rod failure and the design basis fire accident temperature of 725°F, the pressure is calculated by multiplying the 100% rod failure pressure by the inverse ratio of the normal condition temperature (588.7 K) to the accident temperature (658.15 K). The pressure thus calculated is 135 psia (~9.2 atm)

3.5.4.3 25-Rod Maximum Internal Pressure-Cask Cavity

Using the same methodology used to calculate the cavity pressure in Section 3.5.4.2, the pressure from the 100% fuel rod failure and the design basis fire accident temperature of 725°F is calculated using the cask cavity free gas volume (89.32 liters from earlier). The resulting pressure in the cask cavity, assuming that the gases within the canister are released to the cask cavity, is 67 psia (~4.5 atm).

3.5.4.4 TPBAR Shipment Cask Cavity Internal Pressure-Accident Conditions

Employing the normal condition TPBAR result in Section 3.4.4.5 of 276 psig for the 300 production TPBAR content condition and adjusting system pressure to the average accident gas temperature of 358°F yields a maximum accident condition pressure of 322 psig. For a period of one year following the 90-day cooldown, the pressure for this content condition increases to 337 psig. As discussed in Section 3.4.4.5, these values bound those of the up to 25 TPBAR transport

configuration within the 5×5 rod holder. The rod holder combination contains significantly lower releasable gas quantities at similar free volume.

Utilizing the same assumptions as presented in Section 3.4.4.5 and the post-accident thermal conditions discussed above, the pressure for the 55 segmented TPBARs in the waste container will be less than 75 psia and, therefore, bounded by the 300 TPBAR content condition.

3.5.4.5 Maximum Internal Pressure for PULSTAR Fuel Payload

Maximum internal pressures under accident conditions are calculated using the same methodology as that employed in Section 3.4.4.6. The accident condition temperature is set to 394°F, and 100 percent of the fuel rods are assumed to fail. The resulting calculated pressures are summarized as follows.

Description	Free Volume (liters)	Pressure (atm)	Pressure (psia)	Pressure (psig)
Cask Pressure -28 Intact Assemblies	217.0	2.3	34.0	19.3
Cask Pressure -14 Intact Assemblies and 14 Cans	233.0	2.4	35.4	20.7
Can Pressure - PULSTAR Failed Fuel Can	1.53	5.0	73.9	59.2

3.5.4.6 Maximum Internal Pressure for 16 PWR MOX/UO_2 Fuel Rods in a Rod Holder

Using the same methodology used to calculate the cavity pressure in Section 3.4.4.4, the pressure from the 100% fuel rod failure with 100% gas release and the design basis fire accident temperature of 725°F is calculated. The resulting pressure in the cask cavity is 65.3 psig (80.0 psia, 5.4 atm).

3.5.5 Maximum Thermal Stresses

The most severe thermal stress conditions that occur during the fire test and subsequent cooldown have been evaluated. For conservatism, an internal pressure of 168 psig is used, in the analysis that is performed in Section 2.7.3. The temperatures corresponding to the maximum thermal stresses are reported in Table 3.5-1.

3.5.6 Evaluation of Package Performance for Hypothetical Accident Thermal Conditions

The NAC-LWT cask thermal performance has been assessed for the hypothetical accident, as specified in 10 CFR 71. The O-rings and the lead gamma shields remain within their safe

operating ranges. The cask does not suffer any adverse structural consequences as a result of the thermal considerations of the hypothetical accident. The NAC-LWT cask maintains containment and does not exceed the dose rate limits of 49 CFR 173 as a result of the hypothetical accident.

3.5.7 Assessment of the Effects of the Fission Gas Release in the Fire Accident Condition

During the fire, the release of the fission gas is expected to reduce the effective thermal conductivity of the gas in the cavity or inside the sealed canisters. To assess the reduction of the thermal conductivity, the helium conductivity is factored by the ratio of the conservative initial fill pressure of 565 psia (Section 3.4.4) for the PWR fuel assemblies and the end of life pressure (which contains the fill gas plus the fission gas release) of 1,521 psia (Section 3.5.4). This ratio is computed to be 0.37. A conservative ratio of 0.24 is applied to the conductivity of helium, assuming that all fission product gases have a conductivity of zero.

For the temperatures shown, which envelope the maximum temperatures of the cavity gas in the accident condition, the reduced helium properties are larger than the thermal conductivity of air. This is bounding because, as shown in Table 4.2-2, the volume of fission product gas produced by the design basis PWR assembly is higher than that for any other fuel loading.

The data below (Krieth) reflects the comparison of the air conductivity and the factored helium conductivity.

Temperature (°F)	Air Conductivity (K_{air}) (Btu/hr-in-F)	Helium Conductivity (Btu/hr-in-F)	Factored Helium Conductivity (K_{He}) (Btu/hr-in-F)	Ratio K_{He}/K_{air}
300	0.00161	0.00883	0.00212	1.32
400	0.00177	0.00958	0.00230	1.30
500	0.00193	0.01017	0.00244	1.26
600	0.00208	0.01075	0.00258	1.24
700	0.00223	0.01113	0.00267	1.20
800	0.00238	0.01150	0.00276	1.16

The analyses performed for the contents employed air as the gas in the cavity and containers for the accident condition. This demonstrates that the evaluation of the accident condition using air bounds the "reduced helium properties" case.

Figure 3.5-1 Transient Thermal Analysis Finite Element Model of the NAC-LWT

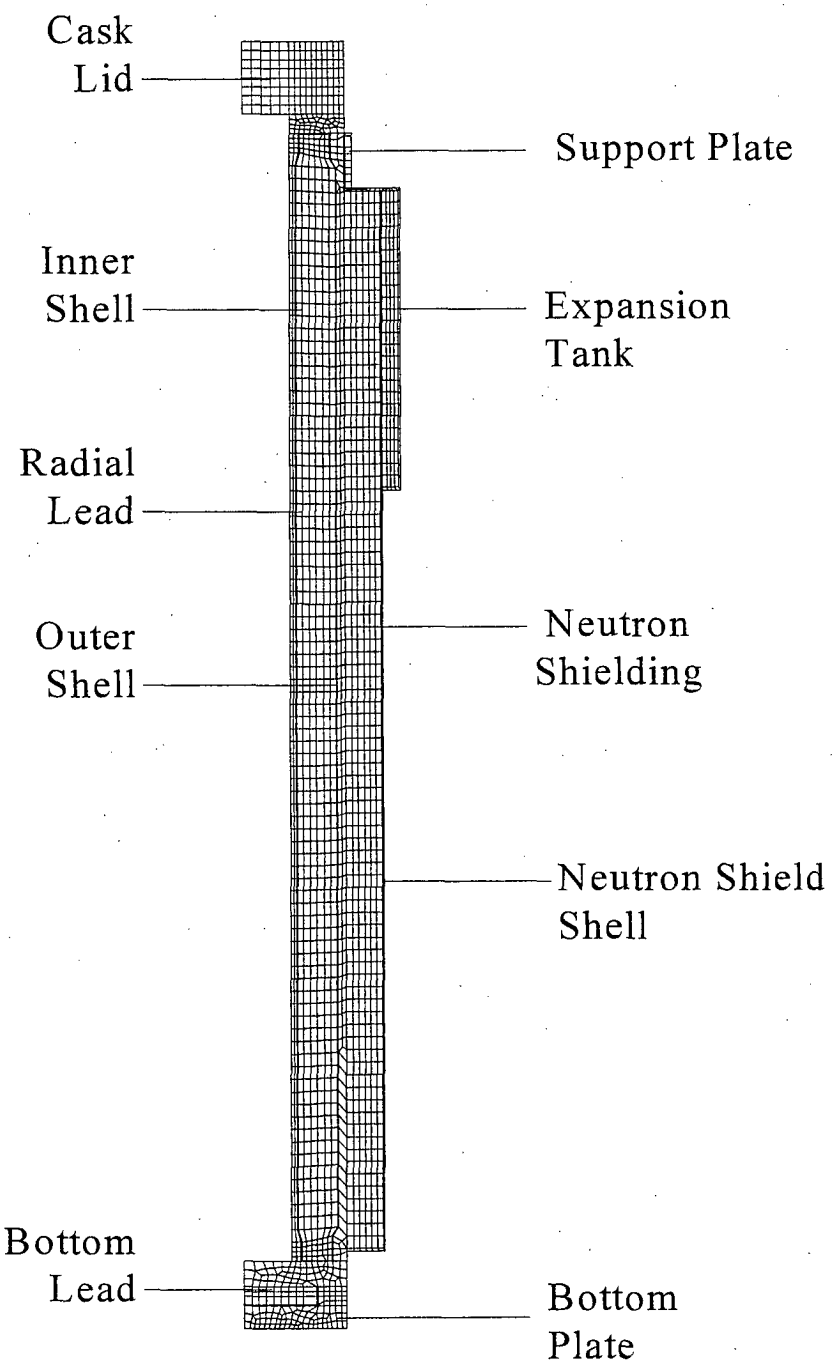
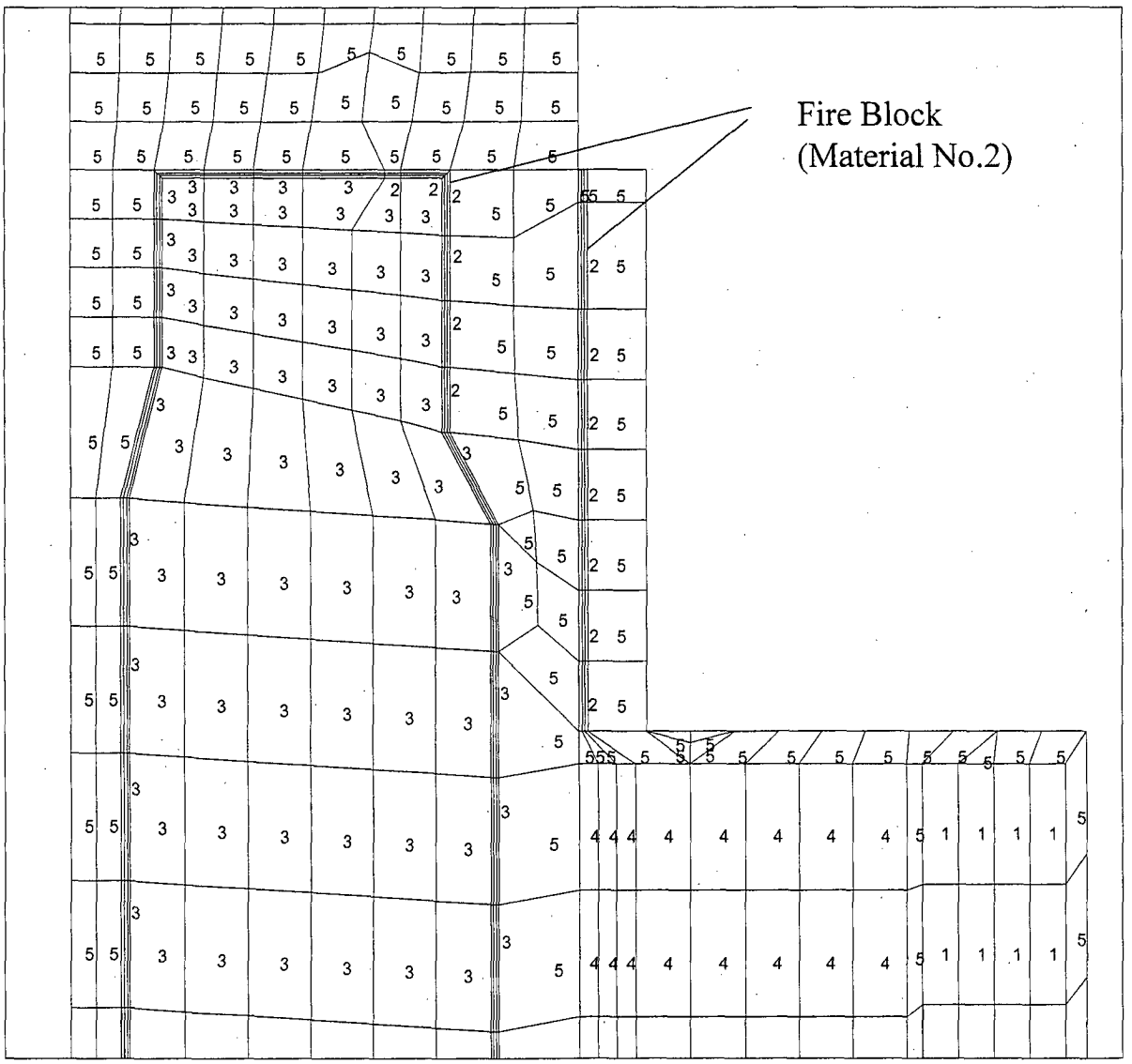
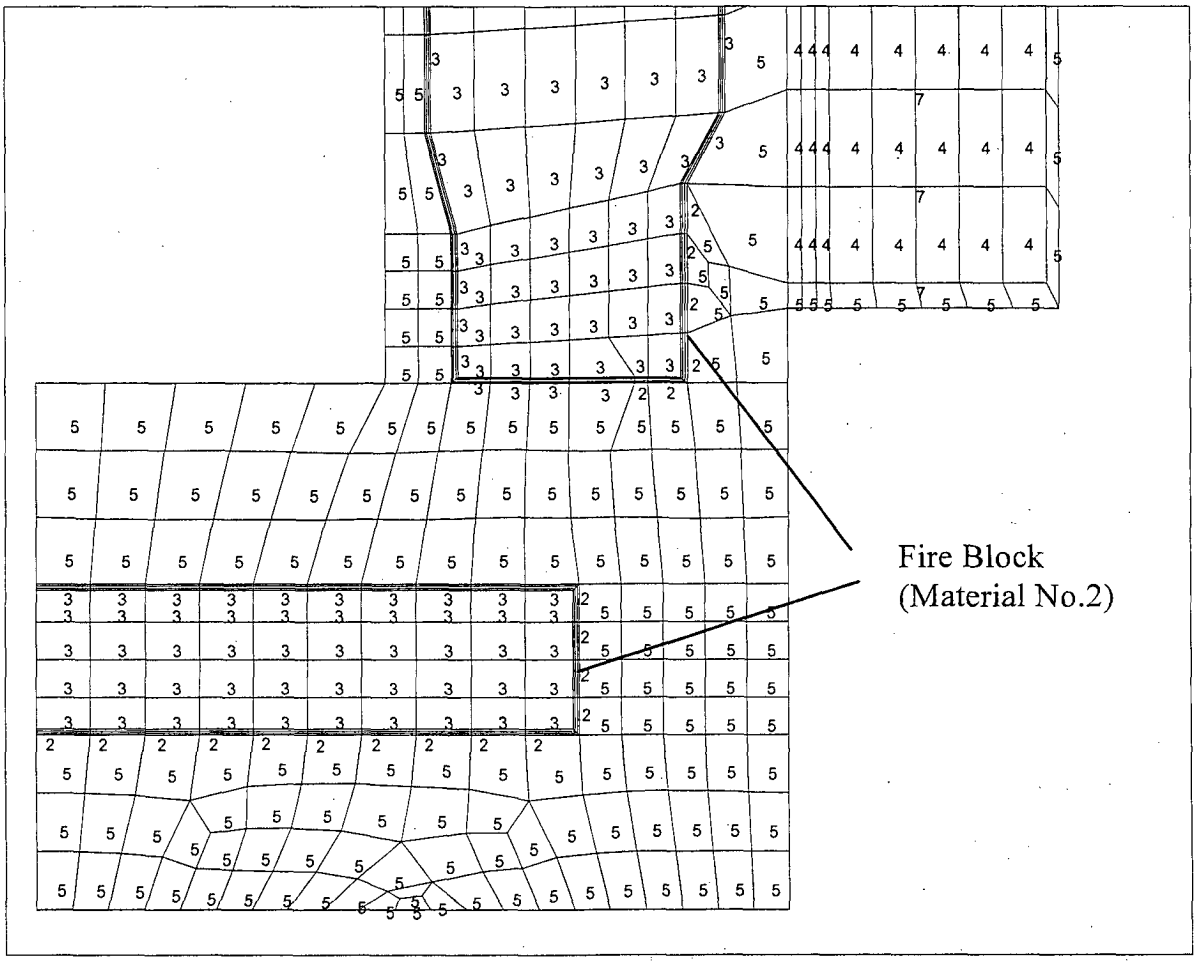


Figure 3.5-2 Top Region of the ANSYS Model



Note: Fire Block is either BISCO FPC or UNIFRAX Fiberfrax Ceramic Fiber Paper

Figure 3.5-3 Bottom Region of the ANSYS Model



Note: Fire Block is either BISCO FPC or UNIFRAX Fiberfrax Ceramic Fiber Paper

Figure 3.5-4 Temperature History of NAC-LWT O-Rings and Valves in the Hypothetical Fire Event

1. Temperature of the Valves
2. Temperature of the O-Rings

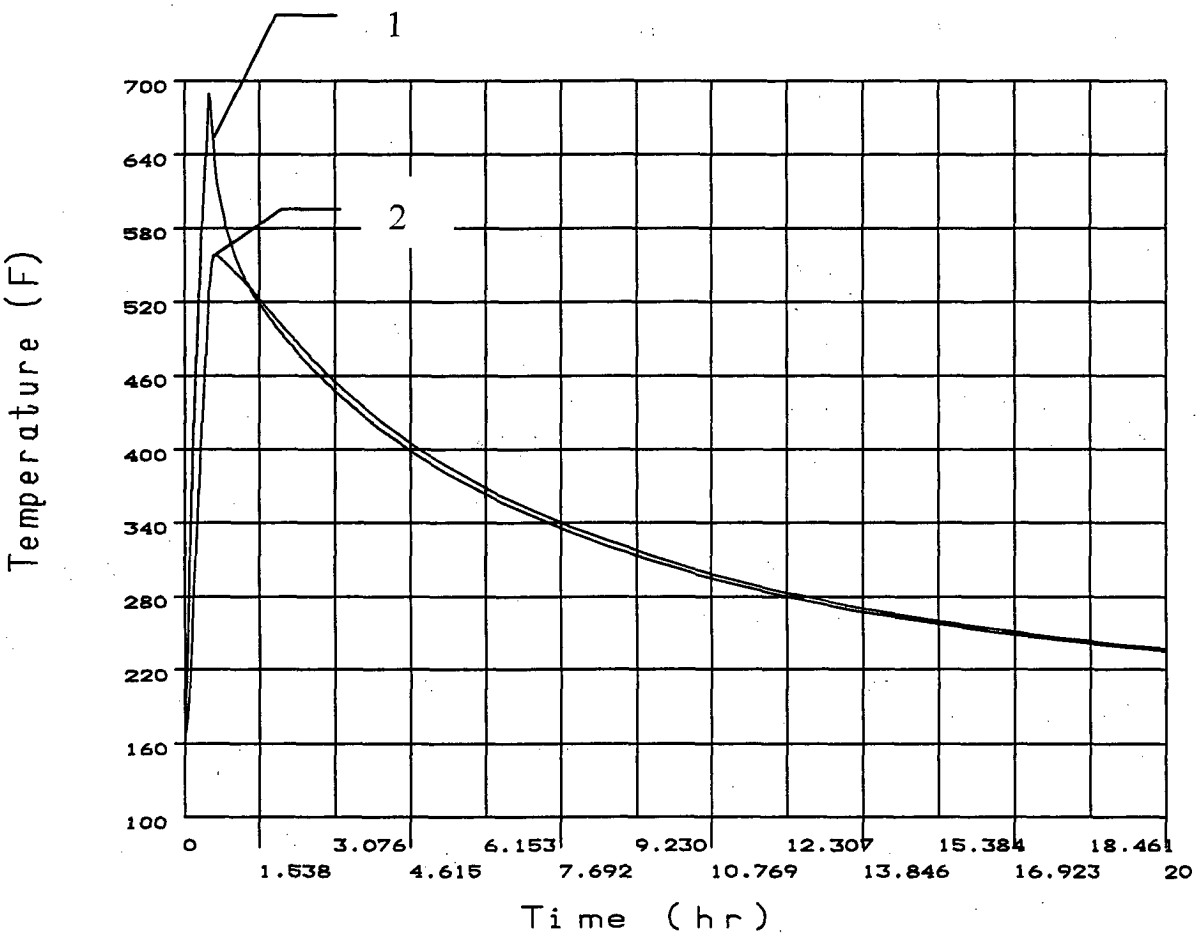


Figure 3.5-5 Temperature History of NAC-LWT Components in the Hypothetical Fire Event

1. Temperature of the Cask Outer Surface
2. Temperature of the Neutron Shield
3. Temperature of the Radial Lead Gamma Shield
4. Temperature of the Bottom Lead Gamma Shield
5. Temperature of the Inner Stainless Steel Shell

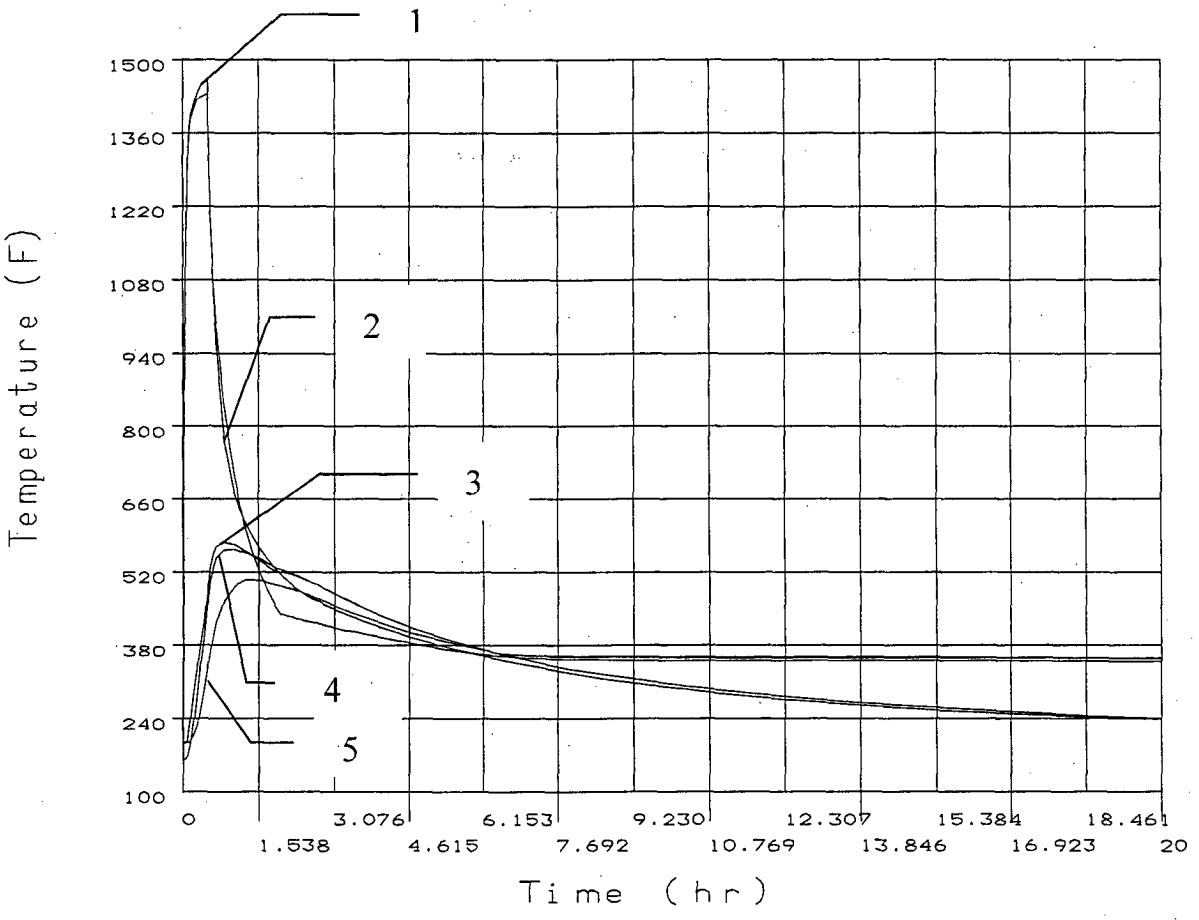


Figure 3.5-6 MTR Fuel Design Basis Heat Load Fire Accident ANSYS Thermal Model (Uniform 30-Watt/Element Configuration Heat Load)

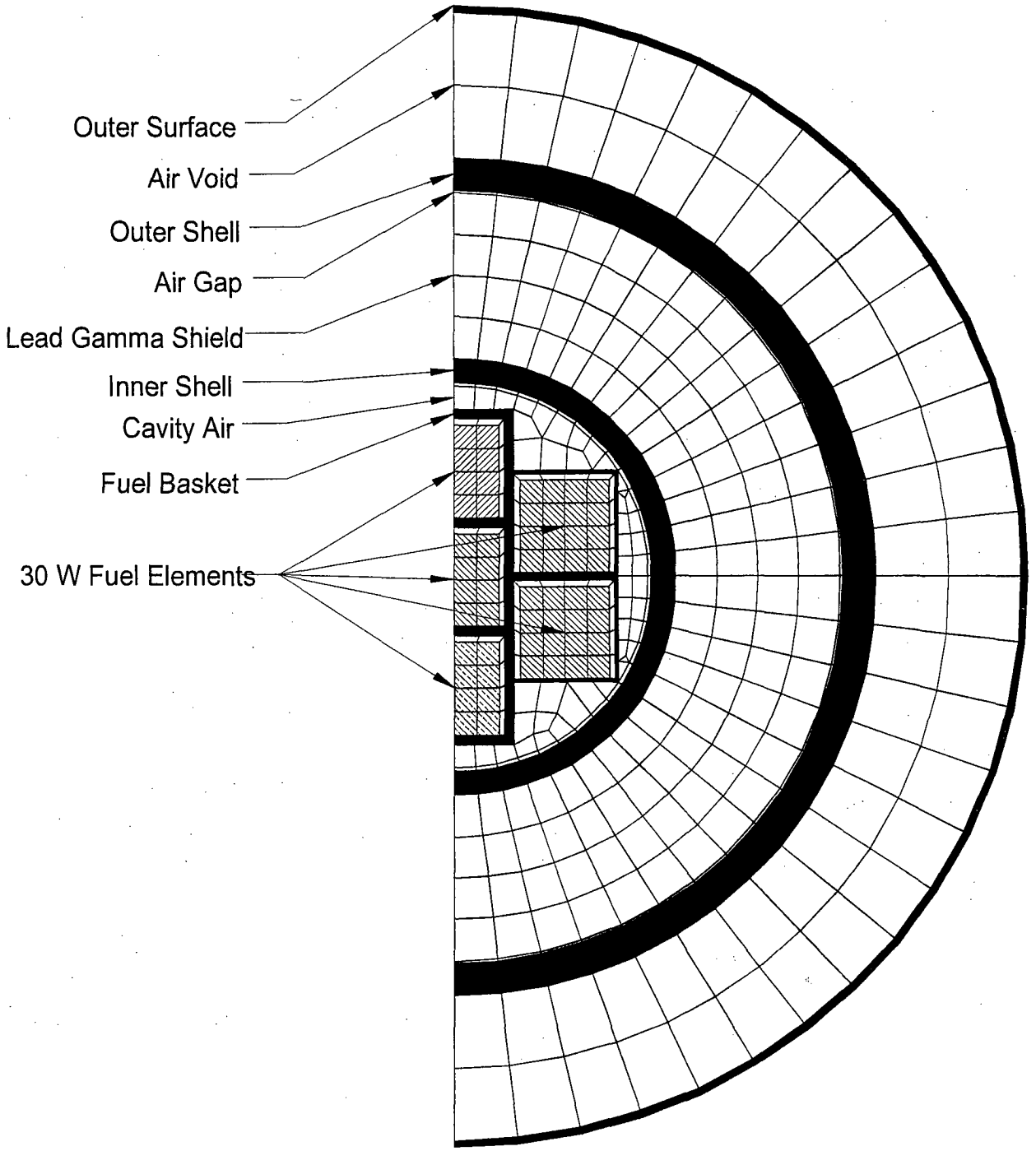


Figure 3.5-7 MTR Fuel Variable Heat Load Fire Accident ANSYS Thermal Model (120-Watt/70-Watt/20-Watt Configuration Heat Load)

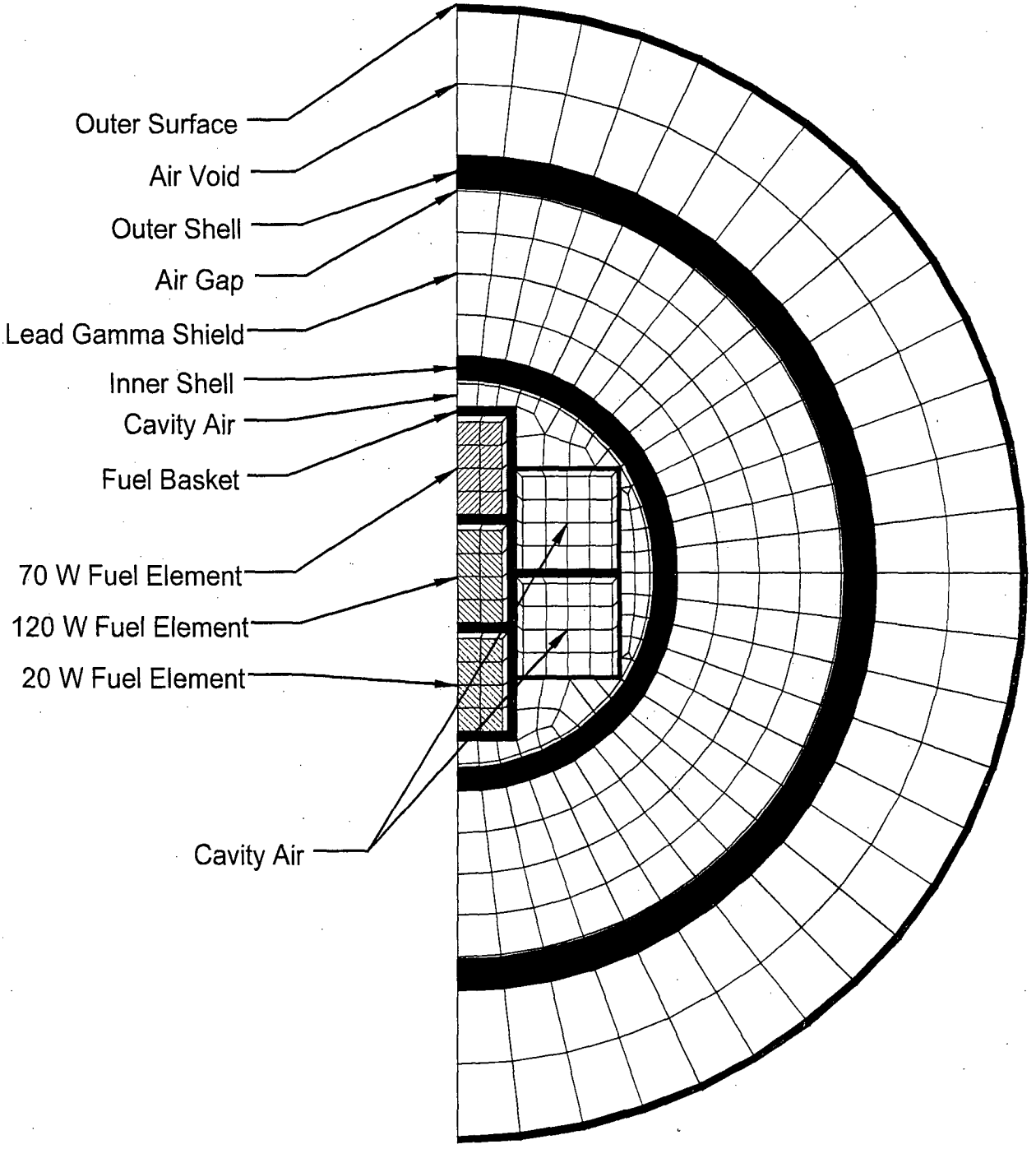
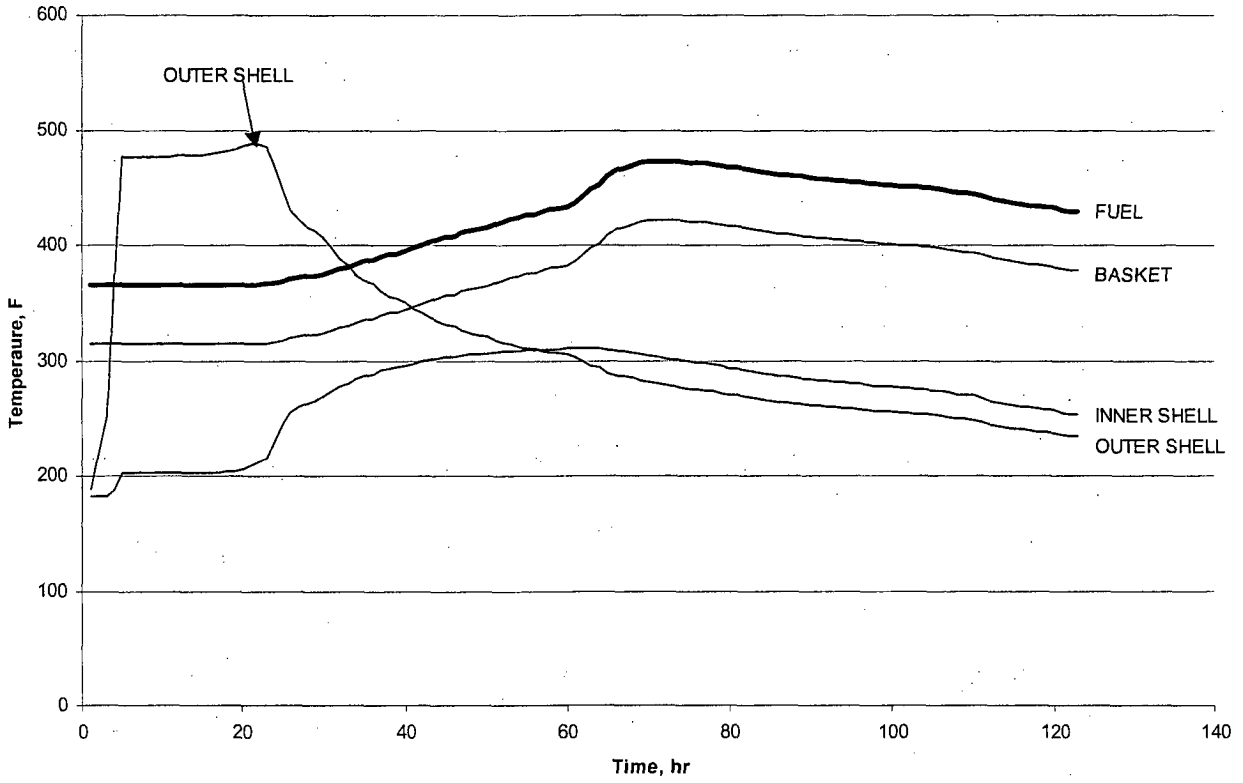


Figure 3.5-8 Temperature History in the MTR Fuel Variable Heat Load Fire Accident Analysis



Note: 120-Watt / 70-Watt / 20-Watt Configuration Heat Load. Cavity gas is air with fire applied to cask surface.

Figure 3.5-9 Location of the Maximum Temperature in the MTR Fuel Variable Heat Load

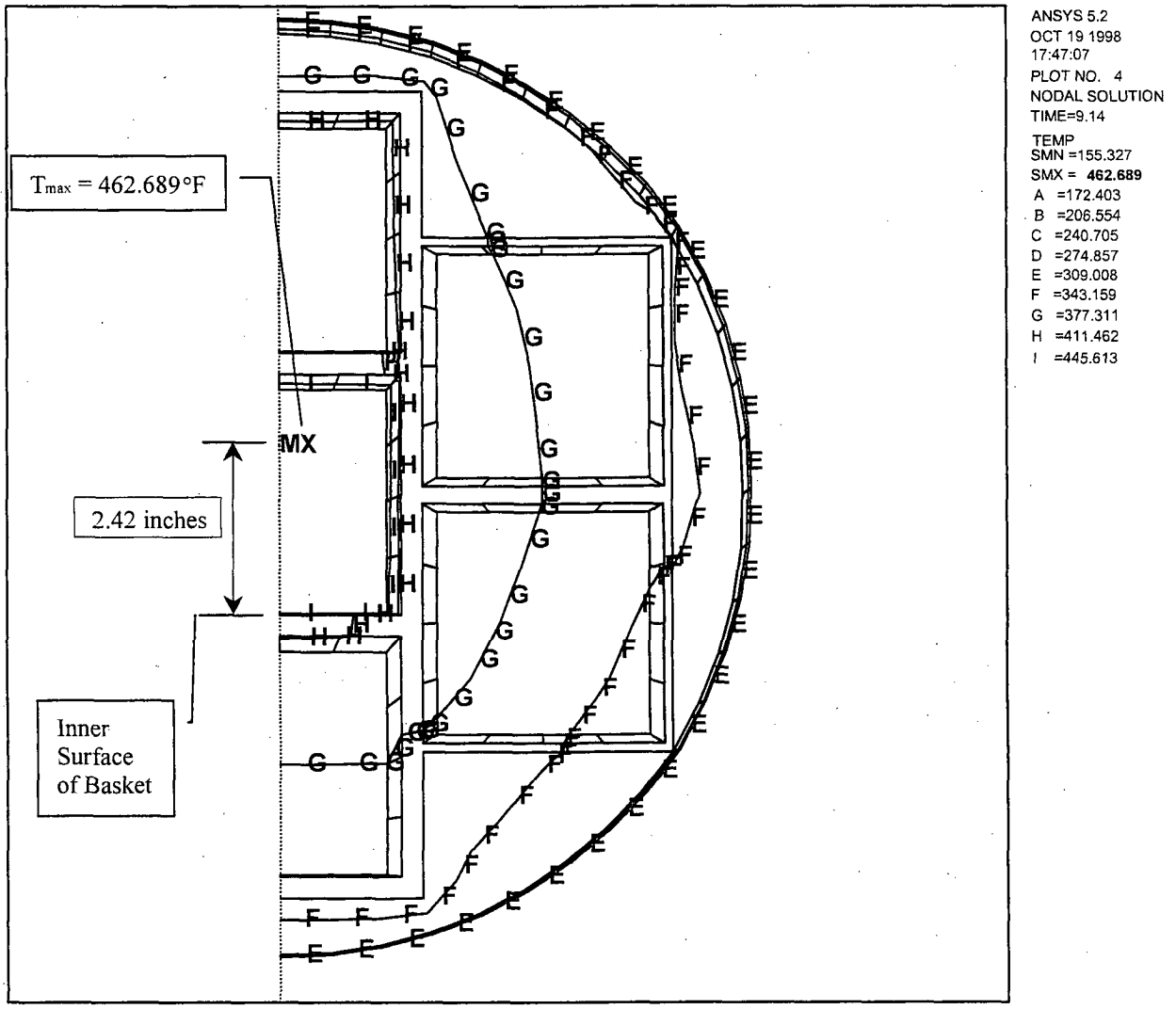


Figure 3.5-10 Temperature History for the TRIGA Fuel Cluster Rods Design Basis Heat Load Fire Accident Analysis

(Uniform 30 watt/basket cell or 210 watt/basket section or 1.05 kW total heat load)
(Cavity gas: Air, Fire is Applied to the Cask Surface)

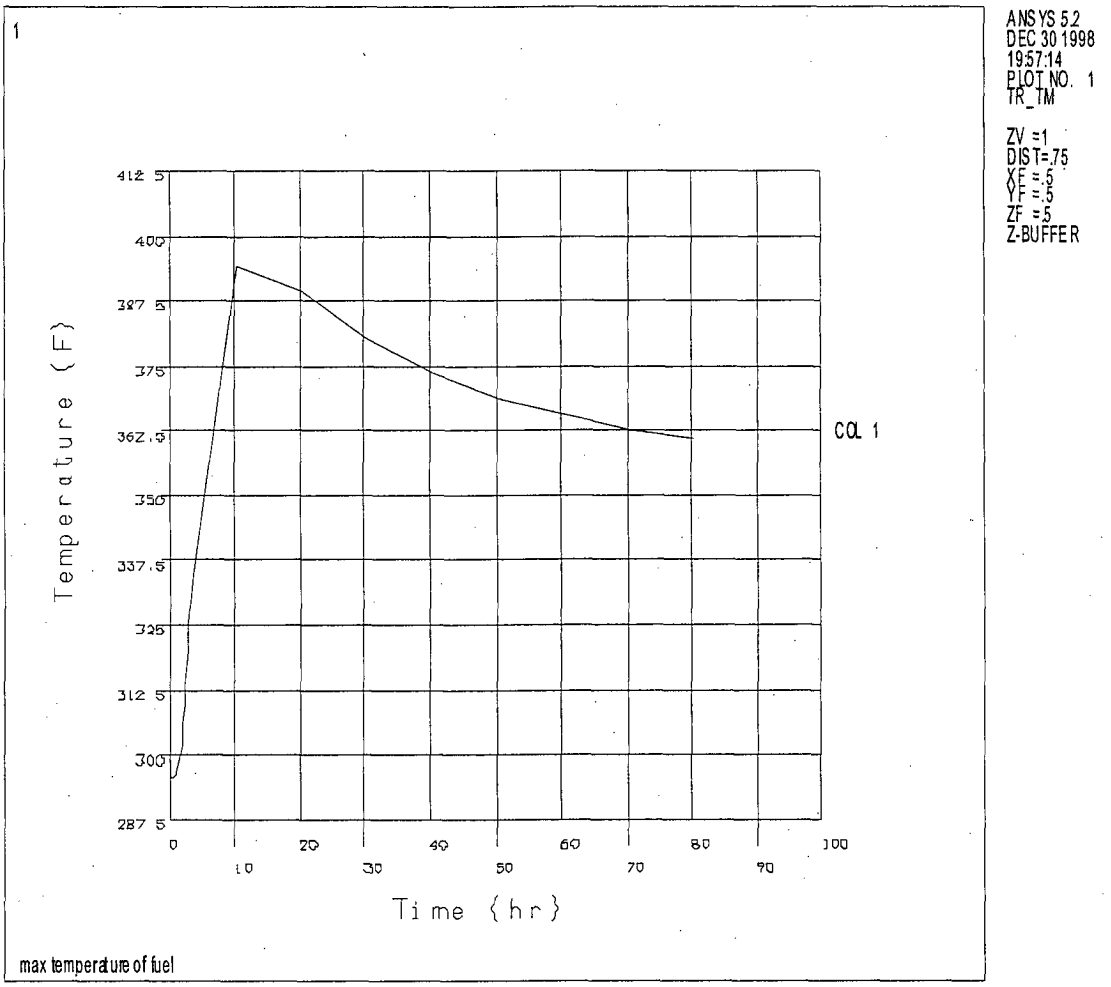


Figure 3.5-11 Temperature History of NAC-LWT Cask Components with PWR and BWR High Burnup Fuel Rods in the Hypothetical Fire Event

1. Average Temperature of Cask Cavity Gas
2. Temperature of the Fuel Cladding
3. Temperature of the Can Weldment
4. Temperature of the Aluminum Structural Component
5. Temperature of the Pin Tube

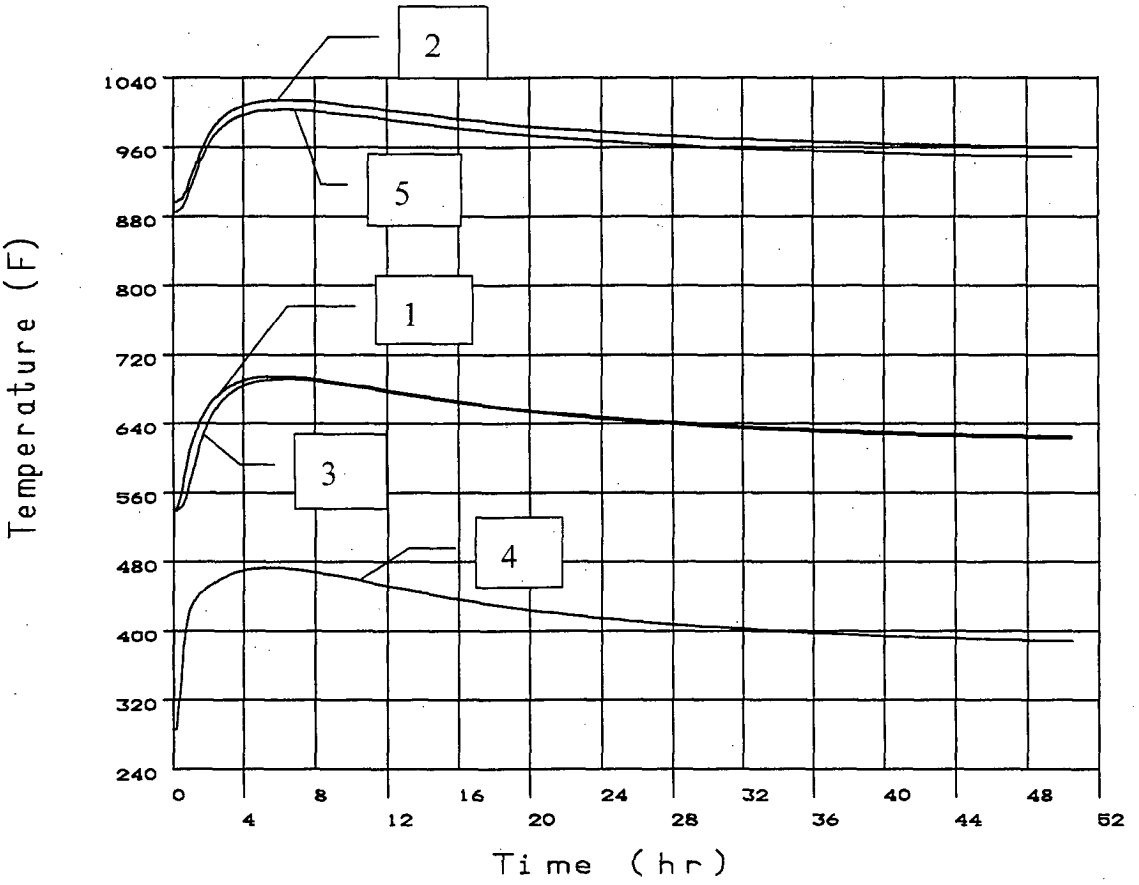


Figure 3.5-12 End of Fire Temperatures of the Alternate Port Cover Components

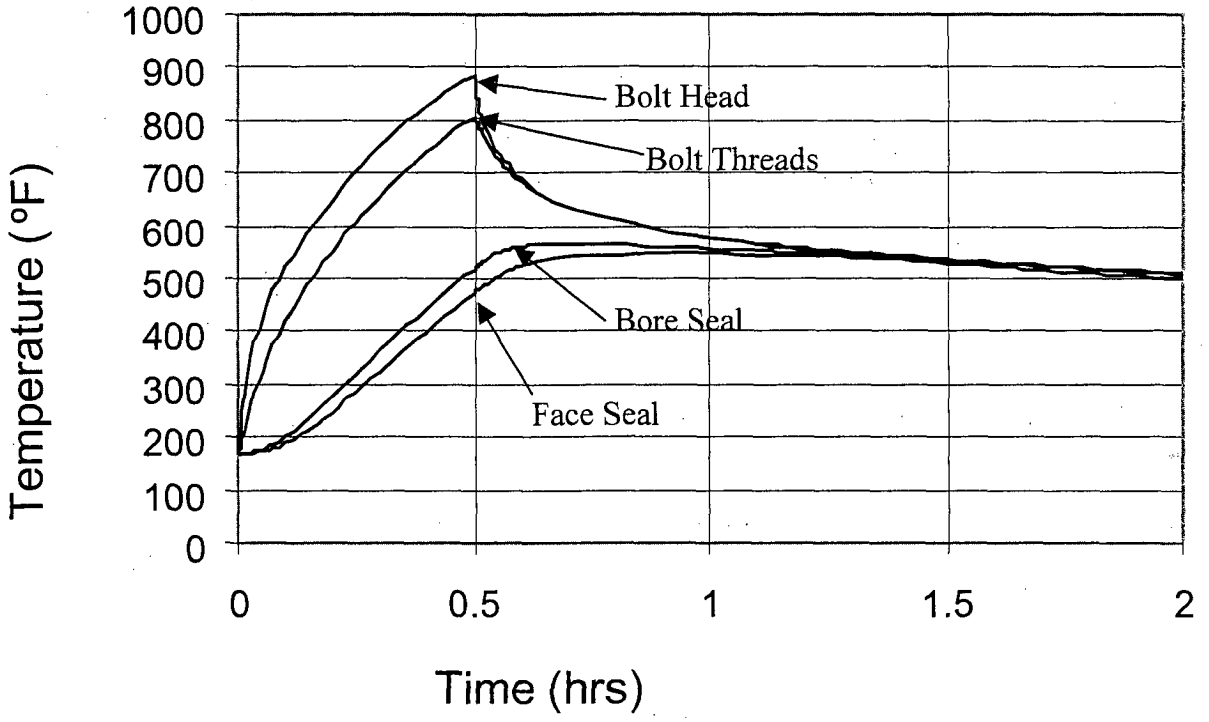


Figure 3.5-13 Transient Temperatures of the Alternate Port Cover Components

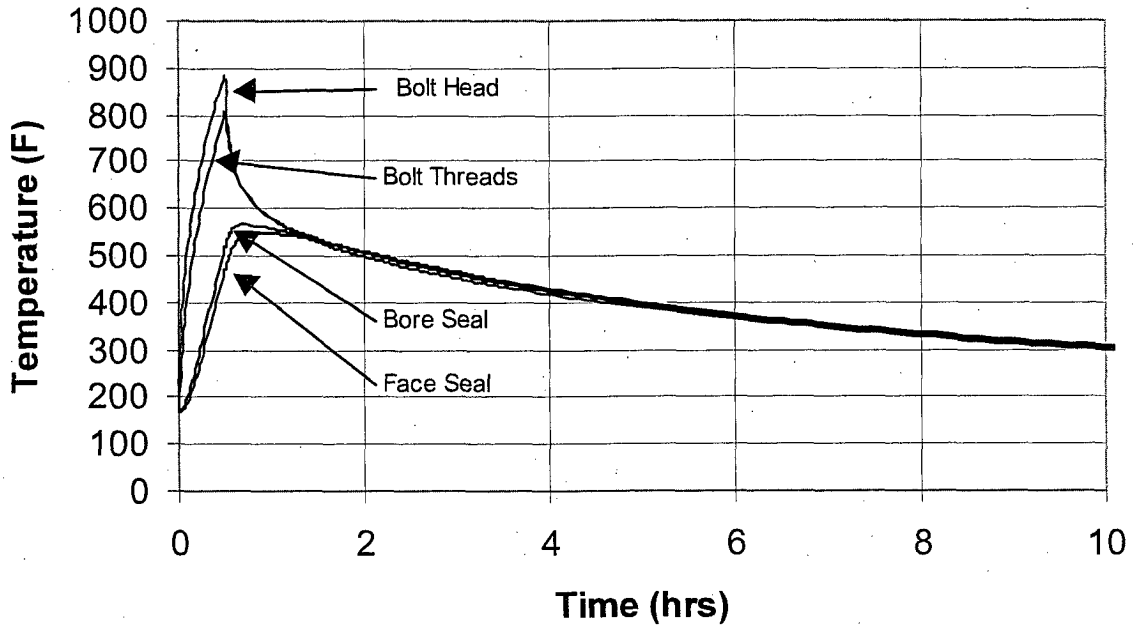


Table 3.5-1 Maximum Component Temperatures (°F) During the Fire Accident (Design Basis PWR Fuel, 2.5 kW Heat Load)

Component	Component Temperature (°F)	Temperature Limit (°F)
O-rings: TFE	558	735
Metallic	571(3)	800
Cask radial outer surface	1460	----(1)
Neutron shield region	1435	----(1)
Radial lead gamma shield	578	600
Bottom lead gamma shield	564	600
Inner stainless steel shell	505	800
Fuel basket outer wall	507	700(2)
Fuel rod cladding	703	1058
Alternate Port Cover	--	--
Bolt head	886	900
Bolt threads	807	900
Alternate Port Cover O-ring – bore	565(4)	550
Alternate Port Cover O-ring – face	547	550
Alternate B Port Cover metallic face seal	547	800

Notes:

(1) No upper limit established. The loss of the liquid neutron shield is assumed under HAC.

(2) The primary consideration in establishing the safe operating range of the aluminum is maintaining the integrity of the aluminum. According to MIL-HDBK-5F, it can be shown that aluminum at 700°F retains component performance.

(3) The maximum port cover seal temperature is conservatively used to bound the maximum temperature of the metallic seal.

(4) Should the bore seal fail post-fire accident, containment would not be breached.

Table 3.5-2 MTR Fuel Fire Accident Maximum Temperatures (°F), 10 Fuel Plate/120W Element Case (Bounding Configuration)

Condition 2: NAC-LWT (Transported via Truck Trailer)
Cavity Gas: Air

Component	Design Basis Heat Loading*	Variable Decay Heat Loading**
Cask Radial Outer Surface	***	***
Lead Shield	***	***
Inner Shell	334	337
Fuel Basket	374	420
Fuel Cladding	385	473

* Uniform 30-Watt/Element Configuration Heat Load.

** 120-Watt/70-Watt/20-Watt Configuration Heat Load.

*** The maximum temperatures for these components are bounded by the design basis reported.

Table 3.5-3 TRIGA Fuel Fire Accident Maximum Temperatures (°F)

Component	Temperature
Fuel Basket	374
Fuel Cladding	433

Table 3.5-4 PWR and BWR High Burnup Fuel Rods Fire Accident Maximum Temperatures (°F)

NAC-LWT (Transported via Truck Trailer)
Cavity Gas: Air

Component	Component Temperature (°F)	Temperature Limit (°F)
Stainless steel Can Weldment	692	800
Fuel Rod Cladding	1,014	1,058[1]

[1] The maximum allowable temperature under HAC for PWR, BWR and PWR MOX fuel rod cladding is 1,058°F per ISG-11, Revision 3.

Table 3.5-5 Maximum Component Temperatures for High Burnup Fuel Rods in a Rod Holder with Damaged Fuel Rods for the Fire Accident

Component	Normal Conditions Temperature[1] (T_{norm})(°F)	Temperature Difference (ΔT) (°F)	Accident Temperature $T_{acc} = T_{norm} + \Delta T$(°F)
Rod Holder Weldment	567	692[2] – 538[3] = 154	721
Fuel Cladding	809	1014[2] – 896[3] = 118	927

[1] Table Table 3.4-14
[2] Table Table 3.5-4
[3] Table Table 3.4-10, Condition 2

Table 3.5-6 TPBAR Fire Accident Maximum Temperatures

Component	Temperature (°F)
TPBARs	402
Aluminum Basket	340
Consolidation Canister	357

March 2009

Revision LWT-09A

NAC-LWT

Legal Weight Truck Cask System

SAFETY ANALYSIS REPORT

Volume 2 of 2

Docket No. 71-9225

NAC INTERNATIONAL

Atlanta Corporate Headquarters: 3930 East Jones Bridge Road, Norcross, Georgia 30092 USA
Phone 770-447-1144, Fax 770-447-1797, www.nacintl.com

List of Effective Pages

LIST OF EFFECTIVE PAGES

Chapter 1

1-i thru 1-iv ..... Revision LWT-09A
1-1 thru 1-5 ..... Revision LWT-09A
1.1-1 thru 1.1-3 ..... Revision LWT-09A
1.2-1 thru 1.2-50 ..... Revision LWT-09A
1.3-1 ..... Revision 39
1.4-1 ..... Revision 39
1.5-1 ..... Revision 39

73 drawings in the
Chapter 1 List of Drawings

Chapter 1 Appendices 1-A
through 1-G

Chapter 2

2-i thru 2-xxiv ..... Revision LWT-09A
2-1 ..... Revision 39
2.1.1-1 thru 2.1.1-2 ..... Revision 39
2.1.2-1 thru 2.1.2-3 ..... Revision 39
2.1.3-1 thru 2.1.3-8 ..... Revision 39
2.2.1-1 thru 2.2.1-4 ..... Revision LWT-09A
2.3-1 ..... Revision 39
2.3.1-1 thru 2.3.1-13 ..... Revision 39
2.4-1 ..... Revision 39
2.4.1-1 ..... Revision 39
2.4.2-1 ..... Revision 39
2.4.3-1 ..... Revision 39
2.4.4-1 ..... Revision 39
2.4.5-1 ..... Revision 39
2.4.6-1 ..... Revision 39
2.5.1-1 thru 2.5.1-11 ..... Revision 39
2.5.2-1 thru 2.5.2-17 ..... Revision 39
2.6.1-1 thru 2.6.1-7 ..... Revision 39
2.6.2-1 thru 2.6.2-7 ..... Revision 39
2.6.3-1 ..... Revision 39
2.6.4-1 ..... Revision 39
2.6.5-1 thru 2.6.5-2 ..... Revision 39
2.6.6-1 ..... Revision 39
2.6.7-1 thru 2.6.7-136 . Revision LWT-09A
2.6.8-1 ..... Revision 39
2.6.9-1 ..... Revision 39
2.6.10-1 thru 2.6.10-15 ..... Revision 39
2.6.11-1 thru 2.6.11-12 ..... Revision 39
2.6.12-1 thru 2.6.12-91 ..... Revision 39
2.7-1 ..... Revision 39
2.7.1-1 thru 2.7.1-117 ..... Revision 39
2.7.2-1 thru 2.7.2-23 ..... Revision 39
2.7.3-1 thru 2.7.3-5 ..... Revision 39
2.7.4-1 ..... Revision 39
2.7.5-1 thru 2.7.5-5 ..... Revision 39
2.7.6-1 thru 2.7.6-4 ..... Revision 39
2.7.7-1 thru 2.7.7-50 ..... Revision 39
2.7.7-51 thru 2.7.7-72 . Revision LWT-09A
2.8-1 ..... Revision 39
2.9-1 thru 2.9-14 ..... Revision LWT-09A
2.10.1-1 thru 2.10.1-3 ..... Revision 39
2.10.2-1 thru 2.10.2-49 ..... Revision 39
2.10.3-1 thru 2.10.3-18 ..... Revision 39
2.10.4-1 thru 2.10.4-11 ..... Revision 39
2.10.5-1 ..... Revision 39
2.10.6-1 thru 2.10.6-19 ..... Revision 39
2.10.7-1 thru 2.10.7-66 ..... Revision 39
2.10.8-1 thru 2.10.8-67 ..... Revision 39
2.10.9-1 thru 2.10.9-9 ..... Revision 39
2.10.10-1 thru 2.10.10-97 ..... Revision 39
2.10.11-1 thru 2.10.11-10 ..... Revision 39
2.10.12-1 thru 2.10.12-31 ..... Revision 39

LIST OF EFFECTIVE PAGES (Continued)

2.10.13-1 thru 2.10.13-17 ..... Revision 39
2.10.14-1 thru 2.10.14-38 .. Revision LWT-09A
2.10.15-1 thru 2.10.15-10 ..... Revision 39
2.10.16-1 thru 2.10.16-5 .... Revision LWT-09A

Chapter 3
3-i thru 3-v ..... Revision LWT-09A
3.1-1 thru 3.1-2 ..... Revision 39
3.2-1 thru 3.2-11 ..... Revision 39
3.3-1 ..... Revision 39
3.4-1 thru 3.4-88 ..... Revision LWT-09A
3.5-1 thru 3.5-35 ..... Revision LWT-09A
3.6-1 thru 3.6-12 ..... Revision 39

Chapter 4
4-i thru 4-iii ..... Revision LWT-09A
4.1-1 thru 4.1-3 ..... Revision LWT-09A
4.2-1 thru 4.2-4 ..... Revision LWT-09A
4.3-1 thru 4.3-4 ..... Revision LWT-09A
4.4-1 ..... Revision 39
4.5-1 thru 4.5-28 ..... Revision 39
4.5-29 thru 4.5-40 ..... Revision LWT-09A

Chapter 5
5-i thru 5-xii ..... Revision LWT-09A
5-1 thru 5-3 ..... Revision 39
5.1.1-1 thru 5.1.1-17 ..... Revision LWT-09A
5.2.1-1 thru 5.2.1-7 ..... Revision 39
5.3.1-1 thru 5.3.1-2 ..... Revision 39
5.3.2-1 ..... Revision 39
5.3.3-1 thru 5.3.3-8 ..... Revision 39
5.3.4-1 thru 5.3.4-19 ..... Revision 39
5.3.5-1 thru 5.3.5-4 ..... Revision 39
5.3.6-1 thru 5.3.6-18 ..... Revision 39
5.3.7-1 thru 5.3.7-19 ..... Revision 39
5.3.8-1 thru 5.3.8-25 ..... Revision 39
5.3.9-1 thru 5.3.9-26 ..... Revision 39
5.3.10-1 thru 5.3.10-14 ..... Revision 39
5.3.11-1 thru 5.3.11-48 ..... Revision 39
5.3.12-1 thru 5.3.12-26 ..... Revision 39
5.3.13-1 thru 5.3.13-18 .. Revision LWT-09A
5.3.14-1 thru 5.3.14-21 ..... Revision 39
5.3.15-1 thru 5.3.15-9 ..... Revision 39
5.3.16-1 thru 5.3.16-5 ..... Revision 39
5.3.17-1 thru 5.3.17-9 ..... Revision 39
5.3.18-1 thru 5.3.18-40 ..... Revision 39
5.4.1-1 thru 5.4.1-6 ..... Revision 39

Chapter 6
6-i thru 6-xiii ..... Revision LWT-09A
6-1 ..... Revision 39
6.1-1 thru 6.1-5 ..... Revision 39
6.2-1 ..... Revision 39
6.2.1-1 thru 6.2.1-3 ..... Revision 39
6.2.2-1 thru 6.2.2-3 ..... Revision 39
6.2.3-1 thru 6.2.3-7 ..... Revision 39
6.2.4-1 ..... Revision 39
6.2.5-1 thru 6.2.5-5 ..... Revision 39
6.2.6-1 thru 6.2.6-3 ..... Revision 39
6.2.7-1 thru 6.2.7-2 ..... Revision 39
6.2.8-1 thru 6.2.8-3 ..... Revision 39
6.2.9-1 thru 6.2.9-4 ..... Revision 39
6.2.10-1 thru 6.2.10-3 ..... Revision 39
6.2.11-1 thru 6.2.11-3 ..... Revision 39
6.2.12-1 thru 6.2.12-4 ..... Revision 39
6.3.1-1 thru 6.3.1-6 ..... Revision 39
6.3.2-1 thru 6.3.2-4 ..... Revision 39
6.3.3-1 thru 6.3.3-9 ..... Revision 39
6.3.4-1 thru 6.3.4-9 ..... Revision 39
6.3.5-1 thru 6.3.5-12 ..... Revision 39

LIST OF EFFECTIVE PAGES (Continued)

6.3.6-1 thru 6.3.6-9 ..... Revision 39
6.3.7-1 thru 6.3.7-4 ..... Revision 39
6.3.8-1 thru 6.3.8-7 ..... Revision 39
6.3.9-1 thru 6.3.9-7 ..... Revision 39
6.4.1-1 thru 6.4.1-10 ..... Revision 39
6.4.2-1 thru 6.4.2-10 ..... Revision 39
6.4.3-1 thru 6.4.3-34 ..... Revision 39
6.4.4-1 thru 6.4.4-24 ..... Revision 39
6.4.5-1 thru 6.4.5-32 ..... Revision 39
6.4.6-1 thru 6.4.6-23 ..... Revision 39
6.4.7-1 thru 6.4.7-14 ..... Revision 39
6.4.8-1 thru 6.4.8-14 ..... Revision 39
6.4.9-1 thru 6.4.9-10 ..... Revision 39
6.4.10-1 thru 6.4.10-18 ..... Revision 39
6.5.1-1 thru 6.5.1-13 ..... Revision 39
6.5.2-1 thru 6.5.2-4 ..... Revision 39
6.5.3-1 thru 6.5.3-2 ..... Revision 39
6.7.1-1 thru 6.7.1-19 ..... Revision LWT-09A
6.7.2-1 thru 6.7.2-47 ..... Revision 39

Appendix 6.6

6.6-i thru 6.6-iii ..... Revision 39
6.6-1 ..... Revision 39
6.6.1-1 thru 6.6.1-111 ..... Revision 39
6.6.2-1 thru 6.6.2-56 ..... Revision 39
6.6.3-1 thru 6.6.3-73 ..... Revision 39
6.6.4.-1 thru 6.6.4-77 ..... Revision 39
6.6.5-1 thru 6.6.5-101 ..... Revision 39
6.6.6-1 thru 6.6.6-158 ..... Revision 39
6.6.7-1 thru 6.6.7-84 ..... Revision 39
6.6.8-1 thru 6.6.8-183 ..... Revision 39
6.6.9-1 thru 6.6.9-52 ..... Revision 39
6.6.10-1 thru 6.6.10-33 ..... Revision 39
6.6.11-1 thru 6.6.11-47 ..... Revision 39
6.6.12-1 thru 6.6.12-20 ..... Revision 39
6.6.13-1 thru 6.6.13-22 ..... Revision 39
6.6.14-1 thru 6.6.14-7 ..... Revision 39
6.6.15-1 thru 6.6.15-45 ..... Revision 39

Chapter 7

7-i thru 7-ii ..... Revision LWT-09A
7.1-1 thru 7.1-56 ..... Revision LWT-09A
7.2-1 thru 7.2-13 ..... Revision LWT-09A
7.3-1 thru 7.3-2 ..... Revision 39

Chapter 8

8-i ..... Revision 39
8.1-1 thru 8.1-11 ..... Revision LWT-09A
8.2-1 thru 8.2-4 ..... Revision LWT-09A
8.3-1 thru 8.3-4 ..... Revision 39

Chapter 9

9-i ..... Revision 39
9-1 thru 9-10 ..... Revision 39

Chapter 4

Table of Contents

4 CONTAINMENT 4.1-1
4.1 Containment Boundary 4.1-1
4.1.1 Containment Penetrations 4.1-1
4.1.2 Seals and Welds 4.1-1
4.1.3 Closure 4.1-3
4.2 Containment Requirements for Normal Conditions of Transport 4.2-1
4.2.1 Containment of Radioactive Material 4.2-1
4.2.2 Pressurization of Containment Vessel 4.2-2
4.2.3 Containment Criteria 4.2-2
4.3 Containment Requirements for Hypothetical Accident Conditions 4.3-1
4.3.1 Fission Gas Products 4.3-1
4.3.2 Containment of Radioactive Materials 4.3-1
4.3.3 Tritium Contamination Issues 4.3-4
4.4 Special Requirements 4.4-1
4.5 Appendices 4.5-1
4.5.1 Tetrafluoroethylene O-Rings 4.5-1
4.5.2 Metallic O-Rings 4.5-10
4.5.3 Viton® O-Rings 4.5-23
4.5.4 Metallic Face Seal 4.5-29

List of Figures

Figure 4.5-1 SAE International Aerospace Standard AS8791 ..... 4.5-2
Figure 4.5-2 Metallic O-rings Technical Bulletin..... 4.5-11
Figure 4.5-3 Parker Seals Material Report on the Viton® Material..... 4.5-25

List of Tables

Table 4.2-1 Containment Analysis Basis Cask Free Volumes and Pressures 4.2-4

4 CONTAINMENT

4.1 Containment Boundary

The containment boundary for the NAC-LWT cask consists of the 0.75-inch thick inner shell, the 4.0-inch thick bottom end plate, the 11.25-inch thick lid, the upper ring forging and the vent and drain port covers. The inner shell is fabricated from Type XM-19 stainless steel and the other components are fabricated from Type 304 stainless steel. The quick-disconnect valves used for filling and draining the cask cavity are not considered to be part of containment and are closed by the port covers. There are two port cover designs: alternate and Alternate B. The alternate port cover is fabricated from SA-705, Grade 630, condition H1150 precipitation-hardened stainless steel. The Alternate B port cover is fabricated from XM-19 stainless steel and is designed to withstand a higher MNOP. The Alternate B port covers are required to be installed for the transport of TPBAR contents.

The closure lid's metallic O-ring seal and the port cover's Viton® O-ring (alternate port cover) or metallic face seal (Alternate B port cover) are also part of the containment boundary. The sealing surfaces for O-rings and seals are machined in accordance with seal manufacturers' recommendations to a finish suitable to achieve reliable leaktight sealing of the containment.

4.1.1 Containment Penetrations

The only containment penetrations in the NAC-LWT cask cavity are the cask lid and the vent and drain ports.

4.1.2 Seals and Welds

4.1.2.1 Seals

The O-rings of the cask lid and the vent and drain port covers are the seals that provide the containment boundary for the radioactive contents of the NAC-LWT cask, as described in Section 4.1. Appendix 4.5.1 contains the military specification that prescribes the physical and chemical properties of the TFE O-rings. Appendix 4.5.2 is the manufacturer's technical bulletin for the metallic O-rings. Appendix 4.5.3 contains a description of the leakage testing performed using the Viton® O-rings on the alternate port cover design at temperatures exceeding the manufacturer's elevated temperature limit. Appendix 4.5.3 also contains the O-ring manufacturer's material report on the Viton® material. Appendix 4.5.9 contains the technical specification on the Alternate B port cover HELICOFLEX® metallic face seal.

Seal testing, prior to cask acceptance from the manufacturer, during routine and annual maintenance, and following assembly prior to transportation, includes the fabrication leakage rate test, the maintenance leakage rate test, and the preshipment leakage rate test. All containment O-ring tests are performed in accordance with the requirements of ANSI N14.5-1997.

4.1.2.1.1 Fabrication Leakage Rate Test

Upon completion of fabrication, the cask containment shall be leakage tested to a leaktight criteria of 1×10^{-7} ref.cm^3/s, per ANSI N14.5-1997, as described in Section 8.1.3. The equivalent allowable helium leakage rate at reference conditions is 2×10^{-7} cm^3/s (helium), with a minimum helium leak test sensitivity of 1×10^{-7} cm^3/s (helium).

4.1.2.1.2 Fabrication Pressure Test

During acceptance testing, the cask containment boundary shall be hydrostatically tested using the pressure test described in Section 8.1.2. This test verifies the sealing integrity of the package with a hydrostatic test pressure of 209 psig.

As an additional post-fabrication test, prior to performing the first TPBAR shipment in a specific NAC-LWT cask, the hydrostatic test described in Section 8.1.2 shall be performed with the Alternate B port covers installed. The test pressure for the hydrostatic test shall be 450 psig, which is 150% MNOP for the TPBAR content conditions.

The hydrostatic tests are further described in Chapter 8.

4.1.2.1.3 Preshipment Leakage Rate Test

Prior to shipment of a loaded NAC-LWT cask, the containment seals of the closure lid and the vent and drain port covers shall be individually leakage tested. For the alternate port covers, a pressure drop test is performed by pressurizing the volume between the containment seal and the test seal. This preshipment leakage rate test assures that the port covers and seals are properly installed and that there is no leakage in excess of the minimum test sensitivity of 1×10^{-3} ref cm^3/s.

If an alternate port cover's Viton® containment O-ring is replaced, a maintenance leakage rate test is required to be performed per Section 8.1.3.2.2.

The closure lid and the Alternate B port cover both utilize metallic O-rings for the containment boundary seal. Metallic O-rings are designed for a single use and must be replaced prior to each loaded transport, if the component is removed. Following installation of the closure lid and

Alternate B port covers, maintenance leakage rate tests are performed on each component in accordance with the helium leak test procedures in Section 8.1.3.

4.1.2.2 Welds

All containment vessel welds are full penetration bevel or groove welds to ensure structural and containment integrity.

4.1.3 Closure

Closure of the containment vessel is provided by the twelve 1-8 UNC closure lid bolts, each tightened to 260 ± 20 ft-lb of torque. The lid bolts are SA-453, Grade 660 high alloy steel bolting material. The lid bolts are preloaded so that the lid seals remain fully compressed for all load conditions. The structural adequacy of the lid bolts is documented in Sections 2.1.3.2.2, 2.6.7.6 and 2.10.9. The closure lid O-ring seals are specified on Drawing No 315-40-02 in Section 1.4. The O-ring seals and grooves are selected based on the manufacturer's specifications to satisfy the pressure and temperature conditions incurred by the NAC-LWT cask.

The leakage tests described in Section 8.1.3 verify that the lid and port cover seal leakage rates do not exceed 2×10^{-7} cm^3/s (helium).

Alternate port covers are retained by three ⅜ - 16 UNC bolts, each tightened to 100 ± 10 in-lb of torque. The bolt material for these port covers is SA-193, Grade B6 high alloy steel. The Alternate B port cover is retained by three ⅜ - 16 UNC bolts, made from SB-637 Grade N07718 nickel alloy steel, each tightened to 280 ± 15 in-lb of torque. The Alternate B port covers are required for the transport of TPBAR contents.

4.2 Containment Requirements for Normal Conditions of Transport

The NAC-LWT cask must maintain a radioactivity release rate less than 10^{-6} A_2/hr under normal conditions of transport, as required by 10 CFR 71.51 and IAEA Transportation Safety Standards (TS-R-1). The maintaining of a leaktight containment for the NAC-LWT cask, per ANSI N14.5-1997, satisfies this condition. ANSI N14.5-1997 specifies and defines a reference (air at standard conditions) leakage rate of 1×10^{-7} ref.cm^3/s as leaktight. The equivalent allowable helium leakage rate at reference conditions is 2×10^{-7} cm^3/s (helium), with a minimum helium leak test sensitivity of 1×10^{-7} cm^3/s (helium).

For the transport of TPBAR contents, a leaktight containment boundary provided by metal containment seals is required. Therefore, for the transport of TPBARs under the package designation of USA/9225/B(M)-96, Alternate B port covers with metal seals are required to be installed.

The structural and thermal evaluations of the NAC-LWT are provided in Chapters 2 and 3, respectively. Results of these evaluations demonstrate that cask containment is maintained leaktight during normal conditions of transport and hypothetical accident conditions. Therefore, the package satisfies the containment requirements of 10 CFR 71.51.

4.2.1 Containment of Radioactive Material

The 10 CFR 71 limit for the release of radioactive material under normal conditions of transport of 10^{-6} A_2/hr is assured by the maintenance of a leaktight containment boundary in accordance with ANSI N14.5-1997.

4.2.2 Pressurization of Containment Vessel

The maximum pressure in the cask during normal conditions of transport for other than TPBAR content payloads is calculated by using the methodology presented in Section 3.4.4. Assumptions underlying this calculation are that during normal conditions of transport, 3% of the fuel rods may fail and that 30% of the fission gases in the rods are releasable. The free volumes and resulting pressures are tabulated in Table 4.2-1. In addition, for LWR high burnup rods, 56% of the rods with oxide layers greater than 70 micrometers (14 rods) are assume to fail during transport. This is conservative since fuel rods classified as damaged may have released fission and charge gases prior to transport. Failed rods are assumed to have released the fission gas prior to transport. The cask cavity is backfilled to 1 atm with 99.9% pure helium gas.

The gas volume (e.g., plenum and pellet to cladding gap) inside the fuel rods is conservatively neglected when calculating the cask free volume. The maximum normal operating pressure (MNOP) of the cavity for the PWR fuel configuration is 1.99 atm. The maximum normal condition cavity pressure for the 25 intact PWR/BWR high burnup fuel rod contents is 2.1 atm. The maximum normal condition cavity pressure with 56% fuel rod failure rate is 3.2 atm for the 25 BWR high burnup rods and 3.0 atm for the 25 PWR high burnup rods.

Pressure evaluations in Section 3.4.4.8 demonstrate that the MNOP is less than 50 psig for aluminum-based nuclear fuels.

MNOP for the transport of up to 300 production TPBARs (including up to 2 prefailed rods) is conservatively determined in Section 3.4.4.5 as 289 psig. The TPBAR normal condition pressure assumed clad failure of all 300 TPBARs during transport. The pressure for the TPBAR content conditions of 55 segmented TPBARs contained in a waste container and 25 TPBARs contained in a PWR/BWR rod transport canister is bounded by the 300 TPBAR MNOP.

4.2.3 Containment Criteria

The standard leak rate for NAC-LWT transports of 1×10^{-7} ref.cm^3/s represents the maximum leak rate allowed if the seals were to be tested with air at an upstream pressure of 1 atm and a downstream pressure of 0.01 atm at a temperature of 25°C. This is the maximum allowable leak rate for the containment system fabrication verification, periodic and maintenance leak tests described in Section 4.1 and in Chapter 8.

The NAC-LWT leaktight containment criteria per ANSI N14.5-1997 is 1×10^{-7} ref cm^3/s, which is equivalent to a helium leak rate of less than or equal to 2×10^{-7} std cm^3/s, (helium) under test conditions. The minimum specified test sensitivity is 1×10^{-7} cm^3/s (helium).

Table 4.2-1 Containment Analysis Basis Cask Free Volumes and Pressures

	Pressure (atm)		Temperature	Free Volume
Fuel Type	Normal	Accident	(K)	(10^5 cm^3)
PWR	1.99[1]	11.4[1]	517.4	1.471
BWR	1.99[2]	11.4[2]	517.4	1.018
Metallic Fuel	1.99[2]	11.4[2]	405.2	1.018
TRIGA[7]	1.99[2]	11.4[2]	571.4[2]	1.717
GA IFM	N/A[6]	N/A[6]	403.2	3.354
25 PWR Rods – 56% Failed Fuel Fraction	3.0	4.3[5]	588.7[4]	0.9681
25 BWR Rods – 56% Failed Fuel Fraction	3.2	4.5[5]	588.7[4]	0.8932

[1] Based on Sections 3.4.4 and 3.5.4, the maximum calculated pressures for the PWR payload are 1.93 atm (28.3 psia) normal condition and 8.56 atm (125.8 psia) accident conditions.

[2] The maximum pressure for the PWR fuel is conservative.

[3] The temperature employed is approximately 4K lower than the maximum fuel clad temperature calculated. The fuel clad temperature is significantly higher than the average gas temperature in the cask.

[4] The normal condition temperature is conservatively applied to the 25 PWR and BWR high burnup rod analysis.

[5] These pressures result from the 100% fuel rod failure plus the design basis fire accident.

[6] Based on the lower temperature and larger free volume of the GA IFM, as compared to the other contents, the pressure, although not explicitly calculated, is lower than that calculated for PWR and BWR fuel.

[7] TRIGA volume and pressure conservatively applied to TRIGA cluster rod analysis. Free volume is higher in the cluster rod configuration.

4.3 Containment Requirements for Hypothetical Accident Conditions

The NAC-LWT cask must maintain a radioactivity release rate of not more than 10 A_2/week ^{85}Kr or 1 A_2/week for other radioactive material under hypothetical accident conditions of transport, as required by 10 CFR 71.51. Maintaining a leaktight containment, per ANSI N14.5-1997, satisfies this condition. ANSI N14.5-1997 specifies and defines a reference (air at standard conditions) leakage rate of 1×10^{-7} ref·cm^3/s or 2×10^{-7} cm^3/s helium at the reference conditions as leaktight.

The structural integrity of the cask containment during hypothetical accident conditions is demonstrated in Section 2.7 and the thermal evaluations are provided in Chapter 3. Therefore, the NAC-LWT cask containment is maintained leaktight under hypothetical accident conditions and satisfies the containment requirements of 10 CFR 71.51.

4.3.1 Fission Gas Products

The accident conditions for maximum fission gas release assumes 100% rod failure and also assume that 30% of the radioactive fission gases, primarily ^{85}Kr, tritium and ^{129}I, are available for release to the cask cavity. The metallic fuels do not contain significant amounts of fission gas that are available for immediate release. TRIGA fuel elements are assumed to release 1% of their fission gas products under accident conditions. With a leaktight containment boundary, only radionuclides related to pressure increases in the containment boundary are relevant to the evaluations.

4.3.2 Containment of Radioactive Materials

The NAC-LWT cask is designed to maintain a release rate of less than 1 A_2/week for the hypothetical accident conditions, as required by 10 CFR 71.51. This is achieved by maintaining a leaktight boundary throughout all hypothetical accident conditions.

4.3.2.1 Containment Criteria

Leaktight cask containment is demonstrated to be maintained under hypothetical accident conditions. Leaktight requirements are used for the establishment of the maximum allowable leak rates for the containment system fabrication and periodic verification leak tests.

4.3.2.2 Tritium Permeation Rate of Seals for TPBAR Shipment

The release of tritium into the cask cavity from all 300 rods, 298 rods that are event-failed and 2 rods defined to be prefailed, has the potential of releasing a significant quantity of tritium (> $1A_2$) into the cask cavity. As shown in the structural analysis, the lid and port cover seals retain their ability to provide cask closure during all accident conditions. To assure that the accident release limit of $1A_2$/week is not exceeded under accident conditions the port and lid seal permeation rates are evaluated.

The formula for permeation through metal is:

$$PR = \Phi \times A / l \times (P_p)^{1/2}$$

where:

PR = equilibrium (steady-state) permeation rate in std cc (permeate) per sec
Φ = permeability in std cc (permeate) per second per material surface area per permeate partial pressure ½ through a unit material thickness
A = material surface area that is "exposed" to the permeate
l = material thickness through which the permeate "passes"
P_p = upstream permeate partial pressure

The formula for permeability is:

$$\Phi = \Phi_0 \times \exp\left(-\frac{E_\Phi}{RT}\right)$$

where:

Φ = permeability as stated previously
Φ_0 = pre-exponential permeation factor in the same units as Φ
E_Φ/R = the activation energy of the permeation process, which has been 'normalized' by the universal gas constant
T = absolute temperature of the metal (K).

Combining the permeation equations with an activity density of 0.16 Ci/cc, resulting from the release of 55 Ci per event failed rod and 0.199 moles of tritiated water for each prefailed rods, and

T = 572K – Maximum accident temperature for the seals per Table 3.5-1

Φ_0 = 7.42×10^{-2} [LLNL Report UCRL-53441] (stainless steel port seal), 2.10×10^{-2} [Fusion Science and Technology] (inconel lid seal)

E_Φ/R = 7,700 (stainless steel port seal), 7490 [Fusion Science and Technology] (inconel lid seal)

l = 0.012 inch for the port cover seal (only considering the stainless steel portion of the seal) and 0.032 inch for the lid seal

P_p = 0.15 atm – tritium partial pressure in the cask cavity based on the cask free volume, accident condition temperature, and a release of 55 Ci of tritium per event failed rod (conservative modeled as isotope not molecular tritium) and 0.199 moles of tritiated water from the prefailed rods)

yields an approximate release through seal permeation of 5 Ci/week compared to the allowable accident release rate of 1.1×10^3 Ci/week ($1A_2$/week based on an A_2 value for tritium of 1.1×10^3 Ci).

Actual permeation release rates would be significantly lower as the accident temperatures are short term, with elevated temperatures at the seal locations returning to normal condition temperatures within an hour of the fire.

Similar calculations are performed for the 55 equivalent TPBARs, in segments and debris, which may release up to 100% of the tritium contained in the pellets during transport. The pellet tritium content represents approximately 40% of the tritium quantity in the TPBAR. At NAC-LWT normal and accident conditions temperatures, the TPBAR components release tritium primarily as tritiated water with only a small fraction (maximum 2%) as gaseous tritium (see Appendix 1-B of Chapter 1). Gaseous tritium represents the basis for the seal permeation evaluation. During a one-year transport, an additional maximum 1% of the tritiated water may undergo radiolysis and dissociate. Conservatively applying a maximum 3% release rate to the 55 equivalent TPBAR total inventory of 66 grams (1.2 grams per rod) yields an inventory of 0.33 moles T_2. Seal permeation rates based on the conservative temperatures discussed in the previous paragraphs and a 3% tritium gas release are 6.5×10^{-6} Ci/hr, normal conditions, and 1.06 Ci/week, accident conditions. A gaseous release of over 90% of the 1.2 grams per rod tritium inventory is required to exceed normal condition allowables at the conservative seal temperature of 222°F. A 100% gaseous release and resulting tritium permeation through the cask seals meets accident condition limits. Reducing seal temperatures less than 5°F, to account for a significantly lower decay heat payload (0.127 kW for the waste container TPBARs versus 1.05 kW on which the 222°F

temperature is based), permits a normal condition release of 100% of the tritium in gaseous form while meeting the 10^{-6} A_2/hr allowable.

4.3.3 Tritium Contamination Issues

Precautions will be taken to minimize the risk of excessive contamination of NAC-LWT casks during the loading and unloading of TPBAR contents to ensure the reusability of the NAC-LWT casks for transport of non-TPBAR contents. In addition to ensuring the safe handling of TPBAR contents, additional cavity gas and internal and external removable contamination surveys for tritium contamination will be implemented at all TPBAR loading and unloading facilities. The specific monitoring methods and levels of contamination to which the cask surfaces must be decontaminated are defined in the TPBAR loading and unloading procedures in Chapter 7. In addition, the TPBAR procedures also include precautions for users to observe when loading, unloading and handling TPBARs.

The procedures and precautions comply with the recommended practices of NUREG-1609, Supplement 2. The results of previous loading and unloading experiences regarding the measurement of tritium gas and contamination levels are provided in the PNNL letter in Section 1.5, Appendix 1-G of this SAR.

NAC-LWT cask units used for TPBAR transports shall comply with the specified contamination levels, or other non-TPBAR users will be advised to incorporate tritium monitoring requirements into their survey procedures and radiological control program.

4.5.4 Metallic Face Seal

This appendix contains the specification that describes the properties of the metallic port cover face seal.

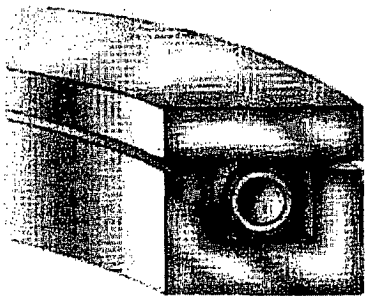
Helicoflex Spring Energized Seals

GENERAL INFORMATION

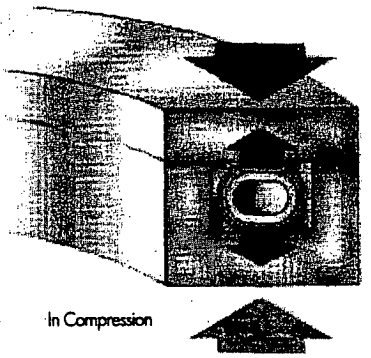
The Helicoflex® seal represents the leading edge in seal technology for high performance sealing applications. Today's extreme sealing requirements have rendered traditional seals & gaskets obsolete. If you can't afford the lost time associated with leaks, put your trust in the leader: Helicoflex®.

SEALING CONCEPT

The sealing principle of the Helicoflex® family of seals is based upon the plastic deformation of a jacket of greater ductility than the flange materials. This occurs between the sealing face of a flange and an elastic core composed of a close-wound helical spring. The spring is selected to have a specific compression resistance. During compression, the resulting specific pressure forces the jacket to yield and fill the flange imperfections while ensuring positive contact with the flange sealing faces. Each coil of the helical spring acts independently and allows the seal to conform to surface irregularities on the flange surface. This combination of elasticity and plasticity makes the Helicoflex seal the best overall performing seal in the industry.



Free State



In Compression

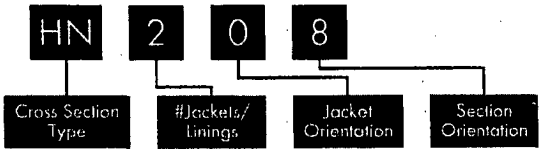
GENERAL CHARACTERISTICS

- Wide range of applications:
  - Dimensional: Diameters from 0.250 inches (6.3 mm) to over 300 inches (7.6 m)
    Cross sections from 0.063 inches (1.6 mm) to over 0.625 inches (15.9 mm)
  - Temperature: Cryogenic to 1800°F (982°C)
  - Pressure: Ultra High Vacuum to 50,000 PSI (100,000 PSI under special conditions)
- Excellent springback: the spring energized Helicoflex is capable of compensating for flange distortions due to temperature and pressure cycling.
- Adaptable to a majority of standard flanges: ANSI, ISO, KF, ASA
- Suited to different types of assemblies: -metal/metal with groove
  -flat flanges with limiter/retainer
  -3 face contact
- Extended shelf life
- Excellent resistance to corrosion and radiation
- Minimum relaxation: the Helicoflex's resilient spring compensates for relaxation ensuring positive seal contact.

For Additional Information, Please Consult Our Engineering Staff
1-800-233-1722

Seal Configurations

CLASSIFICATION OF SEAL TYPE

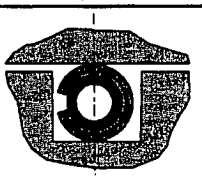


CONFIGURATION GUIDE

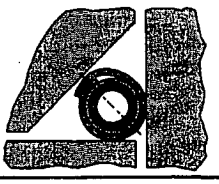
Cross Section Type	HN	single section
	HNR	ground spring for precise load control (Beta Spring)
	HNV	low load (Delta Seal)
	HND	tandem Helicoflex seals
	HNDE	tandem Helicoflex and elastomer seals note: "L" indicates internal limiter (ex: HLDE)
Jacket/Lining	1 = jacket only	
	2 = jacket with inner lining	
Jacket Orientation	0 1 2 3 4 5 6 7 8 9	
Section Orientation	0 1 2 3 4 5 6 7 8 9	

TYPICAL CONFIGURATIONS

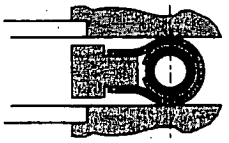
HN200
Groove assemblies



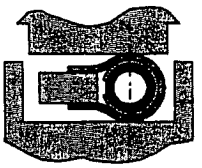
HN240
3 face compression



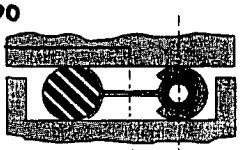
HN208
Raised face flanges - ANSI B16.5



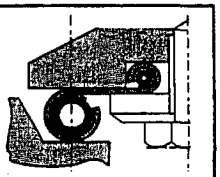
HN203
Tongue & groove



HNDE290
Leak check - inert gas purge



HND229
Valve seats



Garlock Helicoflex

For Additional Information, Please Consult Our Engineering Staff
1-800-233-1722

3

Helicoflex Seal Characteristics

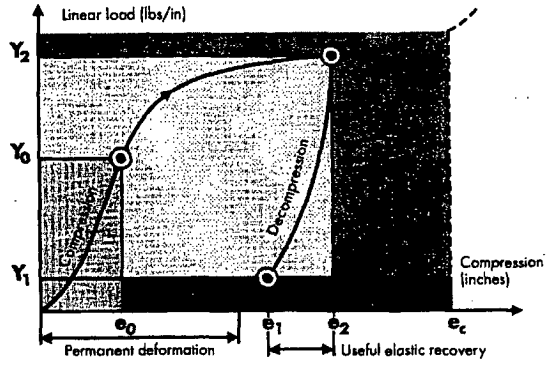
CHARACTERISTIC CURVE

The resilient characteristic of the Helicoflex® seal ensures useful elastic recovery during service. This elastic recovery permits the Helicoflex® seal to accommodate minor distortions in the flange assembly due to temperature and pressure cycling. For most sealing applications the Y_0 value will occur early in the compression curve and the Y_1 value will occur near the end of the decompression curve.

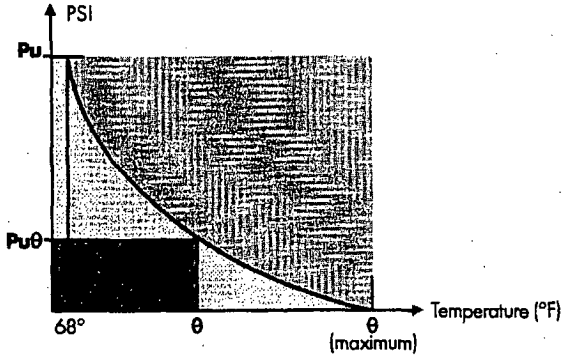
The compression and decompression cycle of the Helicoflex® seal is characterized by the gradual flattening of the compression curve. The decompression curve, which is distinct from the compression curve, is the result of a hysteresis effect and permanent deformation of the spring and jacket.

DEFINITION OF TERMS

- Y_0 = load on the compression curve above which leak rate is at required level
- Y_2 = load required to reach optimum compression e_2
- Y_1 = load on the decompression curve below which leak rate exceeds required level
- e_2 = optimum compression
- e_c = compression limit beyond which there is risk of damaging the spring



INTRINSIC POWER OF THE SEAL



The intrinsic power of the Helicoflex seal reflects its ability to maintain and hold system pressure for a given temperature at Y_2 and e_2. This value is expressed as a specific pressure and is noted by the symbols **Pu** (room temperature) and **Puθ** (at operating temperature). The influence of temperature on Pu is shown in the graph above. The tables on pages 10 and 11 give the values of **Pu** at 68 °F (20 °C), **Puθ** at a given temperature and the maximum temperature where **Puθ** = 0.

Helicoflex Seal Specifications

DEFINITION OF CHARACTERISTIC VALUES

Dj	Mean reaction diameter of the seal. (For a double section seal, $Dj = Dj_1 + Dj_2$)	_____ inches
Y_2	Linear load corresponding to e_2 compression	_____ lbs/inch
Y_1	Linear load on the seal to maintain sealing in service at low pressure ($=Y_{m1}$)	_____ lbs/inch
Pu	Intrinsic power of the seal under pressure at 68 °F (20 °C) when the reaction force of the seal is maintained at Y_2, regardless of the operating conditions.	_____ PSI
Puθ	Value of Pu at temperature θ	_____ PSI
P	Operating or proof pressure	_____ PSI
	Note: if $\frac{P}{Pu \text{ or } Pu\theta} > 1$, the definition of the seal must be modified *This ratio must never exceed 1.*	
Y_{m2}	Linear tightening load on the seal at room temperature to maintain sealing under pressure. $Ym_2 = Y_2 \frac{P}{Pu}$	_____ lbs/inch
$Y_{m2\theta}$	Value of Y_{m2} at temperature θ. $Y_{m2\theta} = Y_2 \frac{P}{Pu\theta}$	_____ lbs/inch
Et	Young's modulus of bolt material at 68 °F (20 °C)	_____ PSI
Et_s	Young's modulus of bolt material at operating temperature	_____ PSI

LOAD CALCULATIONS

Fj	Total tightening load to compress the seal to the operating point (Y_2; e_2) $Fj = \pi \times Dj \times Y_2$	_____ lbs
F_F	Total hydrostatic end force $F_F = \pi/4\ Dj_1^2 \times P$ ($Dj_1 = Dj$ in case of a single section seal)	_____ lbs
Fm	Minimum total load to be maintained on the seal in service to preserve sealing, i.e. $Fm = \pi\ Dj\ Ym$ where: Ym = the greater of the two values: Y_{m1} or $Y_{m2\theta}$ (see note 1 below)	_____ lbs
Fs	Total load to be applied on the bolts to maintain sealing in service. $F_S = F_F + Fm$	_____ lbs
Fs*	Increased value of F_S to compensate for Young's modulus at temperature $Fs^* = Fs\ Et / Et_s$	_____ lbs
F_B	LOAD TO BE APPLIED: If $Fs^* > Fj$ then $Fb = Fs^*$; If $Fj > Fs^*$ then $Fb = Fj$	_____ lbs

Note 1: wherever the working pressure is high and/or seal diameter is big, to such an extent that P•Dj ≥ 32 Ym, in order to remain on the safe side, whatever the inaccuracy on the tightening load may be, it is recommended to take the Fj value in lieu of Fm for the calculation of Fs so that $Fs = F_F + Fj$.

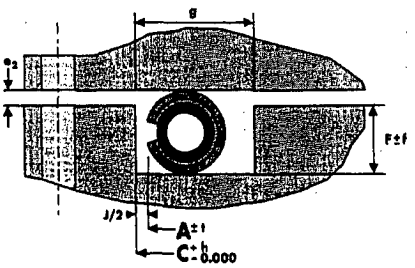
Note 2: this information is provided as a reference only.

Garlock Helicoflex

For Additional Information, Please Consult Our Engineering Staff
1-800-233-1722

5

Groove Design - Radial Pressure



CALCULATIONS

Groove Depth (F)	= Cross Section (CS)-e_2
Depth Tolerance (f)	= e_2 X 0.12
Groove Width (g)	= See table below
Seal OD (A)	= Groove OD (C) - Clearance (J)
Groove Finish	= See table below
Flatness	= See table below

CLEARANCE AND MINIMUM GROOVE WIDTH

Seal Cross Section CS	Pressure < 300 psi (20 bar) Clearance J	Pressure < 300 psi (20 bar) Min Groove Width g	Pressure ≥ 300 psi (20 bar) Clearance J	Pressure ≥ 300 psi (20 bar) Min Groove Width g
0.059 to 0.134 (1.5 to 3.4)	$J = e_2$	$g > CS + 2e_2$	J = 0.012 J = 0.3	$g > CS + 2\ e_2$
0.138 to 0.272 (3.5 to 6.9)	$J = e_2$	$g > CS + 2e_2$	J = 0.020 J = 0.5	$g > CS + 2\ e_2$
0.276 to 0.390 (7.0 to 9.9)	$J = e_2$	$g > CS + 2e_2$	J = 0.028 J = 0.7	$g > CS + 2\ e_2$

SEAL / GROOVE TOLERANCES

Seal Diameter Range	Pressure < 300 psi (20 bar) Seal Tolerance t	Pressure < 300 psi (20 bar) Groove Tolerance h	Pressure ≥ 300 psi (20 bar) Seal Tolerance t	Pressure ≥ 300 psi (20 bar) Groove Tolerance h
0.350 to 2.000 (3.8 to 50.0)	0.005 0.13	0.005 0.13	0.004 0.10	0.004 0.10
2.001 to 12.000 (50.0 to 305.0)	0.010 0.25	0.010 0.25	0.004 0.10	0.004 0.10
12.001 to 25.000 (305.0 to 635.0)	0.010 0.25	0.010 0.25	0.006 0.15	0.006 0.15
25.001 to 48.000 (635.0 to 1220.0)	0.015 0.38	0.015 0.38	0.008 0.20	0.008 0.20
48.001 to 72.000 (1220.0 to 1830.0)	0.020 0.51	0.015 0.38	0.010 0.25	0.008 0.20
> 72.000 (> 1830.0)	Consult our engineering staff		Consult our engineering staff	

SURFACE FINISH

Nr. ICA-CEA	N10	N9	N8	N7	N6	N5	N4
Ra in µm	12.5	6.3	3.2	1.6	0.8	0.4	0.2
Rt in µm	50	37	21	11	6.2	3.4	1.9
RMS	500	250	125	63	32	16	8
Aluminum	o	⊙	⊙	⊙	⊙	o	o
Silver, copper, iron	-	o	⊙	⊙	o	o	-
Nickel, stainless steel	-	o	o	⊙	⊙	o	o

⊙ recommended o consult our engineering staff

Note: Machining/polishing marks must follow seal circumference

SHAPED SEALS

Groove Design: Contact our engineering staff for assistance in designing non-circular grooves.
Groove Finish: Most applications will require a finish of 16-32 RMS (0.4 to 0.8 Ra µm). All machining & polishing marks must follow seal circumference.
Min. Seal Radius: The minimum seal bending radius is six times the seal cross section (CS).
Seating Load: The load (Y2) to seat the seal is approximately 30% higher due to a slightly stiffer spring design.

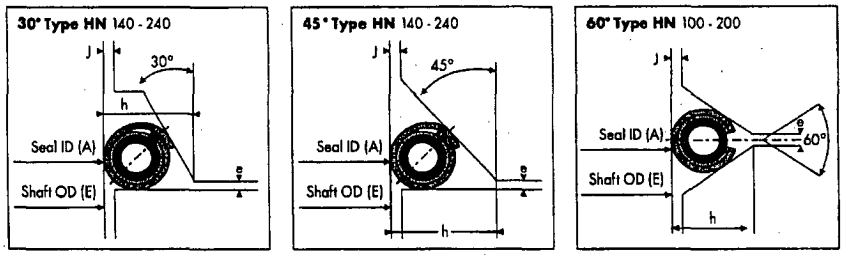
FLATNESS

Seal Diameter Range	Amplitude	Tangential Slope	Radial Slope
0.350 to 20.000 (10 to 500)	0.008 0.2	1:1000	1:100
20.001 to 80.000 (500 to 2000)	0.016 0.4	2:1000	2:100

Dimensions in inches | Dimensions in mm

Cavity Design - Axial Pressure

THREE FACE COMPRESSION



E = Shaft OD $^{+0.000}_{-0.002}$ $^{+0.00}_{-0.05}$ A = Seal D $^{+0.002}_{-0.000}$ $^{+0.05}_{-0.00}$

CALCULATIONS	
Axial Load (Ya)	= K · Y2
Shaft OD (E)	= Seal ID (A)
Clearance (J)	< CS / 10
Axial Compression (e)	= a · e_2
Cavity Finish	< 32 RMS (0.8 um)

COEFFICIENT VALUES			
Coefficient	30°	45°	60°
a	2	1.4	1.15
K	0.9	1.2	1.4



"h" VALUES

Cross Section CS		30° Aluminum Jacket		30° Other Jackets		45° Aluminum Jacket		45° Other Jackets		60° Aluminum Jacket		60° Other Jackets	
in	mm	in	mm	in	mm	in	mm	in	mm	in	mm	in	mm
0.102	2.6	0.130	3.30	0.126	3.20	0.163	4.15	0.157	4.00	0.126	3.20	0.134	3.40
0.126	3.2	0.157	4.00	0.157	4.00	0.199	5.05	0.199	5.05	0.157	4.00	0.165	4.20
0.165	4.2	0.207	5.25	0.207	5.25	0.260	6.60	0.260	6.60	0.213	5.40	0.220	5.60
0.205	5.2	0.260	6.60	0.260	6.60	0.327	8.30	0.327	8.30	0.272	6.90	0.280	7.10
0.252	6.4	0.321	8.15	0.321	8.15	0.402	10.20	0.402	10.20	0.339	8.60	0.346	8.80

Dimensions in inches | Dimensions in mm

TARGET SEALING CRITERIA

The ultimate leak rate of a joint is a function of the seal design, flange design, bolting, surface finish and other factors. Helicoflex seals are designed to provide two levels of service: Helium Sealing or Bubble Sealing.

Helium Sealing: These Helicoflex seals are designed with a target Helium leak rate not to exceed 1×10^{-9} cc/sec.atm under a ΔP of 1 atmosphere. The ultimate leak rate will depend on the factors listed above.

Bubble Sealing: These Helicoflex seals are designed with a target air leak rate not to exceed 1×10^{-4} cc/sec.atm under a ΔP of 1 atmosphere.

Code Calculations

CALCULATIONS ACCORDING TO CODES

	D.I.N. 2505 1990	A.S.M.E. Section VIII Division 1	CODAP 1995	Garlock Helicoflex CEFILAC
Operating load	$F_{DV} = \pi.d_D.k_D.K_{DV}$	$W_{m2} = \pi.b.G.y$	$F_A = \pi.Di.J_E.P_A$	$Fi = \pi.Di.Y_2$
Hydrostatic force	$F_F = \pi.\frac{(d_D)^2}{4}.P$	$H = \pi.\frac{G^2}{4}.P$	$F_F = \pi.\frac{(Di)^2}{4}.P$	$F_F = \pi.\frac{(Di)^2}{4}.P$
Minimum service load	$F_{DB} = \pi.d_D.k_B.P$	$H_p = 2.b.\pi.G.m.P$	$Fi = 2.\pi.Di.J_E.m.P$	$Fm = \pi.Di.Ym$ $Ym = Ym_1 = Y_1.P_e$ $Ym_2 = Y_2.P_{e2}$ Use the greater of the two!
Minimum tightening load to apply on bolts	$F_{BO} = (1)\ F_{DV}$ $(2)\ F_F + F_{BO}$ Use the greater of the two (1) or (2)	$W = (1)\ W_{m2}$ $(2)\ H + Hp = W_{m1}$ Use the greater of the two (1) or (2)	$F_B = (1)\ F_A$ $(2)\ F_F + Fi$ Use the greater of the two (1) or (2)	$F_B = (1)\ Fi$ $(2)\ F_F + Fi = F_B$ Use the greater of the two (1) or (2)

EQUIVALENT SYMBOLS

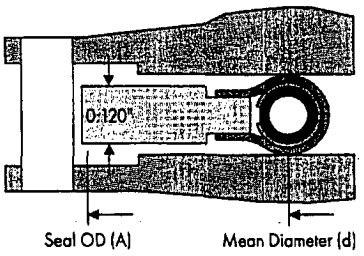
	D.I.N. 2505 1990	A.S.M.E. Section VIII Division 1	CODAP 1995	Garlock Helicoflex CEFILAC
Operating load	$F_{DV} = Fi$ $d_D = Di$ $k_D.K_{DV} = Y_2$ $F_{DV} = \pi.Di.Y_2$	$W_{m2} = Fi$ $b = 1$ $G = Di$ $Y = Y_2$ $W_{m2} = \pi.Di.Y_2$	$F_A = Fi$ $Di = Di$ $J_E = 1$ $P_A = Y_2$ $F_A = \pi.Di.Y_2$	
Hydrostatic force	$F_F = F_F$ $d_D = Di$ $F_F = \pi.\frac{(Di)^2}{4}.P$	$H = F_F$ $G = Di$ $H = \pi.\frac{(Di)^2}{4}.P$	$F_A = F_F$ $Di = Di$ $F_F = \pi.\frac{(Di)^2}{4}.P$	
Minimum service load	$F_{DB} = F_m$ $d_D = Di$ $k_B.P = Y_m$ $F_{DB} = \pi.Di.Y_m$	$Hp = F_m$ $b = 1$ $G = Di$ $2.m.P = Y_m$ $m = \frac{Y_m}{2.P}$ $H_p = \pi.Di.Y_m$	$Fi = F_m$ $Di = Di$ $J_E = 1$ $2.m.P = Y_m$ $m = \frac{Y_m}{2.P}$ $Fi = \pi.Di.Y_m$	
Minimum bolt load	$F_{BO} = FB$ $F_{BO} = (1)\ Fi$ $(2)\ F_F + F_m = F_B$ Use the greater of the two (1) or (2)	$W = F_B$ $W = (1)\ Fi$ $(2)\ F_F + F_m = F_B$ Use the greater of the two (1) or (2)	$F_B = F_B$ $F_B = (1)\ Fi$ $(2)\ F_F + F_m = F_B$ Use the greater of the two (1) or (2)	

Note: Due to its circular cross section, the Helicoflex seal exhibits a "line" load instead of an "area load" typical of traditional gaskets. As a result, "m", "b" and "y" factors are not pertinent when applied to the Helicoflex seal. The above equivalent equations were developed to assist flange designers with their calculations.

Standard Flanges

ANSI B16.5 RAISED FACE FLANGE

The Helicoflex® HN208a is ideally suited for standard raised face flanges. The resilient nature of the seal allows it to compensate for the extremes of high temperature and pressure where traditional spiral wounds and double jacketed seals fail. The jacket and spring combination can be modified to meet most requirements of temperature and pressure. In addition, a large selection of jacket materials ensures chemical compatibility in corrosive and caustic media.



SEAL TYPE: HN208a

Jacket	Availability	Cross Section (inches)	Seating Load (lbs/in)*	Recommended Flange Finish (RMS)
Aluminum	Standard	0.160	1150	63 - 125
Silver	Standard	0.160	1725	63 - 125
Copper	Standard	0.155	2250	63 - 125
Soft Iron	Optional	0.155	2250	32 - 63
Nickel	Standard	0.150	2800	32 - 63
Monel	Optional	0.150	2800	32 - 63
Hastelloy C	Optional	0.150	2800	32 - 63
Stainless Steel	Standard	0.150	3800	32 - 63
Alloy 600	Optional	0.150	3800	32 - 63
Alloy X750	Optional	0.150	4000	32 - 63
Titanium	Optional	0.150	4000	32 - 63

* Note: Seating load only! Does not allow for hydrostatic end force. See page 5 for calculations.

SEAL DIMENSIONS

Nominal Diameter	Mean Diameter (d)	Seal OD (A)						
		150lb	300lb	400lb	600lb	900lb	1500lb	2500lb
1/2	0.827	1.874	2.126	2.126	2.126	2.500	2.500	2.752
3/4	1.102	2.252	2.626	2.626	2.626	2.752	2.752	3.000
1	1.417	2.626	2.874	2.874	2.874	3.122	3.122	3.374
1-1/4	1.890	3.000	3.252	3.252	3.252	3.500	3.500	4.126
1-1/2	2.283	3.374	3.752	3.752	3.752	3.874	3.874	4.626
2	2.913	4.126	4.374	4.374	4.374	5.626	5.626	5.752
2-1/2	3.425	4.874	5.126	5.126	5.126	6.500	6.500	6.626
3	4.173	5.374	5.874	5.874	5.874	6.626	6.874	7.752
3-1/2	4.685	6.374	6.500	6.500	6.374	N/A	N/A	N/A
4	5.256	6.874	7.126	7.000	7.626	8.126	8.252	9.252
5	6.378	7.752	8.500	8.374	9.500	9.752	10.000	11.000
6	7.500	8.752	9.874	9.752	10.500	11.413	11.126	12.500
8	9.567	10.996	12.126	12.000	12.626	14.126	13.874	15.252
10	11.693	13.374	14.252	14.126	15.752	17.126	17.126	18.760
12	13.858	16.126	16.626	16.500	18.000	19.626	20.500	21.626
14	15.098	17.752	19.126	19.000	19.374	20.500	22.752	N/A
16	17.205	20.252	21.252	21.126	22.252	22.626	25.252	N/A
18	19.567	21.626	23.500	23.374	24.126	25.126	27.752	N/A
20	21.575	23.874	25.752	25.500	26.874	27.500	29.752	N/A
24	25.728	28.252	30.500	30.252	31.126	32.996	35.500	N/A

Note: Consult our engineering staff for other available sizes and materials.

Calculation Data - U.S. Customary

Jacket Material	Cross Section In	e_2 in	e_C in	Y_2 lbs/inch	Y_1 lbs/inch	Pu@68°F PSI	Pu@392°F PSI	Y_2 lbs/inch	Y_1 lbs/inch	Pu@68°F PSI	Pu@392°F PSI	Max Temp °F
				HELIUM SEALING				BUBBLE SEALING				
Aluminum	0.063	0.024	0.028	857	114	7250	N/A	514	114	5075	N/A	302
	0.075	0.028	0.033	914	114	7540	N/A	571	114	5800	N/A	302
	0.087	0.028	0.035	942	114	7685	N/A	600	114	5800	N/A	356
	0.098	0.028	0.035	999	114	7975	725	657	114	6090	725	428
	0.118	0.031	0.039	1056	143	7975	1450	742	114	6525	1450	482
	0.138	0.031	0.039	1085	143	7975	2030	799	114	6815	2030	482
	0.157	0.035	0.043	1142	143	8700	2465	857	114	7250	2465	536
	0.177	0.035	0.047	1199	143	8700	2900	914	114	7540	2900	536
	0.197	0.035	0.055	1256	171	9135	3190	971	143	7975	3190	572
	0.217	0.035	0.063	1313	171	9425	3480	1028	143	8265	3480	608
	0.236	0.039	0.071	1399	200	9715	3625	1113	171	8700	3625	644
	0.276	0.039	0.087	1542	228	10150	4060	1171	200	9425	4060	644
	0.315	0.039	0.102	1656	286	10440	4640	1285	228	9860	4495	680
						Pu@482°F				Pu@482°F		
Silver	0.063	0.020	0.024	1142	171	9425	N/A	857	171	5800	N/A	464
	0.075	0.024	0.028	1256	171	9425	N/A	857	171	5800	N/A	464
	0.087	0.024	0.031	1313	200	10150	N/A	914	171	5800	580	536
	0.098	0.028	0.035	1370	257	10875	1160	971	228	6525	725	536
	0.118	0.031	0.039	1485	286	12325	2030	1028	257	7250	1305	572
	0.138	0.031	0.039	1599	286	13775	3190	1085	257	7975	1885	572
	0.157	0.031	0.043	1713	314	15225	3915	1142	286	8700	2320	662
	0.177	0.031	0.043	1827	343	16675	4495	1256	286	10150	2755	698
	0.197	0.031	0.051	1941	343	18125	5220	1313	286	11600	3190	698
	0.217	0.031	0.055	2056	371	19575	5800	1428	343	13050	3625	752
	0.236	0.035	0.067	2284	400	21750	6815	1542	343	13950	4350	842
	0.276	0.035	0.079	2512	457	23200	7830	1713	371	18125	5220	842
	0.315	0.035	0.094	2798	514	24650	8700	1999	400	20300	6090	932
						Pu@572°F				Pu@572°F		
Copper, Soft Iron, Mild Steels	0.063	0.020	0.024	1485	228	7250	1450	1085	171	5075	725	662
	0.075	0.024	0.028	1599	286	7250	1595	1142	228	5075	870	662
	0.087	0.024	0.031	1713	343	7975	1885	1256	286	5075	1160	680
	0.098	0.028	0.035	1827	400	8700	2465	1313	343	5800	1450	716
	0.118	0.028	0.039	1999	457	9425	2900	1428	400	5800	1740	716
	0.138	0.028	0.039	2227	457	10150	3335	1542	400	6525	2175	752
	0.157	0.031	0.043	2455	514	10150	3915	1656	457	6525	2465	788
	0.177	0.031	0.043	2684	571	11600	4350	1827	457	6525	2755	842
	0.197	0.031	0.051	2912	628	12325	4785	1884	514	7250	3045	842
	0.217	0.031	0.055	3141	685	13050	5220	2056	571	7250	3335	896
	0.236	0.035	0.067	3597	799	13775	5800	2284	571	7975	3770	968
	0.276	0.035	0.079	4225	914	14500	6525	2627	628	8700	4205	968
	0.315	0.035	0.094	4911	1085	15950	7105	3026	742	9425	4640	1022
						Pu@662°F				Pu@662°F		
Nickel, Monel, Tantalum	0.063	0.016	0.020	1827	457	10150	1595	1142	343	5800	1015	716
	0.075	0.020	0.024	1999	457	10440	2320	1256	343	6090	1305	716
	0.087	0.020	0.028	2227	514	11020	3045	1313	400	6380	1740	788
	0.098	0.024	0.031	2512	571	11890	3915	1542	400	6815	2320	842
	0.118	0.024	0.035	2512	628	12615	4930	1713	457	7250	2900	896
	0.138	0.024	0.035	2798	685	13485	5800	1941	514	7830	3335	932
	0.157	0.028	0.039	3312	799	13920	6525	2170	571	8265	3915	1022
	0.177	0.028	0.039	4111	857	15225	7540	2398	628	8700	4350	1112
	0.197	0.028	0.043	4454	1028	15950	8265	2627	628	9425	4785	1202
	0.217	0.028	0.051	4625	1142	16675	8990	2855	685	9715	5365	1202
	0.236	0.031	0.063	N/A	N/A	N/A	N/A	3198	742	10440	5945	1202
	0.276	0.031	0.071	N/A	N/A	N/A	N/A	3712	857	11310	6525	1202
	0.315	0.031	0.083	N/A	N/A	N/A	N/A	4168	914	12035	7250	1202
						Pu@752°F				Pu@752°F		
Stainless Steel, Inconel, Titanium	0.063	0.016	0.020	1999	571	13050	3625	1713	457	6815	870	788
	0.075	0.020	0.024	2284	571	13195	3915	1827	457	7250	1160	788
	0.087	0.020	0.028	2570	628	13340	4205	1999	514	7540	1595	896
	0.098	0.024	0.031	2855	685	14065	4640	2170	571	8265	2175	932
	0.118	0.024	0.035	3283	742	14500	5220	2427	628	8990	2900	932
	0.138	0.024	0.035	3769	857	15080	5655	2684	742	9715	3625	1022
	0.157	0.028	0.039	4283	971	15515	6090	2969	857	10440	4350	1112
	0.177	0.028	0.039	4711	1256	15950	6525	3198	1028	11165	4930	1202
	0.197	0.028	0.043	N/A	N/A	N/A	N/A	3426	1085	11890	5365	1292
	0.217	0.028	0.051	N/A	N/A	N/A	N/A	3712	1142	12615	6090	1292
	0.236	0.031	0.063	N/A	N/A	N/A	N/A	4111	1256	13630	6815	1292
	0.276	0.031	0.071	N/A	N/A	N/A	N/A	4568	1485	14790	7540	1292
	0.315	0.031	0.083	N/A	N/A	N/A	N/A	5139	1656	15660	8410	1292

Calculation Data - Metric

Jacket Material	Cross Section mm	e_2 mm	e_C mm	HELIUM SEALING Y_2 daN/cm	Y_1 daN/cm	Pu20°C daN/cm²	Puθ200°C daN/cm²	BUBBLE SEALING Y_2 daN/cm	Y_1 daN/cm	Pu20°C daN/cm²	Puθ200°C daN/cm²	Max Temp °C
Aluminum	1.6	0.6	0.7	150	20	50	N/A	90	20	35	N/A	150
	1.9	0.7	0.85	160	20	52	N/A	100	20	40	N/A	150
	2.2	0.7	0.9	165	20	53	N/A	105	20	40	N/A	180
	2.5	0.7	0.9	175	20	55	5	115	20	42	5	220
	3.0	0.8	1.0	185	25	55	10	130	20	45	10	250
	3.5	0.8	1.0	190	25	55	14	140	20	47	14	250
	4.0	0.9	1.1	200	25	60	17	150	20	50	17	280
	4.5	0.9	1.2	210	25	60	20	160	20	52	20	280
	5.0	0.9	1.4	220	30	63	22	170	25	55	22	300
	5.5	0.9	1.6	230	30	65	24	180	25	57	24	320
	6.0	1.0	1.8	245	35	67	25	195	30	60	25	340
	7.0	1.0	2.2	270	40	70	28	205	35	65	28	340
	8.0	1.0	2.6	290	50	72	32	225	40	68	31	360
							Puθ250°C				Puθ250°C	
Silver	1.6	0.5	0.6	200	30	65	N/A	150	30	40	N/A	240
	1.9	0.6	0.7	220	30	65	N/A	150	30	40	N/A	240
	2.2	0.6	0.8	230	35	70	6	160	30	40	4	280
	2.5	0.7	0.9	240	45	75	8	170	40	45	5	280
	3.0	0.8	1.0	260	50	85	14	180	45	50	9	300
	3.5	0.8	1.0	280	50	95	22	190	45	55	13	300
	4.0	0.8	1.1	300	55	105	27	200	50	60	16	350
	4.5	0.8	1.1	320	60	115	31	220	50	70	19	370
	5.0	0.8	1.3	340	60	125	36	230	50	80	22	370
	5.5	0.8	1.4	360	65	135	40	250	60	90	25	400
	6.0	0.9	1.7	400	70	150	47	270	60	110	30	450
	7.0	0.9	2.0	440	80	160	54	300	65	125	36	450
	8.0	0.9	2.4	490	90	170	60	350	70	140	42	500
							Puθ300°C				Puθ300°C	
Copper, Soft Iron, Mild Steels	1.6	0.5	0.6	260	40	50	10	190	30	35	5	350
	1.9	0.6	0.7	280	50	50	11	200	40	35	6	350
	2.2	0.6	0.8	300	60	55	13	220	50	35	8	360
	2.5	0.7	0.9	320	70	60	17	230	60	40	10	380
	3.0	0.7	1.0	350	80	65	20	250	70	40	12	380
	3.5	0.7	1.0	390	80	70	23	270	70	45	15	400
	4.0	0.8	1.1	430	90	70	27	290	80	45	17	420
	4.5	0.8	1.1	470	100	80	30	320	80	45	19	450
	5.0	0.8	1.3	510	110	85	33	330	90	50	21	450
	5.5	0.8	1.4	550	120	90	36	360	100	50	23	480
	6.0	0.9	1.7	630	140	95	40	400	100	55	26	520
	7.0	0.9	2.0	740	160	100	45	460	110	60	29	520
	8.0	0.9	2.4	860	190	110	49	530	130	65	32	550
							Puθ350°C				Puθ350°C	
Nickel, Monel, Tantalum	1.6	0.4	0.5	320	80	70	11	200	60	40	7	380
	1.9	0.5	0.6	350	80	72	16	220	60	42	9	380
	2.2	0.5	0.7	390	80	76	21	230	70	44	12	420
	2.5	0.6	0.8	440	100	82	27	270	70	47	16	450
	3.0	0.6	0.9	440	110	87	34	300	80	50	20	480
	3.5	0.6	0.9	490	120	93	40	340	90	54	23	500
	4.0	0.7	1.0	580	140	96	45	380	100	57	27	550
	4.5	0.7	1.0	720	150	105	52	420	110	60	30	600
	5.0	0.7	1.1	780	180	110	57	460	110	65	33	650
	5.5	0.7	1.3	810	200	115	62	500	120	67	37	650
	6.0	0.8	1.6	N/A	N/A	N/A	N/A	560	130	72	41	650
	7.0	0.8	1.8	N/A	N/A	N/A	N/A	650	150	78	45	650
	8.0	0.8	2.1	N/A	N/A	N/A	N/A	730	160	83	50	650
							Puθ400°C				Puθ400°C	
Stainless Steel, Inconel, Titanium	1.6	0.4	0.5	350	100	90	25	300	80	47	6	420
	1.9	0.5	0.6	400	100	91	27	320	80	50	8	420
	2.2	0.5	0.7	450	110	92	29	350	90	52	11	480
	2.5	0.6	0.8	500	120	97	32	380	100	57	15	500
	3.0	0.6	0.9	575	130	100	36	425	110	62	20	500
	3.5	0.6	0.9	660	150	104	39	470	130	67	25	550
	4.0	0.7	1.0	750	170	107	42	520	150	72	30	600
	4.5	0.7	1.0	825	220	110	45	560	180	77	34	650
	5.0	0.7	1.1	N/A	N/A	N/A	N/A	600	190	82	37	700
	5.5	0.7	1.3	N/A	N/A	N/A	N/A	650	200	87	42	700
	6.0	0.8	1.6	N/A	N/A	N/A	N/A	720	220	94	47	700
	7.0	0.8	1.8	N/A	N/A	N/A	N/A	800	260	102	52	700
	8.0	0.8	2.1	N/A	N/A	N/A	N/A	900	290	108	58	700

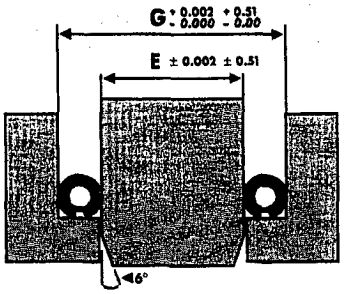
Garlock Helicoflex

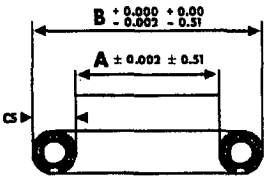
For Additional Information, Please Consult Our Engineering Staff
1-800-233-1722

11

Cavity Design - Axial Pressure

RADIAL COMPRESSION





CALCULATIONS	
Cavity OD (G)	= Seal OD (B)
Shaft OD (E)	= Seal ID (A) +2 e_3
Cavity Finish	< 32 RMS (0.8 um)
Axial Load	= Ya

Note: For best results, the cavity should be lubricated with a product that is compatible with the medium to be sealed.

CHARACTERISTIC VALUES

Aluminum Jacket						Silver Jacket						Nickel Jacket					
CS		e_3		Ya		CS		e_3		Ya		CS		e_3		Ya	
in	mm	in	mm	lb/in	daN/cm	in	mm	in	mm	lb/in	daN/cm	in	mm	in	mm	lb/in	daN/cm
0.063	1.60	0.012	0.30	109	19	0.063	1.60	0.010	0.25	170	30	0.063	1.60	0.008	0.20	228	40
0.102	2.60	0.014	0.35	137	24	0.102	2.60	0.012	0.30	195	34	0.102	2.60	0.010	0.25	308	54
0.118	3.00	0.016	0.40	154	27	0.122	3.10	0.014	0.35	206	36	0.126	3.20	0.012	0.30	343	60
0.157	4.00	0.020	0.50	183	32	0.165	4.20	0.018	0.45	228	40	0.165	4.20	0.016	0.40	434	76
0.200	5.10	0.020	0.50	206	36	0.205	5.20	0.018	0.45	263	46	0.205	5.20	0.016	0.40	525	92
0.260	6.60	0.024	0.60	235	41	0.244	6.20	0.020	0.50	308	54	0.252	6.40	0.018	0.45	640	112

Dimensions in inches | Dimensions in mm

ISO 9001

The technical data contained herein is by way of example and should not be relied on for any specific application. Garlock Helicoflex will be pleased to provide specific technical data or specifications with respect to any customer's particular applications. Use of the technical data or specifications contained herein without the express written approval of Garlock Helicoflex is at user's risk and Garlock Helicoflex expressly disclaims responsibility for such use and the situations which may result therefrom.

Garlock Helicoflex makes no warranty, express or implied, that utilization of the technology or products disclosed herein will not infringe any industrial or intellectual property rights of third parties.

Garlock Helicoflex is constantly involved in engineering and development. Accordingly, Garlock Helicoflex reserves the right to modify, at any time, the technology and product specifications contained herein.

All technical data, specifications and other information contained herein is deemed to be the proprietary intellectual property of Garlock Helicoflex. No reproduction, copy or use thereof may be made without the express written consent of Garlock Helicoflex.

BFGoodrich

Garlock Helicoflex
PO Box 9889
2770 The Boulevard
Columbia, SC 29290 USA
Phone: 1-803-783-1880
Toll Free: 1-800-233-1722
Fax: 1-803-783-4279
www.helicoflex.com
www.garlock.net

Cefilac, S.A.
90 rue de la Roche-du-Geai
42029 Saint-Etienne, FRANCE
Phone: 011-33-4-77-43-51-00
Fax: 011-33-4-77-43-51-52

Garlock Sealing Technologies

Palmyra, NY, USA	1-315-597-4811	Fax: 1-315-597-3216
Paragould, AR, USA	1-870-239-4051	Fax: 1-870-239-4054
Houston, TX USA	1-281-459-7200	Fax: 1-281-458-0502
Sydney, Australia	61-2-9793-2511	Fax: 61-2-9793-2544
São Paulo, Brazil	55-11-884-9680	Fax: 55-11-884-9680
Oakville, Canada	1-905-829-3200	Fax: 1-905-829-3333
Berkshire, England	44-1635-38509	Fax: 44-1635-569573
Neuss, Germany	49-2131-3490	Fax: 49-2131-349-222
Seoul, Korea	822-554-6341	Fax: 822-554-6343
Mexico City, Mexico	52-5-567-7011	Fax: 52-5-368-0418
Singapore	65-284-7873	Fax: 65-284-6089

Catalog Reference: HEL 1

Chapter 5

Table of Contents

5 SHIELDING EVALUATION 5-1
5.1 Discussion and Results 5.1.1-1
5.1.1 NAC-LWT Contents 5.1.1-1
5.2 Gamma and Neutron Sources 5.2.1-1
5.2.1 ORIGEN 5.2.1-1
5.3 Model Specification 5.3.1-1
5.3.1 Description of Radial and Axial Shielding Configuration 5.3.1-1
5.3.2 Shield Regional Densities 5.3.2-1
5.3.3 Metallic Fuel Configuration 5.3.3-1
5.3.4 MTR Fuel Configuration 5.3.4-1
5.3.5 25 PWR Fuel Rods Configuration 5.3.5-1
5.3.6 TRIGA Fuel Element Model Specification and Shielding Evaluation 5.3.6-1
5.3.7 TRIGA Fuel Cluster Rod Model Specification and Shielding Evaluation 5.3.7-1
5.3.8 High Burnup PWR and BWR Rods Shielding Evaluation 5.3.8-1
5.3.9 DIDO Fuel Configuration 5.3.9-1
5.3.10 GA IFM Shielding Evaluation 5.3.10-1
5.3.11 High Burnup PWR and BWR Rods in a Fuel Assembly Lattice 5.3.11-1
5.3.12 Damaged High Burnup PWR and BWR Rods in a Rod Holder 5.3.12-1
5.3.13 TPBAR Shielding Evaluation 5.3.13-1
5.3.14 PULSTAR Fuel Configuration 5.3.14-1
5.3.15 Spiral Fuel Assembly Configuration 5.3.15-1
5.3.16 MOATA Plate Bundle Configuration 5.3.16-1
5.3.17 Irradiated Hardware Shielding Evaluation 5.3.17-1
5.3.18 PWR MOX Rod Fuel Configuration 5.3.18-1
5.4 Shielding Evaluation 5.4.1-1
5.4.1 Shielding Evaluation Codes 5.4.1-1

List of Figures

Figure 5.3.3-1 Three-Dimensional Radial Model 5.3.3-2
Figure 5.3.3-2 End-Fitting Model with Fuel 5.3.3-3
Figure 5.3.3-3 Lead Slump Accident – PWR Top End-Fitting 5.3.3-4
Figure 5.3.3-4 Lead Slump Accident – PWR Bottom End-Fitting 5.3.3-5
Figure 5.3.3-5 Lead Slump Accident – BWR Bottom End-Fitting 5.3.3-6
Figure 5.3.3-6 One-Dimensional Radial Calculational Model 5.3.3-7
Figure 5.3.4-1 MTR Fuel Evaluated Configurations 5.3.4-5
Figure 5.3.4-2 SAS4 Shielding Model for the MTR Fuel Basket in the NAC-LWT (Upper Half) 5.3.4-6
Figure 5.3.4-3 Dose Rates 2 Meters from Transport Vehicle (30 W Uniform Loading) 5.3.4-7
Figure 5.3.6-1 TRIGA Fuel Element One-Dimensional Bounding Radial Dose Rate - Normal Conditions of Transport - Curves and Data Points 5.3.6-7
Figure 5.3.6-2 TRIGA Fuel Element One-Dimensional Bounding Radial Dose Rate - Accident Condition - Curves and Data Points 5.3.6-8
Figure 5.3.6-3 TRIGA SAS4A Radial Model Geometry 5.3.6-9
Figure 5.3.6-4 TRIGA SAS4A Basket Model Geometry 5.3.6-10
Figure 5.3.6-5 TRIGA SAS4A Upper Half Model Geometry (Normal Condition – Shifted Fuel) 5.3.6-11
Figure 5.3.6-6 TRIGA SAS4A Upper Half Model Geometry (Normal Condition) 5.3.6-12
Figure 5.3.6-7 TRIGA SAS4A Lower Half Model Geometry (Normal and Accident Condition) 5.3.6-13
Figure 5.3.7-1 HEU TRIGA Cluster Fuel Rod SAS2H Sample Input (600 GWd/MTU) 5.3.7-3
Figure 5.3.7-2 LEU TRIGA Cluster Fuel Rod SAS2H Sample Input (140 GWd/MTU) 5.3.7-5
Figure 5.3.8-1 PWR Rod SAS2H Model 5.3.8-6
Figure 5.3.8-2 BWR 7×7 SAS2H Model Shown at 80,000 MWd/MTU 5.3.8-6
Figure 5.3.8-3 BWR 8×8 Rod SAS2H Model 5.3.8-7
Figure 5.3.8-4 PWR Rods Axial Burnup and Source Profiles 5.3.8-7
Figure 5.3.8-5 BWR Rods Axial Burnup and Source Profiles 5.3.8-8
Figure 5.3.9-1 SAS2H Input for HEU DIDO Fuel 70% ^{235}U Burnup and 18W Heat Load 5.3.9-5
Figure 5.3.9-2 SAS4 Fuel Gamma Input for HEU DIDO Fuel 70% ^{235}U Burnup and 18W Heat Load – Radial Biasing & Normal Transport Conditions 5.3.9-6
Figure 5.3.9-3 SAS4 Shielding Model for the DIDO Fuel Basket in the NAC-LWT (Upper Half) 5.3.9-12
Figure 5.3.9-4 SAS4 Shielding Model for the DIDO Fuel Basket in the NAC-LWT (Section through Fuel) 5.3.9-13
Figure 5.3.9-5 DIDO LEU Cooling Time vs. Fuel Burnup Basket Module Loading Guidelines for Uniform Loading 5.3.9-14
Figure 5.3.9-6 DIDO MEU Cooling Time vs. Fuel Burnup Basket Module Loading Guidelines for Uniform Loading 5.3.9-14

List of Figures (continued)

Figure 5.3.9-7 DIDO HEU Cooling Time vs. Fuel Burnup Basket Module Loading Guidelines for Uniform Loading 5.3.9-15
Figure 5.3.9-8 DIDO LEU Element Cooling Time vs. ^{235}U % Depletion 5.3.9-15
Figure 5.3.9-9 DIDO MEU Element Cooling Time vs. ^{235}U % Depletion 5.3.9-16
Figure 5.3.9-10 DIDO HEU Element Cooling Time vs. ^{235}U % Depletion 5.3.9-16
Figure 5.3.9-11 Comparison of DIDO Element 25W Minimum Cool Time Curves as a Function of ^{235}U % Depletion 5.3.9-17
Figure 5.3.9-12 Bounding DIDO Element Minimum Cool Time vs. % ^{235}U Depletion 5.3.9-17
Figure 5.3.9-13 18W DIDO HEU Fuel Predicted vs. Actual ^{235}U Depletion Loading Curve 5.3.9-18
Figure 5.3.10-1 ORIGEN-S Input for GA RERTR IFM 5.3.10-3
Figure 5.3.10-2 ORIGEN-S Input for GA HTGR IFM 5.3.10-4
Figure 5.3.10-3 SAS1 Input for GA RERTR IFM 5.3.10-5
Figure 5.3.10-4 SAS1 Input for GA HTGR IFM 5.3.10-6
Figure 5.3.10-5 GA IFM One-Dimensional Radial Model of NAC-LWT 5.3.10-7
Figure 5.3.10-6 One-Dimensional Radial Model of GA RERTR and HTGR IFM 5.3.10-8
Figure 5.3.11-1 PWR Lattice Axial Source Profiles 5.3.11-7
Figure 5.3.11-2 BWR Lattice Axial Source Profiles 5.3.11-7
Figure 5.3.11-3 MCBEND Model of NAC-LWT with Fuel Assembly Lattice – Axial Detail 5.3.11-8
Figure 5.3.11-4 MCBEND Model of NAC-LWT with Fuel Assembly Lattice – Radial Detail 5.3.11-9
Figure 5.3.11-5 Normal Condition Radial Surface Dose Rate Profile by Source Type – Fuel Assembly Lattice 5.3.11-10
Figure 5.3.11-6 Normal Condition Radial 2m Dose Rate Profile by Source Type – Fuel Assembly Lattice 5.3.11-10
Figure 5.3.11-7 Accident Condition Radial 1m Dose Rate Profile by Source Type – Fuel Assembly Lattice 5.3.11-11
Figure 5.3.11-8 MCBEND Input – High Burnup Fuel Lattice – Radial Fuel Gamma 5.3.11-12
Figure 5.3.12-1 MCBEND Model of NAC-LWT with Damaged Fuel Rods – Axial Detail 5.3.12-6
Figure 5.3.12-2 MCBEND Model of NAC-LWT with Damaged Fuel Rods – Radial Detail 5.3.12-7
Figure 5.3.12-3 Normal Condition Axial Surface Dose Rate Profile by Source Type – Damaged Fuel Rods 5.3.12-8
Figure 5.3.12-4 Normal Condition Radial 2m Dose Rate Profile by Source Type – Damaged Fuel Rods 5.3.12-8
Figure 5.3.12-5 Accident Condition Radial 1m Dose Rate Profile by Source Type – Damaged Fuel Rods 5.3.12-9
Figure 5.3.12-6 Sample Input File for Damaged Fuel Evaluation 5.3.12-10
Figure 5.3.13-1 ORIGEN-S Input for TPBARs at 30 Days Cool Time 5.3.13-4

List of Figures (continued)

Figure 5.3.13-2 MCNP Input for 300 TPBARs at 30 Days Cool Time – Normal Conditions & Radial Biasing 5.3.13-5
Figure 5.3.13-3 MCNP Three-Dimensional Model of NAC-LWT with 300 TPBAR Payload – Radial Detail 5.3.13-9
Figure 5.3.13-4 MCNP Three-Dimensional Model of NAC-LWT with 300 TPBAR Payload - Axial Detail 5.3.13-10
Figure 5.3.13-5 Normal Condition Radial Surface Dose Rate Profile for 300 TPBAR Payload 5.3.13-11
Figure 5.3.13-6 Normal Condition Radial 2 Meter Dose Rate Profile for 300 TPBAR Payload 5.3.13-11
Figure 5.3.13-7 Accident Condition Radial 1 Meter Dose Rate Profile for 300 TPBAR Payload 5.3.13-12
Figure 5.3.14-1 PULSTAR Fuel Assembly 5.3.14-6
Figure 5.3.14-2 SAS2H Input for PULSTAR Fuel 5.3.14-7
Figure 5.3.14-3 MCNP Model of NAC-LWT with PULSTAR Fuel – Axial Detail ... 5.3.14-8
Figure 5.3.14-4 MCNP Model of NAC-LWT with PULSTAR Fuel – Radial Detail .. 5.3.14-9
Figure 5.3.14-5 Sample MCNP Input File for Minimum Height Canned PULSTAR Fuel 5.3.14-10
Figure 5.3.14-6 Normal Condition Axial Surface Dose Rate Profile by Source Type – Minimum Height Canned PULSTAR Fuel 5.3.14-14
Figure 5.3.14-7 Normal Condition Radial 2m Dose Rate Profile by Source Type – Minimum Height Canned PULSTAR Fuel 5.3.14-14
Figure 5.3.14-8 Accident Condition Radial 1m Dose Rate Profile by Source Type – Minimum Height Canned PULSTAR Fuel 5.3.14-15
Figure 5.3.15-1 SAS2H Input for Spiral Fuel 70% ^{235}U Depletion and 18-Watt Heat Load 5.3.15-3
Figure 5.3.15-2 Spiral Fuel versus MEU DIDO Gamma Spectrum Comparison (18 Watts, 70% Depletion) 5.3.15-4
Figure 5.3.15-3 Minimum Cool Time Curve for 18-Watt Heat Load (Spiral Fuel and MEU DIDO) 5.3.15-5
Figure 5.3.16-1 SAS2H Input for the MOATA Plate Bundle 5.3.16-3
Figure 5.3.17-1 SAS2H Input for Irradiated Hardware (on a per kg basis) 5.3.17-3
Figure 5.3.17-2 Sample SAS1 Input for Irradiated Hardware (Source 1 kg Material) . 5.3.17-4
Figure 5.3.17-3 Irradiated Hardware One-Dimensional Radial Model of NAC-LWT 5.3.17-5
Figure 5.3.17-4 Irradiated Hardware Normal Condition Surface Dose Rate as a Function of Irradiated Hardware Height 5.3.17-6
Figure 5.3.17-5 Irradiated Hardware Normal Condition 2 Meter Dose Rate as a Function of Irradiated Hardware Height 5.3.17-6
Figure 5.3.17-6 Irradiated Hardware Accident Condition 1 Meter Dose Rate as a Function of Irradiated Hardare Height 5.3.17-7

List of Figures (continued)

Figure 5.3.18-1 Sample SAS2H Input for PWR MOX Fuel 5.3.18-10
Figure 5.3.18-2 PWR Rods Axial Burnup and Source Profiles 5.3.18-11
Figure 5.3.18-3 MCNP Model of NAC-LWT with PWR MOX Fuel – Axial Detail 5.3.18-12
Figure 5.3.18-4 MCNP Model of NAC-LWT with PWR MOX Fuel – Radial Detail 5.3.18-13
Figure 5.3.18-5 Sample MCNP Input File for PWR MOX Fuel (Response Method Benchmark Case) 5.3.18-14
Figure 5.3.18-6 Normal Condition Axial Surface Dose Rate Profile by Source Type – Power Grade MOX at 70 GWd/MTHM, 2% Fissile Material, and 90 Days Cool Time 5.3.18-19
Figure 5.3.18-7 Normal Condition Radial 2m Dose Rate Profile by Source Type – Power Grade MOX at 70 GWd/MTHM, 2% Fissile Material, and 90 Days Cool Time 5.3.18-20
Figure 5.3.18-8 Accident Condition Radial 1m Dose Rate Profile by Source Type – Power Grade MOX at 70 GWd/MTHM, 2% Fissile Material, and 90 Days Cool Time 5.3.18-21
Figure 5.3.18-9 Sample MCNP Input File for Mixed PWR MOX/UO_2 Fuel 5.3.18-22
Figure 5.3.18-10 Comparison of Direct Solution and Response Function Results at Cask Surface for Normal Conditions Model for Discrete Rod Mixed Loading of 8 UO_2 Rods and 8 WG Rods 5.3.18-28
Figure 5.3.18-11 Comparison of Direct Solution and Response Function Results at Cask Surface for Normal Conditions Model for Homogenized WG Material 5.3.18-28
Figure 5.3.18-12 Comparison of Direct Solution and Response Function Results at Cask Surface for Normal Conditions Model for Homogenized LEU Material 5.3.18-29

List of Tables

Table 5.1.1-1 Type, Form, Quantity and Potential Sources of Design Basis Fuel 5.1.1-7
Table 5.1.1-2 Design Basis Fuel for Shielding Evaluation 5.1.1-11
Table 5.1.1-3 Nuclear and Thermal Source Parameters 5.1.1-14
Table 5.1.1-4 Combined Dose Rates for Normal Operations Conditions 5.1.1-15
Table 5.1.1-5 Hypothetical Accident – Loss of Shielding Materials 5.1.1-16
Table 5.1.1-6 Hypothetical Accident –Lead Slump 5.1.1-17
Table 5.2.1-1 LOR-2 Input Data 5.2.1-3
Table 5.2.1-2 Photon Spectrum for Design Basis Fuel 5.2.1-5
Table 5.2.1-3 Fission Product Gas Inventory 5.2.1-6
Table 5.2.1-4 Design Basis Fuel Neutron Spectrum 5.2.1-7
Table 5.3.3-1 Source Material Compositions 5.3.3-8
Table 5.3.3-2 Shield Material Densities and Compositions 5.3.3-8
Table 5.3.4-1 Design Basis MTR Fuel Assembly Characteristics 5.3.4-8
Table 5.3.4-2 MTR Fuel Element Gamma SourceTerms by Thermal Output – 380 grams ^{235}U 5.3.4-9
Table 5.3.4-3 MTR Fuel Element Neutron Source Terms by Thermal Output – 380 grams ^{235}U 5.3.4-10
Table 5.3.4-4 MTR Fuel Element Gamma Source Terms by Thermal Output – 460 grams ^{235}U 5.3.4-11
Table 5.3.4-5 MTR Fuel Element Neutron Source Terms by Thermal Output – 460 grams ^{235}U 5.3.4-12
Table 5.3.4-6 LEU MTR Hardware Source to Fuel Source Comparison 5.3.4-13
Table 5.3.4-7 HEU MTR Hardware Source to Fuel Comparison 5.3.4-14
Table 5.3.4-8 Material Densities for MTR Fuel Shielding Analysis 5.3.4-15
Table 5.3.4-9 LWT Cask Surface Total Dose Rates (Normal Conditions of Transport) 5.3.4-16
Table 5.3.4-10 LWT Cask Plan of Conveyance Dose Rates (Normal Conditions of Transport) 5.3.4-16
Table 5.3.4-11 LWT Cask 2 Meter Off The Plane of Conveyance Dose Rates (Normal Conditions of Transport) 5.3.4-17
Table 5.3.4-12 LWT Cask 1 Meter From the Cask Surface Dose Rates (Normal Conditions of Transport) 5.3.4-17
Table 5.3.4-13 Axial Surface Dose Rates at Cask Lid (Normal Conditions of Transport) 5.3.4-18
Table 5.3.4-14 LWT Cask Dose Rates 5 Meters from the Cask Lid (Back of Tractor Cab) for Normal Conditions of Transport 5.3.4-19
Table 5.3.4-15 LWT Cask Dose Rates – 1 Meter from the Cask Surface (Hypothetical Accident Conditions) 5.3.4-19
Table 5.3.5-1 25 PWR Fuel Rods Design Basis Fuel Source Spectra 5.3.5-2
Table 5.3.5-2 Material Densities for 25 Design Basis PWR Rods Fuel Shielding Analysis 5.3.5-3
Table 5.3.5-3 Cask Radial Dose Rates with 25 Design Basis PWR Fuel Rods (mrem/hr) 5.3.5-4

List of Tables (continued)

Table 5.3.6-1 TRIGA Fuel Element Gamma Source Term - Normal Transport (ACPR, 86,100 MWd/MTU, 231 Days Cooling, 50% ^{235}U Depletion) 5.3.6-14
Table 5.3.6-2 TRIGA Fuel Element Neutron Source Term - Normal Transport (ACPR, 86,100 MWd/MTU, 231 Days Cooling, 50% ^{235}U Depletion) 5.3.6-15
Table 5.3.6-3 TRIGA Fuel Element Gamma Source Term - Accident Conditions (FLIP- LEU-II, 151,100 MWd/MTU, 908 Days Cooling, 80% ^{235}U Depletion) 5.3.6-16
Table 5.3.6-4 TRIGA Fuel Element Neutron Source Term - Accident Conditions (FLIP-LEU-II, 151,100 MWd/MTU, 908 Days Cooling, 80% ^{235}U Depletion) 5.3.6-17
Table 5.3.6-5 Material Densities for TRIGA Fuel Element Shielding Analysis 5.3.6-18
Table 5.3.7-1 TRIGA Fuel Cluster Rod Parameters 5.3.7-7
Table 5.3.7-2 Incoloy 800 Clad Composition 5.3.7-8
Table 5.3.7-3 Representative HEU TRIGA Fuel Cluster Rod Gamma Spectra at 150 GWd/MTU and 1.342 Year Cool Time 5.3.7-9
Table 5.3.7-4 Representative HEU TRIGA Fuel Cluster Rod Neutron Spectrum at 150 GWd/MTU and 1.342 Year Cool Time 5.3.7-10
Table 5.3.7-5 Representative LEU TRIGA Fuel Cluster Rod Gamma Spectra 5.3.7-11
Table 5.3.7-6 Representative LEU TRIGA Fuel Cluster Rod Neutron Spectrum 5.3.7-12
Table 5.3.7-7 Fuel Basket Region Material Composition Used in Shielding Analysis 5.3.7-13
Table 5.3.7-8 Normal Condition Dose Response to Gammas for HEU TRIGA Fuel Cluster Rods 5.3.7-14
Table 5.3.7-9 Normal Condition Dose Response to Neutrons for HEU TRIGA Fuel Cluster Rods 5.3.7-14
Table 5.3.7-10 Accident Condition Dose Response to Gammas for HEU TRIGA Fuel Cluster Rods 5.3.7-15
Table 5.3.7-11 Accident Condition Dose Response to Neutrons for HEU TRIGA Fuel Cluster Rods 5.3.7-15
Table 5.3.7-12 Normal Condition Dose Response to Gammas for LEU TRIGA Fuel Cluster Rods 5.3.7-16
Table 5.3.7-13 Normal Condition Dose Response to Neutrons for LEU TRIGA Fuel Cluster Rods 5.3.7-16
Table 5.3.7-14 Accident Condition Does Response to Gammas for LEU TRIGA Fuel Cluster Rods 5.3.7-17
Table 5.3.7-15 Accident Condition Does Response to Neutrons for LEU TRIGA Fuel Cluster Rods 5.3.7-17
Table 5.3.7-16 HEU TRIGA Fuel Cluster Rod Dose Rate Results at Various Fuel Burnups 5.3.7-18
Table 5.3.7-17 LEU TRIGA Fuel Cluster Rod Dose Rate Results at Various Fuel Burnups 5.3.7-19

List of Tables (continued)

Table 5.3.8-1	High Burnup Fuel Rod Model Parameters	5.3.8-9
Table 5.3.8-2	High Burnup Fuel Assembly Model Parameters	5.3.8-9
Table 5.3.8-3	SCALE 27N18G Neutron Group Structure and ANSI Dose Factors	5.3.8-10
Table 5.3.8-4	SCALE 27N18G Gamma Group Structure and ANSI Dose Factors	5.3.8-11
Table 5.3.8-5	LWT Cask Total Decay Heat [kW] for 25 Rods at Various Cool Times	5.3.8-11
Table 5.3.8-6	PWR 80,000 MWd/MTU Fuel Model Neutron Source Term [n/sec/assy]	5.3.8-12
Table 5.3.8-7	PWR 80,000 MWd/MTU Fuel Model Gamma Source Term [γ/sec/assy]	5.3.8-12
Table 5.3.8-8	BWR 7×7 60,000 MWd/MTU Fuel Model Neutron Source Term [n/sec/assy]	5.3.8-13
Table 5.3.8-9	BWR 7×7 60,000 MWd/MTU Fuel Model Gamma Source Term [γ/sec/assy]	5.3.8-13
Table 5.3.8-10	BWR 7×7 70,000 MWd/MTU Fuel Model Neutron Source Term [n/sec/assy]	5.3.8-14
Table 5.3.8-11	BWR 7×7 70,000 MWd/MTU Fuel Model Gamma Source Term [γ/sec/assy]	5.3.8-14
Table 5.3.8-12	BWR 7×7 80,000 MWd/MTU Fuel Model Neutron Source Term [n/sec/assy]	5.3.8-15
Table 5.3.8-13	BWR 7×7 80,000 MWd/MTU Fuel Model Gamma Source Term [γ/sec/assy]	5.3.8-15
Table 5.3.8-14	BWR 8×8 80,000 MWd/MTU Fuel Model Neutron Source Term [n/sec/assy]	5.3.8-16
Table 5.3.8-15	BWR 8×8 80,000 MWd/MTU Fuel Model Gamma Source Term [γ/sec/assy]	5.3.8-16
Table 5.3.8-16	Fuel Axial Source Profile Parameters	5.3.8-17
Table 5.3.8-17	PWR Fuel Axial Source Profile	5.3.8-17
Table 5.3.8-18	BWR Fuel Axial Source Profile	5.3.8-18
Table 5.3.8-19	Fuel Region Homogenized Material Description [atom/b-cm]	5.3.8-19
Table 5.3.8-20	Basket and Cask Shielding Material Composition [atom/b-cm]	5.3.8-19
Table 5.3.8-21	Basket Model Parameters	5.3.8-20
Table 5.3.8-22	LWT Cask One-Dimensional Model for LWR High Burnup Rod Analysis	5.3.8-20
Table 5.3.8-23	LWT Cask Surface Neutron Dose Response Function	5.3.8-21
Table 5.3.8-24	LWT Cask Surface Gamma Dose Response Function	5.3.8-21
Table 5.3.8-25	LWT Cask 2m Neutron Dose Response Function	5.3.8-22
Table 5.3.8-26	LWT Cask 2m Gamma Dose Response Function	5.3.8-22
Table 5.3.8-27	Surface Dose Responses [mrem/hr] and Cask Decay Heat [kW] for Various Decay Times	5.3.8-23
Table 5.3.8-28	2m Dose Responses [mrem/hr] and Cask Decay Heat [kW] for Various Decay Times	5.3.8-24

List of Tables (continued)

Table 5.3.8-29	Loading Table for PWR and BWR High Burnup Rods Showing Minimum Required Cool Time as a Function of Burnup and Enrichment	5.3.8-25
Table 5.3.9-1	Design Basis DIDO Fuel Assembly Characteristics	5.3.9-19
Table 5.3.9-2	DIDO Fuel Assembly Gamma Source Terms by Thermal Output	5.3.9-20
Table 5.3.9-3	DIDO Fuel Assembly Neutron Source Terms by Thermal Output	5.3.9-21
Table 5.3.9-4	Material Densities for DIDO Fuel Shielding Analysis	5.3.9-22
Table 5.3.9-5	LWT Cask Surface Total Dose Rates - DIDO Fuel (Normal Conditions of Transport)	5.3.9-23
Table 5.3.9-6	LWT Cask Plane of Conveyance Dose Rates – DIDO Fuel (Normal Conditions of Transport)	5.3.9-23
Table 5.3.9-7	LWT Cask 2 Meters Off the Plane of Conveyance Dose Rates – DIDO Fuel (Normal Conditions of Transport)	5.3.9-24
Table 5.3.9-8	LWT Cask 1 Meter from the Cask Surface Dose Rates – DIDO Fuel (Normal Conditions of Transport)	5.3.9-24
Table 5.3.9-9	Axial Surface Dose Rates at Cask Lid – DIDO Fuel (Normal Conditions of Transport)	5.3.9-25
Table 5.3.9-10	LWT Cask Dose Rates - 5 Meters from the Cask Lid – DIDO Fuel (Back of Tractor Cab) for Normal Conditions of Transport	5.3.9-26
Table 5.3.9-11	LWT Cask Dose Rates - 1 Meter from the Radial Cask Surface – DIDO Fuel (Hypothetical Accident Conditions)	5.3.9-26
Table 5.3.10-1	GA IFM Activity Inventory as of January 1, 1996	5.3.10-9
Table 5.3.10-2	GA IFM Neutron and Gamma Spectra in SCALE Format	5.3.10-10
Table 5.3.10-3	GA IFM Primary and Secondary Enclosure Dimensions	5.3.10-11
Table 5.3.10-4	Elemental Constituents of GA IFM	5.3.10-12
Table 5.3.10-5	Material Compositions of GA IFM and NAC-LWT	5.3.10-13
Table 5.3.10-6	Combined Payload Radial Dose Rates for GA IFM	5.3.10-14
Table 5.3.11-1	MCBEND Standard 28 Group Neutron Boundaries	5.3.11-25
Table 5.3.11-2	MCBEND Standard 22 Group Gamma Boundaries	5.3.11-26
Table 5.3.11-3	BWR Fuel Assembly Lattice Three-Dimensional Model Parameters	5.3.11-27
Table 5.3.11-4	PWR Fuel Assembly Lattice Three-Dimensional Model Parameters	5.3.11-28
Table 5.3.11-5	Fuel Assembly Lattice SAS2H Burnup Parameters at 80,000 MWd/MTU	5.3.11-29
Table 5.3.11-6	B&W 15×15 80,000 MWd/MTU, 150 Day Cool Time Source Terms in MCBEND Format	5.3.11-30
Table 5.3.11-7	B&W 17×17 PWR 80,000 MWd/MTU, 150 Day Cool Time Source Terms in MCBEND Format	5.3.11-31
Table 5.3.11-8	CE 14×14 PWR 80,000 MWd/MTU, 150 Day Cool Time Source Terms in MCBEND Format	5.3.11-32
Table 5.3.11-9	Westinghouse 14×14 PWR 80,000 MWd/MTU, 150 Day Cool Time Source Terms in MCBEND Format	5.3.11-33

List of Tables (continued)

Table 5.3.11-10	Westinghouse 15×15 PWR 80,000 MWd/MTU, 150 Day Cool Time Source Terms in MCBEND Format	5.3.11-34
Table 5.3.11-11	Westinghouse 17×17 PWR 80,000 MWd/MTU, 150 Day Cool Time Source Terms in MCBEND Format	5.3.11-35
Table 5.3.11-12	BWR 7×7 80,000 MWd/MTU, 210 Day Cool Time Source Terms in MCBEND Format	5.3.11-36
Table 5.3.11-13	BWR 8×8 80,000 MWd/MTU, 150 Day Cool Time Source Terms in MCBEND Format	5.3.11-37
Table 5.3.11-14	PWR Fuel Lattice Axial Source Profile	5.3.11-38
Table 5.3.11-15	BWR Fuel Lattice Axial Source Profile	5.3.11-39
Table 5.3.11-16	BWR Fuel Assembly Lattice Fuel Region Homogenization	5.3.11-40
Table 5.3.11-17	PWR Fuel Assembly Lattice Fuel Region Homogenization	5.3.11-41
Table 5.3.11-18	Fuel Assembly Lattice Activated Hardware Region Homogenization	5.3.11-43
Table 5.3.11-19	Fuel Lattice Accident Condition Damaged Fuel Material Heights	5.3.11-44
Table 5.3.11-20	BWR Fuel Assembly Lattice Fuel Region Homogenized Material Description	5.3.11-44
Table 5.3.11-21	PWR Fuel Assembly Lattice Fuel Region Homogenized Material Description	5.3.11-45
Table 5.3.11-22	Basket and Cask Shielding Material Composition	5.3.11-45
Table 5.3.11-23	ANSI/ANS 6.1.1-1977 Neutron Flux-to-Dose Conversion Factors	5.3.11-46
Table 5.3.11-24	ANSI/ANS 6.1.1-1977 Gamma Flux-to-Dose Conversion Factors	5.3.11-47
Table 5.3.11-25	Maximum Radial Dose Rates for PWR and BWR Fuel Rods in an Irradiated Fuel Assembly Lattice	5.3.11-48
Table 5.3.11-26	Maximum Axial Dose Rates for PWR and BWR Fuel Rods in an Irradiated Fuel Assembly Lattice	5.3.11-48
Table 5.3.12-1	PWR Rods 80,000 MWd/MTU, 150 Day Cool Time Source Terms in MCBEND Format	5.3.12-20
Table 5.3.12-2	BWR 7×7 Rods 80,000 MWd/MTU, 210 Day Cool Time Source Terms in MCBEND Format	5.3.12-21
Table 5.3.12-3	BWR 8×8 Rods 80,000 MWd/MTU, 150 Day Cool Time Source Terms in MCBEND Format	5.3.12-22
Table 5.3.12-4	Fuel Region Homogenization for PWR Fuel Rods	5.3.12-23
Table 5.3.12-5	Fuel Region Homogenization for BWR 7×7 Fuel Rods	5.3.12-23
Table 5.3.12-6	Region Homogenization for BWR 8×8 Fuel Rods	5.3.12-24
Table 5.3.12-7	Intact/Damaged Fuel Mixture Composition Determinations	5.3.12-24
Table 5.3.12-8	Fuel Region Homogenized Material Description	5.3.12-25
Table 5.3.12-9	Maximum Radial Dose Rates for Damaged PWR and BWR Fuel Rods	5.3.12-26
Table 5.3.12-10	Maximum Axial Dose Rates for Damaged PWR and BWR Fuel Rods	5.3.12-26
Table 5.3.13-1	Single TPBAR Activity Inventory at 30 Days Cool Time	5.3.13-13

List of Tables (continued)

Table 5.3.13-2 TPBAR 30-Day Gamma Source Spectrum 5.3.13-14
Table 5.3.13-3 TPBAR Elemental Constituents 5.3.13-15
Table 5.3.13-4 Material Compositions of NAC-LWT for 300 TPBAR Payload 5.3.13-16
Table 5.3.13-5 Dose Rate Summary for 300 TPBARs at 30 Days Cool Time 5.3.13-17
Table 5.3.13-6 Reactor Operating Conditions for TPBAR Source Term Generation. 5.3.13-18
Table 5.3.14-1 PULSTAR Fuel Geometry 5.3.14-16
Table 5.3.14-2 Source Term Generation Parameters for PULSTAR Fuel 5.3.14-16
Table 5.3.14-3 PULSTAR Fuel Assembly Neutron Source Term for 1 Year Cool Time 5.3.14-17
Table 5.3.14-4 PULSTAR Fuel Assembly Gamma Source Term for 1 Year Cool Time 5.3.14-18
Table 5.3.14-5 Intact Assembly Fuel Homogenization for PULSTAR Fuel 5.3.14-19
Table 5.3.14-6 Nominal Height Can Fuel Homogenization for PULSTAR Fuel 5.3.14-19
Table 5.3.14-7 Minimum Height Can Fuel Homogenization for PULSTAR Fuel 5.3.14-19
Table 5.3.14-8 Fuel Region Homogenized Material Description for PULSTAR Fuel 5.3.14-20
Table 5.3.14-9 Cask/Basket Material Descriptions for PULSTAR Fuel 5.3.14-20
Table 5.3.14-10 Maximum Radial Dose Rates for PULSTAR Fuel 5.3.14-21
Table 5.3.14-11 Maximum Axial Dose Rates for PULSTAR Fuel 5.3.14-21
Table 5.3.15-1 Spiral Fuel Assembly Characteristics 5.3.15-6
Table 5.3.15-2 Spiral Fuel Assembly Neutron and Gamma Source (18 Watt Heat Load) 5.3.15-7
Table 5.3.15-3 Spiral Fuel Assembly Source Comparison to DIDO MEU Fuel (70% Depletion and 18 Watts) 5.3.15-8
Table 5.3.15-4 Spiral Fuel Assembly Source Comparison to DIDO MEU Fuel (70% Depletion and Fixed 2.23-Year Cool Time) 5.3.15-9
Table 5.3.16-1 MOATA Plate Bundle Characteristics 5.3.16-4
Table 5.3.16-2 MOATA Plate Bundle Source Comparison 5.3.16-5
Table 5.3.17-1 Irradiated Hardware Gamma Spectra in SCALE Format (1 kg Activated Stainless Steel) 5.3.17-8
Table 5.3.17-2 Material Compositions of the NAC-LWT 5.3.17-9
Table 5.3.18-1 High Burnup Fuel Rod Model Parameters 5.3.18-30
Table 5.3.18-2 High Burnup MOX Fuel Assembly Model Parameters 5.3.18-30
Table 5.3.18-3 MOX Fuel Material Compositions 5.3.18-31
Table 5.3.18-4 Uranium/Plutonium Fractions in MOX Fuel 5.3.18-31
Table 5.3.18-5 PWR Fuel Axial Source Profile 5.3.18-32
Table 5.3.18-6 Fuel Axial Source Profile Parameters 5.3.18-32
Table 5.3.18-7 MOX Source Term Magnitudes at 70 GWd/MTHM and 90 Days Cool Time (per Rod Basis) 5.3.18-33
Table 5.3.18-8 MOX Fuel Cool Time to Reach 143.75 W/Rod (Days) 5.3.18-34
Table 5.3.18-9 PWR Power Grade MOX Fuel Assembly Neutron Source Term for 70 GWd/MTHM, 2% Fissile Pu, and 90 Days Cooling (16 Rods) 5.3.18-35

List of Tables (continued)

Table 5.3.18-10 PWR Power Grade MOX Fuel Assembly Gamma Source Term for 70 GWd/MTHM, 2% Fissile Pu, and 90 Days Cooling (16 Rods) 5.3.18-36
Table 5.3.18-11 Homogenization for PWR MOX Fuel Rod Regions 5.3.18-37
Table 5.3.18-12 Cask/Basket Material Descriptions for PWR MOX Fuel 5.3.18-38
Table 5.3.18-13 Material Composition Effect Study for PWR MOX Fuel 5.3.18-38
Table 5.3.18-14 Mixed Loading/Material Composition Effect Study for PWR MOX Fuel 5.3.18-39
Table 5.3.18-15 MOX/UO_2 Fuel Material Configuration/Homogenization Study 5.3.18-39
Table 5.3.18-16 Maximum Radial Dose Rates for PWR MOX Fuel – 90 Days Cool Time, 2% Fissile Pu 5.3.18-40
Table 5.3.18-17 Detailed Dose Rates for Bounding Fuel – Power Grade PWR MOX Fuel, 2% Fissile Pu, 70 GWd/MTHM and 90 Days Cool Time 5.3.18-40
Table 5.4.1-1 Discrete Axial Source Distribution 5.4.1-2
Table 5.4.1-2 Flux to Dose Conversion Factors 5.4.1-2

5.1 Discussion and Results

The NAC-LWT cask is designed for the safe transport of spent nuclear fuel from various commercial nuclear installations and research reactors.

5.1.1 NAC-LWT Contents

The following contents constitute the design basis for transport in the NAC-LWT cask:

- 1 PWR assembly;
- up to 2 BWR assemblies;
- up to 15 sound metallic fuel rods;
- up to 9 failed metallic fuel rods;
- up to 3 severely failed metallic fuel rods in filters;
- up to 42 MTR fuel elements;
- up to 42 DIDO fuel assemblies;
- up to 25 PWR fuel rods (including up to 14 rods classified as damaged);
- up to 25 BWR fuel rods (including up to 14 rods classified as damaged)[1];
- up to 25 PWR or BWR UO_2 fueled high burnup (up to 80,000 MWd/MTU) rods
- up to 16 PWR MOX or UO_2 rods in any combination (up to 62,500 MWd/MTHM)
- up to 140 TRIGA fuel elements;
- up to 560 TRIGA fuel cluster rods;
- 2 GA IFM packages;
- up to 300 TPBARs (of which two can be prefailed) in a consolidation canister;
- up to 25 TPBARs (of which two can be prefailed) in a rod holder;
- up to 55 TPBARs segmented during PIE, including segmentation debris;
- up to 700 PULSTAR fuel elements (intact or damaged);
- up to 42 spiral fuel assemblies;
- up to 42 MOATA plate bundles;
- any combination of individual ANSTO basket modules containing either spiral fuel assemblies or MOATA plate bundles up to a total of 42 assemblies/bundles; or
- up to 4,000 lbs of solid, irradiated and contaminated hardware.

The 25 high burnup PWR and BWR rods may be transported in three configurations: 1) a maximum of 25 intact fuel rods loaded in the rod holder; 2) a maximum of 25 fuel rods with up to 14 damaged fuel rods or rod fragments loaded in the rod holder; and 3) a maximum of 25

[1] PWR and BWR fuel rods may be transported in either a fuel assembly lattice (skeleton) or in a fuel rod insert. The fuel rod insert may contain PWR instrument/guide tubes and BWR water/inert rods in addition to the fuel rods.

intact fuel rods housed in a fuel assembly lattice within the NAC-LWT PWR basket. The fuel assembly lattice may be irradiated up to an equivalent burnup of 80,000 MWd/MTU.

The metallic fuel consists of a single rod of uranium metal clad with aluminum. The intact metallic fuel rods are placed into a transport canister that will hold five intact rods. The cask can hold three transport canisters for a total of 15 intact metallic fuel rods. In the event the metallic fuel has failed or is suspected of having failed, each fuel rod is sealed in its own container. The failed metallic fuel is loaded into either one of the three holes in the metallic fuel basket or into one of the six openings in the failed metallic fuel basket.

MTR research reactor fuel elements are typically 33 to 57 inches long, including lower nozzle and upper handle. The fuel plates typically consist of U-Al, U_3O_8-Al, or USi-Al clad with aluminum. The fuel plates are held in a parallel arrangement with two thick aluminum slotted pieces to form a fuel element. Standard fuel elements have between 10 and 23 fuel plates. The active fuel region is typically 22.75 inches in height, and the fuel meat is typically 0.023-inch thick. The highly enriched uranium (HEU) fuel has been analyzed conservatively with an enrichment of 90 wt % ^{235}U and fuel loading per element up to 380 g ^{235}U, with a separate analysis performed to accommodate up to 460 g ^{235}U. The design basis fuel parameters are provided in Table 5.1.1-1. The fuel characteristics are presented in Table 5.1.1-2. The dose rates produced from the design basis 470 g ^{235}U and 640 g ^{235}U LEU and 380 g ^{235}U MEU MTR fuel are bounded by the HEU MTR design basis fuel. Therefore, a mixed loading of LEU, MEU and HEU MTR fuel elements are also bounded by a full HEU MTR fuel element loading.

The source term characteristics of the design basis PWR fuel assembly, BWR fuel assembly, metallic rods, 25 PWR rods, 16 PWR MOX rods, and MTR fuels are given in Table 5.1.1-3. The design basis PWR and BWR fuels require two years of cooling after discharge to meet the neutron and gamma source, and decay heat limits of the cask. The MOX rods require 90 days of cooling. The design basis metallic fuel requires one year cooling. The design basis MTR fuel requires a variable number of years cooling, after discharge, to meet the decay heat limits of the cask. Loading configurations must conform to the limits stated in Section 7.1.5.

DIDO research reactor fuel elements typically consist of U-Al, U_3O_8-Al, or U_3Si_2-Al that is aluminum clad. The fuel elements are held in a concentric arrangement inside an outer aluminum cylinder to form a fuel assembly. Fuel assemblies have 4 fuel elements. The active fuel region is typically 23.6 inches in height, and the fuel meat is typically 0.026 inch thick. The highly enriched uranium (HEU) fuel has been analyzed with a minimum enrichment of 90 wt % ^{235}U and fuel loading per assembly up to 190 g ^{235}U. Low enriched (LEU) and medium enriched (MEU) assemblies are evaluated at 190 g ^{235}U with minimum enrichments of 19 and 40 wt % ^{235}U, respectively. The design basis fuel parameters are provided in Table 5.1.1-1. The fuel characteristics are presented in Table 5.1.1-2. As discussed in Section 5, the dose rates produced

from the design basis LEU and MEU DIDO fuel are bounded by the HEU DIDO design basis fuel. Therefore, a mixed loading of LEU, MEU and HEU DIDO fuel assemblies is also bounded by a full HEU DIDO fuel assembly loading.

Two GA IFM Fuel Handling Units (packages) are intended for a single shipment in the NAC-LWT. The first package is composed of Reduced-Enrichment Research and Test Reactor (RERTR) type fuel, which is an Incoloy clad TRIGA fuel. The second is composed of High-Temperature Gas-Cooled Reactor (HTGR) type fuel. Each set of IFM is packaged into stainless steel weld-encapsulated primary and secondary enclosures. Design basis fuel parameters are summarized in Table 5.1.1-1, with fuel characteristics presented in Table 5.1.1-2. Design basis source terms are provided in Table 5.1.1-3. NAC-LWT combined dose rates for GA IFM are bounded by the dose rates for PWR fuel shown in Table 5.1.1-4 through Table 5.1.1-6.

An inventory of up to 300 production TPBARs (of which two can be prefailed) is intended for multiple shipments in the NAC-LWT. A separate content condition is for the transport of up to 55 segmented TPBARs and associated segmentation debris from PIE contained in a waste container. Each TPBAR is a Type 316 stainless steel rod with a 0.381-inch outer diameter and a 0.336-inch inner diameter and a post-irradiation length of approximately 154 inches. Tritium is produced by irradiation of ^{6}Li. Design basis fuel parameters are summarized in Table 5.1.1-1 with characteristics presented in Table 5.1.1-2. Design basis source terms are provided in Table 5.1.1-3. NAC-LWT dose rates for the payloads of up to 300 production TPBARs in a consolidation canister, or up to 55 segmented TPBARs in the waste container, are bounded by the dose rates for PWR fuel shown in Table 5.1.1-4 through Table 5.1.1-6.

Source terms for the high burnup PWR and BWR rods are developed using the SCALE SAS2H code package. Cask dose rates are evaluated using the SCALE SAS1 shielding analysis sequence. Results presented in Section 5.3.8 give the required cool time for PWR and BWR rods as a function of burnup for up to 25 intact fuel rods loaded in the NAC-LWT rod holder. The results presented in Sections 5.3.11 and 5.3.12 demonstrate that dose rate limits are met for the shipment of fuel rods in an irradiated fuel assembly lattice and damaged fuel rods in a rod holder, respectively.

Source terms for the 62,500 MWd/MTHM MOX rods, and the UO_2 rods evaluated in the same section, are developed using the SCALE 5.0 SAS2H code package. Source terms were conservatively calculated for a 70,000 MWd/MTHM burnup. Cask dose rates are evaluated using the MCNP5 Monte Carlo code. Results presented in Section 5.3.18 require the MOX and UO_2 rods to be cooled 90 days prior to shipment (low quality, power grade, MOX fuel requires 120 days to meet heat load limits, but produces dose rates below limits at 90 days).

As can be seen from Table 5.1.1-3, the PWR fuel assembly has the largest source terms and was used as the design basis fuel for shielding analysis of PWR and BWR fuel in the NAC-LWT presented in this section. The metallic fuel shielding analysis is presented in Section 5.3.3. Metallic fuel is shipped with the neutron shield drained and the analysis reflects this. The MTR fuel shielding analysis is presented in Section 5.3.4. The design basis source terms for 25 PWR rods at 60,000 MWd/MTU are well below the design basis PWR fuel assembly. However, the self shielding of 25 PWR rods is less than the 204 rod design basis PWR fuel assembly. Thus, a shielding evaluation of 25 design basis PWR rods is presented in Section 5.3.5. Similarly, the self shielding for either the 25 high burnup PWR or BWR rods at 80,000 MWd/MTU is lower than that of the design basis assemblies. Shielding evaluations for these rods are presented in Sections 5.3.8, 5.3.11 and 5.3.12.

The transport of up to 140 TRIGA fuel elements is evaluated in Section 5.3.6. TRIGA fuel is a solid metal hydride, U-ZrH and may be high enriched (70%), or low enriched (20%). The fuel clad is either aluminum or stainless steel. TRIGA fuel is fabricated in several configurations, as described in Section 1.2.3.1, that vary in weight, active fuel length and overall length. The typical fuel element length and weight is 28.3 inches and 8.82 pounds. The fuel follower control rod element (FFCR) establishes the upper bound weight (13.2 pounds) and length (approximately 45 inches). These elements can only be loaded in the top module of the TRIGA fuel basket. The design basis TRIGA fuel parameters are presented in Table 5.1.1-1 and Table 5.1.1-2. Source term characteristics are presented in Table 5.1.1-3. Cooling time for TRIGA fuel is variable, down to a minimum of 90 days, based on the time required for the decay heat to reach 7.5 watts.

In addition, the transport of TRIGA fuel cluster rods is evaluated in Section 5.3.7. These rods are obtained from the disassembly of the 5×5 (25 rod) arrays comprising the cluster-type TRIGA fuel as shown in Figure 1.2-6. Only the shipment of the fuel cluster rods is analyzed here; no other activated components of the TRIGA cluster assembly are considered for shipment in this analysis. The TRIGA fuel cluster rod is considered to contain a maximum design-basis fuel mass of 50.5 g of U (evaluated at 92 wt % ^{235}U) for HEU cluster rods and 289.4 g of U (19 wt % ^{235}U) for LEU elements. Both elements are modeled with a nominal H to Zr ratio of 1.6. A manufacturing tolerance produced H to Zr ratio of 1.7 is evaluated in Chapter 6 for criticality. The manufacturing tolerances have no significant effect on the shielding evaluations. The HEU fuel contains 10 wt % uranium in the U-ZrH_x fuel meat, while the LEU material contains 45 wt % uranium. The rods are clad in Incoloy 800 and contain upper and lower stainless steel end plugs with a mass of approximately 60.5 g each. For shipment, each rod is placed inside an aluminum tube (ID 0.625 in, OD 0.750 in), with 16 rods occupying each LWT basket opening for a total of up to 112 rods per basket or 560 rods per cask.

The basis for the dose rate evaluation of the TRIGA fuel cluster rods is a source term and one-dimensional shielding analysis in which the minimum cooling time required for the dose rates produced by the TRIGA fuel cluster rods to fall below the dose rates produced by the design basis TRIGA fuel elements. Cooling time results are determined at a large number of fuel burnup values (at approximately every 2.5% increment in ^{235}U depletion).

PULSTAR fuel elements are zirconium alloy-clad UO_2 pellets with a physical design characteristic as listed in Table 5.1.1-1 and Table 5.1.1-2. PULSTAR fuel assemblies are a 5×5 rectangular array of elements surrounded by a zirconium alloy box, with aluminum upper and lower fittings. The element pitch is nominally 0.524 × 0.606 inch. PULSTAR fuel elements are analyzed at a loading of 32 grams ^{235}U per element, an initial enrichment of 6 wt % ^{235}U, and 45% ^{235}U burnup. For conservatism, a cool time of one year from discharge is employed in the shielding analysis; a cool time of at least 1.5 years is required to meet the basket cell heat load limit of 30 W. Source term characteristics are presented in Table 5.1.1-3

Spiral fuel assemblies typically consist of 10 curved plates (also referred to as elements) of metallic U-Al fuel meat that is aluminum clad. The fuel elements are held in a spiral arrangement between an inner and outer aluminum cylinder to form a fuel assembly. The active fuel region is typically 60.325 cm in height, and the fuel meat is typically 0.061 cm thick. The elements are nominally enriched to 80 wt % ^{235}U and were conservatively evaluated at 75 wt % ^{235}U. Maximum fuel loading per assembly is evaluated at 160 g ^{235}U. The design basis fuel parameters are provided in Table 5.1.1-1. The fuel characteristics are presented in Table 5.1.1-2. Applying MEU DIDO fuel assembly minimum cool time curves, which are based on a 40 wt % ^{235}U enriched 190 g ^{235}U fuel assembly, to the spiral fuel elements produces source terms that are bounded by the DIDO MEU fuel. Given similar basket designs, the dose rates produced by the spiral fuel elements are bounded by the MEU DIDO evaluation set.

MOATA fuel bundles consist of a maximum of 14 flat MTR type fuel plates. The fuel plates are composed of a metallic U-Al fuel meat that is aluminum clad. The fuel elements are held in place with aluminum outer plates and pins through the top and bottom of the plate stack in their shipment configuration. The plates are held in a typical MTR plate (12 plates per assembly) with a comb side plate configuration during reactor operations. The active fuel region is typically 58.4 cm in height, and the fuel meat is typically 0.1016-cm thick. The elements are nominally enriched to 90 wt % ^{235}U and were conservatively evaluated at 80 wt % ^{235}U. Maximum fuel loading per plate is evaluated at 25 g ^{235}U (nominal loading is 22 g ^{235}U). The design basis fuel parameters are provided in Table 5.1.1-1. The fuel characteristics are presented in Table 5.1.1-2. The gamma radiation source for the 14 fuel plate bundle is approximately 2% of the DIDO MEU

assembly. Since the basket designs are similar, the dose rates produced by the plate bundle are bounded by the MEU DIDO evaluation set.

The shield materials are selected and arranged to minimize cask weight while maintaining overall shield effectiveness. Lead and steel are chosen as effective gamma radiation shields, and a water tank on the outside of the cask is provided to efficiently moderate and absorb the neutron radiation.

The total neutron and gamma dose rates calculated for the normal operations conditions are shown in Table 5.1.1-4. Note that the maximum dose rate is on the cask lid surfaces at the top end of the cask and does not exceed the design limit of 200 mrem/hour for the surface of the cask. The 10 CFR 71 limits of 10 mrem/hour at two meters from the cask surface and the design limit of 200 mrem/hour on the cask surface are met. Table 5.1.1-4 contains the total dose rates for the hypothetical accident conditions. These dose rates are well under the 49 CFR 173 limit of 1000 mrem/hour at one meter from the cask surface. The dose rates for the lead slump accident are shown in Table 5.1.1-5. These dose rates show that even with the lead slumped, the hypothetical accident dose rate limits have not been exceeded and the cask is safe for transport.

The cask surface fuel centerline normal operations and hypothetical accident dose rates calculated include neutrons and gammas originating from the fuel, neutrons and gammas scattered from the ground and secondary gammas resulting from neutron capture in the neutron shield. All of the other dose locations also include the contribution from the ^{60}Co in the end-fittings.

Table 5.1.1-1 Type, Form, Quantity and Potential Sources of Design Basis Fuel

Fuel Type	-	PWR, Assembly
	-	3.7 wt % ^{235}U maximum initial enrichment
	-	35,000 MWd/MTU maximum burnup
	-	2.5 kW per assembly maximum decay heat
	-	2 years (or more) decay time after reactor discharge
Fuel Form	-	Intact assemblies
Quantity	-	1 design basis fuel assembly
Source of Fuel	-	Commercial PWR nuclear power reactors
Transport Index	-	35
Fuel Type	-	BWR, Assembly
	-	4.0 wt % ^{235}U maximum initial enrichment
	-	30,000 MWd/MTU maximum burnup
	-	1.1 kW per assembly maximum decay heat, 2.2 kW per cask for 2 assemblies
	-	2 years (or more) decay time after reactor discharge
Fuel Form	-	Intact assemblies
Quantity	-	2 design basis fuel assemblies
Source of Fuel	-	Commercial BWR nuclear power reactors
Transport Index	-	35
Fuel Type		High Burnup PWR or BWR rods
	-	5.0 wt % maximum ^{235}U initial enrichment
	-	80,000 MWd/MTU maximum average burnup
	-	2.3 kW /cask maximum decay heat
	-	Minimum cool time dependent on burnup (See Table 5.3.8-29)
Fuel Form	-	Intact rods in a fuel assembly lattice or rod holder and intact rods with up to 14 fuel rods classified as damaged in a rod holder
Quantity	-	Up to 25
Source of Fuel	-	Commercial PWR or BWR nuclear power reactor
Transport Index	-	36 (intact rods) 28 (intact rods in a fuel assembly lattice) 37 (intact rods with 14 rods classified as damaged)
Fuel Type	-	Uranium metal fuel rods
	-	Natural wt % ^{235}U
	-	1,600 MWd/MTU maximum burnup
	-	0.0357 kW per sound rod maximum decay heat, 0.54 kW per cask for 15 sound fuel rods
	-	1 year (or more) decay time after reactor discharge
Fuel Form	-	Intact or encapsulated failed fuel rods
Quantity	-	15 design basis fuel rods, or 6 design basis failed fuel rods
Source of Fuel	-	Research reactors
Transport Index	-	25

Table 5.1.1-1 Type, Form, Quantity and Potential Sources of Design Basis Fuel (cont'd)

Fuel Type	- Material Test Reactor (MTR) Fuel Elements
	- HEU: 90 wt % ^{235}U, Maximum burnup variable up to 660,000 MWd/MTU for 380 g ^{235}U and 577,500 MWd/MTU for 460 g ^{235}U
	- MEU: 40 wt % ^{235}U, Maximum burnup variable up to 293,300 MWd/MTU for 380 g ^{235}U
	- LEU: 19 wt % ^{235}U, Maximum burnup variable up to 139,300 MWd/MTU for 470 g ^{235}U and 640 g ^{235}U
	- 210 W per basket decay heat
	- Variable cool time down to 90 days using the procedure in Section 7.1.5
Fuel Form	- Intact aluminum clad parallel plates
Quantity	- Up to 42 fuel elements
Source of Fuel	- Research and Material Test Reactors
Transport Index	- 45
Fuel Type	- TRIGA Fuel Element
	- 20 to 70 wt % ^{235}U
	- 80% ^{235}U depletion (approximately 151 GWd/MTU for LEU fuel and 460 GWd/MTU HEU fuel)
	- 7.5 watts per element decay heat
	- Variable cool time down to 90 days
Fuel Form	- Aluminum or stainless steel (304) clad rods, intact, failed or as debris
Quantity	- Up to 140 fuel elements
Source of Fuel	- Test, Research and Isotope Reactors
Transport Index	- 25
Fuel Type	- HEU and LEU TRIGA Fuel Cluster Rods
	- Minimum 92 wt % ^{235}U (HEU) and minimum 19 wt % ^{235}U (LEU)
	- 80% ^{235}U depletion (approximately 600 GWd/MTU for HEU and approximately 140 GWd/MTU for LEU)
	- 1.875 watts per rod decay heat
	- Variable cool time down to 90 days
Fuel Form	- Incoloy 800 clad damaged or undamaged rods
Quantity	- Up to 560 fuel rods
Source of Fuel	- Test, Research and Isotope Reactors
Transport Index	- 17.9
Fuel Type	- DIDO Fuel Assemblies
	- HEU: 90 wt % ^{235}U, Maximum burnup variable up to 577,460 MWd/MTU or 70% ^{235}U depletion
	- MEU: 40 wt % ^{235}U, Maximum burnup variable up to 256,650 MWd/MTU or 70% ^{235}U depletion
	- LEU: 19 wt % ^{235}U, Maximum burnup variable up to 121,910 MWd/MTU or 70% ^{235}U depletion
	- 175 or 126 W per basket decay heat
	- Variable cool time down to 180 days using the procedure in Section 7.1.4

Table 5.1.1-1 Type, Form, Quantity and Potential Sources of Design Basis Fuel (cont'd)

Fuel Form	-	Intact aluminum clad concentric fuel tubes
Quantity	-	Up to 42 fuel assemblies
Source of Fuel	-	Research Reactors
Transport Index	-	40.1
Fuel Type	-	General Atomics (GA) Irradiated Fuel Material (IFM)
	-	RERTR (see activity inventory in Table 5.3.10-1)
	-	HTGR (see activity inventory in Table 5.3.10-1)
	-	<13.05 W
	-	Transport after 1/1/96
Fuel Form	-	RERTR: 13 intact TRIGA elements, 7 sectioned elements
	-	HTGR: Spherical loose fuel particles, cylindrical fuel rods, 2 fuel pebbles
Quantity	-	1 Fuel Handling Unit holding RERTR IFM and 1 Fuel Handling Unit holding HTGR IFM
Source of Fuel	-	Research reactors, commercial LWR reactors
Transport Index	-	<1
Maximum Activity	-	3,403 Ci
Material Type	-	Tritium Producing Burnable Absorber Rods (TPBARs)
	-	3.35 W/TPBARs; 1.005 kW total[1] (max. for 300 TPBARs)
	-	30 days minimum cool time
Material Form	-	Type 316 stainless steel clad TPBARs
Quantity	-	Up to 300 TPBARs (of which two can be prefailed) in consolidation canister
	-	Up to 25 TPBARs (of which two can be prefailed) in rod holder
Source of Material	-	Commercial LWR reactors
Transport Index	-	22
Maximum Activity	-	12,800 Ci/TPBAR; 3,840,000 Ci total[1] (max. for 300 TPBARs)
Material Type	-	Tritium Producing Burnable Poison Rods (TPBARs)
	-	2.31 W/TPBAR, 127 W total
	-	90 days
Material Form	-	Type 316 stainless steel clad TPBARs segmented for PIE
Quantity	-	Up to 55 segmented TPBARs
Source of Material	-	Commercial LWRs
Transport Index	-	22[2]
Maximum Activity	-	12,000 Ci/TPBAR, 665,500 Ci total

[1] Conservatively calculated for 30-day minimum cooling time. Actual minimum cooling period for thermal requirements is 90 days.

[2] Conservatively applied 300 TPBAR shipment transport index.

Table 5.1.1-1 Type, Form, Quantity and Potential Sources of Design Basis Fuel (cont'd)

Fuel Type	-	PULSTAR Fuel Elements
	-	6 wt % ^{235}U
	-	32 grams ^{235}U per element
	-	45% ^{235}U depletion (burnup)
	-	210 W per basket decay heat (30 watts per basket cell) × 4 = 840W
		Minimum cool time from discharge of 1.5 years[3]
Fuel Form	-	Intact assemblies; intact elements in fuel rod insert; canned intact or failed elements
Quantity	-	Up to 700 elements (25 elements per cell)
Sources of Fuel	-	Research reactors
Transport Index	-	25
Fuel Type	-	Spiral Fuel Assemblies
	-	75 wt % ^{235}U, maximum burnup variable up to 70% ^{235}U depletion
	-	18 W per assembly , 126 W per basket (at given cool time and burnup limits, maximum heat load is 15.7 W per assembly or 110 W per basket)
		Variable cool time down to 270 days using the procedure in Section 7.1.4 for 18 W DIDO MEU fuel
Fuel Form	-	Intact aluminum clad fuel plates within concentric aluminum inner and outer shells
Quantity	-	Up to 42 fuel assemblies
Sources of Fuel	-	Research reactors
Transport Index	-	40.1 (applied bounding MEU DIDO limit)
Fuel Type	-	MOATA Plate Bundles
	-	80 wt % ^{235}U, maximum burnup variable up to a 30,000 MWd/MTU or 4.1% ^{235}U depletion
Fuel Form	-	Intact aluminum-clad fuel plates
Quantity	-	Up to 42 bundles
Sources of Fuel	-	Research reactors
Transport Index	-	40.1 (applied bounding MEU DIDO limit)
Fuel Type	-	PWR MOX or UO_2 rods (including up to 9 BPRAs)
	-	5.0 wt % maximum ^{235}U initial enrichment for UO_2 rods
		7.0 wt % fissile Pu for MOX rods
	-	62,500 MWd/MTHM maximum average burnup
	-	2.3 kW/cask maximum decay heat
	-	Minimum cool time 90 days (120 days for Power Grade MOX)
Fuel Form	-	Undamaged rods in a rod holder
Quantity	-	Up to 16 (any combination of UO_2 or MOX) fuel rods plus up to 9 BPRAs
Source of Fuel	-	Commercial PWR nuclear power reactor
Transport Index	-	28

[3] Conservatively evaluated at a one-year cool time and 38 watts per basket cell.

Table 5.1.1-2 Design Basis Fuel for Shielding Evaluation

Parameter	PWR	BWR	Metallic	MTR (HEU)	MTR (MEU)	MTR (LEU)	DIDO
Assembly Array	15 × 15	7 × 7	N/A	Parallel Plates	Parallel Plates	Parallel Plates	Fuel Tubes
Assembly or Element Weight (lbs)	1650	750	1805 (15 rods)	13.0 (max)	13.0 (max)	13.0 (max)	15.0 (max)
Assembly/Element/Rod Length (in)	162	176	120.5	25.23[5]	26.14[5]	26.14[5]	24.6
Active Fuel Length (in)	144	144	120.0	24.80	25.59	25.59	23.6
No. Rods per Assembly	204	49	N/A	N/A	N/A	N/A	N/A
No. of Plates per Element	N/A	N/A	N/A	23	23	23	4
Fuel Rod Diameter/Plate Thickness (in)	0.422	0.563	1.36	0.050	0.050	0.050	0.059
Clad Material	Zr-4	Zr-4	Al	Al	Al	Al	Al
Clad Thickness (in)	0.0243	0.032	0.080	0.0150	0.0150	0.0150	0.0167
Pellet Diameter/Meat Thickness (in)	0.3659	0.487	1.36	0.020	0.020	0.020	0.026
Fuel Material	UO_2	UO_2	U metal	U_3O_8-Al; U-Al; or U_3Si_2-Al	U_3O_8-Al; U-Al; or U_3Si_2-Al	U_3O_8-Al; U-Al; or U_3Si_2-Al	U_3O_8-Al; U-Al; or U_3Si_2-Al
Percent Theoretical Density	95	95	100	N/A	N/A	N/A	N/A
Enrichment (wt % ^{235}U)	3.7	4.0	Natural	90[8]	40[8]	19[8]	90 (HEU) 400 (MEU) 199 (LEU)
Maximum Average Burnup (MWd/MTU)	35,000	30,000	1,600	Variable up to 660,000[2,9]	Variable up to 293,300[2]	Variable up to 139,300[2]	Variable up to 577,460 (HEU) 256,650 (MEU) 121,910 (LEU)
Minimum Cool Time	2 Years	2 Years	1 Year	Variable down to 90 days[2]	Variable down to 90 days[2]	Variable down to 90 days[2]	Variable down to 180 days[10]
U Weight (kg/assembly)	475	198	N/A	N/A	N/A	N/A	N/A
U Weight (kg/element)	N/A	N/A	54.5	0.422 0.511	0.950	2.4737 3.3684	0.2111 (HEU) 0.4750 (MEU) 1.0000 (LEU)
UO_2 Weight (kg/assembly)	538.9	224.3	N/A	N/A	N/A	N/A	N/A

Notes:

1. Up to 2 of the PWR rods may have a maximum average burnup of 65,000 MWd/MTU.
2. Variable cool time down to 90 days using the procedure in Section 7.1.4.
3. Design Basis normal condition source term is for ACPR fuel with 86,100 MWd/MTU (50% ^{235}U depletion) and accident condition source term is for FLIP-LEU-II with 151,100 MWd/MTU (80% ^{235}U depletion).
4. Detailed fuel data is presented in Tables 1.2-1 and 6.2.5-1. The values presented here are the physical values for the bounding source terms of the ACPR and FLIP-LEU-II fuel types.
5. For MTR fuel assemblies, which are cut to remove non-fuel bearing hardware prior to transport, a nominal 0.28 inch of nonfuel hardware will remain above and below the active fuel region to allow for fuel handling operations
6. Minimum cool time varies with burnup such that maximum decay heat is 1.875 watts/rod.
7. Varies with burnup – see Table 5.3.8-29.
8. For the shielding evaluation, lower values are conservatively assumed.
9. Maximum burnup of 660,000 MWd/MTU for 380 g ^{235}U and 577,500 MWd/MTU for 460 g ^{235}U.
10. Variable cool time down to 180 days using the procedure in Section 7.1.4.

Table 5.1.1-2 Design Basis Fuel for Shielding Evaluation (continued)

Parameter	PWR Rods	High B/U PWR Rods	High B/U BWR Rods	PWR MOX/UO_2 Rods	TRIGA[4]	TRIGA Fuel Cluster Rods	TPBARs
Assembly Array	N/A	N/A	N/A	N/A	N/A	N/A	N/A
Assembly or Element Weight (lbs)	N/A	N/A	N/A	N/A	8.82 (nominal) 13.2 (max)		2.655
Assembly/Element/Rod Length (in)	162	162	176.1	162	45	31.0	153.035 (pre-irradiation)
Active Fuel Length (in)	144	150	150	153.5	15	22	N/A
No. Rods per Assembly per Shipment	25	25	25	16	1	1	300 Production or 55 Segmented
No. of Plates per Element	N/A	N/A	N/A	N/A	N/A	N/A	N/A
Fuel Rod Diameter/Plate Thickness (in)	0.422	0.440	0.570 (7×7) 0.4961 (other)	0.440	1.478	0.542	0.381
Clad Material	Zr-4	Zr-4	Zr-2	Zirc Alloy	304SS	Incoloy 800	316 SS
Clad Thickness (in)	0.242	0.026	0.036 (7×7) 0.0343 (other)	0.026	0.02	0.016	0.0225
Pellet Diameter/Meat Thickness (in)	0.3659	0.3805	0.4900 (7×7) 0.4213 (other)	0.3805	1.435 (max)	0.510	N/A
Fuel Material	UO_2	UO_2	UO_2	UO_2 – PuO_2/ UO_2	U-ZrH	U-ZrH	N/A
Percent Theoretical Density	97	95	95	95	95	95	N/A
Enrichment (wt % ^{235}U)	5.0	5.0	5.0	5.0 (UO_2) 7.0 fissile Pu (MOX))	20	92 (HEU) 19 (LEU)	N/A
Maximum Average Burnup (MWd/MTHM)	60,000[1]	80,000	60,000 – 80,000	62,500	ACPR 86,100 (50% ^{235}U)[3] FLIP-LEU-II 151,100 (80% ^{235}U)[3]	Variable up to 600,000 (HEU) Variable up to 140,000 (LEU)	N/A
Minimum Cool Time	150 days	150 days	Varies with burnup[7]	90 days (Power Grade MOX – 120 days)	ACPR 231 days FLIP-LEU-II 908 days	Varies with burnup[6]	30 days for production TPBAR; 90 days for PIE TPBAR
U Weight (kg/assembly)	58.2	65.6	108.8 (7×7) 91.3 (other)	N/A	N/A	N/A	N/A
HM Weight (kg/element)	N/A	N/A	N/A	2.63[11]	ACPR 0.280 FLIP-LEU-II 0.824	0.0505 (HEU) 0.2894 (LEU)	N/A
UO_2 Weight (kg/assembly)	66.0	66.0	74.5	N/A	N/A	N/A	N/A

Notes:

1. Up to 2 of the PWR rods may have a maximum average burnup of 65,000 MWd/MTU.
2. Variable cool time down to 90 days using the procedure in Section 7.1.4.
3. Design Basis normal condition source term is for ACPR fuel with 86,100 MWd/MTU (50% ^{235}U depletion) and accident condition source term is for FLIP-LEU-II with 151,100 MWd/MTU (80% ^{235}U depletion).
4. Detailed fuel data is presented in Tables 1.2-1 and 6.2.5-1. The values presented here are the physical values for the bounding source terms of the ACPR and FLIP-LEU-II fuel types.
5. For MTR fuel assemblies, which are cut to remove nonfuel-bearing hardware prior to transport, a nominal 0.28 inch of nonfuel hardware will remain above and below the active fuel region to allow for fuel handling operations.
6. Minimum cool time varies with burnup such that maximum decay heat is 1.875 watts/rod.
7. Varies with burnup – see Table 5.3.8-29.
8. For the shielding evaluation, lower values are conservatively assumed.
9. Maximum burnup of 660,000 MWd/MTU for 380 g ^{235}U and 577,500 MWd/MTU for 460 g ^{235}U.
10. Variable cool time down to 180 days using the procedure in Section 7.1.4.
11. Heavy metal weight per rod.

Table 5.1.1-2 Design Basis Fuel for Shielding Evaluation (continued)

Parameter	GA IFM RERTR	GA IFM HTGR	PULSTAR Fuel	Spiral Fuel Assembly	MOATA Plate Bundle
Assembly Array	N/A	N/A	5×5	Spiral Plates	Parallel Plates
Assembly or Element Weight (lbs)	23.73	23.52	45 (assembly); 1.3 (element)	7.9	13.6[12]
Assembly/Element/Rod Length (in)	29.92	N/A	38 (assembly) 26.2 (element)	63.5 cm	58.4 cm[13]
Active Fuel Length (in)	22.05	N/A	24.1	60.325 cm	58.4 cm
No. Rods per Assembly	13 intact; 7 sectioned	N/A	25	N/A	N/A
No. of Plates per Element	N/A	N/A	N/A	10	maximum 14
Fuel Rod Diameter/Plate Thickness (in)	0.543	N/A	0.47	0.147 cm	0.203 cm
Clad Material	Incoloy	N/A	Zirconium alloy	Al	Al
Clad Thickness (in)	0.031	N/A	0.0185	0.043 cm	N/A
Pellet Diameter/Meat Thickness (in)	0.512	N/A	0.423	0.061 cm	0.1016 cm
Fuel Material	U-ZrH	UC_2; UCO; UO_2; $(Th,U)C_2$; or $(Th,U)O_2$	UO_2	U-Al	U-Al
Percent Theoretical Density	N/A	N/A	94.9% (nominal); 99.5% (analyzed)	N/A	N/A
Enrichment (wt % ^{235}U)	19.7	93.15 (maximum)	6	75	80
Maximum Average Burnup (MWd/MTU)	N/A	N/A	45	70% ^{235}U depletion	30,000 MWd/MTU 4.1% ^{235}U depletion
Minimum Cool Time	None	None	1.0 Year	see MEU DIDO	10 yr
U Weight (kg/assembly)	8.49	0.45	13.33	0.213[14]	0.4375[15]
U Weight (kg/element)	0.42	N/A	0.53	0.0213[16]	0.03125[17]
UO_2 Weight (kg/assembly)	N/A	N/A	15.13	N/A	N/A

Notes: (cont'd)

12. For 14-fuel plate bundle.
13. Not available for in-core configuration. Analysis input restricted to active fuel length.
14. Based on a 160 g ^{235}U fissile material load and listed enrichment.
15. Based on fuel mass per plate multiplied by 14 plates.
16. Based on 10 plates per assembly.
17. Based on 25 g ^{235}U and listed enrichment.

Table 5.1.1-3 Nuclear and Thermal Source Parameters

Payload	Decay Heat (kW)	Gamma Source (g/sec)	Neutron Source (n/sec)	Top End-Fitting (g/sec)	Bottom End-Fitting (g/sec)
1 PWR Assembly	2.5	1.27E+16	2.21E+08	1.49E+13	1.25E+13
2 BWR Assemblies	2.2	1.04E+16	1.34E+08	1.16E+12	2.78E+12
15 Sound Metallic Fuel Rods[2]	0.532	4.37E+15	1.61E+05	N/A	N/A
6 Failed Metallic Fuel Rods[1]	0.03	1.75E+15	6.44E+04	N/A	N/A
42 HEU MTR Elements[3,9]	1.26	7.42E+15	1.40E+08	N/A[15]	N/A[15]
42 MEU MTR Elements[3,8]	1.26	7.86E+15	2.88E+07	N/A[15]	N/A[15]
42 LEU MTR Elements[3,8,14]	1.26	7.51E+15	3.96E+07	N/A[15]	N/A[15]
42 DIDO Assemblies[10]	1.05	6.07E+15	9.73E+04	N/A	N/A
25 PWR Rods[2]	1.41	8.39E+15	1.40E+08	N/A	N/A
TRIGA (140 Elements) Normal Condition	1.05	6.52E+15[4]	1.57E+06	Note 6	Note 6
TRIGA (140 Elements) Accident Condition	1.05	5.97E+15[5]	1.06E+08	Note 6	Note 6
HEU TRIGA Cluster Rod[7]	1.875E-03	1.12E+13	4.918E+01	N/A	N/A
LEU TRIGA Cluster Rod[7]	1.875E-03	1.11E+13	4.005E+02	N/A	N/A
General Atomics Irradiated Fuel Material	0.013	3.429E+13	1.279E+04	Note 11	Note 11
300 Production TPBARs	1.005	6.681E+15	N/A	N/A	N/A
55 PIE TPBARs	1,005	5.6E+13	N/A	N/A	N/A
PULSTAR Fuel	1.05[12]	6.206E+15	2.115E+07	N/A	N/A
Spiral Fuel Assembly[13]	0.756	1.07E+14	4.54E+03	N/A	N/A
MOATA Plate Bundle	0.042	2.2E+12	< 1E+03	N/A	N/A
16 PWR MOX Rods	2.3	1.14E+16	1.17E+09	N/A	N/A

Notes:

1. Gamma and neutron source terms conservatively calculated based on design basis sound metallic fuel rods.
2. 23 rods with 60,000 MWd/MTU burnup and two rods with 65,000 MWd/MTU burnup. Source terms as a function of cool time for the 80,000 MWd/MTU burnup PWR and BWR rods are presented in Section 5.3.8.
3. Bounding values of the gamma and neutron source terms presented for 30W uniform loading for 80% burnup.
4. Based on TRIGA ACPR fuel (86,100 MWd/MTU, 231 days cooling, 50% ^{235}U depletion).
5. Based on TRIGA FLIP-LEU-II fuel (151,100 MWd/MTU, 908 days cooling, 80% ^{235}U depletion).
6. Total hardware gamma is 7.64E+14 gamma/second for ACPR fuel (86,100 MWd/MTU, 231 days cooling, 50% ^{235}U depletion).
7. Source term at TRIGA cluster rods maximum dose rate burnup/cool time combination. For HEU fuel, 150 GWd/MTU, 1.34 years cooled. For LEU fuel, 30 GWd/MTU, 1.5 years cooled. Gamma source includes source from activated inconel clad.
8. Moderator used is light water, H_2O.
9. Moderator used is heavy water, D_2O.
10. Bounding values of the gamma and neutron source terms presented for 25W uniform loading for 70% burnup HEU fuel.
11. Hardware activation, including end-fitting sources, for the TRIGA elements included in the total gamma source for GA IFM.
12. Cool time required to meet 30 watt per cell heat load limit is 1.5 years.
13. Based on 18 W per assembly heat load.
14. Fuel source represents maximum magnitude gamma source obtained from the 470 g ^{235}U analysis, and the maximum neutron source obtained from the 640 g ^{235}U analysis.
15. A maximum 100 grams of cadmium may be included as part of the MTR fuel element or plate construction. Activation of the cadmium produces no significant source per Section 5.3.4.

Table 5.1.1-4 Combined Dose Rates for Normal Operations Conditions

(1 PWR assembly, 35,000 MWd/MTU, 2-year cool time)

Location	Detector I.D.	Radiation	Normal Dose Rate (mrem/hr)
Radial at 2 m from personnel barrier, Fuel midplane	1	Neutron	1.25
		Secondary Gamma	0.18
		Primary Gamma	6.71
		TOTAL	8.14
Radial surface, Fuel midplane	2	Neutron	6.53
		Secondary Gamma	1.37
		Primary Gamma	43.44
		TOTAL	51.34
Bottom surface, Axial centerline	3	Neutron	0.33
		Primary Gamma	35.51
		End-fitting Gamma	17.02
		TOTAL	52.86
Bottom at 2 m from impact limiter, Axial centerline	4	Neutron	0.03
		Primary Gamma	2.19
		End-fitting Gamma	0.79
		TOTAL	3.01
Top surface, Axial centerline	5	Neutron	0.12
		Primary Gamma	54.17
		End-fitting Gamma	41.45
		TOTAL	95.74
Top at 2 m from impact limiter, Axial centerline	6	Neutron	0.01
		Primary Gamma	3.82
		End-fitting Gamma	2.17
		TOTAL	6.00
Top at Cab	7	Neutron	0.00135
		Primary Gamma	0.47
		End-fitting Gamma	0.25
		TOTAL	0.72

Table 5.1.1-5 Hypothetical Accident – Loss of Shielding Materials

(1 PWR assembly, 35,000 MWd/MTU, 2-year cool time)

Location	Detector I.D.	Radiation	Normal Dose Rate (mrem/hr)
Radial surface, Fuel midplane, With neutron shield	8	Neutron Secondary Gamma Primary Gamma TOTAL	6.53 1.37 43.44 51.34
Radial surface, Fuel midplane, Without neutron shield	9	Neutron Secondary Gamma Primary Gamma TOTAL	177.13 0.39 75.00 252.52
Radial at 1 m from surface, Fuel midplane, Without neutron shield	10	Neutron Secondary Gamma Primary Gamma TOTAL	50.93 1.52 54.59 107.04

Table 5.1.1-6 Hypothetical Accident –Lead Slump

Location	Detector I.D.	Radiation	Normal Dose Rate (mrem/hr)
Radial at 1 m from surface, PWR top end-fitting	11	End-fitting Gamma	3.60
		TOTAL	3.60
Radial at 1 m from surface, PWR top end-fitting	12	End-fitting Gamma	1.31
		TOTAL	1.31
Radial at 1 m from surface, PWR top end-fitting	13	End-fitting Gamma	0.80
		TOTAL	0.80
Radial at 1 m from surface, PWR bottom end-fitting	14	End-fitting Gamma	0.01
		TOTAL	0.01
Radial at 1 m from surface, PWR bottom end-fitting	15	End-fitting Gamma	0.35
		TOTAL	0.35
Radial at 1 m from surface, PWR bottom end-fitting	16	End-fitting Gamma	1.48
		TOTAL	1.48
Radial at 1 m from surface, BWR bottom end-fitting	17	End-fitting Gamma	0.10
		TOTAL	0.10
Radial at 1 m from surface, BWR bottom end-fitting	18	End-fitting Gamma	0.54
		TOTAL	0.54
Radial at 1 m from surface, BWR bottom end-fitting	19	End-fitting Gamma	0.84
		TOTAL	0.84

5.3.13 TPBAR Shielding Evaluation

The content condition of up to 300 production TPBARs (of which two can be prefailed) loaded into a consolidation canister and cooled a minimum of 30 days is analyzed for transport in the NAC-LWT cask. Two other NAC-LWT content conditions are evaluated and are shown to be conservatively bounded by the reported results for the 300 TPBARs. The second content condition is for 30-day-cooled transport of up to 25 TPBARs in a rod holder. The third content condition is 55 segmented TPBARs and associated segmentation debris from PIE loaded in a welded waste container and cooled a minimum of 90 days. All TPBAR transport configurations employ the same TPBAR basket, but invoke variations of shipping container/canister within the basket.

A production TPBAR source spectrum is calculated using the activity inventory for a cool time of 30 days from reactor discharge. Source spectra are generated using ORIGEN 2.1 with the PWRU cross-section library. Reactor operating conditions used to generate the activity inventory are summarized in Table 5.3.13-6 (also see Chapter 1, Appendix 1-C). The activity inventory is input into ORIGEN-S, which outputs a gamma spectrum in the 22-group spectrum employed in the analysis.

Table 5.3.13-1 (also see Chapter 1, Appendix 1-C) gives the activity inventory for a single TPBAR at 30 days cool time. Using the table, an ORIGEN-S input is created in order to produce a gamma spectrum in the employed 22-group format. ORIGEN-S input is shown in Figure 5.3.13-1; the resulting spectrum is summarized in Table 5.3.13-2. In the MCNP analysis, a uniform peaking factor of 1.15 is applied over the entire TPBAR length to bound the actual discharge irradiation profile. The application of the peaking factor results in a source of 7.683E+15 photons/sec being employed in the analysis.

The geometric description of the TPBARs is based on the consolidation canister cavity width of 8.15 inches, the modeled TPBAR height of 154 inches, and a TPBAR mass of 1.25 kg/rod. Based on these dimensions, a homogenized source region is modeled, with a material density of 2.24 g/cm^3. The material description in MCNP is based on the element masses given in Table 5.3.13-3 (also see Chapter 1, Appendix 1-C), which also summarizes the resultant number densities of each element. Table 5.3.13-3contains trace elements contained in the TPBAR components, such as uranium in the Zircaloy clad. The listed TPBAR mass and activation source represent a bounding source description and is larger than the structural bounding weight of 1.2 kg/rod.

The NAC-LWT cavity model explicitly considers the axial position of the TPBARs and the consolidation canister as determined by the basket upper and lower fittings and the TPBAR spacer. The TPBARs are modeled at their highest position in the cask cavity, which is the difference of the cavity height, TPBAR height, and spacer height. The resultant axial offset positions the rods 11.87 inches from the cavity bottom and 12.13 inches from the cavity top. For conservatism, the cavity model considers only the extents of the upper and lower basket fittings and the basket spacer; these regions are modeled as voids. Radial shielding in the cavity is provided by the 0.135-inch thick consolidation canister and the aluminum basket shell.

MCNP input for the normal conditions model with radial biasing is shown in Figure 5.3.13-2; sketches of key radial and axial dimensions are shown in Figure 5.3.13-3 and Figure 5.3.13-4, respectively. In the accident analysis, the neutron shield and shell are conservatively modeled as void. Material descriptions of the NAC-LWT constituent volumes are summarized in Table 5.3.13-4.

Normal and hypothetical accident condition radial and axial maximum and average dose rates for a payload of 300 production TPBARs at 30 days cool time are shown in Table 5.3.13-5. Dose rates are below regulatory limits at the surface and 2 meters from the truck bed. The transport index, based on the normal conditions dose rate at 1 meter from the package, is 22. Significant margin exists to the 1000 mrem/hr 1 meter hypothetical accident condition dose rate limit.

Dose rates for the 300 TPBAR consolidation canister bound those of 25 TPBARs in the rod holder (located in the PWR/BWR Transport Canister). The source term for the 25 TPBAR rod holder configuration is 1/12 the source of the 300 rod consolidation canister payload. The PWR/BWR canister lid structure provides source offset and shielding to minimize streaming above the lead shield and limits the evaluation to a radial dose comparison. Cask internal radial shielding of the consolidation canister payload is limited to the thin basket and consolidation canister shells. The 25 TPBAR configuration provides significant additional shielding due to the 5×5 rod holder mass, canister internal spacer, canister shell, PWR/BWR basket insert and basket shell. Combining the reduced source with increased shielding will produce lower dose rates for the rod holder configuration than those calculated for the consolidation canister with 300 TPBARs. The transport index of 22 calculated for the 300 TPBARs is conservatively assigned to the 25 TPBAR payload.

The significantly smaller source term of 55 segmented TPBARs cooled for a minimum of 90 days is bounded by the source term of 300 TPBARs cooled 30 days and the associated dose analysis reported herein. The 55 segmented TPBAR dose rates will be significantly below the regulatory limits for normal conditions of transport and hypothetical accident conditions. The transport index applied to this content is 22.

Figure 5.3.13-5 through Figure 5.3.13-7 show radial dose rate profiles under normal and hypothetical accident conditions.

Dose conversion and quality factors used in the analysis are those from ANSI/ANS-6.1.1-1977.

The three-dimensional Monte Carlo code MCNP (version 4C) is employed in the shielding analysis (ORNL). Significant validation literature is available on MCNP and it represents an industry standard tool for spent fuel cask evaluations. Confirmatory calculations against other validated shielding codes (SCALE and MCBEND) on NAC casks have further validated the use of MCNP for shielding evaluations of the NAC-LWT.

Figure 5.3.13-1 ORIGEN-S Input for TPBARs at 30 Days Cool Time

```
#ORIGENS
0$$  A11 71  E T
DECAY CASE
3$$ 21 1 1 28  A16 4  A33 22  E T
35$$ 0 T
54$$ A8 1  E
56$$ A2 1  A6 1  A10  0  A13 84  A14 5  A15 3 E
57** 0 E T
TPBAR Spectrum Generation
Cool Time of 30 Days
60** 1.E-20
61** F1E-20
65$$
'GRAM-ATOMS    GRAMS     CURIES      WATTS-ALL  WATTS-GAMMA
  21R1
  21R1
  21R1
81$$ 2 0 26 1  E
82$$  2
83**  1.40E+7  1.20E+7  1.00E+7  8.00E+6  6.50E+6
      5.00E+6  4.00E+6  3.00E+6  2.50E+6  2.00E+6
      1.66E+6  1.44E+6  1.22E+6  1.00E+6  8.00E+5
      6.00E+5  4.00E+5  3.00E+5  2.00E+5  1.00E+5
      5.00E+4  2.00E+4  1.00E+4
84**  1.460E+7 1.350E+7 1.250E+7 1.125E+7 1.000E+7
      8.500E+6 7.000E+6 6.070E+6 4.720E+6 3.680E+6
      2.870E+6 1.740E+6 6.000E+5 3.900E+5 1.100E+5
      6.740E+4 2.480E+4 9.120E+3 2.950E+3 9.610E+2
      3.540E+2 1.660E+2 4.810E+1 1.600E+1 4.000E+0
      1.500E+0 5.500E-1 7.090E-2 0.000E+0
73$$  10030 60140 110240 150320 160350 180370 180390
      190420 200410 200450 200470 210460 210470 240510
      250540 260550 260590 270580 270600 280590 280630
      280660 290640 290660 300650 330760 340750 350820
      380890 390891 390900 390910 400890 400930 400950
      400970 410920 410931 410940 410950 410951 410960
      410970 410971 420930 420990 430990 441030 481150
      481151 491131 491140 491141 501130 501171 501191
      501210 501211 501230 501250 511220 511240 511250
      511260 521231 521251 551310 561310 561330 561331
      561351 571400 711770 721750 721810 731820 731830
      741810 741850 741870 741880 751860 751880 761910
74**  1.15E+04 1.42E-03  1.65E-13 3.38E-01 1.15E-02 2.40E-01 9.49E-03
      8.34E-12 7.51E-05  2.84E-01 4.66E-06 6.78E-03 1.76E-05 5.44E+02
      3.98E+01 2.12E+02  1.39E+01 2.15E+02 3.57E+01 1.68E-01 2.29E+01
      1.38E-07 1.04E-16  1.38E-07 3.87E-03 4.25E-07 7.77E-01 2.25E-08
      5.48E-02 4.18E-06  1.30E-03 1.46E-01 4.18E-06 1.13E-04 5.12E+01
      1.65E-11 6.34E-02  4.02E-06 4.76E-04 6.50E+01 3.80E-01 9.19E-11
      1.78E-11 1.57E-11  1.04E-03 5.11E-02 4.36E-05 2.14E-03 2.27E-07
      1.28E-04 1.14E+00  9.13E-02 9.54E-02 1.14E+00 2.63E+00 7.89E+00
      4.66E-08 5.53E-04  4.22E-01 4.21E-01 2.99E-04 1.43E-02 1.66E+00
      1.56E-02 2.65E-03  3.40E-01 2.34E-02 9.53E-03 7.40E-04 1.95E-09
      4.49E-10 1.86E-07  1.99E-04 2.59E-02 6.06E-01 9.33E+00 1.12E+00
      5.16E-03 1.69E-01  2.99E-09 1.31E-02 4.66E-04 1.33E-02 1.73E-05
75$$  84R1 T
TPBAR Spectrum Generation - Cool Time of 30 Days
56$$ F0 T
END
```

Figure 5.3.13-2 MCNP Input for 300 TPBARs at 30 Days Cool Time – Normal Conditions & Radial Biasing

```
NAC-LWT Cask - Tpbar_030d - Normal Transport Conditions
C Radial Biasing - Fuel Gamma Source
C Cells - TPBARs in Consolidation Canister & Basket - v1.4
1  1  -2.1515  -1          u=2  $ TPBARS
2  0     -2  +1        u=2  $ Can void
3  6  -7.9200  -3  +2        u=2  $ Consol. Can
4  0     -4  +3  +1       u=2  $ Basket void
5  4  -2.7000  -5  +4  -6       u=2  $ Basket shell
6  0     -6  +5        u=2  $ Void
7  0     +6          u=2  $ Outside
C Cells - LWT Cask Normal Conditions v1.4
8  5  -11.3440  -10          u=1  $ BotPb
9  0     -9  fill=2        u=1  $ Cavity
10  6  -7.9200  -8  +10        u=1  $ Bottom
11  6  -7.9200  -7  +8  +12  +15  +9  u=1  $ OuterShell
12  6  -7.9200  -11  +14  +9       u=1  $ InnerShellTaper
13  6  -7.9200  -13  +9        u=1  $ InnerShell
14  5  -11.3440  -14  +13         u=1  $ Lead
15  5  -11.3440  -12  +11  +14       u=1  $ LeadTaper
16  0     -15  +14         u=1  $ LeadGap
17  3  -0.9669  -17  +7        u=1  $ NeutronShield
18  6  -7.9200  -16  +7  +17       u=1  $ NSShell
19  7  -0.4997  -18  +7        u=1  $ UpperLimiter
20  7  -0.4997  -19  +7        u=1  $ LowerLimiter
21  0     -20  +7  +16  +18  +19  u=1  $ Container
22  0     +20          u=1  $ Outside
C Detector Cells - Radial Biasing
100  0  -100  fill=1  $ Surface
200  0  -200  +100  $ 1ft
300  0  -300  +200  $ 1m
400  0  -400  +300  $ 2m
500  0  -500  +400  $ 2m+Convey
600  0  +500  $ Exterior
C Surfaces - TPBARs in Consolidation Canister & Basket - v1.4
1  RPP  -10.3505  10.3505  -10.3505  10.3505  30.1498  421.3098    $ TPBARS
2  RPP  -10.3505  10.3505  -10.3505  10.3505  17.7800  383.5400    $ Consol. can inner
3  RPP  -10.6934  10.6934  -10.6934  10.6934  17.7800  383.5400    $ Consol. can outer
4  RPP  -11.2713  11.2713  -11.2713  11.2713  17.7800  427.9900    $ Basket void
5  RPP  -12.5413  12.5413  -12.5413  12.5413  17.7800  427.9900    $ Basket shell
6  CZ  16.8275              $ Basket OD
C Surfaces - LWT Cask Normal Conditions v1.4
7  RCC  0.0000  0.0000  -26.6700  0.0000  0.0000  507.3650  36.5189  $ Lwt
8  RCC  0.0000  0.0000  -26.6700  0.0000  0.0000  26.6700  36.5189  $ Bottom
9  RCC  0.0000  0.0000  0.0000  0.0000  0.0000  452.1200  16.9863  $ Cavity
10  RCC  0.0000  0.0000  -17.7800  0.0000  0.0000  7.6200  26.3525  $ Bottom gamma shield
11  RCC  0.0000  0.0000  0.0000  0.0000  0.0000  444.5000  20.1740  $ Lead id - taper
12  RCC  0.0000  0.0000  0.0000  0.0000  0.0000  444.5000  31.5976  $ Lead od - taper
13  RCC  0.0000  0.0000  13.8176  0.0000  0.0000  416.8648  18.9103  $ Lead id
14  RCC  0.0000  0.0000  13.8176  0.0000  0.0000  416.8648  33.3271  $ Lead od
15  RCC  0.0000  0.0000  13.8176  0.0000  0.0000  416.8648  33.4645  $ Lead gap
16  RCC  0.0000  0.0000  3.8100  0.0000  0.0000  419.1000  49.8183  $ Neutron shield shell
17  RCC  0.0000  0.0000  5.0800  0.0000  0.0000  416.5600  49.2189  $ Neutron shield
18  RCC  0.0000  0.0000  450.2150  0.0000  0.0000  70.5612  49.8183  $ Upper limiter
19  RCC  0.0000  0.0000  -68.0212  0.0000  0.0000  71.8312  49.8183  $ Lower limiter
20  RCC  0.0000  0.0000  -68.0212  0.0000  0.0000  588.7974  49.8183  $ Container
C Radial Detector DRA (Surface)
100  RCC  0.0000  0.0000  -68.1212  0.0000  0.0000  588.9974  49.9183
101  PZ  -38.6713
102  PZ  -9.2215
103  PZ  20.2284
104  PZ  49.6783
105  PZ  79.1282
106  PZ  108.5780
107  PZ  138.0279
108  PZ  167.4778
109  PZ  196.9276
110  PZ  226.3775
111  PZ  255.8274
112  PZ  285.2772
113  PZ  314.7271
114  PZ  344.1770
115  PZ  373.6269
116  PZ  403.0767
117  PZ  432.5266
118  PZ  461.9765
119  PZ  491.4263
C Radial Detector DRB (1ft)
200  RCC  0.0000  0.0000  -98.6012  0.0000  0.0000  649.9574  80.2983
201  PZ  -66.1033
202  PZ  -33.6055
203  PZ  -1.1076
204  PZ  31.3903
205  PZ  63.8882
206  PZ  96.3860
207  PZ  128.8839
208  PZ  161.3818
209  PZ  193.8796
210  PZ  226.3775
211  PZ  258.8754
212  PZ  291.3732
213  PZ  323.8711
214  PZ  356.3690
215  PZ  388.8669
216  PZ  421.3647
```

Figure 5.3.13-2 MCNP Input for 300 TPBARs at 30 Days Cool Time – Normal Conditions & Radial Biasing (Continued)

```
217  PZ  453.8626
218  PZ  486.3605
219  PZ  518.8583
C Radial Detector DRC (1m)
300  RCC  0.0000  0.0000  -168.1212  0.0000  0.0000  788.9974  149.8183
301  PZ  -135.2463
302  PZ  -102.3714
303  PZ  -69.4965
304  PZ  -36.6216
305  PZ  -3.7467
306  PZ  29.1282
307  PZ  62.0030
308  PZ  94.8779
309  PZ  127.7528
310  PZ  160.6277
311  PZ  193.5026
312  PZ  226.3775
313  PZ  259.2524
314  PZ  292.1273
315  PZ  325.0022
316  PZ  357.8771
317  PZ  390.7520
318  PZ  423.6269
319  PZ  456.5017
320  PZ  489.3766
321  PZ  522.2515
322  PZ  555.1264
323  PZ  588.0013
C Radial Detector DRD (2m)
400  RCC  0.0000  0.0000  -268.1212  0.0000  0.0000  988.9974  249.8183
401  PZ  -226.9130
402  PZ  -185.7048
403  PZ  -144.4965
404  PZ  -103.2883
405  PZ  -62.0801
406  PZ  -20.8719
407  PZ  20.3364
408  PZ  61.5446
409  PZ  102.7528
410  PZ  143.9611
411  PZ  185.1693
412  PZ  226.3775
413  PZ  267.5857
414  PZ  308.7940
415  PZ  350.0022
416  PZ  391.2104
417  PZ  432.4186
418  PZ  473.6269
419  PZ  514.8351
420  PZ  556.0433
421  PZ  597.2515
422  PZ  638.4598
423  PZ  679.6680
C Radial Detector DRE (2m+Convey)
500  RCC  0.0000  0.0000  -269.1212  0.0000  0.0000  990.9974  321.9200
501  PZ  -227.8296
502  PZ  -186.5381
503  PZ  -145.2465
504  PZ  -103.9550
505  PZ  -62.6634
506  PZ  -21.3719
507  PZ  19.9197
508  PZ  61.2113
509  PZ  102.5028
510  PZ  143.7944
511  PZ  185.0859
512  PZ  226.3775
513  PZ  267.6691
514  PZ  308.9606
515  PZ  350.2522
516  PZ  391.5437
517  PZ  432.8353
518  PZ  474.1269
519  PZ  515.4184
520  PZ  556.7100
521  PZ  598.0015
522  PZ  639.2931
523  PZ  680.5846
C
C Materials List - Common Materials - v1.4
C
C Homogenized TPBARs
m1      3000   -2.138E+01  $ Li
       26000   -3.500E+02  $ Fe
       24000   -1.020E+02  $ Cr
       28000   -3.350E+02  $ Ni
        8000   -1.020E+02  $ O
       13000   -8.660E+01  $ Al
       33000   -2.750E-01  $ As
        5000   -1.140E-02  $ B
       56000   -1.680E-01  $ Ba
        6000   -7.120E-01  $ C
       20000   -8.400E-01  $ Ca
       48000   -1.080E-04  $ Cd
```

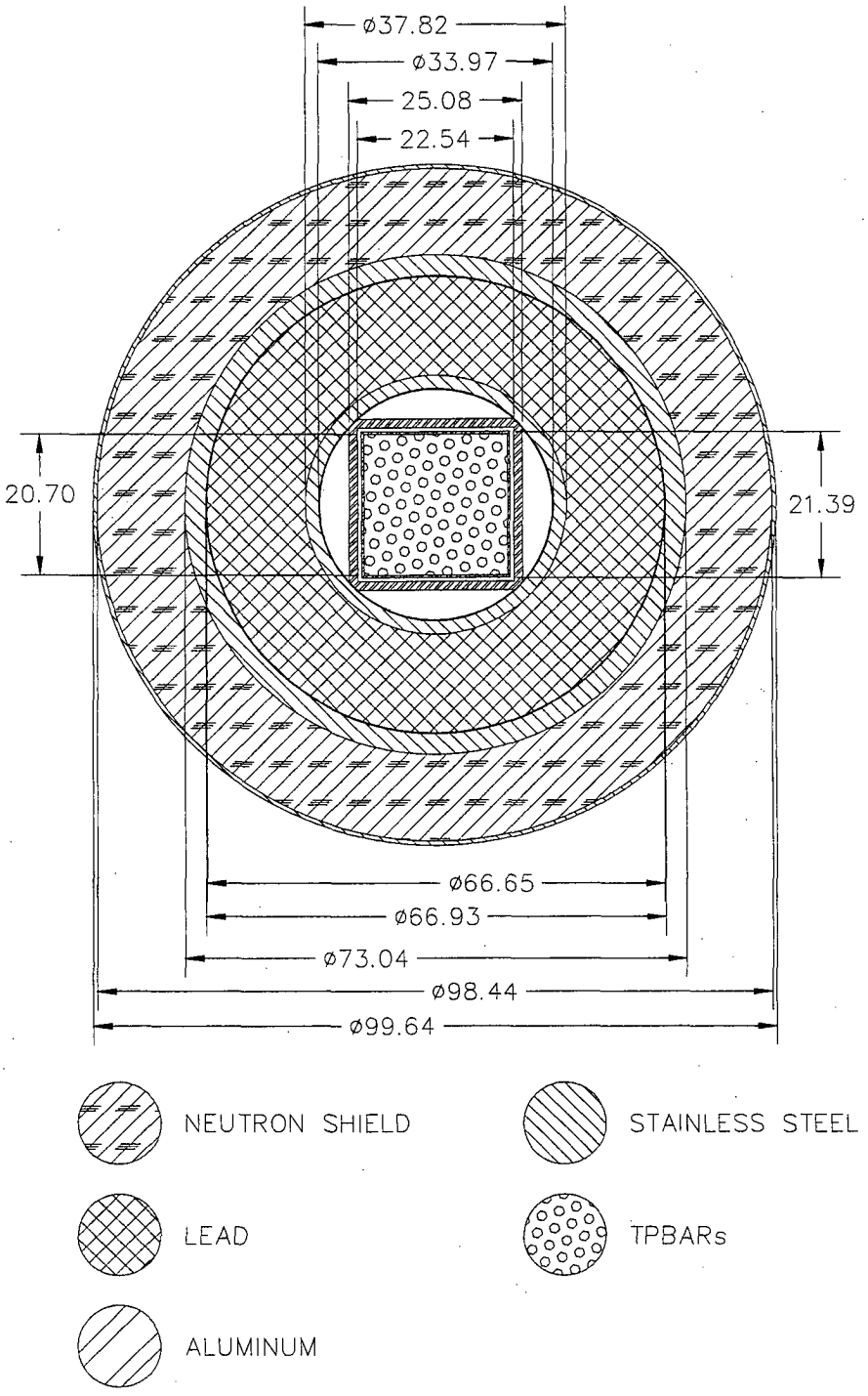
Figure 5.3.13-2 MCNP Input for 300 TPBARs at 30 Days Cool Time – Normal Conditions & Radial Biasing (Continued)

```
        27000  -2.870E-01  $ Co
        29000  -2.370E-01  $ Cu
         1000  -5.380E-03  $ H
        72000  -2.150E-02  $ Hf
        19000  -1.050E+00  $ K
        12000  -4.240E-01  $ Mg
        25000  -1.130E+01  $ Mn
        42000  -1.700E+01  $ Mo
         7000  -7.370E-02  $ N
        11000  -1.050E+00  $ Na
        41000  -2.830E-01  $ Nb
        15000  -2.260E-01  $ P
        82000  -8.400E-02  $ Pb
        16000  -5.650E-02  $ S
        34000  -7.350E-02  $ Se
        14000  -6.360E+00  $ Si
        50000  -3.660E+00  $ Sn
        73000  -1.130E-01  $ Ta
        22000  -1.080E-02  $ Ti
        23000  -2.830E-01  $ V
        74000  -2.150E-02  $ W
        40000  -2.100E+02  $ Zr
        92000  -7.530E-04  $ U
C Water
m2      1001  6.6667E-01  $ H
        8016  3.3333E-01  $ O
mt2  lwtr.01
C Water/Glycol
m3      1001  -1.03651E-01
        8016  -6.75619E-01
        6000  -2.20730E-01
C Aluminum
m4     13027  -1.0
C Lead
m5     82000  -1.0
C Stainless Steel 304
m6     26000  -0.695
       24000  -0.190
       28000  -0.095
       25000  -0.020
C Aluminum Honeycomb Impact Limiter
m7  13027  -1.0
nonu  $ No subcritical multiplication
C
C Cell Importances
C
imp:p 1 26r 0
C
C Source Definition - Fuel Gamma - Tpbar_030d
C
sdef  x=d1  y=d2  z=d3  erg=d4
si1  -10.3505  10.3505
sp1  0  1
si2  -10.3505  10.3505
sp2  0  1
si3  30.1498  421.3098
sp3  0  1
si4  1.000E-02  2.000E-02  5.000E-02  1.000E-01  2.000E-01  3.000E-01
     4.000E-01  6.000E-01  8.000E-01  1.000E+00  1.220E+00  1.440E+00
     1.660E+00  2.000E+00  2.500E+00  3.000E+00  4.000E+00  5.000E+00
     6.500E+00  8.000E+00  1.000E+01  1.200E+01  1.400E+01
sp4  0.0000E+00  3.0175E+11  4.7611E+11  4.4009E+11  2.9577E+11  1.0398E+11
     1.8282E+12  2.5002E+12  4.6571E+12  8.5647E+12  1.6438E+12  1.4198E+12
     1.5788E+08  3.8151E+10  2.2794E+08  4.3234E+04  1.8781E+00  4.8373E-08
     0.0000E+00  0.0000E+00  0.0000E+00  0.0000E+00  0.0000E+00
mode p
nps  40000000
C
C ANSI/ANS-6.1.1-1977 - Gamma Flux-to-Dose Conversion Factors
C (mrem/hr)/(photons/cm2-sec)
C
de0  0.01  0.03  0.05  0.07  0.1  0.15  0.2
     0.25  0.3  0.35  0.4  0.45  0.5  0.55
     0.6  0.65  0.7  0.8  1  1.4  1.8
     2.2  2.6  2.8  3.25  3.75  4.25  4.75
     5  5.25  5.75  6.25  6.75  7.5  9
     11  13  15
df0  3.96E-03  5.82E-04  2.90E-04  2.58E-04  2.83E-04  3.79E-04  5.01E-04
     6.31E-04  7.59E-04  8.78E-04  9.85E-04  1.08E-03  1.17E-03  1.27E-03
     1.36E-03  1.44E-03  1.52E-03  1.68E-03  1.98E-03  2.51E-03  2.99E-03
     3.42E-03  3.82E-03  4.01E-03  4.41E-03  4.83E-03  5.23E-03  5.60E-03
     5.80E-03  6.01E-03  6.37E-03  6.74E-03  7.11E-03  7.66E-03  8.77E-03
     1.03E-02  1.18E-02  1.33E-02
C
C Weight Window Generation - Radial
C
wwg  2 0 0 0 0
wwp:p  5 3 5 0 -1 0
mesh  geom=cyl ref=0 0 226 origin=0.1 0.1 -568
      imesh  15.1 17.0 18.9 33.3 36.5 49.2 49.8 549.8
      iints  5 1 1 5 1 1 1 1
      jmesh  500 541 550 558 568 598 989 1020 1049 1089 1589
      jints  1 1 1 1 1 1 1 1 1 1
      kmesh  0.5 1
```

Figure 5.3.13-2 MCNP Input for 300 TPBARs at 30 Days Cool Time – Normal Conditions & Radial Biasing (Continued)

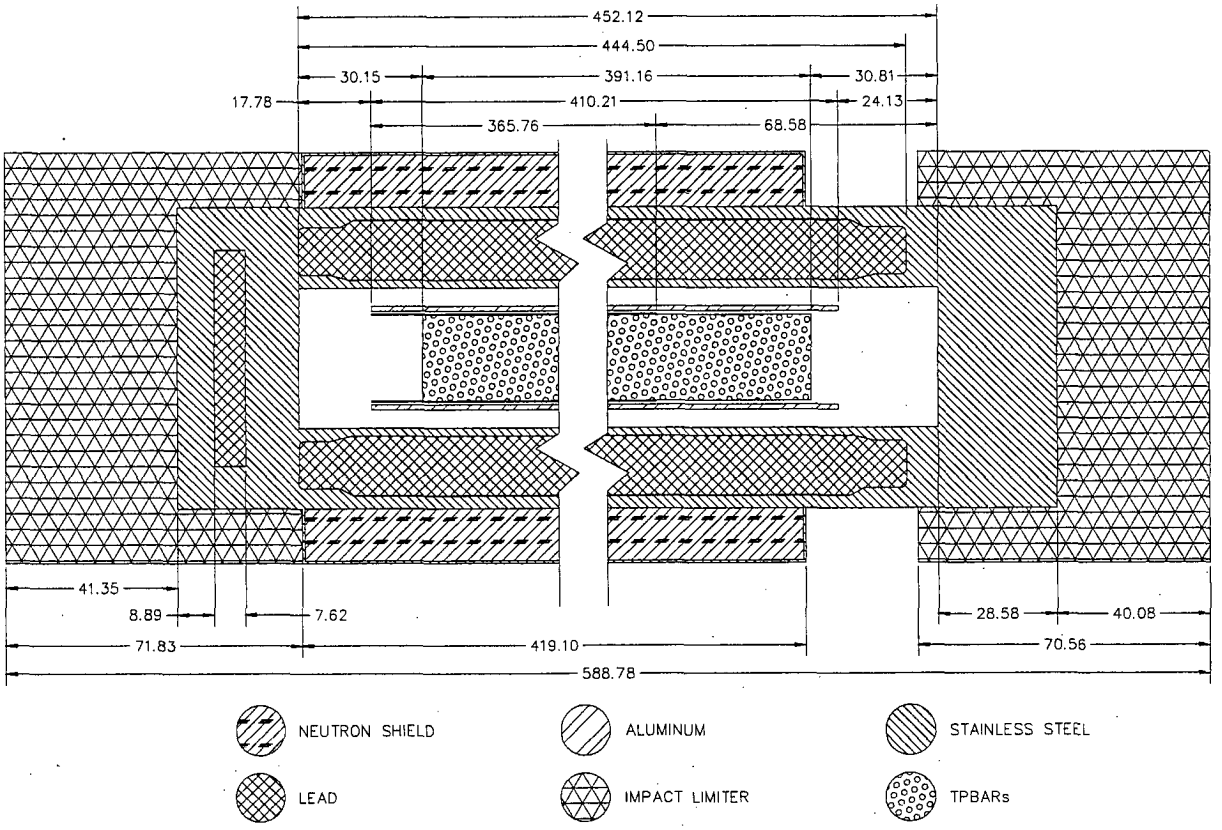
```
      kints  1 1
wwge:p  1e-3 1 20
fc2 Radial Surface Tally
f2:p 100.1
fm2 7.6832E+15
fs2  -101  -102  -103  -104  -105  -106
     -107  -108  -109  -110  -111  -112
     -113  -114  -115  -116  -117  -118
     -119  T
tf2
fc12 Radial 1ft Tally
f12:p 200.1
fm12 7.6832E+15
fs12  -201  -202  -203  -204  -205  -206
     -207  -208  -209  -210  -211  -212
     -213  -214  -215  -216  -217  -218
     -219  T
tf12
fc22 Radial 1m Tally
f22:p 300.1
fm22 7.6832E+15
fs22 -301  -302  -303  -304  -305  -306
     -307  -308  -309  -310  -311  -312
     -313  -314  -315  -316  -317  -318
     -319  -320  -321  -322  -323  T
tf22
fc32 Radial 2m Tally
f32:p 400.1
fm32 7.6832E+15
fs32 -401  -402  -403  -404  -405  -406
     -407  -408  -409  -410  -411  -412
     -413  -414  -415  -416  -417  -418
     -419  -420  -421  -422  -423  T
tf32
fc42 Radial 2m+Convey Tally
f42:p 500.1
fm42 7.6832E+15
fs42 -501  -502  -503  -504  -505  -506
     -507  -508  -509  -510  -511  -512
     -513  -514  -515  -516  -517  -518
     -519  -520  -521  -522  -523  T
tf42
C
C
C Print Control
C
prdmp  -30 -60 1 2
print
```

Figure 5.3.13-3 MCNP Three-Dimensional Model of NAC-LWT with 300 TPBAR Payload – Radial Detail



Dimensions in cm.

Figure 5.3.13-4 MCNP Three-Dimensional Model of NAC-LWT with 300 TPBAR Payload - Axial Detail



Dimensions in cm.

Figure 5.3.13-5 Normal Condition Radial Surface Dose Rate Profile for 300 TPBAR Payload

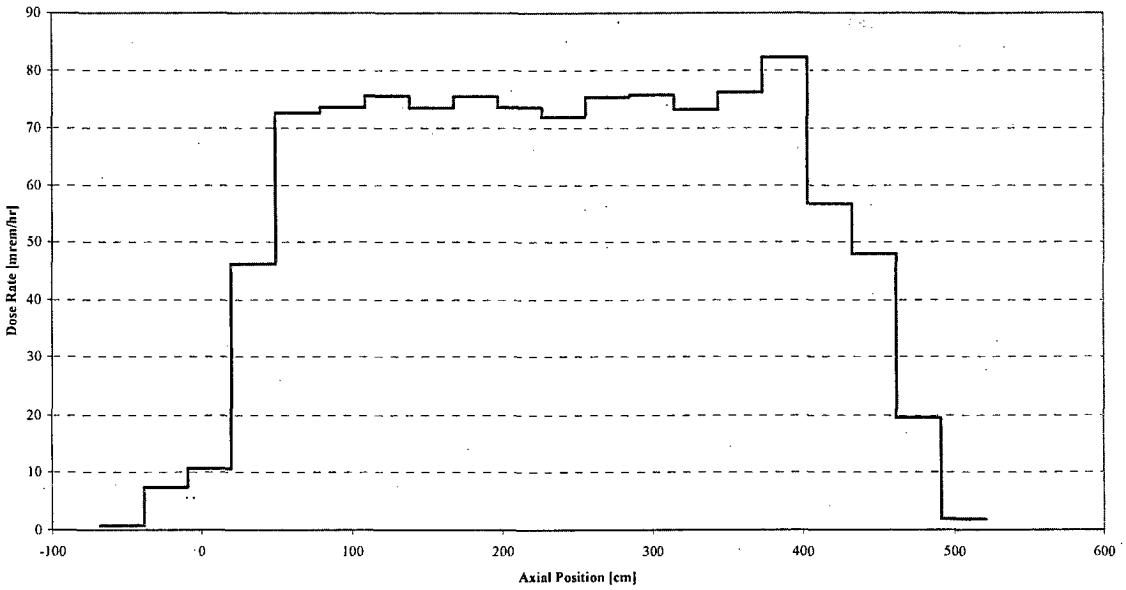


Figure 5.3.13-6 Normal Condition Radial 2 Meter Dose Rate Profile for 300 TPBAR Payload

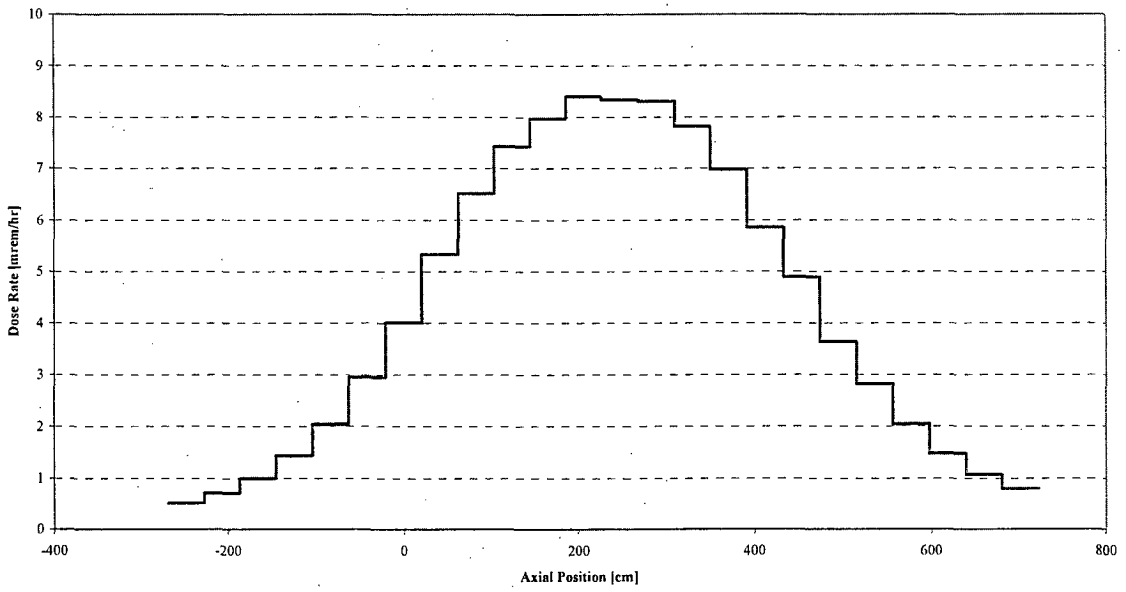


Figure 5.3.13-7 Accident Condition Radial 1 Meter Dose Rate Profile for 300 TPBAR Payload

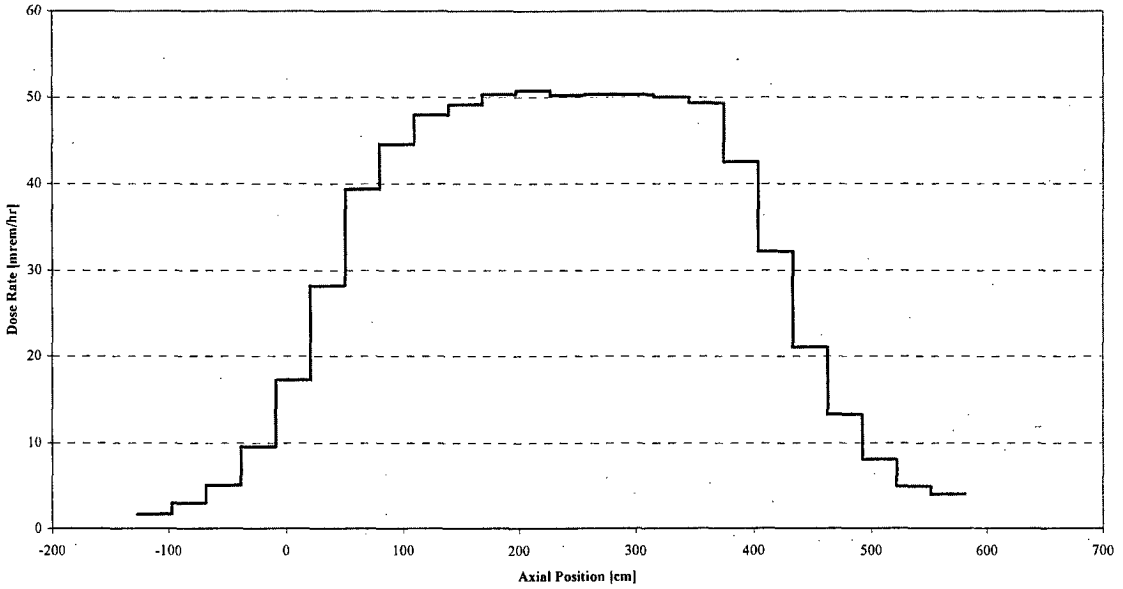


Table 5.3.13-1 Single TPBAR Activity Inventory at 30 Days Cool Time

Isotope	Activity [Ci]	Isotope	Activity [Ci]
^{3}H	1.15E+04	^{97m}Nb	1.57E-11
^{14}C	1.42E-03	^{93}Mo	1.04E-03
^{24}Na	1.65E-13	^{99}Mo	5.11E-02
^{32}P	3.38E-01	^{99}Tc	4.36E-05
^{35}S	1.15E-02	^{103}Ru	2.14E-03
^{37}Ar	2.40E-01	^{115}Cd	2.27E-07
^{39}Ar	9.49E-03	^{115m}Cd	1.28E-04
^{42}K	8.34E-12	^{113m}In	1.14E+00
^{41}Ca	7.51E-05	^{114}In	9.13E-02
^{45}Ca	2.84E-01	^{114m}In	9.54E-02
^{47}Ca	4.66E-06	^{113}Sn	1.14E+00
^{46}Sc	6.78E-03	^{117m}Sn	2.63E+00
^{47}Sc	1.76E-05	^{119m}Sn	7.89E+00
^{51}Cr	5.44E+02	^{121}Sn	4.66E-08
^{54}Mn	3.98E+01	^{121m}Sn	5.53E-04
^{55}Fe	2.12E+02	^{123}Sn	4.22E-01
^{59}Fe	1.39E+01	^{125}Sn	4.21E-01
^{58}Co	2.15E+02	^{122}Sb	2.99E-04
^{60}Co	3.57E+01	^{124}Sb	1.43E-02
^{59}Ni	1.68E-01	^{125}Sb	1.66E+00
^{63}Ni	2.29E+01	^{126}Sb	1.56E-02
^{66}Ni	1.38E-07	^{123m}Te	2.65E-03
^{64}Cu	1.04E-16	^{125m}Te	3.40E-01
^{66}Cu	1.38E-07	^{131}Cs	2.34E-02
^{65}Zn	3.87E-03	^{131}Ba	9.53E-03
^{76}As	4.25E-07	^{133}Ba	7.40E-04
^{75}Se	7.77E-01	^{133m}Ba	1.95E-09
^{82}Br	2.25E-08	^{135m}Ba	4.49E-10
^{89}Sr	5.48E-02	^{140}La	1.86E-07
^{89m}Y	4.18E-06	^{177}Lu	1.99E-04
^{90}Y	1.30E-03	^{175}Hf	2.59E-02
^{91}Y	1.46E-01	^{181}Hf	6.06E-01
^{89}Zr	4.18E-06	^{182}Ta	9.33E+00
^{93}Zr	1.13E-04	^{183}Ta	1.12E+00
^{95}Zr	5.12E+01	^{181}W	5.16E-03
^{97}Zr	1.65E-11	^{185}W	1.69E-01
^{92}Nb	6.34E-02	^{187}W	2.99E-09
^{93m}Nb	4.02E-06	^{188}W	1.31E-02
^{94}Nb	4.76E-04	^{186}Re	4.66E-04
^{95}Nb	6.50E+01	^{188}Re	1.33E-02
^{95m}Nb	3.80E-01	^{191}Os	1.73E-05
^{96}Nb	9.19E-11	Total	1.28E+04
^{97}Nb	1.78E-11		

Table 5.3.13-2 TPBAR 30-Day Gamma Source Spectrum

Energy Group	E_{Lower} [MeV]	E_{Upper} [MeV]	Source [gamma/sec/TPBAR]
1	1.200E+01	1.400E+01	0.000E+00
2	1.000E+01	1.200E+01	0.000E+00
3	8.000E+00	1.000E+01	0.000E+00
4	6.500E+00	8.000E+00	0.000E+00
5	5.000E+00	6.500E+00	0.000E+00
6	4.000E+00	5.000E+00	4.837E-08
7	3.000E+00	4.000E+00	1.878E+00
8	2.500E+00	3.000E+00	4.323E+04
9	2.000E+00	2.500E+00	2.279E+08
10	1.660E+00	2.000E+00	3.815E+10
11	1.440E+00	1.660E+00	1.579E+08
12	1.220E+00	1.440E+00	1.420E+12
13	1.000E+00	1.220E+00	1.644E+12
14	8.000E-01	1.000E+00	8.565E+12
15	6.000E-01	8.000E-01	4.657E+12
16	4.000E-01	6.000E-01	2.500E+12
17	3.000E-01	4.000E-01	1.828E+12
18	2.000E-01	3.000E-01	1.040E+11
19	1.000E-01	2.000E-01	2.958E+11
20	5.000E-02	1.000E-01	4.401E+11
21	2.000E-02	5.000E-02	4.761E+11
22	1.000E-02	2.000E-02	3.018E+11
Total			2.227E+13

Table 5.3.13-3 TPBAR Elemental Constituents

Nuclide	Mass[g]	Number Density [atom/b-cm]
Li	2.14E+01	3.3198E-03
Fe	3.50E+02	6.7548E-03
Cr	1.02E+02	2.1143E-03
Ni	3.10E+02	5.6925E-03
O	1.02E+02	6.8712E-03
Al	8.66E+01	3.4592E-03
As	2.75E-01	3.9560E-06
B	1.14E-02	1.1365E-06
Ba	1.68E-01	1.3185E-06
C	7.05E-01	6.3261E-05
Ca	8.40E-01	2.2589E-05
Cd	1.08E-04	1.0355E-09
Co	2.87E-01	5.2487E-06
Cu	2.37E-01	4.0197E-06
H	5.38E-03	5.7530E-06
Hf	2.15E-02	1.2982E-07
K	1.05E+00	2.8944E-05
Mg	4.24E-01	1.8802E-05
Mn	1.13E+01	2.2168E-04
Mo	1.70E+01	1.9098E-04
N	7.37E-02	5.6709E-06
Na	1.05E+00	4.9224E-05
Nb	2.83E-01	3.2830E-06
P	2.26E-01	7.8639E-06
Pb	8.40E-02	4.3694E-07
S	5.65E-02	1.8991E-06
Se	7.35E-02	1.0032E-06
Si	6.36E+00	2.4406E-04
Sn	3.66E+00	3.3229E-05
Ta	1.13E-01	6.7305E-07
Ti	1.08E-02	2.4317E-07
V	2.83E-01	5.9874E-06
W	2.15E-01	1.2605E-07
Zr	1.86E+02	2.1975E-03
U	7.53E-04	3.4095E-09
Total	1.25E+03	3.2074E-02

Table 5.3.13-4 Material Compositions of NAC-LWT for 300 TPBAR Payload

Material	Density [g/cm³]	MCNP Isotope/Element	Mass Fraction	Number Density [atom/b-cm]
Neutron Shield	9.6690E-01	Hydrogen	1.0365E-01	5.9884E-02
		Oxygen-16	6.7562E-01	2.4595E-02
		Carbon	2.2073E-01	1.0701E-02
Aluminum	2.7000E+00	Aluminum-27	1.0000E+00	6.0262E-02
Lead	1.1344E+01	Lead	1.0000E+00	3.2970E-02
Stainless Steel	7.9200E+00	Iron	6.9500E-01	5.9357E-02
		Chromium	1.9000E-01	1.7428E-02
		Nickel	9.5000E-02	7.6845E-03
		Manganese	2.0000E-02	1.7363E-03
Impact Limiters	4.9970E-01	Aluminum-27	1.0000E+00	1.1153E-02

Table 5.3.13-5 Dose Rate Summary for 300 TPBARs at 30 Days Cool Time

Transport Condition	Dose Rate Location	Maximum		Average	
		[mrem/hr]	FSD	[mrem/hr]	FSD
Normal	Side Surface of Cask	82.3	1.8%	54.5	2.4%
	Top Surface of Cask	14.2	3.7%	7.5	4.2%
	Bottom Surface of Cask	3.8	3.9%	2.0	4.3%
	Side 1m	21.6	1.2%	12.0	1.5%
	2m from Truck - Radial	8.4	1.0%	4.3	1.3%
	2m from Top	0.6	3.5%	0.3	7.5%
	2m from Bottom	0.2	3.6%	0.1	8.9%
Accident	Side Surface of Cask	253.7	2.1%	178.6	2.6%
	Top Surface of Cask	110.7	3.5%	45.3	4.9%
	Bottom Surface of Cask	29.5	4.7%	11.2	6.7%
	Side 1m	50.8	1.2%	30.1	1.7%
	Top 1m	6.9	2.9%	2.7	6.1%
	Bottom 1m	1.8	3.8%	0.7	5.5%

Table 5.3.13-6 Reactor Operating Conditions for TPBAR Source Term Generation

Parameter	Value
Mass of U [kg/assembly]	462
Number of Assemblies	193
Reactor Power [MW]	3,459
Irradiation Time [days]	510
Maximum Assembly Burnup [MWd/MTU]	29,700
^{235}U enrichment [wt %]	3.000
Mass ^{235}U [g/MTU]	30,000
Mass ^{238}U [g/MTU]	970,000
Assembly Specific Power [MW/MTU]	58.24
Radial Assembly Peaking Factor	1.50

Chapter 6

Table of Contents

6 CRITICALITY EVALUATION 6-1
6.1 Discussion and Results 6.1-1
6.2 Package Fuel Loading 6.2-1
6.2.1 PWR Fuel Assemblies 6.2.1-1
6.2.2 BWR Fuel Assemblies 6.2.2-1
6.2.3 MTR Fuel Elements 6.2.3-1
6.2.4 PWR and BWR Rods in a Rod Holder or Fuel Assembly Lattice 6.2.4-1
6.2.5 TRIGA Fuel Elements 6.2.5-1
6.2.6 TRIGA Fuel Cluster Rods 6.2.6-1
6.2.7 Metallic Fuel Rods 6.2.7-1
6.2.8 DIDO Fuel Assemblies 6.2.8-1
6.2.9 General Atomics Irradiated Fuel Material 6.2.9-1
6.2.10 PULSTAR Fuel Elements 6.2.10-1
6.2.11 Spiral Fuel Assemblies 6.2.11-1
6.2.12 MOATA Plate Bundles 6.2.12-1
6.3 Criticality Model Specifications 6.3.1-1
6.3.1 PWR Fuel Assemblies 6.3.1-1
6.3.2 BWR Fuel Assemblies 6.3.2-1
6.3.3 MTR Fuel Elements 6.3.3-1
6.3.4 PWR and BWR Rods in a Rod Holder or Fuel Assembly Lattice 6.3.4-1
6.3.5 TRIGA Fuel Elements and Cluster Rods 6.3.5-1
6.3.6 DIDO Fuel Assemblies 6.3.6-1
6.3.7 General Atomics Irradiated Fuel Material 6.3.7-1
6.3.8 PULSTAR Fuel Contents 6.3.8-1
6.3.9 ANSTO Basket Payload 6.3.9-1
6.4 Criticality Calculations 6.4.1-1
6.4.1 PWR Fuel Assemblies 6.4.1-1
6.4.2 BWR Fuel Assemblies 6.4.2-1
6.4.3 MTR Fuel Elements 6.4.3-1
6.4.4 PWR and BWR Rods in a Rod Holder or Fuel Assembly Lattice 6.4.4-1
6.4.5 TRIGA Fuel Elements 6.4.5-1
6.4.6 TRIGA Fuel Cluster Rods 6.4.6-1
6.4.7 DIDO Fuel Assemblies 6.4.7-1
6.4.8 General Atomics Irradiated Fuel Material 6.4.8-1
6.4.9 PULSTAR Fuel Contents 6.4.9-1
6.4.10 ANSTO Basket Payloads 6.4.10-1
6.5 Critical Benchmarks 6.5.1-1
6.5.1 PWR and BWR Fuel Assemblies 6.5.1-1
6.5.2 MTR and DIDO Fuel Elements 6.5.2-1
6.5.3 TRIGA Fuel Elements 6.5.3-1
6.7 Payload Specific Details 6.7.1-1
6.7.1 PWR Mixed Oxide Fuel Rods 6.7.1-1
6.7.2 Critical Benchmarks 6.7.2-1

Note: See separate Section 6.6 for Appendices to this chapter.

List of Figures

Figure 6.2.3-1 Design Basis HFBR MTR Fuel Element 6.2.3-2
Figure 6.2.5-1 Aluminum Clad TRIGA Fuel Element 6.2.5-2
Figure 6.2.5-2 Stainless Steel Clad TRIGA Fuel Element 6.2.5-3
Figure 6.2.6-1 TRIGA Fuel Cluster Rod Details 6.2.6-2
Figure 6.2.8-1 DIDO Fuel Assembly 6.2.8-2
Figure 6.2.10-1 PULSTAR Fuel Assembly 6.2.10-2
Figure 6.2.11-1 Spiral Fuel Assembly Cross-Section Sketch 6.2.11-2
Figure 6.2.12-1 MOATA Plate Bundle Sketch 6.2.12-2
Figure 6.3.1-1 KENO-Va Model of the NAC-LWT Cask Model with PWR Basket and 15×15 PWR Assembly 6.3.1-4
Figure 6.3.1-2 KENO-Va Model of the NAC-LWT Cask with PWR Basket and Westinghouse 17×17 OFA Assembly 6.3.1-5
Figure 6.3.2-1 KENO-Va Model of the NAC-LWT Cask Model with BWR Basket and 2 Exxon 9×9-2/80 Assemblies 6.3.2-3
Figure 6.3.3-1 KENO-Va Fuel/Basket Unit Cell Model for MTR Fuel 6.3.3-4
Figure 6.3.3-2 KENO-Va Model of NAC-LWT Cask with MTR Fuel 6.3.3-5
Figure 6.3.3-3 Intermediate MTR 42 Basket Module 6.3.3-6
Figure 6.3.3-4 Full Length NAC-LWT Cask Model with 42 MTR Fuel Elements 6.3.3-7
Figure 6.3.3-5 MTR Fuel Basket Module Loading Pattern 6.3.3-8
Figure 6.3.4-1 Triangular Pitch Lattice Formation of 25 PWR Rods 6.3.4-4
Figure 6.3.4-2 KENO-Va Model of the NAC-LWT Cask with 25 PWR Rods 6.3.4-5
Figure 6.3.4-3 Maximum Reactivity Triangular Pitch Lattice Formation of Damaged Fuel Rods 6.3.4-6
Figure 6.3.4-4 KENO-Va Model of the NAC-LWT Cask with Damaged Fuel Rods – Radial Detail 6.3.4-7
Figure 6.3.4-5 KENO-Va Model of the NAC-LWT Cask with Damaged Fuel Rods – Axial Detail 6.3.4-8
Figure 6.3.5-1 Fuel Rod Handling Insert for TRIGA Fuel Cluster Rods 6.3.5-5
Figure 6.3.5-2 Fuel/Basket Unit Cell Model for TRIGA Fuel Elements 6.3.5-6
Figure 6.3.5-3 NAC-LWT Cask with TRIGA Fuel, Nonpoisoned Basket - Radial View 6.3.5-7
Figure 6.3.5-4 KENO-Va Model of NAC-LWT with Poisoned Basket - Radial View 6.3.5-8
Figure 6.3.5-5 NAC-LWT Cask Model with TRIGA Fuel Elements, Nonpoisoned Basket – Axial View 6.3.5-9
Figure 6.3.5-6 Full-Length NAC-LWT Cask Model with TRIGA Fuel Elements, Nonpoisoned Basket – Axial View 6.3.5-10
Figure 6.3.6-1 Intermediate DIDO 42 Basket Module 6.3.6-3
Figure 6.3.6-2 KENO-Va DIDO Fuel in Fuel Tube and Basket Cross-Section 6.3.6-4
Figure 6.3.6-3 KENO-Va Model of NAC-LWT Cask Cross-Section with DIDO Fuel 6.3.6-5
Figure 6.3.6-4 Full Length NAC-LWT Cask Model with 42 DIDO Fuel Assemblies 6.3.6-6
Figure 6.3.7-1 PICTURE Representation of NAC-LWT Cavity with 'Rectangular' Array of GA IFM TRIGA Elements 6.3.7-2
Figure 6.3.7-2 PICTURE Representation of NAC-LWT Cavity with 'Square' Array of GA IFM TRIGA Elements 6.3.7-2

List of Figures (continued)

Figure 6.3.7-3 KENO-Va Model of NAC-LWT Cask Cross-Section with GA IFM 6.3.7-3
Figure 6.3.8-1 PICTURE Representation of NAC-LWT Cavity with PULSTAR Assemblies 6.3.8-3
Figure 6.3.8-2 PICTURE Representation of NAC-LWT Cavity with PULSTAR Elements in 4×4 Rod Insert 6.3.8-3
Figure 6.3.8-3 PICTURE Representation of NAC-LWT Cavity with Canned Discrete PULSTAR Elements 6.3.8-4
Figure 6.3.8-4 PICTURE Representation of NAC-LWT Cavity with Canned Homogenized PULSTAR Elements 6.3.8-4
Figure 6.3.8-5 KENO-Va Model of NAC-LWT Cask Cross-Section with 28 MTR 7-Element Basket 6.3.8-5
Figure 6.3.8-6 Finite Length KENO-Va Model of NAC-LWT Cask with 700 PULSTAR Fuel Elements 6.3.8-6
Figure 6.3.9-1 Intermediate ANSTO Basket Module 6.3.9-3
Figure 6.3.9-2 KENO-Va ANSTO Payloads and Basket Cross-Section 6.3.9-4
Figure 6.3.9-3 KENO-Va Model of NAC-LWT Cask Cross-Section with ANSTO Basket 6.3.9-5
Figure 6.4.3-1 Cask Interior Moderator Density and Blocked Cell Study Results 6.4.3-16
Figure 6.4.4-1 Maximum Reactivity Pitch Determination for Damaged BWR Rod Arrays – Water Exterior 6.4.4-8
Figure 6.4.4-2 Maximum Reactivity Pitch Determination for Damaged PWR Rod Arrays – Water Exterior 6.4.4-8
Figure 6.4.4-3 Maximum Reactivity Determination for Homogenized UO_2/Water Mixture 6.4.4-9
Figure 6.4.5-1 Finite Cask Array Reactivity versus Fuel Zirconium Mass (Dry Cask Cavity) 6.4.5-14
Figure 6.4.5-2 Finite Cask Array Reactivity versus H/Zr Ratio (Dry Cask Cavity) 6.4.5-14
Figure 6.4.5-3 Finite Cask Array Reactivity versus Fuel Mass (Study of ZrH Displacement of Fissile Material for a Fixed Fuel Geometry) 6.4.5-15
Figure 6.4.5-4 Intact Fuel Optimum Moderator Study – 70 wt % ^{235}U Various Zirconium Masses 6.4.5-15
Figure 6.4.5-5 Detailed Intact Fuel Optimum Moderator Study – H/Zr Ratio, Fuel Element Characteristics and Location Varied 6.4.5-16
Figure 6.4.5-6 Screened and Sealed Can Optimum Moderator Study – Maximum Reactivity Fuel Configuration – 70 wt% ^{235}U Steel Clad 6.4.5-16
Figure 6.4.5-7 Screened and Sealed Can Debris Height Study – Maximum Reactivity Fuel Configuration – 70 wt% ^{235}U Steel Clad 6.4.5-17
Figure 6.4.5-8 Screened Can – 4 Elements per Can – Maximum Reactivity Fuel Configuration – 70 wt% ^{235}U Steel Clad 6.4.5-17
Figure 6.4.6-1 HEU Cluster Rod Reactivity versus H/Zr Ratio – Accident Condition Cask Array 6.4.6-9

List of Figures (continued)

Figure 6.4.6-2 LEU Cluster Rod Reactivity versus H/Zr Ratio – Accident Condition Cask Array 6.4.6-9
Figure 6.4.6-3 HEU TRIGA Cluster Rod System Reactivity versus Cask Cavity Moderator 6.4.6-10
Figure 6.4.6-4 LEU TRIGA Cluster Rod System Reactivity versus Cask Cavity Moderator 6.4.6-10
Figure 6.4.6-5 TRIGA Cluster Rod Reactivity versus Damaged Fuel Can Moderator (Pref Flood – Dry Cask Cavity) 6.4.6-11
Figure 6.4.9-1 PICTURE Schematic of Modified PULSTAR Fuel Assembly Alignment Configuration 6.4.9-5
Figure 6.4.9-2 PULSTAR Intact Assembly Model Moderator Density Study Graphical Results 6.4.9-6
Figure 6.4.10-1 Spiral Fuel - Moderator Density Plot 6.4.10-7
Figure 6.4.10-2 MOATA Plate Bundle -Moderator Density Plot 6.4.10-8
Figure 6.5.1-1 KENO-Va Validation—27 Group Library Results: Frequency Distribution of k_{eff} Values 6.5.1-6
Figure 6.5.1-2 KENO-Va Validation—27-Group Library Results: k_{eff} versus Enrichment. 6.5.1-7
Figure 6.5.1-3 KENO-Va Validation—27-Group Library Results: k_{eff} versus Rod Pitch ... 6.5.1-8
Figure 6.5.1-4 KENO-Va Validation—27-Group Library Results: k_{eff} versus H/U Volume Ratio 6.5.1-9
Figure 6.5.1-5 KENO-Va Validation—27-Group Library Results: k_{eff} versus Average Group of Fission 6.5.1-10
Figure 6.7.1-1 MCNP Model Sketch of the NAC-LWT Cask with PWR MOX/UO_2 Rods 6.7.1-3
Figure 6.7.1-2 VISED Sketch of LWT Radial View – Hex Rod Array– Normal Conditions 6.7.1-4
Figure 6.7.1-3 VISED Sketch of LWT Radial View – Square Rod Pitch - Accident Conditions 6.7.1-5
Figure 6.7.1-4 VISED Sketch of LWT Axial View – Accident Conditions 6.7.1-6
Figure 6.7.1-5 PWR MOX Rod Shipment - Reactivity versus Rod Pitch 6.7.1-12
Figure 6.7.1-6 Moderator Density Study – UO_2 Fuel Material – 3.0 cm Rod Pitch 6.7.1-12
Figure 6.7.1-7 Moderator Density Study – MS Fuel Material – 3.6 cm Rod Pitch 6.7.1-13
Figure 6.7.1-8 Moderator Density Study – PWR MOX ^{241}Pu Fuel Material – 3.6 cm Rod Pitch 6.7.1-13
Figure 6.7.2-1 LEU USLSTATS Output for EALCF 6.7.2-5
Figure 6.7.2-2 k_{eff} versus Fuel Enrichment (LEU) 6.7.2-10
Figure 6.7.2-3 k_{eff} versus Rod Pitch (LEU) 6.7.2-10
Figure 6.7.2-4 k_{eff} versus Fuel Pellet Diameter (LEU) 6.7.2-11
Figure 6.7.2-5 k_{eff} versus Fuel Rod Outside Diameter (LEU) 6.7.2-11
Figure 6.7.2-6 k_{eff} versus Hydrogen/^{235}U Atom Ratio (LEU) 6.7.2-12
Figure 6.7.2-7 k_{eff} versus Soluble Boron Concentration (LEU) 6.7.2-12
Figure 6.7.2-8 k_{eff} versus Cluster Gap Thickness (LEU) 6.7.2-13

List of Figures (continued)

Figure 6.7.2-9 k_{eff} versus ^{10}B Plate Loading (LEU) 6.7.2-13
Figure 6.7.2-10 k_{eff} versus Energy of Average Neutron Lethargy Causing Fission (LEU) 6.7.2-14
Figure 6.7.2-11 PWR MOX USLSTATS Output for Water to Fuel Volume Ratio 6.7.2-37
Figure 6.7.2-12 Adjusted k_{eff} vs. Energy of Average Neutron Lethargy Causing Fission 6.7.2-42
Figure 6.7.2-13 Adjusted k_{eff} vs. $^{235}U/^{238}U$ Ratio 6.7.2-42
Figure 6.7.2-14 Adjusted k_{eff} vs. $^{238}Pu/^{238}U$ Ratio 6.7.2-43
Figure 6.7.2-15 Adjusted k_{eff} vs. $^{239}Pu/^{238}U$ Ratio 6.7.2-43
Figure 6.7.2-16 Adjusted k_{eff} vs. $^{240}Pu/^{238}U$ Ratio 6.7.2-44
Figure 6.7.2-17 Adjusted k_{eff} vs. $^{241}Pu/^{238}U$ Ratio 6.7.2-44
Figure 6.7.2-18 Adjusted k_{eff} vs. $^{242}Pu/^{238}U$ Ratio 6.7.2-45
Figure 6.7.2-19 Adjusted k_{eff} vs. Water-to-Fuel Volume Ratio 6.7.2-45

Note: See separate Section 6.6 for Appendices to this chapter, along with the List of Figures for the Appendices.

List of Tables

Table 6.2.1-1 B&W, CE and Westinghouse PWR Fuel Assembly Data....6.2.1-2
Table 6.2.1-2 Exxon/ANF PWR Fuel Assembly Data....6.2.1-3
Table 6.2.2-1 GE BWR Fuel Assembly Data....6.2.2-2
Table 6.2.2-2 Exxon BWR Fuel Assembly Data....6.2.2-2
Table 6.2.2-3 BWR Fuel Assembly Data....6.2.2-3
Table 6.2.3-1 Characteristics of Design Basis HEU MTR Fuels....6.2.3-3
Table 6.2.3-2 Characteristics of Design Basis LEU MTR Fuel....6.2.3-6
Table 6.2.3-3 Characteristics of Design Basis MEU MTR Fuel....6.2.3-7
Table 6.2.5-1 Characteristics of Design Basis TRIGA Fuels Elements....6.2.5-4
Table 6.2.5-2 Characteristics of Design Basis TRIGA Fuels -Fuel Compositions....6.2.5-5
Table 6.2.6-1 Characteristics of TRIGA Fuel Cluster Rods....6.2.6-3
Table 6.2.6-2 Characteristics of TRIGA Fuel Cluster Rods - Fuel Compositions....6.2.6-3
Table 6.2.7-1 Characteristics of Design-Basis Metallic Fuel Rods....6.2.7-2
Table 6.2.8-1 Characteristics of DIDO Fuel Assemblies....6.2.8-3
Table 6.2.8-2 DIDO Fuel Assembly Tolerances....6.2.8-3
Table 6.2.9-1 GA IFM RERTR/TRIGA Fuel Parameters....6.2.9-3
Table 6.2.9-2 GA IFM RERTR/TRIGA Fuel Composition....6.2.9-3
Table 6.2.9-3 GA IFM RERTR/TRIGA Clad Composition....6.2.9-3
Table 6.2.9-4 GA IFM Elemental Constituents....6.2.9-4
Table 6.2.9-5 GA IFM Primary and Secondary Enclosure Dimensions....6.2.9-4
Table 6.2.10-1 PULSTAR Fuel Characteristics....6.2.10-3
Table 6.2.11-1 Spiral Fuel Assemblies Characteristics....6.2.11-3
Table 6.2.11-2 Spiral Fuel Assemblies Tolerances Applied....6.2.11-3
Table 6.2.12-1 MOATA Plate Bundle Characteristics....6.2.12-3
Table 6.2.12-2 MOATA Plate Bundle Tolerances Applied....6.2.12-4
Table 6.3.1-1 Compositions and Number Densities Used in the Criticality Analysis of PWR Fuel Assemblies....6.3.1-6
Table 6.3.2-1 Compositions and Number Densities Used in the Criticality Analysis of BWR Fuel Assemblies....6.3.2-4
Table 6.3.3-1 Composition Densities Used in Criticality Analysis of MTR Fuel....6.3.3-9
Table 6.3.4-1 Compositions and Number Densities Used in the Criticality Analysis of PWR and BWR Rods....6.3.4-9
Table 6.3.5-1 Sample Compositions and Number Densities Used in Criticality Analysis of TRIGA Fuel Elements....6.3.5-11
Table 6.3.5-2 Sample Composition and Number Densities Used in Criticality Analysis of TRIGA Fuel Cluster Rods....6.3.5-12
Table 6.3.6-1 DIDO Fuel Parameters....6.3.6-7
Table 6.3.6-2 DIDO Basket and Cask Parameters....6.3.6-8
Table 6.3.6-3 Composition Densities Used in Criticality Analysis of DIDO Fuel....6.3.6-9
Table 6.3.7-1 Composition Densities Used in Criticality Analysis of GA IFM....6.3.7-4
Table 6.3.8-1 Composition Densities Used in Criticality Analysis of PULSTAR Fuel....6.3.8-7
Table 6.3.9-1 ANSTO Basket and Cask Parameters....6.3.9-6

List of Tables (continued)

Table 6.3.9-2 Composition Densities Used in Criticality Analysis of ANSTO Basket Payloads 6.3.9-7
Table 6.4.1-1 PWR Fuel Assembly at 3.7% Enrichment Most Reactive Assembly Results 6.4.1-5
Table 6.4.1-2 PWR Fuel Assembly at 3.5% Enrichment Most Reactive Assembly Results 6.4.1-6
Table 6.4.1-3 Westinghouse 17×17 OFA Assembly Geometric Tolerances and Mechanical Perturbations Results 6.4.1-7
Table 6.4.1-4 Exxon 15×15 Geometric Tolerances and Mechanical Perturbations Results 6.4.1-7
Table 6.4.1-5 Reactivity with Design Basis PWR Fuel vs. Basket Moderator Density, Normal Conditions 6.4.1-8
Table 6.4.1-6 Reactivity with Design Basis PWR Fuel vs. Basket Moderator Density, Accident Conditions 6.4.1-9
Table 6.4.1-7 PWR Single Package 10 CFR 71.55(b)(3) Evaluation k_{eff} Summary for 3.5% Enrichment 6.4.1-10
Table 6.4.1-8 PWR Single Package 10 CFR 71.55(b)(3) Evaluation k_{eff} Summary for 3.7% Enrichment 6.4.1-10
Table 6.4.2-1 BWR Most Reactive Assembly Analysis Results 6.4.2-5
Table 6.4.2-2 BWR Basket Tolerances 6.4.2-6
Table 6.4.2-3 BWR Fuel Assembly Geometric Tolerances and Mechanical Perturbations Results 6.4.2-7
Table 6.4.2-4 Reactivity with BWR Fuel vs. Basket Moderator Density, Normal Conditions, Array of 20 Casks 6.4.2-8
Table 6.4.2-5 Reactivity with BWR Fuel vs. Basket Moderator Density, Accident Conditions, Array of 20 Casks 6.4.2-9
Table 6.4.2-6 BWR Single Package 10 CFR 71.55(b)(3) Evaluation k_{eff} Summary 6.4.2-10
Table 6.4.3-1 Fuel/Basket Unit Cell k_{eff} versus MTR Fuel Element Type 6.4.3-17
Table 6.4.3-2 Cask k_{eff} versus Fuel Plate Spacing 6.4.3-17
Table 6.4.3-3 MTR Basket Geometric Tolerances 6.4.3-18
Table 6.4.3-4 MTR Basket/Intact Fuel Element Geometric Tolerances and Mechanical Perturbations Results 6.4.3-18
Table 6.4.3-5 MTR Basket/Optimally Spaced Fuel Plates Geometric Tolerances and Mechanical Perturbations Results 6.4.3-18
Table 6.4.3-6 Reactivity with MTR Fuel vs. Basket Moderator Density, Normal Conditions, Dry Exterior, Infinite Array of Casks 6.4.3-19
Table 6.4.3-7 Reactivity with MTR Fuel vs. Basket Moderator Density, Accident Conditions, Dry Exterior, Infinite Array of Casks 6.4.3-20
Table 6.4.3-8 MTR Fuel Element Rotation Perturbation Study 6.4.3-21
Table 6.4.3-9 MTR Basket/Center Fuel Element Perturbation Study 6.4.3-21
Table 6.4.3-10 Mixed HEU/LEU MTR Fuel Perturbation Study 6.4.3-21
Table 6.4.3-11 MTR Single Package 10 CFR 71.55(b)(3) Evaluation k_{eff} Summary 6.4.3-21
Table 6.4.3-12 MTR Fuel Uranium Weight Percentage Perturbations 6.4.3-22

List of Tables (continued)

Table 6.4.3-13 MEU MTR Unit Cell k_{eff} Comparison (Enrichment Variation) 6.4.3-22
Table 6.4.3-14 MEU MTR Basket k_{eff} Comparison (Plate Location) 6.4.3-23
Table 6.4.3-15 Physical Characteristics of McMaster MTR Fuels 6.4.3-23
Table 6.4.3-16 Reactivity of Various Parameter Variations for 10-Plate McMaster Element 6.4.3-24
Table 6.4.3-17 Reactivity of Various Parameter Variations for 18-Plate McMaster Element 6.4.3-24
Table 6.4.3-18 MTR Limiting Fuel Configurations 6.4.3-25
Table 6.4.3-19 Initial Fuel Configurations for MTR Bounding Evaluations 6.4.3-25
Table 6.4.3-20 Reactivity Impact of Parameter Variations in the Finite Cask Model 6.4.3-26
Table 6.4.3-21 Baseline MTR Bounding Configurations 6.4.3-27
Table 6.4.3-22 High Fissile Mass MTR Fuel – Bounding Parameter Analysis 6.4.3-28
Table 6.4.3-23 MTR High Fissile Content Loading Evaluation (460 g ^{235}U) 6.4.3-29
Table 6.4.3-24 LEU MTR Active Fuel Width Increase Evaluation 6.4.3-29
Table 6.4.3-25 Summary of LEU MTR Bounding Configurations 6.4.3-30
Table 6.4.3-26 Summary of Previous Bounding Configurations for Use in High Mass LEU Calculations 6.4.3-31
Table 6.4.3-27 High Fissile Mass LEU (32 g ^{235}U per Plate) Analysis Results 6.4.3-32
Table 6.4.3-28 LEU High Fissile Mass Bounding Configuration 6.4.3-33
Table 6.4.3-29 Cask Interior Moderator Density and Blocked Cell Study Results 6.4.3-34
Table 6.4.4-1 NAC-LWT Cask with 25 PWR Rods, k_{eff} versus Fuel Rod Pitch, 5.0 wt % ^{235}U Initial Enrichment 6.4.4-10
Table 6.4.4-2 Reactivity with 25 PWR Rods vs. Basket Moderator Density, Normal Conditions, Infinite Array of Casks 6.4.4-11
Table 6.4.4-3 Reactivity with 25 PWR Rods vs. Basket Moderator Density, Accident Conditions, Infinite Array of Casks 6.4.4-12
Table 6.4.4-4 PWR Rods, Single Package 10 CFR 71.55(b)(3) Evaluation k_{eff} Summary 6.4.4-13
Table 6.4.4-5 NAC-LWT Cask with 25 BWR rods, k_{eff} versus Fuel Rod Pitch, 5.0 wt % ^{235}U Initial Enrichment 6.4.4-13
Table 6.4.4-6 Reactivity with 25 BWR Rods vs. Basket Moderator Density, Normal Conditions, Infinite Array of Casks 6.4.4-14
Table 6.4.4-7 Reactivity with 25 BWR Rods vs. Basket Moderator Density, Accident Conditions, Infinite Array of Casks 6.4.4-15
Table 6.4.4-8 BWR Rods, Single Package 10 CFR 71.55(b)(3) Evaluation k_{eff} Summary 6.4.4-16
Table 6.4.4-9 Maximum Reactivity Pitch Determination for 25 BWR Rods – Water Exterior 6.4.4-16
Table 6.4.4-10 Maximum Reactivity Pitch Determination for 25 PWR Rods – Water Exterior 6.4.4-17
Table 6.4.4-11 Maximum Reactivity Pitch Determination for 37 BWR Rods – Water Exterior 6.4.4-17

List of Tables (continued)

Table 6.4.4-12 Maximum Reactivity Pitch Determination for 37 PWR Rods – Water Exterior 6.4.4-18
Table 6.4.4-13 Maximum Reactivity Pitch Determination for 61 BWR Rods – Water Exterior 6.4.4-18
Table 6.4.4-14 Maximum Reactivity Pitch Determination for 61 PWR Rods – Water Exterior 6.4.4-19
Table 6.4.4-15 Maximum Reactivity Pitch Determination for 61 BWR Rods – Void Exterior 6.4.4-19
Table 6.4.4-16 Maximum Reactivity Pitch Determination for 61 PWR Rods – Void Exterior 6.4.4-20
Table 6.4.4-17 Maximum Reactivity Pitch Determination for 61 BWR Rods – Void Exterior and Preferential Flooding of Cask Cavity 6.4.4-20
Table 6.4.4-18 Maximum Reactivity Pitch Determination for 61 PWR Rods – Void Exterior and Preferential Flooding of Cask Cavity 6.4.4-21
Table 6.4.4-19 Damaged Rod Array Area Calculation – Flooded Cask Cavity 6.4.4-21
Table 6.4.4-20 Damaged Rod Array Area Calculation – Preferential Flooding 6.4.4-22
Table 6.4.4-21 Maximum Reactivity Determination for Homogenized UO_2/Water Mixture 6.4.4-22
Table 6.4.4-22 Homogenized UO_2/Water Cask Cavity Moderator Density Study Results - Void Exterior 6.4.4-22
Table 6.4.4-23 Homogenized UO_2/Water Cask Cavity Moderator Density Study Results - Water Exterior 6.4.4-23
Table 6.4.4-24 Homogenized UO_2/Water Exterior Moderator Density Study Results – Void Cask Cavity 6.4.4-23
Table 6.4.4-25 Homogenized UO_2/Water Exterior Moderator Density Study Results – Water Cask Cavity 6.4.4-24
Table 6.4.4-26 Single Cask Containment Reflected Results Comparison for Homogenized UO_2/Water Model 6.4.4-24
Table 6.4.5-1 Parametric Study – Fuel / Basket k-infinity versus TRIGA Fuel Element Type, Nonpoisoned Basket 6.4.5-18
Table 6.4.5-2 Parametric Study – Cask k_{eff} versus TRIGA Fuel Element Type, Poisoned Basket 6.4.5-19
Table 6.4.5-3 Axially Infinite Cask k_{eff} with TRIGA Fuel Elements- Fuel Element Placement Perturbations, Nonpoisoned Basket 6.4.5-20
Table 6.4.5-4 Axially Infinite Cask k_{eff} with TRIGA Fuel Elements - Fuel Element Placement Perturbations, Poisoned Basket 6.4.5-20
Table 6.4.5-5 Axially Infinite Cask k_{eff} with TRIGA Fuel Elements – Basket Manufacturing Tolerance Perturbations, Nonpoisoned Basket 6.4.5-21
Table 6.4.5-6 Axially Infinite Cask k_{eff} with TRIGA Fuel Elements – Basket Manufacturing Tolerance Perturbations, Poisoned Basket 6.4.5-21
Table 6.4.5-7 Screened Can Preferential Flooding and Partial Loading Reactivity Evaluations for TRIGA Fuel Elements, Nonpoisoned and Poisoned Baskets 6.4.5-22

List of Tables (continued)

Table 6.4.5-8 Sealed Can Preferential Flooding and Partial Loading Reactivity Evaluations for TRIGA Fuel Elements, Nonpoisoned and Poisoned Baskets 6.4.5-23
Table 6.4.5-9 Summary of Most Reactive Configurations, TRIGA Fuel Elements, Nonpoisoned Basket 6.4.5-24
Table 6.4.5-10 Summary of Most Reactive Configurations, TRIGA Fuel Elements, Poisoned Basket 6.4.5-24
Table 6.4.5-11 Reactivity Results for TRIGA Fuel Elements, Sealed Cans, Normal Conditions, Nonpoisoned Basket 6.4.5-25
Table 6.4.5-12 Reactivity Results for TRIGA Fuel Elements, Sealed Cans, Accident Conditions, Nonpoisoned Basket 6.4.5-26
Table 6.4.5-13 Reactivity Results for TRIGA Fuel Elements, Screened Cans, Normal Conditions, Poisoned Basket 6.4.5-27
Table 6.4.5-14 Reactivity Results for TRIGA Fuel Elements, Screened Cans, Accident Conditions, Poisoned Basket 6.4.5-28
Table 6.4.5-15 Single Package 10 CFR 71.55(b)(3) Evaluation k_{eff} Summary, TRIGA Fuel Element, Nonpoisoned Basket 6.4.5-29
Table 6.4.5-16 Single Package 10 CFR 71.55(b)(3) Evaluation k_{eff} Summary, TRIGA Fuel Element, Poisoned Basket 6.4.5-29
Table 6.4.5-17 Fuel Element Physical Characteristics Evaluation 6.4.5-30
Table 6.4.5-18 Element Variation to Reduce k_s Below 0.95 ..... 6.4.5-31
Table 6.4.5-19 General Model Configuration – Dry to Wet System Reactivity Changes, 70 wt% ^{235}U Stainless Steel Clad Fuel - Nominal Fuel Parameters 6.4.5-31
Table 6.4.5-20 Primary Fuel Type Reactivity Comparison – Accident Conditions Eight-Cask Array (No Cans) 6.4.5-32
Table 6.4.5-21 Normal Condition Maximum System Reativities (No Cans) 6.4.5-32
Table 6.4.6-1 Cask k_{eff} with TRIGA Fuel Cluster Rods – Fuel Rod Placement Perturbations, Nonpoisoned Basket 6.4.6-12
Table 6.4.6-2 Cask k_{eff} with TRIGA Fuel Cluster Rods – Fuel Rod Placement Perturbations, Poisoned Basket 6.4.6-12
Table 6.4.6-3 Axially Infinite Cask k_{eff} with TRIGA Fuel Cluster Rods – Basket and Insert Manufacturing Tolerance Perturbations, Nonpoisoned Basket 6.4.6-13
Table 6.4.6-4 Axially Infinite Cask k_{eff} with TRIGA Fuel Cluster Rods – Basket and Insert Manufacturing Tolerance Perturbations, Poisoned Basket 6.4.6-14
Table 6.4.6-5 Sealed Can Preferential Flooding and Partial Loading Reactivity Evaluations for TRIGA Fuel Rod Clusters, Nonpoisoned Basket 6.4.6-15
Table 6.4.6-6 Sealed Can Preferential Flooding and Partial Loading Reactivity Evaluations for TRIGA Fuel Rod Clusters, Poisoned Basket 6.4.6-15
Table 6.4.6-7 Summary of Most Reactive Configurations, TRIGA Fuel Cluster Rods, Nonpoisoned Basket 6.4.6-16
Table 6.4.6-8 Summary of Most Reactive Configurations, TRIGA Fuel Cluster Rods, Poisoned Basket 6.4.6-16

List of Tables (continued)

Table 6.4.6-9 Reactivity Results for TRIGA Fuel Cluster Rods, Sealed Cans, Normal Conditions, Nonpoisoned Basket 6.4.6-17
Table 6.4.6-10 Reactivity Results for TRIGA Fuel Cluster Rods, Sealed Can, Accident Conditions, Nonpoisoned Basket 6.4.6-18
Table 6.4.6-11 Reactivity Results for TRIGA Fuel Cluster Rods, Sealed Cans, Normal Conditions, Poisoned Basket 6.4.6-19
Table 6.4.6-12 Reactivity Results for TRIGA Fuel Cluster Rods, Sealed Cans, Accident Conditions, Poisoned Basket 6.4.6-20
Table 6.4.6-13 Single Package 10 CFR 71.55(b)(3) Evaluation k_{eff} Summary, TRIGA Fuel Cluster Rod, Nonpoisoned Basket 6.4.6-21
Table 6.4.6-14 Single Package 10 CFR 71.55(b)(3) Evaluation k_{eff} Summary, TRIGA Fuel Cluster Rod, Poison Basket 6.4.6-21
Table 6.4.6-15 Increased Fuel Dimensional Parameter k_{eff} Summary, TRIGA Fuel Cluster Rod, Nonpoisoned Basket 6.4.6-21
Table 6.4.6-16 TRIGA Cluster Rod Reactivities – Accident Conditions 6.4.6-22
Table 6.4.6-17 TRIGA Cluster Rod Reactivities – Normal Conditions 6.4.6-22
Table 6.4.6-18 TRIGA Cluster Rod Reactivities – Single Cask with Containment Fully Water Reflected 6.4.6-22
Table 6.4.6-19 Summary of TRIGA Cluster Rod Maximum Reactivity Configuration .. 6.4.6-23
Table 6.4.6-20 Licensing Parameters for TRIGA Cluster Rods 6.4.6-23
Table 6.4.7-1 Normal Condition HEU, LEU, MEU DIDO Evaluation 6.4.7-7
Table 6.4.7-2 HEU DIDO Accident Evaluation – Radial Shift and Exterior Moderator Density Variation 6.4.7-8
Table 6.4.7-3 DIDO Heat Shunt and Aluminum Shell Evaluation Results 6.4.7-8
Table 6.4.7-4 DIDO Basket Geometric Tolerance Study Results 6.4.7-8
Table 6.4.7-5 DIDO Fuel Assembly Tolerance Study Results 6.4.7-9
Table 6.4.7-6 DIDO Fuel Maximum Reactivity Combinations 6.4.7-10
Table 6.4.7-7 Moderator Density Study for the Infinite Array of Casks (Nominal Fuel and Basket Configuration) 6.4.7-11
Table 6.4.7-8 DIDO Single Package 10 CFR 71.55(b)(3) Evaluation k_{eff} Summary 6.4.7-12
Table 6.4.7-9 DIDO Fuel Assembly Tolerance Study Results (Reduced Clad Thickness) 6.4.7-12
Table 6.4.7-10 DIDO Fuel Maximum Reactivity Combinations (Reduced Clad Thickness) 6.4.7-12
Table 6.4.7-11 DIDO Fuel Maximum Reactivity Combinations (Reduced Clad and Maximum Pitch) 6.4.7-13
Table 6.4.7-12 DIDO Bounding Configurations 6.4.7-14
Table 6.4.8-1 GA IFM Payload Evaluation Result Summary 6.4.8-5
Table 6.4.8-2 GA IFM TRIGA Rectangular Array Pitch Evaluation Result Summary ... 6.4.8-6
Table 6.4.8-3 GA IFM TRIGA Square Array Pitch Evaluation Result Summary 6.4.8-6
Table 6.4.8-4 GA IFM Interior Moderator Density Evaluation Result Summary 6.4.8-7
Table 6.4.8-5 GA IFM HTGR Matrix Moderator Density Evaluation Result Summary . 6.4.8-8
Table 6.4.8-6 GA IFM Exterior Moderator Density Evaluation Result Summary 6.4.8-9

List of Tables (continued)

Table 6.4.8-7 GA IFM Partial Flooding Comparison Result Summary 6.4.8-10
Table 6.4.8-8 GA IFM Partial Flooding Interior Moderator Density, Void Exterior Result Summary 6.4.8-10
Table 6.4.8-9 GA IFM Partial Flooding Interior Moderator Density, Water Exterior Result Summary 6.4.8-11
Table 6.4.8-10 GA IFM Partial Flooding Exterior Moderator Density, Void Interior Result Summary 6.4.8-12
Table 6.4.8-11 GA IFM Partial Flooding Exterior Moderator Density, Water Interior Result Summary 6.4.8-13
Table 6.4.8-12 GA IFM Partial Flooding Single Cask Result Comparison 6.4.8-13
Table 6.4.8-13 GA IFM Damaged TRIGA Fuel Result Summary 6.4.8-14
Table 6.4.9-1 PULSTAR Intact Assembly Shift Results 6.4.9-7
Table 6.4.9-2 PULSTAR Intact Assembly Mechanical Perturbation Results 6.4.9-7
Table 6.4.9-3 PULSTAR Intact Assembly Lattice Moderator Ratio Results 6.4.9-8
Table 6.4.9-4 PULSTAR Canned Intact Element Results 6.4.9-8
Table 6.4.9-5 PULSTAR Canned Homogenized Element Results 6.4.9-9
Table 6.4.9-6 PULSTAR Maximum Reactivity Summary 6.4.9-10
Table 6.4.10-1 Spiral Fuel Assembly - Base Data Comparisons 6.4.10-9
Table 6.4.10-2 Spiral Fuel Assembly - Basket Tolerance Evaluations 6.4.10-10
Table 6.4.10-3 Spiral Fuel Assembly - Fuel Tolerance Evaluations 6.4.10-11
Table 6.4.10-4 Spiral Fuel Assembly - Moderator Density Variations 6.4.10-12
Table 6.4.10-5 Spiral Fuel Assembly - Maximum Reactivity Case Summary 6.4.10-13
Table 6.4.10-6 MOATA Plate Bundle - Base Data Comparisons 6.4.10-14
Table 6.4.10-7 MOATA Plate Bundle – Basket Tolerance Evaluations 6.4.10-15
Table 6.4.10-8 MOATA Plate Bundle - Fuel Tolerance Evaluations 6.4.10-16
Table 6.4.10-9 MOATA Plate Bundle - Moderator Density Variations 6.4.10-17
Table 6.4.10-10 MOATA Plate Bundle - Maximum Reactivity Case Summary 6.4.10-18
Table 6.5.1-1 KENO-Va and 27-Group Library Validation Statistics 6.5.1-11
Table 6.5.2-1 Criticality Results for High Enrichment Uranium Systems 6.5.2-3
Table 6.7.1-1 PWR MOX Fuel Analysis Compositions and Number Densities 6.7.1-7
Table 6.7.1-2 PWR MOX Fuel Analysis Isotope Weight Fraction 6.7.1-7
Table 6.7.1-3 PWR MOX Rod Shipment - Reactivitiy as a Function of Geometry and Material 6.7.1-14
Table 6.7.1-4 PWR MOX Fuel Shipment - Fuel Rod Pitch Study 6.7.1-15
Table 6.7.1-5 PWR MOX Fuel Shipment - Optimum Moderator Study Maximum Reactivity Summary 6.7.1-15
Table 6.7.1-6 PWR MOX Fuel Shipment Reactivity Summary for Single Cask Containment Fully Reflected Cases 6.7.1-16
Table 6.7.1-7 PWR MOX Fuel Shipment Reactivity Summary for Normal Condition Array Cases 6.7.1-16
Table 6.7.1-8 PWR MOX Fuel Shipments - Summary of Maximum Reactivity Configurations 6.7.1-17

List of Tables (continued)

Table 6.7.1-9 PWR MOX Fuel Shipments – PWR MOX Comparison to Area of Applicabilitly 6.7.1-17
Table 6.7.1-10 PWR MOX Fuel Shipments – UO_2 Comparison to Area of Applicability 6.7.1-18
Table 6.7.1-11 Bounding Parameters for PWR MOX/UO_2 Rod Shipments 6.7.1-18
Table 6.7.1-12 B&W, CE and Westinghouse PWR Fuel Assembly Data 6.7.1-19
Table 6.7.1-13 Exxon/ANF PWR Fuel Assembly Data 6.7.1-19
Table 6.7.2-1 LEU Range of Applicability for Complete Set of 186 Benchmark Experiments 6.7.2-7
Table 6.7.2-2 LEU Correlation Coefficients and USLs for Bechmark Experiments 6.7.2-8
Table 6.7.2-3 LEU MCNP Validation Statistics 6.7.2-15
Table 6.7.2-4 PWR MOX Range of Applicability for Complete Set of 59 Benchmark Experiments 6.7.2-39
Table 6.7.2-5 PWR MOX Correlation Coefficients and USLs for Benchmark Experiments 6.7.2-40
Table 6.7.2-6 MCNP Validation Statistics 6.7.2-46

6.7 Payload Specific Details

This section contains NAC-LWT cask payload specific evaluation detail.

6.7.1 PWR Mixed Oxide Fuel Rods

This section includes input, analysis method, results, and critical benchmark evaluations for the NAC-LWT cask containing a payload of up to 16 PWR rods. The PWR rods may be composed of uranium oxide fuel pellets or mixed oxide fuel pellets (depleted or natural uranium oxide with plutonium oxide contributing the primary quantity of fissile material).

6.7.1.1 Package Fuel Loading

The NAC-LWT cask may transport up to 16 undamaged PWR fuel rods in a fuel rod holder. To bound all PWR MOX rods that may be transported in the NAC-LWT cask, UO_2 rods are evaluated with enrichments up to 5.0 wt % ^{235}U, while MOX rods were evaluated up to 7 wt % fissile plutonium. Characteristics of the design basis PWR rods are presented in Table 6.7.1-12 and Table 6.7.1-13. Given a fixed fissile material density, defined by a maximum UO_2 enrichment or fissile plutonium weight percent, the most reactive rod has the greatest fissile mass, i.e., the rod with the largest pellet radius. Therefore, the CE 14×14 pellet diameter of 0.3765 inch is chosen as the base radius for the most reactive PWR fuel rod evaluated here. A conservative maximum fissile material length of 153.5 inches is also applied. As a maximum reactivity fuel pitch is established, and the zirconium alloy is essentially transparent to neutrons, the clad thickness has no significant effect on the analysis.

6.7.1.2 Criticality Model Specifications

This section describes the models that are used in the criticality analyses for the NAC-LWT cask containing up to 16 PWR rods. PWR rods are either low enriched uranium oxide (maximum 5 wt % ^{235}U) fueled or MOX fueled. The models are analyzed separately under normal conditions and hypothetical accident conditions to ensure that all possible configurations are subcritical.

The model uses the MCNP5 code package with the ENDF/B-VI cross-section set. No cross-section pre-processing is required prior to MCNP implementation. MCNP uses the Monte Carlo technique to calculate the k_{eff} of a system. In these analyses, approximately 530 cycles with 1,000 neutron histories per cycle are tracked through the system.

Description of Calculational Models

The MCNP model of the NAC-LWT cask with 16 undamaged PWR rods includes triangular and square lattice formation of design basis rods centered in the cask cavity. No credit is taken for geometry control provided by the rod holder. The fuel rods, cask cavity and radial shields are explicitly modeled as shown in the Figure 6.7.1-1 model sketch.

The model of the NAC-LWT cask takes advantage of the universe structure of MCNP. Each universe defines an infinite space, bounded after its insertion into a containing cell. Four universes are employed herein. The "0" universe defines the cask universe. The remaining universes are discussed in the following sections. Each universe is developed independently as surfaces and cells. Fuel rod array surfaces and cells are configured to place the rods in either a rectangular (square) pitch array or a hex (triangular) pitch array. The rod pitch is a variable input into the model and is modified to achieve a maximum reactivity configuration. In the basket universe, the rod array is placed into a square (RPP) body that allows the moderator density outside the rod array to be adjusted independently.

The modeled accident condition completely removes the neutron shielding, the neutron shield tank and the cask impact limiters. In the normal conditions model, the impact limiter diameter is modeled as identical to the neutron shield tank diameter. This allows for closer packing for the cask array than physically possible.

VISED sketches of the assembled geometry are shown in Figure 6.7.1-2 through Figure 6.7.1-4. The cask outer surface is surrounded by a rectangular body with reflecting boundary conditions. The boundary conditions are imposed on the sides, top and bottom, which simulates an infinite array of casks.

Package Regional Densities

The composition densities (g/cc) and nuclide number densities (atm/b-cm) used in the subsequent criticality analyses are shown in Table 6.7.1-1. The various isotope weight compositions used in the MOX/UO_2 rod analysis are listed in Table 6.7.1-2.

Figure 6.7.1-1 MCNP Model Sketch of the NAC-LWT Cask with PWR MOX/UO_2 Rods

(Dimensions in centimeters)

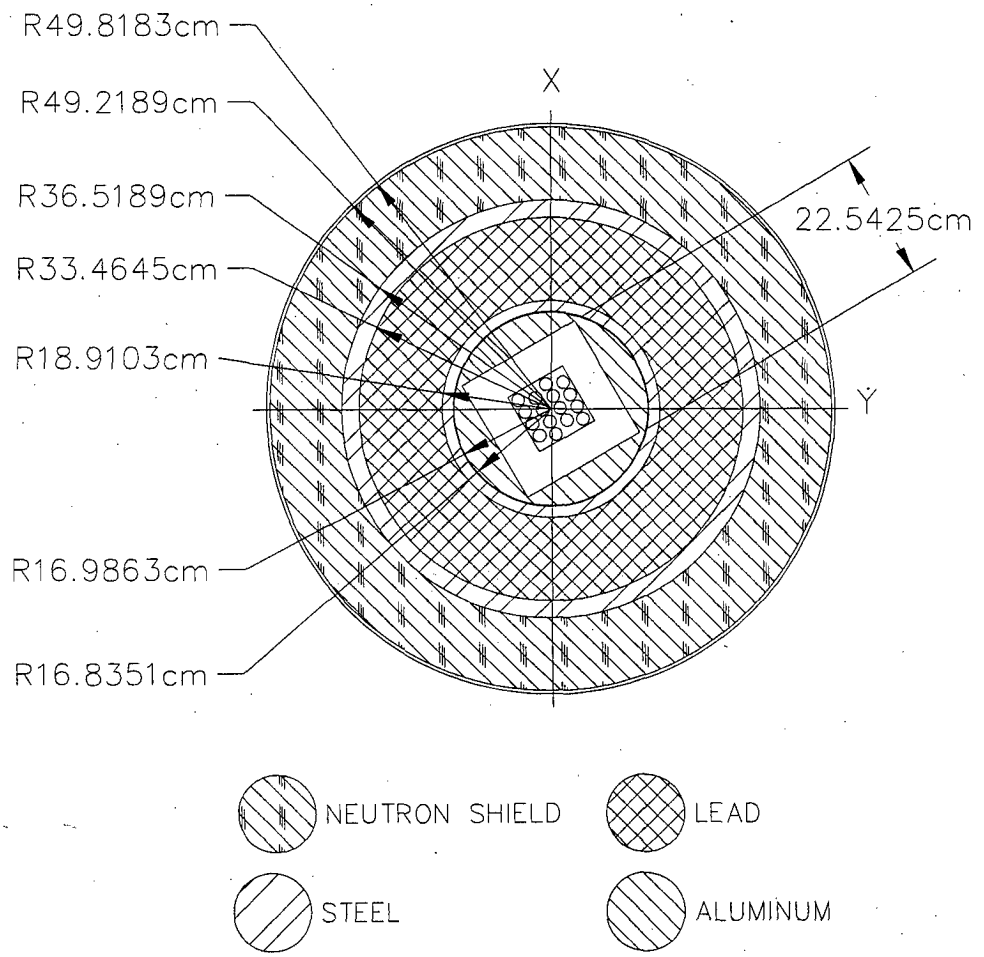


Figure 6.7.1-2 VISED Sketch of LWT Radial View – Hex Rod Array– Normal Conditions

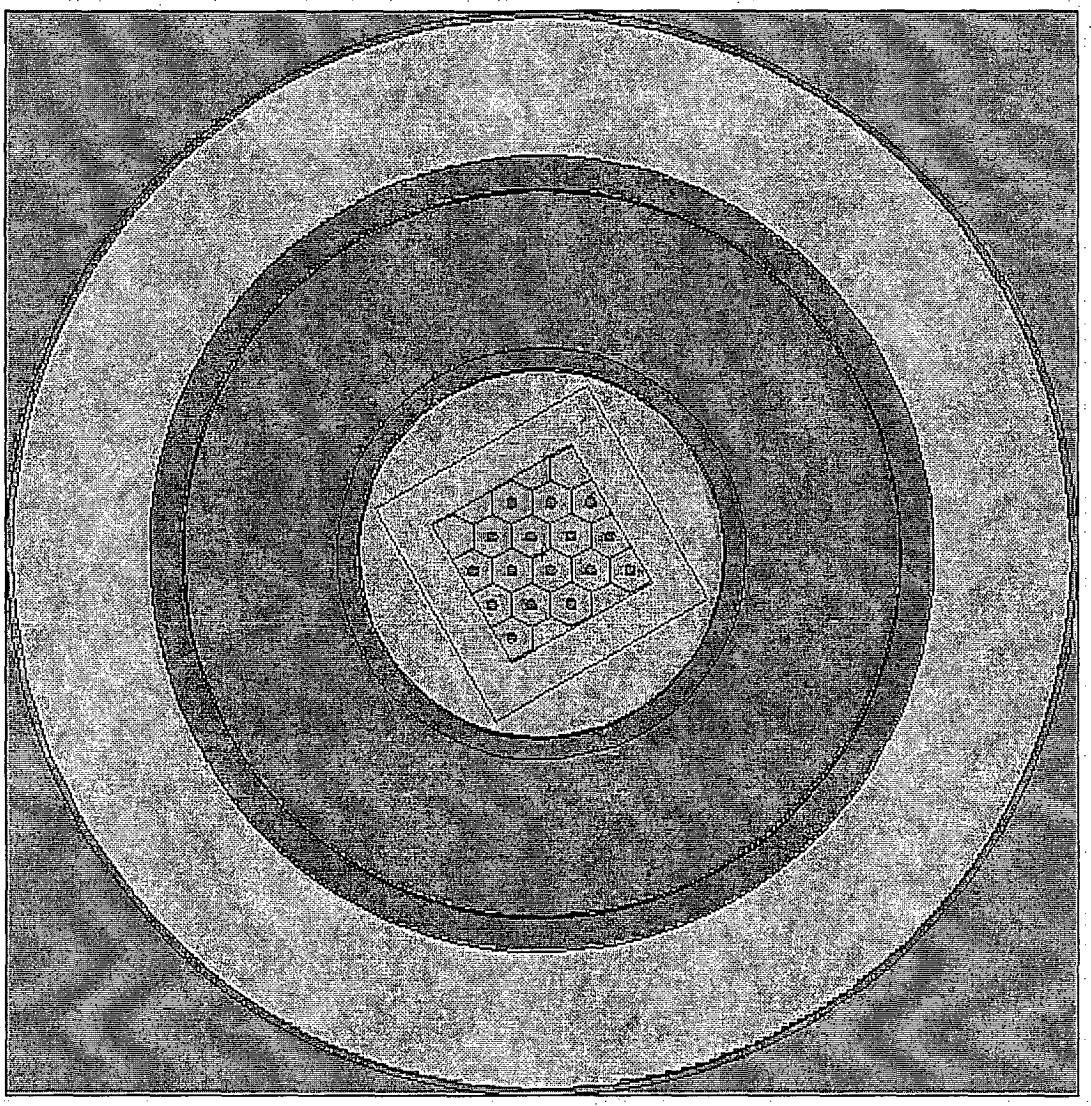


Figure 6.7.1-3 VISED Sketch of LWT Radial View – Square Rod Pitch - Accident Conditions

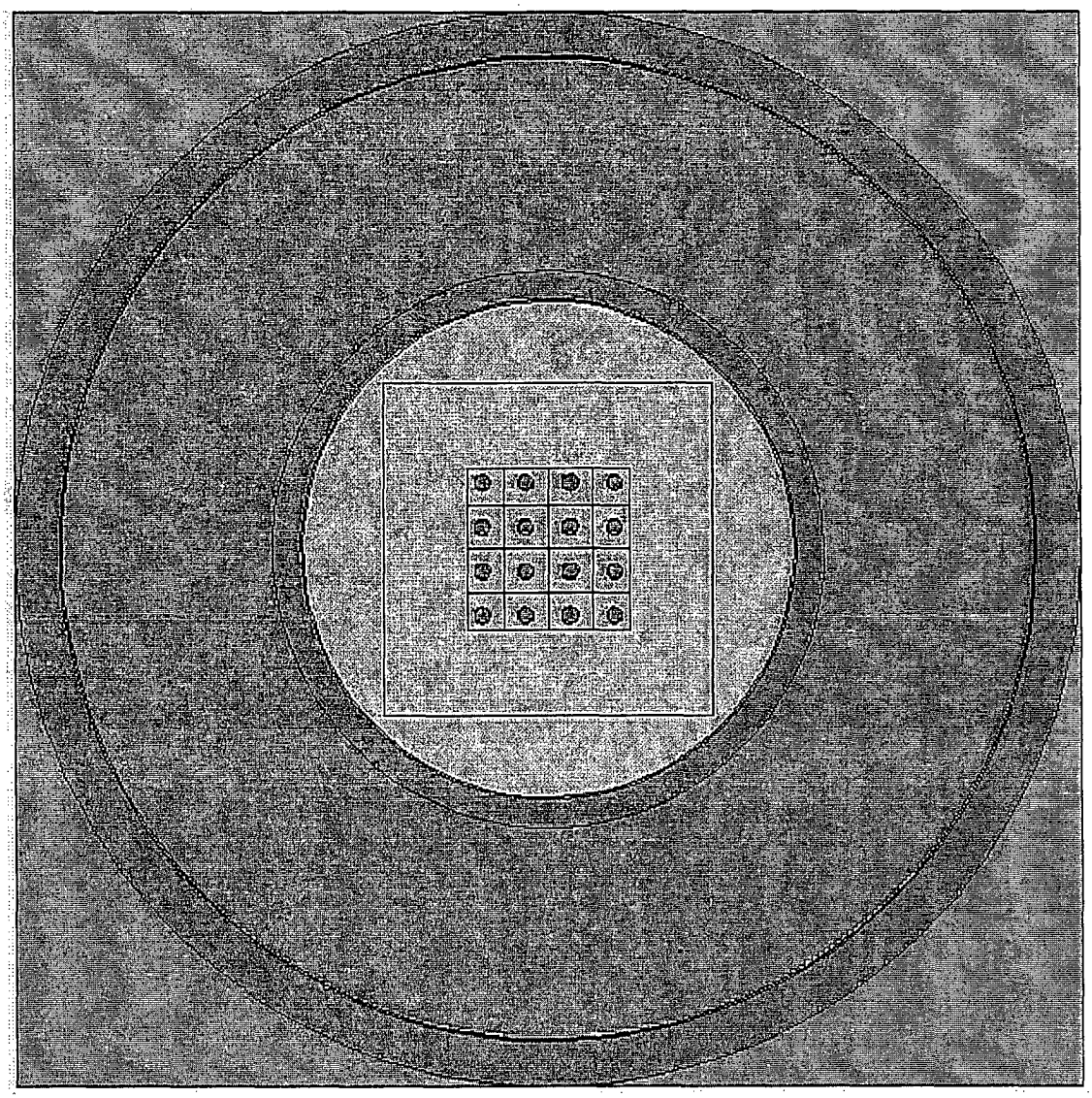


Figure 6.7.1-4 VISED Sketch of LWT Axial View – Accident Conditions

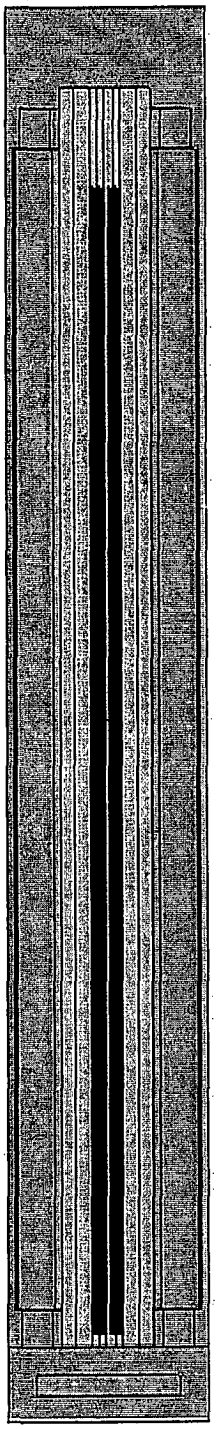


Table 6.7.1-1 PWR MOX Fuel Analysis Compositions and Number Densities

Material	5.0% Enriched UO_2	Weapons Grade (7 wt % Fissile Pu)[1]	Zirconium Alloy	H_2O	304 Stainless Steel	Pb	Al
Density, g/cc	10.522	10.556	6.56	0.9982	7.920	11.344	2.702
Density	atoms/b-cm						
Uranium-235	1.19E-03	1.54E-04					
Uranium-238	2.23E-02	2.16E-02					
Plutonium-238		9.15E-07					
Plutonium-239		1.70E-03					
Plutonium-240		1.09E-04					
Plutonium-241		7.23E-06					
Plutonium-242		9.00E-07					
Oxygen	4.70E-02	4.70E-02		3.338E-2			
Hydrogen				6.677E-2			
Zirconium Alloy			4.331E-2				
Iron					5.936E-2		
Chromium					1.743E-2		
Nickel					7.721E-3		
Manganese					1.736E-3		
Lead						3.297E-2	
Aluminum							6.031E-2

Table 6.7.1-2 PWR MOX Fuel Analysis Isotope Weight Fraction[2]

Isotope	UO_2	Weapon Grade	Fuel Grade	Power Grade	MOX Services
^{235}U	5	0.7	0.7	0.7	0.7
^{238}U	95	99.3	99.3	99.3	99.3
^{238}Pu	0	0.05	0.1	1	0.05
^{239}Pu	0	93.5	86.1	62	95
^{240}Pu	0	6	12	22	4.5
^{241}Pu	0	0.4	1.6	12	0.4
^{242}Pu	0	0.05	0.2	3	0.05

[1] Sample composition.
[2] Typical fresh fuel MOX material is composed of depleted uranium at 0.2 to 0.3 wt % ^{235}U. A bounding natural uranium enrichment of 0.7 wt % ^{235}U is used in the criticality evaluations.

6.7.1.3 Criticality Calculations

This section presents the criticality analysis for the NAC-LWT cask with up to 16 PWR UO_2 or MOX rods. UO_2 rods are enriched up to 5.0 wt % ^{235}U initial enrichment, while MOX rods contain up to 7 wt % fissile plutonium. No credit is taken for geometry control that is provided by the rod holder and no rod positions are specified for the rods in the lattice. Since various fuel rod arrangements may be shipped, the criticality of the PWR MOX rods in the NAC-LWT cask cavity is studied to determine the optimum pitch and, therefore, the maximum k_{eff} for the cask.

Criticality results are divided into individual sets of analyses.

- Evaluate the NAC-LWT accident configuration to demonstrate that, at a fixed fissile plutonium content, the maximum fissile percentage material (MOX Services definition) produces the maximum reactivity configuration.
- Determine the maximum reactivity pitch of the most reactive fuel material.
- Run the optimum moderator density evaluation.
- Evaluate normal condition and single cask "containment reflected" cases.

Included in all analyses are hypothetical plutonium compositions solely to justify the removal of the plutonium compositions as a licensing limit.

Rod Geometry and Material Composition Studies

Each of the material compositions is evaluated for the maximum fissile material mass rod. Fissile material in the uranium oxide rods is limited by the 5 wt % ^{235}U enrichment constraint, while the MOX material is limited by the 7 wt % fissile plutonium input. In addition to the physically realistic MOX material descriptions, three hypothetical MOX materials are evaluated: one containing all fissile plutonium (adding into ^{241}Pu the remaining plutonium weight fractions), an all ^{239}Pu material and an all ^{241}Pu material. The following nomenclature is used to describe the various plutonium fuel materials.

Abbreviation	Material
PG	Power grade plutonium isotopic distribution
FG	Fuel grade plutonium isotopic distribution
WG	Weapons grade plutonium isotopic distribution
MS	MOX Services "WG type" material
FP	Plutonium is modeled as all fissile plutonium
P9	Plutonium is modeled as all ^{239}Pu
P1	Plutonium is modeled as all ^{241}Pu

All cases are evaluated at a hexagonal pitch of 3.0 and 3.6 cm. Based on scoping evaluations, as validated in the following section, these fuel rod pitches approximate maximum reactivity configurations over a range of material composition.

As shown in later moderator density studies, maximum reactivity moderation is achieved by a preferentially flooded lattice with a void gap to the cask cavity. Fuel material and pitch studies are based on a flooded cask cavity. As these studies primarily rely on the interaction between rods in the lattice, rather than between casks, applying the results of the flooded cavity to the dry cavity/wet lattice is acceptable.

As seen in Table 6.7.1-3, maximum reactivity for physically realistic plutonium compositions is achieved by the MOX Services material. This result was expected as the MOX Services composition model contains the maximum fissile material within the plutonium oxide matrix. For the hypothetical compositions, the all ^{241}Pu case produces maximum reactivity. As the ^{241}Pu isotope has the highest fission cross-section, this result is to be expected.

Maximum Reactivity Rod Pitch Evaluation

The maximum fissile mass rod configuration is evaluated with uranium oxide, MOX Services (95 wt % ^{239}Pu in Pu), and 100% ^{241}Pu at a range of rod pitches to determine the maximum (optimum) pitch for a flooded cask cavity. This evaluation takes no credit for the actual pitch of the encapsulating stainless steel rod (11/16 inch at 1.75 cm OD) structure into which the rods are placed. As seen in Figure 6.7.1-5 and Table 6.7.1-4, the maximum reactivity pitch is approximately 3.4 to 3.6 cm for the MOX rods and around 3 cm for the uranium oxide rods, with a "flat" peak extending approximately 0.4 to 0.6 cm in width depending on material and configuration. Based on a three sigma uncertainty band, maximum reactivities do not statistically differ between hexagonal and square pitch configurations. The base case for the optimum moderator density studies will be the 3.6 cm hexagonal pitch for the MOX rods and the 3.0 cm hexagonal pitch for the UO_2 rods.

Optimum Moderator Density Evaluation

The maximum fissile mass rod is evaluated at various internal and external moderator densities, including preferential flooding of the fuel region. For the preferential flooding scenarios, the square container containing the rod array will be evaluated at a moderator density independent of that in the remainder of the cask cavity. Figure 6.7.1-6 through Figure 6.7.1-8 contain the moderator density plots of the uranium oxide, MOX Services, and all ^{241}Pu material configurations. All results produce identical trends in that maximum reactivity is achieved by a preferentially flooded fuel region and void cavity and cask exterior. This result was to be

expected as it provides maximum neutronic coupling within the reflective boundary (infinite array) model.

Maximum system reactivities are summarized in Table 6.7.1-5 for the UO_2 fuel compostion, the MOX Services defined fuel composition, and the hypothetical fissile material composition (100% ^{241}Pu) at the bounding fissile configuration—a maximum fuel material rod (0.3765-in pellet OD, 153.5-in active fuel length).

Single Cask Containment (Fully Reflected) and Normal Condition Array Evaluations

A single cask evaluation is performed to comply with 10 CFR 71.55(b)(3).

The containment for the NAC-LWT is the cask inner shell. While no operating condition results in a removal of the cask outer shell and lead gamma shield, the most reactive preferential flooded and fully flooded cases are reevaluated by removing the lead and outer shells (including neutron shield), and reflecting the system by 20 cm water at full density on the X, Y, and Z faces. Single cask, containment fully reflected reactivities are summarized in Table 6.7.1-6.

A normal condition infinite cask array is also evaluated. As indicated by the evaluations of the accident conditions array, including the radial neutron shield reduces system reactivity by eliminating neutronic interaction between casks. Normal condition cask array results are summarized in Table 6.7.1-7.

Maximum Reactivities and Comparison to USL

The maximum $k_{eff} + 2\sigma$ results for three primary analysis groups (single cask, normal array and accident array) are summarized in Table 6.7.1-8. Two normal condition array cases are included as the cask remains dry through all operating conditions, while 10 CFR 71 requires a normal condition maximum reactivity moderator density case. The listed values represent the maximum system reactivity adjusted for Monte Carlo run uncertainty and are significantly below the lower of system USL.

No benchmarks for mixed heterogeneous UO_2 and MOX rod systems are publically available. Therefore, individual benchmarks are established for UO_2 and MOX systems. The more limiting USL is applied to the results of the MOX/UO_2 rod calculations. Per Section 6.7.2, the USL for an array of UO_2 rods is 0.9376 and 0.9331 for an array of MOX rods for a Δk of 0.0045 between the two fuel types. The evaluations demonstrated that MCNP, with its associated cross-sections, accurately predicts system reactitities containing either fuel rod type.

The focus of the evaluations is a wet (flooded) system, as no reasonable extrapolation of the data provided would indicate a safety concern for a dry system at the requested fissile material levels.

While it is recognized that code performance and bias are potentially affected by the difference in the energy level of neutron causing fission, the benchmarks accounted for the basic phenomena, and the computer code is capable of tracking particles at their relevant energy levels.

Analyses have demonstrated that the UO_2 rod payload, calculated to be at maximum reactivity flooded with an EALCF of 0.13 eV (3.0 cm pitch study UO_2 case), are significantly lower in reactivity than the MOX payload with an EALCF of 0.13 eV (note systems have identical EALCF at optimum pitch). Insertion of the lower reactivity UO2 rods and corresponding replacement of higher reactivity MOX rods will reduce system reactivity.

Given the significant margin (Δk of 0.13) between maximum calculated reactivity for a hypothetical fuel material (all ^{241}Pu) at maximum reactivity pitch, without inclusion of the tube insert that retains the rods in a fixed position, the evaluations demonstrate that the system meets regulatory requirements. No mixed fuel evaluations are, therefore, performed and no mixed bias is discussed.

Table 6.7.1-9 compares the physical and hypothetical rod/material combinations to the area of applicability for the MOX material and maximum reactivity ^{241}Pu material. The MOX Services fuel material is within the area of applicability. No pure ^{241}Pu benchmark exists; therefore, the hypothetical configuration is significantly outside the area of applicability of the benchmark calculation. Compliance with regulatory limits is assured, as there is no significant reactivity trend versus plutonium isotopic composition. There is a significant margin to limits (0.13 Δk) versus a typical code bias in the 1-2% range, and the results are obtained from a hypothetical (conservative) isotope composition (all ^{241}Pu).

As the shipment includes uranium oxide rods, the maximum reactivity uranium oxide rod configuration characteristics are compared to the area of applicability in Table 6.7.1-10. The USL for UO_2 evaluations is 0.9372. Exceeding the area of applicability for enrichment and fuel to moderator ratios (expressed as rod pitch and H/U ratio) in the UO_2 benchmark cases is acceptable as neither function has a trend that is statistically significant and the margin to limits is large (> 0.4). A similar argument is applied to slightly lower fission energy for the maximum reactivity case than covered by the benchmark analysis. There is no statistically significant trend of reactivity versus energy, and any relative changes in USL postulated from the extrapolation is not significant versus the subcritical margin of the UO_2 rod shipment.

Evaluations of a mixed shipment of enriched UO_2 rods and MOX rods are not required, as the reactivity of the evaluated MOX rods are significantly higher than those of the UO_2 rods. Mixed shipments are, therefore, permitted.

Table 6.7.1-11 lists the bounding characteristics for the MOX/UO_2 PWR fuel rods evaluated in this section.

Figure 6.7.1-5 PWR MOX Rod Shipment - Reactivity versus Rod Pitch

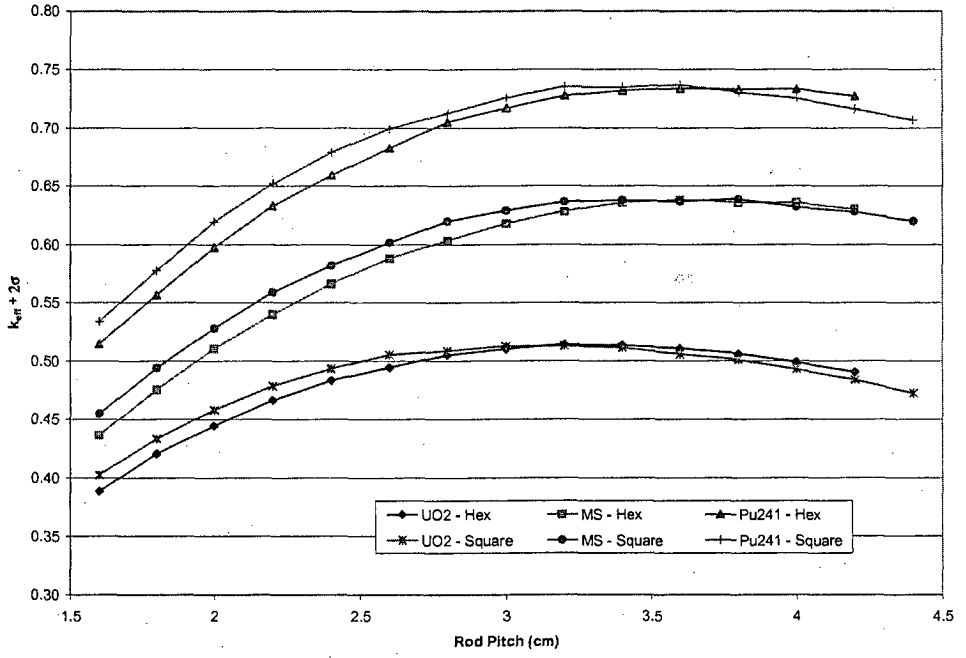


Figure 6.7.1-6 Moderator Density Study – UO_2 Fuel Material – 3.0 cm Rod Pitch

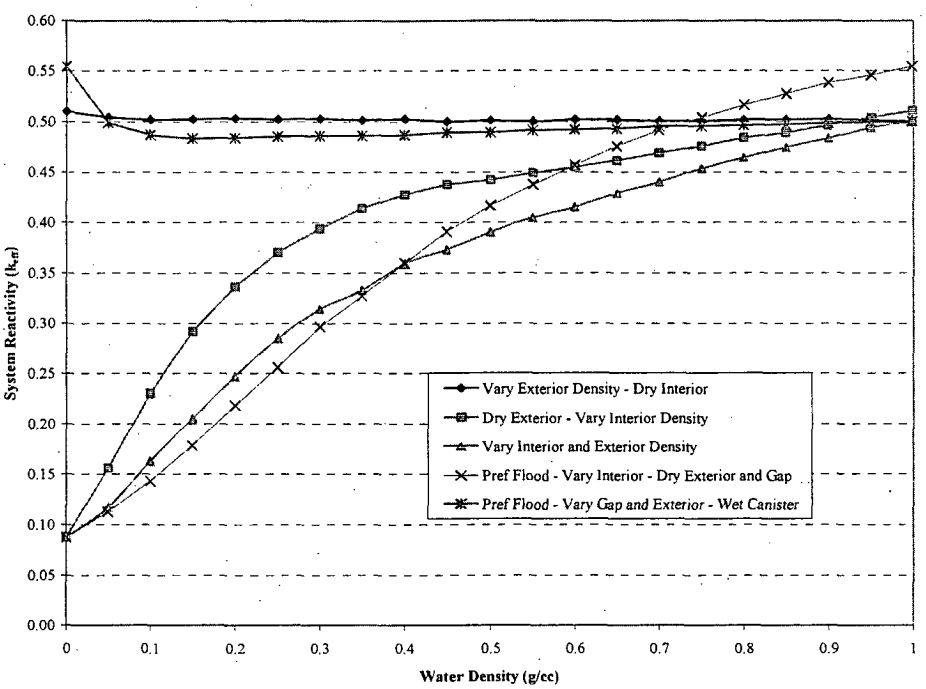


Figure 6.7.1-7 Moderator Density Study – MS Fuel Material – 3.6 cm Rod Pitch

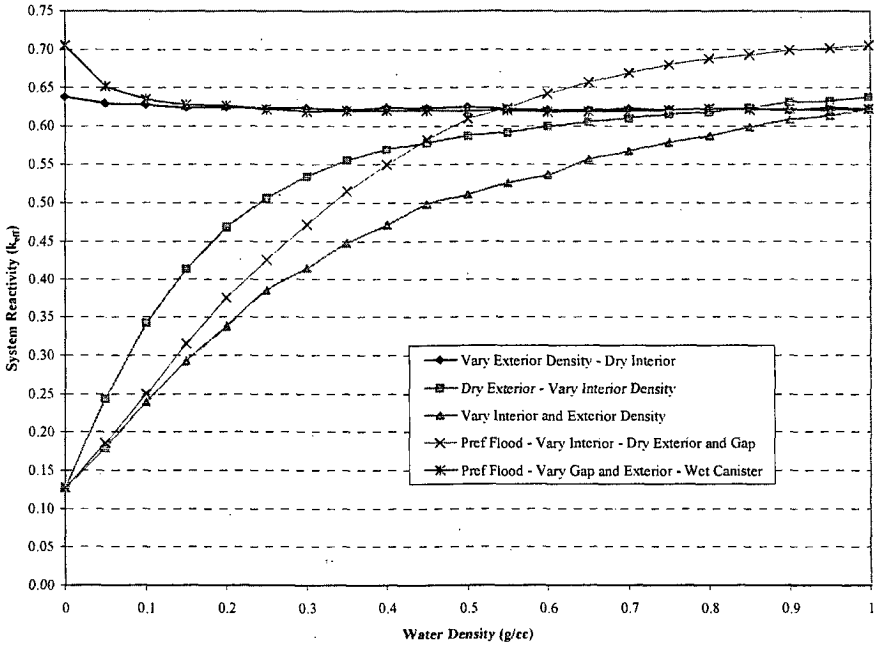


Figure 6.7.1-8 Moderator Density Study – PWR MOX ^{241}Pu Fuel Material – 3.6 cm Rod Pitch

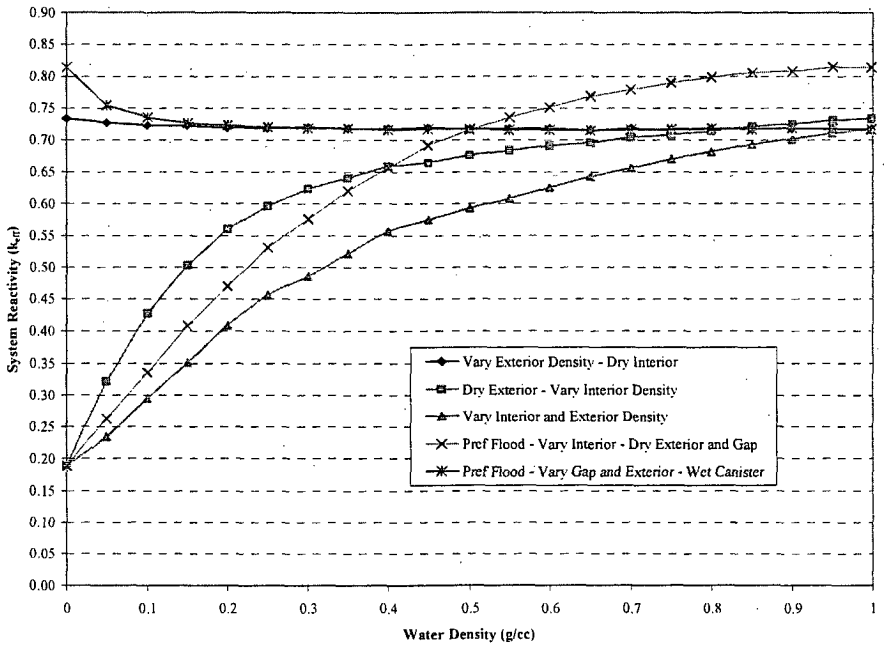


Table 6.7.1-3 PWR MOX Rod Shipment - Reactivity as a Function of Geometry and Material

Fuel Material	Rod Pitch	k_{eff}	σ	$k_{eff}+2\sigma$	vs. MS or P1 Composition	
					Δk_{eff}	$\Delta k_{eff}/\sigma$
UO_2	3.0	0.50837	0.00087	0.51011	-0.10728	-81.4
WG	3.0	0.61442	0.00106	0.61654	-0.00123	-0.8
FG	3.0	0.60516	0.00097	0.60710	-0.01049	-7.6
PG	3.0	0.59390	0.00104	0.59598	-0.02175	-15.1
MS	3.0	0.61565	0.00099	0.61763	--	--
FP	3.0	0.63359	0.00107	0.63573	-0.08132	-51.8
P9	3.0	0.62715	0.00111	0.62937	-0.08776	-54.9
P1	3.0	0.71491	0.00115	0.71721	--	--
UO_2	3.6	0.50911	0.00084	0.51079	-0.12688	-96.0
WG	3.6	0.63252	0.00098	0.63448	-0.00347	-2.5
FG	3.6	0.62282	0.00099	0.62480	-0.01317	-9.3
PG	3.6	0.61299	0.00105	0.61509	-0.02300	-15.7
MS	3.6	0.63599	0.00102	0.63803	--	--
FP	3.6	0.65225	0.00100	0.65425	-0.07909	-50.1
P9	3.6	0.64517	0.00107	0.64731	-0.08617	-53.1
P1	3.6	0.73134	0.00122	0.73378	--	--

Table 6.7.1-4 PWR MOX Fuel Shipment – Fuel Rod Pitch Study

Rod Pitch	Pitch Config	Fuel Material	k_{eff}	Fuel Material	k_{eff}	Fuel Material	k_{eff}
1.8	Hexagonal	UO_2	0.41843	MS	0.47357	^{241}Pu	0.55466
2.0	Hexagonal	UO_2	0.44262	MS	0.50841	^{241}Pu	0.59542
2.2	Hexagonal	UO_2	0.46448	MS	0.53761	^{241}Pu	0.63030
2.4	Hexagonal	UO_2	0.48147	MS	0.56403	^{241}Pu	0.65675
2.6	Hexagonal	UO_2	0.49260	MS	0.58626	^{241}Pu	0.68060
2.8	Hexagonal	UO_2	0.50325	MS	0.60145	^{241}Pu	0.70293
3.0	Hexagonal	UO_2	0.50837	MS	0.61565	^{241}Pu	0.71491
3.2	Hexagonal	UO_2	0.51224	MS	0.62593	^{241}Pu	0.72528
3.4	Hexagonal	UO_2	0.51156	MS	0.63376	^{241}Pu	0.72957
3.6	Hexagonal	UO_2	0.50911	MS	0.63599	^{241}Pu	0.73134
3.8	Hexagonal	UO_2	0.50464	MS	0.63360	^{241}Pu	0.73067
4.0	Hexagonal	UO_2	0.49718	MS	0.63359	^{241}Pu	0.73097
4.2	Hexagonal	UO_2	0.48894	MS	0.62789	^{241}Pu	0.72504
1.8	Square	UO_2	0.43146	MS	0.49220	^{241}Pu	0.57531
2.0	Square	UO_2	0.45613	MS	0.52574	^{241}Pu	0.61729
2.2	Square	UO_2	0.47678	MS	0.55687	^{241}Pu	0.64902
2.4	Square	UO_2	0.49150	MS	0.57989	^{241}Pu	0.67677
2.6	Square	UO_2	0.50343	MS	0.59949	^{241}Pu	0.69695
2.8	Square	UO_2	0.50669	MS	0.61768	^{241}Pu	0.71049
3.0	Square	UO_2	0.51090	MS	0.62688	^{241}Pu	0.72343
3.2	Square	UO_2	0.51089	MS	0.63415	^{241}Pu	0.73285
3.4	Square	UO_2	0.50965	MS	0.63544	^{241}Pu	0.73257
3.6	Square	UO_2	0.50429	MS	0.63440	^{241}Pu	0.73463
3.8	Square	UO_2	0.49939	MS	0.63658	^{241}Pu	0.72833
4.0	Square	UO_2	0.49120	MS	0.63003	^{241}Pu	0.72326
4.2	Square	UO_2	0.48232	MS	0.62576	^{241}Pu	0.71403

Table 6.7.1-5 PWR MOX Fuel Shipment – Optimum Moderator Study Maximum Reactivity Summary

Fuel Material	$k_{eff} + 2\sigma$
UO_2	0.55404
MOX Services	0.70523
^{241}Pu	0.81451

Table 6.7.1-6 PWR MOX Fuel Shipment Reactivity Summary for Single Cask Containment Fully Reflected Cases

Fuel Mat'l	Rod Gap (g/cc)	Array (g/cc)	Cavity (g/cc)	Exterior (g/cc)	k_{eff}	σ	$k_{eff} + 2\sigma$
UO_2	0.0001	0.0001	0.0001	0.9982	0.03394	0.00018	0.03430
UO_2	0.9982	0.9982	0.9982	0.9982	0.49629	0.00085	0.49799
UO_2	0.9982	0.9982	0.0001	0.9982	0.43536	0.00091	0.43718
MS	0.0001	0.0001	0.0001	0.9982	0.04527	0.00028	0.04583
MS	0.9982	0.9982	0.9982	0.9982	0.61686	0.00100	0.61886
MS	0.9982	0.9982	0.0001	0.9982	0.58689	0.00102	0.58893
^{241}Pu	0.0001	0.0001	0.0001	0.9982	0.04895	0.00036	0.04967
^{241}Pu	0.9982	0.9982	0.9982	0.9982	0.71168	0.00115	0.71398
^{241}Pu	0.9982	0.9982	0.0001	0.9982	0.67957	0.00121	0.68199

Table 6.7.1-7 PWR MOX Fuel Shipment Reactivity Summary for Normal Condition Array Cases

Fuel Mat'l	Rod Gap (g/cc)	Array (g/cc)	Cavity (g/cc)	Exterior (g/cc)	k_{eff}	σ	$k_{eff} + 2\sigma$
UO_2	0.0001	0.0001	0.0001	0.0001	0.03393	0.00016	0.03425
UO_2	0.9982	0.9982	0.9982	0.9982	0.49757	0.00089	0.49935
UO_2	0.9982	0.9982	0.9982	0.0001	0.49624	0.00092	0.49808
UO_2	0.9982	0.9982	0.0001	0.0001	0.43382	0.00087	0.43556
MS	0.0001	0.0001	0.0001	0.0001	0.04576	0.00025	0.04626
MS	0.9982	0.9982	0.9982	0.9982	0.61761	0.00101	0.61963
MS	0.9982	0.9982	0.9982	0.0001	0.61581	0.00102	0.61785
MS	0.9982	0.9982	0.0001	0.0001	0.58588	0.00099	0.58786
^{241}Pu	0.0001	0.0001	0.0001	0.0001	0.04905	0.00032	0.04969
^{241}Pu	0.9982	0.9982	0.9982	0.9982	0.71149	0.00112	0.71373
^{241}Pu	0.9982	0.9982	0.9982	0.0001	0.71256	0.0012	0.71496
^{241}Pu	0.9982	0.9982	0.0001	0.0001	0.68189	0.00118	0.68425

Table 6.7.1-8 PWR MOX Fuel Shipments - Summary of Maximum Reactivity Configurations

Fuel Material	Result	Accident Array – Preferentially Flooded	Normal Array – Preferentially Flooded	Normal Array – Dry	Single Cask Fully (Water) Reflected
UO_2	$k_{eff} + 2\sigma$	0.55404	0.49808	0.03425	0.49799
	EALCF (eV)	9.79E-02	8.83E-02	2.95E+05	8.81E-02
MS	$k_{eff} + 2\sigma$	0.70523	0.61963	0.04626	0.61886
	EALCF (eV)	1.25E-01	1.17E-01	2.14E+05	1.17E-01
^{241}Pu	$k_{eff} + 2\sigma$	0.81386	0.71496	0.04969	0.71398
	EALCF (eV)	1.33E-01	1.21E-01	8.72E+04	1.22E-01

Table 6.7.1-9 PWR MOX Fuel Shipments – PWR MOX Comparison to Area of Applicability

Parameter	Min	Max	MOX Services Materials	^{241}Pu Materials
EALCF (eV)	8.10E-02	8.99E-01	0.13	0.13
$^{235}U/^{238}U$ Weight Ratio	1.58E-03	1.51E+00	7.05E-03	7.05E-03
$^{238}Pu/^{238}U$ Weight Ratio	1.88E-06	1.54E-04	4.17E-05	0.0
$^{239}Pu/^{238}U$ Weight Ratio	1.39E-02	7.77E-01	7.92E-02	0.0
$^{240}Pu/^{238}U$ Weight Ratio	1.20E-03	8.48E-02	3.75E-03	0.0
$^{241}Pu/^{238}U$ Weight Ratio	7.90E-05	7.59E-03	3.34E-04	7.94E-02
$^{242}Pu/^{238}U$ Weight Ratio	4.63E-06	6.38E-04	4.17E-05	0.0
Water to Fuel Volume Ratio	1.10E+00	2.07E+01	1.43E+01	

Table 6.7.1-10 PWR MOX Fuel Shipments – UO_2 Comparison to Area of Applicability

Parameter	Min	Max	UO_2 Case
Enrichment (wt % ^{235}U)	2.35	4.738	5.0
Fuel rod pitch (cm)	1.3	2.54	3.0
Fuel pellet outer diameter (cm)	0.79	1.265	0.85/0.96
Fuel rod diameter (cm)	0.94	1.4172	0.93/1.12
H/^{235}U atom ratio	106.2	403.9	627 to 2140[1]
EALCF (eV)	0.09781	0.3447	0.0874

Table 6.7.1-11 Bounding Parameters for PWR MOX/UO_2 Rod Shipments

Parameter	Value
Fuel Form	Clad UO_2 or MOX rod
Number of Rods	16[2]
Clad Material	Zirconium Alloy
UO_2 Rods – Max. Enrichment (wt % ^{235}U)	5
MOX Rods – Max. Fissile Pu Content (wt %)	7[3]
Maximum Heavy Metal Content Per Rod (kg)	2.60
Maximum Pellet Diameter (inch)	0.3765
Maximum Active Fuel Length (inch)	153.5

[1] Dependent on pitch configuration (square or hexagonal).
[2] Mixture of UO_2 and MOX rods is permitted.
[3] Sum of ^{239}Pu and ^{241}Pu.

Table 6.7.1-12 B&W, CE and Westinghouse PWR Fuel Assembly Data

Fuel Type/ Parameter	B&W 15×15 Mark B4	B&W 17×17 Mark C	CE 14×14	CE 16×16 SYS 80	WE 14×14 Std	WE 14×14 OFA	WE 15×15	WE 17×17	WE 17×17 OFA
Fuel Rod Data									
Rod Dia. (in)	0.43	0.379	0.44	0.382	0.422	0.4	0.422	0.374	0.36
Clad Thick. (in)	0.0265	0.024	0.028	0.025	0.0225	0.0243	0.0242	0.0225	0.0225
Clad Mat.	Zirc	Zirc	Zirc	Zirc	Zirc	Zirc	Zirc	Zirc	Zirc
Pellet Dia. (in)	0.3686	0.3232	0.3765	0.325	0.3674	0.3444	0.3659	0.3225	0.3088
Act. Length (in)	144	143	137	150	145.2	144	144	144	144

Table 6.7.1-13 Exxon/ANF PWR Fuel Assembly Data

Fuel Type/ Parameter	WE Ex/ANF 14×14	WE Ex/ANF 15×15	WE Ex/ANF 17×17	CE Ex/ANF 14×14
Fuel Rod Data				
# Rods	179	204	264	176
Pin Pitch (in)	0.556	0.563	0.496	0.58
Rod Dia. (in)	0.424	0.424	0.36	0.44
Clad Thick. (in)	0.03	0.03	0.025	0.031
Clad Mat.	Zirc	Zirc	Zirc	Zirc
Pellet Dia. (in)	0.3505	0.3565	0.303	0.37
Act. Length (in)	142	144	144	134

Chapter 7

Table of Contents

7 OPERATING PROCEDURES 7.1-1
7.1 Procedures for Loading Packages 7.1-2
7.1.1 Procedures for Wet Loading of LWR Fuel Assemblies and Canistered LWR Fuel Rods 7.1-3
7.1.2 Procedures for Dry Loading of Metallic Fuel 7.1-7
7.1.3 Procedures for Loading Metallic Fuel and Filters Containing Severely Damaged Metallic Fuel into Damaged Fuel Canisters 7.1-10
7.1.4 Procedures for Dry Loading of DIDO, Spiral, MOATA and MTR Fuel Elements in Basket Modules into the NAC-LWT Cask 7.1-12
7.1.5 MTR General and Preferential Loading Procedures 7.1-18
7.1.6 Procedure for Dry Loading of TRIGA Fuel Basket Modules and GA IFM Modules into the NAC-LWT Cask 7.1-33
7.1.7 Procedure for Loading TRIGA Damaged Fuel or Fuel Debris into a TRIGA Sealed Damaged Fuel Can (DFC) 7.1-38
7.1.8 Procedure for Wet Loading of PWR/BWR Fuel Rods or TPBARs into the PWR/BWR Transport Canister 7.1-39
7.1.9 Procedure for Wet Loading of TPBAR Consolidation Canister or PWR/BWR Rod Transport Canister into the NAC-LWT Cask 7.1-41
7.1.10 Procedure for the Dry Loading of PULSTAR Fuel into the NAC-LWT Cask 7.1-44
7.1.11 Procedure for Dry Loading of TPBAR Waste Container 7.1-49
7.1.12 Procedure for Wet Loading PWR MOX Fuel Rods in a Transport Canister into the NAC-LWT Cask 7.1-51
7.2 Procedures for Unloading Package 7.2-1
7.2.1 Procedures for Wet Unloading of LWR Fuel and PWR, PWR MOX and BWR Fuel Rods in Transport Canisters 7.2-1
7.2.2 Procedures for Wet Unloading of Metallic Fuel 7.2-3
7.2.3 Procedure for Wet Unloading of MTR, TRIGA, DIDO, ANSTO or PULSTAR Fuel Basket Contents 7.2-6
7.2.4 Procedure for Dry Unloading of MTR, TRIGA, DIDO, ANSTO or PULSTAR Fuel Contents 7.2-8
7.2.5 Procedure for Dry Unloading of TPBAR Contents 7.2-10
7.2.6 Procedure for Dry Unloading of PWR/BWR/MOX Fuel Rod Contents 7.2-12
7.3 Procedures for Preparation of the Empty Package for Transport 7.3-1

List of Figures

Figure 7.1-1 MTR Fuel Basket Module Loading Pattern (Top View) 7.1-22
Figure 7.1-2 LEU MTR Fuel Basket Loading Guidelines for 30 W Uniform Loading 7.1-23
Figure 7.1-3 MEU MTR Fuel Basket Loading Guidelines for 30 W Uniform Loading 7.1-24
Figure 7.1-4 HEU MTR Fuel Basket Loading Guidelines for 30 W Uniform Loading – Maximum 380 grams ^{235}U 7.1-25
Figure 7.1-5 HEU MTR Fuel Basket Loading Guidelines for 30 W Uniform Loading – Maximum 460 grams ^{235}U 7.1-26
Figure 7.1-6 HEU MTR Fuel Basket Loading Guidelines for Preferential Loading – Maximum 380 grams ^{235}U 7.1-27
Figure 7.1-7 HEU MTR Fuel Basket Loading Guidelines for Preferential Loading – Maximum 460 grams ^{235}U 7.1-28
Figure 7.1-8 DIDO LEU Cooling Time vs. Fuel Burnup Basket Module Loading Guidelines for Uniform Loading 7.1-29
Figure 7.1-9 DIDO MEU Cooling Time vs. Fuel Burnup Basket Module Loading Guidelines for Uniform Loading 7.1-30
Figure 7.1-10 DIDO HEU Cooling Time vs. Fuel Burnup Basket Module Loading Guidelines for Uniform Loading 7.1-31
Figure 7.1-11 Bounding DIDO Element Minimum Cool Time vs. wt % ^{235}U Depletion 7.1-32

List of Tables

Table 7.3-1 Bolt and Torque Table 7.3-2

7 OPERATING PROCEDURES

This chapter describes the generic operating procedures for loading, unloading and preparing the NAC-LWT package for transport. These procedures shall be implemented to ensure the package is used in accordance with Certificate of Compliance (CoC) No. 9225 for the NAC-LWT packaging.

These procedures are based on generic site conditions and assume that the package arrives at the handling site with the appropriate internals installed in the cask. Additional operations and/or modifications (i.e., sequence of operations, use of parallel operations, etc.) to these procedures to address site-specific conditions may be required for each user's facility. These additional operations and/or modifications will be documented in site-specific procedures.

In addition, site-specific procedures may incorporate signoffs for activities or operational sequences as they are performed. Oversight organizations, such as Quality Assurance or Quality Control, may participate in certain package handling operations. The use of signoffs can assist the user in assuring that critical steps are not overlooked, that the package is handled in accordance with the CoC and Safety Analysis Report (SAR), and that appropriate records are retained as required by 10 CFR 71.91.

The NAC-LWT package is designed and certified to transport numerous fissile and radioactive contents, as described in the CoC, as a Type B(U)F-96 package in a leaktight containment boundary configuration.

The NAC-LWT is also certified for the transport of Tritium Producing Burnable Absorber Rod (TPBAR) contents, as described in the CoC, as a Type B(M)-96 package in a leaktight containment boundary configuration. NAC-LWT cask units designated for the transport of TPBAR contents shall be configured with Alternate B vent and drain port covers in accordance with the license drawings, and subjected to the additional hydrostatic test per the requirements of Section 8.1.2.

Loaded shipments received at U.S. Department of Energy (DOE) facilities shall be receipt surveyed and monitored in accordance with DOE regulations. As required, the shipper will be notified of any survey or shipping discrepancy and the shipper will ensure appropriate regulatory notifications are completed.

When the package is handled in accordance with the procedures provided herein, and is loaded within the conditions of the CoC and the SAR, the resulting occupational exposures will be maintained as low as reasonably achievable (ALARA), as required by 10 CFR 20.

7.1 Procedures for Loading Packages

For the shipment of loaded packages, the cavity shall be dry, the contents and nameplate package identification, corresponding to the contents, shall be verified as correct, and the other applicable conditions of the Certificate of Compliance (CoC) shall be verified as met. Site-specific procedures for dry handling and loading of fuel assemblies and other authorized contents will be prepared to incorporate the dry transfer system components required to safely and efficiently load the NAC-LWT at each loading facility. Dry loading and transfer procedures are not specifically described in the individual loading procedures due to these facility and required equipment variations. Content configurations may require spacers, baskets, basket inserts, canisters, etc., to support and/or control the content geometry during transport. The transport configurations identifying the specific contents and components required are specified in the license drawings. Solid, irradiated and contaminated hardware will generally be loaded wet utilizing the procedure guidance of Section 7.1.1. Alternatively, the solid, irradiated and contaminated hardware can be loaded dry utilizing dry loading procedures (i.e., per Section 7.1.2) modified to the requirements of the dry loading facilities.

Two port cover designs are available for use. The alternate port cover has an O-ring along the barrel and a Viton® O-ring on the inner end of the port cover. The alternate port cover was developed to provide a leaktight containment boundary and to facilitate ease of installation. The second port cover design is the Alternate B port cover that has two face seals on the inner end of the port cover. The Alternate B port cover was developed to provide a high-pressure and leaktight containment boundary and is required to be installed for the transport of TPBAR contents. The two port cover designs can be used interchangeably for authorized contents not requiring a high-pressure containment boundary capability.

The alternate port cover bolts are torqued to 100 ± 10 inch-pounds. The Alternate B port cover bolts are torqued to 285 ± 15 inch-pounds to ensure compression of the metallic containment O-ring seal.

As required for the TPBAR contents, procedures will specify the use of the Alternate B port covers. In these loading procedures, the more restrictive Alternate B port cover helium leakage rate testing is described. For other content loading procedures, either port cover design can be used. However, if the Alternate B port covers are used, the metallic O-ring seal will be replaced for each transport following component removal and the helium maintenance leakage rate test is required to be performed.

For cask loading operations performed under water or when water is introduced into the cask cavity, the cask cavity is required to be blown down to remove the cavity water, vacuum dried, verified as dry, and helium backfilled prior to final closure and leakage testing. The cavity is vacuum dried by attaching a vacuum pump to the vent and/or drain port and evacuating the cavity to a pressure of less than 10 torr (13 mbar), and continuing to vacuum pump for an additional 15 minutes. If the cavity pressure rise is less than 5 torr (6.7 mbar) during a 10-minute isolation and hold period, there is no free water in the cavity and the cask cavity is verified as dry. Final containment closure and leakage testing operations in preparation for transport can proceed. If the pressure rise is >5 torr (6.7 mbar), the vacuum drying will be continued until the dryness verification criteria are met. The successful performance of the dryness verification and backfilling the cavity with helium ensures that there is no free water in the cavity and oxidation of the cask's contents is precluded. When the cask is loaded in a dry cell or under other conditions where no water is introduced into the cask cavity, the procedure sequences for cavity blow down, vacuum drying and dryness verification can be eliminated and the loading sequence can proceed directly to final closure, containment boundary leakage testing and helium backfill operations.

7.1.1 Procedures for Wet Loading of LWR Fuel Assemblies and Canistered LWR Fuel Rods

The procedures for wet loading the NAC-LWT with LWR fuel are as follows:

1. Perform a receipt inspection of the empty cask and trailer/ISO container, inspecting for transport damage.
2. Position the trailer in the designated cask unloading area. Set the trailer brakes and chock the wheels to prevent unintended movement. If site-specific conditions exist that require the trailer to move to allow the cask to be uprighted on its rotation trunnions, release brakes and remove the chocks when required to complete uprighting operations. If an ISO container is used, it may be removed from the trailer and secured in the unloading area.
3. Remove the personnel barrier or the roof and roof cross-members from the ISO container.

   Note: Verify that the package nameplate displays the correct package identification number in accordance with the CoC.

4. Perform a Health Physics survey of the cask and adjacent surfaces of the trailer.

   Note: A receiving survey of the cask and transporter must be performed as soon as practicable after arrival at the site to assure compliance with 10 CFR 20, 10 CFR 71.87(i) and 10 CFR 71.47, and to assure timely reporting of any reportable noncompliance.

5. Remove the top and bottom impact limiters.
6. Remove the cask tie-down strap.
7. Using the lifting yoke with the guides removed, engage the lifting trunnions. Raise the cask to vertical by rotating the cask rotation sockets on the rear cask supports, moving the crane and/or trailer as required to keep the lift yoke engaged to the trunnions and the cask engaged in the rear supports. When the cask is fully vertical, lift the cask from the supports and remove it from the trailer/container.
8. Place the cask in the cask preparation area or other designated location. Disengage the lifting yoke. Clean cask surfaces of road dirt as required for entry into the spent fuel pool.
9. Visually inspect the neutron shield tank fill, drain and level inspection plugs for signs of neutron shield fluid leakage. If leakage is detected or suspected, verify shield tank fluid level and correct, as required.
10. Remove the vent and drain valve port covers. Prior to reinstallation of the port covers, carefully inspect the valve port cover O-ring seals and, if the O-rings show any damage, replace them with approved spares. Ensure that the replacement O-rings are properly installed and seated. Visually inspect the valved quick-disconnect nipples and replace them, if necessary.

    Note: For Alternate B port covers, replace the metallic O-ring with an approved spare prior to reinstallation.

11. Remove closure lid bolts. Attach the lid lift slings to the closure lid. Remove the closure lid and set it on a support that is suitable for radiological control and for maintaining the cleanliness of the closure lid. Prior to reinstallation of the lid, carefully inspect the Teflon O-ring seal in the underside of the closure lid and, if it shows any damage, replace it. Remove the metallic O-ring and replace it with an approved spare. Ensure that the replacement O-rings are properly installed and seated. Inspect the lid bolts and replace any that are damaged.
12. Visually inspect the inner cavity for foreign material or damage. Install or verify the presence of the proper drain tube and basket assembly.
13. Fill the cask cavity with clean water.
14. Install lift yoke arm guides and remote actuation component on the cask lifting yoke.
15. Engage the cask lifting yoke with the cask lifting trunnions and pick up the cask. Carefully lower the cask to the bottom of the cask loading area. Rinse the cask surfaces with clean water to minimize cask surface contamination.
16. Disengage the lifting yoke from the cask and remove the yoke from the pool, if necessary, to provide fuel loading clearance.
17. Identify the fuel assembly(ies) or canistered LWR fuel rods to be loaded. Verify the identified materials comply with the content conditions and authorized quantities as specified in the CoC.

18. Pick up the fuel assembly or transport canister containing individual fuel rods, using the required grapple system.

    Note: See Section 7.1.8 procedures for instructions for loading and preparing PWR or BWR rods in a transport canister.

19. Position the fuel contents over the cask and carefully lower them into the cask to avoid damage to the cask sealing surfaces. Confirm that the fuel assembly (or transport canister and insert, or material container) is fully seated, then release the grapple from the fuel assembly (or transport canister and insert) and raise the grapple to the full up position. Repeat this step as necessary to load multiple assemblies or containers (if required).

20. Position the cask lifting yoke over the cask closure lid. Attach the slings to the closure lid and cask lifting yoke. Lower the yoke over the cask.

21. Position the closure lid over the cask and slowly lower it into place using the cask and lid match marks as guides. Visually confirm that the closure lid is seated.

22. Lower the cask handling yoke to slack the closure lid cables. Engage the cask lifting trunnions with the yoke and begin lifting.

    Note: Visually verify the yoke engagement before lifting the cask.

23. Raise the cask until the lid is slightly above the surface of the pool. At the option of the licensee/user, a number of closure lid bolts (i.e., 4 to 12) may be installed hand tight.

24. Raise the cask clear of the pool, rinsing the yoke and cask with clean water.

25. Transfer the cask to the decontamination pit or other work area. Remove the yoke and lid lift slings.

26. Install and tighten the 12 closure lid bolts to 260 ± 20 ft-lb in three passes, using the torque sequence stamped on the closure lid.

27. At the option of the licensee/user, a 25 to 50 gallon clean water flush of the cask cavity may be performed by connecting a valved, clean water line to the drain valve and a valved drain line to the vent valve. After the cavity flushing is completed, if performed, disconnect the water supply and drain lines.

28. Connect a gas supply line to the vent valve and the drain line to the drain valve.

29. Open the nitrogen or helium gas supply valve and pressurize the cask cavity (< 30 psig) to force any residual water out the drain line. Continue to supply pressurized gas to the cask for a minimum of five minutes after the last residual free water discharges from the drain. Remove the drain and gas supply lines and attach a vacuum drying system (VDS) to the vent.

30. Evacuate the cask cavity to less than or equal to 10 torr (13 mbar) and continue vacuum pumping for a minimum of 15 minutes.

31. At the end of the vacuum pumping period, isolate the cask cavity from the vacuum pump and stop the vacuum pump. Monitor the cask cavity pressure for a minimum of 10 minutes. If the pressure rise is less than 5 torr (6.7 mbar), the cavity is verified as dry of

free water. If the pressure rise is >5 torr (6.7 mbar), repeat vacuum drying until the dryness verification results are satisfactory.

32. Backfill the cask cavity with helium to 0 psig (1 atmosphere, absolute), +1, -0 psi and disconnect the VDS from the vent valve.

33. Perform a helium leakage test of the closure lid containment O-ring using a Helium Mass Spectrometer Leak Detector (He MSLD) in accordance with the procedural requirements of Section 8.1.3.1, Steps 3 through 10.

34. Install the vent and drain alternate port covers and torque the bolts to 100 ±10 inch-pounds.

35. If an alternate port cover containment O-ring seal was replaced, perform a helium leakage test on the affected port cover using a He MSLD in accordance with the requirements of Section 8.1.3.2.2.

36. If the alternate port cover containment seal was inspected and accepted for reuse, perform a gas pressure drop leakage test on the affected port cover as follows.

    a. Install a pressure test fixture to the port cover test port, including a calibrated pressure gauge with a minimum sensitivity of 0.25 psi.

    b. Pressurize the port cover seal annulus to 15 psig, +1, -0 psi.

    c. Isolate the gas supply and observe the pressure gauge for a minimum of five minutes.

    d. The acceptance criterion for the test is no measurable drop in pressure during the minimum test time. An acceptable test assures that the minimum assembly verification leakage test sensitivity is achieved.

    Note: Alternate B port covers, if used, require the satisfactory completion of a helium maintenance leakage rate test to confirm a leaktight seal condition for each loaded transport. Install the Alternate B port cover and perform the maintenance leakage rate test per the requirements of Section 8.1.3.3.2.

37. Decontaminate the cask surfaces. Survey the cask for surface contamination and radiation dose rates.

    Note: Ensure compliance with 10 CFR 71.87(i) and 10 CFR 71.47.

38. Remove lift yoke arm guides. Engage the cask lifting yoke to the lifting trunnions.

39. Lift the cask and position the cask rotation sockets in the rear rotation trunnions of the rear support structure. Carefully lower the cask to the horizontal transport orientation resting on the front saddle by moving the crane and/or the trailer as required to maintain cask engagement to the rear supports.

40. Disengage the lifting yoke from the lifting trunnions and remove it from the area.

41. Install the cask tie-down strap. Install the top and bottom impact limiters.

42. Install tamper-indicating device (TID) to an attachment point on the top impact limiter.

43. Install ISO container bracing and lid or personnel barrier.

44. Complete radiation and contamination surveys of the external surfaces of the package and record the data. Ensure removable contamination and radiation dose rate survey results comply with the limits specified in 10 CFR 71.87(i) and (j).
45. Measure the dose rate in millirems per hour at one meter from the package surface to determine the Transport Index (TI). Indicate the TI on the Radioactive Material labels applied to the package in accordance with 49 CFR 172, Subpart E.
46. Determine the appropriate Criticality Safety Index (CSI) assigned to the package contents in accordance with the CoC, and indicate the correct CSI on the Fissile Material label applied to the package per 49 CFR 172, Subpart E.
47. Apply appropriate placards to the transport vehicle in accordance with 49 CFR 172, Subpart F.
48. Complete the shipping documents and provide the carrier with instructions regarding the requirements for maintaining an exclusive use shipment.

7.1.2 Procedures for Dry Loading of Metallic Fuel

The procedures for dry loading the package with metallic fuel are as follows:

1. Perform a receipt inspection of the empty cask and trailer/ISO container, inspecting for transport damage.
2. Position the trailer in the designated cask unloading area. Set the trailer brakes and chock the wheels to prevent unintended movement. If site-specific conditions exist that require the trailer to move to allow the cask to be uprighted on its rotation trunnions, release brakes and remove the chocks when required to complete uprighting operations. If an ISO container is used, it may be removed from the trailer and secured in the unloading area.
3. Remove the roof from the ISO container and open the front and rear ISO doors. Remove roof cross-members, if installed.

   Note: Verify that the package nameplate displays the correct package identification number in accordance with the CoC.
4. Perform a Health Physics survey of the cask and adjacent surfaces of the container.

   Note: A receiving survey of the cask and transporter must be performed as soon as practicable after arrival at the site to ensure compliance with 10 CFR 20, 10 CFR 71.87(i) and 10 CFR 71.47, and to ensure timely reporting of any reportable noncompliance.
5. Remove the top and bottom impact limiters.
6. Remove the cask tie-down strap.
7. Using the lifting yoke with the guides removed, engage the lifting trunnions. Raise the cask to vertical by rotating the cask rotation sockets on the rear cask supports, moving the crane and/or trailer as required to keep the lift yoke engaged to the

trunnions and the cask engaged in the rear supports. When the cask is fully vertical, lift the cask from the supports and remove it from the trailer/container.

8. Place the cask in the dry loading stand. Disengage the lifting yoke.

9. Remove the vent and drain valve port covers. Prior to reinstallation of the port covers, carefully inspect the O-rings and, if the O-rings show any damage, replace them with approved spares. Ensure that the replacement O-rings are properly installed and seated. Visually inspect the valved quick-disconnect nipples and replace them, if necessary.

   Note: For Alternate B port covers, replace the metallic O-ring with an approved spare prior to reinstallation.

10. Remove closure lid bolts. Attach the lid lift slings to the closure lid. Remove the closure lid and set it on a support that is suitable for radiological control and for maintaining the cleanliness of the closure lid. Prior to reinstallation of the lid, carefully inspect the Teflon O-ring seal in the underside of the closure lid and, if it shows any damage, replace it. Remove the metallic O-ring and replace it with an approved spare. Ensure that the replacement O-rings are properly installed and seated. Inspect the lid bolts and replace any that are damaged.

11. Visually inspect the inner cavity for foreign material or damage. Install, or verify the presence of the proper drain tube assembly and basket, as required.

12. Install the required dry transfer system components to the top of the cask.

13. Position the shielded transfer cask system components for fuel loading, as appropriate.

14. Identify the fuel to be loaded and verify that the fuel contents comply with the content conditions and authorized quantities as specified in the CoC. Up to five sound metallic fuel rods may be placed in an unsealed canister. Damaged rods may be placed in a sealed 2.75-inch or 4.0-inch failed fuel canister (FFC). Up to 10 filters containing oxide powder from severely damaged metallic fuel rods may be placed in one FFC. The FFC(s) containing filters may be loaded with up to two FFCs containing failed fuel rods to fill the three–element basket. The FFCs must be vacuum dried and sealed as described in Section 7.1.3.

15. Load the shielded transfer cask with the selected fuel contents.

16. Place the shielded transfer cask, containing a fuel canister, onto the dry transfer system components positioned on the top of the cask.

17. Lower the fuel canister from the transfer cask into the shipping cask.

18. Repeat the loading and transfer of fuel canisters until the approved cask loading plan is completed.

19. Install the closure lid onto the cask. Visually verify that the lid is properly seated.

20. Remove the dry transfer system components from the top of the cask.

21. Install and tighten the 12 closure lid bolts to 260 ± 20 ft-lb in three passes, using the torque sequence stamped on the closure lid.

22. This step applies only if the cask contains damaged metallic fuel or severely damaged metallic fuel.

    a. Attach the vacuum pump to the cask vent valve.

    b. Evacuate the cask cavity to ≤ 10 torr (13 mbar) and maintain for a minimum of 15 minutes.

    c. Stop the vacuum pump and monitor pressure for a minimum of 10 minutes. If the pressure rise is less than 5 torr (6.5 mbar), the cask is adequately dried for shipment. If not, repeat vacuum drying and pressure rise verification.

    d. Remove the vacuum pump and backfill the cask cavity with helium to 1 atmosphere (absolute) +1, -0 psi.

    e. Remove the gas supply line.

23. Perform the helium mass spectrometer leakage rate test on the cask lid in accordance with the requirements of Section 8.1.3.1, Steps 3 through 10.

24. Install the vent and drain alternate port covers and torque the bolts to 100 ±10 inch-pounds.

25. If an alternate port cover containment O-ring seal was replaced, perform a helium leakage test on the affected port cover using a He MSLD in accordance with the requirements of Section 8.1.3.2.2.

26. If the alternate port cover containment seal was inspected and accepted for reuse, perform a gas pressure drop leakage test on the affected port cover as follows.

    a. Install a pressure test fixture to the port cover test port, including a calibrated pressure gauge with a minimum sensitivity of 0.25 psi.

    b. Pressurize the port cover seal annulus to 15 psig, +1, -0 psi.

    c. Isolate the gas supply and observe the pressure gauge for a minimum of five minutes.

    d. The acceptance criterion for the test is no measurable drop in pressure during the minimum test time. An acceptable test assures that the minimum assembly verification leakage test sensitivity is achieved.

    Note: Alternate B port covers, if used, require the satisfactory completion of a helium maintenance leakage rate test to confirm a leaktight seal condition for each loaded transport. Install the Alternate B port cover and perform the maintenance leakage rate test per the requirements of Section 8.1.3.3.2.

27. Decontaminate the cask. Survey the cask for surface contamination and radiation dose rates.

    Note: Ensure compliance with 10 CFR 71.87(i) and 10 CFR 71.47.

28. Remove lift yoke arm guides. Engage the cask lifting yoke to the lifting trunnions.
29. Lift the cask and position the cask rotation sockets in the rear rotation trunnions of the rear support structure. Carefully lower the cask to the horizontal transport orientation resting on the front saddle by moving the crane and/or the trailer as required to maintain cask engagement to the rear supports.
30. Disengage the lifting yoke from the lifting trunnions and remove it from the area.
31. Install the cask tie-down strap. Install the top and bottom impact limiters.
32. Install a TID to an attachment point on the top impact limiter.
33. Install ISO container bracing and lid or personnel barrier.
34. Complete radiation and contamination surveys of the external surfaces of the package and record the data. Ensure removable contamination and radiation dose rate survey results comply with the limits specified in 10 CFR 71.87(i) and (j).
35. Measure the dose rate in millirems per hour at one meter from the package surface to determine the Transport Index (TI). Indicate the TI on the Radioactive Material labels applied to the package in accordance with 49 CFR 172, Subpart E.
36. Determine the appropriate Criticality Safety Index (CSI) assigned to the package contents in accordance with the CoC, and indicate the correct CSI on the Fissile Material label applied to the package per 49 CFR 172, Subpart E.
37. Apply appropriate placards to the transport vehicle in accordance with 49 CFR 172, Subpart F.
38. Complete the shipping documents and provide the carrier with instructions regarding the requirements for maintaining an exclusive use shipment.

7.1.3 Procedures for Loading Metallic Fuel and Filters Containing Severely Damaged Metallic Fuel into Damaged Fuel Canisters

7.1.3.1 Small Diameter Canisters (Damaged Metallic Fuel)

1. Examine the small diameter failed fuel canister (FFC) and check it for damage.
2. Place the FFC inside the containment barrier portion of the pool. Position the FFC in the failed rod loading station.
3. After verifying the accountability records, place the designated failed fuel rod into the FFC. If the rod is broken into two or more pieces, verify that the lid thread and seal area is not fouled during rod insertion.
4. When the can is loaded, install the lid using the FFC Lid Installation Tool.
5. Using the FFC handling tool, move the loaded FFC through the containment barrier door and place the FFC horizontally into the upender.
6. Operate the hand winch to move the FFC to the vertical position.

7. Torque the FFC lid to 100 ± 10 ft-lb for the small canister.
8. Connect the nitrogen supply line to the vent valve.
9. Open nitrogen supply valve and pressurize the FFC to force out the water. Blow gas through the FFC for at least 5 minutes after the first visible bubbles appear. Remove the gas supply line.
10. Invert the FFC in the upender and install the pipe plug.
11. Re-invert the FFC in the upender.
12. Attach the vacuum pump to the FFC vent valve. Evacuate the FFC to a pressure below 25 torr (33 mbar) for a minimum of 15 minutes. Remove the vacuum pump and backfill with nitrogen.
13. Remove the FFC from the upender and place it into temporary storage.

7.1.3.2 Large Diameter Canisters (Damaged Metallic Fuel)

1. Examine the large diameter FFC and check it for damage.
2. Place the FFC inside the containment barrier portion of the pool. Position the FFC in the failed rod loading station.
3. This step is to be used when loading up to three uncanned or canned fuel rods into the large diameter canister. After verifying the accountability records, remove the ceramic filter from the top of the original failed rod can. Position the can plug with aluminum screen onto the open can. Install the plug.
4. Verify the accountability records for the fuel to be loaded.
5. Place the designated fuel into the FFC. If the rod is broken into two or more pieces, verify that the lid thread and seal area is not fouled during rod or can insertion. If more than one failed rod is to be installed, repeat steps 3 through 5.
6. After the canister is loaded with fuel, install the lid using the FFC Lid Installation Tool.
7. Using the FFC handling tool, move the loaded FFC through the containment barrier door and place the FFC horizontally into the upender.
8. Operate the hand winch to move the FFC to the vertical position.
9. Torque the FFC lid to 130 ± 10 ft-lb for the large canister.
10. Connect the nitrogen supply line to the vent valve.
11. Open the nitrogen supply valve and pressurize the FFC to force out the water. Blow gas through the FFC for at least 5 minutes after the first visible traces of bubbles appear. Remove the gas supply line.
12. Invert the FFC in the upender and install the pipe plug.
13. Reinvert the FFC in the upender.

14. Attach the vacuum pump to the FFC vent valve. Evacuate the FFC to a pressure below 25 torr (33 mbar) for a minimum of 15 minutes. Remove the vacuum pump and backfill with nitrogen.
15. Remove the FFC from the upender and place it into temporary storage.

7.1.3.3 Large Diameter Canisters (Severely Damaged Metallic Fuel)

1. Examine the large diameter FFC and check it for damage.
2. Place the FFC inside the containment barrier portion of the pool. Position the FFC in the failed rod loading station.
3. Verify the accountability records for the fuel in the filter set (up to 10 filters) to be loaded into the FFC.
4. After verifying the accountability records, load the filter set into the FFC and place aluminum wool on top of the last filter.
5. Verify that the lid thread and seal area is not fouled during insertion of the filter set.
6. After the canister is loaded with fuel, insert the lid using the FFC Lid Installation Tool.
7. Using the FFC handling tool, move the loaded FFC through the containment barrier door and place the FFC horizontally into the upender.
8. Operate the hand winch to move the FFC to the vertical position.
9. Torque the FFC lid to 130 ± 10 ft-lb for the large canister.
10. Connect the nitrogen supply line to the vent valve.
11. Open the nitrogen supply valve and pressurize the FFC to force out the water. Continue to blow gas through the FFC for at least 5 minutes after the first visible traces of bubbles appear. Remove the gas supply line.
12. Invert the FFC in the upender and install the pipe plug.
13. Re-invert the FFC in the upender.
14. Attach the vacuum pump to the FFC vent valve. Evacuate the FFC to a pressure below 25 torr (33 mbar) for a minimum of 15 minutes. Remove the vacuum pump and backfill with nitrogen.
15. Remove the FFC from the upender and place it into temporary storage.

7.1.4 Procedures for Dry Loading of DIDO, Spiral, MOATA and MTR Fuel Elements in Basket Modules into the NAC-LWT Cask

This procedure presents the steps for dry loading of fuel basket modules into the NAC-LWT cask using a transfer cask, which can contain various types of reactor fuel elements such as MTR, DIDO, spiral and plate assemblies (i.e., MOATA elements). The design, materials, use and

function of the various modular fuel basket assemblies such as MTR, DIDO and ANSTO are similar, and all can be loaded into the NAC-LWT utilizing these procedures.

The modular fuel basket assemblies all consist of three types of modules: a base module, intermediate modules, and a top module. Each basket module contains seven fuel element locations, consisting of a center cell and six peripheral cells. The top basket module interfaces with the cask lid to limit the axial movement of the basket assembly. The base module interfaces with the bottom of the cask cavity. The base and intermediate modules are provided with guide pins to provide for and maintain the proper alignment between basket modules. Each of the basket module types is provided with a guide bar assembly to provide for the proper interface of the basket assembly with the drain tube assembly.

Depending on the fuel type, the basket assembly may consist of 4, 5 or 6 modules, with a varying number of intermediate modules. For the DIDO, MOATA and spiral fuel types, the DIDO and ANSTO (the basket assembly identification for MOATA and spiral fuel types) basket assemblies consist of a top module, four intermediate modules and a base module. In the case of MTR fuel elements, the basket assembly can include 2, 3 or 4 intermediate modules, depending on the length and conditions of the fuel contents. Axial fuel spacers and plates may be used as dunnage to axially position the MTR fuel elements in the basket module to facilitate fuel unloading operations.

The fuel content condition (i.e., heat load, fissile mass, minimum cool time, etc.) limits for the various fuel types are discussed or referenced in the following paragraphs.

MTR fuel elements shall be selected and loaded in accordance with the MTR General and Preferential Loading Procedures in Section 7.1.5. The MTR plate canister, if required, shall be loaded in accordance with Section 7.1.4.1.

DIDO fuel elements shall meet the following loading conditions:

- The maximum decay heat per DIDO fuel element shall not exceed 25 W.
- The maximum decay heat load for a loaded DIDO fuel basket assembly shall not exceed 1.05 kW.
- The heat load for each DIDO fuel element shall be verified by use of cool time versus burnup (MWd/MTU) curves in Figure 7.1-8 (LEU fuel), Figure 7.1-9 (MEU fuel), and Figure 7.1-10 (HEU fuel) or by use of minimum cool time versus ^{235}U depletion curves in Figure 7.1-11 (generic for LEU, MEU and HEU fuels). Note that significantly lower uranium content for a loaded assembly compared to the design basis assembly may result in a loaded assembly calculated burnup higher than that included in Figure 7.1-8 through Figure 7.1-10. Use of Figure 7.1-11 ^{235}U depletion curves is required for fuel assemblies in this category.

- An additional requirement for fuel element loading of the top module limits the heat load to 18 W per element, unless there is a spacer bolted to the underside of the closure lid, or there is sufficient fuel element hardware to ensure that axial movement of the fuel element is limited, to ensure that the active fuel region is radially shielded by the gamma shield lead layer. A lid spacer, if required, shall be as shown on NAC Drawing No. 315-40-113.

Spiral and MOATA fuel elements shall meet the content conditions specified in the Certificate of Compliance for loading into the ANSTO fuel basket assembly. Full spiral fuel loads or mixed spiral and MOATA fuel loads are authorized with separate basket modules containing the two fuel types.

The procedures for loading the NAC-LWT cask with MTR, DIDO or ANSTO fuel baskets in a dry configuration or using a dry transfer system are as follows:

1. Perform a receipt inspection of the empty cask and trailer/ISO container, inspecting for transport damage.
2. Position the trailer in the designated cask unloading area. Set the trailer brakes and chock the wheels to prevent unintended movement. If site-specific conditions exist that require the trailer to move to allow the cask to be uprighted on its rotation trunnions, release brakes and remove the chocks when required to complete uprighting operations. If an ISO container is used, it may be removed from the trailer and secured in the unloading area.
3. Remove the personnel barrier or the roof and roof cross-members from the ISO container.

   Note: Verify that the package nameplate displays the correct package identification number in accordance with the CoC.
4. Perform a Health Physics survey of the cask and adjacent surfaces of the trailer.

   Note: A receiving survey of the cask and transporter must be performed as soon as practicable after arrival at the site to assure compliance with 10 CFR 20, 10 CFR71.87(i) and 10 CFR 71.47, and to assure timely reporting of any reportable noncompliance.
5. Remove the top and bottom impact limiters.
6. Remove the cask tie-down strap.
7. Using the lifting yoke with the guides removed, engage the lifting trunnions. Raise the cask to vertical by rotating the cask rotation sockets on the rear cask supports, moving the crane and/or trailer as required to keep the lift yoke engaged to the trunnions and the cask engaged in the rear supports. When the cask is fully vertical, lift the cask from the supports and remove it from the trailer/container.
8. Place the cask onto the dry loading station/stand. Disengage the lifting yoke and move clear.

9. Visually inspect the neutron shield tank fill, drain and level inspection plugs for signs of neutron shield fluid leakage. If leakage is detected or suspected, verify shield tank fluid level and correct, as required.

10. Remove the vent and drain valve port covers. Prior to reinstallation of the port covers, carefully inspect the O-ring seals and, if the O-rings show any damage, replace them with approved spares. Ensure that the replacement O-rings are properly installed and seated. Visually inspect the valved quick-disconnect nipples and replace them, if necessary.

    Note: For Alternate B port covers, replace the metallic O-ring with an approved spare prior to reinstallation.

11. Remove closure lid bolts. Attach the lid lift slings to the closure lid. Remove the closure lid and set it on a support that is suitable for radiological control and for maintaining the cleanliness of the closure lid. Prior to reinstallation of the lid, carefully inspect the Teflon O-ring seal in the underside of the closure lid and, if it shows any damage, replace it. Remove the metallic O-ring and replace it with an approved spare. Ensure that the replacement O-rings are properly installed and seated. Inspect the lid bolts and replace any that are damaged.

12. Visually inspect the inner cavity for foreign material or damage. Install or verify presence of a proper drain tube including drain tube alignment ring, as required.

13. Install the required dry transfer system components on the top of the cask.

14. Position the shielded transfer cask system components for fuel loading, as appropriate.

15. Identify the fuel to be loaded into each fuel basket module. Fuel elements loaded into each basket and/or module shall comply with the approved content conditions specified in Condition 5.(b)(1) and 5.(b)(2) of CoC No. 9225. Specific guidance on fuel selection, use of loading diagrams and preferential loading procedures is provided in Section 7.1.5. Perform an independent verification of the loading diagrams and fuel loading operations per Section 7.1.5.3.

    Note: If a basket module is to be loaded with a LEU MTR fuel element having ^{235}U content >470 g (>22 g ^{235}U per plate), cell black spacers, as shown on Drawing 315-40-085, shall be installed in basket module cell positions 1, 2 and 3 to prevent inadvertent loading of more than four LEU MTR fuel elements.

    Note: For the loading of HEU MTR fuel elements having ^{235}U content >380 g, a minimum of 2.0 cm of nonfuel hardware and /or spacer plates shall be provided at both ends of the fuel element to meet criticality control analysis requirements.

16. Load the shielded transfer cask and basket module with the selected fuel contents.

17. Place the shielded transfer cask containing a loaded fuel basket module onto the dry transfer system components positioned on the top of the cask.

18. Lower the loaded basket module from the transfer cask into the shipping cask.

19. Repeat the loading and transfer of loaded basket modules until the approved cask loading plan is completed.

20. Install the closure lid onto the cask using the dry transfer system. Visually verify that the lid is properly seated.
21. Remove the dry transfer system components from the top of the cask.
22. Install and tighten the 12 closure bolts to 260 ± 20 ft-lb in three passes, using the sequence stamped on the lid.
23. Connect a gas supply line to the vent valve and the drain line to the drain valve.
24. Open the air, nitrogen or helium gas supply valve and pressurize the cask cavity (< 30 psig) to force any residual water out the drain line. Continue to supply pressurized gas to the cask for a minimum of five minutes after the last residual free water discharges from the drain. Remove the drain and gas supply lines and attach a vacuum drying system (VDS) to the vent.
25. Evacuate the cask cavity to less than or equal to 10 torr (13 mbar) and continue vacuum pumping for a minimum of 15 minutes.
26. At the end of the vacuum pumping period, isolate the cask cavity from the vacuum pump and stop the vacuum pump. Monitor the cask cavity pressure for a minimum of 10 minutes. If the pressure rise is less than 5 torr (6.7 mbar), the cavity is verified as dry of free water. If pressure rise is >5 torr (6.7 mbar), repeat vacuum drying until the dryness verification results are satisfactory.
27. Backfill the cask cavity with helium to 0 psig (1 atmosphere, absolute), +1, -0 psi and disconnect the VDS from the vent valve.
28. Perform a helium leakage test of the closure lid containment O-ring using a Helium Mass Spectrometer Leak Detector (He MSLD) in accordance with the procedural requirements of Section 8.1.3.1, Steps 3 through 10.
29. Install the vent and drain alternate port covers and torque the bolts to 100 ±10 inch-pounds.
30. If an alternate port cover containment O-ring seal was replaced, perform a helium leakage test on the affected port cover using a He MSLD in accordance with the requirements of 8.1.3.2.2.
31. If the alternate port cover containment seal was inspected and accepted for reuse, perform a gas pressure drop leakage test on the affected port cover as follows.
    a. Install a pressure test fixture to the port cover test port including a calibrated pressure gauge with a minimum sensitivity of 0.25 psi.
    b. Pressurize the port cover seal annulus to 15 psig, +1, -0 psi.
    c. Isolate the gas supply and observe the pressure gauge for a minimum of five minutes.
    d. The acceptance criterion for the test is no measurable drop in pressure during the minimum test time. An acceptable test assures that the minimum assembly verification leakage test sensitivity is achieved.

Note: Alternate B port covers, if used, require the satisfactory completion of a helium maintenance leakage rate test to confirm a leaktight seal condition for each loaded transport. Install the Alternate B port cover and perform the maintenance leakage rate test per the requirements of Section 8.1.3.3.2.

32. Decontaminate the cask surfaces. Survey the cask for surface contamination and radiation dose rates.

    Note: Ensure compliance with 10 CFR 71.87(i) and 10 CFR 71.47

33. Remove lift yoke arm guides. Engage the cask lifting yoke to the lifting trunnions.
34. Lift the cask and position the cask rotation sockets in the rear rotation trunnions of the rear support structure. Carefully lower the cask to the horizontal transport orientation resting on the front saddle by moving the crane and/or the trailer as required to maintain cask engagement to the rear supports.
35. Disengage the lifting yoke from the lifting trunnions and remove it from the area.
36. Install the cask tie-down strap. Install the top and bottom impact limiters.
37. Install a TID to an attachment point on the top impact limiter.
38. Install ISO container bracing and lid, or personnel barrier.
39. Complete radiation and contamination surveys of the external surfaces of the package and record the data. Ensure removable contamination and radiation dose rate survey results comply with the limits specified in 10 CFR 71.87(i) and (j).
40. Measure the dose rate in millirems per hour at one meter from the package surface to determine the Transport Index (TI). Indicate the TI on the Radioactive Material labels applied to the package in accordance with 49 CFR 172, Subpart E.
41. Determine the appropriate Criticality Safety Index (CSI) assigned to the package contents in accordance with the CoC, and indicate the correct CSI on the Fissile Material label applied to the package per 49 CFR 172, Subpart E.
42. Apply appropriate placards to the transport vehicle in accordance with 49 CFR 172, Subpart F.
43. Complete the shipping documents and provide the carrier with instructions regarding the requirements for maintaining an exclusive use shipment.

7.1.4.1 Procedure for Loading MTR Fuel Plates into MTR Plate Canister

1. Examine the MTR plate canister and inspect for damage. Visually verify that one end of the canister is installed, the six associated bolts are installed and the other end is removed.
2. Place the can in the loading fixture.
3. Load the fuel plates into the canister. Verify that the number of fuel plates in the canister is no more than the maximum number of plates in an intact MTR fuel element of its type.

4. Install the lid and lid bolts.

7.1.5 MTR General and Preferential Loading Procedures

Up to 42 LEU, MEU, and HEU MTR fuel elements may be loaded into the NAC-LWT MTR Fuel Basket, i.e., 7 fuel elements per basket module × 6 basket modules per fuel basket, except for LEU MTR fuel elements with greater than 470 g ^{235}U, which are limited to 4 elements per basket module as detailed in the following paragraphs. Each MTR basket module has 7 fuel element positions. The MTR basket module loading diagram presented in Figure 7.1-1 has a center position (Position 1), two exterior positions (Positions 2 and 3) that are in line with the center position, and four exterior positions (Positions 4, 5, 6, and 7) that are adjacent to the center row positions. The basket module's fuel element locations are specifically identified to ensure loading of each location with the appropriate fuel element. Ensuring MTR fuel loadings are performed in strict accordance with the procedures presented herein will ensure that the MTR fuel content conditions of the Certificate of Compliance (CoC) are met and that the analyses presented in this SAR are bounding.

MTR fuel elements are selected for loading into specific fuel element locations based on the decay heat of each individual fuel element at the time of loading. Figure 7.1-2 through Figure 7.1-5 are provided to assist in determining the acceptability of a MTR fuel element for loading in a 30 W uniform loading pattern depending on enrichment (i.e., LEU, MEU or HEU) or ^{235}U content (i.e. 380 or 460 grams). For determining the acceptability of higher heat load HEU fuel elements, Figure 7.1-6 and Figure 7.1-7 are provided for 380 and 460 grams of ^{235}U, respectively. The use of the fuel element cool time versus fuel burnup figures are described in Section 7.1.5.4. LEU MTR fuel elements with a ^{235}U content greater than 470 grams, but not exceeding 640 grams, are restricted to baskets containing a maximum of four fuel elements (or an equivalent number of fuel plates per opening). The four element per basket module is in effect even if only one LEU MTR assembly exceeds 470 g per element. Specific basket locations and restrictions for the high load LEU elements are described in Section 7.1.5.1.

The procedural steps and sequence to ensure the MTR fuel loading and content condition limits are met are: 1) determine ^{235}U content weight per element; 2) determine fuel element decay heat load per Section 7.1.5.4; 3) determine basket module loading position for each element and overall basket loading pattern; and 4) individual basket module loading and assembly of the fuel basket in the NAC-LWT. Each of these steps is independently verified.

Attention to the overall cask loading pattern allows the decay heat load of the cask to be maintained as uniform, as is practical and within CoC total heat load limits. Loading diagrams for each individual module and the complete cask assembly shall be developed and used during

the basket module and cask loading operations. After the decay heat load of each of the MTR fuel elements to be loaded and transported is calculated or determined and verified, the loading and content considerations of Sections 7.1.5.1 through 7.1.5.3 shall be met or complied with to establish the final acceptable loading pattern and sequence.

7.1.5.1 General Loading Requirements

1. The maximum decay heat load per MTR fuel basket module shall not exceed 210 W and the maximum decay heat load per cask (package) shall not exceed 1.26 kW. A MTR fuel element with a decay heat greater than 120 W shall not be loaded.
2. LEU, MEU and HEU MTR fuel elements with decay heat not exceeding 30 W per element may be loaded in any basket module fuel element location in any combination.
3. HEU MTR fuel elements with decay heats exceeding 30 W shall be preferentially loaded in a basket module in decreasing decay heat order according to the loading diagram in Figure 7.1-1, with the highest heat load element loaded in fuel location one. Fuel elements with heat loads of up to 120 W shall only be loaded in the center fuel element location of any MTR fuel basket module. The decay heat of the fuel element in either of the two fuel element locations (i.e., number 2 or 3), in line with the center fuel element location of a MTR fuel basket module, shall not exceed 70 W.
4. LEU MTR fuel elements (or canistered fuel plates) with a ^{235}U content greater than 470 g, and not exceeding 640 g, shall only be loaded into basket positions 4, 5, 6 and 7 shown in Figure 7.1-1. In order to ensure that baskets containing the high fissile mass LEU MTR elements (>470 g ^{235}U) will not be loaded with fuel elements (or fuel plates) in basket opening positions 1, 2 and 3, a cell block spacer shall be installed in each of these three basket openings. The cell block spacer, as shown on Drawing 315-40-085, is of sufficient height and diameter to ensure that LEU MTR fuel elements are prevented from being placed in these openings. The capacity limitation of a maximum of four MTR fuel elements per module is in effect even if a single LEU MTR fuel elements (or canistered fuel plates) having >470 g ^{235}U is to be loaded.
5. An MTR plate canister may be loaded into any fuel basket module fuel element location. The contents of each plate canister shall be limited to the number of fuel plates, dimensions and masses of an equivalent intact MTR fuel element.
6. MTR fuel elements with corrosion and/or mechanically damaged cladding may be loaded, provided that the total surface area of through-clad corrosion and/or mechanical damage does not exceed 2,775 cm^2 per package.

7.1.5.2 Determination of Basket Module Loading Pattern

1. Perform an evaluation of the full inventory of fuel elements to be loaded into the NAC-LWT cask(s) and develop an overall loading plan that minimizes overall dose rates to minimize general population dose and operator dose. The loading of LEU MTR fuel elements with greater than 470 g ^{235}U shall be governed by the loading restrictions in item 4 of Section 7.1.5.1, and cell block spacers shall be placed in basket loading

positions 1, 2 and 3 to prevent inadvertent loading of more than four high fissile mass LEU MTR elements.

2. Select up to seven MTR fuel elements to be loaded in a basket module meeting the general loading requirements of Section 7.1.5.1. Identify if spacers or spacer plates are required to properly position the MTR elements axially in the basket module.
3. Rank the fuel elements in order of decreasing decay heat load from 1 to 7. (i.e., the assembly with the highest decay heat is designated number 1.)
4. Generate loading diagrams for each basket module based on Figure 7.1-1, by placing the numbered assemblies in the matching numbered basket module positions, except that fuel elements ranked 4,5,6 or 7 may be loaded in any of the outer (i.e., 4-7) basket module positions.
5. Repeat steps 1 through 4 for all of the basket modules to be loaded.
6. Independently verify the basket module loading diagrams.
7. The loading diagrams shall be used to direct the loading of the basket modules per Section 7.1.5.3.

Once the basket module loading charts are complete, they are used to direct the loading of the basket modules.

7.1.5.3 Basket Loading Procedure

1. Locate the MTR fuel element to be loaded into the basket module per the loading diagram prepared for that module type (i.e., base, intermediate or top).
2. Independently verify the element identification.
3. Load the element into the predetermined fuel basket module fuel element location using the loading diagram. Ensure spacers are installed in positions 1, 2 and 3 of any basket module containing a high fissile mass LEU MTR element.
4. Independently verify that the fuel element and spacer loading in the basket module complies with the loading diagram.
5. Repeat steps 1 through 4 until all identified fuel elements have been loaded into basket modules in compliance with the loading diagrams.

7.1.5.4 Estimating Assembly Decay Heat

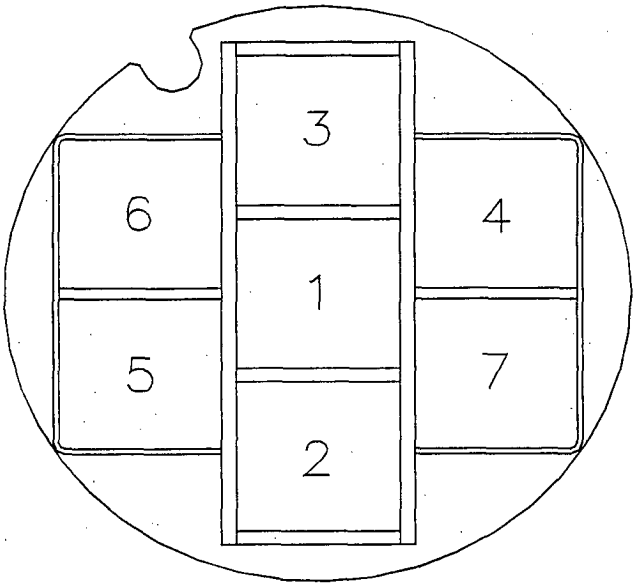
When the decay heat of a fuel element is not known, the assembly burnup (MWd/MTU) and cooling time (years) can be used to define the allowable basket module positions using Figure 7.1-2 through Figure 7.1-7, depending on fuel enrichment (i.e., LEU, MEU or HEU) or ^{235}U content.

HEU MTR fuel elements may be loaded with heat loads greater than 30 W. HEU elements exceeding 30 W shall be preferentially loaded, and Figure 7.1-6 and Figure 7.1-7 identify the appropriate cooling times and burnup limits for 120 W, 70 W and 20 W HEU elements, having a

^{235}U mass of up to 380 grams and a ^{235}U mass of up to 460 grams, respectively. The following steps are used to develop the appropriate loading patterns.

1. Locate the point on Figure 7.1-6 or Figure 7.1-7 for the fuel element burnup and cooling time, and ^{235}U content.
2. If the located point is above the 20 W line, there are no restrictions on fuel element placement in the basket module.
3. If the located point is between the 20 W and 70 W lines, the element is loaded as a 70 W element.
4. If the located point is between the 70 W and 120 W lines, the element is loaded as a 120 W element.
5. If the located point is below the 120 W line, the element shall not be loaded in the NAC-LWT cask.
6. The maximum total decay heat load for a preferentially loaded basket module shall not exceed 210 W and 1.26 kW for a loaded NAC-LWT cask.
7. Each shipper shall ensure that the Certificate of Compliance maximum decay heat load limits of 210 W per basket module and 1.26 kW per cask are not exceeded.

Figure 7.1-1 MTR Fuel Basket Module Loading Pattern (Top View)



Loading Diagram

Figure 7.1-2 LEU MTR Fuel Basket Loading Guidelines for 30 W Uniform Loading

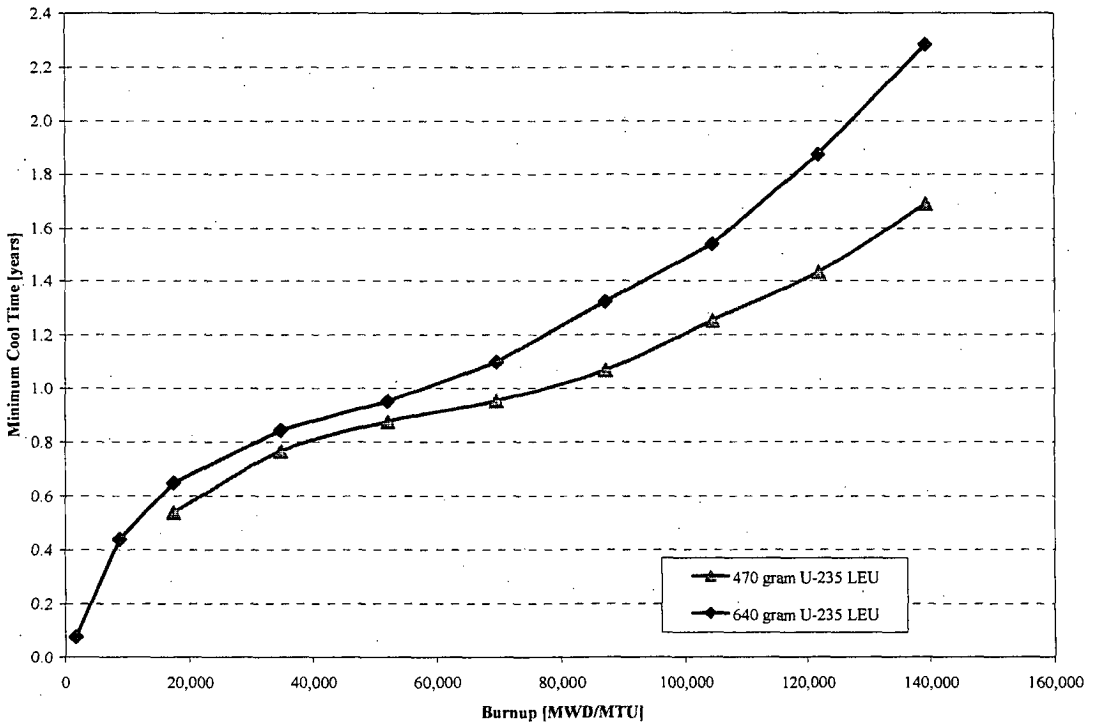


Figure 7.1-3 MEU MTR Fuel Basket Loading Guidelines for 30 W Uniform Loading

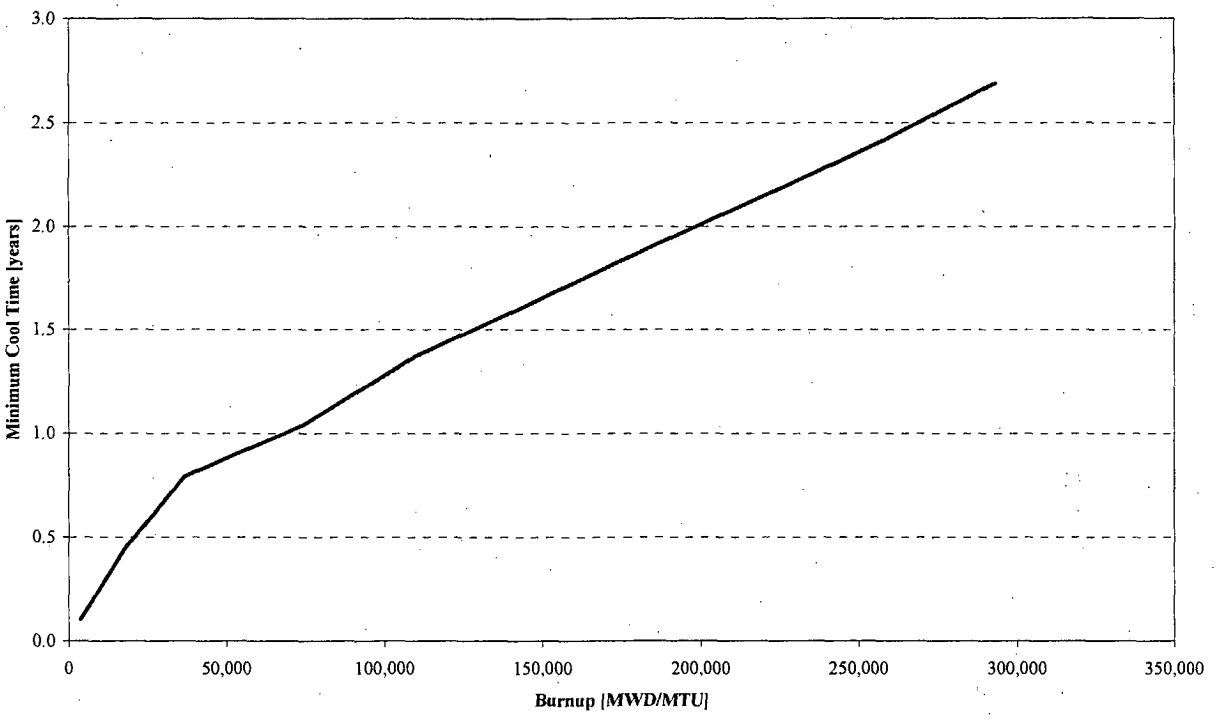


Figure 7.1-4 HEU MTR Fuel Basket Loading Guidelines for 30 W Uniform Loading – Maximum 380 grams ^{235}U

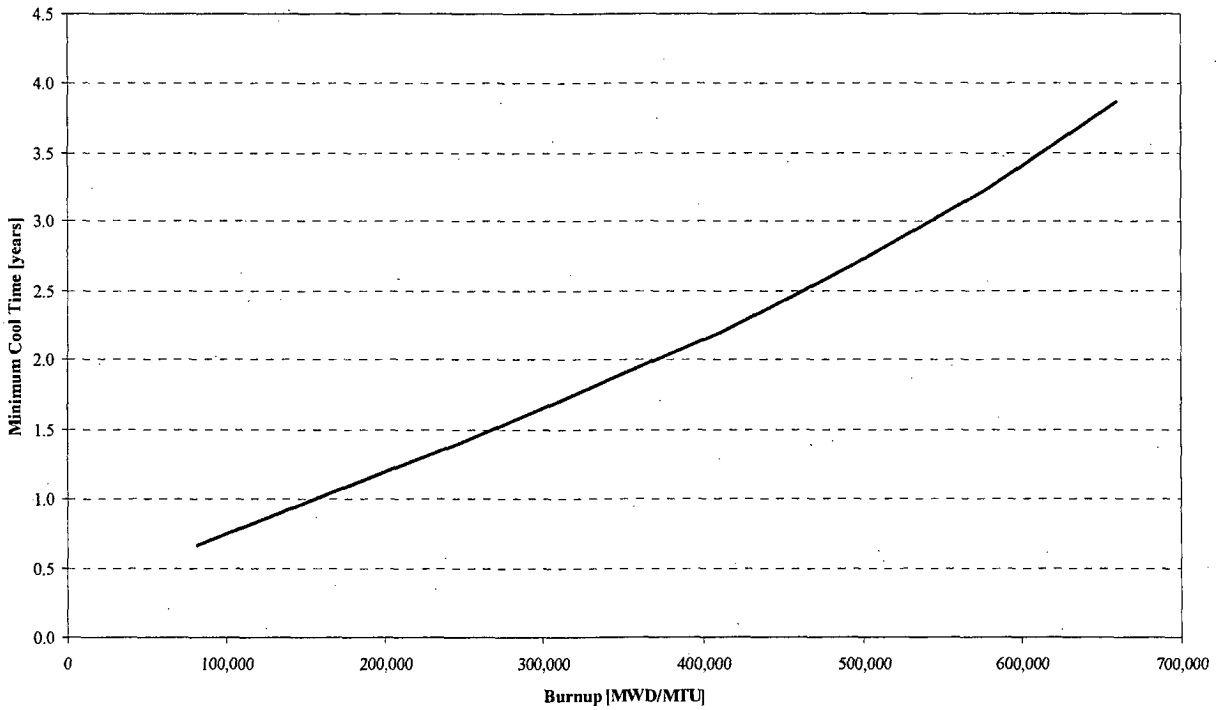


Figure 7.1-5 HEU MTR Fuel Basket Loading Guidelines for 30 W Uniform Loading – Maximum 460 grams ^{235}U

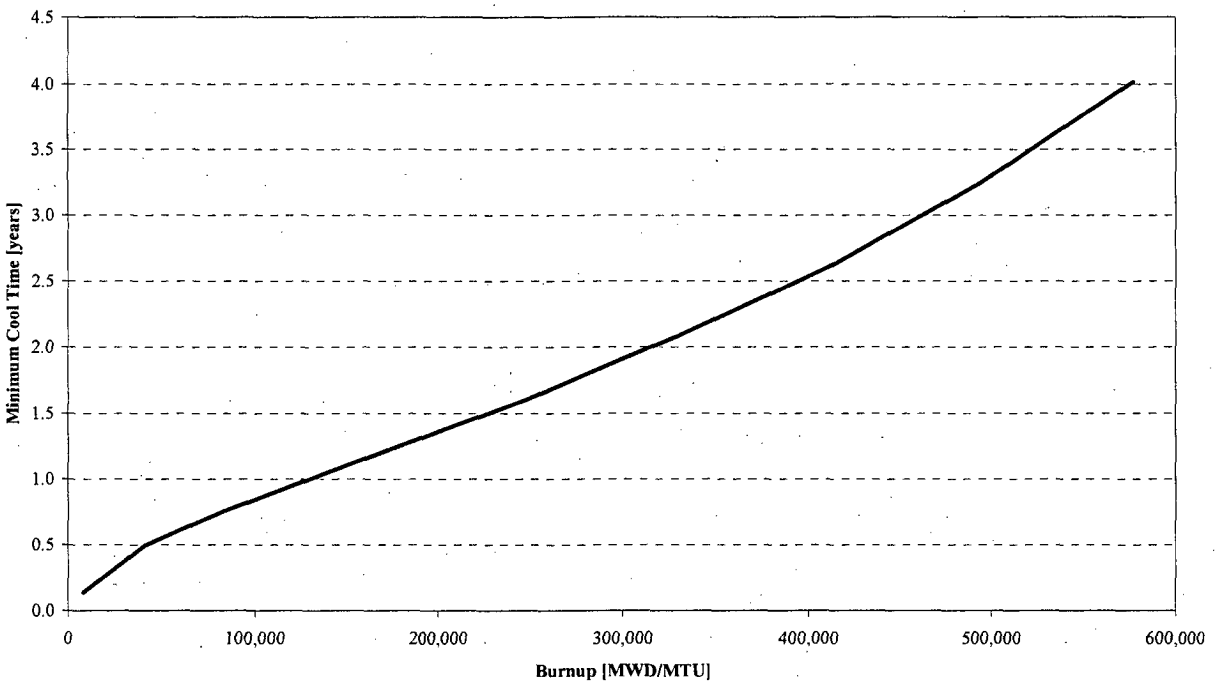


Figure 7.1-6 HEU MTR Fuel Basket Loading Guidelines for Preferential Loading – Maximum 380 grams ^{235}U

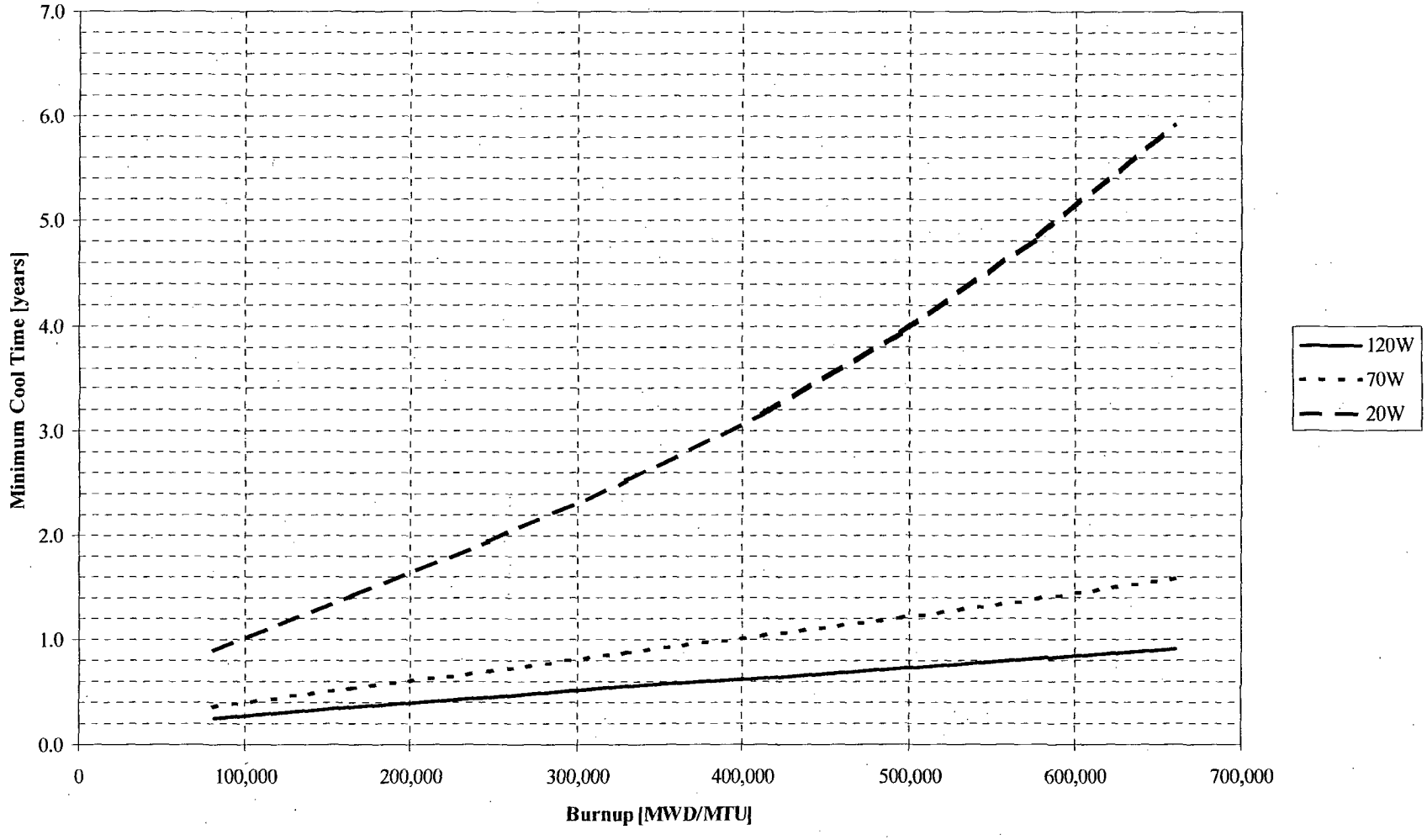


Figure 7.1-7 HEU MTR Fuel Basket Loading Guidelines for Preferential Loading – Maximum 460 grams ^{235}U

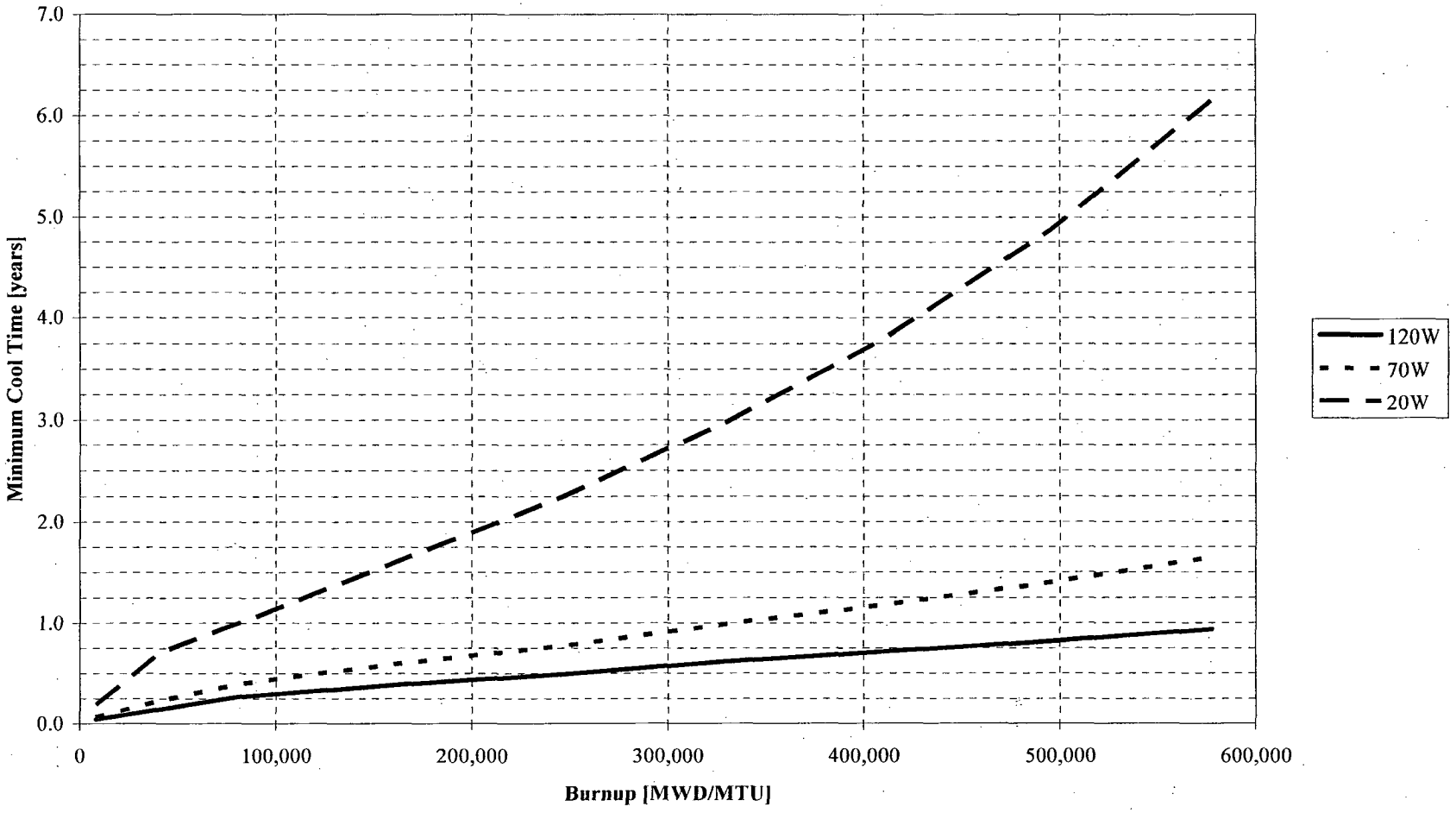


Figure 7.1-8 DIDO LEU Cooling Time vs. Fuel Burnup Basket Module Loading Guidelines for Uniform Loading

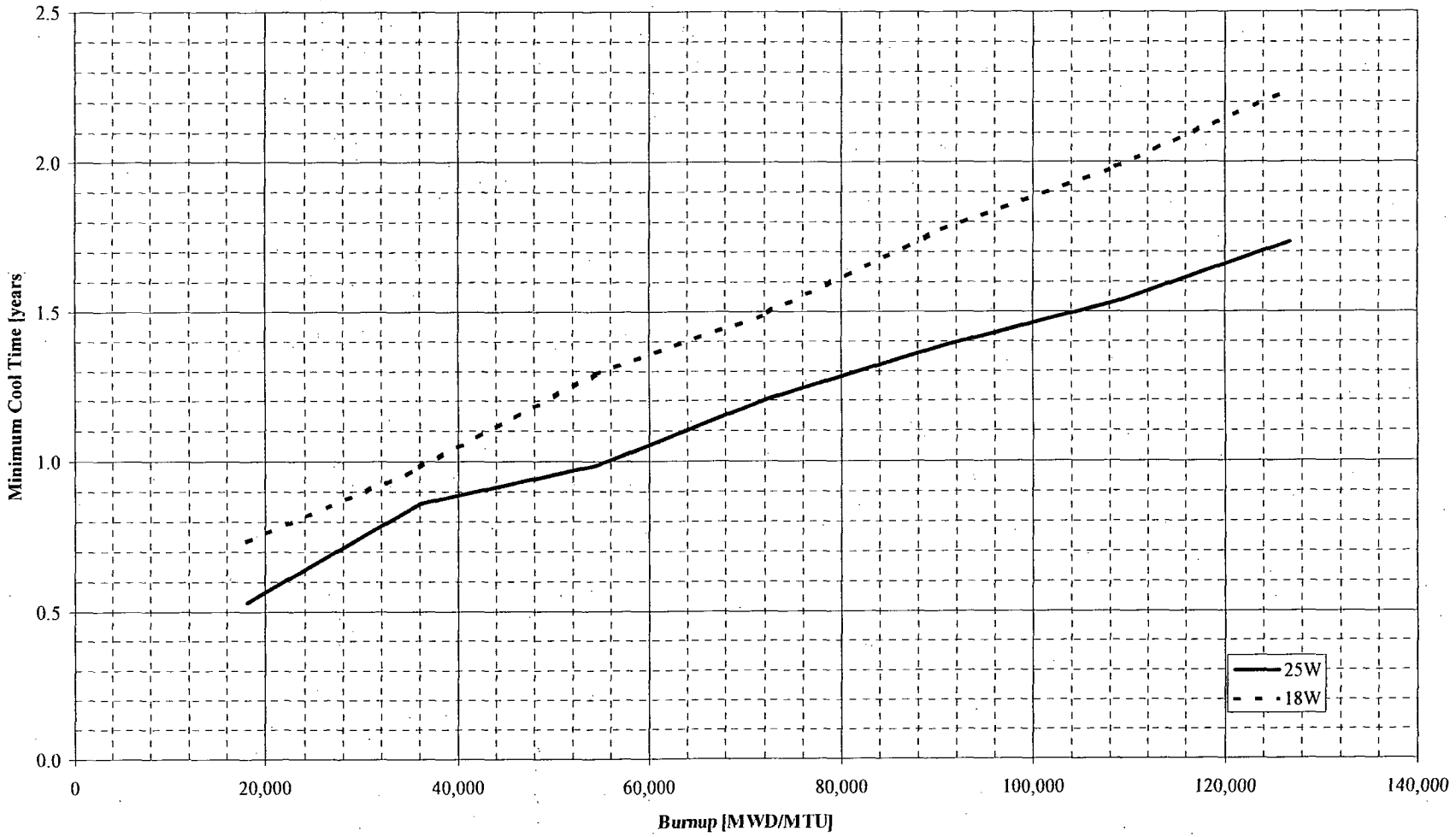


Figure 7.1-9 DIDO MEU Cooling Time vs. Fuel Burnup Basket Module Loading Guidelines for Uniform Loading

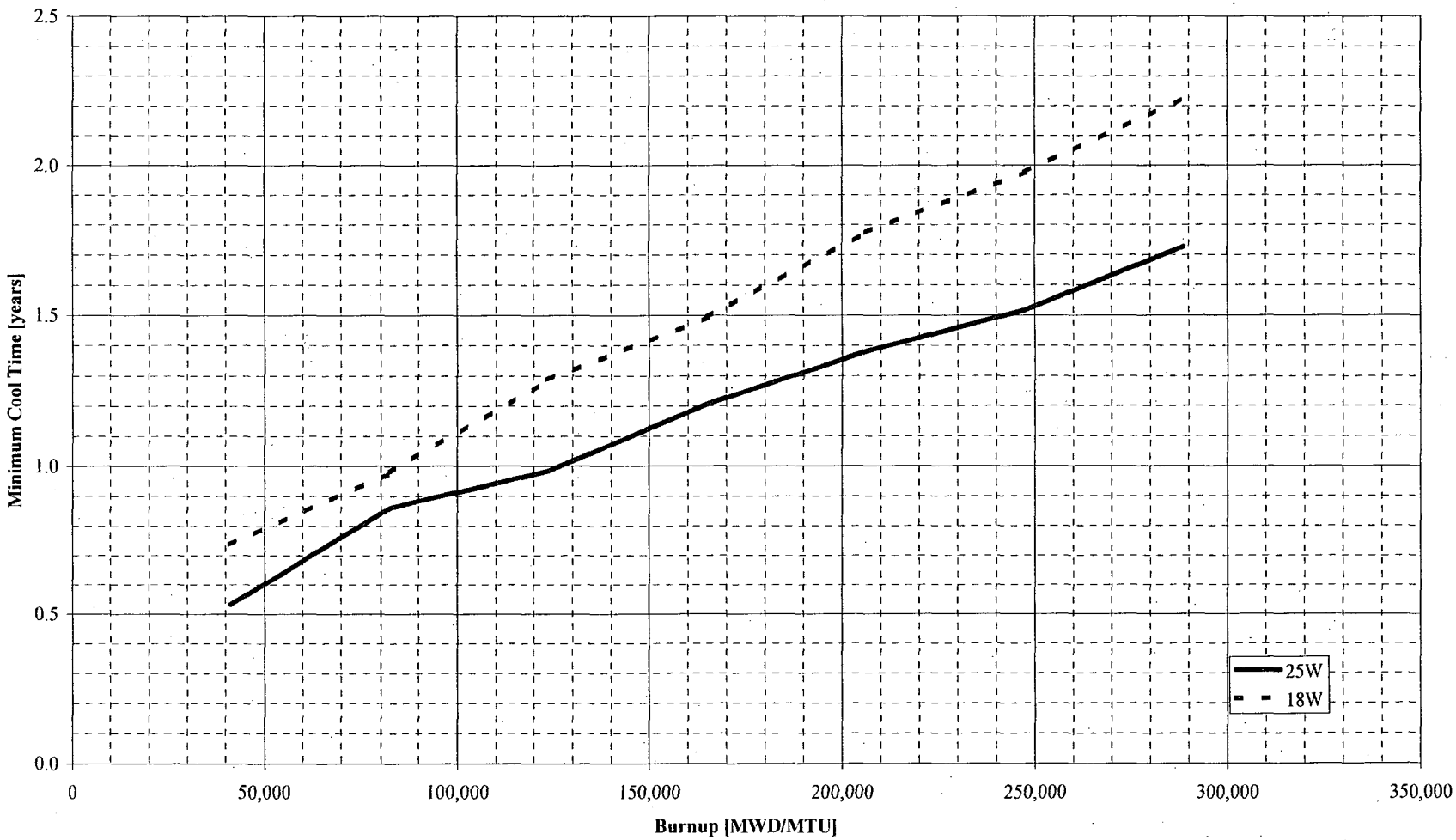


Figure 7.1-10 DIDO HEU Cooling Time vs. Fuel Burnup Basket Module Loading Guidelines for Uniform Loading

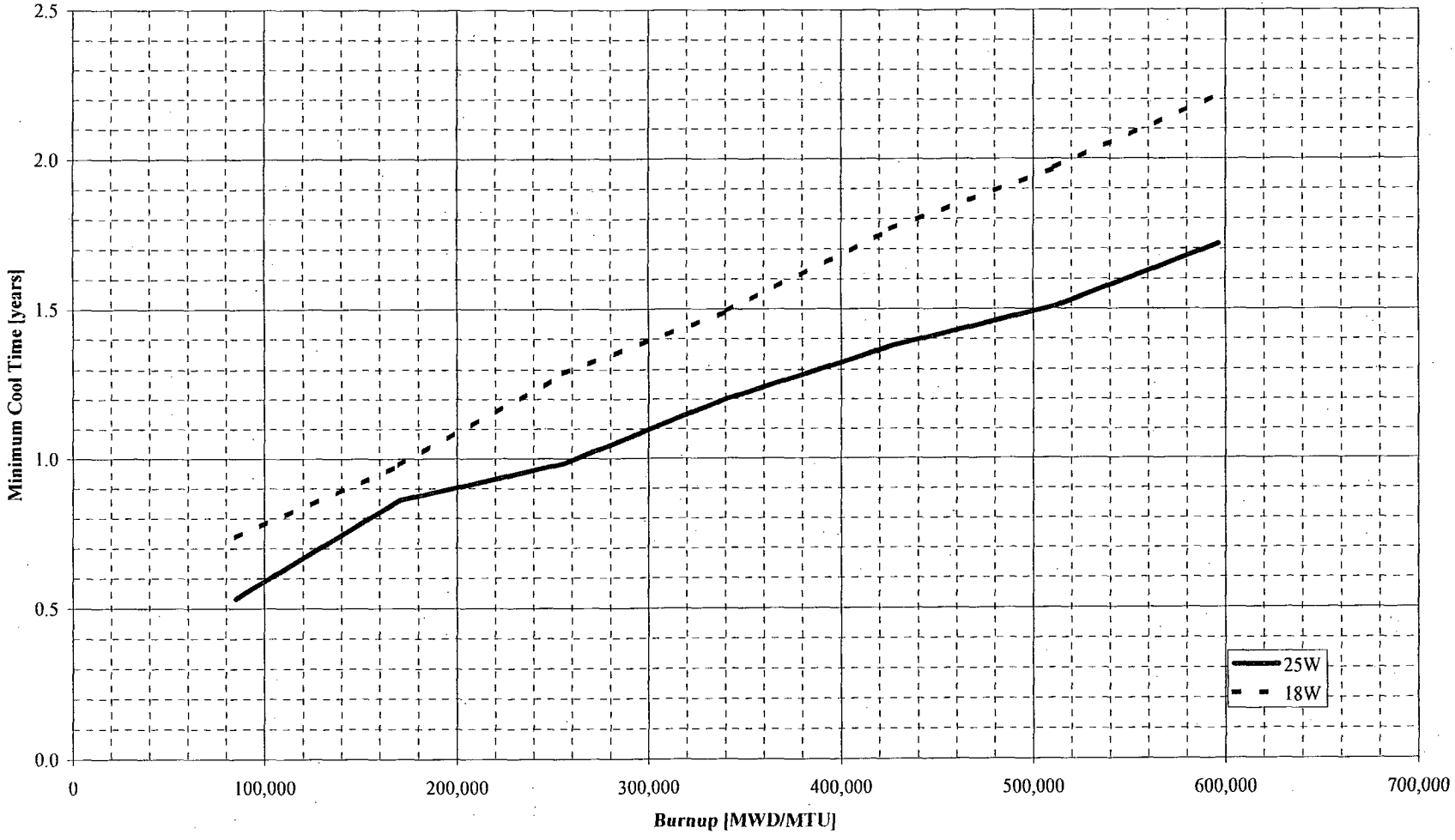
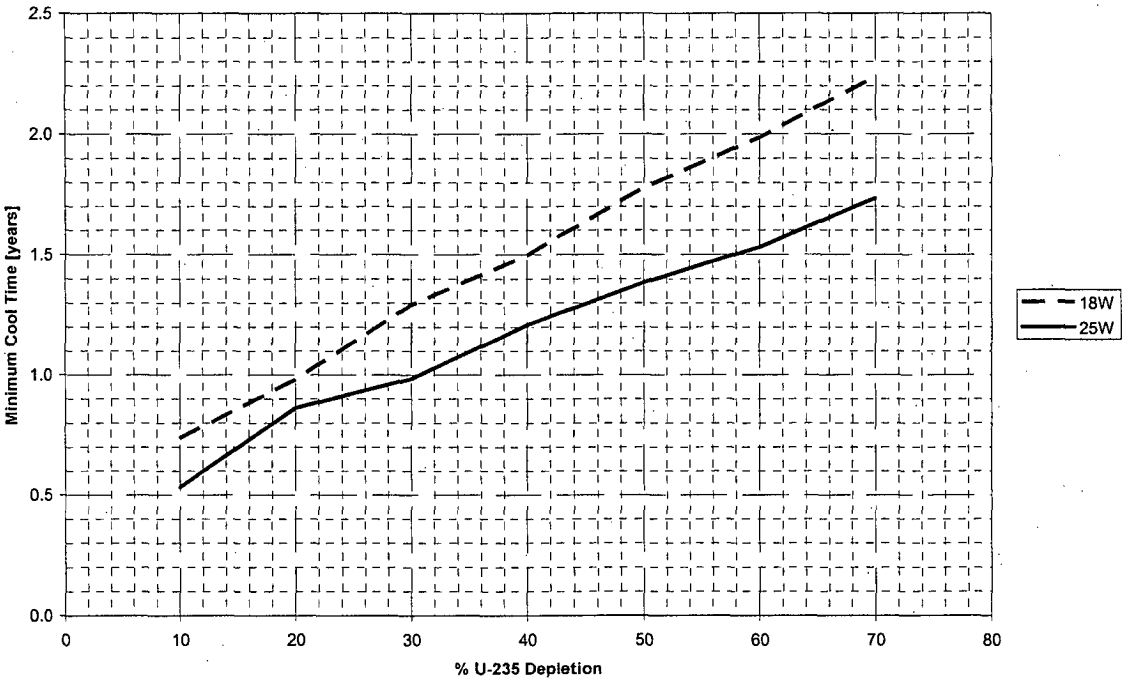


Figure 7.1-11 Bounding DIDO Element Minimum Cool Time vs. wt % ^{235}U Depletion



7.1.6 Procedure for Dry Loading of TRIGA Fuel Basket Modules and GA IFM Modules into the NAC-LWT Cask

This procedure presents the steps for dry loading, using a transfer cask, of the nonpoisoned or poisoned TRIGA fuel basket modules into the NAC-LWT. For transport, five TRIGA fuel basket modules, consisting of a top module, a base module, and three intermediate modules must be loaded into the NAC-LWT. An alternative loading option is available for the poisoned TRIGA basket modules. This configuration, Configuration 2, consists of 1 base module and 4 intermediate modules. A spacer attached to the underside of the NAC-LWT lid is used with Configuration 2. Each basket module consists of seven cells, a center cell, and six peripheral cells. The center cell of the nonpoisoned basket design is blocked and cannot be loaded. Each unblocked cell may contain up to four TRIGA fuel elements, or up to 16 TRIGA fuel cluster rods within a fuel rod insert placed into the cell prior to loading. Each nonpoisoned basket module may contain up to 24 TRIGA fuel elements, for a total of 120 elements, or up to 96 TRIGA fuel cluster rods, for a total of 480 rods per basket assembly. Each poisoned basket module may contain up to 28 TRIGA fuel elements, for a total of 140 elements, or up to 112 TRIGA fuel cluster rods, for a total of 560 rods per basket assembly. The maximum decay heat load of any TRIGA fuel element is 7.5 watts, while the maximum decay heat load of a TRIGA fuel cluster rod is 1.875 watts. An alternative loading option is available for the General Atomics (GA) Irradiated Fuel Material (IFM) Fuel Handling Units (FHU). This configuration consists of one GA IFM top module and one GA IFM spacer. The GA IFM top module, based on the TRIGA basket design, has two canister storage tubes that hold the GA IFM FHU.

TRIGA fuel elements may be transported directly in the basket module cell, or in a sealed damaged fuel can (DFC). TRIGA fuel cluster rods may be transported within the fuel rod insert in a basket cell, or a sealed DFC. The sealed DFCs fit in a module cell. The sealed DFC holds up to two equivalent TRIGA elements as damaged fuel or fuel debris, or up to six equivalent TRIGA fuel cluster rods as damaged rods or fuel debris. Damaged TRIGA fuel and fuel debris contained in sealed DFCs.

When loading TRIGA fuel elements directly into the basket cells of a TRIGA basket module, the fuel elements may be loaded with either 4 elements per cell, or one element per cell, without shoring. If a basket cell is loaded with 2 or 3 intact elements, dummy rods will be inserted as necessary to fill the remaining space in the cell.

Damaged TRIGA fuel elements and cluster rods and fuel debris are required to be loaded into sealed DFCs. The sealed DFCs are provided in two lengths. The short sealed DFC may be used in the base or top basket module. The long sealed DFC may be used in only the top module. The

sealed DFCs are vacuum dried prior to loading into a TRIGA fuel basket (see sealed DFC loading procedure in Section 7.1.7).

There are two separate GA IFM FHU designs. One FHU is designed to hold research reactor fuel and the other is designed to hold High-Temperature Gas-Cooled Reactor fuel pellets. Each FHU consists of a sealed inner canister within a sealed outer canister. Each FHU contains irradiated fuel materials as described in Chapter 1. When loading the GA IFM FHUs, each individual sealed FHU will be loaded separately into a single GA IFM basket. This single basket containing two GA IFM FHUs and a spacer will comprise the entire cask load. Loading of the GA IFM basket into the NAC-LWT cask will utilize the TRIGA dry configuration loading procedure that is described in the following paragraphs.

TRIGA fuel elements that can be loaded into the cask are limited to a maximum decay heat of 7.5 watts per element, as discussed in Section 1.2.3. The decay heat load of the element must be calculated, and verified to be equal to or less than 7.5 watts per element prior to loading. TRIGA fuel cluster rods that can be loaded into the cask are limited to a maximum decay heat of 1.875 watts per element, as discussed in Section 1.2.3 (by reference to Table 5.1.1). The decay heat load of the fuel cluster rod must be calculated, and verified to be equal to or less than 1.875 watts per element prior to loading.

The procedure for loading the package with TRIGA fuel in a dry configuration is as follows:

1. Perform a receipt inspection of the empty cask and trailer/ISO container, inspecting for transport damage.
2. Position the trailer in the designated cask unloading area. Set the trailer brakes and chock the wheels to prevent unintended movement. If site-specific conditions exist that require the trailer to move to allow the cask to be uprighted on its rotation trunnions, release brakes and remove the chocks when required to complete uprighting operations. If an ISO container is used, it may be removed from the trailer and secured in the unloading area.
3. Remove the personnel barrier or the roof and roof cross-members from the ISO container.

   Note: Verify that the package nameplate displays the correct package identification number in accordance with the CoC.

4. Perform a Health Physics survey of the cask and adjacent surfaces of the trailer.

   Note: A receiving survey of the cask and transporter must be performed as soon as practicable after arrival at the site to assure compliance with 10 CFR 20, 10 CFR 71.87(i) and 10 CFR 71.47, and to assure timely reporting of any reportable noncompliance.

5. Remove the top and bottom impact limiters.

6. Remove the cask tie-down strap.

7. Using the lifting yoke with the guides removed, engage the lifting trunnions. Raise the cask to vertical by rotating the cask rotation sockets on the rear cask supports, moving the crane and/or trailer as required to keep the lift yoke engaged to the trunnions and the cask engaged in the rear supports. When the cask is fully vertical, lift the cask from the supports and remove it from the trailer/container.

8. Place the cask onto the dry loading station. Disengage the lifting yoke and move clear.

9. Visually inspect the neutron shield tank fill, drain and level inspection plugs for signs of neutron shield fluid leakage. If leakage is detected or suspected, verify shield tank fluid level and correct, as required.

10. Remove the vent and drain valve port covers. Prior to reinstallation of the port covers, carefully inspect the O-rings and, if the O-rings show any damage, replace them with approved spares. Ensure that the replacement O-rings are properly installed and seated. Visually inspect the valve quick-disconnect nipples and replace them, if necessary.

    Note: For Alternate B port covers, replace the metallic O-ring with an approved spare prior to reinstallation.

11. Remove closure lid bolts. Attach the lid lift slings to the closure lid. Remove the closure lid and set it on a support that is suitable for radiological control and for maintaining the cleanliness of the closure lid. Prior to reinstallation of the lid, carefully inspect the Teflon O-ring seal in the underside of the closure lid and, if it shows any damage, replace it. Remove the metallic O-ring and replace it with an approved spare. Ensure that the replacement O-rings are properly installed and seated. Inspect the lid bolts and replace any that are damaged.

12. Visually inspect the inner cavity for foreign material or damage. Install, or verify the presence of the proper drain tube and drain alignment ring.

13. Install the required dry transfer system components on the top of the cask.

14. Position the shielded transfer cask system components for fuel loading, as appropriate.

15. Identify the TRIGA fuel basket modules to be loaded. Modular baskets consisting of one base unit, three intermediate units, and one top unit, may be loaded into the cask cavity. The base unit must be the first unit loaded and the top unit must be the last unit loaded. The intermediate modules may be loaded in any of the other loading operations. If the poisoned basket Configuration 2 is used, ensure that the TRIGA spacer is bolted and torqued to 40 ft-lbs to the underside of the NAC-LWT lid. If TRIGA fuel cluster rods are to be transported, ensure that fuel rod inserts are placed into each cell location that will contain fuel cluster rods. For the GA IFM basket load, install the GA IFM spacer, shown on NAC drawing 315-40-123, prior to inserting the loaded GA IFM top module.

Notes:
a. When utilizing nonpoisoned TRIGA baskets, visually verify that the center blocking plate is welded in place on each basket module.
b. When utilizing poisoned TRIGA baskets, visually inspect each cell of each basket module for foreign material or damage and verify the presence of the neutron poison material (borated stainless steel plates) as shown on NAC Drawings 315-40-080, -081, and -082.
c. When utilizing the GA IFM top module, follow the TRIGA loading procedure below, noting that this is a single basket load.

16. Identify the TRIGA fuel contents to be loaded and verify that the fuel contents comply with the content, heat load and quantity conditions as specified in the CoC.
17. Load a TRIGA fuel basket module into the shielded transfer cask.
18. Place the shielded transfer cask containing the loaded basket module onto the dry transfer system components positioned on the top of the cask.
19. Lower the fuel basket from the shielded transfer cask into the shipping cask.
20. Repeat the loading and transfer of loaded basket modules until the approved cask loading plan is completed.
21. Install the closure lid onto the cask. Visually verify that the lid is properly seated.
22. Remove the dry transfer system components from the top of the cask.
23. Install and tighten the 12 closure bolts to 260 ± 20 ft-lbs in three passes, using the torque sequence stamped on the closure lid.
24. Connect a gas supply line to the vent valve and the drain line to the drain valve.
25. Open the air, nitrogen or helium gas supply valve and pressurize the cask cavity (< 30 psig) to force any residual water out the drain line. Continue to supply pressurized gas to the cask for a minimum of five minutes after the last residual free water discharges from the drain. Remove the drain and gas supply lines and attach a vacuum drying system (VDS) to the vent.
26. Evacuate the cask cavity to less than or equal to 10 torr (13 mbar) and continue vacuum pumping for a minimum of 15 minutes.
27. At the end of the vacuum pumping period, isolate the cask cavity from the vacuum pump and stop the vacuum pump. Monitor the cask cavity pressure for a minimum of ten minutes. If the pressure rise is less than 5 torr (6.7 mbar), the cavity is verified as dry of free water. If pressure rise is >5 torr (6.7 mbar), repeat vacuum drying until the dryness verification results are satisfactory.
28. Backfill the cask cavity with helium to 0 psig (1 atmosphere, absolute), +1, -0 psi and disconnect the VDS from the vent valve.

29. Perform a helium leakage test of the closure lid containment O-ring using a Helium Mass Spectrometer Leak Detector (He MSLD) in accordance with the procedural requirements of Section 8.1.3.1, Steps 3 through 10.

30. Install the vent and drain alternate port covers and torque the bolts to 100 ±10 inch-pounds.

31. If an alternate port cover containment O-ring seal was replaced, perform a helium leakage test on the affected port cover using a He MSLD in accordance with the requirements of 8.1.3.2.2.

32. If the alternate port cover containment seal was inspected and accepted for reuse, perform a gas pressure drop leakage test on the affected port cover as follows.

    a. Install a pressure test fixture to the port cover test port including a calibrated pressure gauge with a minimum sensitivity of 0.25 psi.

    b. Pressurize the port cover seal annulus to 15 psig, +1, -0 psi.

    c. Isolate the gas supply and observe the pressure gauge for a minimum of five minutes.

    d. The acceptance criterion for the test is no measurable drop in pressure during the minimum test time. An acceptable test assures that the minimum assembly verification leakage test sensitivity is achieved.

    Note: Alternate B port covers, if used, shall have a helium maintenance leakage rate test performed to confirm a leaktight containment closure. Install the Alternate B port cover and perform the maintenance leakage rate test per the requirements of Section 8.1.3.3.2.

33. Decontaminate the cask surfaces. Survey the cask for surface contamination and radiation dose rates.

    Note: Ensure compliance with 10 CFR 71.87(i) and 10 CFR 71.47.

34. Engage the cask lifting yoke to the lifting trunnions.

35. Lift the cask and position the cask rotation sockets in the rear rotation trunnions of the rear support structure. Carefully lower the cask to the horizontal transport orientation resting on the front saddle by moving the crane and/or the trailer as required to maintain cask engagement to the rear supports.

36. Disengage the lifting yoke from the lifting trunnions and remove it from the area. Install the cask tie-down strap. Install the top and bottom impact limiters. Install a TID to an attachment point on the top impact limiter.

37. Install ISO container bracing and lid, or personnel barrier.

38. Complete radiation and contamination surveys of the external surfaces of the package and record the data. Ensure removable contamination and radiation dose rate survey results comply with the limits specified in 10 CFR 71.87(i) and (j).

39. Measure the dose rate in millirems per hour at one meter from the package surface to determine the Transport Index (TI). Indicate the TI on the Radioactive Material labels applied to the package in accordance with 49 CFR 172, Subpart E.

40. Determine the appropriate Criticality Safety Index (CSI) assigned to the package contents in accordance with the CoC, and indicate the correct CSI on the Fissile Material label applied to the package per 49 CFR 172, Subpart E.

41. Apply appropriate placards to the transport vehicle in accordance with 49 CFR 172, Subpart F.

42. Complete the shipping documents and provide the carrier with instructions regarding the requirements for maintaining an exclusive use shipment.

7.1.7 Procedure for Loading TRIGA Damaged Fuel or Fuel Debris into a TRIGA Sealed Damaged Fuel Can (DFC)

1. Examine the sealed damaged fuel can (DFC) body and inspect for damage. Verify that the lid sealing surface is clean and free of defects. Visually verify that the drain plug seal is installed and the drain plug is partially threaded into the drain plug adapter to allow for draining.

2. Lower the DFC into the pool and position it for fuel loading.

3. Load the damaged TRIGA fuel cluster rods or fuel debris into the DFC. Verify that no more than the equivalent of 2 fuel elements, or 6 fuel cluster rods, as damaged fuel or fuel debris are loaded into the sealed DFC as specified in the CoC. Visually verify that there is no debris in the lid sealing surface and thread areas.

4. Examine the DFC lid and inspect for damage. Visually verify that the sealing surface is clean and free of defects. Lubricate the lid bolts, install the lid seal and verify that the lid valve is in the open position and the valve lock set screw is retracted.

5. Attach the testing hose to the lid test connection and ensure that the fitting is properly seated.

6. Install the lid and torque the lid bolts to 150 ± 10 inch-pound.

   Note: Torque any two diametrically opposed bolts first, then torque the remaining two bolts. Complete the torque sequence by verifying the torque of all four bolts in a clockwise direction.

7. Pressurize the sealed DFC with air or helium to 5-15 psig to remove the water. Continue the purge for at least 5 minutes after bubbles appear from the base of the DFC.

8. Access and torque the DFC drain plug to 50 ± 10 inch-pound.

9. Evacuate the DFC to a pressure below 10 torr (13 mbar) and continue vacuum pumping for 10 minutes.

10. Stop and isolate the vacuum pump and monitor the DFC vacuum pressure for a minimum of 10 minutes. If the pressure rise is <5 torr (6.7 mbar) in 10 minutes, the DFC is verified as dry of free water. If the pressure rise is >5 torr (6.7 mbar) in 10 minutes or less, the DFC is not considered dry of free water. Repeat vacuum drying and pressure rise testing until the dryness verification results are satisfactory.
11. Backfill the DFC with helium to a pressure of 1 atmosphere (0 psig), +1, -0 psi.
12. Shut and lock the lid diaphragm valve. The DFC is now sealed, dried and backfilled.
13. Disconnect the testing hose from the lid test connection.
14. The sealed DFC is now ready for loading into a TRIGA basket module.

7.1.8 Procedure for Wet Loading of PWR/BWR Fuel Rods or TPBARs into the PWR/BWR Transport Canister

For the shipment of PWR and BWR fuel rods, the PWR/BWR transport canister has three configurations: sealed canister, screened canister, and free flow canister. All three canister configurations may be used to contain either intact or damaged fuel rods, or a combination of both damaged and intact fuel rods. The loaded transport canisters are loaded into the NAC-LWT cask containing a LWT PWR basket assembly with an appropriate bottom weldment spacer. For transport canisters containing any damaged fuel rod contents, a can and an insert spacer are required to be installed and bolted to the underside of the closure lid to limit the axial movement of the canister. The use of the can and insert spacer requires the use of the PWR basket assembly fitted with the Alternate B spacer. Transport canisters containing intact rods may be placed in any of the three types of PWR basket assemblies.

For the shipment of TPBARs, only the screened or free flow PWR/BWR Rod Transport Canister containing the 5 × 5 rod insert may be used.

Upon completion of loading the transport canister, the canister and the insert spacer are loaded, either together or individually, into the basket assembly in a manner similar to loading a PWR assembly.

1. If the transport canister is to be shipped in a sealed configuration, verify the five drain plugs are installed and torqued to 50 ± 2 foot-pound. If the transport canister is to be shipped in the free flow configuration, verify the five drain plugs are not installed. If the transport canister is to be shipped in the screened configuration, verify the screened plugs are installed and torqued to 50 ± 2 foot-pound in the bottom of the canister.
2. Lower the transport canister (and insert) into the fuel pool for loading.
3. Load the spent fuel rods into the transport canister in accordance with site-specific procedures. Separate failed fuel rod capsules may be used to contain either intact or damaged fuel rods within the canister. The capsules are intended to limit dispersal of

radioactive material to the canister internals. Visually upon completion of loading, verify that there is no debris on the lid sealing surface and threaded areas.

4. Using the appropriate lid (sealed, screened or free-flow), examine and inspect for damage. Visually verify that the sealing surface is clean and free of defects. Lubricate the lid bolts.

5. Install the lid and torque the lid bolts to 35 ± 5 inch-pound.

Note: Torque any two diametrically opposed bolts first, then torque the remaining six bolts. Complete the torque sequence by verifying the torque of all eight bolts in a clockwise direction.

6. If the transport canister is being shipped in either the screened or free-flow configuration, it is now ready for shipment. To ship PWR and BWR rods, the transport canister shall be loaded into the NAC-LWT cask in accordance with Section 7.1.1, Procedures for Wet Loading of LWR Fuel Assemblies and Canistered LWR Fuel Rods. To ship TPBARs, the transport canister shall be loaded in accordance with Section 7.1.9, Procedure for Wet Loading of TPBAR Consolidation Canister or PWR/BWR Rod Transport Canister into the NAC-LWT Cask. If the transport canister is being shipped in the sealed configuration, complete steps 7-14 of this section.

7. Connect vent and drain lines to the respective quick-disconnect fittings on the sealed transport canister lid. The drain hose discharge should be directed to the plant drain system for radiological wastewater or another appropriate collection point.

8. Pressurize and purge the transport canister using helium. (Caution do not exceed 25 psig. while dewatering the transport canister.) Secure the purge once no fluid is observed exiting the discharge for at least 10 minutes.

9. Connect the vent line to a suitable vacuum pump. Maintain connection of drain line to the can, but isolate the line to allow vacuum drying of the sealed failed fuel can.

10. Evacuate the can to a pressure below 10 torr (13 mbar) and continue vacuum pumping for 10 minutes.

11. Stop and isolate the vacuum pump and monitor the cask cavity vacuum pressure for a minimum of 10 minutes. If the pressure rise is less than 5 torr (6.7 mbar), the cavity is verified as dry of free water. If the pressure rise is >5 torr (6.7 mbar), repeat vacuum drying until the dryness verification results are satisfactory.

12. Backfill the transport canister cavity with helium to 1 atmosphere (absolute), +1, -0 psi.

13. Disconnect the vent and drain lines from the transport canister.

14. The sealed transport canister is now ready for shipment and may be loaded into the NAC-LWT cask in accordance with Section 7.1.1.

7.1.9 Procedure for Wet Loading of TPBAR Consolidation Canister or PWR/BWR Rod Transport Canister into the NAC-LWT Cask

This section describes the procedures for loading the NAC-LWT with a TPBAR consolidation canister or with a screened or free flow PWR/BWR Rod Transport Canister. The consolidation canister can contain up to 300 TPBARs, two of which may be prefailed. Dunnage (i.e., spacer grids, stainless steel tubes, etc.) may be used in consolidation canisters containing fewer than 300 TPBARs. The total weight and volume of the contents (i.e., dunnage and reduced number of TPBARs) must be less than, or equal to, the weight and volume of the full load of 300 TPBARs.

The PWR/BWR Rod Transport Canister may contain up to 25 TPBARs.

Appropriate radiological controls and procedures addressing tritium shall be utilized by the licensee, including appropriate personnel monitoring for tritium exposure.

NAC-LWT casks to be used to transport the TPBAR consolidation canisters shall be configured as shown on Drawing No. 315-40-128, including Alternate B port covers. NAC-LWT casks to be used to transport a PWR/BWR Rod Transport Canister shall be configured as shown on Drawing No. 315-40-104, Assembly 95, including Alternate B port covers.

1. Perform a receiving survey of the empty cask and inspect for damage. Verify, by cask serial number, that the cask is approved for TPBAR shipment.
2. Position a trailer in the designated cask unloading area. Set the trailer brakes and chock the wheels to prevent unintended movement. If site-specific conditions exist that require the trailer to move to allow the cask to be uprighted on its rotation trunnions, release brakes and remove the chocks when required to complete uprighting operations. If an ISO is used, it may be removed from the trailer and secured in the unloading area.
3. Remove the roof from the ISO container and open the front and rear ISO doors. Remove roof cross-members, if installed.

   Note: Verify that the package nameplate displays the package identification number, USA/9225/B(M)-96, as required by the CoC for TPBAR contents.
4. Perform a Health Physics survey of the cask and adjacent surfaces of the trailer.

   Note: A receiving survey of the cask and transporter must be performed as soon as practical after arrival at the site to assure compliance with 10 CFR 71.87(i) and 10 CFR 71.47, and to assure timely reporting of any reportable noncompliance.
5. Remove the top and bottom impact limiters.
6. Remove the cask tie-down strap.
7. Using the lifting yoke with the guides removed, engage the lifting trunnions. Raise the cask to vertical by rotating the cask rotation sockets on the rear cask supports, moving the crane and/or trailer as required to keep the lift yoke engaged to the

trunnions and the cask engaged in the rear supports. When the cask is fully vertical, lift the cask from the supports and remove it from the trailer/container.

8. Place the cask in the decontamination pit or other designated area. Disengage the lifting yoke. Clean cask surfaces of road dirt as required for entry into the spent fuel pool.

9. Visually inspect the neutron shield tank fill, drain and level inspection plugs for signs of neutron shield fluid leakage. If leakage is detected, verify shield tank fluid level and correct, as required.

10. Remove the Alternate B vent and drain valve port covers. Prior to reinstallation of the port covers, replace the metallic O-ring seal with an approved spare and inspect the Viton® O-ring seal for each port cover. If the Viton® O-ring shows any damage, replace it. Ensure that the replacement O-rings are properly installed and seated. Store the port covers to protect the seal surfaces. Visually inspect the valved quick-disconnect nipples and replace them, if necessary.

11. Remove closure lid bolts. Attach the lid lift slings to the closure lid. Remove the closure lid and set it on a support that is suitable for radiological control and for maintaining the cleanliness of the closure lid. Prior to reinstallation of the lid, carefully inspect the Teflon O-ring seal in the underside of the closure lid. If the O-ring shows any damage, replace it. Remove the metallic O-ring and replace it with an approved spare. Ensure that the replacement O-rings are properly installed and seated. Inspect the lid bolts and replace any that are damaged. Ensure that the TPBAR spacer is installed on the bottom of the cask lid for consolidation canister transports and not damaged when the lid is set down.

12. Visually inspect the inner cavity for foreign material or damage. Install or verify the presence of the standard drain tube and the TPBAR basket assembly (Drawing No. 315-40-10, Assembly 96 or Assembly 95) for loading of the consolidation canister; or the standard drain tube, TPBAR basket assembly (Drawing No. 315-40-10, Assembly 95), and the PWR Insert (Drawing No. 315-40-105, Assembly 99) for the loading of the PWR/BWR Rod Transport Canister containing TPBARs.

    Note: The PWR insert may be installed during the placement of the loaded PWR/BWR Rod Transport Canister into the NAC-LWT cask.

13 Fill the cask cavity with clean water. Install lift yoke arm guides and remote actuation components on the cask lifting yoke.

14. Engage the cask lifting yoke with the cask lifting trunnions and pick up the cask. Carefully lower the cask to the bottom of the cask loading area while spraying the cask down with clean water.

15. Disengage the lifting yoke from the cask and remove the yoke from the pool.

16. Identify the TPBAR consolidation canister or the PWR/BWR Rod Transport Canister containing TPBARs to be loaded.

17. Pick up the consolidation canister or the PWR/BWR Rod Transport Canister using the required grapple system.

18. Position the container over the cask and then carefully lower it into the cask to avoid damage to the cask sealing surfaces. Orient the consolidation canister bail so that it is aligned with the drain tube location. Confirm that the container is fully seated, then release and raise the grapple to the full up position.

19. Position the cask lifting yoke over the cask closure lid. Attach the slings to the closure lid and cask lifting yoke. Lower the yoke over the cask.

20. Position the closure lid over the cask and slowly lower it into place. For the consolidation canister, ensure the bail is properly aligned to the TPBAR spacer on the bottom of the lid. Use the cask and lid match marks as guides to properly align the lid. Visually confirm that the closure lid is seated.

21. Lower the cask handling yoke to slack the closure lid cables. Engage the lift yoke to the lifting trunnions and begin lifting.

    Note: Visually verify the yoke engagement before lifting the cask.

22. Raise the cask until the lid is slightly above the surface of the pool. At the option of the licensee/user, a number of closure lid bolts (4 to 12) may be installed hand tight.

23. Raise the cask clear of the pool, rinsing the yoke and cask with clean water.

24. Transfer the cask to the decontamination pit or other work area. Remove the yoke and lid lift slings.

25. Install and tighten the 12 closure lid bolts to 260 ± 20 ft-lb in three passes, using the torque sequence stamped on the closure lid.

26. At the option of the licensee/user, a 25 to 50 gallon clean water flush of the cask cavity may be performed by connecting a valved clean water line to the drain valve and a valved drain line to the vent valve. After the cavity flushing is completed, if performed, disconnect the water supply and drain lines.

27. Connect a gas supply line to the vent valve and the drain line to the drain valve.

28. Open the air, nitrogen or helium gas supply valve and pressurize the cask cavity (<30 psig) to force out the water. Continue to supply pressurized gas to the cask for a minimum of five minutes after the last residual free water discharges from the drain line. Remove the drain and gas supply lines and attach a vacuum drying system (VDS) to the cask vent valve.

29. Evacuate the cask cavity to a vacuum pressure of less than 10 torr (13 mbar) and continue vacuum pumping for a minimum of 15 minutes.

30. At the end of the vacuum pumping period, isolate the cask cavity from the vacuum pump and stop the pump. Monitor the cask cavity pressure for a minimum of ten (10) minutes. If the pressure rise is less than 5 torr (6.7 mbar), the cavity is verified as dry of free water. If the pressure rise >5 torr (6.7 mbar), repeat vacuum drying until the dryness verification results are satisfactory.

31. Backfill the cask cavity with helium to 0 psig (1 atmosphere, absolute), +1, -0 psi. Disconnect the VDS.

32. Perform the helium leakage test of the closure lid containment O-ring using a Helium Mass Spectrometer Leak Detector (He MSLD) in accordance with the requirements of Section 8.1.3.1, Steps 3 through 10.
33. Install and helium leakage test the Alternate B vent and drain port covers to leaktight criteria in accordance with Section 8.1.3.3.2.
34. Decontaminate the cask. Survey the cask for surface contamination and radiation dose rates.

    Note: Ensure compliance with 10 CFR 71.87(i) and 10 CFR 71.47.
35. Remove lift yoke arm guides. Engage the cask lifting yoke to the lifting trunnions.
36. Lift the cask and position the cask rotation sockets in the rear rotation trunnions of the rear support structure. Carefully lower the cask to the horizontal transport orientation resting on the front saddle by moving the crane and/or trailer, as required, to maintain cask engagement to the rear supports.
37. Disengage the cask lifting yoke from the cask lifting trunnions and remove it from the area.
38. Install the cask tie-down strap. Install the top and bottom impact limiters.
39. Install a TID to an attachment point on the top impact limiter.
40. Install roof cross-members, close ISO container doors, and replace ISO container roof.
41. Complete radiation and contamination surveys of the external surfaces of the package and record the data. Ensure removable contamination and radiation dose rate survey results comply with the limits specified in 10 CFR 71.87(i) and (j).
42. Measure the dose rate in millirems per hour at one meter from the package surface to determine the Transport Index (TI). Indicate the TI on the Radioactive Material labels applied to the package in accordance with 49 CFR 172, Subpart E.
43. Determine the appropriate Criticality Safety Index (CSI) assigned to the package contents in accordance with the CoC, and indicate the correct CSI on the Fissile Material label applied to the package per 49 CFR 172, Subpart E.
44. Apply appropriate placards to the transport vehicle in accordance with 49 CFR 172, Subpart F.
45. Complete the shipping documents and provide the carrier with instructions regarding the requirements for maintaining an exclusive use shipment.

7.1.10 Procedure for the Dry Loading of PULSTAR Fuel Into the NAC-LWT Cask

This section describes the procedures for loading the NAC-LWT cask with intact PULSTAR fuel assemblies, intact PULSTAR fuel rods in fuel rod inserts, and intact or damaged PULSTAR fuel assemblies, fuel rods, fuel debris, and nonfuel components of PULSTAR fuel assemblies in

either sealed or screened PULSTAR cans. Up to 28 PULSTAR fuel assemblies, rod inserts, and sealed or screened cans can be loaded in the 28 MTR (four module × seven cells/module) basket assembly. The 28 MTR basket assembly consists of a base module, two intermediate modules, and a top module.

Damaged PULSTAR fuel assemblies, damaged fuel rods, fuel debris, and nonfuel components of fuel assemblies are required to be loaded in either a sealed failed fuel or screened PULSTAR can. Intact PULSTAR fuel rods may be loaded into either one of the cans at the option of the licensee. The PULSTAR cans are limited to being loaded in any cell in either the top or the base module. The top and base basket modules can also contain intact PULSTAR fuel assemblies and fuel rod inserts containing intact PULSTAR fuel rods.

The NAC-LWT cask will be loaded dry, utilizing a transfer cask for loading each of the four basket modules. The basket modules will be preloaded with the PULSTAR fuel contents. The damaged fuel cans will be preloaded, closed, drained and dried, if applicable, prior to loading in either the top or base basket module. The PULSTAR cans shall be loaded and prepared for transport in accordance with the applicable steps of Section 7.1.7.

The NAC-LWT dry PULSTAR fuel loading and preparation for transport procedures are as follows.

1. Perform a receipt inspection of the empty cask and trailer/ISO container, inspecting for transport damage.
2. Position the trailer in the designated cask unloading area. Set the trailer brakes and chock the wheels to prevent unintended movement. If site-specific conditions exist that require the trailer to move to allow the cask to be uprighted on its rotation trunnions, release brakes and remove the chocks when required to complete uprighting operations. If an ISO container is used, it may be removed from the trailer and secured in the unloading area.
3. Remove the lid/top of the ISO container and remove any bracing.

   Note: Verify that the package nameplate displays the correct package identification number in accordance with the CoC.

4. Perform a Health Physics survey of the cask and adjacent surfaces of the trailer.

   Note: A receiving survey of the cask and transporter must be performed as soon as practical after arrival at the site to assure compliance with 10 CFR 71.87(i) and 10 CFR 71.47, and to assure timely reporting of any reportable noncompliance.

5. Remove the top and bottom impact limiters.
6. Remove the cask tie-down strap.

7. Using the lifting yoke with the guides removed, engage the lifting trunnions. Raise the cask to vertical by rotating the cask rotation sockets on the rear cask supports, moving the crane and/or trailer as required to keep the lift yoke engaged to the trunnions and the cask engaged in the rear supports. When the cask is fully vertical, lift the cask from the supports and remove it from the trailer/container.

8. Place the cask into the dry loading station.

9. Disengage the lift yoke.

10. Visually inspect the neutron shield tank fill, drain and level inspection plugs for signs of neutron shield fluid leakage. If leakage is detected or suspected, verify shield tank fluid level and correct, as required.

11. Remove the vent and drain port covers. Prior to reinstallation of the port covers, carefully inspect the port cover O-ring seals and, if the O-rings show any damage, replace them with approved spares. Ensure that the replacement O-rings are properly installed and seated. Visually inspect the vent and drain quick-disconnect nipples and replace them, if necessary.

    Note: For Alternate B port covers, replace the metallic O-ring with an approved spare prior to reinstallation.

12. Remove closure lid bolts. Attach the lid lift slings to the closure lid. Remove the closure lid and set it on a support that is suitable for radiological control and for maintaining the cleanliness of the closure lid. Prior to reinstallation of the lid, carefully inspect the Teflon O-ring seal in the underside of the closure lid. If the O-ring shows any damage, replace it. Remove the metallic O-ring and replace it with an approved spare. Ensure that the replacement O-rings are properly installed and seated. Inspect the lid bolts and replace any that are damaged.

13. Visually inspect the cask cavity for foreign material or damage. Clean as necessary. Install or verify the presence of a correct drain tube assembly including alignment ring.

14. Install the required dry transfer system components to the top of the cask.

15. Position the shielded transfer cask components for basket module loading, as appropriate.

16. Identify the PULSTAR fuel assemblies, fuel rod holders, and fuel cans to be loaded, and verify that the PULSTAR fuel contents comply with the authorized content, heat load and quantity conditions of the CoC. Four basket modules (e.g., one base module, two intermediate modules, and a top module) constitute the 28 MTR basket assembly. Spacers will be used as provided to position the PULSTAR fuel contents, as required.

17. Each module is capable of containing up to seven intact fuel assemblies, fuel rod inserts or a PULSTAR fuel can. Fuel cans are restricted to being loaded into the top and base modules, where the cans may be loaded with intact fuel assemblies or fuel rod holders without loading preference. There are no limitations on loading location for intact fuel assemblies or fuel rod holders in any of the four basket modules.

The base module is loaded into the cask first, followed by the two intermediate modules and the top module is loaded last.

18. Load the shielded transfer cask with the loaded base basket module.
19. Place the shielded transfer cask containing the base module unit onto the dry transfer system components positioned on the top of the cask.
20. Lower the fuel basket from the transfer cask into the NAC-LWT cask cavity.
21. Repeat the loading and transfer of loaded basket modules until the approved cask loading plan is completed.
22. Install the closure lid onto the cask using the dry transfer system. Visually verify that the lid is properly seated.
23. Remove the dry transfer cask system components from the top of the cask.
24. Install and torque the 12 closure lid bolts to 260 ± 20 ft-lb in three passes using the torquing sequence stamped on the lid.
25. Connect a gas supply line to the vent valve and a drain line to the drain valve.
26. Open the nitrogen or helium gas supply valve and pressurize the cask cavity (< 30 psig) to force any residual water out the drain line. Continue to supply pressurized gas to the cask for a minimum of five minutes after the last residual free water discharges form the drain. Remove the drain and gas supply lines and attach a vacuum drying system (VDS) to the vent.
27. Evacuate the cask cavity to less than or equal to 10 torr (13 mbar) and continue vacuum pumping for a minimum of 15 minutes.
28. At the end of the vacuum pumping period, isolate the cask cavity from the vacuum pump and stop the vacuum pump, and monitor the cask cavity pressure for a minimum of 10 minutes. If the pressure rise is less than 5 torr (6.7 torr), the cavity is verified dry of free water. If the pressure rise is >5 torr (6.7 mbar), continue vacuum drying until the dryness verification is completed satisfactorily.
29. Backfill the cask cavity with helium to 0 psig (1 atmosphere, absolute), +1, -0 psi. Disconnect the VDS from the vent valve.
30. Perform the helium leakage test of the closure lid containment O-ring using a Helium Mass Spectrometer Leak Detector (He MSLD) in accordance with the requirements of Section 8.1.3.1, Steps 3 through 10.
31. Install the vent and drain alternate port covers and torque the bolts to 100 ±10 inch-pounds.
32. If an alternate port cover containment O-ring seal was replaced, perform a helium leakage test on the affected port cover using a He MSLD in accordance with the requirements of Section 8.1.3.2.2.
33. If the alternate port cover containment seal was inspected and accepted for reuse, perform an air pressure drop leakage test on the affected port cover as follows.

a. Install a pressure test fixture to the port cover test port, including a calibrated pressure gauge with a minimum sensitivity of 0.25 psi.

b. Pressurize the port cover seal annulus to 15 psig, +1, -0 psi.

c. Isolate the gas supply and observe the pressure gauge for a minimum of five minutes.

d. The acceptance criterion for the test is no measurable drop in pressure during the minimum test time. An acceptable test assures that the minimum assembly verification leakage test sensitivity is achieved.

Note: Alternate B port covers, if used, require the satisfactory completion of a helium maintenance leakage rate test for each loaded transport. Install the Alternate B port cover and perform the maintenance leakage rate test per the requirements of 8.1.3.3.2.

34. Decontaminate the cask. Survey the cask for surface contamination and radiation dose rates.

Note: Ensure compliance with 10 CFR 71.87(i) and 10 CFR 71.47.

35. Engage the cask lifting yoke to the lifting trunnions.

36. Lift the cask and position the cask rotation sockets in the rear rotation trunnions of the rear support structure. Carefully lower the cask to the horizontal transport orientation resting on the front saddle by moving the crane and/or the trailer as required to maintain cask engagement to the rear supports.

37. Disengage the lifting yoke from the lifting trunnions and remove it from the area.

38. Install the cask tie-down strap. Install the top and bottom impact limiters.

39. Install a TID to an attachment point on the top impact limiter.

40. Install ISO container bracing and lid.

41. Complete radiation and contamination surveys of the external surfaces of the package and record the data. Ensure removable contamination and radiation dose rate survey results comply with the limits specified in 10 CFR 71.87(i) and (j).

42. Measure the dose rate in millirems per hour at one meter from the package surface to determine the Transport Index (TI). Indicate the TI on the Radioactive Material labels applied to the package in accordance with 49 CFR 172, Subpart E.

43. Determine the appropriate Criticality Safety Index (CSI) assigned to the package contents in accordance with the Certificate of Compliance, and indicate the correct CSI on the Fissile Material label applied to the package per 49 CFR 172, Subpart E.

44. Apply appropriate placards to the transport vehicle in accordance with 49 CFR 172, Subpart F.

45. Complete the shipping documents and provide the carrier with instructions regarding the requirements for maintaining an exclusive use shipment.

7.1.11 Procedure for Dry Loading of TPBAR Waste Container

This section describes the procedure for the loading of a TPBAR Waste Container into a NAC-LWT cask in a dry loading facility. Appropriate radiological controls and procedures addressing tritium shall be utilized by the licensee, including appropriate monitoring for tritium exposure.

NAC-LWT casks to be used for the transport of TPBARs shall be configured as shown on Drawing No. 315-40-128, including Alternate B port covers.

1. Perform a receiving survey of the ISO and trailer, and inspect for damage.
2. Position the trailer in the designated cask unloading area. Set the trailer brakes and chock the wheels to prevent unintended movement. If site-specific conditions exist that require the trailer to move to allow the cask to be uprighted on its rotation trunnions, release the brakes and remove the chocks when required to complete the uprighting operations. If necessary, the ISO container may be removed from the trailer and secured in the unloading area.
3. Licensees shall receive and survey the package for radiation and removable contamination (for both gross beta-gamma and tritium) per 10 CFR 20 and 49 CFR 173. Record the survey results. If radiation or contamination levels exceed the limits of 49 CFR 173.441 or 173.443, respectively, the licensee shall notify the shipper and ensure the appropriate notifications are completed.
4. Remove the roof from the ISO container and open the front and rear ISO doors. Remove the ISO roof cross members, if installed.
5. Remove the top and bottom impact limiters.
6. Remove the cask tie-down strap. Complete the radiation and contamination surveys of the package as additional surfaces become accessible. Clean the cask surfaces as required for entry into the dry loading facility.
7. Using the cask lifting yoke with lift yoke arm guides removed, engage the lifting trunnions of the front end of the cask. Raise the cask to a vertical position on the rear cask supports, moving the crane and/or trailer, as required, to keep the cask engaged in the rear cask supports and the crane cable vertical. When the cask is vertical, block the trailer wheels and lift the cask from the container.
8. Place the cask in a transfer cart or a loading fixture. Disengage the lifting yoke.
9. Remove the Alternate B vent and drain valve port covers. Replace the metallic seal with an approved spare and inspect the Viton® O-ring seal on each cover. If the Viton® O-ring shows any damage, replace it. Ensure the replacement O-rings are properly installed and seated. Store the port cover to protect the seal surfaces. Visually inspect the vent and drain valved quick-disconnect nipples and replace, if necessary.
10. Loosen and remove all closure lid bolts.
11. Attach the lid removal fixture to the closure lid.
12. Use a transfer cart or loading fixture and move the cask into the loading position.

13. Remove the closure lid and set it on a support that is suitable for radiological control and for maintaining the cleanliness of the closure lid. Carefully inspect the Teflon O-ring seal in the underside of the closure lid. If the O-ring shows any damage, replace it. Remove the metallic O-ring and replace it with an approved spare. Ensure the replacement O-rings are properly installed and seated. Inspect the lid bolts and replace any that are damaged. Verify that the TPBAR spacer is installed on the bottom of the cask lid and not damaged when the lid is set down.
14. Install the seal surface protector in the lid cavity, if required.
15. Load the TPBAR Waste Container into the TPBAR basket positioned in the cask cavity using the required grapple or handling system. Verify the contents of the Waste Container comply with the CoC content conditions.
16. Remove the cask seal surface protector, if used, and install the cask closure lid.
17. Use the transfer cart or loading fixture and remove the cask from the loading area.
18. Inspect, install and tighten all 12 closure lid bolts to 260 ± 20 ft-lbs in three passes using the torque sequence indicated on the closure lid.
19. Connect a vacuum pump to the cask vent valve.
20. Install the drain port cover, if drain valve is not required for operations, and torque the port cover bolts to 285 ± 15 in-lbs.
21. Perform the helium mass spectrometer maintenance leakage rate test on the cask lid to leaktight criteria in accordance with the requirements of Section 8.1.3.1, Steps 3 through 10.
22. Following successful completion of the helium backfill and helium leak testing of the lid seal, monitor the cavity volume for tritium and record the results.

    Note: Tritium monitoring system shall have a minimum sensitivity of 5×10^{-3} micro curies/cc.
23. Install Alternate B port covers on the vent and drain openings and torque each port cover bolt to 285 ± 15 in-lbs. Perform a helium leakage rate test on each port cover to leaktight criteria in accordance with Section 8.1.3.3.2.
24. Decontaminate the cask. Survey the cask surface for gross beta-gamma and tritium removable contamination levels, and radiation dose rates.

    Note: Removable contamination levels and radiation levels shall comply with 49 CFR 173.443 and 173.441, respectively.
25. Using the cask lifting yoke with the guide arms removed, lift and position the cask in the rear cask supports on the ISO/trailer. Engage the trunnion pockets in the bottom end of the cask with the rotation trunnions. Lower the cask to rest on the front tiedown saddle, moving the crane, and/or trailer, as required, to keep the crane cables vertical. Disengage the cask lifting yoke from the cask lifting trunnions and set it aside.
26. Install and attach the cask tiedown strap. Install the cask top and bottom impact limiters.

27. Install a TID to an attachment point on the top impact limiter.
28. Install roof cross-members, close ISO container doors, and replace ISO container roof.
29. Complete a Health Physics survey on the external surface of the package and record the results. Complete dose rate measurements at the cask surface, at 1 meter from the cask surface, and at 2 meters from the vertical plane of the side of the transport vehicle. The maximum dose rate at 1 meter from the cask is the transport index (TI). Ensure compliance with 10 CFR 71.87(i) and observe the following criteria.

    - If the dose rate is less than 2 mSv/h (200 mrem/hr) at all accessible points on the external surface of the cask, and the TI is less than 10, the package must meet the requirements of 10 CFR 71.47 (a).
    - If the dose rate is greater than 2 mSv/h (200 mrem/hr), but is less than 10 mSv/h (1000 mrem/hr) at any point on the external surface of the package, or the TI is greater than 10, the package must be shipped as "exclusive use" and meet the requirements of 10 CFR 71.47 (b), (c) and (d). If the dose rate and shipping requirements of 10 CFR 71.47 (b), (1), (2), (3) and (4) cannot be met, the package cannot be shipped.

    Note: 10 CFR 71.47 (c) and (d) require the shipper to provide the carrier with written instructions for maintenance of the exclusive use shipment. The instructions must be included with the shipping paper information. The instructions must be sufficient so that, when followed, they cause the carrier to avoid actions that unnecessarily delay delivery or unnecessarily result in increased radiation levels or radiation exposures to transport workers or members of the general public.

    - If the dose rate is > 10 mSv/h (1000 mrem/hr) at any point on the external surface of the cask, the cask exceeds the limits of 10 CFR 71.47 and cannot be shipped.
30. Complete the shipping document, carrier instructions (if required), and apply appropriate placards and labels.

7.1.12 Procedure for Wet Loading PWR MOX Fuel Rods in a Transport Canister Into the NAC-LWT Cask

PWR MOX fuel rods (or combinations of PWR MOX and UO_2 PWR fuel rods) are required to be loaded into a screened or free flow PWR/BWR Rod Transport Canister prior to loading into the NAC-LWT cask for transport. Although a maximum quantity of 16 MOX fuel rods may be shipped, it is required that the 5 × 5 rod insert be used to position the rods in the transport canister (i.e., the 4 × 4 insert is not authorized for use for the transport of MOX fuel rods).

In order to satisfy the increased potential for release of significant quantities of radioactive materials, and as recommended by NUREG-1617, Supplement 1, the NAC-LWT cask assembly

specified for the transport of PWR MOX fuel rods contained in a transport canister provides a leaktight containment boundary.

The screened or free flow transport canister with a 5 × 5 rod insert will be loaded with up to 16 PWR MOX fuel rods (or a combination of up to 16 PWR MOX and UO_2 PWR fuel rods). In addition to the 16 PWR MOX fuel rods, up to 9 zirconium alloy-based burnable poison rods (BPRs) may be loaded into the unused insert openings.

NAC-LWT casks to be used for the transport of MOX fuel rods shall be configured as shown on Drawing No. 315-40-104, Assembly 97.

1. Perform a receiving survey of the empty cask and inspect for damage.
2. Position a trailer in the designated cask unloading area. Set the trailer brakes and chock the wheels to prevent unintended movement. If site-specific conditions exist that require the trailer to move to allow the cask to be uprighted on its rotation trunnions, release brakes and remove the chocks when required to complete uprighting operations. If an ISO is used, it may be removed from the trailer and secured in the unloading area.
3. Remove the roof from the ISO container and open the front and rear ISO doors. Remove roof cross-members, if installed.

   Note: Verify that the package nameplate displays the package identification number, USA/9225/B(U)F-96, as required by the CoC for PWR MOX fuel rods.
4. Perform a Health Physics survey of the cask and adjacent surfaces of the trailer.

   Note: A receiving survey of the cask and transporter must be performed as soon as practical after arrival at the site to assure compliance with 10 CFR 71.87(i) and 10 CFR 71.47, and to assure timely reporting of any reportable noncompliance.
5. Remove the top and bottom impact limiters.
6. Remove the cask tie-down strap.
7. Using the lifting yoke with the guides removed, engage the lifting trunnions. Raise the cask to vertical by rotating the cask rotation sockets on the rear cask supports, moving the crane and/or trailer as required to maintain the lift yoke engaged to the trunnions and the cask engaged in the rear supports. When the cask is fully vertical, lift the cask from the supports and remove it from the trailer/container.
8. Place the cask in the decontamination pit or other designated area. Disengage the lifting yoke. Clean cask surfaces of road dirt, as required, for entry into the spent fuel pool.
9. Visually inspect the neutron shield tank fill, drain and level inspection plugs for signs of neutron shield fluid leakage. If leakage is detected, verify shield tank fluid level and correct, as required.

10. Remove the vent and drain valve port covers. Prior to reinstallation of the port covers, carefully inspect the valve port cover O-ring seals and, if the O-rings show any damage, replace them with approved spares. Ensure that the replacement O-rings are properly installed and seated. Visually inspect the valved quick-disconnect nipples and replace them, if necessary.

    Note: For Alternate B port covers, replace the metallic O-ring with an approved spare prior to reinstallation.

11. Remove closure lid bolts. Attach the lid lift slings to the closure lid. Remove the closure lid and set it on a support that is suitable for radiological control and for maintaining the cleanliness of the closure lid. Prior to reinstallation of the lid, carefully inspect the Teflon O-ring seal in the underside of the closure lid. If the O-ring shows any damage, replace it. Remove the metallic O-ring and replace it with an approved spare. Ensure that the replacement O-ring(s) is properly installed and seated. Inspect the lid bolts and replace any that are damaged. Ensure that the Rod Transport Canister spacer is not damaged when the lid is set down.

12. Visually inspect the inner cavity for foreign material or damage. Install or verify the presence of the drain tube and the PWR basket assembly.

13 Fill the cask cavity with clean water. Install lift yoke arm guides and remote actuation components on the cask lifting yoke.

14. Engage the cask lifting yoke with the cask lifting trunnions and pick up the cask. Carefully lower the cask to the bottom of the cask loading area while spraying the cask down with clean water.

15. Disengage the lifting yoke from the cask and remove the yoke from the pool.

16. Identify the PWR/BWR Rod Transport Canister to be loaded and verify that a 5 × 5 rod insert is located in the canister.

17. Identify the PWR MOX fuel rods (and standard PWR rods and BPRs, as applicable) to be loaded into the PWR/BWR Rod Transport Canister. Verify that the fuel rods and BPRs comply with the content type, form, heat load, minimum cooling time and quantity conditions of the NAC-LWT CoC. Load the screened or free flow PWR/BWR transport canister with up to 16 PWR MOX fuel rods, a combination of MOX and standard PWR rods, and up to 9 BPRs in the open tube locations in the 5 × 5 insert. Perform an independent verification of the fuel rod selection and loading process.

18. Install the transport canister lid and torque the lid bolts to 35 ± 5 inch-pounds.

19. Position the loaded PWR/BWR Rod Transport Canister over the cask and then carefully lower it into the cask to avoid damage to the cask sealing surfaces. Note that the transport canister may be loaded into the cask with the PWR basket insert.

20. Position the cask lifting yoke over the cask closure lid. Attach the slings to the closure lid and cask lifting yoke. Lower the yoke over the cask.

21. Position the closure lid over the cask and verify that the appropriate lid spacer is installed per the approved PWR MOX fuel rod transport arrangement in Drawing 315-40-104, Section 1.4. Lower the closure lid into the lid recess using the lid match marks as guides to align the lid. Visually confirm that the closure lid is flush with the top of the cask and properly seated.

22. Lower the cask handling yoke to slack the closure lid cables. Engage the lift yoke to the lifting trunnions and begin lifting the cask.

    Note: Visually verify the yoke engagement before lifting the cask.

23. Raise the cask until the lid is slightly above the surface of the pool. At the option of the licensee/user, a number of closure lid bolts (4 to 12) may be installed hand tight.

24. Raise the cask clear of the pool, rinsing the yoke and cask with clean water and transfer the cask to the decontamination pit or other work area. Remove the yoke and lid lift slings.

25. Install and tighten the 12 closure lid bolts to 260 ± 20 ft-lb in three passes, using the torque sequence stamped on the closure lid.

26. At the option of the licensee/user, a 25 to 50 gallon clean water flush of the cask cavity may be performed by connecting a valved clean water line to the drain valve and a valved drain line to the vent valve. After the cavity flushing is completed, if performed, disconnect the water supply and drain lines.

27. Connect a nitrogen or helium gas supply line to the vent valve and the drain line to the drain valve.

28. Open the nitrogen or helium gas supply valve and pressurize the cask cavity (<30 psig) to force out the water. Continue to supply pressurized helium to the cask for a minimum of five minutes after the last residual free water discharges from the drain line. Remove the drain and gas supply lines and attach a vacuum drying system (VDS) to the cask vent valve.

29. Evacuate the cask cavity to a vacuum pressure of less than 10 torr (13 mbar) and continue vacuum pumping for a minimum of 15 minutes.

30. At the end of the vacuum pumping period, isolate the cask cavity from the vacuum pump and stop the pump. Monitor the cask cavity pressure for a minimum of 10 minutes. If the pressure rise is less than 5 torr (6.7 mbar), the cavity is verified as dry of free water. If the pressure rise is greater than 5 torr (6.7 mbar), repeat vacuum drying until the dryness verification results are satisfactory.

31. Backfill the cask cavity with helium to 0 psig (1 atmosphere, absolute), +2, -0 psi. Disconnect the VDS.

32. Perform the helium leakage test of the closure lid containment O-ring using a Helium Mass Spectrometer Leak Detector (He MSLD) in accordance with the requirements of Section 8.1.3.1, Steps 6 through 10.

33. Install the vent and drain port covers and torque the bolts to 100 ± 10 inch-pounds.

34. If an alternate port cover containment O-ring seal was replaced, perform a helium leakage test on the affected port cover using a He MSLD in accordance with the requirements of Section 8.1.3.2.2.

35. If the alternate port cover containment seal was inspected and accepted for reuse, perform a gas pressure drop leakage test on the affected port cover as follows.

    a. Install a pressure test fixture to the port cover test port, including a calibrated pressure gauge with a minimum sensitivity of 0.25 psi.

    b. Pressurize the port cover seal annulus to 15 psig, +1, -0 psi.

    c. Isolate the gas supply and observe the pressure gauge for a minimum of five minutes.

    d. The acceptance criterion for the test is no measurable drop in pressure during the minimum test time. An acceptable test assures that the minimum assembly verification leakage test sensitivity is achieved.

    Note: Alternate B port covers, if used, require the satisfactory completion of a helium maintenance leakage rate test to confirm a leaktight seal condition for each loaded transport. Install the Alternate B port cover and perform the maintenance leakage rate test per the requirements of Section 8.1.3.3.2.

36. Decontaminate the cask. Survey the cask for surface contamination and radiation dose rates.

    Note: Ensure compliance with 10 CFR 71.87(i) and 10 CFR 71.47.

37. Remove lift yoke arm guides. Engage the cask lifting yoke to the lifting trunnions.

38. Lift the cask and position the cask rotation sockets in the rear rotation trunnions of the rear support structure. Carefully lower the cask to the horizontal transport orientation resting on the front saddle by moving the crane and/or trailer, as required, to maintain cask engagement to the rear supports.

39. Disengage the cask lifting yoke from the cask lifting trunnions and remove it from the area.

40. Install the cask tie-down strap. Install the top and bottom impact limiters.

41. Install a TID to an attachment point on the top impact limiter.

42. Install roof cross-members, close ISO container doors, and replace ISO container roof.

43. Complete radiation and contamination surveys of the external surfaces of the package and record the data. Ensure removable contamination and radiation dose rate survey results comply with the limits specified in 10 CFR 71.87(i) and (j).

44. Measure the dose rate in millirems per hour at one meter from the package surface to determine the Transport Index (TI). Indicate the TI on the Radioactive Material labels applied to the package in accordance with 49 CFR 172, Subpart E.

45. Determine the appropriate Criticality Safety Index (CSI) assigned to the package contents in accordance with the CoC, and indicate the correct CSI on the Fissile Material label applied to the package per 49 CFR 172, Subpart E.

46. Apply appropriate placards to the transport vehicle in accordance with 49 CFR 172, Subpart F.

47. Complete the shipping documents and provide the carrier with instructions regarding the requirements for maintaining an exclusive use shipment.

7.2 Procedures for Unloading Package

In general, the procedure for unloading the package is the reverse of that presented for loading the package (Section 7.1). Specific generic procedures are provided in this section for the wet and dry unloading of various authorized contents from the NAC-LWT cask. As required to accommodate specific facilities and equipment, site-specific procedures shall be prepared and utilized for the unloading operations as appropriate to the contents.

7.2.1 Procedures for Wet Unloading of LWR Fuel and PWR, PWR MOX and BWR Fuel Rods in Transport Canisters

The procedures for unloading the package are as follows:

1. Perform a receipt inspection of the cask and trailer/ISO container, inspecting for transport damage.
2. Position the trailer in the designated cask unloading area. Set the trailer brakes and chock the wheels to prevent unintended movement. If site-specific conditions exist that require the trailer to move to allow the cask to be uprighted on its rotation trunnions, release brakes and remove the chocks when required to complete uprighting operations. If an ISO container is used, it may be removed from the trailer and secured in the unloading area.
3. Remove the lid/top of the ISO container and remove any bracing, or the personnel barrier.

   Note: Verify that the package nameplate displays the correct package identification number in accordance with the CoC.

4. Licensees shall monitor the package for radioactive contamination and radiation levels in accordance with 10 CFR 20.1906. If contamination levels exceed 10 CFR 71.87(i) or radiation levels exceed the limits of 10 CFR 71.47, the licensee shall notify the NRC Operations Center.
5. Verify the TID identification number on the top impact limiter to confirm tampering with the package did not occur.
6. Remove the top and bottom impact limiters.
7. Remove the cask tie-down strap.
8. Using the lifting yoke with the guides removed, engage the lifting trunnions. Raise the cask to vertical by rotating the cask rotation sockets on the rear cask supports, moving the crane and/or trailer as required to keep the lift yoke engaged to the trunnions and the cask engaged in the rear supports. When the cask is fully vertical, lift the cask from the supports and remove it from the trailer/container.

9. Place the cask in the decontamination pit or other designated area. Disengage the lifting yoke. Clean cask surfaces of road dirt as required for entry into the spent fuel pool.
10. Remove the vent and drain valve port covers. Connect a pressure gauge and isolation valve assembly to the cask vent valve.
11. Connect vent and clean water fill lines to the vent and drain valves.
12. Open the water supply valve to allow water to slowly enter the cask cavity.

    Note: The hot gases exiting from the vent valve could be highly radioactive. The exhaust gases must, therefore, be routed to an off-gas process system. The cask cavity does not contain a relief valve; therefore, any system for cooling down the package must be provided with a pressure relief device set so that the maximum pressure in the cask cavity does not exceed 100 psig. Coolant flow rates should be controlled to avoid thermal shock to the cask internals.

13. Continue the filling procedure until the cask cavity is filled with water. Remove fill and vent lines.
14. Loosen and remove the closure lid bolts. At the option of licensee/user, some bolts (i.e., 4-12) may be left installed hand tight for the cask movement to the spent fuel pool.
15. Engage the cask lifting yoke (with slings, yoke arm guides and remote actuation system components attached) with the cask lifting trunnions and connect the closure lid to the lifting yoke slings.
16. Position the cask over the spent fuel pool and lower the cask until the top of the cask is at an elevation that permits access to the closure lid bolts.
17. Remove any remaining closure lid bolts.
18. Carefully lower the cask to rest on the bottom of the cask unloading area while spraying the cask's exterior surfaces with clean water to minimize contamination.
19. Disengage the lifting yoke from the cask and slowly raise the yoke until the closure lid is raised clear of the cask. Remove the yoke from the vicinity of the cask to provide clearance for unloading the cask.
20. Unload the contents of the cask cavity (i.e., fuel assemblies or Rod Transport Canisters) using the required grapple system. Verify that the unloaded contents conform to the contents described in the cask loading report. Place the fuel assemblies or transport canisters into storage or prepare them for further processing.
21. Position the cask lifting yoke with the cask closure lid over the cask cavity and slowly lower it into place using the cask and closure lid match marks as guides. Visually confirm that the closure lid is seated.
22. Engage the cask lifting yoke with the cask trunnions and raise the cask.

    Note: Verify yoke engagement before lifting the cask.

23. Raise the cask until the lid is slightly above the surface of the pool. At the option of the licensee/user, several of the closure lid bolts (i.e., 4-12) may be installed hand tight.
24. Raise the cask clear of the pool, rinsing the yoke and cask with clean water.
25. Transfer the cask to the decontamination pit or other work area. Remove the yoke and lid lift slings.
26. Install and tighten all 12 closure lid bolts to 260 ± 20 ft-lb in three passes, using the torque sequence stamped on the closure lid.
27. At the option of the licensee/user, a 25 to 50 gallon clean water flush of the cask cavity may be performed by connecting a valved, clean water line to the drain valve and a valved drain line to the vent valve. After the cavity flushing is completed, if performed, disconnect the water supply and drain lines.
28. Connect a gas (air, nitrogen or helium) supply line to the vent valve and the drain line to the drain valve.
29. Open the gas supply valve and pressurize the cask cavity (<30 psig) to force out the water. Continue to supply gas to the cask cavity for a minimum of five minutes after the last residual free water discharges from the drain line.
30. Remove the gas supply and drain lines.
31. Install the alternate port covers over the vent and drain valves and tighten the port cover bolts to 100 ± 10 inch-pounds. For Alternate B port covers, install and torque the high-strength bolts to 285 ± 15 inch-pounds.

    Note: It is not necessary to inspect or replace the port cover seals. Seal inspection and replacement, if required, will be performed prior to the next loaded transport.

7.2.2 Procedures for Wet Unloading of Metallic Fuel

The procedure for unloading the metallic fuel from the package in a spent fuel pool is as follows.

1. Perform a receipt inspection of the cask and trailer/ISO container, inspecting for transport damage.
2. Position the trailer in the designated cask unloading area. Set the trailer brakes and chock the wheels to prevent unintended movement. If site-specific conditions exist that require the trailer to move to allow the cask to be uprighted on its rotation trunnions, release brakes and remove the chocks when required to complete uprighting operations. If an ISO container is used, it may be removed from the trailer and secured in the unloading area.
3. Remove the lid/top of the ISO container and remove any bracing, or the personnel barrier.

   Note: Verify that the package nameplate displays the correct package identification number in accordance with the CoC.

4. Licensees shall monitor the package for radioactive contamination and radiation levels in accordance with 10 CFR 20.1906. If contamination levels exceed 10 CFR 71.87(i) or radiation levels exceed the limits of 10 CFR 71.47, the licensee shall notify the NRC Operations Center.
5. Verify the TID identification number on the top impact limiter to confirm tampering with the package did not occur.
6. Remove the top and bottom impact limiters.
7. Remove the cask tie-down strap.
8. Using the lifting yoke with the guides removed, engage the lifting trunnions. Raise the cask to vertical by rotating the cask rotation sockets on the rear cask supports, moving the crane and/or trailer as required to keep the lift yoke engaged to the trunnions and the cask engaged in the rear supports. When the cask is fully vertical, lift the cask from the supports and remove it from the trailer/container.
9. Place the cask in the decontamination pit or other designated area. Disengage the lifting yoke. Clean cask surfaces of road dirt as required for entry into the spent fuel pool.
10. Remove the vent valve and drain valve port covers. Connect a pressure gauge and isolation valve assembly to the cask vent valve. Open the isolation valve and record the internal pressure reading (if any). Using a suitable air line and the gauge/valve assembly, vent the cask cavity to an off-gas handling unit.
11. Connect vent and clean water fill lines to the vent and drain valves.
12. Open the water supply valve to allow water to slowly enter the cask cavity.

    Note: The hot gases exiting from the vent valve could be highly radioactive. The exhaust gases must, therefore, be routed to an off-gas process system. The cask cavity does not contain a relief valve; therefore, any system for cooling down the package must be provided with a pressure relief device set so that the maximum pressure in the cask cavity does not exceed 100 psig. Coolant flow rates should be controlled to avoid thermal shock to the cask internals.

13. Continue the filling procedure until the cask cavity is filled with water. Remove fill and vent lines.
14. Loosen and remove the 12 closure lid bolts. At the option of licensee/user, some bolts (i.e., 4-12) may be left installed hand tight for the cask movement to the spent fuel pool.
15. Engage the cask lifting yoke (with slings, lift yoke arm guides and remote actuation system components attached) with the cask lifting trunnions and connect the closure lid to the lifting yoke slings.
16. Position the cask over the spent fuel pool and lower the cask until the top of the cask is at an elevation, which permits access to the closure lid bolts.
17. Remove any remaining closure lid bolts, inspect and store.

18. Carefully lower the cask to rest on the bottom of the cask unloading area while spraying the exterior surfaces of the cask with clean water to minimize contamination.
19. Disengage the lifting yoke from the cask and slowly raise the yoke until the closure lid is raised clear of the cask. Remove the yoke from the vicinity of the cask to provide clearance for unloading the cask.

    Note: Closure lid may be brought out of the pool and later assembled to the empty cask.
20. Unload the contents of the cask cavity using the required grapple system.
21. Position the cask lifting yoke with the cask closure lid over the cask cavity and slowly lower it into place using the cask and closure lid match marks as guides. Visually confirm that the closure lid is seated.
22. Engage the cask lifting yoke with the cask trunnions and raise the cask.
23. Raise the cask until the lid is slightly above the surface of the pool. At the option of the licensee/user, several of the closure lid bolts (i.e., 4-12) may be installed hand tight.
24. Raise the cask clear of the pool, rinsing the yoke and cask with clean water.
25. Transfer the cask to the decontamination pit or other work area. Remove the yoke and lid lift slings.
26. Install and tighten the 12 closure lid bolts to 260 ± 20 ft-lb in three passes, using the torque sequence stamped on the closure lid.
27. At the option of the licensee/user, a 25 to 50 gallon clean water flush of the cask cavity may be performed by connecting a valved, clean water line to the drain valve and a valved drain line to the vent valve. After the cavity flushing is completed, if performed, disconnect the water supply and drain lines.
28. Connect a gas (air, nitrogen or helium) supply line to the vent valve and the drain line to the drain valve.
29. Open the gas supply valve and pressurize the cask cavity (<30 psig) to force out the water. Continue to supply gas to the cask cavity for a minimum of five minutes after the last residual free water discharges from the drain line.
30. Remove the gas supply and drain lines.
31. Install the alternate port covers over the vent and drain valves and tighten the port cover bolts to 100 ± 10 in-lb. For Alternate B port covers, install and torque the high-strength bolts to 285 ± 15 inch-pound.

    Note: It is not necessary to inspect or replace the port cover seals. Seal inspection and replacement, if required, will be performed prior to the next loaded transport.

7.2.3 Procedure for Wet Unloading of MTR, TRIGA, DIDO, ANSTO or PULSTAR Fuel Basket Contents

The procedure for the unloading of MTR, TRIGA, DIDO, ANSTO or PULSTAR fuel basket contents from the package in a spent fuel pool is as follows:

1. Perform a receiving survey of the cask and inspect for transport damage.
2. Position the trailer in the designated cask unloading area. Set the trailer brakes and chock the wheels to prevent unintended movement. If site-specific conditions exist that require the trailer to move to allow the cask to be uprighted on its rotation trunnions, release the brakes and remove the chocks when required to complete the uprighting operations. If an ISO container is used, it may be removed from the trailer and secured in the loading area.
3. Remove the roof from the ISO container, and open the front and rear ISO doors. Remove roof cross-members, if installed.

   Note: Verify that the package nameplate displays the correct package identification number in accordance with the CoC.
4. Licensees shall monitor the package for radioactive contamination and radiation levels in accordance with 10 CFR 20.1906. If contamination levels exceed 10 CFR 71.87(i) or radiation levels exceed the limits of 10 CFR 71.47, the licensee shall notify the NRC Operations Center.
5. Verify the TID identification number on the top impact limiter to confirm tampering with the package did not occur.
6. Remove the top and bottom impact limiters.
7. Remove the cask tie-down strap.
8. Using the cask lifting yoke with left yoke arm guides removed, engage the lifting trunnions of the front end of the cask. Raise the cask to a vertical position on the rear cask support, moving the crane as necessary to keep the cask engaged in the rear rotation supports and the crane cable vertical. When the cask is vertical, lift the cask from the container supports.
9. Place the cask in the decontamination pit or other site designated area. Disengage the lifting yoke. Clean cask surfaces of road dirt as required for entry into the spent fuel pool.
10. Remove the vent valve and drain valve port covers. Connect a pressure gauge and isolation valve assembly to the cask vent valve. Open the isolation valve and record the internal pressure reading (if any). Using a suitable air line and the gauge/valve assembly, vent the cask cavity to an off-gas handling unit.
11. Connect vent and clean water fill lines to the vent and drain valves.
12. Open the water supply valve to allow water to slowly enter the cask cavity.

Note: Gases or steam exiting the vent may be radioactive. The vent line should be routed to an off-gas process system or a HEPA filter. The system for cooling down the package shall contain a pressure relief device set to ensure that the cask internal pressure is maintained below 100 psig. Coolant flow rates are to be controlled to avoid thermal shock to the fuel contents.

13. Continue the filling procedure until the cask cavity is filled with water. Remove fill and vent lines.
14. Loosen and remove the 12 closure lid bolts. At the option of licensee/user, some bolts (i.e., 4-12) may be left installed hand tight for the cask movement to the spent fuel pool.
15. Engage the cask lifting yoke (with slings, yoke arm guides and remote actuation system components attached) with the cask lifting trunnions and connect the closure lid to the lifting yoke slings.
16. Position the cask over the spent fuel storage pool and lower the cask until the top of the cask is at an elevation which allows access for the removal of the closure lid bolts.
17. Remove any remaining closure lid bolts, inspect and store.
18. Carefully lower the cask to rest on the bottom of the cask unloading area while spraying the exterior surfaces of the cask with clean water to minimize contamination. Disengage the lifting yoke from the lifting trunnions and slowly raise the yoke until the closure lid is raised clear of the cask. Remove the yoke from the vicinity of the cask to provide for clearance for unloading the cask.

    Note: The closure lid may be brought out of the pool and later assembled to the empty cask.

19. Unload the MTR, TRIGA, DIDO, spiral, MOATA plate or PULSTAR fuel assemblies or fuel cans from the top basket module using the appropriate grapple or handling system. As required, remove empty basket modules from the cask cavity to allow access to the next basket module. Continue fuel unloading operations until all fuel assemblies, fuel cans, and empty basket modules are removed from the cavity. Alternatively, each basket module containing fuel assemblies or damaged fuel cans may be unloaded from the cask cavity and stored in the spent fuel pool. Continue unloading until all basket modules have been removed.
20. Position the cask lifting yoke with guide arms and remote actuation components installed over the cask closure lid. Attach the slings to the cask closure lid and cask lifting yoke.
21. Position the cask lifting yoke and closure lid over the cask cavity and slowly lower it into place using the cask and closure lid match marks as guides. Visually confirm that the closure lid is seated.

    Note: The closure lid may be installed separately after the empty cask is removed from the spent fuel pool.

22. Engage the cask lifting yoke with the cask trunnions and raise the cask.

23. Raise the cask until the lid is slightly above the surface of the pool. At the option of the licensee/user, several of the closure lid bolts (i.e., 4-12) may be installed hand tight.
24. Raise the cask clear of the pool, rinsing the yoke and cask with clean water.
25. Transfer the cask to the decontamination pit or other work area. Remove the yoke and lid lift slings.
26. Install and tighten four closure lid bolts to 100 ± 10 ft-lb using the torque sequence stamped on the closure lid.
27. At the option of the licensee/user, a 25 to 50 gallon clean water flush of the cask cavity may be performed by connecting a valved, clean water line to the drain valve and a valved drain line to the vent valve. After the cavity flushing is completed, if performed, disconnect the water supply and drain lines.
28. Connect a gas (air, nitrogen or helium) supply line to the vent valve and the drain line to the drain valve.
29. Open the gas supply valve and pressurize the cask cavity (<30 psig) to force out the water. Continue to supply gas to the cask cavity for a minimum of five minutes after the last residual free water discharges from the drain line.
30. Remove the gas supply and water drain lines.
31. Remove the four closure lid bolts and lift the lid clear of the cask.

    Note: It is not necessary to inspect or replace the closure lid metallic seal. A new metallic seal will be installed and tested prior to the next loaded transport.

32. Remove the drain tube assembly and drain tube alignment ring from the cask cavity.
33. Reinstall the closure lid and install the 12 closure lid bolts. Torque the bolts to 260 ± 20 ft-lbs in three passes using the torque sequence indicated in the closure lid.
34. Install the alternate port covers over the vent and drain valves and tighten the port cover bolts to 100 ± 10 inch-pounds. For Alternate B port covers, install and torque the high-strength bolts to 285 ± 15 inch-pounds.

    Note: It is not necessary to inspect or replace the port cover seals. Seal inspection and replacement, if required, will be performed prior to the next loaded transport.

7.2.4 Procedure for Dry Unloading of MTR, TRIGA, DIDO, ANSTO or PULSTAR Fuel Contents

This section describes the procedure for unloading of MTR, TRIGA, DIDO, ANSTO or PULSTAR fuel basket contents from the NAC-LWT in a cell or a dry unloading fixture.

1. Perform a receiving survey of the cask and inspect for transport damage.
2. Position the trailer in the designated cask unloading area. Set the trailer brakes and chock the wheels to prevent unintended movement. If site-specific conditions exist that require the trailer to move to allow the cask to be uprighted on its rotation trunnions,

release the brakes and remove the chocks when required to complete the uprighting operations. If an ISO container is used, the ISO container may be removed from the trailer and secured in the unloading area.

3. Remove the roof from the ISO container and open the front and rear ISO doors. Remove roof cross-members, if installed.

   Note: Verify that the package nameplate displays the correct package identification number in accordance with the CoC.

4. Licensees shall monitor the package for radioactive contamination and radiation levels in accordance with 10 CFR 20.1906. If contamination levels exceed 10 CFR 71.87(i) or radiation levels exceed the limits of 10 CFR 71.47, the licensee shall notify the NRC Operations Center.

5. Verify the TID identification number on the top impact limiter to confirm tampering with the package did not occur.

6. Remove the top and bottom impact limiters.

7. Remove the cask tie-down strap. Clean the cask surfaces as required for entry into the hot cell.

8. Using the cask lifting yoke with lift yoke arm guides removed, engage the lifting trunnions of the front end of the cask. Raise the cask to a vertical position on the rear cask support, moving the crane and/or trailer, as required, to keep the cask engaged in the rear rotation supports and the crane cable vertical. When the cask is vertical, block the trailer wheels and lift the cask from the container.

9. Place the cask in the cell transfer cart or unloading fixture. Disengage the lifting yoke.

10. Remove the vent valve port cover.

11. Connect vent line to the vent valve.

    Note: The hot gases exiting from the vent may be highly radioactive and the exhaust gas should be routed to an off-gas process system or to a HEPA filter.

12. Allow the cask to vent. Remove vent line.

13. Loosen and remove the 12 closure lid bolts. Visually inspect and store the bolts.

14. Attach the lid removal fixture.

15. Using the hot cell transfer cart or unloading fixture, move the cask into the unloading position.

16. Remove the cask lid.

    Note: It is not necessary to inspect or replace the closure lid metallic seal. A new metallic seal will be installed and tested prior to the next loaded shipment.

17. Install the seal surface protector in the lid cavity, if required.

18. Unload the MTR, TRIGA, DIDO, ANSTO or PULSTAR fuel basket modules from the cask cavity using the required grapple or handling system.

19. Remove the cask seal surface protector, if installed, and replace the cask lid.
20. Using the cell transfer cart or unloading fixture, remove the cask.
21. Remove the lid from the cask and remove the drain tube and drain tube alignment ring
22. Replace the cask lid and remove the lid removal fixture.
23. Install and tighten all 12 closure lid bolts to 260 ± 20 ft-lbs in three passes using the torque sequence indicated on the closure lid.
24. Install the port covers over the vent and drain valves and tighten the port cover bolts to 100 ±10 inch-pounds. For Alternate B port covers, install and torque the high-strength bolts to 285 ±10 inch-pounds.

    Note: It is not necessary to inspect or replace the port cover seals. Seal inspection replacement and leak testing will be performed prior to the next loaded transport.

7.2.5 Procedure for Dry Unloading of TPBAR Contents

This section describes the procedure for the unloading of a consolidation canister, a PWR/BWR Rod Transport Canister or a waste container that contains TPBARs from the NAC-LWT in a dry unloading facility.

1. Perform a receiving survey of the ISO container and trailer, and inspect for damage.
2. Position the trailer in the designated cask unloading area. Set the trailer brakes and chock the wheels to prevent unintended movement. If site-specific conditions exist that require the trailer to move to allow the cask to be uprighted on its rotation trunnions, release the brakes and remove the chocks when required to complete the uprighting operations. If necessary, the ISO container may be removed from the trailer and secured in the unloading area.
3. Licensees shall receive and survey the package for radiation and removable contamination (for both gross beta-gamma and tritium) per 10 CFR 20 and 49 CFR 173. Record the survey results. If radiation or contamination levels exceed the limits of 49 CFR 173.441 or 173.443, respectively, the licensee shall notify the shipper and ensure the appropriate notifications are completed.
4. Remove the roof from the ISO container and open the front and rear ISO doors. Remove the ISO roof cross members, if installed.
5. Verify the TID identification number on the top impact limiter to confirm tampering with the package did not occur.
6. Remove the top and bottom impact limiters.
7. Remove the cask tie-down strap. Complete the radiation and contamination surveys of the package as additional surfaces become accessible. Clean the cask surfaces as required for entry into the dry unloading facility.

8. Using the cask lifting yoke with lift yoke arm guides removed; engage the lifting trunnions of the front end of the cask. Raise the cask to a vertical position on the rear cask support, moving the crane and/or trailer, as required, to keep the cask engaged in the rear rotation supports and the crane cable vertical. When the cask is vertical, block the trailer wheels and lift the cask from the container.
9. Place the cask in a transfer cart or an unloading fixture. Disengage the lifting yoke.
10. Remove the vent and drain valve port covers.
11. Connect a tritium monitoring system to the vent and drain quick-disconnect valves, and operate the device in accordance with the manufacturer's instructions. The tritium monitoring system shall have a minimum sensitivity of 5×10^{-3} micro curie/cc.
12. Monitor the cavity gas for tritium. If the gas sample measurement indicates a tritium gas concentration greater than 1×10^{-2} micro curie/cc, the cask internals must be decontaminated after unloading is completed and prior to subsequent use in transporting non-TPBAR contents.

    Note: The gases exiting from the cavity may be radioactive and contaminated with tritium, and at an elevated temperature. Cavity gases should be controlled per the site requirements.
13. Vent the cask cavity. Remove the gas lines and monitoring system from the vent and drain valves.
14. Loosen and remove all closure lid bolts.
15. Attach the lid removal fixture.
16. Use a transfer cart or unloading fixture and move the cask into the unloading position.
17. Remove the cask lid.

    Note: Replacement of the closure lid metallic seal is not required. A new metallic seal will be installed and leak tested prior to the next loaded shipment.
18. Install the seal surface protector in the lid cavity, if required.
19. Unload the TPBAR contents from the cask cavity using the required grapple or handling system.
20. Using the transfer cart or unloading fixture, remove the cask from the unloading area.
21. Collect an ambient air sample near the cask cavity opening. If the measured tritium gas concentration exceeds 1×10^{-2} micro curie/cc, the cask cavity must be decontaminated after unloading and prior to subsequent use in transporting non-TPBAR contents.
22. Survey the accessible inside surfaces of the cask cavity and internal components (i.e., upper 2 feet) for tritium contamination. If measured tritium removable contamination is greater than $2.2 \times 10^{+4}$ dpm/100 cm^2, the cask must be decontaminated after unloading is completed and prior to subsequent use in transporting non-TPBAR contents.

    Note: If significantly higher tritium contamination levels and the need for repeated decontamination become indicative of residual tritium contamination in the

crystalline structure of the cask interior with potential for weeping, NAC will notify the NRC of the condition and its action.

23. Remove the cask seal surface protector, if used, and install the cask lid.
24. Inspect, install and tighten all 12 closure lid bolts to 260 ± 20 ft-lbs in three passes using the torque sequence indicated on the closure lid.

    Note: Replacement of the vent and drain port cover metallic seals is not required. New metallic seals will be installed and leak tested prior to the next loaded shipment.

25. Install the port covers on the vent and drain ports and torque the port cover bolts to 285 ± 15 inch-pounds.

7.2.6 Procedure for Dry Unloading of PWR/BWR/MOX Fuel Rod Contents

This section describes the procedure for the unloading of a PWR/BWR Rod Transport Canister from the NAC-LWT cask in a dry unloading facility.

1. Perform a receiving survey of the ISO container and trailer, and inspect for damage.
2. Position the trailer in the designated cask unloading area. Set the trailer brakes and chock the wheels to prevent unintended movement. If site-specific conditions exist that require the trailer to move to allow the cask to be uprighted on its rotation trunnions, release the brakes and remove the chocks when required to complete the uprighting operations. If necessary, the ISO container may be removed from the trailer and secured in the unloading area.
3. Licensees shall receive and survey the package for radiation and removable contamination per 10 CFR 20 and 49 CFR 173. Record the survey results. If radiation or contamination levels exceed the limits of 49 CFR 173.441 or 173.443, respectively, the licensee shall notify the shipper and ensure the appropriate notifications are completed.
4. Remove the roof from the ISO container and open the front and rear ISO doors. Remove the ISO roof cross members, if installed.
5. Verify the TID identification number on the top impact limiter to confirm tampering with the package did not occur.
6. Remove the top and bottom impact limiters.
7. Remove the cask tie-down straps. Complete the radiation and contamination surveys of the package as additional surfaces become accessible. Clean the cask surfaces as required for entry into the dry unloading facility.
8. Using the cask lifting yoke with lift yoke arm guides removed, engage the lifting trunnions of the front end of the cask. Raise the cask to a vertical position on the rear cask support, moving the crane and/or trailer, as required, to keep the cask engaged in the rear rotation supports and the crane cable vertical. When the cask is vertical, block the trailer wheels and lift the cask from the container.

9. Place the cask in a transfer cart or an unloading fixture. Disengage the lifting yoke.
10. Remove the vent and drain valve port covers.
11. Connect the vent line with pressure gauge and isolation valve to the vent port quick disconnect coupling.

    Note: At the discretion of the receiving facility, a gas sample may be taken prior to cavity venting to determine if leakage from the fuel rods occurred during transport.

    Note: The gases exiting from the cavity may be radioactive and at an elevated temperature and pressure. Cavity gases should be controlled and vented to radioactive gas treatment systems per site requirements.

12. Vent the cask cavity. Remove the vent line from the vent valves.
13. Attach the lid removal fixture.
14. Loosen and remove all closure lid bolts.
15. Use the transfer cart or unloading fixture and move the cask into the unloading position.
16. Remove the cask lid.

    Note: Replacement of the closure lid metallic seal is not required. A new metallic seal will be installed and leak tested prior to the next loaded shipment.

17. Install the seal surface protector in the lid cavity, if required.
18. Unload the PWR/BWR Rod Transport Canister and/or its contents using the appropriate grapple or handling system.
19. Using the transfer cart or unloading fixture, remove the cask from the unloading area.
20. Remove the cask seal surface protector, if used, and install the cask lid.
21. Inspect, install and tighten all 12 closure lid bolts to 260 ± 20 ft-lbs in three passes using the torque sequence indicated on the closure lid.

    Note: Inspection or replacement of the vent and drain port cover metallic seals is not required. New metallic seals will be installed and leak tested prior to the next loaded shipment.

22. Install the port covers on the vent and drain ports and torque the port cover bolts to 100 ± 10 inch-pounds for the alternate port covers or 285 ± 15 inch-pounds for the Alternate B port covers.

Chapter 8

8 ACCEPTANCE TESTS AND MAINTENANCE PROGRAM

This chapter discusses the acceptance test and maintenance program to be used for the NAC-LWT cask, in compliance with 10 CFR 71, Subpart G.

Where required, specific procedures for testing will be developed in conjunction with the cask fabrication, in accordance with an approved Quality Assurance program.

8.1 Acceptance Tests

This section discusses the tests to be performed prior to first use of the cask.

Two port cover designs are available for use. The alternate port cover has a face seal containment boundary Viton® O-ring and a secondary test boundary O-ring seal along the barrel of the port cover. The alternate port cover was developed to facilitate ease in installation and removal in the field. The Alternate B port cover has two face seals on the inner end of the port cover, one metallic containment boundary seal and one Viton® test boundary seal. The Alternate B port cover was developed to provide a high-pressure containment boundary for TPBAR contents. The Alternate B port covers utilize higher strength bolts and a higher installed torque value. Both port cover designs provide a leaktight containment boundary.

To simplify the testing procedures below, when "port cover" or "port cover O-ring" is mentioned, it is intended to mean the port cover which has been chosen for that specific fabrication or cask configuration, either the alternate or the Alternate B and their respective O-rings. The different testing procedures are described in the applicable sections.

8.1.1 Visual Inspection

All components making up the cask lid, body, and baskets are to be visually inspected. This inspection verifies that all items are properly cleaned, free of nicks, gouges and damage, and are assembled in accordance with the license drawings. Each item is compared to the appropriate drawing to verify that it is in the correct orientation, position, and location.

All dirt, oil residue, metal chips or other forms of debris are removed by appropriate cleaning methods. Any entrapped water is removed. Any component found to deviate from its drawing is re-installed, replaced, or otherwise reworked as necessary in order to bring it into conformance.

Acceptance criteria require complete cask cleanliness, that foreign objects are removed, and that nicks or gouges that might preclude sealing or cask closure are not permitted. Valve and system components are visually inspected for leaks during pressure checks. Leaks are not permitted. Any case of noncompliance shall be corrected prior to final acceptance. All welds are visually inspected in accordance with the methods of Article 9, Section V of the "ASME Boiler and

Pressure Vessel Code." The acceptance criteria are in accordance with part NB-4424, Section III, and parts UW-35 or UW-36, Section VIII, of the "ASME Boiler and Pressure Vessel Code."

8.1.2 Structural and Pressure Tests

Following completion of fabrication, a hydrostatic test is performed on the cask cavity in accordance with the "ASME Boiler and Pressure Vessel Code," Section III, Subsection NB, Article NB-6000, to 209 (+5/-0) psig. This test is performed in accordance with a procedure prepared by the fabricator and approved by NAC International (NAC). For casks intended for transport of TPBARs, an additional post-fabrication hydrostatic test is performed to 450 +15/-0 psig (1.5 × MNOP of 289 psig = 434 psig). Alternate B port covers are installed for the 450 +15/-0 psig test. The test requirements and acceptance criteria for both tests are described below.

The cask cavity is hydrostatically tested using demineralized water. The test is conducted with the closure lid and valve port covers installed in accordance with the cask handling procedure for loaded casks, but with the quick-disconnect valves removed. During these two 30-minute pressure tests (conducted alternately with one port cover installed and the other removed for access to the cavity), an inspection is made to detect any visual or other evidence of leakage. Any evidence of leakage, including drop of gauge pressure, is cause for rejection.

Following the hydrostatic test, the cask cavity, lid, and port covers are dried and made ready for visual and dye penetrant testing (PT) inspections.

The cask cavity (containment boundary including lid and port covers) is visually inspected. All accessible welds within the cask cavity are examined by PT in accordance with ASME Code, Section V, Article 6, with acceptance criteria in accordance with ASME Code, Section III, Subsection NB, Article NB-5350. Any evidence of cracking, permanent deformation, or exceeding of material yield strength is cause for rejection.

Following completion of the fabrication pressure test or the postfabrication TPBAR-required pressure test, the cask containment boundary is leakage tested in accordance with the requirements of Section 8.1.3.

The neutron shield tank and the expansion tank are hydrostatically tested simultaneously, since they are joined by a siphon tube. The test is in accordance with the "ASME Boiler and Pressure Vessel Code," Section VIII, Division 1, to 248 (+5/-0) psig (165 psig maximum hypothetical accident pressure × 1.5). The neutron shield relief valve is replaced by a plug during the test. All tank seams and joints are inspected for evidence of leakage. The pressure is monitored by use of a pressure gauge. Any evidence of leakage or drop in pressure is cause for rejection. All accessible welds on the neutron shield structure are PT examined following the hydrostatic test.

Each of the two pairs of the cask lift trunnions is load tested. The load test is performed for one pair and, then, repeated for the other pair.

The test consists of applying a vertical load of 159,375 lbs + 3,000 lbs, -0 lbs (300 % of the maximum service load), to each trunnion pair. The load is applied in a vertical direction and equally distributed between the two trunnions.

This test may be carried out by the use of calibrated hydraulic rams combined with a beam, or the cask lifting yoke, and appropriate dead weight attached to the trunnion pair. The load is held for a minimum of 10 minutes.

Following the load test, all welds and material are visually inspected for plastic deformation and cracking and liquid penetrant inspected in accordance with the "ASME Boiler and Pressure Vessel Code," Section V, Article 6, and Section III, Division I, Subsection NF, Article NF-5350, as called for in ANSI N14.6-1993.

Any evidence of permanent deformation or any evidence of cracking, galling, or exceeding of yield strength is cause for rejection of that item.

The rotation sockets at the lower end of the cask are not load tested, being monolithic steel block with a suitably machined opening. Prior to first use, each socket is visually inspected for cleanliness and signs of deformation or other unsuitability. Accessible welds are inspected in accordance with the standards for the cask trunnions.

8.1.3 Leak Tests

The cask containment boundary is subjected to a fabrication leakage rate test, as described in the sections below, to verify containment following fabrication. The test is performed using helium inside the cask cavity and a helium mass spectrometer connected to the test port of the lid or one of the port covers. The mass spectrometer has a minimum sensitivity such that it is capable of detecting a leak rate of at least 1×10^{-9} ref cm^3/sec and is calibrated before and after the test with a standard having a known leak rate between 4×10^{-7} and 1×10^{-9} ref cm^3/sec. The procedure is performed between 40°F and 125°F and is temperature corrected. New O-rings are to be used. The basic procedures for the cask lid and for the vent and drain port covers are provided in the following sections.

A required maintenance leakage rate test adheres to the criteria listed above and follows the replacement of any containment component or seal. Containment components having single-use metallic containment seals (i.e., closure lid and Alternate B port covers) require a maintenance leakage rate test prior to each loaded transport. All containment components shall be subjected to a periodic leakage rate test annually while the cask is in service, or prior to returning the cask

to service if the period since the last leakage rate test exceeds 12 months. The acceptance criteria for the fabrication, maintenance, and periodic leakage rate tests appear in the following sections.

8.1.3.1 Closure Lid Leakage Rate Test

The following procedure shall be used to perform the fabrication, maintenance, periodic and pre-shipment leakage rate tests on the closure lid. Steps 1 and 2 are not performed for the pre-shipment leakage rate test performed during cask loading operations as described in Chapter 7.

1. Remove the vent and drain port covers and install the closure lid fitted with a new metallic seal on the cask body.
2. Install the 12 lid bolts and torque them to 260 ± 20 ft-lb in three passes, using the torque sequence stamped on the lid.
3. Connect the vacuum pump to the vent valve and evacuate the cask cavity to a pressure ≤ 100 torr (130 mbar).
4. Backfill the cask cavity with 99.9% (minimum) pure helium to atmospheric pressure.
5. Repeat Steps 3 and 4 to ensure that the cask cavity helium concentration is approximately 98%.
6. Remove the test port plug from the lid.
7. Connect a helium mass spectrometer leak detector (MSLD) to the cask lid test port. Start the helium MSLD.

   Note: The specific test procedure depends on the helium MSLD used. The test commences when a vacuum is pulled on the test port by the MSLD and the MSLD is placed in the "test" mode.

8. Monitor the test leakage rate until the leakage rate is stable or a minimum of 30 seconds.
9. The acceptance criteria for the helium leakage test shall be a measured leakage rate of $\leq 2 \times 10^{-7}$ cm^3/s (helium), i.e., leaktight per ANSI N14.5-1997 under the test conditions.
10. Remove helium MSLD from test port plug and reinstall port plug and torque to 60 ± 6 inch-pounds.

8.1.3.2 Alternate Port Cover Leakage Rate Tests

8.1.3.2.1 Fabrication and Periodic Leakage Rate Tests

The following procedure shall be used to perform the fabrication and periodic leakage rate tests on the alternate port covers.

1. If the port cover leakage rate tests are not performed immediately following the closure lid leakage rate test of Section 8.1.3.1, evacuate the cask cavity to ≤ 100 torr (130 mbar) and backfill to atmospheric pressure with 99.9% (minimum) pure helium. Reevacuate to ≤ 100 torr (130 mbar) and perform the final helium backfill to atmospheric pressure.
2. Install new O-rings on the port cover.
3. Remove the port valve (either vent or drain valve) and install the port cover.
4. Install and torque the port cover bolts to 100 ± 10 inch-pounds.
5. Remove the test port plug from the port cover.
6. Connect a helium MSLD to the test port. Start the helium MSLD.
7. Monitor the test leakage rate until the leakage rate is stable or for a minimum of 30 seconds.
8. The acceptance criteria for the helium leakage rate test shall be ≤ 2×10^{-7} cm^3/s (helium), i.e., leaktight per ANSI N14.5-1997 under the test conditions.
9. Remove helium MSLD from the test port and reinstall port plug and torque to 60 ± 6 inch-pounds.
10. Repeat Steps 1 through 9 for the second port cover.

8.1.3.2.2 Maintenance Leakage Rate Test

The following procedure shall be used to perform the maintenance leakage rate test on the alternate port covers following the field replacement of a port cover containment face seal during cask loading operations.

1. Replace the affected seal(s).
2. Insert port cover in a plastic test bag and seal the bag to the cask body around the port opening using suitable tape.
3. Evacuate test bag and backfill with 99.9% (minimum) pure helium to one atmosphere absolute.
4. Reevacuate test bag and perform final helium backfill to one atmosphere absolute.
5. Without breaking the seal of the plastic bag to the cask body, insert the port cover into the port opening and hand tighten the bolts.
6. Torque the bolts to 100 ± 10 inch-pounds. Remove the plastic bag.
7. Remove the test port plug from the port plug.

8. Attach helium MSLD to the port cover test port and evacuate the volume between the seals.
9. Monitor the test leakage rate until stable or for a minimum of 30 seconds.
10. The test is acceptable if the measured leakage rate is $\leq 2 \times 10^{-7}$ cm^3/s (helium), i.e., leaktight per ANSI N14.5-1997 under the test conditions.
11. Remove helium MSLD from test port and reinstall the test port plug and torque to 60 ± 6 inch-pounds.

8.1.3.3 Alternate B Port Cover Leakage Rate Tests

8.1.3.3.1 Fabrication and Periodic Leakage Rate Tests

The following test procedure shall be used to perform the fabrication and periodic leakage rate tests for the Alternate B port cover. For NAC-LWT casks to be used to transport TPBARS, the fabrication leakage rate test shall be performed immediately following the post-fabrication hydrostatic test to 450 +15/-0 psig required for transport of TPBAR contents. The Alternate B port covers shall be installed for the 450 +15/-0 psig hydrostatic test. The periodic leakage rate test will be performed as part of a cask's annual maintenance and certification program.

1. If the Alternate B port cover leakage rate tests are not performed immediately after the closure lid leakage rate test in Section 8.1.3.1, evacuate the cask cavity to ≤ 100 torr (130 mbar) and perform the final helium backfill to atmospheric pressure with 99.9% (minimum) pure helium. Reevacuate to ≤ 100 torr (130 mbar) and perform final helium backfill to atmospheric pressure.
2. Install the new metallic O-ring on the Alternate B port cover.
3. Remove the port nipple (either vent or drain valve) and install the Alternate B port cover.
4. Install and torque the port cover bolts to 285 ± 15 inch-pounds.
5. Remove the test port plug from the port cover.
6. Connect a helium MSLD to the test port. Start the helium MSLD.
7. Monitor the test leakage rate until the leakage rate is stable or for a minimum of 30 seconds.
8. The test is acceptable if the measured leakage rate is $\leq 2 \times 10^{-7}$ cm^3/s (helium), i.e., leaktight per ANSI N14.5-1997 under the test conditions.
9. Remove helium MSLD from the test port and reinstall the test port plug and torque to 60 ± 6 inch-pounds.
10. Repeat Steps 1 through 9 for the second Alternate B port cover.

8.1.3.3.2 Maintenance and Preshipment Leakage Rate Tests

The following maintenance leakage rate test procedure for the Alternate B port cover is used after metallic O-ring replacement during each cask loading operation, or if another containment component of an Alternate B port cover is replaced, for contents requiring leaktight containment per ANSI N14.5-1997, such as TPBARs, damaged TRIGA fuel in sealed DFCs and MOX fuel rods.

1. Replace metallic seal.
2. Insert Alternate B port cover in plastic test bag and seal to cask body around port opening with suitable tape.
3. Evacuate test bag and backfill with 99.9% (minimum) pure helium to one atmosphere absolute.
4. Reevacuate test bag and perform final helium backfill to one atmosphere absolute.
5. Without breaking seal of plastic bag to the cask body, insert the Alternate B port cover into the port opening and tighten bolts hand tight.
6. Remove plastic bag and torque bolts to 285 ± 15 inch-pounds.
7. Remove test port plug from the Alternate B port cover.
8. Attach helium mass spectrometer to the Alternate B port cover test port and evacuate the volume between the seals.
9. Monitor the leakage rate test until stable or a minimum of 30 seconds.
10. The test is acceptable if the indicated leakage rate is $\leq 2 \times 10^{-7}$ cm^3/s (helium), i.e., leaktight per ANSI N14.5-1997 under test conditions.
11. Repeat Steps 1 through 10 for the second Alternate B port cover.

8.1.4 Component Tests

Tests performed on individual components are designed to ensure that the components meet the design requirements for correct operation of the cask system.

Acceptance criteria are functions of the purpose of the component being tested.

8.1.4.1 Valves, Pressure Relief Device, and Fluid Transport Devices

Overpressurization protection is afforded the neutron shield tank in the form of a relief valve that is designed to open at 165 psig (plus or minus 10 percent), and reseat. The relief valve is removed from the cask and hydraulically pressure tested using a calibrated system to verify relief valve opening and closing pressures. Failure to operate within tolerance is cause for rejection. Rejected valves are rebuilt or replaced and retested prior to use.

The cask cavity does not contain overpressurization protection because the maximum pressures developed in the worst case (fuel or TPBAR rupture) are well below the structural capability of the cask structure, lid, port covers, and seals.

The cask ports for vent/drain operations (two ports) contain valved quick disconnect fittings. These valves do not require testing to verify valved operation, because no credit is taken for these valves in the cask analyses. The valves provide a convenient method of attaching lines and fixtures, but serve no safety-related function.

The NAC-LWT cask package does not use rupture disks.

A siphon tube is used to connect the neutron shield tank to the neutron shield expansion tank. The tube is a passive device and allows expanding fluid to enter the expansion tank and returns the fluid as the liquid cools. It contains no moving parts and cannot be inspected after installation. The tube will be inspected for cleanliness and to verify that its passage is free of debris and clear prior to installation.

8.1.4.2 Gaskets

Cask closure lid and port cover O-rings will be hydrostatically pressure tested to verify suitability for use and for operation in the Maximum Normal Operating Pressure (MNOP) condition. The O-rings are arranged in pairs with an annulus between them. The annulus is connected by a drilled passageway to a test port. In the acceptance test, each of the three O-ring sets (one closure lid set, one vent port cover set, and one drain port cover set) is pressurized to 209 (+5/-0) psig for 30 minutes. Casks having TPBARs as approved contents are subjected to additional hydrostatic tests at 450 +15/-0 psig (one with the vent cover installed and one with the drain port cover installed). Loss of pressure or any other sign of leakage is cause for rejection.

8.1.4.3 Sealed Canisters

Prior to underwater application of sealed canisters, each design shall be qualified by testing to demonstrate the ability of the canister to be vacuum dried and to stay sealed during subsequent underwater handling and storage. The qualification tests performed will simulate underwater vacuum drying and subsequent handling/storage. Acceptance criteria include no residual water in, or water ingress to, the sealed canister.

8.1.4.4 Miscellaneous

The cask impact limiter structures contain a two-part, aluminum honeycomb that is fabricated to have dynamic crush strengths of 3,500 psi. (plus 5 percent, minus 10 percent) and 250 psi (plus 10 percent, minus 10 percent), respectively. Sample lots of honeycomb material are subjected to dynamic crush testing to verify the crush strength of the impact limiter material. A dynamic crush strength of a sample outside of the allowable variation is cause for rejection of the batch lot of honeycomb material.

8.1.5 Tests for Shielding Integrity

A gamma scan inspection of all steel and lead shielding is conducted in order to verify shielding integrity. This inspection is performed on the cask body, including the cask bottom.

The test is conducted by continuous scanning or probing over 100 percent of all accessible surfaces, using a 3-inch detector and a ^{60}Co source of sufficient strength to produce a count rate that equals or exceeds three times the background count rate.

Scan path spacing is 2.5 inches. Scan speed is 4.5 feet-per-minute or less. All probing is on a 2-inch grid pattern (when using a 3-inch detector) and the count time is a minimum of one minute.

Acceptance is based on a lead and steel mock-up, where the material thicknesses are equivalent to the minimum thicknesses specified by the drawings. The lead and steel mock-up is produced using the same pouring technique as that approved for the cask.

Any area that produces a count rate over that established by the mock-up is considered rejected and must be corrected and retested prior to use.

Test equipment is checked before and after each use to ensure that shield test results are accurate.

8.1.6 Thermal Acceptance Tests

8.1.6.1 Thermal Test

A heat transfer acceptance test is conducted to test the integrity of the lead/stainless steel interface and to establish the heat rejection capability of the cask. The test is conducted with the neutron shield tank full[1] and the pressurized water reactor (PWR) basket located in the dry cask cavity.

[1] The neutron shield tank is filled with a liquid consisting of 58 weight percent ethylene glycol, 39 weight percent demineralized water and 3 weight percent potassium tetraborate ($K_2B_4O_7$).

The cask is internally heated at a rate of 8,500 BTU per hour (± 1,000 BTU per hour). A minimum of 12 internal and 12 external temperatures on the cask are measured with thermocouples. A test closure lid is used to allow penetrations for electric heaters and thermocouples. The steady state heat rate, transient cask temperatures, and ambient temperature are recorded. The test is conducted with the cask 3 feet (approximately) above the ground, horizontal and in still air.

8.1.6.2 Retest

If any equipment should fail during the test, such that the test must be aborted, the test is repeated.

8.1.6.3 Heat Source

The heat source for the thermal test is an electrical heater (cal-rod type) with an active length of 144 to 150 inches and is capable of generating at least 2.5 kilowatts.

8.1.7 Neutron Absorber Tests

8.1.7.1 General

Neutron absorber material in the form of borated stainless steel sheets is used in the TRIGA poison basket modules. After manufacturing, test samples from each batch of neutron absorber (poison) sheets shall be tested using neutron absorption techniques to verify the presence, proper distribution, and minimum weight percent of enriched boron. The tests shall be performed in accordance with approved written procedures.

8.1.7.2 Preparation of Samples for Spectroscopic Examination

Detailed written procedures to perform neutron absorption tests of each batch of neutron absorber sheets shall be established by the manufacturer and approved by NAC. For each batch of neutron absorber sheets, a sample shall be taken from each sheet. The samples shall be indelibly marked and recorded for identification.

At least 2 percent of the sheets in a batch shall be tested using a grid pattern of locations covering the entire surface of the sheet. Each of the remaining sheets in a batch shall be tested at one random location to ensure the presence of boron.

8.1.7.3 Neutron Absorption Test Performance

An approved facility with a neutron source and neutron detection capability shall be selected to perform the described tests. The tests will assure that the neutron absorption capacity of the material tested is equal to, or higher than, the given reference value and will verify the uniformity of boron distribution of a batch of neutron absorber sheets. The principle of measurement of neutron absorption is that the presence of boron results in a slowing down of neutron flux between the neutron sources, the reflector, and the neutron detector – depending on the material thickness and boron content.

Typical test equipment will consist of a neutron source/neutron detector, a reflector, and a counting instrument. The test equipment is calibrated using approved reference sheet(s), whose ^{10}B content has been checked and verified by an independent method such as chemical analysis. The highest permissible counting rate is determined from the neutron counting rates of the reference sheet(s), which should be ground to the minimum allowable plate thickness. This calibration process shall be repeated daily (at least once every 24 hours) while tests are being performed.

8.1.7.4 Acceptance Criteria

The neutron absorption test shall be considered acceptable if the neutron count determined for each test specimen is less than or equal to the highest permissible neutron count rate determined from the reference sheet(s). The poison sheets shall have a minimum of 1.04 weight-percent enriched boron content, with ^{10}B being a minimum of 93.88 atom percent. Any specimen not meeting the acceptance criteria for maximum neutron count shall be rejected and all of the sheets from that lot shall be similarly rejected.

8.2 Maintenance Program

Each NAC-LWT cask is subjected to a series of tests and inspections prior to each loaded shipment and annually, as shown in the Maintenance Program Schedule (Table 8.2-1).

Prior to each loaded transport, the metallic O-rings of the closure lid and Alternate B port covers, if used, are replaced. The O-ring seals of the alternate port covers are inspected and replaced as necessary. The cask cavity, trunnions, and all removable components (i.e., closure lid, port covers, attachment bolts, impact limiters, etc.) are visually inspected for damage. Following loading, the closure lid and port covers are installed and the bolting torqued. Leakage rate tests are performed on the closure lid and port covers as detailed in the cask loading procedures of Chapter 7.1. Depending on the port cover design and content conditions, helium leakage rate tests and air pressure drop tests verify the pre-shipment integrity of the containment boundary.

The completion of the annual maintenance and test program is required for each NAC-LWT cask while it is in service. The completion of the annual maintenance is documented on an annual inspection certification document. Each NAC-LWT cask must have a current annual certification before it can be used. The required annual cask maintenance test program is performed during or before the calendar month in which the annual program is due, but it is required to be performed no later than 30 days following the due date. During periods when the cask is not in use, the annual maintenance program may be deferred provided that the annual maintenance is completed and documented prior to the cask's next use.

For NAC-LWT casks to be used to transport TPBAR contents, a one-time post-fabrication hydrostatic test of the cask containment boundary shall be performed to a pressure of 450 + 15/-0 psig.

NAC-LWT cask closure lid and port cover containment seals are helium leakage rate tested to the leaktight criteria of ANSI N14.5-1997.

The annual maintenance program certification documentation shall specifically identify that a NAC-LWT packaging has been qualified by testing for TPBAR contents.

Engineering approval is required prior to making any repairs of damaged areas or areas that need refurbishing as a result of normal wear and tear. All such repairs shall be fully documented in accordance with NAC's approved Quality Assurance program. The replacement of valves, fittings, seals, thread fasteners, or use of calibrated pressure gauges are considered normal maintenance and do not require engineering approval.

Testing of the cask shielding and heat rejection capabilities is conducted during original packaging acceptance testing. The structures that provide shielding and heat rejection are passive and do not require verification during routine use of the package. Consequently, the

efficiency of these systems is not tested during the annual maintenance program. Radiation surveys conducted at the time of cask loading provide verification of continued shielding effectiveness.

Testing of the neutron absorber material utilized in TRIGA poisoned basket modules are conducted prior to fabrication of the basket modules. The neutron absorber material is in the form of borated stainless steel sheets that are visually inspected for wear or damage prior to each use, and do not require routine maintenance.

Table 8.2-1 Maintenance Program Schedule

Cask Cavity (Including Port Cover and Lid Seals Annulus)	
Annually	Visual Inspection Lid and Port Cover Seal Replacement Helium Leak Tests (per Section 8.1.3)
Valve Port Covers	
Each Loaded Shipment	Visual Inspection Air Pressure Drop Test at 15 +1/-0 psig (Alternate port covers) Helium Leakage Testing (Alternate B port covers) Seal Replacement as Necessary[1]
Drain Line Gasket	
Each Shipment	Seal Replacement as Necessary
Annually	Seal Replacement
Water Jacket and Expansion Tank	
Annually	Visual Inspection Check Fluid Level, Specific Gravity, and Boron Concentration[2]
Each Shipment	Visually Inspect Fill, Drain and Inspection Port Plugs for Leakage
Cask Lid Bolts	
Each Shipment	Visually Inspect for Damage and Replace, as required.
Long Term Maintenance	Bolt replacement upon reaching 20-year life or 550 operational cycles.

[1] Helium leak testing (per Section 8.1.3.2.2) is required following replacement of alternate port cover seals. For Alternate B port covers, seal replacement and leak testing are required for each shipment per the requirements specified in the Operating Procedures in Chapter 7 and Section 8.1.3.2.2.

[2] The neutron shield fluid must be verified to contain greater than 1.0 wt % boron and the specific gravity must be such that the solution does not freeze at temperatures above -40°F.

Table 8.2-1 Maintenance Program Schedule (continued)

Water Jacket Relief Valve	
Annually	Replace With New Pre-set Valve, or Verify Opening and Reseating Pressure (Allowable variation is ± 10 psig of Nominal Valve Opening Pressure, 165 psig)
Fasteners, Valved Nipples, Washers, Reusable O-rings, and Helicoils	
Each Shipment	Inspect and Replace as necessary
Lid and Alternate B Port Cover Metallic O-rings	
Each Loaded Shipment	Replace and perform helium leakage rate testing to the criteria specified in Section 8.1.3.